frontiers | Research Topics

Targeting signals in protein trafficking and transport

Edited by
Markus Kunze, Andrey L. Karamyshev, Inhwan Hwang,
Anastassios Economou and Nathan Alder

Published in
Frontiers in Physiology
Frontiers in Cell and Developmental Biology
Frontiers in Microbiology

ISSN 1664-8714
ISBN 978-2-8325-4172-2
DOI 10.3389/978-2-8325-4172-2

About Frontiers

Frontiers is more than just an open access publisher of scholarly articles: it is a pioneering approach to the world of academia, radically improving the way scholarly research is managed. The grand vision of Frontiers is a world where all people have an equal opportunity to seek, share and generate knowledge. Frontiers provides immediate and permanent online open access to all its publications, but this alone is not enough to realize our grand goals.

Frontiers journal series

The Frontiers journal series is a multi-tier and interdisciplinary set of open-access, online journals, promising a paradigm shift from the current review, selection and dissemination processes in academic publishing. All Frontiers journals are driven by researchers for researchers; therefore, they constitute a service to the scholarly community. At the same time, the *Frontiers journal series* operates on a revolutionary invention, the tiered publishing system, initially addressing specific communities of scholars, and gradually climbing up to broader public understanding, thus serving the interests of the lay society, too.

Dedication to quality

Each Frontiers article is a landmark of the highest quality, thanks to genuinely collaborative interactions between authors and review editors, who include some of the world's best academicians. Research must be certified by peers before entering a stream of knowledge that may eventually reach the public - and shape society; therefore, Frontiers only applies the most rigorous and unbiased reviews. Frontiers revolutionizes research publishing by freely delivering the most outstanding research, evaluated with no bias from both the academic and social point of view. By applying the most advanced information technologies, Frontiers is catapulting scholarly publishing into a new generation.

What are Frontiers Research Topics?

Frontiers Research Topics are very popular trademarks of the *Frontiers journals series*: they are collections of at least ten articles, all centered on a particular subject. With their unique mix of varied contributions from Original Research to Review Articles, Frontiers Research Topics unify the most influential researchers, the latest key findings and historical advances in a hot research area.

Find out more on how to host your own Frontiers Research Topic or contribute to one as an author by contacting the Frontiers editorial office: frontiersin.org/about/contact

Targeting signals in protein trafficking and transport

Topic editors

Markus Kunze — Medical University of Vienna, Austria

Andrey L. Karamyshev — Texas Tech University Health Sciences Center, United States

Inhwan Hwang — Pohang University of Science and Technology, Republic of Korea

Anastassios Economou — KU Leuven, Belgium

Nathan Alder — University of Connecticut, United States

Citation

Kunze, M., Karamyshev, A. L., Hwang, I., Economou, A., Alder, N., eds. (2023). *Targeting signals in protein trafficking and transport*. Lausanne: Frontiers Media SA. doi: 10.3389/978-2-8325-4172-2

Table of contents

frontiers | Frontiers in Physiology

TYPE Editorial
PUBLISHED 06 December 2023
DOI 10.3389/fphys.2023.1338852

OPEN ACCESS

EDITED AND REVIEWED BY
Christoph Fahlke,
Helmholtz Association of German Research Centres (HZ), Germany

*CORRESPONDENCE
Markus Kunze,
markus.kunze@meduniwien.ac.at

RECEIVED 15 November 2023
ACCEPTED 23 November 2023
PUBLISHED 06 December 2023

CITATION
Kunze M, Alder NN, Hwang I, Roussel G and Karamyshev AL (2023), Editorial: Targeting signals in protein trafficking and transport.
Front. Physiol. 14:1338852.
doi: 10.3389/fphys.2023.1338852

Editorial: Targeting signals in protein trafficking and transport

Markus Kunze[1]*, Nathan N. Alder[2], Inhwan Hwang[3], Guillaume Roussel[4] and Andrey L. Karamyshev[5]

[1]Department of Pathobiology of the Nervous System, Center for Brain Research, Medical University of Vienna, Vienna, Austria, [2]Department of Molecular and Cell Biology, University of Connecticut, Storrs, CT, United States, [3]Department of Life Sciences, Pohang University of Science and Technology, Pohang, Republic of Korea, [4]Laboratory of Molecular Bacteriology, Department of Microbiology, Immunology, and Transplantation, Rega Institute, Katholieke Universiteit-Leuven, Leuven, Belgium, [5]Department of Cell Biology and Biochemistry, Texas Tech University Health Sciences Center, Lubbock, TX, United States

KEYWORDS

protein transport, targeting signals, mitochondria, chloroplasts, endoplasmic reticulum, peroxisomes, bacterial secretion

Editorial on the Research Topic
Targeting signals in protein trafficking and transport

"This Research Topic of Frontiers in Physiology is dedicated to the memory of Professor Anastassios (Tassos) Economou, one of the guest editors of this issue, who recently passed away during its formation."

Introduction

The distribution of proteins among the different compartments of cells and the ability to export proteins to the extracellular space is critically dependent on protein transport processes. In most cases these processes are governed by the interaction between targeting signals encoded in the primary sequence of proteins to be transported (cargo proteins) and receptor proteins linking them with the general transport machinery. This Research Topic is a collection of original articles and reviews covering transport processes into peroxisomes, mitochondria and chloroplasts, into the endoplasmic reticulum (ER) and across the secretory pathway, and protein secretion in bacteria. Remarkably, some targeting signals, particularly the N-terminal ones, are structurally similar, which raises questions of the relation between similarity and specificity (Kunze and Berger, 2015) and the conservation through evolution.

Peroxisomes

Peroxisomes are single membrane bound organelles with two types of peroxisomal targeting signals for matrix proteins (PTS1 and PTS2) and another for peroxisomal membrane proteins (mPTS), which are recognized by the receptor proteins PEX5, PEX7 together with a co-receptor, and PEX19, respectively (Rudowitz and Erdmann, 2023). Krishna et al. describe targeting signals encoded in the peroxisomal membrane protein PEX11 from the protozoon *Trypanosoma brucei*, which not only has binding sites for the cognate peroxisomal receptor PEX19 but also for the mitochondrial receptor

TOM20 although mitochondrial targeting is only observed when no peroxisomes are present. The first comprehensive inventory of peroxisomal proteins of the zebrafish (*Danio rerio*) by Kamoshita et al. reveals extensive similarity to the mammalian peroxisomal proteome and of the PTS1 and PTS2 motifs encoded in the homologous enzymes, which confirms *D. rerio* as promising model organism for chordates. Based on a PTS2-tagged EGFP reporter protein Lu et al. studied the peroxisomal dynamics in the fungus *Alternaria alternata* as a developmentally interesting model system for rapidly changing organismal states confirming previous studies on the relevance of peroxisomes for fungal developmental and infectious processes.

Mitochondria

Mitochondria contain two membranes and several distinct subcompartments, each one with its own defined set of proteins (Iovine et al., 2021). These organelles have their own genome and biosynthetic machinery to produce some resident proteins. But the vast majority of mitochondrial proteins are encoded in nuclear DNA, synthesized on cytosolic ribosomes, and trafficked to the organelle. Targeting mitochondrial proteins to their correct subcompartments requires a diversity of import pathways, each one having its own type of targeting signal. Most nuclear-encoded proteins, however, are directed to mitochondria by N-terminal presequences that engage the TOM and TIM23 complexes of the outer and inner mitochondrial membranes, respectively. In this Research Topic, Genge and Mokranjac review what is currently known about the import of presequence-containing proteins into mitochondria with particular emphasis on the cooperation of the TOM and TIM23 complexes. Reed et al. review evidence for a more non-canonical role of TIM23-mediated import in neurodegenerative diseases, describing how amyloidogenic proteins bearing cryptic targeting signals may import into mitochondria as part of the pathogenic process, or perhaps as a quality control mechanism.

Chloroplasts

Chloroplasts are an endosymbiotic organelle found in plants and algae. For their function, chloroplasts contain a large number of proteins, with estimates ranging from 2,000 to 5,000 different proteins. Over 95% of these proteins are targeted from the cytosol to various suborganellar compartments after translation (Peltier et al., 2000; Schleiff and Becker, 2011). The protein targeting mechanisms for chloroplasts are complex and diverse; each of the suborganellar compartments of chloroplasts employs specific protein targeting mechanisms. In this Research Topic, Jeong et al. review the diverse nature of transit peptides for specific targeting to chloroplasts and also provide analysis on how the targeting specificity is determined between chloroplasts and mitochondria. Zheng et al. summarize the properties and significance of liquid-liquid phase separation in the sorting of chloroplast twin arginine transport substrate proteins. Zhu et al. review the various protein transport systems from the chloroplast stroma to the thylakoid membrane and also describe the targeting of chloroplast-encoded proteins to the thylakoid membranes. Finally, Ballabani et al. review the common features of targeting sequences in routing preproteins to and across the chloroplast envelope as well as the thylakoid membrane and lumen. They also summarize recent findings on components of the import machinery at outer and inner envelopes, thylakoid membranes, and stroma.

Secretory pathway

In humans, about 30%–40% of proteins are secretory and membrane proteins. These proteins need to be transported to different cellular organelles, inserted into membranes or transported outside of the cells. Many of these proteins use signal recognition particle (SRP) and SEC61 complex in ER for their transport (Kellogg et al., 2021). This process is tightly regulated, and its dysregulation is associated with multiple diseases. Secretory proteins have N-terminal targeting signals called signal peptides which are recognized by SRP, and mutations in them often lead to diseases (Gutierrez Guarnizo et al., 2023). In this Research Topic, Lang et al. review molecular mechanisms of ER protein targeting and translocation and analyze signal peptide features that determine the specificity of protein transport. Karamysheva and Karamyshev describe how cells protect themselves from aberrant secretory proteins by activating the RAPP protein quality control on the ribosome and discuss molecular mechanisms of human diseases associated with dysregulation of protein transport. Štepihar et al. focus on the late steps in protein transport—cell-specific secretory granule sorting mechanism and role of MAGEL2 protein in regulated secretion.

Bacterial transport

Amongst the numerous secretion systems in bacteria, each secretory protein follows a dedicated pathway and therefore need to indicate to the cell its journey and destination (Loos et al., 2019). Evolution selected the signal peptide, a short amino-acid sequence, to direct the client to the appropriate secretion system. The review from Kaushik et al. examines in detail the complete journey of the signal peptide during secretion; from the cytoplasm where it delays the folding, then to the network of chaperones sorting it to the appropriate secretion system to be exported or inserted in the membrane; and finally, its degradation by the signal peptidase; and how this critical step can be used as a novel strategy for antibiotics development. While the key role of the signal peptide has largely been attributed to its amino acid sequence, the work of Spitz et al. on signal peptides from clients of the Type 1 secretion system introduces an interesting concept where a structural feature, a conserved amphipathic helix, is encoded in the signal peptide and is more important than the sequence itself.

Altogether, this Research Topic allows an up-to-date synopsis of various transport systems covering all phylogenetic kingdoms and

providing a plethora of information on different targeting signals, the cognate receptor proteins, and their relevance for complex transport processes. Highlighting the benefits of a systematic analysis of the vast majority of proteins harboring the same type of targeting signal either by experimental approaches or by computational prediction of organellar proteomes from different species and their comparison, fostering a comparison of targeting signals directing proteins to different compartments in spite of similar structural properties, and emphasizing the relevance of protein transport systems and their associated quality controls for human diseases, this Research Topic pinpoints critical research questions of the field of protein transport today.

Author contributions

MK: Conceptualization, Writing–original draft, Writing–review and editing. NA: Writing–original draft, Writing–review and editing. IH: Writing–original draft, Writing–review and editing. GR: Writing–original draft, Writing–review and editing. AK: Writing–original draft, Writing–review and editing.

In memoriam

Professor Economou was a renowned scientist in bacterial protein secretion, known for its significant and numerous contributions to the Sec and Type III translocase mechanisms. Native from Alexandroupolis in Greece, Tassos graduated in Biology in Thessaloniki, and then earned his PhD in Molecular Microbiology in 1990 from the John Innes Institute and University of East Anglia in the United-Kingdom. He then pursued his career as a postdoctoral researcher at the University of California in Los Angeles (United States), and then the Medical School of Dartmouth (United States). In 1999, he established his lab at the Institute of Molecular Biology and Biotechnology—Foundation of Research and Technology (IMBB-FORTH) at the University of Crete in Greece, where he also founded the MINOTECH Biotechnology company and Proteomics facility, and acted as a consultant for Pfizer and Integrated Genomics. Tassos played a significant role in the development and recognition of IMBB-FORTH as a center of excellence and led to extensive funding for large European and international programs in Greece. In 2013, Tassos changed to a more temperate climate and moved his lab to Belgium. He became professor of Molecular Biology and Biochemistry and the Head of the Molecular Bacteriology division, at the REGA institute, KU Leuven—Since his first publication in 1986, he collaborated on over 130 research articles, making notable contributions to top-ranking scientific journals such as Cell, Nature, and Science. He had an extraordinarily wide knowledge of the field of molecular biology, specifically on the molecular basis of protein secretion and folding. Over the years he created a unique infrastructure that encompasses not only cutting-edge molecular biology but also a multi-disciplinary biophysical toolset including single-molecule FRET and hydrogen deuterium exchange mass spectrometry, using his words, "A unique combination of tools that allow us to dissect the intricate mechanisms involved in protein secretion". Tassos' deep involvement in science extends beyond his publications, involving active participation in departmental boards, advisory committees, and diligent service as a reviewer and editor for renowned scientific journals. He had an extraordinary passion for science which was a profound source of inspiration and motivation for his students and collaborators. He mentored his students with the utmost dedication and fervor, instilling them with a lifelong love for science and the pursuit of knowledge. Outside of his research lab, Tassos was a great father of three kids, a dedicated husband for over three decades, a caring friend, and an excellent cook (always bringing Greek delicacies during the lab dinners). His legacy as a mentor and scientist will continue to inspire the next generation of scientists, forever grateful for the passion and enthusiasm with which he guided them on their scientific and life journeys.

Conflict of interest

The authors declare that the research was conducted in the absence of any commercial or financial relationships that could be construed as a potential conflict of interest.

Publisher's note

References

Gutierrez Guarnizo, S. A., Kellogg, M. K., Miller, S. C., Tikhonova, E. B., Karamysheva, Z. N., and Karamyshev, A. L. (2023). Pathogenic signal peptide variants in the human genome. *Nar. Genom Bioinform* 5, lqad093. doi:10.1093/nargab/lqad093

Iovine, J. C., Claypool, S. M., and Alder, N. N. (2021). Mitochondrial compartmentalization: emerging themes in structure and function. *Trends Biochem. Sci.* 46, 902–917. doi:10.1016/j.tibs.2021.06.003

Kellogg, M. K., Miller, S. C., Tikhonova, E. B., and Karamyshev, A. L. (2021). SRPassing Co-translational targeting: the role of the signal recognition particle in protein targeting and mRNA protection. *Int. J. Mol. Sci.* 22. doi:10.3390/ijms22126284

Kunze, M., and Berger, J. (2015). The similarity between N-terminal targeting signals for protein import into different organelles and its evolutionary relevance. *Front. Physiol.* 6, 259. doi:10.3389/fphys.2015.00259

Loos, M. S., Ramakrishnan, R., Vranken, W., Tsirigotaki, A., Tsare, E. P., Zorzini, V., et al. (2019). Structural basis of the subcellular topology landscape of *Escherichia coli*. *Front. Microbiol.* 10, 1670. doi:10.3389/fmicb.2019.01670

Peltier, J. B., Friso, G., Kalume, D. E., Roepstorff, P., Nilsson, F., Adamska, I., et al. (2000). Proteomics of the chloroplast: systematic identification and targeting analysis of lumenal and peripheral thylakoid proteins. *Plant Cell* 12, 319–341. doi:10.1105/tpc.12.3.319

Rudowitz, M., and Erdmann, R. (2023). Import and quality control of peroxisomal proteins. *J. Cell Sci.* 136. doi:10.1242/jcs.260999

Schleiff, E., and Becker, T. (2011). Common ground for protein translocation: access control for mitochondria and chloroplasts. *Nat. Rev. Mol. Cell Biol.* 12, 48–59. doi:10.1038/nrm3027

frontiers in Physiology

MINI REVIEW
published: 22 November 2021
doi: 10.3389/fphys.2021.795156

Functional Organization of Sequence Motifs in Diverse Transit Peptides of Chloroplast Proteins

Jinseung Jeong[1], Inhwan Hwang[2] and Dong Wook Lee[1,3]**

[1]*Department of Integrative Food, Bioscience and Biotechnology, Chonnam National University, Gwangju, South Korea,* [2]*Department of Life Sciences, Pohang University of Science and Technology, Pohang, South Korea,* [3]*Department of Bioenergy Science and Technology, Chonnam National University, Gwangju, South Korea*

Although the chloroplasts in plants are characterized by an inherent genome, the chloroplast proteome is composed of proteins encoded by not only the chloroplast genome but also the nuclear genome. Nuclear-encoded chloroplast proteins are synthesized on cytosolic ribosomes and post-translationally targeted to the chloroplasts. In the latter process, an N-terminal cleavable transit peptide serves as a targeting signal required for the import of nuclear-encoded chloroplast interior proteins. This import process is mediated *via* an interaction between the sequence motifs in transit peptides and the components of the TOC/TIC (translocon at the outer/inner envelope of chloroplasts) translocons. Despite a considerable diversity in primary structures, several common features have been identified among transit peptides, including N-terminal moderate hydrophobicity, multiple proline residues dispersed throughout the transit peptide, preferential usage of basic residues over acidic residues, and an absence of N-terminal arginine residues. In this review, we will recapitulate and discuss recent progress in our current understanding of the functional organization of sequence elements commonly present in diverse transit peptides, which are essential for the multi-step import of chloroplast proteins.

Keywords: chloroplast, transit peptide, sequence motif, protein targeting, protein translocation

OPEN ACCESS

Edited by:
Walter Sandtner,
Medical University of Vienna, Austria

Reviewed by:
Carmela Giglione,
Centre National de la Recherche Scientifique (CNRS), France

****Correspondence:***
Inhwan Hwang
ihhwang@postech.ac.kr
Dong Wook Lee
ldw4844@jnu.ac.kr

Specialty section:
This article was submitted to Membrane Physiology and Membrane Biophysics, a section of the journal Frontiers in Physiology

Received: *15 October 2021*
Accepted: *28 October 2021*
Published: *22 November 2021*

Citation:
Jeong J, Hwang I and Lee DW (2021) Functional Organization of Sequence Motifs in Diverse Transit Peptides of Chloroplast Proteins. Front. Physiol. 12:795156. doi: 10.3389/fphys.2021.795156

INTRODUCTION

The chloroplast, a type of plastid, is an organelle uniquely present in plants and is believed to have been derived *via* the endosymbiosis of ancient cyanobacteria (Dyall et al., 2004; Zimorski et al., 2014; Lee and Hwang, 2021). During the subsequent evolution of chloroplasts as subcellular organelles, more than 90% of the original cyanobacterial genes were transferred to the host nuclear genome (Ponce-Toledo et al., 2019). Consequently, both chloroplastic and nuclear genome systems now contribute to assembly of the chloroplast proteome in plants. Most of the nuclear-encoded chloroplast proteins are synthesized on cytosolic ribosomes and targeted to chloroplasts post-translationally (Inaba and Schnell, 2008; Li and Chiu, 2010; Lee et al., 2013). These nuclear-encoded chloroplast proteins can be broadly categorized based on their sub-organellar locations. Proteins localized to the outer membrane of chloroplasts are primarily inserted directly into the outer membrane from the cytosol, with a few exceptions (Lee et al., 2014, 2017; Day et al.,

2019; Gross et al., 2021). However, most chloroplast interior proteins, which are localized to the inner membrane, stroma, or thylakoids, are imported into chloroplasts in a process mediated by the TOC/TIC (translocon at the outer/inner envelope of chloroplasts) translocons (Li and Chiu, 2010; Richardson et al., 2017, 2018). The chloroplast interior proteins are characterized by the presence of N-terminal cleavable targeting signals, called transit peptides (Bruce, 2000; Lee and Hwang, 2018), one of the hallmarks of which is the considerable diversity in their primary structure (Bruce, 2000; Lee et al., 2008, 2015; Li and Teng, 2013). It has previously been proposed that these diverse transit peptides might have been generated *via* the selective assembly of short sequence motifs that are critical for interactions with the components of the TOC/TIC translocons (Li and Teng, 2013; Lee et al., 2015; Lee and Hwang, 2018). Indeed, it has been established that different transit peptides contain distinct sequence motifs that play vital roles during the multi-step import process (Lee et al., 2006, 2008; Li and Teng, 2013; Lee and Hwang, 2018). Moreover, a previous study indicated that diverse transit peptides can be classified into multiple subgroups based on their sequence motifs (Lee et al., 2008).

Conversely, in addition to the inherent diversity of transit peptides, recent studies have revealed the presence of common sequence elements among different chloroplast transit peptides. In this review, we will discuss how these common features contribute to the appropriate functioning of transit peptides and provide an overview of the organization of these sequence features in transit peptides.

SEQUENCE MOTIFS IN THE RUBISCO SMALL SUBUNIT TRANSIT PEPTIDE AS A MODEL SYSTEM

Ribulose-1,5-bisphosphate carboxylase/oxygenase (Rubisco) is acknowledged to be the most abundant protein in nature, accounting for approximately 30% of total leaf proteins (Jensen, 2000). As an enzyme that is prominently involved in CO_2 fixation, Rubisco plays a central role in photosynthesis. The Rubisco complex comprises the Rubisco small subunit (RbcS) and Rubisco large subunit. Within the chloroplast stroma, the Rubisco large subunit produced in the chloroplast is assembled with the RbcS that is encoded in the nuclear genome and imported into the chloroplasts *via* the TOC/TIC translocons (Lee et al., 2006; Chotewutmontri et al., 2012; Holbrook et al., 2016). Given the abundance and essential roles of the RbcS in chloroplasts, the mechanisms underlying the import of RbcS have been extensively studied in several species as a representative chloroplast cargo protein, thereby providing a new perspective regarding our understanding of chloroplast biogenesis (Karlin-Neumann and Tobin, 1986; Reiss et al., 1987; Becker et al., 2004; Smith et al., 2004; Lee et al., 2006, 2015; Chotewutmontri et al., 2012; Holbrook et al., 2016; Richardson et al., 2018; Chen et al., 2019).

Early attempts to elucidate the organization of the RbcS transit peptide led to the conclusion that it contains multiple domains that play important roles during protein import into chloroplasts (Karlin-Neumann and Tobin, 1986; von Heijne et al., 1989; Bruce, 2001; Becker et al., 2004). Subsequently, extensive mutagenesis analysis of the *Arabidopsis* RbcS transit peptide revealed the presence of distinct sequence motifs, each of which proved to be essential for the correct cytosolic navigation, chloroplast binding, or translocation of chloroplast preproteins across the envelope membranes (Lee et al., 2006; **Figure 1**). Among these sequences, the sequence motif FP/RK was identified as the most important with respect to the efficient targeting of proteins to the chloroplasts (**Figure 1**). Furthermore, this motif has been established to be fully functional in sequence contexts other than that of RbcS transit peptides (Lee et al., 2015), and has been shown to facilitate the import of preproteins with less-efficient transit peptides (Lee et al., 2009; Razzak et al., 2017). Interestingly, the findings of a site-specific cross-linking approach have indicated that the segment encompassing this motif displays a strong cross-linking patterns with not only the TOC translocon, but also Tic20, which functions as a translocation channel in the TIC translocon, thereby indicating that the FP/RK motif plays an essential role in protein translocation across TOC/TIC translocons (Richardson et al., 2018; **Figure 1**).

Another study identified the presence of a semi-conserved motif, FGLK, to be crucial for the interaction with TOC34 (Chotewutmontri et al., 2012; Holbrook et al., 2016; **Figure 1**). Together with TOC159, TOC34 is assumed to function as a receptor for chloroplast transit peptides on the outer membrane. Although the RbcS transit peptide of *Chlamydomonas reinhardtii*, a unicellular lower eukaryote, also has sequence motifs partially homologous to the *Arabidopsis* FNGLK and FP/RK motifs, this algal transit peptide proved to be non-functional when examined in *Arabidopsis* protoplasts (Razzak et al., 2017). Interestingly, the restoration of *Arabidopsis* FNGLK and FP/RK motifs in the *Chlamydomonas* RbcS transit peptide was found to markedly enhance the delivery of GFP (green fluorescent protein) to chloroplasts in *Arabidopsis* protoplasts (Razzak et al., 2017). Moreover, a synthetic transit peptide, in which the FNGLK and FP/RK motifs of the *Arabidopsis* RbcS transit peptide were incorporated, was demonstrated to deliver a vacuolar protein to chloroplasts, thereby confirming the importance of these motifs in chloroplast protein targeting (Lee et al., 2015).

A further important feature of the RbcS transit peptide sequence is its N-terminal hydrophobicity. The N-terminal region of transit peptides is characterized by a higher proportion of hydroxylated amino acids, such as serine or threonine, than that of hydrophobic amino acids (Zybailov et al., 2008). However, it has been found that when hydroxylated residues in the N-terminal region of the RbcS transit peptide are substituted with alanines, there is no corresponding perturbation of protein import into chloroplasts (Lee et al., 2006). Contrastingly, hydrophobic residues in the N-terminal region of the RbcS transit peptide (MLM motif) have been established to be essential for protein targeting from the cytosol to the chloroplasts (Lee et al., 2006; **Figure 1**). Moreover, this region has also been proposed to function in preprotein translocation across the chloroplast membranes by interacting with stromal Hsp70, an ATP-driven molecular motor protein (Chotewutmontri and Bruce, 2015; **Figure 1**).

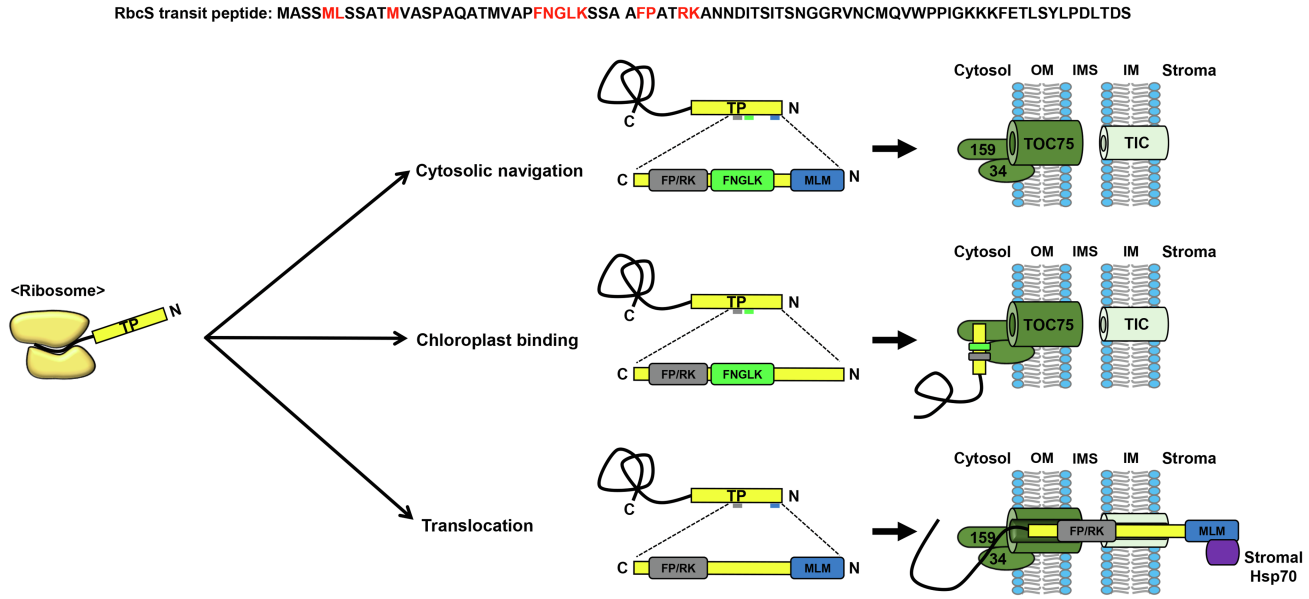

FIGURE 1 | Sequence motifs in the Rubisco small subunit transit peptide. Among the sequence motifs in the Rubisco small subunit (RbcS) transit peptide, the motifs, MLM, FNGLK, and FP/RK have been extensively characterized. The MLM motif is vital not only for cytosolic navigation, but also for translocation across chloroplast membranes, by interacting with stromal Hsp70. The FNGLK and FP/RK motifs have been demonstrated to mediate chloroplast binding *via* interactions with Toc34. The segment containing the FP/RK motif lies in close proximity to the TOC/TIC translocons during preprotein translocation, which may be essential for the efficient translocation of RbcS. TP, transit peptide; OM, outer membrane; IMS, intermembrane space; IM, inner membrane.

Collectively, we have accumulated considerable knowledge regarding the organization of sequence motifs in RbcS transit peptides, which will help in elucidating the import mechanisms of chloroplast proteins and in designing more efficient transit peptides to deliver proteins into the chloroplast.

SEQUENCE FEATURES REQUIRED FOR CHLOROPLAST-SPECIFIC TARGETING

The mitochondrion, another example of an endosymbiotic organelle, is universally present in all eukaryotic cells and is believed to have evolved prior to the chloroplast (Dyall et al., 2004). Interestingly, the protein import mechanisms of these two endosymbiotic organelles are remarkably similar, implying that plant cells possess appropriate sorting mechanisms that facilitate the site-specific targeting of proteins to chloroplasts and mitochondria (Schleiff and Becker, 2011; Lee and Hwang, 2021). A recent study accordingly sought to elucidate the putative mechanisms underlying the specificity of chloroplastic and mitochondrial protein targeting, by constructing several hybrid targeting signals consisting of segments derived from both chloroplast transit peptides and mitochondrial presequences (Lee et al., 2019). On the basis of the observed import behaviors of GFP-fused hybrid targeting signals, a simple but sophisticated principle has been deduced. Both transit peptides and presequences comprise two domains, one of which is the N-terminal specificity domain, which determines specific targeting to chloroplasts or mitochondria, and the other is the C-terminal translocation domain, which is interchangeable between the transit peptide and presequence (Lee et al., 2019; Lee and Hwang, 2021).

With regard to the common features of the N-terminal specificity domain of transit peptides, as stated in the previous section, the moderate hydrophobicity of the N-terminal region of transit peptides is critical for efficient protein import into chloroplasts. Contrastingly, however, the findings of numerous previous studies have indicated that the N-terminal region of mitochondrial presequences contains multiple arginine residues (Bhushan et al., 2006; Huang et al., 2009; Ge et al., 2014; Garg and Gould, 2016; Lee et al., 2020; **Figure 2A**). Surprisingly, the removal of these multiple arginine residues was sufficient to switch the final destination of cargo proteins from mitochondria to chloroplasts (Lee et al., 2019, 2020; Lee and Hwang, 2021; **Figure 2A**). Moreover, although mitochondrial presequences obtained from fungi and humans, which lack chloroplasts, have no need of a mechanism that discriminates between chloroplast and mitochondrial proteins, they could deliver GFP to chloroplasts when multiple arginines in the N-terminal region were substituted with alanines (Lee et al., 2020). These observations clearly indicate that the multiple arginine residues in mitochondrial presequences play a vital role in evading chloroplast targeting.

THE ROLES OF PROLINE AND BASIC AMINO ACID RESIDUES COMMONLY PRESENT IN DIVERSE TRANSIT PEPTIDES

Despite the considerable diversity among the primary structures of transit peptides, there are certain amino acids that are

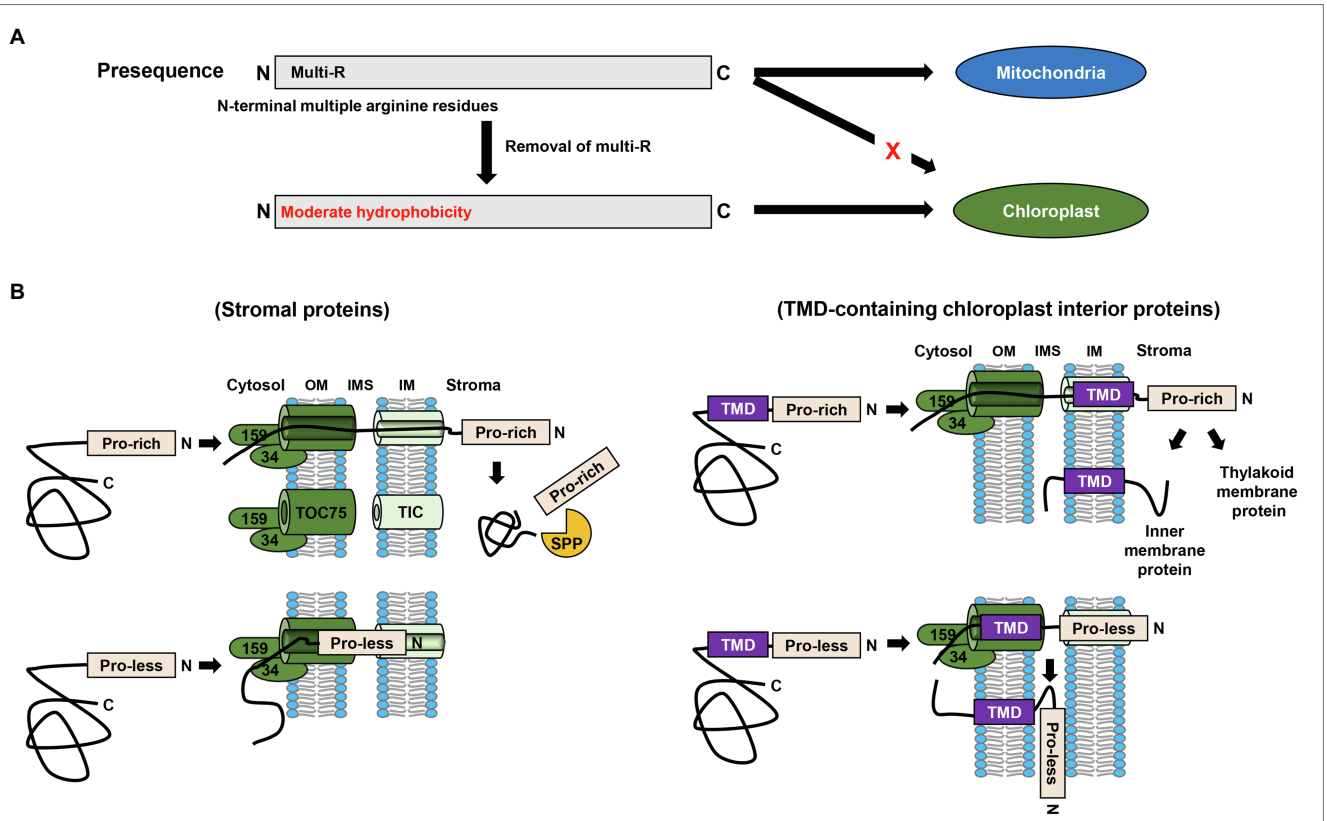

FIGURE 2 | Common characteristics of different transit peptides. **(A)** Multiple arginine residues in the N-terminal region of targeting signals function as a chloroplast evasion signal. Removal of the arginine residues from the N-terminal region of mitochondrial presequences is sufficient to switch the final destination of proteins from the mitochondria to chloroplasts. **(B)** Multiple proline residues in transit peptides are essential for preprotein translocation into chloroplasts. In the case of soluble stromal proteins, preproteins with proline-less transit peptides are trapped within the TOC/TIC translocons, whereas for transmembrane domain (TMD)-containing chloroplast internal proteins, the preproteins are laterally inserted into the chloroplast outer membrane when the preproteins harbor proline-less transit peptides. TP, transit peptide; OM, outer membrane; IMS, intermembrane space; IM, inner membrane; TMD, transmembrane domain.

preferentially incorporated into the transit peptides. Among these, the roles of multiple proline residues (which are commonly present in transit peptides) in chloroplast targeting have recently been investigated (Lee et al., 2018). Proline is a unique amino acid in that it breaks the local secondary structure, thereby conferring an unstructured property to polypeptides such as transit peptides (Guzzo, 1965). Interestingly, whereas chloroplast preproteins containing proline-less transit peptides show no defects in early cytosolic steps, their translocation into chloroplasts is typically compromised (Lee et al., 2018). In this regard, the fate of unimported preproteins harboring proline-less mutant transit peptides has been found to differ depending on the characteristics of preproteins. In the case of soluble stromal proteins, unimported precursors have been found to be trapped within the TOC/TIC translocons (**Figure 2B**). Contrastingly, preproteins harboring hydrophobic transmembrane domain(s), such as Tic110 and Tha4 (thylakoid assembly-4), and thus destined for the inner membrane and thylakoid membrane, respectively, have been found to be integrated into the outer membrane when the transit peptides lacked proline residues (Lee et al., 2018; **Figure 2B**). This aberrant insertion appears to occur during preprotein translocation through the Toc75 channel *via* lateral insertion, as opposed to direct insertion from the cytosol. Notably, it was found that in the wild-type cells, the behavior of Tha4 with a proline-less transit peptide was practically similar to that of Tha4 with a proline-rich transit peptide in *hsp93-V* mutant cells (Lee et al., 2018). Given that the translocation of preproteins is compromised in the *hsp93-V* mutant, these observations provide further evidence in support of the crucial role of proline residues in preprotein translocation (Lee et al., 2015, 2018; Huang et al., 2016).

Unlike the TOM/TIM (translocase of the outer/inner membrane) translocons in the mitochondria, TOC/TIC translocons in the chloroplasts can translocate small fully folded preproteins (Ganesan et al., 2018). Even a precursor with aggregation-prone GFP[V29A], a variant of GFP, was observed to be efficiently imported into chloroplasts, which was mediated by proline-rich transit peptides (Lee et al., 2018). However, the GFP[V29A] harboring a proline-less transit peptide was found to be aggregated to a greater extent, thereby markedly compromising translocation (Lee et al., 2018). Collectively, the aforementioned observations provide compelling evidence to indicate the essential roles of multiple proline residues in transit peptides, with respect to efficient translocation of chloroplast proteins, particularly hydrophobic TMD-containing or aggregation-prone proteins.

A further common feature of different transit peptides is their preference for positively charged basic residues over negatively charged acidic residues (Bhushan et al., 2006; Zybailov et al., 2008). Indeed, it has been shown that substitution of basic residues in some transit peptides with acidic residues markedly disrupts protein import into chloroplasts (Razzak et al., 2017; Lee and Hwang, 2019). Other studies have demonstrated that a sequence motif, consisting of two consecutive basic residues, and thus referred to as a twin-positive motif, play a role in specifically facilitating the import of plastid preproteins into leucoplasts, another type of plastid (Teng et al., 2012; Chu et al., 2020). Furthermore, recent *in silico* analysis of 1,153 *Arabidopsis* plastid proteins revealed that the presence of these twin-positive motifs is significantly correlated with a higher protein abundance in root leucoplasts (Chu et al., 2020).

CONCLUSION AND FUTURE PERSPECTIVES

We have now begun to understand the complex nature of the diverse range of chloroplast transit peptides. Transit peptides may have been generated *via* the assembly of distinct sequence motifs, each playing a pivotal role during interactions with the components of the TOC/TIC translocons, either sequentially or in concert. In addition to the specific short sequence motifs, there are several common sequence elements that make an essential contribution to the functionality of transit peptides. These include a lack of arginine residues in the N-terminal region, the presence of multiple proline residues, and the preferential usage of positively charged basic residues. In the future, it will be necessary to investigate how these common features coordinate the interactions of preproteins with the TOC/TIC translocons to facilitate the efficient import of proteins into chloroplasts.

AUTHOR CONTRIBUTIONS

DL and IH conceived this review article. JJ, DL, and IH participated in the writing of the manuscript. JJ prepared the figures. All authors contributed to the article and approved the submitted version.

FUNDING

DL has been supported by an NRF grant funded by the MSIT (grant NRF-2020R1A2C4002294) and a grant from Chonnam National University (2021–2118). IH has been supported by a National Research Foundation of Korea (NRF) grant funded by the Korean government (MSIT; No. 2019R1A2B5B03099982).

ACKNOWLEDGMENTS

We would like to thank Editage (www.editage.co.kr) for English language editing.

REFERENCES

Becker, T., Jelic, M., Vojta, A., Radunz, A., Soll, J., and Schleiff, E. (2004). Preprotein recognition by the Toc complex. *EMBO J.* 23, 520–530. doi: 10.1038/sj.emboj.7600089

Bhushan, S., Kuhn, C., Berglund, A. K., Roth, C., and Glaser, E. (2006). The role of the N-terminal domain of chloroplast targeting peptides in organellar protein import and miss-sorting. *FEBS Lett.* 580, 3966–3972. doi: 10.1016/j.febslet.2006.06.018

Bruce, B. D. (2000). Chloroplast transit peptides: structure, function and evolution. *Trends Cell Biol.* 10, 440–447. doi: 10.1016/S0962-8924(00)01833-X

Bruce, B. D. (2001). The paradox of plastid transit peptides: conservation of function despite divergence in primary structure. *Biochim. Biophys. Acta* 1541, 2–21. doi: 10.1016/s0167-4889(01)00149-5

Chen, L., Wang, X., Wang, L., Fang, Y., Pan, X., Gao, X., et al. (2019). Functional characterization of chloroplast transit peptide in the small subunit of Rubisco in maize. *J. Plant Physiol.* 237, 12–20. doi: 10.1016/j.jplph.2019.04.001

Chotewutmontri, P., and Bruce, B. D. (2015). Non-native, N-terminal Hsp70 molecular motor recognition elements in transit peptides support plastid protein translocation. *J. Biol. Chem.* 290, 7602–7621. doi: 10.1074/jbc.M114.633586

Chotewutmontri, P., Reddick, L. E., Mcwilliams, D. R., Campbell, I. M., and Bruce, B. D. (2012). Differential transit peptide recognition during preprotein binding and translocation into flowering plant plastids. *Plant Cell* 24, 3040–3059. doi: 10.1105/tpc.112.098327

Chu, C. C., Swamy, K., and Li, H. M. (2020). Tissue-specific regulation of plastid protein import via transit-peptide motifs. *Plant Cell* 32, 1204–1217. doi: 10.1105/tpc.19.00702

Day, P. M., Inoue, K., and Theg, S. M. (2019). Chloroplast outer membrane beta-barrel proteins use components of the general import apparatus. *Plant Cell* 31, 1845–1855. doi: 10.1105/tpc.19.00001

Dyall, S. D., Brown, M. T., and Johnson, P. J. (2004). Ancient invasions: from endosymbionts to organelles. *Science* 304, 253–257. doi: 10.1126/science.1094884

Ganesan, I., Shi, L. X., Labs, M., and Theg, S. M. (2018). Evaluating the functional pore size of chloroplast TOC and TIC protein translocons: import of folded proteins. *Plant Cell* 30, 2161–2173. doi: 10.1105/tpc.18.00427

Garg, S. G., and Gould, S. B. (2016). The role of charge in protein targeting evolution. *Trends Cell Biol.* 26, 894–905. doi: 10.1016/j.tcb.2016.07.001

Ge, C., Spanning, E., Glaser, E., and Wieslander, A. (2014). Import determinants of organelle-specific and dual targeting peptides of mitochondria and chloroplasts in *Arabidopsis thaliana*. *Mol. Plant* 7, 121–136. doi: 10.1093/mp/sst148

Gross, L. E., Klinger, A., Spies, N., Ernst, T., Flinner, N., Simm, S., et al. (2021). Insertion of plastidic beta-barrel proteins into the outer envelopes of plastids involves an intermembrane space intermediate formed with Toc75-V/OEP80. *Plant Cell* 33, 1657–1681. doi: 10.1093/plcell/koab052

Guzzo, A. V. (1965). The influence of amino-acid sequence on protein structure. *Biophys. J.* 5, 809–822. doi: 10.1016/S0006-3495(65)86753-4

Holbrook, K., Subramanian, C., Chotewutmontri, P., Reddick, L. E., Wright, S., Zhang, H., et al. (2016). Functional analysis of semi-conserved transit peptide motifs and mechanistic implications in precursor targeting and recognition. *Mol. Plant* 9, 1286–1301. doi: 10.1016/j.molp.2016.06.004

Huang, P. K., Chan, P. T., Su, P. H., Chen, L. J., and Li, H. M. (2016). Chloroplast Hsp93 directly binds to transit peptides at an early stage of the preprotein import process. *Plant Physiol.* 170, 857–866. doi: 10.1104/pp.15.01830

Huang, S. B., Taylor, N. L., Whelan, J., and Millar, A. H. (2009). Refining the definition of plant mitochondrial presequences through analysis of sorting signals, N-terminal modifications, and cleavage motifs. *Plant Physiol.* 150, 1272–1285. doi: 10.1104/pp.109.137885

Inaba, T., and Schnell, D. J. (2008). Protein trafficking to plastids: one theme, many variations. *Biochem. J.* 413, 15–28. doi: 10.1042/BJ20080490

Jensen, R. G. (2000). Activation of Rubisco regulates photosynthesis at high temperature and CO2. *Proc. Natl. Acad. Sci. U. S. A.* 97, 12937–12938. doi: 10.1073/pnas.97.24.12937

Karlin-Neumann, G. A., and Tobin, E. M. (1986). Transit peptides of nuclear-encoded chloroplast proteins share a common amino acid framework. *EMBO J.* 5, 9–13. doi: 10.1002/j.1460-2075.1986.tb04170.x

Lee, D. W., and Hwang, I. (2018). Evolution and design principles of the diverse chloroplast transit peptides. *Mol. Cell* 41, 161–167. doi: 10.14348/molcells.2018.0033

Lee, D. W., and Hwang, I. (2019). Protein import into chloroplasts via the Tic40-dependent and -independent pathways depends on the amino acid composition of the transit peptide. *Biochem. Biophys. Res. Commun.* 518, 66–71. doi: 10.1016/j.bbrc.2019.08.009

Lee, D. W., and Hwang, I. (2021). Understanding the evolution of endosymbiotic organelles based on the targeting sequences of organellar proteins. *New Phytol.* 230, 924–930. doi: 10.1111/nph.17167

Lee, D. W., Jung, C., and Hwang, I. (2013). Cytosolic events involved in chloroplast protein targeting. *Biochim. Biophys. Acta* 1833, 245–252. doi: 10.1016/j.bbamcr.2012.03.006

Lee, D. W., Kim, J. K., Lee, S., Choi, S., Kim, S., and Hwang, I. (2008). Arabidopsis nuclear-encoded plastid transit peptides contain multiple sequence subgroups with distinctive chloroplast-targeting sequence motifs. *Plant Cell* 20, 1603–1622. doi: 10.1105/tpc.108.060541

Lee, D. W., Lee, J., and Hwang, I. (2017). Sorting of nuclear-encoded chloroplast membrane proteins. *Curr. Opin. Plant Biol.* 40, 1–7. doi: 10.1016/j.pbi.2017.06.011

Lee, D. W., Lee, S., Lee, G. J., Lee, K. H., Kim, S., Cheong, G. W., et al. (2006). Functional characterization of sequence motifs in the transit peptide of *Arabidopsis* small subunit of rubisco. *Plant Physiol.* 140, 466–483. doi: 10.1104/pp.105.074575

Lee, D. W., Lee, S., Lee, J., Woo, S., Razzak, M. A., Vitale, A., et al. (2019). Molecular mechanism of the specificity of protein import into chloroplasts and mitochondria in plant cells. *Mol. Plant* 12, 951–966. doi: 10.1016/j.molp.2019.03.003

Lee, D. W., Lee, S., Min, C. K., Park, C., Kim, J. M., Hwang, C. S., et al. (2020). Cross-species functional conservation and possible origin of the N-terminal specificity domain of mitochondrial presequences. *Front. Plant Sci.* 11:64. doi: 10.3389/fpls.2020.00064

Lee, D. W., Lee, S., Oh, Y. J., and Hwang, I. (2009). Multiple sequence motifs in the rubisco small subunit transit peptide independently contribute to Toc159-dependent import of proteins into chloroplasts. *Plant Physiol.* 151, 129–141. doi: 10.1104/pp.109.140673

Lee, D. W., Woo, S., Geem, K. R., and Hwang, I. (2015). Sequence motifs in transit peptides act as independent functional units and can be transferred to new sequence contexts. *Plant Physiol.* 169, 471–484. doi: 10.1104/pp.15.00842

Lee, D. W., Yoo, Y. J., Razzak, M. A., and Hwang, I. (2018). Prolines in transit peptides are crucial for efficient preprotein translocation into chloroplasts. *Plant Physiol.* 176, 663–677. doi: 10.1104/pp.17.01553

Lee, J., Kim, D. H., and Hwang, I. (2014). Specific targeting of proteins to outer envelope membranes of endosymbiotic organelles, chloroplasts, and mitochondria. *Front. Plant Sci.* 5:173. doi: 10.3389/fpls.2014.00173

Li, H. M., and Chiu, C. C. (2010). Protein transport into chloroplasts. *Annu. Rev. Plant Biol.* 61, 157–180. doi: 10.1146/annurev-arplant-042809-112222

Li, H. M., and Teng, Y. S. (2013). Transit peptide design and plastid import regulation. *Trends Plant Sci.* 18, 360–366. doi: 10.1016/j.tplants.2013.04.003

Ponce-Toledo, R. I., Lopez-Garcia, P., and Moreira, D. (2019). Horizontal and endosymbiotic gene transfer in early plastid evolution. *New Phytol.* 224, 618–624. doi: 10.1111/nph.15965

Razzak, M. A., Lee, D. W., Yoo, Y. J., and Hwang, I. (2017). Evolution of rubisco complex small subunit transit peptides from algae to plants. *Sci. Rep.* 7:9279. doi: 10.1038/s41598-017-09473-x

Reiss, B., Wasmann, C. C., and Bohnert, H. J. (1987). Regions in the transit peptide of SSU essential for transport into chloroplasts. *Mol. Gen. Genet.* 209, 116–121. doi: 10.1007/BF00329845

Richardson, L. G. L., Singhal, R., and Schnell, D. J. (2017). The integration of chloroplast protein targeting with plant developmental and stress responses. *BMC Biol.* 15:118. doi: 10.1186/s12915-017-0458-3

Richardson, L. G. L., Small, E. L., Inoue, H., and Schnell, D. J. (2018). Molecular topology of the transit peptide during chloroplast protein import. *Plant Cell* 30, 1789–1806. doi: 10.1105/tpc.18.00172

Schleiff, E., and Becker, T. (2011). Common ground for protein translocation: access control for mitochondria and chloroplasts. *Nat. Rev. Mol. Cell Biol.* 12, 48–59. doi: 10.1038/nrm3027

Smith, M. D., Rounds, C. M., Wang, F., Chen, K., Afitlhile, M., and Schnell, D. J. (2004). atToc159 is a selective transit peptide receptor for the import of nucleus-encoded chloroplast proteins. *J. Cell Biol.* 165, 323–334. doi: 10.1083/jcb.200311074

Teng, Y. S., Chan, P. T., and Li, H. M. (2012). Differential age-dependent import regulation by signal peptides. *PLoS Biol.* 10:e1001416. doi: 10.1371/journal.pbio.1001416

Von Heijne, G., Steppuhn, J., and Herrmann, R. G. (1989). Domain structure of mitochondrial and chloroplast targeting peptides. *Eur. J. Biochem.* 180, 535–545. doi: 10.1111/j.1432-1033.1989.tb14679.x

Zimorski, V., Ku, C., Martin, W. F., and Gould, S. B. (2014). Endosymbiotic theory for organelle origins. *Curr. Opin. Microbiol.* 22, 38–48. doi: 10.1016/j.mib.2014.09.008

Zybailov, B., Rutschow, H., Friso, G., Rudella, A., Emanuelsson, O., Sun, Q., et al. (2008). Sorting signals, N-terminal modifications and abundance of the chloroplast proteome. *PLoS One* 3:e1994. doi: 10.1371/journal.pone.0001994

Conflict of Interest: The authors declare that the research was conducted in the absence of any commercial or financial relationships that could be construed as a potential conflict of interest.

Publisher's Note: All claims expressed in this article are solely those of the authors and do not necessarily represent those of their affiliated organizations, or those of the publisher, the editors and the reviewers. Any product that may be evaluated in this article, or claim that may be made by its manufacturer, is not guaranteed or endorsed by the publisher.

frontiers in Physiology

MINI REVIEW
published: 24 December 2021
doi: 10.3389/fphys.2021.801212

Liquid-Liquid Phase Separation Phenomenon on Protein Sorting Within Chloroplasts

*Canhui Zheng, Xiumei Xu, Lixin Zhang and Dandan Lu**

State Key Laboratory of Crop Stress Adaptation and Improvement, School of Life Sciences, Henan University, Kaifeng, China

In higher plants, chloroplasts are vital organelles possessing highly complex compartmentalization. As most chloroplast-located proteins are encoded in the nucleus and synthesized in the cytosol, the correct sorting of these proteins to appropriate compartments is critical for the proper functions of chloroplasts as well as plant survival. Nuclear-encoded chloroplast proteins are imported into stroma and further sorted to distinct compartments via different pathways. The proteins predicted to be sorted to the thylakoid lumen by the chloroplast twin arginine transport (cpTAT) pathway are shown to be facilitated by STT1/2 driven liquid-liquid phase separation (LLPS). Liquid-liquid phase separation is a novel mechanism to facilitate the formation of membrane-less sub-cellular compartments and accelerate biochemical reactions temporally and spatially. In this review, we introduce the sorting mechanisms within chloroplasts, and briefly summarize the properties and significance of LLPS, with an emphasis on the novel function of LLPS in the sorting of cpTAT substrate proteins. We conclude with perspectives for the future research on chloroplast protein sorting and targeting mechanisms.

Keywords: chloroplast, protein sorting, STTs, liquid-liquid phase separation, liquid droplets

OPEN ACCESS

Edited by:
Inhwan Hwang,
Pohang University of Science and Technology, South Korea

Reviewed by:
Dong Wook Lee,
Chonnam National University, South Korea
Alessandro Vitale,
National Research Council (CNR), Italy

****Correspondence:***
Dandan Lu
ludandan@henu.edu.cn

Specialty section:
This article was submitted to Membrane Physiology and Membrane Biophysics, a section of the journal Frontiers in Physiology

Received: *25 October 2021*
Accepted: *09 December 2021*
Published: *24 December 2021*

Citation:
Zheng C, Xu X, Zhang L and Lu D (2021) Liquid-Liquid Phase Separation Phenomenon on Protein Sorting Within Chloroplasts. Front. Physiol. 12:801212. doi: 10.3389/fphys.2021.801212

INTRODUCTION

Chloroplasts are essential semi-autonomous organelles that are primarily responsible for photosynthesis as well as many other functions, such as synthesis of amino acids, fatty acids, pigments, and hormones (Jarvis and Lopez-Juez, 2013). Chloroplasts contain highly complex sub-organellar compartments, including three membrane systems (the outer and inner envelope membrane and the thylakoid membrane) delineating three aqueous compartments (the intermembrane space, the stroma, and the thylakoid lumen) (Kirchhoff, 2019). Chloroplasts are estimated to contain approximately 3000 different proteins, but only about 100 proteins are encoded by the chloroplast genome (Jarvis and Robinson, 2004; Bouchnak et al., 2019). The vast majority of proteins are encoded in the nucleus and synthesized in the cytosol as precursors before being imported into chloroplasts post-translationally. Upon arrival at the stroma, some proteins reside and function therein, while other proteins are further sorted and targeted to the inner envelope or thylakoids depending on their specific targeting signals. Previous investigations have revealed different sorting pathways and numerous factors involved in intra-chloroplast protein sorting and targeting (Jarvis and Lopez-Juez, 2013; New et al., 2018; Ziehe et al., 2018; Xu et al., 2021a). However, how the targeting signals are recognized and how the substrates are sorted in the stroma are not yet fully elucidated.

Liquid-liquid phase separation (LLPS) is a basic physicochemical phenomenon, referred to a state transition in which a homogeneous liquid spontaneously de-mixes into two or more

coexisting liquids (Alberti, 2017). However, recent investigations have shown that LLPS is a universal organizing principle of liquid condensates or membrane-less compartments in living cells, offering an exciting novel mechanism for intracellular organization (Brangwynne et al., 2009; Shin and Brangwynne, 2017). Intriguingly, LLPS has also been found within the chloroplast to facilitate formation of intraorganellar liquid droplets for protein sorting to thylakoid lumen (Ouyang et al., 2020).

In this review, we provide an overview of the current knowledge of protein sorting within chloroplasts, and briefly summarize the significance and key components of liquid condensates formed by LLPS, with a focus on the function of LLPS on protein sorting within the chloroplast. Finally, we prospect for the future research on intra-chloroplast protein sorting and targeting.

PROTEIN SORTING WITHIN THE CHLOROPLAST

Nuclear-encoded chloroplast proteins are synthesized in the cytoplasm as precursors with an N-terminal cleavable targeting signal, known as the transit peptide (Bruce, 2000; Lee and Hwang, 2021). The transit peptide is recognized by the chloroplast protein import machinery, translocons at the outer (TOC) and inner (TIC) envelope membrane of chloroplasts, which facilitate the translocation of the protein across the outer and inner envelope. Some chloroplast inner membrane proteins, such as albino or pale green mutant 1 (APG1), are laterally released and thus inserted into the membrane by stop-transfer mechanism during translocation through TIC translocon (Viana et al., 2010; Lee et al., 2017). For other proteins, the N-terminal transit peptide is removed by the stroma processing peptidase (SPP) (Richardson et al., 2014). These proteins may stay in the stroma or be further sorted to other sub-organellar compartments, including the inner envelope membrane, thylakoid membrane, or thylakoid lumen (Jarvis and Lopez-Juez, 2013; Paila et al., 2015). Some inner envelope proteins, such as FTSH12 and TIC40, are translocated by the translocase SEC2 (Li et al., 2015, 2017; Lee et al., 2017), whereas thylakoid proteins are sorted and targeted by distinct pathways depending on the associated chaperones and energy required.

Thylakoid membrane-located proteins may be sorted by the following pathways: the chloroplast signal recognition particle (RP) pathway, the chloroplast Guided Entry of Tail-anchored protein (cpGET) pathway, or the "spontaneous insertion" pathway. The cpSRP pathway is involved in the insertion of light-harvesting chlorophyll-binding proteins (LHCPs) into thylakoid membranes. The 14 amino-acid sequence located at the beginning of the third transmembrane domain (TMD3) of LHCPs, T14, is recognized by a stromal ankyrin protein LHCP TRANSLOCATION DEFECT (LTD), which interacts with cpSRP43 and subsequently routes LHCPs from the TIC translocon to the cpSRP pathway (Ouyang et al., 2011). The unique plastid chaperone cpSRP43 binds LHCPs with their unique motif between TMD2 and TMD3, named the L18 peptide, and together with the cpSRP54 GTPase, protects the substrates from aggregation in the aqueous stroma (Stengel et al., 2008; Falk and Sinning, 2010). Subsequently, cpSRP43 and cpSRP54 interact with the membrane receptor CHLOROPLAST FILAMENTOUS TEMPERATURE SENSITIVE Y (cpFtsY), and the latter mediates the membrane insertion of LHCPs by integrase Albino3 (Abl3) in a GTP-dependent manner (Lee et al., 2017; Ziehe et al., 2018).

Chloroplast tail-anchored (TA) proteins, which possess a stroma-exposed N-terminus proceeding a single TMD and a short C-terminal tail (Abell and Mullen, 2011), can be targeted to the thylakoid membrane via the cpGET pathway. This pathway is assisted by targeting factor Get3B that binds the TMD of the TA protein in its hydrophobic groove (Anderson et al., 2021). The analog of the cpGET pathway in the cytoplasm, the GET pathway, is distributed throughout all eukaryotic cells and targets numerous TA proteins to the membranes exposed to the cytosol (Borgese et al., 2019). But thus far, the only known substrate of the cpGET pathway is CHLOROPLAST SECRETORY TRANSLOCASE E1 (cpSECE1), which appears to be sorted based on the characteristics of its TMD and C-terminal tail (Anderson et al., 2021). Further investigation is required to understand whether more substrates are translocated by the cpGET pathway and also the detailed regulatory mechanisms for protein targeting.

Some thylakoid membrane proteins are presumably inserted into the thylakoid membrane via the "spontaneous insertion" pathway, which is supposed to require no energy input or the assistance of other proteins for substrate insertion (Jarvis and Robinson, 2004; Schunemann, 2007). The proteins, such as THYLAKOID ASSEMBLY 4 (Tha4), HIGH CHLOROPHYLL FLUORESCENCE 106 (Hcf106), CF0 II, PsbX, PsbY, PsaG, and PsaK, are targeted by this pathway (Schleiff and Klösgen, 2001; Lee et al., 2017). However, spontaneous membrane insertion of these proteins could be only apparent: chaperones involved in the process or assembly into complexes with other subunits may actually occur but remain still unidentified. Examples include the Plsp1, a plastidic type I signal peptidase, which can insert into membrane spontaneously *in vitro* but is assisted by a large complex containing chaperonin 60 (Cpn60) in the stroma and cpSECY1 during insertion into thylakoid membranes (Endow et al., 2015; Klasek et al., 2020).

The thylakoid lumen proteins are translocated by the chloroplast secretory (cpSEC) pathway or the chloroplast twin-arginine translocase (cpTAT) pathway. These proteins carry an N-terminal bipartite targeting sequence, i.e., a standard transit peptide followed by a lumen targeting peptide (LTP) (Lee et al., 2017; Xu et al., 2021a). The cpSEC pathway involves the SECA1 ATPase and the thylakoid membrane-localized cpSECY1/E1 translocon, and tends to handle unfolded proteins (Albiniak et al., 2012; Fernandez, 2018). The cpTAT pathway comprises three membrane components, Hcf106, Tha4, and cpTatC, which work together as the translocon (Celedon and Cline, 2012; Ma et al., 2018). Compared to the cpSEC pathway, substrates of the cpTAT pathway are folded proteins or proteins assembled into complexes with co-factors, and their transmembrane translocation is promoted by the thylakoidal proton gradient (Jarvis and Lopez-Juez, 2013; New et al., 2018).

Besides the conformational differences, substrates of the cpSEC and cpTAT pathways have similar but different LTPs. Specifically, while LTPs of both pathways contain three distinct regions: an N-terminal charged region, a hydrophobic core, and a polar C-terminal domain, the cpTAT LTPs possess a twin arginine (RR) motif in the N-terminal region, which functions as the "cpSEC avoidance" motif (Fernandez, 2018; New et al., 2018). While the LTPs and the protein conformation required by the two lumen targeting pathways are quite clear, the underlying molecular mechanisms of targeting signal recognition and protein translocation through the aqueous stroma were almost completely unknown until recently, when Ouyang et al. (2020) revealed a novel mechanism for the cpTAT substrate sorting facilitated by STTs driven LLPS.

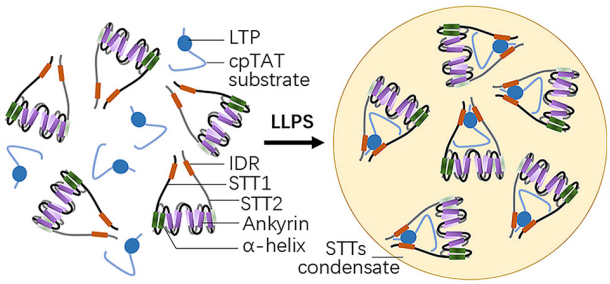

FIGURE 1 | Structure of STT1/2 and LLPS driven by STT1/2. Both STT1 and STT2 have an N-terminal intrinsically disordered region (IDR) and five C-terminal ankyrin repeat domains following two α-helixes. STT1 and STT2 form an ellipsoidal-like core structure via the antiparallel interaction of their five ankyrin repeat domains and two adjacent N-terminal helixes. STT1 and STT2 complex binds the lumen targeting peptide (LTP) of the cpTat substrate by their IDRs and undergo liquid-liquid phase separation (LLPS).

SIGNIFICANCE AND COMPOSITION OF LIQUID CONDENSATES

Liquid-liquid phase separation (LLPS) is a prevalent mechanism that drives intracellular membrane-less compartments formation across kingdoms of life and accelerates biochemical reactions spatiotemporally via concentrating macromolecules locally. In humans, animals, plants, and many other organisms, LLPS participates in various biological processes, such as ribosome biogenesis, gene expression, RNA processing, heterochromatin formation, etc. (Zhang et al., 2020; Emenecker et al., 2021; Kim et al., 2021; Xu et al., 2021b). Disturbing the process of LLPS may lead to liquid condensates vanishing or transforming into other material states, which are associated with many human diseases, including infectious diseases, neurodegeneration, and cancer (Alberti et al., 2019). Several liquid droplets appear to be plant specific, such as photobodies, which are sophisticated subnuclear condensates that robustly induce light signal transduction (Pardi and Nusinow, 2021), AUXIN RESPONSE FACTOR (ARF) condensates, which are cytoplasmic condensates regulating auxin transcriptional responses in Arabidopsis tissues that are no longer actively growing (Powers et al., 2019), and the pyrenoid, which is the liquid droplet for CO_2 concentration and fixation found in the chloroplast of most unicellular algae (Freeman Rosenzweig et al., 2017).

Most liquid condensates formed via LLPS are composed of a heterogeneous mixture of macromolecules, and phase separation is driven by weak intermolecular forces between specific macromolecular components, based on multivalent protein-protein or protein-RNA interactions (Li et al., 2012; Emenecker et al., 2021). Emerging evidence indicates that proteins undergoing LLPS usually contain intrinsically disordered regions (IDRs) and low-complexity regions (LCRs) (Zhang et al., 2020). Intrinsically disordered regions fail to fold into a fixed three-dimensional structure but instead exhibit flexible and versatile conformations (Zhang et al., 2020). The net electric charge and hydrophilicity/hydrophobicity of IDRs are variable, due to the various biased amino acid compositions (Oldfield and Dunker, 2014). Some IDRs contain the LCR, a domain enriched in a specific subset of amino acid residues, such as poly-glycine, poly-serine, and poly-glutamine (Kato et al., 2012; Wright and Dyson, 2015). The flexible conformations of IDRs and the multitude of identical or highly similar residues in LCRs fulfill the requirement for weak multivalent interactions to drive LLPS (Posey et al., 2018).

STTs CONDENSATES AND THE cpTAT PATHWAY

In Arabidopsis, both STT1 and its homolog, STT2, are IDR-containing proteins. They interact specifically with cpTAT substrates OXYGEN EVOLVING COMPLEX SUBUNIT 23 kD (OE23), OE17, and the photosystem I subunit PSI-N (PsaN), but not with the cpSEC substrate OE33. Although STT1 and STT2 can physically interact with OE23 individually, together they promote the targeting and binding of iOE23 (the intermediate form of OE23 containing the LTP but without the transit peptide) to thylakoid membranes. This result was further confirmed by analyzing knock-down lines of STT1 and STT2. In this experiment, cpTAT specific substrates were dramatically reduced while other proteins were only moderately affected (Ouyang et al., 2020).

STT1 and STT2 are two plant-specific proteins with an N-terminal IDR and five C-terminal ankyrin repeat domains (**Figure 1**). While individual STT1 or STT2 tends to aggregate, bimolecular fluorescence complementation (BiFC) experiments indicated STT1 directly interacts with STT2, facilitated by their ankyrin repeat domains to form a STTs complex. This is consistent with the results of crystal structure analysis, which showed that truncated STT1 and STT2, lacking the transit peptide and the IDR, form an ellipsoidal-like core structure through the antiparallel interaction of their two N-terminal helixes and five ankyrin repeat domains. Meanwhile, the conserved positively charged residues within the ankyrin repeat domains are crucial for STTs oligomer formation (Ouyang et al., 2020).

Pull-down assays, isothermal titration calorimetry (ITC) analyses, together with residue-substitution mutation assays

showed that the STTs complex binds the cpTAT substrate OE23 or its LTP at an approximately 1:1 protein: protein or protein: peptide ratio, and that both the RR residues in the N-terminal charged region and the hydrophobic core of OE23 LTP, as well as the negatively charged residues of the WEEPD motif in the STT1 IDR and the hydrophobic residues of the LVP-W motif in the STT2 IDR, are required for STTs-OE23 heterotrimers formation and subsequent cpTAT substrate targeting (Ouyang et al., 2020).

Considering that STT1 and STT2 contain IDRs, the STTs complexes may undergo LLPS. As speculated, microscopy imaging assays and photobleaching showed that STTs complexes lead to spherical liquid condensates through LLPS at high concentration *in vitro*, when mixed with OE23 LTPs at the ratio of 1:1 (**Figure 1**). STTs complex formation is a prerequisite for LLPS, as shown by the observations that liquid condensates after mixing with LTPs do not form when individual STT1 or STT2 are used or when the STTs complex formation is disrupted by mutating the electropositive residues within the ankyrin repeat domains. The STTs-LTP binding reaction is also required for LLPS, as substitution of the residues of the LTP binding motif within the STTs, such as the RR residues in the N-terminal charged region and residues in the hydrophobic core, severely compromised liquid condensates formation. Thus, multivalent interactions and hydrophobic interactions between STT1, STT2, and LTP drive LLPS and form STTs condensates (Ouyang et al., 2020).

BiFC and pull-down assays further revealed that STT1 and STT2 interact with the stromal domain of cpTAT translocon component Hcf106. Binding to Hcf106 hinders STTs oligomerization and LLPS, thereby releasing and docking cpTAT substrates to the cpTatC-Hcf106 receptor complex and facilitating substrate translocation across the thylakoid membrane (Ouyang et al., 2020).

In general, the STT1 and STT2 complex undergoes cpTAT substrate-induced LLPS and form the STTs condensates to facilitate the substrate targeting and translocation into the thylakoid lumen. Along with the STTs, many other targeting factors were predicted to contain IDRs. These factors include but are not limited to the following (Ouyang et al., 2020): (1) SECA1 in Arabidopsis and rice, and SECA2 in Arabidopsis but not rice. These proteins are assistants of substrate translocation to the thylakoid lumen and the inner chloroplast envelope, respectively; (2) cpSRP43 and cpSRP54 in Arabidopsis and rice. These proteins are the components of the cpSRP pathway; (3) SRP54 in *Escherichia coli*, yeast, Arabidopsis and mice. This protein is a cytosolic translocation factor for secreted proteins; (4) PEX5 and PEX13 in Arabidopsis and mice. These proteins are components of the peroxisomal protein translocation machinery; (5) AKR2A in Arabidopsis and mice. This protein is a cytosolic targeting factor. As IDR-containing proteins have been widely implicated in mediating phase separation (Li et al., 2012; Molliex et al., 2015), these factors mentioned above probably undergo LLPS and lead to liquid condensate formation, implicating that LLPS may be a universal and conserved mechanism for substrate sorting not only in the chloroplast of the plant but also in the cytoplasm across kingdoms (Lee and Hwang, 2020; Ouyang et al., 2020).

PERSPECTIVES

Within cells, LLPS is tightly regulated by various mechanisms for proper functions. Physical conditions that can change affinities of biomolecular multivalent interactions, such as pH, temperature, redox state, ionic strength, and osmotic pressure, are known to have an effect on LLPS of biomolecular systems (Banani et al., 2017). Within the chloroplast, the redox state, which interplays with the photosynthetic light reactions, fluctuates rapidly with light intensity changes, biotic and abiotic stresses suffered, diurnal variation, and other environmental stimuli (Foyer, 2018; Kuzniak and Kopczewski, 2020; Sachdev et al., 2021). And the stromal pH oscillates during light-dark transition. In the dark both the cytoplasmic and stromal pH is close to 7, but upon illumination the stroma becomes alkaline and the pH increases to about 8.0, as a consequence of H^+-pumping into the thylakoid lumen (Heldt et al., 1973; Hohner et al., 2016). In addition, dynamics of many ions in the stroma have been observed in response to stress stimuli and also at the transition between light and darkness, especially Mg^{2+} and Ca^{2+}, which play a critical role in regulating enzyme activity and other numerous physiological and biochemical processes (Szabo and Spetea, 2017; Frank et al., 2019; Li et al., 2020; Marti Ruiz et al., 2020). In summary, physical conditions within the chloroplast change frequently through variations of environmental and metabolic conditions. In addition, various post-translational modifications alter the interactions among macromolecules and can modulate LLPS (Bah and Forman-Kay, 2016; Zhang et al., 2020). While post-translational modifications in the chloroplasts have been poorly investigated compared to whole plant cells, animal cells, and yeast, numerous types of post-translational modification have been identified and are believed to occur in the chloroplast, such as phosphorylation, oxidation-reduction, acetylation, methylation, and glutathionylation (Lehtimaki et al., 2015; Grabsztunowicz et al., 2017). However, whether or not STTs driven LLPS is regulated by any physical condition changes or post-translational modifications within the chloroplast is still unclear. Further studies on this topic will expand our knowledge of the regulation of intra-chloroplast protein sorting.

The TAT system has been found in prokaryotes, chloroplasts, and some mitochondria, allowing folded proteins to be transported across membranes (Berks, 2015). The TAT pathway in both chloroplasts and bacteria comprise similar membrane located translocon components, cpTatC (TatC), Hcf106 (TatB), and Tha4 (TatA) (New et al., 2018), but each has different chaperones. In bacteria, some substrates of TAT pathway have specific cytosolic chaperones, whereas some are assisted by the general chaperones, such as DnaK and DnaJ in *E. coli* (Robinson et al., 2011). In Arabidopsis, cpTAT passenger proteins are assisted by the general chaperones, STT1 and STT2. However, orthologs of STTs could be identified only in the angiosperm and gymnosperm lineages, and none was detected in animals, microorganisms, or even other photosynthetic species including

cyanobacteria, eukaryotic unicellular algae and mosses (Garcion et al., 2006), indicating STTs-driven LLPS as an emerging mechanism for cpTAT substrate sorting during plant evolution. Phylogenetic analyses should be taken to find the origin of STTs and chaperones for cpTAT pathway in lower plants need to be identified, which are important challenges for the future to decipher the sorting process and the mechanism for regulating the cpTAT pathway.

AUTHOR CONTRIBUTIONS

CZ and DL led the writing effort with substantial contributions from XX and LZ. All the authors read and approved the submitted version.

FUNDING

The authors have received funding from the following: a grant (No. 2020YFA0907600) from the National Key Research and Development Program of China, the 111 Project (D16014), the Program for Innovative Research Teams (in Science and Technology) in Universities of Henan Province (22IRTSTHN024), and the Outstanding Talents Fund of Henan University, China.

ACKNOWLEDGMENTS

We thank Leonard Krall from Yunnan University for critical reading of this manuscript.

REFERENCES

Abell, B. M., and Mullen, R. T. (2011). Tail-anchored membrane proteins: exploring the complex diversity of tail-anchored-protein targeting in plant cells. *Plant Cell Rep.* 30, 137–151. doi: 10.1007/s00299-010-0925-6

Alberti, S. (2017). Phase separation in biology. *Curr. Biol.* 27, R1097–R1102. doi: 10.1016/j.cub.2017.08.069

Alberti, S., Gladfelter, A., and Mittag, T. (2019). Considerations and challenges in studying liquid-liquid phase Sseparation and biomolecular condensates. *Cell* 176, 419–434. doi: 10.1016/j.cell.2018.12.035

Albiniak, A. M., Baglieri, J., and Robinson, C. (2012). Targeting of lumenal proteins across the thylakoid membrane. *J. Exp. Bot.* 63, 1689–1698. doi: 10.1093/jxb/err444

Anderson, S. A., Satyanarayan, M. B., Wessendorf, R. L., Lu, Y., and Fernandez, D. E. (2021). A homolog of GuidedEntry of Tail-anchored proteins3 functions in membrane-specific protein targeting in chloroplasts of Arabidopsis. *Plant Cell.* 33, 2812–2833. doi: 10.1093/plcell/koab145

Bah, A., and Forman-Kay, J. D. (2016). Modulation of intrinsically disordered protein function by post-translational modifications. *J. Biol. Chem.* 291, 6696–6705. doi: 10.1074/jbc.R115.695056

Banani, S. F., Lee, H. O., Hyman, A. A., and Rosen, M. K. (2017). Biomolecular condensates: organizers of cellular biochemistry. *Nat. Rev. Mol. Cell. Biol.* 18, 285–298. doi: 10.1038/nrm.2017.7

Berks, B. C. (2015). The twin-arginine protein translocation pathway. *Annu. Rev. Biochem.* 84, 843–864. doi: 10.1146/annurev-biochem-060614-034251

Borgese, N., Coy-Vergara, J., Colombo, S. F., and Schwappach, B. (2019). The ways of Tails: the GET pathway and more. *Protein J.* 38, 289–305. doi: 10.1007/s10930-019-09845-4

Bouchnak, I., Brugiere, S., Moyet, L., Le Gall, S., Salvi, D., Kuntz, M., et al. (2019). Unraveling hidden components of the chloroplast envelope proteome: opportunities and limits of better MS sensitivity. *Mol. Cell Proteomics* 18, 1285–1306. doi: 10.1074/mcp.RA118.000988

Brangwynne, C. P., Eckmann, C. R., Courson, D. S., Rybarska, A., Hoege, C., Gharakhani, J., et al. (2009). Germline P granules are liquid droplets that localize by controlled dissolution/condensation. *Science* 324, 1729–1732. doi: 10.1126/science.1172046

Bruce, B. D. (2000). Chloroplast transit peptides: structure, function and evolution. *Trends Cell. Biol.* 10, 440–447. doi: 10.1016/s0962-8924(00)01833-x

Celedon, J. M., and Cline, K. (2012). Stoichiometry for binding and transport by the twin arginine translocation system. *J. Cell. Biol.* 197, 523–534. doi: 10.1083/jcb.201201096

Emenecker, R. J., Holehouse, A. S., and Strader, L. C. (2021). Biological phase separation and biomolecular condensates in plants. *Annu. Rev. Plant Biol.* 72, 17–46. doi: 10.1146/annurev-arplant-081720-015238

Endow, J. K., Singhal, R., Fernandez, D. E., and Inoue, K. (2015). Chaperone-assisted post-translational transport of plastidic type I signal peptidase 1. *J. Biol. Chem.* 290, 28778–28791. doi: 10.1074/jbc.M115.684829

Falk, S., and Sinning, I. (2010). cpSRP43 is a novel chaperone specific for light-harvesting chlorophyll a,b-binding proteins. *J. Biol. Chem.* 285, 21655–21661. doi: 10.1074/jbc.C110.132746

Fernandez, D. E. (2018). Two paths diverged in the stroma: targeting to dual SEC translocase systems in chloroplasts. *Photosynth Res.* 138, 277–287. doi: 10.1007/s11120-018-0541-9

Foyer, C. H. (2018). Reactive oxygen species, oxidative signaling and the regulation of photosynthesis. *Environ. Exp. Bot.* 154, 134–142. doi: 10.1016/j.envexpbot.2018.05.003

Frank, J., Happeck, R., Meier, B., Hoang, M. T. T., Stribny, J., Hause, G., et al. (2019). Chloroplast-localized BICAT proteins shape stromal calcium signals and are required for efficient photosynthesis. *New Phytol.* 221, 866–880. doi: 10.1111/nph.15407

Freeman Rosenzweig, E. S., Xu, B., Kuhn Cuellar, L., Martinez-Sanchez, A., Schaffer, M., Strauss, M., et al. (2017). The eukaryotic CO2-concentrating organelle is liquid-like and exhibits dynamic reorganization. *Cell* 171, 148–162.e19. doi: 10.1016/j.cell.2017.08.008

Garcion, C., Guilleminot, J., Kroj, T., Parcy, F., Giraudat, J., and Devic, M. (2006). AKRP and EMB506 are two ankyrin repeat proteins essential for plastid differentiation and plant development in Arabidopsis. *Plant J.* 48, 895–906. doi: 10.1111/j.1365-313X.2006.02922.x

Grabsztunowicz, M., Koskela, M. M., and Mulo, P. (2017). Post-translational modifications in regulation of chloroplast function: recent advances. *Front. Plant Sci.* 8:240. doi: 10.3389/fpls.2017.00240

Heldt, H. W., Werdan, K., Milovancev, M., and Geller, G. (1973). Alkalization of the chloroplast stroma caused by light-dependent proton flux into the thylakoid space. *Biochim. Biophys. Acta* 314, 224–241. doi: 10.1016/0005-2728(73)90137-0

Hohner, R., Aboukila, A., Kunz, H. H., and Venema, K. (2016). Proton gradients and proton-dependent transport processes in the chloroplast. *Front. Plant Sci.* 7:218. doi: 10.3389/fpls.2016.00218

Jarvis, P., and Lopez-Juez, E. (2013). Biogenesis and homeostasis of chloroplasts and other plastids. *Nat. Rev. Mol. Cell. Biol.* 14, 787–802. doi: 10.1038/nrm3702

Jarvis, P., and Robinson, C. (2004). Mechanisms of protein import and routing in chloroplasts. *Curr. Biol.* 14, R1064–R1077. doi: 10.1016/j.cub.2004.11.049

Kato, M., Han, T. W., Xie, S., Shi, K., Du, X., Wu, L. C., et al. (2012). Cell-free formation of RNA granules: low complexity sequence domains form dynamic fibers within hydrogels. *Cell* 149, 753–767. doi: 10.1016/j.cell.2012.04.017

Kim, J., Lee, H., Lee, H. G., and Seo, P. J. (2021). Get closer and make hotspots: liquid-liquid phase separation in plants. *EMBO Rep.* 22:e51656. doi: 10.15252/embr.202051656

Kirchhoff, H. (2019). Chloroplast ultrastructure in plants. *New Phytol.* 223, 565–574. doi: 10.1111/nph.15730

Klasek, L., Inoue, K., and Theg, S. M. (2020). Chloroplast chaperonin-mediated targeting of a thylakoid membrane protein. *Plant Cell* 32, 3884–3901. doi: 10.1105/tpc.20.00309

Kuzniak, E., and Kopczewski, T. (2020). The chloroplast reactive oxygen species-redox system in plant immunity and disease. *Front. Plant. Sci.* 11:572686. doi: 10.3389/fpls.2020.572686

Lee, D. W., and Hwang, I. (2020). Liquid-liquid phase transition as a new means of protein targeting in chloroplasts. *Mol. Plant* 13, 679–681. doi: 10.1016/j.molp.2020.04.001

Lee, D. W., and Hwang, I. (2021). Understanding the evolution of endosymbiotic organelles based on the targeting sequences of organellar proteins. *New Phytol.* 230, 924–930. doi: 10.1111/nph.17167

Lee, D. W., Lee, J., and Hwang, I. (2017). Sorting of nuclear-encoded chloroplast membrane proteins. *Curr. Opin. Plant Biol.* 40, 1–7. doi: 10.1016/j.pbi.2017.06.011

Lehtimaki, N., Koskela, M. M., and Mulo, P. (2015). Posttranslational modifications of chloroplast proteins: an emerging field. *Plant Physiol.* 168, 768–775. doi: 10.1104/pp.15.00117

Li, J., Yokosho, K., Liu, S., Cao, H. R., Yamaji, N., Zhu, X. G., et al. (2020). Diel magnesium fluctuations in chloroplasts contribute to photosynthesis in rice. *Nat Plants* 6, 848–859. doi: 10.1038/s41477-020-0686-3

Li, P., Banjade, S., Cheng, H. C., Kim, S., Chen, B., Guo, L., et al. (2012). Phase transitions in the assembly of multivalent signalling proteins. *Nature* 483, 336–340. doi: 10.1038/nature10879

Li, Y., Martin, J. R., Aldama, G. A., Fernandez, D. E., and Cline, K. (2017). Identification of putative substrates of SEC2, a chloroplast inner envelope translocase. *Plant Physiol.* 173, 2121–2137. doi: 10.1104/pp.17.00012

Li, Y., Singhal, R., Taylor, I. W., McMinn, P. H., Chua, X. Y., Cline, K., et al. (2015). The Sec2 translocase of the chloroplast inner envelope contains a unique and dedicated SECE2 component. *Plant J.* 84, 647–658. doi: 10.1111/tpj.13028

Ma, Q., Fite, K., New, C. P., and Dabney-Smith, C. (2018). Thylakoid-integrated recombinant Hcf106 participates in the chloroplast twin arginine transport system. *Plant Direct* 2:e00090. doi: 10.1002/pld3.90

Marti Ruiz, M. C., Jung, H. J., and Webb, A. A. R. (2020). Circadian gating of dark-induced increases in chloroplast- and cytosolic-free calcium in Arabidopsis. *New Phytol.* 225, 1993–2005. doi: 10.1111/nph.16280

Molliex, A., Temirov, J., Lee, J., Coughlin, M., Kanagaraj, A. P., Kim, H. J., et al. (2015). Phase separation by low complexity domains promotes stress granule assembly and drives pathological fibrillization. *Cell* 163, 123–133. doi: 10.1016/j.cell.2015.09.015

New, C. P., Ma, Q., and Dabney-Smith, C. (2018). Routing of thylakoid lumen proteins by the chloroplast twin arginine transport pathway. *Photosynth Res.* 138, 289–301. doi: 10.1007/s11120-018-0567-z

Oldfield, C. J., and Dunker, A. K. (2014). Intrinsically disordered proteins and intrinsically disordered protein regions. *Annu. Rev. Biochem.* 83, 553–584. doi: 10.1146/annurev-biochem-072711-164947

Ouyang, M., Li, X., Ma, J., Chi, W., Xiao, J., Zou, M., et al. (2011). LTD is a protein required for sorting light-harvesting chlorophyll-binding proteins to the chloroplast SRP pathway. *Nat. Commun.* 2:277. doi: 10.1038/ncomms1278

Ouyang, M., Li, X., Zhang, J., Feng, P., Pu, H., Kong, L., et al. (2020). Liquid-liquid phase transition drives intra-chloroplast cargo sorting. *Cell* 180, 1144–1159.e20. doi: 10.1016/j.cell.2020.02.045

Paila, Y. D., Richardson, L. G. L., and Schnell, D. J. (2015). New insights into the mechanism of chloroplast protein import and its integration with protein quality control, organelle biogenesis and development. *J. Mol. Biol.* 427, 1038–1060. doi: 10.1016/j.jmb.2014.08.016

Pardi, S. A., and Nusinow, D. A. (2021). Out of the dark and into the light: a new view of phytochrome photobodies. *Front. Plant Sci.* 12:732947. doi: 10.3389/fpls.2021.732947

Posey, A. E., Holehouse, A. S., and Pappu, R. V. (2018). Phase separation of intrinsically disordered proteins. *Methods Enzymol.* 611, 1–30. doi: 10.1016/bs.mie.2018.09.035

Powers, S. K., Holehouse, A. S., Korasick, D. A., Schreiber, K. H., Clark, N. M., Jing, H., et al. (2019). Nucleo-cytoplasmic partitioning of ARF proteins controls auxin responses in Arabidopsis thaliana. *Mol. Cell* 76, 177–190.e5. doi: 10.1016/j.molcel.2019.06.044

Richardson, L. G., Paila, Y. D., Siman, S. R., Chen, Y., Smith, M. D., and Schnell, D. J. (2014). Targeting and assembly of components of the TOC protein import complex at the chloroplast outer envelope membrane. *Front. Plant Sci.* 5:269. doi: 10.3389/fpls.2014.00269

Robinson, C., Matos, C. F., Beck, D., Ren, C., Lawrence, J., Vasisht, N., et al. (2011). Transport and proofreading of proteins by the twin-arginine translocation (Tat) system in bacteria. *Biochim. Biophys. Acta* 1808, 876–884. doi: 10.1016/j.bbamem.2010.11.023

Sachdev, S., Ansari, S. A., Ansari, M. I., Fujita, M., and Hasanuzzaman, M. (2021). Abiotic stress and reactive oxygen species: generation, signaling, and defense mechanisms. *Antioxidants* 10:277. doi: 10.3390/antiox10020277

Schleiff, E., and Klösgen, R. B. (2001). Without a little help from 'my' friends: direct insertion of proteins into chloroplast membranes? *Biochim. Biophys. Acta* 1541, 22–33. doi: 10.1016/s0167-4889(01)00152-5

Schunemann, D. (2007). Mechanisms of protein import into thylakoids of chloroplasts. *Biol. Chem.* 388, 907–915. doi: 10.1515/BC.2007.111

Shin, Y., and Brangwynne, C. P. (2017). Liquid phase condensation in cell physiology and disease. *Science* 357:eaaf4382. doi: 10.1126/science.aaf4382

Stengel, K. F., Holdermann, I., Cain, P., Robinson, C., Wild, K., and Sinning, I. (2008). Structural basis for specific substrate recognition by the chloroplast signal recognition particle protein cpSRP43. *Science* 321, 253–256. doi: 10.1126/science.1158640

Szabo, I., and Spetea, C. (2017). Impact of the ion transportome of chloroplasts on the optimization of photosynthesis. *J. Exp. Bot.* 68, 3115–3128. doi: 10.1093/jxb/erx063

Viana, A. A., Li, M., and Schnell, D. J. (2010). Determinants for stop-transfer and post-import pathways for protein targeting to the chloroplast inner envelope membrane. *J. Biol. Chem.* 285, 12948–12960. doi: 10.1074/jbc.M110.109744

Wright, P. E., and Dyson, H. J. (2015). Intrinsically disordered proteins in cellular signalling and regulation. *Nat. Rev. Mol. Cell. Biol.* 16, 18–29. doi: 10.1038/nrm3920

Xu, X., Ouyang, M., Lu, D., Zheng, C., and Zhang, L. (2021a). Protein sorting within chloroplasts. *Trends Cell. Biol.* 31, 9–16. doi: 10.1016/j.tcb.2020.09.011

Xu, X., Zheng, C., Lu, D., Song, C. P., and Zhang, L. (2021b). Phase separation in plants: new insights into cellular compartmentalization. *J. Integr. Plant Biol.* 63, 1835–1855. doi: 10.1111/jipb.13152

Zhang, H., Ji, X., Li, P., Liu, C., Lou, J., Wang, Z., et al. (2020). Liquid-liquid phase separation in biology: mechanisms, physiological functions and human diseases. *Sci. China Life Sci.* 63, 953–985. doi: 10.1007/s11427-020-1702-x

Ziehe, D., Dunschede, B., and Schunemann, D. (2018). Molecular mechanism of SRP-dependent light-harvesting protein transport to the thylakoid membrane in plants. *Photosynth Res.* 138, 303–313. doi: 10.1007/s11120-018-0544-6

Conflict of Interest: The authors declare that the research was conducted in the absence of any commercial or financial relationships that could be construed as a potential conflict of interest.

Publisher's Note: All claims expressed in this article are solely those of the authors and do not necessarily represent those of their affiliated organizations, or those of the publisher, the editors and the reviewers. Any product that may be evaluated in this article, or claim that may be made by its manufacturer, is not guaranteed or endorsed by the publisher.

frontiers in Physiology

MINI REVIEW
published: 06 January 2022
doi: 10.3389/fphys.2021.806426

Coordinated Translocation of Presequence-Containing Precursor Proteins Across Two Mitochondrial Membranes: Knowns and Unknowns of How TOM and TIM23 Complexes Cooperate With Each Other

*Marcel G. Genge and Dejana Mokranjac**

Biozentrum — Department of Cell Biology, LMU Munich, Munich, Germany

The vast majority of mitochondrial proteins are encoded in the nuclear genome and synthesized on cytosolic ribosomes as precursor proteins with specific mitochondrial targeting signals. Mitochondrial targeting signals are very diverse, however, about 70% of mitochondrial proteins carry cleavable, N-terminal extensions called presequences. These amphipathic helices with one positively charged and one hydrophobic surface target proteins to the mitochondrial matrix with the help of the TOM and TIM23 complexes in the outer and inner membranes, respectively. Translocation of proteins across the two mitochondrial membranes does not take place independently of each other. Rather, in the intermembrane space, where the two complexes meet, components of the TOM and TIM23 complexes form an intricate network of protein–protein interactions that mediates initially transfer of presequences and then of the entire precursor proteins from the outer to the inner mitochondrial membrane. In this Mini Review, we summarize our current understanding of how the TOM and TIM23 complexes cooperate with each other and highlight some of the future challenges and unresolved questions in the field.

Keywords: mitochondria, protein translocation, presequence pathway, TOM-TIM23 contacts, precursor transfer, intermembrane space, TOM complex, TIM23 complex

OPEN ACCESS

Edited by:
Nathan Alder, University of Connecticut, United States

Reviewed by:
Johannes M. Herrmann, University of Kaiserslautern, Germany

****Correspondence:***
Dejana Mokranjac
mokranjac@bio.lmu.de

Specialty section:
This article was submitted to Mitochondrial Research, a section of the journal Frontiers in Physiology

Received: *31 October 2021*
Accepted: *03 December 2021*
Published: *06 January 2022*

Citation:
Genge MG and Mokranjac D (2022) Coordinated Translocation of Presequence-Containing Precursor Proteins Across Two Mitochondrial Membranes: Knowns and Unknowns of How TOM and TIM23 Complexes Cooperate With Each Other. Front. Physiol. 12:806426. doi: 10.3389/fphys.2021.806426

INTRODUCTION

Eukaryotic cells are defined by the presence of different membrane-enclosed compartments, cell organelles, that contain specific sets of proteins and provide specific chemical milieus. The obvious advantage of the subcellular compartmentalization is that a wide variety of cellular processes can take place simultaneously under vastly different conditions. The obvious disadvantage, however, is that eukaryotic cells needed to develop very precise mechanisms that would ensure that each protein is correctly sorted to the specific organelle where it can perform its function. In general, intracellular protein sorting relies on the presence of specific targeting signals within the proteins and on the respective receptors, usually localized on the surface of the organelle, that recognize these signals (Blobel, 2000). Upon recognition of targeting signals,

proteins are translocated across or inserted into the organelle membrane, usually through some form of the translocation channel and with the input of energy. Though this basic concept also applies to protein translocation into mitochondria, the complex structure of this organelle brings many additional challenges. One of them is the need to translocate the majority of its proteins across two membranes in a coordinated manner. In this Mini Review, we briefly summarize and discuss our current understanding of this process.

The Presequence Pathway

Mitochondria are double-membrane-bounded organelles with four subcompartments: two membranes, the outer membrane (OM) and the inner membrane (IM), that define two aqueous subcompartments, the intermembrane space (IMS) and the innermost matrix. Though mitochondria possess their own genome, the mitochondrial DNA (mtDNA), and a complete apparatus for its expression, out of *ca.* 1,000–1,500 mitochondrial proteins, only 8 in yeast *Saccharomyces cerevisiae* and 13 in humans are encoded in the mtDNA. The vast majority of mitochondrial proteins are encoded by nuclear genes and translated on cytosolic ribosomes as precursor proteins with specific mitochondrial targeting signals. Upon initial recognition by cytosol-exposed receptors in the OM of mitochondria, precursor proteins are imported into their final place of function with the help of highly specific protein translocases present in all mitochondrial subcompartments (Neupert, 2015; Wiedemann and Pfanner, 2017; Hansen and Herrmann, 2019). The mitochondrial targeting signals are very diverse, mirroring the complex structure of the organelle. Still, about 70% of the mitochondrial precursor proteins carry at their N-termini typically 15–55 amino acids long, cleavable extensions called presequences (Vögtle et al., 2009). Presequences are characterized by the ability to form an amphipathic helix with a net positive charge (typically +3 to +6) on one side and a hydrophobic surface on the opposite side. By default, presequences target precursor proteins to the mitochondrial matrix, however, in combination with additional targeting signals, presequence-containing precursor proteins can also be targeted to the IM, IMS, and even OM. Translocation of presequence-containing precursor proteins across the two mitochondrial membranes is mediated by the TOM and TIM23 complexes in the outer and inner membranes, respectively (**Figure 1**). This import pathway is also termed the "presequence pathway." As the main entry gate of mitochondria, the TOM complex is not only involved in the presequence pathway but also in import of essentially all nuclear-encoded mitochondrial proteins along other mitochondrial protein import pathways involving TOB/SAM, MIM, MIA and TIM22 complexes (Neupert, 2015; Schulz et al., 2015; Wiedemann and Pfanner, 2017; Hansen and Herrmann, 2019; Pfanner et al., 2019).

Newly synthesized mitochondrial precursor proteins are bound to cytosolic chaperones that keep them in a largely unfolded, import-competent state (Becker et al., 2019; Avendaño-Monsalve et al., 2020; Bykov et al., 2020). Presequences are recognized on the cytosolic surface of the OM, the so-called *cis* site, by the receptors of the TOM complex, Tom20 and Tom22 (**Figure 1**). The TOM complex has an additional receptor, Tom70. Though initial data suggested that Tom70 is specifically involved in recognition of internal targeting signals within mitochondrial proteins, recent work shows that its predominant function is in tethering cytosolic chaperones to the surface of mitochondria (Backes et al., 2021), suggesting a more general role for Tom70 in protein translocation into mitochondria. After initial recognition by Tom20 and Tom22, presequences are transferred to the translocation channel of the TOM complex formed by the β-barrel protein Tom40. Transmembrane segments of Tom22 and of three small Tom proteins, Tom5, Tom6, and Tom7, are bound on the outer surface of the Tom40 barrel. On the IMS face of the channel, presequences bind to the so-called *trans* site of the TOM complex formed by the IMS-exposed segments of Tom22, Tom40, and Tom7. Already at this stage, presequences are recognized by the IMS-exposed receptors of the TIM23 complex, Tim50 and Tim23 (**Figure 1**). In a membrane-potential dependent step, presequences are subsequently inserted into the still mysterious translocation channel of the TIM23 complex, formed by the membrane-embedded segments of Tim23 and Tim17. Once in the matrix, presequences are proteolytically removed by the mitochondrial processing peptidase. Translocation of the complete polypeptide chain into the matrix requires the ATP-dependent action of the import motor (Craig, 2018; Mokranjac, 2020). The peripheral membrane protein Tim44 recruits mtHsp70 (Ssc1), the ATP-consuming subunit of the motor, and its cochaperones Tim14 (Pam18), Tim16 (Pam16), and Mge1, to the translocation channel in the inner membrane. If the presequence is the only targeting signal present, precursor proteins will be completely translocated into the matrix. However, if an additional hydrophobic sorting signal ("stop-transfer signal") is present downstream of the presequence, translocation into the matrix will be arrested and the hydrophobic segment will be inserted laterally into the IM. The TIM23 complex contains three nonessential subunits, Pam17, Tim21, and Mgr2, that appear to play a role in the differential sorting of proteins into the matrix and the IM.

It is likely that all major players of the presequence pathway are identified by now. However, molecular understanding of how presequences are recognized and handed over along this pathway is still very rudimentary – the only high-resolution structure of the receptor bound to the presequence peptide is that of the cytosolic domain of Tom20 (Abe et al., 2000; Saitoh et al., 2007). Below we present and discuss our current knowledge of how TOM and TIM23 cooperate during transfer of presequences between outer and inner mitochondrial membranes.

Cooperation of TOM and TIM23 Complexes During Transfer of Precursor Proteins

Upon solubilization of mitochondria, the TOM complex does not interact in a stable manner with the TIM23 complex, or with any other of the downstream translocases. Studies with isolated OM vesicles and purified and reconstituted TOM complex showed that the TOM complex is able to recognize presequence-containing precursor proteins and initiate their

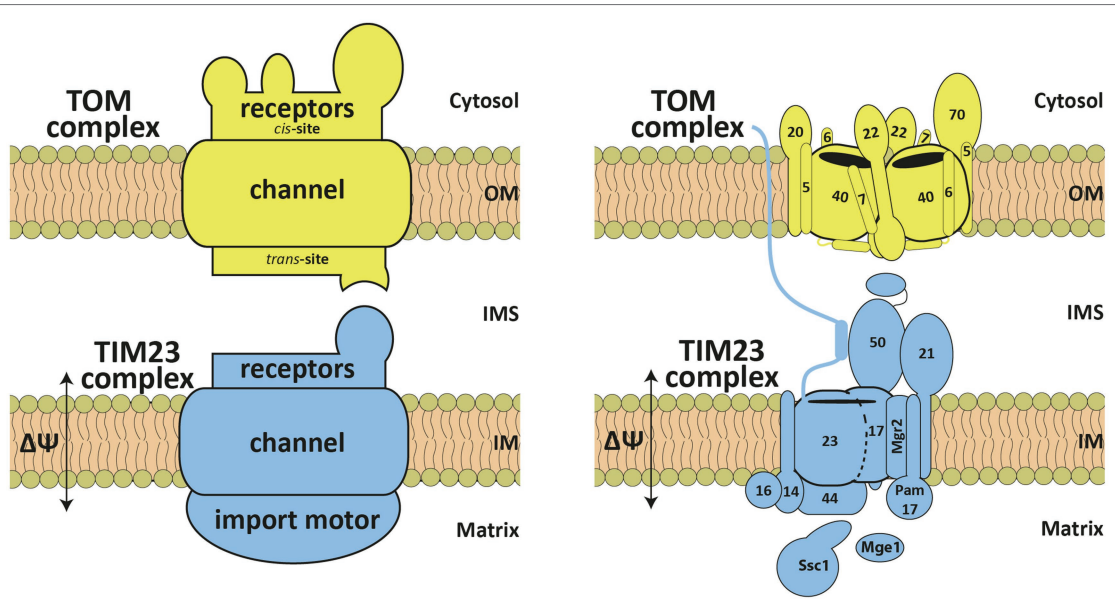

FIGURE 1 | Schematic representation of the TOM and TIM23 complexes. The TOM complex consists of the receptors, Tom20, Tom22, and Tom70, and a channel unit, formed by Tom40, associated with three small proteins Tom5, Tom6 and Tom7. It possesses *cis* and *trans* presequence-binding sites. The TIM23 complex can be functionally divided into receptors, translocation channel and import motor – Tim23, Tim17, Tim50, Tim44, Tim14, Tim16, mtHsp70 (Ssc1), Mge1, Tim21, Mgr2, and Pam17. See text for details. OM, outer membrane; IMS, intermembrane space; IM, inner membrane.

translocation across the OM; however, they also showed that the TOM complex on its own is not able to translocate proteins completely across the membrane (Mayer et al., 1995; Künkele et al., 1998). On the other hand, experiments performed with mitoplasts, mitochondria in which the OM was artificially removed, showed that the TIM23 complex is, on its own, able to recognize and import precursor proteins across the IM (Hwang et al., 1989). In intact mitochondria, however, N-terminal presequences can be proteolytically removed in the matrix while the C-terminal part of the protein is still in the cytosol. Also, the TOM-TIM23 supercomplex can be stabilized with precursor proteins arrested as the TOM-TIM23 spanning intermediates (Chacinska et al., 2003; Popov-Celeketić et al., 2008). These experiments show that the TOM and TIM23 complexes do not operate as isolated units but rather mediate import of presequence-containing precursor proteins in a tightly controlled and coordinated manner. The cooperation of the TOM and TIM23 complexes is likely to take place in the IMS where the two complexes meet. The subunits implicated in TOM and TIM23 cooperation are Tom22, Tom7, and Tom40, from the TOM side, and Tim50, Tim23, and Tim21, from the TIM23 side (**Figure 2A**).

Biochemical and genetic experiments suggested that the *trans* site of the TOM complex is formed by the IMS-facing segments of Tom22, Tom7, and Tom40. All three proteins can be crosslinked to precursor proteins arrested in the TOM complex (Kanamori et al., 1999; Esaki et al., 2004). Simultaneous deletion of Tom7 and the IMS segment of Tom22 leads to the accumulation of precursor forms of mitochondrial proteins in the cytosol, indicative of impaired import. These cells are not able to grow on a fermentable carbon source at higher temperatures and not at all on nonfermentable carbon sources (Esaki et al., 2004). The recently determined cryo-EM structure of the TOM complex indeed suggests that they are all found close to each other at the Tom40 dimer interface (Araiso et al., 2019; Tucker and Park, 2019). Unfortunately, the actual IMS-exposed segments of Tom40 and Tom22, where the presequences most likely bind, were not resolved in the structure. However, biochemical evidence has been presented that the presequence-containing precursor proteins exit the channel in the middle of the dimer where the *trans* site of the TOM complex is expected to be (Araiso et al., 2019).

Experiments performed in intact mitochondria and with isolated recombinant proteins showed that the TIM23 complex interacts with the *trans* site of the TOM complex even in the absence of protein translocation (**Figure 2A**). Using chemical and/or site-specific UV crosslinking, Tim23 and Tim50 were crosslinked to the IMS-exposed segments of Tom22 and Tom40 (Tamura et al., 2009; Shiota et al., 2011; Waegemann et al., 2015; Araiso et al., 2019; Günsel et al., 2020). Recombinantly expressed and purified IMS segments of Tim23 and Tim21 bound to the IMS segment of Tom22 *in vitro* (Chacinska et al., 2005; Mokranjac et al., 2005; Albrecht et al., 2006; Bajaj et al., 2014). A direct interaction of any of these TIM23 subunits with Tom7 has not been demonstrated yet, however, considering the recently shown proximity of Tom7 to the IMS-exposed segments of Tom22 and Tom40 (Araiso et al., 2019; Tucker and Park, 2019), it is likely that Tom7 is present in the vicinity of and/or interacts with at least one of the three TIM23 subunits. Indeed, Tom7 genetically interacts with the N-terminal segment of Tim23, as does the IMS segment of Tom22 (Waegemann et al., 2015). The unique feature of the N-terminal segment of Tim23 is that it is accessible to externally added proteases

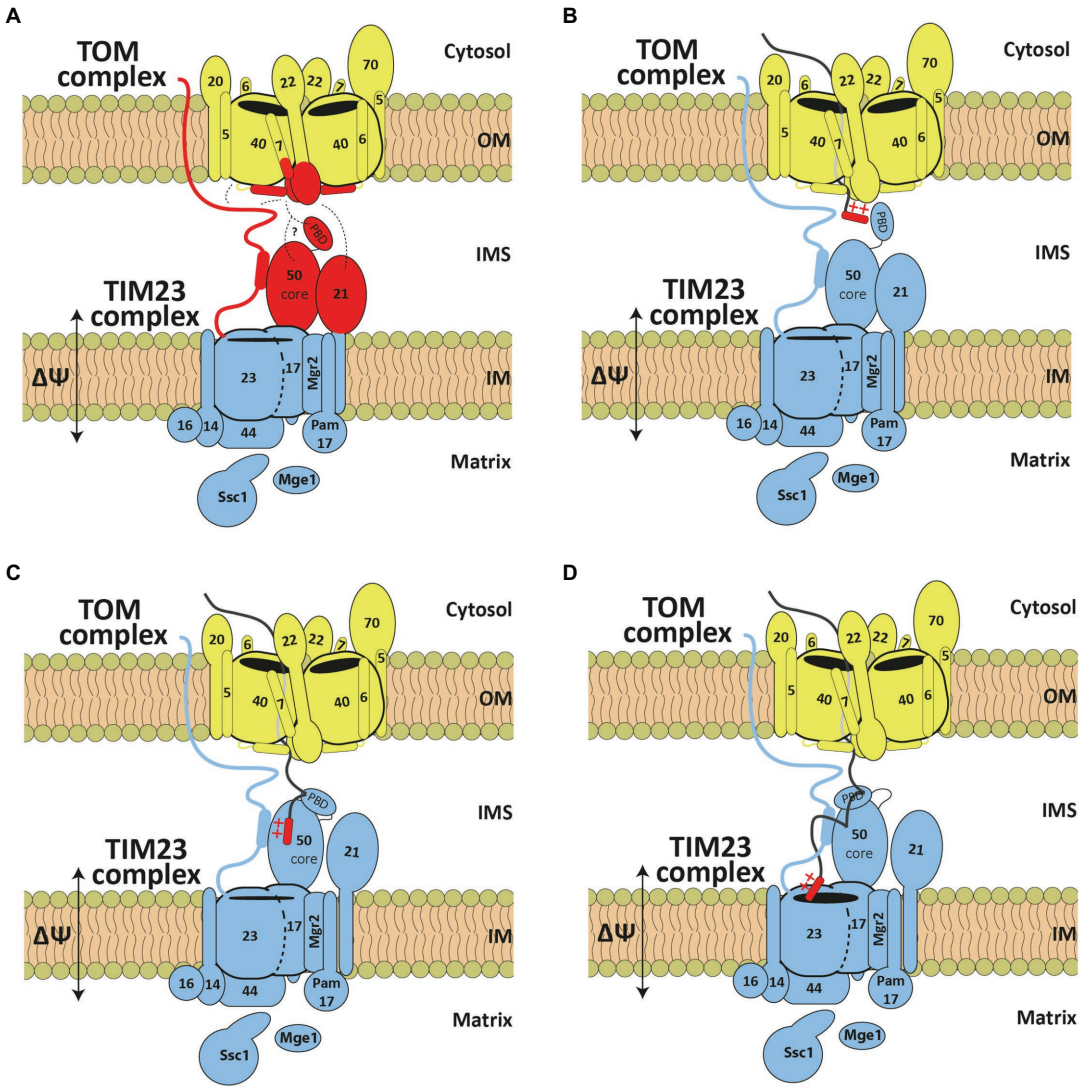

FIGURE 2 | TOM and TIM23 cooperation during precursor translocation across two mitochondrial membranes. **(A)** Subunits implicated in TOM and TIM23 cooperation are highlighted in red. Dashed lines represent identified interaction points. **(B–D)** Current working model for transfer of precursors from the TOM to the TIM23 complex. See text for details. OM, outer membrane; IMS, intermembrane space; IM, inner membrane.

in intact mitochondria (Donzeau et al., 2000). Though still controversial, the exposure of Tim23 on the mitochondrial surface depends on the interaction between Tim23 and Tim50 in the IMS (Yamamoto et al., 2002; Gevorkyan-Airapetov et al., 2009; Tamura et al., 2009), the dynamics of the TOM complex (Waegemann et al., 2015), the energetic state of the inner membrane (Günsel et al., 2020) and the translocation activity of the TIM23 complex (Popov-Celeketić et al., 2008). Whether Tim23 reaches the cytosol through the lipid bilayer, through the TOM channel or by some other, still unknown mechanism remains unclear. Even though this segment of Tim23 is not essential for cell viability (Chacinska et al., 2003; Waegemann et al., 2015), it is only logical that, by crossing two mitochondrial membranes, Tim23 would bring them closer, facilitating transfer of proteins between TOM and TIM23 complexes.

The IMS-exposed segments of the TIM23 subunits not only interact with the *trans* site of the TOM complex but also with each other. The high-resolution structural information on these interactions is unfortunately still missing. Still, biochemical experiments showed that Tim21 binds to Tim23 and to Tim50, as judged by both *in organello* crosslinking and interactions between recombinantly expressed and purified proteins (Tamura et al., 2009; Lytovchenko et al., 2013; Bajaj et al., 2014). The interaction between Tim23 and Tim50 has been extensively analyzed *in vivo*, *in organello*, and *in vitro*, and residues in both proteins have been identified that contribute to their interaction (Geissler et al., 2002; Yamamoto et al., 2002; Mokranjac et al., 2003, 2009; Meinecke et al., 2006; Alder et al., 2008; Gevorkyan-Airapetov et al., 2009; Tamura et al., 2009; Qian et al., 2011; Schulz et al., 2011; Lytovchenko et al., 2013; Günsel

et al., 2020; Gomkale et al., 2021). Interestingly, Tim23 seems to bind to two distinct patches on the surface of Tim50 (Tamura et al., 2009; Qian et al., 2011; Dayan et al., 2019). Also, lipids seem to play an important role in the interaction between the two proteins (Malhotra et al., 2017). Despite many efforts, the picture of Tim23-Tim50 interaction and particularly its dynamics remains blurry, likely due to the intrinsically disordered character of the Tim23 segment involved in the interaction (Gevorkyan-Airapetov et al., 2009; de La Cruz et al., 2010; Günsel et al., 2020).

Presequences are recognized by several components of the presequence pathway and precursor proteins influence not only the interactions between TOM and TIM23 complexes but also the interactions among the TIM23 subunits. Precursor proteins arrested at the *trans* site of the TOM complex can already be crosslinked to Tim50 (Yamamoto et al., 2002; Mokranjac et al., 2003, 2009), making it the first subunit of the TIM23 complex to recognize and bind presequences. The actual binding of presequences to the IMS segment of Tim50 was subsequently confirmed in a reconstituted system (Marom et al., 2011). Details of how translocating precursor proteins are transferred from the *trans* site of the TOM complex to Tim50 remain unclear. Precursor proteins increased the efficiency of chemical crosslinking between Tim50 and Tom22 (Waegemann et al., 2015), but they decreased a site-specific crosslink between the two proteins (Shiota et al., 2011). The situation got complicated even further when it was shown that the IMS segment of Tim50 consists of two domains: the highly evolutionary conserved core domain and the fungi-specific presequence-binding domain (PBD; Schulz et al., 2011). Though PBD was initially suggested to be solely responsible for recognizing and binding presequences, subsequent experiments showed that the core domain also binds presequences and even with similar affinity as PBD (Schulz et al., 2011; Lytovchenko et al., 2013). Recent NMR experiments indicate that the two domains of Tim50 bind to each other and that their interaction is modulated by presequences (Rahman et al., 2014). The receptor function of Tim50 depends on its interaction with Tim23 (Mokranjac et al., 2009; Tamura et al., 2009). Tim23 on its own also binds to presequences, however, with far lower affinity than Tim50 (Bauer et al., 1996; de La Cruz et al., 2010; Marom et al., 2011; Lytovchenko et al., 2013). Presequences dissociated the interaction of Tim50 with Tim21, indicating that Tim21 modulates the dynamic interplay of the TOM and TIM23 subunits in the IMS with presequences (Lytovchenko et al., 2013). Recent purification of the TOM-TIM23 supercomplex followed by crosslinking and mass spectrometry identified many new potential TOM-TIM23 interactions (Gomkale et al., 2021). Particularly interesting are the multiple contacts between Tim21 and Tom22 as well as the ones between Tim23 and Tom5 and Tom40. Unfortunately, these new contacts were not yet analyzed in intact mitochondria. It is also surprising that the TOM-TIM23 crosslinks previously identified in intact mitochondria were not recapitulated in this work.

Based on the available data, the current working model of how presequences are transferred from the *trans* site of the TOM complex to the translocation channel in the inner membrane would suggest the following scenario. Precursor proteins exit the TOM channel at the *trans* site where presequences are recognized by Tim50 (**Figure 2B**). The changes in multiple interactions between TOM and TIM23 complexes, induced by the recognition of presequences, would allow the presequences to be released from the *trans* site of the TOM complex, likely, to the PBD of Tim50. Binding of presequences to the PBD would then induce structural rearrangements within Tim50 so that presequences are further transferred to the core domain of Tim50 and the IMS-exposed segment of Tim23 (**Figure 2C**). In a membrane-potential dependent step, presequences are finally inserted into the TIM23 channel for translocation across the IM (**Figure 2D**).

CONCLUDING REMARKS

Even *ca.* 30 years after identification of its first components, the presequence pathway still withholds many of its secrets. The major players involved in cooperation between the TOM and TIM23 complexes are probably all identified; however, we are only beginning to understand their multiple and dynamic interactions that underlie transfer of precursor proteins between two mitochondrial membranes and many open questions remain. Many of the TOM-TIM23 contacts have only been identified and their dynamics during translocation of proteins have not yet been analyzed. The different steps during transfer of presequences from the TOM to TIM23 complex remain speculative and unclear even on the level of components involved at different proposed steps. Understanding of presequence recognition in the IMS is still very limited, both on the level of the TOM and TIM23 complexes. Do the two domains of Tim50 bind presequences individually, do they together form a presequence-binding site or are they maybe involved in recognition of presequences during different stages of protein translocation? How does Tim23 contribute to presequence recognition in the IMS? Which domain of Tim50 is involved in which of the identified interactions of Tim50 and how do they change during translocation of proteins into mitochondria? If PBD of Tim50 is indeed only fungi-specific, how do higher eukaryotes deal with the lack of this domain? On a more general note, it will be interesting to know whether newly synthesized precursor proteins in the cytosol already know which TOM complexes are associated with TIM23 complexes or if the coordination of the two complexes predominantly happens after the presequences have reached the *trans* site of the TOM complex. If former, what distinguishes TOM complexes bound to TIM23 from the rest?

The successful use of the recent developments in the cryo-EM to solve the high-resolution structure of the TOM complex (Araiso et al., 2019; Tucker and Park, 2019; Wang et al., 2020) represents a milestone toward understanding the molecular mechanisms of protein import through the TOM complex and its coordination with other protein translocases. The structure of at least part of the TIM23 complex will hopefully become available soon (Sim et al., 2021). The ability to generate and purify the TOM-TIM23 supercomplex gives hope that the same developments can also be used to solve the structure of the supercomplex. The structures will certainly help in putting all the already available data in the structural

context but also in raising novel hypotheses that can then be tested in careful biochemical experiments. The secrets of the presequence pathway seem less out of reach now than they were just few years ago.

AUTHOR CONTRIBUTIONS

MG and DM wrote the manuscript together and authors approved the submitted version. MG made the figures with the input from DM.

FUNDING

This work was supported by the Deutsche Forschungs gemeinschaft (MO1944/3-1 to DM).

ACKNOWLEDGMENTS

We would like to thank the present and past members of the Mokranjac group and the Mito Club for the stimulating and inspiring discussions on mitochondrial biogenesis.

REFERENCES

Abe, Y., Shodai, T., Muto, T., Mihara, K., Torii, H., Nishikawa, S., et al. (2000). Structural basis of presequence recognition by the mitochondrial protein import receptor Tom20. *Cell* 100, 551–560. doi: 10.1016/s0092-8674(00)80691-1

Albrecht, R., Rehling, P., Chacinska, A., Brix, J., Cadamuro, S. A., Volkmer, R., et al. (2006). The Tim21 binding domain connects the preprotein translocases of both mitochondrial membranes. *EMBO Rep.* 7, 1233–1238. doi: 10.1038/sj.embor.7400828

Alder, N. N., Sutherland, J., Buhring, A. I., Jensen, R. E., and Johnson, A. E. (2008). Quaternary structure of the mitochondrial TIM23 complex reveals dynamic association between Tim23p and other subunits. *MBoC* 19, 159–170. doi: 10.1091/mbc.e07-07-0669

Araiso, Y., Tsutsumi, A., Qiu, J., Imai, K., Shiota, T., Song, J., et al. (2019). Structure of the mitochondrial import gate reveals distinct preprotein paths. *Nature* 575, 395–401. doi: 10.1038/s41586-019-1680-7

Avendaño-Monsalve, M. C., Ponce-Rojas, J. C., and Funes, S. (2020). From cytosol to mitochondria: the beginning of a protein journey. *Biol. Chem.* 401, 645–661. doi: 10.1515/hsz-2020-0110

Backes, S., Bykov, Y. S., Flohr, T., Räschle, M., Zhou, J., Lenhard, S., et al. (2021). The chaperone-binding activity of the mitochondrial surface receptor Tom70 protects the cytosol against mitoprotein-induced stress. *Cell Rep.* 35:108936. doi: 10.1016/j.celrep.2021.108936

Bajaj, R., Jaremko, Ł., Jaremko, M., Becker, S., and Zweckstetter, M. (2014). Molecular basis of the dynamic structure of the TIM23 complex in the mitochondrial intermembrane space. *Structure* 22, 1501–1511. doi: 10.1016/j.str.2014.07.015

Bauer, M. F., Sirrenberg, C., Neupert, W., and Brunner, M. (1996). Role of Tim23 as voltage sensor and Presequence receptor in protein import into mitochondria. *Cell* 87, 33–41. doi: 10.1016/S0092-8674(00)81320-3

Becker, T., Song, J., and Pfanner, N. (2019). Versatility of Preprotein transfer from the cytosol to mitochondria. *Trends Cell Biol.* 29, 534–548. doi: 10.1016/j.tcb.2019.03.007

Blobel, G. (2000). Protein targeting (Nobel lecture). *Chembiochem* 1, 86–102. doi: 10.1002/1439-7633(20000818)1:2<86::AID-CBIC86>3.0.CO;2-A

Bykov, Y. S., Rapaport, D., Herrmann, J. M., and Schuldiner, M. (2020). Cytosolic events in the biogenesis of mitochondrial proteins. *Trends Biochem. Sci.* 45, 650–667. doi: 10.1016/j.tibs.2020.04.001

Chacinska, A., Lind, M., Frazier, A. E., Dudek, J., Meisinger, C., Geissler, A., et al. (2005). Mitochondrial presequence translocase: switching between TOM tethering and motor recruitment involves Tim21 and Tim17. *Cell* 120, 817–829. doi: 10.1016/j.cell.2005.01.011

Chacinska, A., Rehling, P., Guiard, B., Frazier, A. E., Schulze-Specking, A., Pfanner, N., et al. (2003). Mitochondrial translocation contact sites: separation of dynamic and stabilizing elements in formation of a TOM-TIM-preprotein supercomplex. *EMBO J.* 22, 5370–5381. doi: 10.1093/emboj/cdg532

Craig, E. A. (2018). Hsp70 at the membrane: driving protein translocation. *BMC Biol.* 16:11. doi: 10.1186/s12915-017-0474-3

Dayan, D., Bandel, M., Günsel, U., Nussbaum, I., Prag, G., Mokranjac, D., et al. (2019). A mutagenesis analysis of Tim50, the major receptor of the TIM23 complex, identifies regions that affect its interaction with Tim23. *Sci. Rep.* 9:2012. doi: 10.1038/s41598-018-38353-1

de La Cruz, L., Bajaj, R., Becker, S., and Zweckstetter, M. (2010). The intermembrane space domain of Tim23 is intrinsically disordered with a distinct binding region for presequences. *Protein Sci.* 19, 2045–2054. doi: 10.1002/pro.482

Donzeau, M., Káldi, K., Adam, A., Paschen, S., Wanner, G., Guiard, B., et al. (2000). Tim23 links the inner and outer mitochondrial membranes. *Cell* 101, 401–412. doi: 10.1016/S0092-8674(00)80850-8

Esaki, M., Shimizu, H., Ono, T., Yamamoto, H., Kanamori, T., Nishikawa, S., et al. (2004). Mitochondrial protein import. Requirement of presequence elements and tom components for precursor binding to the TOM complex. *J. Biol. Chem.* 279, 45701–45707. doi: 10.1074/jbc.M404591200

Geissler, A., Chacinska, A., Truscott, K. N., Wiedemann, N., Brandner, K., Sickmann, A., et al. (2002). The mitochondrial presequence translocase. *Cell* 111, 507–518. doi: 10.1016/S0092-8674(02)01073-5

Gevorkyan-Airapetov, L., Zohary, K., Popov-Celeketic, D., Mapa, K., Hell, K., Neupert, W., et al. (2009). Interaction of Tim23 with Tim50 is essential for protein translocation by the mitochondrial TIM23 complex. *J. Biol. Chem.* 284, 4865–4872. doi: 10.1074/jbc.M807041200

Gomkale, R., Linden, A., Neumann, P., Schendzielorz, A. B., Stoldt, S., Dybkov, O., et al. (2021). Mapping protein interactions in the active TOM-TIM23 supercomplex. *Nat. Commun.* 12:5715. doi: 10.1038/s41467-021-26016-1

Günsel, U., Paz, E., Gupta, R., Mathes, I., Azem, A., and Mokranjac, D. (2020). In vivo dissection of the intrinsically disordered receptor domain of Tim23. *J. Mol. Biol.* 432, 3326–3337. doi: 10.1016/j.jmb.2020.03.031

Hansen, K. G., and Herrmann, J. M. (2019). Transport of proteins into mitochondria. *Protein J.* 38, 330–342. doi: 10.1007/s10930-019-09819-6

Hwang, S., Jascur, T., Vestweber, D., Pon, L., and Schatz, G. (1989). Disrupted yeast mitochondria can import precursor proteins directly through their inner membrane. *J. Cell Biol.* 109, 487–493. doi: 10.1083/jcb.109.2.487

Kanamori, T., Nishikawa, S., Nakai, M., Shin, I., Schultz, P. G., and Endo, T. (1999). Uncoupling of transfer of the presequence and unfolding of the mature domain in precursor translocation across the mitochondrial outer membrane. *Proc. Natl. Acad. Sci.* 96, 3634–3639. doi: 10.1073/pnas.96.7.3634

Künkele, K.-P., Heins, S., Dembowski, M., Nargang, F. E., Benz, R., Thieffry, M., et al. (1998). The preprotein translocation channel of the outer membrane of mitochondria. *Cell* 93, 1009–1019. doi: 10.1016/S0092-8674(00)81206-4

Lytovchenko, O., Melin, J., Schulz, C., Kilisch, M., Hutu, D. P., and Rehling, P. (2013). Signal recognition initiates reorganization of the presequence translocase during protein import. *EMBO J.* 32, 886–898. doi: 10.1038/emboj.2013.23

Malhotra, K., Modak, A., Nangia, S., Daman, T. H., Gunsel, U., Robinson, V. L., et al. (2017). Cardiolipin mediates membrane and channel interactions of the mitochondrial TIM23 protein import complex receptor Tim50. *Sci. Adv.* 3:e1700532. doi: 10.1126/sciadv.1700532

Marom, M., Dayan, D., Demishtein-Zohary, K., Mokranjac, D., Neupert, W., and Azem, A. (2011). Direct interaction of mitochondrial targeting presequences with purified components of the TIM23 protein complex. *J. Biol. Chem.* 286, 43809–43815. doi: 10.1074/jbc.M111.261040

Mayer, A., Neupert, W., and Lill, R. (1995). Mitochondrial protein import: reversible binding of the presequence at the trans side of the outer membrane drives partial translocation and unfolding. *Cell* 80, 127–137. doi: 10.1016/0092-8674(95)90457-3

Meinecke, M., Wagner, R., Kovermann, P., Guiard, B., Mick, D. U., Hutu, D. P., et al. (2006). Tim50 maintains the permeability barrier of the mitochondrial inner membrane. *Science* 312, 1523–1526. doi: 10.1126/science.1127628

Mokranjac, D. (2020). How to get to the other side of the mitochondrial inner membrane – the protein import motor. *Biol. Chem.* 401, 723–736. doi: 10.1515/hsz-2020-0106

Mokranjac, D., Paschen, S. A., Kozany, C., Prokisch, H., Hoppins, S. C., Nargang, F. E., et al. (2003). Tim50, a novel component of the TIM23 preprotein translocase of mitochondria. *EMBO J.* 22, 816–825. doi: 10.1093/emboj/cdg090

Mokranjac, D., Popov-Celeketić, D., Hell, K., and Neupert, W. (2005). Role of Tim21 in mitochondrial translocation contact sites. *J. Biol. Chem.* 280, 23437–23440. doi: 10.1074/jbc.C500135200

Mokranjac, D., Sichting, M., Popov-Celeketić, D., Mapa, K., Gevorkyan-Airapetov, L., Zohary, K., et al. (2009). Role of Tim50 in the transfer of precursor proteins from the outer to the inner membrane of mitochondria. *MBoC* 20, 1400–1407. doi: 10.1091/mbc.e08-09-0934

Neupert, W. (2015). A perspective on transport of proteins into mitochondria: a myriad of open questions. *J. Mol. Biol.* 427, 1135–1158. doi: 10.1016/j.jmb.2015.02.001

Pfanner, N., Warscheid, B., and Wiedemann, N. (2019). Mitochondrial proteins: from biogenesis to functional networks. *Nat. Rev. Mol. Cell Biol.* 20, 267–284. doi: 10.1038/s41580-018-0092-0

Popov-Celeketić, D., Mapa, K., Neupert, W., and Mokranjac, D. (2008). Active remodelling of the TIM23 complex during translocation of preproteins into mitochondria. *EMBO J.* 27, 1469–1480. doi: 10.1038/emboj.2008.79

Qian, X., Gebert, M., Höpker, J., Yan, M., Li, J., Wiedemann, N., et al. (2011). Structural basis for the function of Tim50 in the mitochondrial presequence translocase. *J. Mol. Biol.* 411, 513–519. doi: 10.1016/j.jmb.2011.06.020

Rahman, B., Kawano, S., Yunoki-Esaki, K., Anzai, T., and Endo, T. (2014). NMR analyses on the interactions of the yeast Tim50 C-terminal region with the presequence and Tim50 core domain. *FEBS Lett.* 588, 678–684. doi: 10.1016/j.febslet.2013.12.037

Saitoh, T., Igura, M., Obita, T., Ose, T., Kojima, R., Maenaka, K., et al. (2007). Tom20 recognizes mitochondrial presequences through dynamic equilibrium among multiple bound states. *EMBO J.* 26, 4777–4787. doi: 10.1038/sj.emboj.7601888

Schulz, C., Lytovchenko, O., Melin, J., Chacinska, A., Guiard, B., Neumann, P., et al. (2011). Tim50's presequence receptor domain is essential for signal driven transport across the TIM23 complex. *J. Cell Biol.* 195, 643–656. doi: 10.1083/jcb.201105098

Schulz, C., Schendzielorz, A., and Rehling, P. (2015). Unlocking the presequence import pathway. *Trends Cell Biol.* 25, 265–275. doi: 10.1016/j.tcb.2014.12.001

Shiota, T., Mabuchi, H., Tanaka-Yamano, S., Yamano, K., and Endo, T. (2011). In vivo protein-interaction mapping of a mitochondrial translocator protein Tom22 at work. *Proc. Natl. Acad. Sci. U. S. A.* 108, 15179–15183. doi: 10.1073/pnas.1105921108

Sim, S.I., Chen, Y., and Park, E. (2021). Structural basis of mitochondrial protein import by the TIM complex. *BioRxiv*. [ahead of preprint]. doi:10.1101/2021.10.10.463828

Tamura, Y., Harada, Y., Shiota, T., Yamano, K., Watanabe, K., Yokota, M., et al. (2009). Tim23-Tim50 pair coordinates functions of translocators and motor proteins in mitochondrial protein import. *J. Cell Biol.* 184, 129–141. doi: 10.1083/jcb.200808068

Tucker, K., and Park, E. (2019). Cryo-EM structure of the mitochondrial protein-import channel TOM complex at near-atomic resolution. *Nat. Struct. Mol. Biol.* 26, 1158–1166. doi: 10.1038/s41594-019-0339-2

Vögtle, F.-N., Wortelkamp, S., Zahedi, R. P., Becker, D., Leidhold, C., Gevaert, K., et al. (2009). Global analysis of the mitochondrial N-proteome identifies a processing peptidase critical for protein stability. *Cell* 139, 428–439. doi: 10.1016/j.cell.2009.07.045

Waegemann, K., Popov-Čeleketić, D., Neupert, W., Azem, A., and Mokranjac, D. (2015). Cooperation of TOM and TIM23 complexes during translocation of proteins into mitochondria. *J. Mol. Biol.* 427, 1075–1084. doi: 10.1016/j.jmb.2014.07.015

Wang, W., Chen, X., Zhang, L., Yi, J., Ma, Q., Yin, J., et al. (2020). Atomic structure of human TOM core complex. *Cell Discov.* 6:67. doi: 10.1038/s41421-020-00198-2

Wiedemann, N., and Pfanner, N. (2017). Mitochondrial machineries for protein import and assembly. *Annu. Rev. Biochem.* 86, 685–714. doi: 10.1146/annurev-biochem-060815-014352

Yamamoto, H., Esaki, M., Kanamori, T., Tamura, Y., Nishikawa, S., and Endo, T. (2002). Tim50 is a subunit of the TIM23 complex that links protein translocation across the outer and inner mitochondrial membranes. *Cell* 111, 519–528. doi: 10.1016/S0092-8674(02)01053-X

Conflict of Interest: The authors declare that the research was conducted in the absence of any commercial or financial relationships that could be construed as a potential conflict of interest.

Publisher's Note: All claims expressed in this article are solely those of the authors and do not necessarily represent those of their affiliated organizations, or those of the publisher, the editors and the reviewers. Any product that may be evaluated in this article, or claim that may be made by its manufacturer, is not guaranteed or endorsed by the publisher.

frontiers in Physiology

REVIEW
published: 12 January 2022
doi: 10.3389/fphys.2021.802057

Protein Targeting Into the Thylakoid Membrane Through Different Pathways

*Dan Zhu, Haibo Xiong, Jianghao Wu, Canhui Zheng, Dandan Lu, Lixin Zhang and Xiumei Xu**

State Key Laboratory of Crop Stress Adaptation and Improvement, School of Life Sciences, Henan University, Kaifeng, China

In higher plants, chloroplasts are essential semi-autonomous organelles with complex compartments. As part of these sub-organellar compartments, the sheet-like thylakoid membranes contain abundant light-absorbing chlorophylls bound to the light-harvesting proteins and to some of the reaction center proteins. About half of the thylakoid membrane proteins are encoded by nuclear genes and synthesized in the cytosol as precursors before being imported into the chloroplast. After translocation across the chloroplast envelope by the Toc/Tic system, these proteins are subsequently inserted into or translocated across the thylakoid membranes through distinct pathways. The other half of thylakoid proteins are encoded by the chloroplast genome, synthesized in the stroma and integrated into the thylakoid through a cotranslational process. Much progress has been made in identification and functional characterization of new factors involved in protein targeting into the thylakoids, and new insights into this process have been gained. In this review, we introduce the distinct transport systems mediating the translocation of substrate proteins from chloroplast stroma to the thylakoid membrane, and present the recent advances in the identification of novel components mediating these pathways. Finally, we raise some unanswered questions involved in the targeting of chloroplast proteins into the thylakoid membrane, along with perspectives for future research.

Keywords: chloroplast protein import, cpSRP pathway, cpGet pathway, spontaneous pathway, cotranslational protein transport

OPEN ACCESS

Edited by:
Inhwan Hwang, Pohang University of Science and Technology, South Korea

Reviewed by:
Chiung-Chih Chu, Academia Sinica, Taiwan
Dong Wook Lee, Chonnam National University, South Korea

****Correspondence:***
Xiumei Xu
xuxiumei@vip.henu.edu.cn

Specialty section:
This article was submitted to Membrane Physiology and Membrane Biophysics, a section of the journal Frontiers in Physiology

Received: *26 October 2021*
Accepted: *07 December 2021*
Published: *12 January 2022*

Citation:
Zhu D, Xiong H, Wu J, Zheng C, Lu D, Zhang L and Xu X (2022) Protein Targeting Into the Thylakoid Membrane Through Different Pathways. Front. Physiol. 12:802057. doi: 10.3389/fphys.2021.802057

INTRODUCTION

Chloroplasts of higher plants, the semi-autonomous organelles with internal sheet-like membrane-bound structure, are not only the sites for photosynthesis, but also for the synthesis of many essential metabolites, such as fatty acids, amino acids, vitamins, tetrapyrroles, and some phytohormones (Neuhaus and Emes, 2000; Wicke et al., 2011). Chloroplasts are believed to have evolved from an ancient cyanobacteria-like endosymbiont. Following this endosymbiosis most of the endosymbiont genes were transferred to the host nuclear genome. As a result, ∼3,000 chloroplast proteins are encoded by nuclear genes, while only ∼100 proteins are encoded by the chloroplast genome and synthesized in the stroma (Lee et al., 2017; Sjuts et al., 2017; Nakai, 2018; Richardson and Schnell, 2020). Chloroplasts contain three distinct membranes: outer envelope, inner envelope, and thylakoid membranes, which separate the chloroplast into three compartments:

the intermembrane space, chloroplast stroma and thylakoid lumen (Staehelin, 2003; Kirchhoff, 2019). The thylakoid contains several photosynthetic complexes including photosystem I (PSI), photosystem II (PSII), the cytochrome b_6f complex (Cyt b_6f), and ATP synthase (ATPase), which are responsible for the primary reactions of photosynthesis. About half of the subunits of these complexes are encoded by the nuclear genome, synthesized in the cytosol, imported into chloroplasts and transported to the thylakoids. However, the complex structure of chloroplasts makes translocation of these proteins across the membrane system for correct targeting to their specific sub-compartment highly challenging.

The nuclear-encoded thylakoid proteins with an N-terminal transit peptide (TP) are first imported into the stroma by the Toc/Tic (translocon at the outer/inner envelope membrane of chloroplasts) complexes, and then the TP is removed by the stromal processing peptidase, and the proteins are targeted into or across the thylakoid membranes through sophisticated targeting pathways (Martin et al., 2002; Leister, 2003). To date, several independent pathways have been reported, of which the chloroplast signal recognition particle (cpSRP) pathway, the spontaneous insertion pathway and the recently discovered chloroplast Guided Entry of TA proteins (cpGET) pathway are responsible for inserting proteins into the thylakoid membrane (**Figure 1**), while the chloroplast secretory (cpSec) and the chloroplast twin-arginine translocase (cpTat) pathways are needed for translocating proteins into the thylakoid lumen (Schünemann, 2007; Ouyang et al., 2020; Anderson et al., 2021; Xu et al., 2021a,b). In contrast, proteins encoded by the chloroplast genome are cotranslationally transported from the stroma to thylakoids (**Figure 1**). Although several translocation events can be distinguished through their components and energy requirements, how the imported chloroplast proteins are recognized and sorted exactly to their distinct pathways is still largely unknown. In this review, we describe the distinct transport mechanisms for targeting nuclear- and chloroplast-encoded proteins from the stroma to the thylakoid membrane. Moreover, we review recent advances and the discovery of novel components of these transport systems. Finally, we discuss current challenges and present new perspectives in this promising field.

PATHWAYS FOR INSERTING THE NUCLEAR-ENCODED PROTEINS INTO THE THYLAKOID MEMBRANE

The thylakoid membrane harbors the photosynthetic apparatus composed of PSI, PSII, Cyt b_6f, and ATP synthase. Besides, several proteins involved in thylakoid biogenesis and homeostasis are also anchored in the thylakoid membrane. These proteins are encoded by both the nuclear and chloroplast genomes, of which the nuclear-encoded proteins are translocated into thylakoid membranes through the cpSRP pathway, the spontaneous insertion pathway, and the cpGET pathway, whereas chloroplast-encoded proteins are inserted into the thylakoid membrane cotranslationally (**Figure 1**).

Posttranslational Insertion Into the Thylakoid Membrane Through the Chloroplast Signal Recognition Particle Pathway

The classical SRP system is responsible for cotranslationally delivering newly synthesized proteins to their correct cellular membranes. The functional core of cytosolic SRP is composed of the SRP54 GTPase and SRP RNA, which is tightly bound to SRP54. Notably, the cpSRP system in green plants is different from all other SRP systems because the cpSRP lacks the associated RNA and instead consists of a conserved cpSRP54 and a unique chloroplast-specific cpSRP43 subunit. Contrary to the universally conserved cytosolic SRP system which only binds to the short nascent polypeptide chains and functions cotranslationally, the cpSRP system evolved posttranslational activity to target the light-harvesting chlorophyll a/b binding proteins (LHCPs) from the stroma to the thylakoid membrane (Ziehe et al., 2017, 2018; Costa et al., 2018). LHCP membrane integration requires the cpSRP43/cpSRP54 complex and its receptor cpFtsY, the integral translocase Alb3, and GTP, which is hydrolyzed by the cpSRP54 and cpFtsY GTPases (Moore et al., 2003; Ziehe et al., 2018; **Figure 1**).

It was first confirmed that the L18 region between the second and third transmembrane domain (TMD) of LHCP is the binding site for cpSRP43 (DeLille et al., 2000; Tu et al., 2000; Stengel et al., 2008). Recently, however, McAvoy et al. (2018) found that cpSRP43 makes more extensive interactions with all the TMDs within LHCP, thus protecting the hydrophobic LHCP from aggregation in the stroma. These new interaction sites are important for the chaperone activity of cpSRP43 based on the result that a class of cpSRP43 mutants are specifically deficient in their ability of chaperoning full-length LHCP but are not affected in their association activity with the L18 region. NMR analysis showed three conformations of cpSRP43. Interaction with cpSRP54 produces the active state through structural rearrangement, thereby improving the substrate binding efficiency of cpSRP43 (Gao et al., 2015; Liang et al., 2016). The assembly of cpSRP54 to the cpSRP43/LHCP complex leads to a much smaller LHCP/cpSRP transit complex (∼170 kDa) than the cpSRP43/LHCP complex (∼450 kDa), most likely to enable efficient LHCP insertion (Dünschede et al., 2015).

Upon formation of the cpSRP/LHCP transit complex, it is guided to the thylakoid membrane and docks to the membrane-bound cpSRP receptor cpFtsY, and then transfers LHCP to the integrase Alb3 for insertion into the thylakoid membrane. cpFtsY and cpSRP54 form a complex by association of their homologous NG domains (the N-terminal four-helix bundle and the GTPase domain), and stabilization of the cpSRP54/cpFtsY complex is dramatically activated by anionic phospholipids and the Alb3 translocase (Chandrasekar and Shan, 2017). Moreover, a new interaction site between a positively charged cluster within the cpFtsY G-domain (the GTPase domain) and a negatively charged

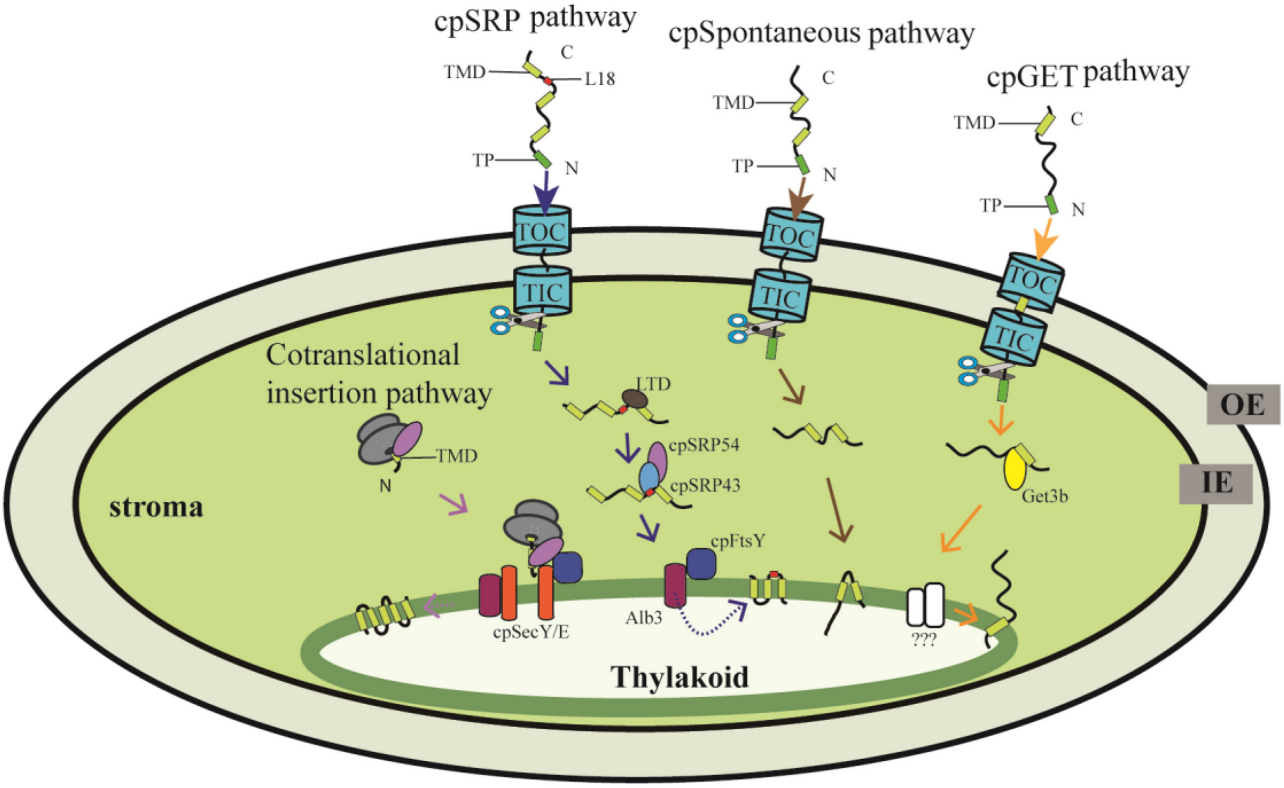

FIGURE 1 | Proteins targeting into thylakoid membranes through distinct pathways. The nuclear-encoded preprotein with an N-terminal transit peptide (TP) is translocated into the chloroplast stroma through the Toc/Tic system, and then the TP is cleaved by stromal processing peptidase. The thylakoid membrane proteins are further targeted mainly through the cpSRP pathway, cpGET pathway and the spontaneous pathway. In the cpSRP-dependent pathway, LHCP is transferred from the Toc/Tic system to the SRP43/SRP54 complex with the help of LTD., cpSRP43 interacts with the L18 region between the second and third TMD of LHCP. Then the cpSRP/LHCP complex interacts with cpFtsY and finally LHCP is insert into the thylakoid membrane by the integrase Alb3. In the cpGET pathway, imported TA proteins are transferred to the targeting factor Get3b, followed by transferr to the unknown integrases. Some proteins are translocated into thylakoid membranes spontaneously. On the other hand, the chloroplast-encoded proteins are synthesized in the stroma, and cotranslationally integrated into the thylakoid membrane with the requirement of cpSec and cpSRP components. OE, outer chloroplast envelope; IE, inner chloroplast envelope. TP, transit peptide. TMD, transmembrane domain.

cluster in the cpSRP54 M-domain has been identified, in which the M domain of cpSRP54 plays a similar role as the classical SRP RNA to enhance the cpSRP54/cpFtsY complex assembly (Chandrasekar et al., 2017; **Figure 2**).

The recruitment of the transit complex to the Alb3 translocase for LHCP insertion is mediated through the cpSRP43/Alb3 interaction. The linear motif in the Alb3 C-terminal tail (A3CT) interacts with the C-terminal chromodomains CD2 and CD3 of cpSRP43, which enables the efficient delivery of LHCP to the Alb3 integrase (Falk et al., 2010; Horn et al., 2015; **Figure 2**). A novel model has been proposed in which the conformational dynamics of cpSRP43 enables LHCP capture and release. Distinct conformations of cpSRP43 allow it to be activated by cpSRP54 assembly in the stroma to capture LHCP and inactivated by association with Alb3 translocase in the thylakoid membrane to release LHCP (Liang et al., 2016). Interestingly, cpSRP43 also directly interacts with the N-terminal of glutamyl-tRNA reductase (GluTR), a rate-limiting enzyme in tetrapyrrole biosynthesis (TBS), chaperones and stabilizes GluTR, and consequently optimizes chlorophyll biosynthesis. This interaction between cpSRP43 and GluTR reveals a posttranslational coordination for LHCP insertion with chlorophyll biosynthesis (Wang et al., 2018). More strikingly, high temperature drives the dissociation of the cpSRP43/54 complex, thus freeing cpSRP43 to interact with GluTR, CHLH (Mg-chelatase H subunit) and GUN4 (Genomes uncoupled 4) to protect them from heat-induced aggregation (Ji et al., 2021). Taken together, cpSRP43 not only functions as the hub for LHCP membrane insertion since it recruits cpSRP54, chaperones LHCP, and provides the docking site for Alb3 translocase, but also chaperones proteins for chlorophyll biosynthesis and thus coordinates the assembly of chlorophyll and LHCP into the light-harvesting complex.

Several new components of the cpSRP pathway have also been identified. An *Arabidopsis* ankyrin protein, LTD., which is located in the stroma and interacts with the Tic complex, LHCP and cpSRP43, was demonstrated to handover LHCP from the Tic translocon to the cpSRP43/cpSRP54 complex (Ouyang et al., 2011). In addition, *STIC1* (suppressor of *tic40*) and *STIC2* were revealed to act in the cpSRP54/cpFtsY-involved transport pathway. The *STIC1* gene encodes the Alb3 paralog protein, Alb4, while *STIC2* encodes a novel stromal protein that associates

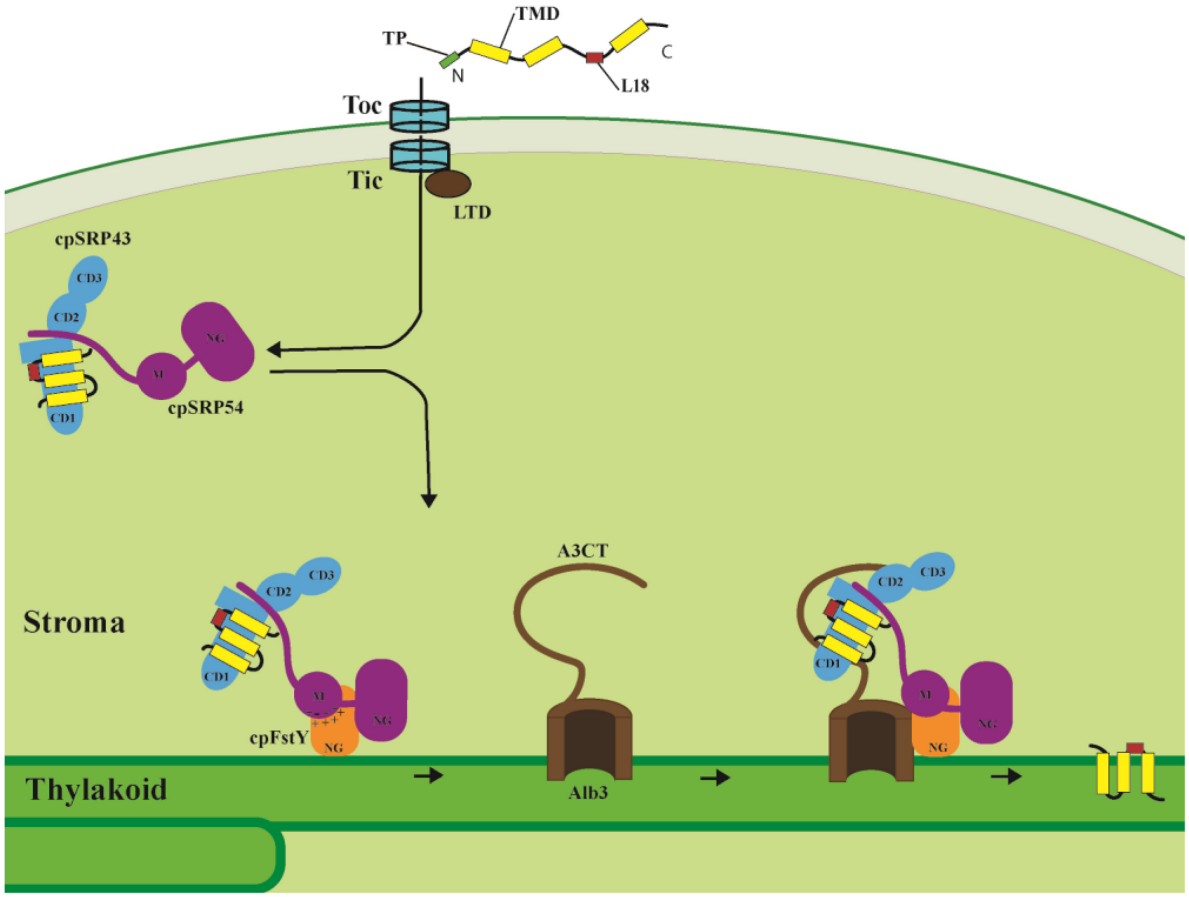

FIGURE 2 | LHCPs targeting into thylakoid membranes through the cpSRP pathway. After import into the stroma through the Toc/Tic system, the LHCPs are transferred to the cpSRP43/cpSRP54 complex with the help of LTD. The L18 region between the second and third TMD of LHCP is the binding site for cpSRP43. Then cpSRP54 interacts with cpFtsY through their homologous NG domains, while the negatively charged cluster of cpSRP54 M domain interacts with the positively charged cluster of cpFtsY G domain and enhances the cpSRP54/cpFtsY complex assembly. Finally, Alb3 C-terminal tail (A3CT) interacts with the C-terminal chromodomains CD2 and CD3 of cpSRP43, and thus facilitates LHCP delivery to the Alb3 translocase and insertion into the thylakoid membrane. TP, transit peptide. TMD, transmembrane domain.

with Alb3 and Alb4. Loss of STIC1/Alb4 and STIC2 proteins may mitigate the defect of protein import caused by the *TIC40* mutation, thus revealing a potential link between the envelope and thylakoid protein transport systems (Bédard et al., 2017).

Direct Insertion Into the Thylakoid Membrane Through the Spontaneous Pathway

Many proteins such as the photosystem subunit PsaG, PsaK, PsbW, PsbX, and PsbY, the ATPase subunit CFo-II, and the cpTat translocase subunits Tha4 and Hcf106, are integrated into the thylakoid membrane *via* the spontaneous insertion pathway which does not need any energy or proteinaceous components. This direct insertion pathway was first proposed for CFo-II, a nuclear-encoded single-membrane-spanning component of the ATP synthase. Treatments that disrupt the cpSRP, cpSec and cpTat dependent pathways do not affect the integration of CFo-II, suggesting a direct interaction of CFo-II with the lipid components of the membrane (Michl et al., 1994; Robinson et al., 1996). CFo-II, PsbW, and PsbX all span the thylakoid membrane with a single hydrophobic domain, whereas PsaG and PsaK insert into the membrane with two transmembrane spans (Lorkovic et al., 1995; Kim et al., 1998; Thompson et al., 1998; Mant et al., 2001; Zygadlo et al., 2006; Aldridge et al., 2009). For PsbY, the two transmembrane spans partition into the lipid bilayer of the thylakoid membrane and provide the driving force required for the translocation of the intervening charged region through hydrophobic interactions (Thompson et al., 1999).

The mechanism of insertion of the M13 procoat protein into the cytoplasmic membrane of *E. coli* was also originally proposed to be by the spontaneous pathway. However, it was subsequently found that YidC, the homolog of the chloroplast Alb3 insertase, is actually required for the insertion of the M13 procoat protein, which raised the question if there exists a truly spontaneous insertion pathway (Kuhn et al., 1986; Samuelson et al., 2000). PsbW and PsbX have remarkable structural similarities with the M13 procoat protein. However,

inactivation of Alb3 did not affect PsbW and PsbX insertion into the thylakoid membrane, suggesting a direct insertion pathway for these proteins (Woolhead et al., 2001).

Insertion of Tail-Anchored Proteins Into the Thylakoid Membrane Through the Chloroplast Guided Entry of TA Proteins Pathway

In a typical eukaryote cell, 3%∼5% of the membrane proteins are tail-anchored (TA) proteins with the feature of a cytosolic-facing N-terminal domain and a single C-terminal TMD followed by a tail within 30 amino acids. In these proteins TMD acts both as a membrane anchor and a targeting signal (Shigemitsu et al., 2016; Mateja and Keenan, 2018). TA proteins are found in all cellular membranes and play key roles in protein translocation, membrane fusion, vesicular trafficking, apoptosis, organelle biogenesis, and other essential cellular processes (Denic et al., 2013).

The posttranslational insertion of TA proteins from the cytosol to cellular membranes depends on the GET pathway in yeast and the TRC (Transmembrane Recognition Complex) pathway in mammals (Farkas et al., 2019; Farkas and Bohnsack, 2021). The yeast cytosolic GET machinery includes a pretargeting complex consisting of Sgt2, a small glutamine-rich tetratricopeptide repeat (TPR)-containing protein (SGTA in mammals), Get4 (TRC35 in mammals), and Get5 (UBL4 in mammals), of which Sgt2 captures newly synthesized TA proteins from the ribosomal exit tunnel and is considered the most upstream factor in the GET pathway (Wang et al., 2010; Shao et al., 2017; Zhang et al., 2021). Subsequently Get4 and Get5 build up a "scaffolding complex" by recruiting Get3 and the Sgt2-TA complex, respectively. This scaffolding complex prevents aggregation and promotes loading of TA proteins onto Get3 (Bat3 in mammals), the central targeting factor that forms a closed structure after binding ATP. The resulting hydrophobic groove recognizes the TMD of TA proteins. At the endoplasmic reticulum (ER) membrane, Get2 (CAML in mammals) aids Get1 (WRB in mammals) to form a tight complex with nucleotide-free Get3, resulting in the release of the TA protein for insertion into the membranes. Finally, Get3 is recycled to the cytosol to initiate a new round of targeting (Schuldiner et al., 2008; Gristick et al., 2014; Rome et al., 2014; Wang et al., 2014; Rao et al., 2016; **Figure 3A**). A recent study showed that the cytoplasmic helix α3′ of Get2/CAML forms a "gating" interaction with Get3/TRC40, which is important for guiding TA proteins insertion into membranes (McDowell et al., 2020).

While the GET pathway was originally identified in mammals and yeasts, it was recently found to be partially conserved in higher plants as well. Orthologs of Get1, Get3, Get4, Get5, and Sgt2, but not Get2 have been identified in plant genomes through bioinformatic approaches *Get1*, *Get3*, *Get4*, *Get5*, and *Sgt2*, *Get2* (Paul et al., 2013; Srivastava et al., 2017). Further phylogenetic analysis of 18 species revealed two Get3 clades termed Get3a and Get3bc, of which *At*Get3a, *At*Get3b, and *At*Get3c are localized in the cytosol, chloroplast and mitochondria, respectively. Loss of *AtGet1* or *AtGet3a* results in a significant reduction of the root hair-specific protein SYP123, and thus leads to root hair growth defects in these *Atget* mutant lines (Xing et al., 2017). Most surprisingly, overexpression of *AtGet3a* in the *Atget1* mutant causes a more severe phenotype in root, silique and seed development compared with the parental lines. The absence of GET pathway components may trigger alternative insertion pathways. However, overexpression of *AtGet3a* in the receptor mutant *Atget1* might cause cytosolic *At*Get3a/TA protein aggregates and a consequent TA protein insertion block through the alternative insertion pathway (Xing et al., 2017).

Recently, *Arabidopsis* Get2 was also discovered by an immunoprecipitation-mass spectrometry (IP-MS) method. Using the *AtGet1-GFP* transgenic plants, G1IP (*At*Get1-interacting protein) was identified. G1IP exhibits low sequence similarity but high structural similarity to Get2/CAML (Asseck et al., 2021). Both G1IP and *At*Get1 show a subcellular ER localization and share the same expression profile. The *g1ip* mutant shows reduced root hair elongation, which is similar to other *Atget* lines. Moreover, G1IP interacts with *At*Get1 and *At*Get3a, and expression of G1IP and *At*Get1 together can complement the yeast GET receptor mutant Δ*get1get2* strain. Besides, the G1IP N terminus contains a conserved cluster of positively charged amino acids which is essential for the binding of Get3/TRC40, and alteration of this motif in G1IP is sufficient to inhibit TA protein transport. These results strongly suggest that *Arabidopsis* G1IP encodes the functional ortholog of Get2, although only a small part of its sequence is conserved between yeasts, plants and mammals (Asseck et al., 2021).

Based on the facts that only Get3b and Get3c, but no other Get system components are found in organelles, and that Get3bc cannot rescue the growth defect of the *Atget3a* mutant, it was previously considered to be unlikely that the organellar Get3 homologs were involved in TA protein insertion (Xing et al., 2017). However, Anderson et al. recently demonstrated that *At*Get3b is structurally similar to the cytosolic Get3 protein and serves as a targeting factor to deliver TA proteins from the chloroplast stroma to the thylakoid membrane (Anderson et al., 2021; **Figure 3B**). Chloroplast membranes contain several TA proteins, such as cpSecE1, a component of the thylakoid Sec1 translocase and cpSecE2, a component of the chloroplast inner envelope Sec2 translocase (Schüenemann et al., 1999; Li et al., 2015). Both *in vitro* and *in vivo* assays indicated that *At*Get3b interacts with cpSecE1 rather than cpSecE2 to form a homodimer or oligomer in the chloroplast stroma, mediated by the C-X-X-C zinc coordination motif of *At*Get3b (Anderson et al., 2021). A domain-swapping strategy used between cpSecE1 and cpSecE2 suggests that the TMDs and C-terminal tails of TA proteins are key factors that specify the interaction between *At*Get3b and its client TA proteins (Anderson et al., 2019). The physicochemical features of the TMD and C-terminal regions of cpSecE2 make it incompatible with the hydrophobic groove formed by *At*Get3b oligomerization (Anderson et al., 2021).

Loss of *get3b* in *Arabidopsis* displays a visually indistinguishable phenotype from the wild type. Similar observations have been made with the yeast *get3* mutant, suggesting that the Get system may operate in parallel or at least be partially redundant with other insertion pathways

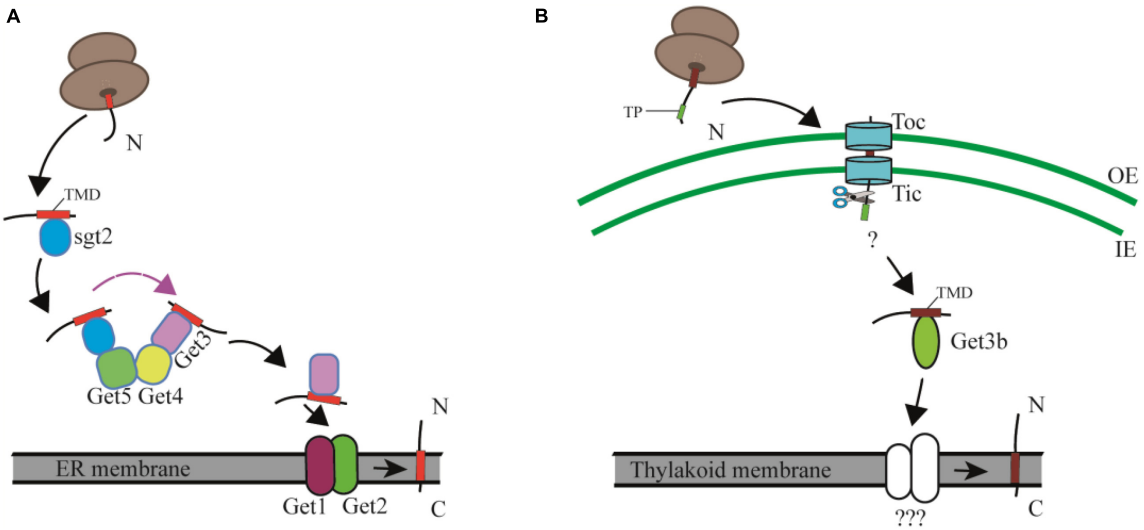

FIGURE 3 | Comparison of the cytosolic and chloroplast GET pathway. **(A)** In the cytosolic GET pathway, the newly synthesized TA proteins are firstly captured by Sgt2, and then transferred to the targeting factor Get3 by the Get4/Get5 scaffold complex, and finally integrated into ER membranes with the facilitation of Get1 and Get2. TMD, transmembrane domain. **(B)** In the cpGET pathway, imported TA proteins are transferred to the targeting factor Get3b, and then integrated into the thylakoid membrane with the aid of unknown integrases. OE, outer chloroplast envelope; IE, inner chloroplast envelope. TP, transit peptide. TMD, transmembrane domain.

(Anderson et al., 2021). Consistent with this notion, the *get3bsrp54* double mutant and the *get3bsrp43srp54* triple mutant show much more severe defects in growth, including pronounced dwarfism, obvious chlorosis and dramatically reduced PSI and PSII activities. These results demonstrate synergistic interactions between cpGET and the cpSRP pathways in delivering proteins into thylakoid membranes (Anderson et al., 2021).

COTRANSLATIONAL INSERTION OF THE CHLOROPLAST-ENCODED PROTEINS INTO THE THYLAKOID MEMBRANE

Chloroplast genes encode ∼37 thylakoid membrane proteins such as the PSII reaction center protein D1 and D2, and the PSI subunits PsaA and PsaB, which are synthesized in the stroma and integrated into thylakoid membranes through a cotranslational process (Zoschke and Barkan, 2015). However, little is known about the mechanisms that target these proteins into the thylakoid membrane. The *cpSRP54* (*ffc*) mutant contains much lower levels of D1, D2, PsaA, and PsaB proteins, suggesting the involvement of *cpSRP54* in the cotranslational pathway (Amin et al., 1999). Cross-linking experiments revealed an interaction between the D1-ribosome nascent chain complex and cpSRP54, but not cpSRP43 (Nilsson et al., 1999). cpSRP54 is present in two stroma pools. In one of them it is recruited by cpSRP43 to function in the posttranslational targeting for LHCPs, and in the other pool it is associated with 70S ribosomes to function in the cotranslational import of proteins such as D1 (Franklin and Hoffman, 1993; Schüenemann et al., 1998). The interaction between cpSRP54 and D1 involves the first TMD of D1, and only occurs when the D1 nascent chain is still attached to ribosomes, suggesting that cpSRP54 functions in the early steps of D1 biogenesis (Nilsson and van Wijk, 2002).

Besides cpSRP54, the SRP receptor cpFtsY is also considered to function in the cotranslational integration process of chloroplast-encoded thylakoid membrane proteins, based on the observation of a strong reduction of D1 in the *cpftsy* mutant (Tzvetkova-Chevolleau et al., 2007; Asakura et al., 2008). Zhang et al. (2001) demonstrated a direct interaction between D1 elongation intermediates and the chloroplast Sec translocon component cpSecY, suggesting that the cpSec pathway not only functions in posttranslational targeting of nuclear-encoded proteins, but also in cotranslational insertion of chloroplast-encoded proteins. The Alb3 integrase of the cpSRP pathway is also reported to act in a later insertion process, facilitate release of D1 from the cpSecY translocase, and promote the assembly of D1 into PSII (Ossenbühl et al., 2004; Walter et al., 2015). Thus, the integration of D1 into the thylakoid membrane suggests a functional link between the cpSRP and the cpSec translocation machinery. Further evidence for this speculation comes from the integration of Cytochrome f. Cytochrome f insertion into the thylakoid membrane was initially thought to be mediated through the cpSec translocon. However, further analysis showed a severely decreased level of Cytochrome f in the *cpftsy* mutant, indicating a coordinated mechanism between the cpSRP and cpSec translocation pathways (Nohara et al., 1996; Asakura et al., 2008).

Recently, Zoschke and Barkan performed a comprehensive analysis of chloroplast ribosome profiling with separated soluble and membrane fractions in maize. They found that about half of the chloroplast-encoded thylakoid membrane proteins are targeted cotranslationally while the other half is targeted

posttranslationally. Synthesis of these cotranslationally integrated proteins are initiated on stromal ribosomes, and then transferred to the thylakoid-attached ribosomes in a nuclease-resistant fashion shortly after the emergence of the first transmembrane segment of the nascent peptide. In contrast, membrane proteins whose translation terminates before a transmembrane segment emerge from the ribosome's exit channel will be integrated into thylakoid membranes posttranslationally. These results suggest a key role of the first transmembrane segment in linking ribosomes to the thylakoid membrane for cotranslational targeting (Zoschke and Barkan, 2015).

CONCLUSION AND FUTURE PERSPECTIVES

In the past decades, much progress has been made in understanding the molecular details of targeting both nuclear- and chloroplast-encoded proteins into the thylakoid membranes. However, several central issues still need to be further investigated in the future. One avenue of study will be to explore novel components of these translocation pathways. During evolution, ancient translocation systems acquired and developed new proteins and mechanisms to facilitate the correct targeting of chloroplast preproteins. Thus, identification of these novel components may provide new insights into how plant cells have adapted prokaryotic mechanisms to the eukaryotic environment. Another area yet to be examined is the overall structure of these distinct translocases, a challenging task given their highly dynamic and transient nature. Furthermore, the recent discovered cpGET pathway has broadened our understanding of protein targeting into thylakoid membranes. However, only Get3b in this system has been identified, thus the search for the remaining components of the cpGET pathway constitutes an important task for the future.

AUTHOR CONTRIBUTIONS

DZ and XX designed and wrote the manuscript. DZ, JW, CZ, and DL collected and analyzed the data. LZ and XX revised the manuscript. HX produced the figures. All authors contributed to the article and approved the submitted version.

FUNDING

This study was supported by the National Natural Science Foundation of China (32170258), CAS Interdisciplinary Innovation Team (JCTD-2020-06), the 111 Project of China (D16014), and Program for Innovative Research Team (in Science and Technology) in University of Henan Province (22IRTSTHN024).

ACKNOWLEDGMENTS

We thank Jean-David Rochaix (University of Geneva) and Leonard Krall (Yunnan University) for critical reading of this manuscript.

REFERENCES

Aldridge, C., Cain, P., and Robinson, C. (2009). Protein transport in organelles: protein transport into and across the thylakoid membrane. *FEBS J.* 276, 1177–1186.

Amin, P., Sy, D. A., Pilgrim, M. L., Parry, D. H., Nussaume, L., and Hoffman, N. E. (1999). *Arabidopsis* mutants lacking the 43- and 54-kilodalton subunits of the chloroplast signal recognition particle have distinct phenotypes. *Plant Physiol.* 121, 61–70. doi: 10.1104/pp.121.1.61

Anderson, S. A., Satyanarayan, M. B., Wessendorf, R. L., Lu, Y., and Fernandez, D. E. (2021). A homolog of GuidedEntry of Tail-anchored proteins3 functions in membrane-specific protein targeting in chloroplasts of *Arabidopsis*. *Plant Cell* 33, 2812–2833. doi: 10.1093/plcell/koab145

Anderson, S. A., Singhal, R., and Fernandez, D. E. (2019). Membrane specific targeting of tail-anchored proteins SECE1 and SECE2 within chloroplasts. *Front. Plant Sci.* 10:1401. doi: 10.3389/fpls.2019.01401

Asakura, Y., Kikuchi, S., and Nakai, M. (2008). Non-identical contributions of two membrane-bound cpSRP components, cpFtsY and Alb3, to thylakoid biogenesis. *Plant J.* 56, 1007–1017. doi: 10.1111/j.1365-313X.2008.03659.x

Asseck, L. Y., Mehlhorn, D. G., Monroy, J. R., Ricardi, M. M., Breuninger, H., Wallmeroth, N., et al. (2021). Endoplasmic reticulum membrane receptors of the GET pathway are conserved throughout eukaryotes. *Proc. Natl. Acad. Sci. U.S.A.* 118:e2017636118. doi: 10.1073/pnas.2017636118

Bédard, J., Trösch, R., Wu, F., Ling, Q., Flores-Pérez, Ú, and Töpel, M. (2017). Suppressors of the chloroplast protein import mutant tic40 reveal a genetic link between protein import and thylakoid biogenesis. *Plant Cell* 29, 1726–1747. doi: 10.1105/tpc.16.00962

Chandrasekar, S., and Shan, S. O. (2017). Anionic phospholipids and the albino3 translocase activate signal recognition particle-receptor interaction during light-harvesting chlorophyll a/b-binding protein targeting. *J. Biol. Chem.* 292, 397–406. doi: 10.1074/jbc.M116.752956

Chandrasekar, S., Sweredoski, M. J., Sohn, C. H., Hess, S., and Shan, S. (2017). Co-evolution of two GTPases enables efficient protein targeting in an RNA-less chloroplast signal recognition particle pathway. *J. Biol. Chem.* 292, 386–396. doi: 10.1074/jbc.M116.752931

Costa, E. A., Subramanian, K., Nunnari, J., and Weissman, J. S. (2018). Defining the physiological role of SRP in protein-targeting efficiency and specificity. *Science* 359, 689–692. doi: 10.1126/science.aar3607

DeLille, J., Peterson, E. C., Johnson, T., Moore, M., Kight, A., and Henry, R. (2000). A novel precursor recognition element facilitates posttranslational binding to the signal recognition particle in chloroplasts. *Proc. Natl. Acad. Sci. U.S.A.* 97, 1926–1931. doi: 10.1073/pnas.030395197

Denic, V., Dötsch, V., and Sinning, I. (2013). Endoplasmic reticulum targeting and insertion of tail-anchored membrane proteins by the GET pathway. *Cold Spring Harb. Perspect. Biol.* 5:a013334. doi: 10.1101/cshperspect.a013334

Dünschede, B., Träger, C., Schröder, C. V., Ziehe, D., Walter, B., Funke, S., et al. (2015). Chloroplast SRP54 was recruited for posttranslational protein transport via complex formation with chloroplast SRP43 during land plant evolution. *J. Biol. Chem.* 290, 13104–13114. doi: 10.1074/jbc.M114.597922

Falk, S., Ravaud, S., Koch, J., and Sinning, I. (2010). The C terminus of the Alb3 membrane insertase recruits cpSRP43 to the thylakoid membrane. *J. Biol. Chem.* 285, 5954–5962. doi: 10.1074/jbc.M109.084996

Farkas, Á, and Bohnsack, K. E. (2021). Capture and delivery of tail-anchored proteins to the endoplasmic reticulum. *J. Cell Biol.* 220:e202105004. doi: 10.1083/jcb.202105004

Farkas, Á, De Laurentiis, E. I., and Schwappach, B. (2019). The natural history of Get3-like chaperones. *Traffic* 20, 311–324. doi: 10.1111/tra.12643

Franklin, A. E., and Hoffman, N. E. (1993). Characterization of a chloroplast homologue of the 54-kDa subunit of the signal recognition particle. *J. Biol. Chem.* 268, 22175–22180. doi: 10.1016/s0021-9258(20)80664-4

Gao, F., Kight, A. D., Henderson, R., Jayanthi, S., Patel, P., Murchison, M., et al. (2015). Regulation of structural dynamics within a signal recognition particle promotes binding of protein targeting substrates. *J. Biol. Chem.* 290, 15462–15474. doi: 10.1074/jbc.M114.624346

Gristick, H. B., Rao, M., Chartron, J. W., Rome, M. E., Shan, S. O., and Clemons, W. M. (2014). Crystal structure of ATP-bound Get3-Get4-Get5 complex reveals regulation of Get3 by Get4. *Nat. Struct. Mol. Biol.* 21, 437–442. doi: 10.1038/nsmb.2813

Horn, A., Hennig, J., Ahmed, Y. L., Stier, G., Wild, K., and Sattler, M. (2015). Structural basis for cpSRP43 chromodomain selectivity and dynamics in Alb3 insertase interaction. *Nat. Commun.* 6:8875. doi: 10.1038/ncomms9875

Ji, S., Siegel, A., Shan, S. O., Grimm, B., and Wang, P. (2021). Chloroplast SRP43 autonomously protects chlorophyll biosynthesis proteins against heat shock. *Nat. Plants* 7, 1420–1432. doi: 10.1038/s41477-021-00994-y

Kim, S. J., Robinson, C., and Mant, A. (1998). Sec/SRP-independent insertion of two thylakoid membrane proteins bearing cleavable signal peptides. *FEBS Lett.* 424, 105–108. doi: 10.1016/s0014-5793(98)00148-3

Kirchhoff, H. (2019). Chloroplast ultrastructure in plants. *New Phytol.* 223, 565–574. doi: 10.1111/nph.15730

Kuhn, A., Wickner, W., and Kreil, G. (1986). The cytoplasmic carboxy terminus of M13 procoat is required for the membrane insertion of its central domain. *Nature* 322, 335–339. doi: 10.1038/322335a0

Lee, D. W., Lee, J., and Hwang, I. (2017). Sorting of nuclear-encoded chloroplast membrane proteins. *Curr. Opin. Plant Biol.* 40, 1–7. doi: 10.1016/j.pbi.2017.06.011

Leister, D. (2003). Chloroplast research in the genomic age. *Trends Genet.* 19, 47–56. doi: 10.1016/s0168-9525(02)00003-3

Li, Y., Singhal, R., Taylor, I. W., McMinn, P. H., Chua, X. Y., Cline, K., et al. (2015). The Sec2 translocase of the chloroplast inner envelope contains a unique and dedicated SECE2 component. *Plant J.* 84, 647–685. doi: 10.1111/tpj.13028

Liang, F. C., Kroon, G., McAvoy, C. Z., Chi, C., Wright, P. E., and Shan, S. (2016). Conformational dynamics of a membrane protein chaperone enables spatially regulated substrate capture and release. *Proc. Natl. Acad. Sci. U.S.A.* 22, 1615–1624. doi: 10.1073/pnas.1524777113

Lorkovic, Y. J., Schroder, W. P., Pakrasi, H. B., Irrgang, K. D., Herrmann, R. G., and Oelmuller, R. (1995). Molecular characterization of PsbW, a nuclear-encoded component of the photosystem II reaction center complex in spinach. *Proc. Natl. Acad. Sci. U.S.A.* 92, 8930–8934. doi: 10.1073/pnas.92.19.8930

Mant, A., Woolhead, C. A., Moore, M., Henry, R., and Robinson, C. (2001). Insertion of PsaK into the thylakoid membrane in a "Horseshoe" conformation occurs in the absence of signal recognition particle, nucleoside triphosphates, or functional albino3. *J. Biol. Chem.* 276, 36200–36206. doi: 10.1074/jbc.M102914200

Martin, W., Rujan, T., Richly, E., Hansen, A., Cornelsen, S., Lins, T., et al. (2002). Evolutionary analysis of *Arabidopsis*, *cyanobacterial*, and chloroplast genomes reveals plastid phylogeny and thousands of *cyanobacterial* genes in the nucleus. *Proc. Natl. Acad. Sci. U.S.A.* 99, 12246–12251. doi: 10.1073/pnas.182432999

Mateja, A., and Keenan, R. J. (2018). A structural perspective on tail-anchored protein biogenesis by the GET pathway. *Curr. Opin. Struct. Biol.* 51, 195–202. doi: 10.1016/j.sbi.2018.07.009

McAvoy, C. Z., Siegel, A., Piszkiewicz, S., Miaou, E., Yu, M. S., Nguyen, T., et al. (2018). Two distinct sites of client protein interaction with the chaperone cpSRP43. *J. Biol. Chem.* 293, 8861–8873. doi: 10.1074/jbc.RA118.002215

McDowell, M. A., Heimes, M., Fiorentino, F., Mehmood, S., Farkas, Á, Coy-Vergara, J., et al. (2020). Structural basis of tail-anchored membrane protein biogenesis by the GET Insertase complex. *Mol. Cell* 80, 72–86. doi: 10.1016/j.molcel.2020.08.012

Michl, D., Robinson, C., Shackleton, J. B., Herrmann, R. G., and Klösgen, R. B. (1994). Targeting of proteins to the thylakoids by bipartite presequences: CFoII is imported by a novel, third pathway. *EMBO J.* 13, 1310–1317.

Moore, M., Goforth, R. L., Mori, H., and Henry, R. (2003). Functional interaction of chloroplast SRP/FtsY with the ALB3 translocase in thylakoids: substrate not required. *J. Cell Biol.* 162, 1245–1254. doi: 10.1083/jcb.200307067

Nakai, M. (2018). New perspectives on chloroplast protein import. *Plant Cell Physiol.* 59, 1111–1119. doi: 10.1093/pcp/pcy083

Neuhaus, H. E., and Emes, M. J. (2000). Nonphotosynthetic metabolism in plastids. *Annu. Rev. Plant Physiol. Plant Mol. Biol.* 51, 111–140. doi: 10.1146/annurev.arplant.51.1.111

Nilsson, R., and van Wijk, K. J. (2002). Transient interaction of cpSRP54 with elongating nascent chains of the chloroplast-encoded D1 protein; 'cpSRP54 caught in the act'. *FEBS Lett.* 524, 127–133. doi: 10.1016/s0014-5793(02)03016-8

Nilsson, R., Brunner, J., Hoffman, N. E., and van Wijk, K. J. (1999). Interactions of ribosome nascent chain complexes of the chloroplast-encoded D1 thylakoid membrane protein with cpSRP54. *EMBO J.* 18, 733–742. doi: 10.1093/emboj/18.3.733

Nohara, T., Asai, T., Nakai, M., Sugiura, M., and Endo, T. (1996). Cytochrome f encoded by the chloroplast genome is imported into thylakoids via the SecA-dependent pathway. *Biochem. Biophys. Res. Commun.* 224, 2474–2478. doi: 10.1006/bbrc.1996.1051

Ossenbühl, F., Göhre, V., Meurer, J., Krieger-Liszkay, A., Rochaix, J. D., and Eichacker, L. A. (2004). Efficient assembly of photosystem II in Chlamydomonas reinhardtii requires Alb3.1p, a homolog of *Arabidopsis* ALBINO3. *Plant Cell* 16, 1790–1800. doi: 10.1105/tpc.023226

Ouyang, M., Li, X., Ma, J., Chi, W., Xiao, J., Zou, M., et al. (2011). LTD is a protein required for sorting light-harvesting chlorophyll-binding proteins to the chloroplast SRP pathway. *Nat. Commun.* 2:277. doi: 10.1038/ncomms1278

Ouyang, M., Li, X., Zhang, J., Feng, P., Pu, H., Kong, L., et al. (2020). Liquid-liquid phase transition drives intra-chloroplast cargo sorting. *Cell* 180, 1144–1159. doi: 10.1016/j.cell.2020.02.045

Paul, P., Simm, S., Blaumeiser, A., Scharf, K. D., Fragkostefanakis, S., Mirus, O., et al. (2013). The protein translocation systems in plants-composition and variability on the example of *Solanum lycopersicum*. *BMC Genom.* 14:189. doi: 10.1186/1471-2164-14-189

Rao, M., Okreglak, V., Chio, U. S., Cho, H., Walter, P., and Shan, S. O. (2016). Multiple selection filters ensure accurate tail-anchored membrane protein targeting. *Elife.* 5:e21301. doi: 10.7554/eLife.21301

Richardson, L. G. L., and Schnell, D. J. (2020). Origins, function, and regulation of the TOC-TIC general protein import machinery of plastids. *J. Exp. Bot.* 71, 1226–1238. doi: 10.1093/jxb/erz517

Robinson, D., Karnauchov, I., Herrmann, R. G., Klosgen, R. B., and Robinson, C. (1996). Protease-sensitive thylakoidal import machinery for the Sec-, ΔpH- and signal recognition particle-dependent protein targeting pathways, but not for CFoII integration. *Plant J.* 10, 149–155. doi: 10.1046/j.1365-313x.1996.10010149.x

Rome, M. E., Chio, U. S., Rao, M., Gristick, H., and Shan, S. O. (2014). Differential gradients of interaction affinities drive efficient targeting and recycling in the GET pathway. *Proc. Natl. Acad. Sci. U.S.A.* 111, E4929–E4935. doi: 10.1073/pnas.1411284111

Samuelson, J. C., Chen, M., Jiang, F., Moller, I., Wiedmann, M., Kuhn, A., et al. (2000). YidC mediates membrane protein insertion in bacteria. *Nature* 406, 575–577. doi: 10.1038/35020586

Schüenemann, D., Amin, P., Hartmann, E., and Hoffman, N. E. (1999). Chloroplast SecY is complexed to SecE and involved in the translocation of the 33-kDa but not the 23-kDa subunit of the oxygen-evolving complex. *J. Biol. Chem.* 274, 12177–12182. doi: 10.1074/jbc.274.17.12177

Schüenemann, D., Gupta, S., Persello-Cartieaux, F., Klimyuk, V. I., Jones, J. D. G., Nussaume, L., et al. (1998). A novel signal recognition particle targets light-harvesting proteins to the thylakoid membranes. *Proc. Natl. Acad. Sci. U.S.A.* 95, 10312–10316. doi: 10.1073/pnas.95.17.10312

Schuldiner, M., Metz, J., Schmid, V., Denic, V., Rakwalska, M., Schmitt, H. D., et al. (2008). The GET complex mediates insertion of tail-anchored proteins into the ER membrane. *Cell* 134, 634–645. doi: 10.1016/j.cell.2008.06.025

Schünemann, D. (2007). Mechanisms of protein import into thylakoids of chloroplasts. *Biol. Chem.* 388, 907–915. doi: 10.1515/BC.2007.111

Shao, S., Rodrigo-Brenni, M. C., Kivlen, M. H., and Hegde, R. S. (2017). Mechanistic basis for a molecular triage reaction. *Science* 355, 298–302. doi: 10.1126/science.aah6130

Shigemitsu, S., Cao, W., Terada, T., Shimizu, K., Kutay, U., Hartmann, E., et al. (2016). Development of a prediction system for tail-anchored proteins. *BMC Bioinform.* 17:378. doi: 10.1186/s12859-016-1202-7

Sjuts, I., Soll, J., and Bölter, B. (2017). Import of soluble proteins into chloroplasts and potential regulatory mechanisms. *Front. Plant Sci.* 8:168. doi: 10.3389/fpls.2017.00168

Srivastava, R., Zalisko, B. E., Keenan, R. J., and Howell, S. H. (2017). The GET system inserts the tailanchored protein. SYP72, into endoplasmic reticulum membranes. *Plant Physiol.* 173, 1137–1145. doi: 10.1104/pp.16.00928

Staehelin, L. A. (2003). Chloroplast structure: from chlorophyll granules to supramolecular architecture of thylakoid membranes. *Photosynth. Res.* 76, 185–196. doi: 10.1023/A:1024994525586

Stengel, K. F., Holdermann, I., Cain, P., Robinson, C., Wild, K., and Sinning, I. (2008). Structural basis for specific substrate recognition by the chloroplast signal recognition particle protein cpSRP43. *Science* 321, 253–256. doi: 10.1126/science.1158640

Thompson, S. J., Kim, S. J., and Robinson, C. (1998). Sec-independent insertion of thylakoid membrane proteins. Analysis of insertion forces and identification of a loop intermediate involving the signal peptide. *J. Biol. Chem.* 273, 18979–18983. doi: 10.1074/jbc.273.30.18979

Thompson, S. J., Robinson, C., and Mant, A. (1999). Dual signal peptides mediate the signal recognition particle/Sec-independent insertion of a thylakoid membrane polyprotein, PsbY. *J. Biol. Chem.* 274, 4059–4066. doi: 10.1074/jbc.274.7.4059

Tu, C. J., Peterson, E. C., Henry, R., and Hoffman, N. E. (2000). The L18 domain of light-harvesting chlorophyll proteins binds to chloroplast signal recognition particle 43. *J. Biol. Chem.* 275, 13187–13190. doi: 10.1074/jbc.c000108200

Tzvetkova-Chevolleau, T., Hutin, C., Noel, L. D., Goforth, R., Carde, J. P., and Caffarri, S. (2007). Canonical signal recognition particle components can be bypassed for posttranslational protein targeting in chloroplasts. *Plant Cell* 19, 1635–1648. doi: 10.1105/tpc.106.048959

Walter, B., Hristou, A., Nowaczyk, M. M., and Schünemann, D. (2015). In vitro reconstitution of co-translational D1 insertion reveals a role of the cpSec-Alb3 translocase and Vipp1 in photosystem II biogenesis. *Biochem. J.* 468, 315–324. doi: 10.1042/BJ20141425

Wang, F., Brown, E. C., Mak, G., Zhuang, J., and Denic, V. (2010). A chaperone cascade sorts proteins for posttranslational membrane insertion into the endoplasmic reticulum. *Mol. Cell* 40, 159–171. doi: 10.1016/j.molcel.2010.08.038

Wang, F., Chan, C., Weir, N. R., and Denic, V. (2014). The Get1/2 transmembrane complex is an endoplasmic-reticulum membrane protein insertase. *Nature* 512, 441–444. doi: 10.1038/nature13471

Wang, P., Liang, F. C., Wittmann, D., Siegel, A., Shan, S. O., and Grimm, B. (2018). Chloroplast SRP43 acts as a chaperone for glutamyl-tRNA reductase, the rate-limiting enzyme in tetrapyrrole biosynthesis. *Proc. Natl. Acad. Sci. U.S.A.* 115, E3588–E3596. doi: 10.1073/pnas.1719645115

Wicke, S., Schneeweiss, G. M., Pamphilis, C. W., Müller de, K. F., and Quandt, D. (2011). The evolution of the plastid chromosome in land plants: gene content, gene order, gene function. *Plant Mol. Biol.* 76, 273–297. doi: 10.1007/s11103-011-9762-4

Woolhead, C. A., Thompson, S. J., Moore, M., Tissier, C., Mant, A., Rodger, A., et al. (2001). Distinct Albino3-dependent and-independent pathways for thylakoid membrane protein insertion. *J. Biol. Chem.* 276, 40841–40846. doi: 10.1074/jbc.M106523200

Xing, S., Mehlhorn, D. G., Wallmeroth, N., Asseck, L. Y., Kar, R., Voss, A., et al. (2017). Loss of GET pathway orthologs in *Arabidopsis thaliana* causes root hair growth defects and affects SNARE abundance. *Proc. Natl. Acad. Sci. U.S.A.* 114, E1544–E1553. doi: 10.1073/pnas.1619525114

Xu, X., Ouyang, M., Lu, D., Zheng, C., and Zhang, L. (2021a). Protein sorting within chloroplasts. *Trends Cell Biol.* 31, 9–16. doi: 10.1016/j.tcb.2020.09.011

Xu, X., Zheng, C., Lu, D., Song, C. P., and Zhang, L. (2021b). Phase separation in plants: new insights into cellular compartmentalization. *J. Integr. Plant Biol.* 63, 1835–1855. doi: 10.1111/jipb.13152

Zhang, L., Paakkarinen, V., Suorsa, M., and Aro, E. M. (2001). A SecY homologue is involved in chloroplast-encoded D1 protein biogenesis. *J. Biol. Chem.* 276, 37809–37814. doi: 10.1074/jbc.M105522200

Zhang, Y., De Laurentiis, E., Bohnsack, K. E., Wahlig, M., Ranjan, N., Gruseck, S., et al. (2021). Ribosome-bound Get4/5 facilitates the capture of tail-anchored proteins by Sgt2 in yeast. *Nat. Commun.* 12:782. doi: 10.1038/s41467-021-20981-3

Ziehe, D., Dünschede, B., and Schünemann, D. (2017). From bacteria to chloroplasts: evolution of the chloroplast SRP system. *Biol. Chem.* 398, 653–661. doi: 10.1515/hsz-2016-0292

Ziehe, D., Dünschede, B., and Schünemann, D. (2018). Molecular mechanism of SRP-dependent light-harvesting protein transport to the thylakoid membrane in plants. *Photosynth. Res.* 138, 303–313. doi: 10.1007/s11120-018-0544-6

Zoschke, R., and Barkan, A. (2015). Genome-wide analysis of thylakoid-bound ribosomes in maize reveals principles of cotranslational targeting to the thylakoid membrane. *Proc. Natl. Acad. Sci. U.S.A.* 112, E1678–E1687. doi: 10.1073/pnas.1424655112

Zygadlo, A., Robinson, C., Scheller, H. V., Mant, A., and Jensen, P. E. (2006). The properties of the positively charged loop region in PSI-G are essential for its 'spontaneous' insertion into thylakoids and rapid assembly into the photosystem I complex. *J. Biol. Chem.* 281, 10548–10554. doi: 10.1074/jbc.M512687200

Conflict of Interest: The authors declare that the research was conducted in the absence of any commercial or financial relationships that could be construed as a potential conflict of interest.

Publisher's Note: All claims expressed in this article are solely those of the authors and do not necessarily represent those of their affiliated organizations, or those of the publisher, the editors and the reviewers. Any product that may be evaluated in this article, or claim that may be made by its manufacturer, is not guaranteed or endorsed by the publisher.

frontiers in Physiology

ORIGINAL RESEARCH
published: 10 February 2022
doi: 10.3389/fphys.2021.804646

Identity Determinants of the Translocation Signal for a Type 1 Secretion System

*Olivia Spitz[1], Isabelle N. Erenburg[1], Kerstin Kanonenberg[1†], Sandra Peherstorfer[1], Michael H. H. Lenders[1], Jens Reiners[2], Miao Ma[3], Ben F. Luisi[3], Sander H. J. Smits[1,2] and Lutz Schmitt[1]**

[1] Institute of Biochemistry, Heinrich Heine University Düsseldorf, Düsseldorf, Germany, [2] Center for Structural Studies, Heinrich Heine University Düsseldorf, Düsseldorf, Germany, [3] Department of Biochemistry, University of Cambridge, Cambridge, United Kingdom

OPEN ACCESS

Edited by:
Markus Kunze,
Medical University of Vienna, Austria

Reviewed by:
Michael Freissmuth,
Medical University of Vienna, Austria
Ian Kerr,
University of Nottingham,
United Kingdom

***Correspondence:**
Lutz Schmitt
lutz.schmitt@hhu.de

†Present address:
Kerstin Kanonenberg,
CALIXAR,
Lyon, France

Specialty section:
This article was submitted to Membrane Physiology and Membrane Biophysics, a section of the journal Frontiers in Physiology

Received: 29 October 2021
Accepted: 31 December 2021
Published: 10 February 2022

Citation:
Spitz O, Erenburg IN, Kanonenberg K, Peherstorfer S, Lenders MHH, Reiners J, Ma M, Luisi BF, Smits SHJ and Schmitt L (2022) Identity Determinants of the Translocation Signal for a Type 1 Secretion System. Front. Physiol. 12:804646. doi: 10.3389/fphys.2021.804646

The toxin hemolysin A was first identified in uropathogenic *E. coli* strains and shown to be secreted in a one-step mechanism by a dedicated secretion machinery. This machinery, which belongs to the Type I secretion system family of the Gram-negative bacteria, is composed of the outer membrane protein TolC, the membrane fusion protein HlyD and the ABC transporter HlyB. The N-terminal domain of HlyA represents the toxin which is followed by a RTX (Repeats in Toxins) domain harboring nonapeptide repeat sequences and the secretion signal at the extreme C-terminus. This secretion signal, which is necessary and sufficient for secretion, does not appear to require a defined sequence, and the nature of the encoded signal remains unknown. Here, we have combined structure prediction based on the AlphaFold algorithm together with functional and *in silico* data to examine the role of secondary structure in secretion. Based on the presented data, a C-terminal, amphipathic helix is proposed between residues 975 and 987 that plays an essential role in the early steps of the secretion process.

Keywords: bacterial secretion systems, secretion signal, ABC transporter, amphipathic helix, ATPase activity, protein secretion

INTRODUCTION

Type 1 secretion systems (T1SS) are widespread in Gram-negative bacteria and translocate a large variety of mainly proteinaceous substrates (Holland et al., 2016). The general blueprint of such a nanomachinery consists of an ABC transporter, a membrane fusion protein (MFP) and an outer membrane protein (OMP). In the presence of a substrate, the three components form a continuous channel across the inner and outer membrane, which allows the translocation of the substrate from the cytosol into the extracellular space in one step.

A well-known member of sub-family 2 of T1SS is the hemolysin A (HlyA) T1SS, which is composed of the ABC transporter HlyB, the membrane fusion protein HlyD and the outer membrane protein TolC [for recent reviews see Kanonenberg et al. (2013)], which was first identified in uropathogenic *E. coli* strains (Felmlee et al., 1985). The secretion signal of the substrate is located at the extreme C-terminus and is not cleaved prior, during or after transport (Gray et al., 1986). Additionally, these substrates are characterized by Gly- and Asp-rich nonapeptide

repeats, the so-called GG-repeats (Welch, 2001). These GG-repeats with the consensus sequence GGxGxDxUx (x: any amino acid, U: large, hydrophobic amino acid) bind Ca^{2+} ions with an affinity of approximately 150 μM (Sanchez-Magraner et al., 2007). As the concentration of free Ca^{2+} ions in the cytosol is around 300 nM (Jones et al., 1999), orders of magnitude below the K_D, substrates of sub-family 2 remain unfolded in the cytosol, as demonstrated for HlyA (Bakkes et al., 2010). In contrast, Ca^{2+} concentration in the extracellular space is around 2 mM. This results in binding of Ca^{2+} ions to the GG-repeats, which induces folding of the entire protein and formation of a β-roll structure similar to that first identified in *Pseudomonas aeruginosa* alkaline protease (Baumann et al., 1993). The GG repeats in the β-roll defines the Repeat in ToXins (RTX) domain that is found in a large family of T1SS-secreted proteins, and these are accordingly referred to as RTX proteins.

With the exception of sub-family 1 (Kanonenberg et al., 2013), all other substrates of T1SS contain a C-terminal secretion signal at the extreme C-terminus that is necessary and sufficient for secretion (Mackman et al., 1987). Mutational studies of HlyA revealed that the secretion "information" is located in the last 50 to 60 residues (Nicaud et al., 1986; Mackman et al., 1987; Koronakis et al., 1989; Jarchau et al., 1994). However, despite extensive research, the exact nature of the information or code remains enigmatic. Based on sequence comparisons, no real conservation on the level of primary structure was evident within all sub-families (Holland et al., 2016). This was confirmed by random mutagenesis of the secretion signal of HlyA, indicating a high level of redundancy with only eight positions showing drastic influences on secretion efficiencies (Kenny et al., 1994). This redundancy led to the proposal that secondary structures might be encoded in the secretion signal. A putative amphipathic α-helix located between residues 973 and 987 of HlyA was first proposed by *in silico* approaches and subsequently supported by mutagenesis studies (Koronakis et al., 1989; Stanley et al., 1991) that indicated a larger α-helix between residues 976 and 1001. However, the presence of such a helix remained under debate, and a series of studies either supported or contradicted the theory (Stanley et al., 1991; Kenny et al., 1992, 1994; Chervaux and Holland, 1996). A combinatorial approach combined with structural studies provided further support for the importance of an amphipathic helix, now situated between residues 975 and 988 (Yin et al., 1995; Hui et al., 2000; Hui and Ling, 2002). Unfortunately, the crystal structure of the C-terminal part of the RTX domain of CyaA did not provide further information, as the last 33 C-terminal amino acids covering the corresponding region in CyaA were disordered in the structure (Bumba et al., 2016). Thus, the nature of the code of the secretion signal is still unclear, and it is also an open question whether all RTX proteins use the same code to initiate secretion: secondary structure predictions as well as the few crystal structures of proteases and lipases of the RTX family indicate rather the presence of β-strand structures, but not an α-helical content of the C-terminus (Baumann et al., 1993; Meier et al., 2007).

In this study, we re-examined the role of C-terminal secretion signal of HlyA based on a set of mutants (Chervaux and Holland, 1996) within the proposed amphipathic α-helix, but extended the number of mutants by including proline residues. Since the hemolytic activities of all mutants were not affected, we focused on the initial steps of secretion and determined the rate of secretion per transporter. Here, important differences became apparent pointing toward an essential role of a putative amphipathic α-helix in the secretion of HlyA. Additionally, we further supported the hypothesis by an *in silico* analyses of the primary sequence and by modeling the structure of HlyA using AlphaFold (Jumper et al., 2021). Overall, our results strongly support the essential role of this amphipathic α-helix in the initiation step of the secretion process of HlyA.

MATERIALS AND METHODS

AlphaFold Prediction of the HlyA Structure

AlphaFold (Jumper et al., 2021) was used to predict the structure of HlyA (Uniprot entry P08715) employing the ColabFold web interface[1] using standard settings (five models and no templates).

Cloning of Pro-HlyA Mutants

Mutations were introduced in the pro-HlyA plasmid pSU-HlyA (Thomas et al., 2014a) by applying the quick-change PCR method using primers listed in **Table 1** and following the protocol of the manufacturer (New England Biolabs).

Overexpression and Purification of Pro-HlyA and Mutants From Inclusion Bodies

Overexpression and purification was performed as described in Thomas et al. (2014a). In brief, the expression of pro-HlyA was induced by adding 1 mM IPTG to cultures. Incubation was continued for 4 h and cells were harvested by centrifugation (8000 g, 10 min, 4°C). For the purification of pro-HlyA, cells were resuspended in 50 mM HEPES pH 7.4, 150 mM NaCl, 10% (w/v) glycerol, 0.05% (w/v) NaN_3 and lysed by passing three times through a cell disruptor at 1.5 kbar (M-110P, Microfluidics). Inclusion bodies were collected by centrifugation at 18,000 g for 30 min. Pellets were washed and centrifuged successively in (1) 50 mM HEPES, pH 7.4, 50 mM EDTA, 1% (w/v) Triton X-100, 0.05% (w/v) NaN_3 and (2) 50 mM HEPES, pH 7.4, 1 mM EDTA, 1 M NaCl, 0.05% (w/v) NaN_3. The pellet was solubilized overnight in 20 mM HEPES pH 7.4, 20 mM NaCl, 6 M urea) at room temperature. Insoluble material was removed by ultra-centrifugation (150,000 g, 30 min, 4°C) and the urea-solubilized inclusion bodies were stored at −80°C.

Small Angle X-ray Scattering Measurements

Size exclusion chromatography coupled small angle x-ray scattering (SEC-SAXS) data of refolded proHlyA were collected on beamline BM29 at the ESRF Grenoble (Pernot et al., 2010,

[1]https://colab.research.google.com/github/sokrypton/ColabFold/blob/main/AlphaFold2.ipynb

TABLE 1 | Primers used for quick-change polymerase chain reaction.

Mutant	Forward primer	Reverse primer
P975G	CAGGGTGATCTTAATGGAT TAATTAATGAAATCAGC	GCTGATTTCATTAATTAA TCCATTAAGATCACCCTG
N978G	GATCTTAATCCATTAATTGG TGAAATCAGCAAAATC	GATTTTGCTGATTTCACC AATTAATGGATTAAGATC
E979G	CCATTAATTAATGGAATCA GCAAAATCATTTCAGCTGC	GCAGCTGAAATGATTTTGC TGATTCCATTAATTAATGG
E979P	CCATTAATTAATCCAATCA GCAAAATCATTTCAGCTGC	GCAGCTGAAATGATTTTGC TGATTGGATTAATTAATGG
I980S	CCATTAATTAATGAATCCA GCAAAATCATTTCAGCTGC	GCAGCTGAAATGATTTTGC TGGATTCATTAATTAATGG
I980P	CCATTAATTAATGAACCCA GCAAAATCATTTCAGCTGC	GCAGCTGAAATGATTTTGC TGGGTTCATTAATTAATGG
S981I	CATTAATTAATGAAATC ATCAAAATCATTTCAGC	GCTGAAATGATTTTGATG ATTTCATTAATTAATG
S981P	CATTAATTAATGAAATCC CCAAAATCATTTCAGCTG	CAGCTGAAATGATTTTGG GGATTTCATTAATTAATG
K982T	CCATTAATTAATGAAATCA GCACAATCATTTCAGCTGC	GCAGCTGAAATGATTGTG CTGATTTCATTAATTAATGG
K982P	CCATTAATTAATGAAATCAG CCCAATCATTTCAGCTGC	GCAGCTGAAATGATTGGGC TGATTTCATTAATTAATGG
I983S	GAAATCAGCAAAAGC ATTTCAGCTGCAG	CTGCAGCTGAAATG CTTTTGCTGATTTC
I984S	GAAATCAGCAAAATC AGCTCAGCTGCAGG	CCTGCAGCTGAGCTG ATTTTGCTGATTTC
I984P	GAAATCAGCAAAATC CCTTCAGCTGCAG	CTGCAGCTGAAGGGAT TTTGCTGATTTC
S985A	CAGCAAAATCATTG CAGCTGCAGG	CCTGCAGCTGCAA TGATTTTGCTG
S985P	CAGCAAAATCATTC CAGCTGCAGG	CCTGCAGCTGGAA TGATTTTGCTG
F990P	CATTTCAGCTGCAGGTAGCC CCGATGTTAAAGAGGAAAG	CTTTCCTCTTTAACATCGGGG CTACCTGCAGCTGAAATG
I983P	GAAATCAGCAAACC CATTTCAGCTGCAG	CTGCAGCTGAAATG GGTTTGCTGATTTC
A986P	GCAAAATCATTTCA CCTGCAGGTAGC	GCTACCTGCAGGT GAAATGATTTTGC
E979G-I980S -K982T	CCATTAATTAATGGATCCAG CACAATCATTTCAGCTGC	GCAGCTGAAATGATTGTGC TGGATCCATTAATTAATGG
E979G-K982T	CCATTAATTAATGGAATCA GCACAATCATTTCAGCTGC	GCAGCTGAAATGATTGTGC TGATTCCATTAATTAATGG
E979P-I980P -K982P	CCATTAATTAATCCACCCA GCCCAATCATTTCAGCTGC	GCAGCTGAAATGATTGGG CTGGGTGGATTAATTAATGG
E979G-I980S	CCATTAATTAATGGAAGCA GCAAAATCATTTCAGCTG	CAGCTGAAATGATTTTGC TGCTTCCATTAATTAATGG
I980S-K982T	CCATTAATTAATGAAAGCA GCACAATCATTTCAGCTGC	GCAGCTGAAATGATTGTG CTGCTTTCATTAATTAATGG

2013). The BM29 beamline was equipped with a PILATUS 1M detector (Dectris) at a fixed distance of 2.869 m. The measurement of refolded pro-HlyA (8.0 mg/ml, 110 µL inject) were performed at 10°C on a Superose 6 increase 10/300 column, preequilibrated with 100 mM HEPES pH 8.0, 250 mM NaCl, 10 mM $CaCl_2$. with a flowrate of 0.5 ml/min, collecting one frame every 2 s. Data were scaled to absolute intensity against water.

All programs used for data processing were part of the ATSAS Software package (Version 3.0.4) (Manalastas-Cantos et al., 2021). Primary data analysis was performed with the program CHROMIXS (Panjkovich and Svergun, 2017) and PRIMUS (Konarev et al., 2003). With the Guinier approximation (Guinier, 1939), the forward scattering *I(0)* and the radius of gyration (R_g) were determined. The program GNOM (Svergun, 1992) was used to estimate the maximum particle dimension (D_{max}) with the pair-distribution function *p(r)*. Low resolution *ab initio* models were calculated with GASBORMX (Svergun et al., 2001; Petoukhov et al., 2012) (P2 Symmetry). Dimer docking of the calculated AlphaFold (Jumper et al., 2021) monomer model was done with SASREFMX (Petoukhov and Svergun, 2005; Petoukhov et al., 2012). Superimposing of the calculated dimer model was done with the program SUPCOMB (Kozin and Svergun, 2001). The monomer/dimer content of the scattering data was determined with OLIGOMER (Konarev et al., 2003) using the AlphaFold monomer and the SASREFMX dimer as input.

In vitro Acylation Assay and Hemolytic Activity of HlyA

An *in vitro* acylation protocol was applied as described in Thomas et al. (2014b). Briefly, the pro-HlyA mutants were unfolded in 6 M urea and any divalent cations were removed by adding 10 mM EDTA. Pro-HlyA was mixed with HlyC and acyl-carrier protein (ACP) and the hemolysis-efficiency on erythrocytes was quantified by measuring the hemoglobin release at 544 nm (Thomas et al., 2014b) at a final concentration of HlyA of 18 µg/ml (160 nM). 1 µl of 16% SDS solution in 74 µl assay was used as positive control to determine the value of 100% cell lysis. The concentration of wildtype HlyA and the mutants was chosen as it represents the lowest concentration of wildtype HlyA with the highest lytic activity (Thomas et al., 2014b).

Secretion Assay of Pro-HlyA-Mutants

The secretion rate of the pro-HlyA mutants was determined as described before (Lenders et al., 2016). Briefly, cells were grown for a total of 4 h. Every hour, samples were taken and the supernatants were analyzed by SDS-PAGE. Pro-HlyA as well as the secretion apparatus was subsequently quantified and the secretion rates were determined as amino acids per second and transporter as described in detail in (Lenders et al., 2016).

Secondary Structure Prediction

Quick2D (Zimmermann et al., 2018) and AmphipaSeeK (Combet et al., 2000; Sapay et al., 2006) were used to predict the secondary structures. Quick2D is able to predict α-, π- and TM-helices, β-strands, coiled coils, as well as disordered regions (Zimmermann et al., 2018). AmphipaSeeK, on the other hand, is specifically designed to identify amphipathic helices (Sapay et al., 2006). The output includes a secondary structure prediction, a predicted membrane topology (in-plane or not in-plane), a prediction score for the proposed membrane topology and an amphipathy score for each residue in dependence to the neighboring residues.

Structure Prediction of HlyA Derived Peptides

PEP-FOLD3 was used to model peptides of HlyA (Thevenet et al., 2012; Shen et al., 2014; Lamiable et al., 2016).

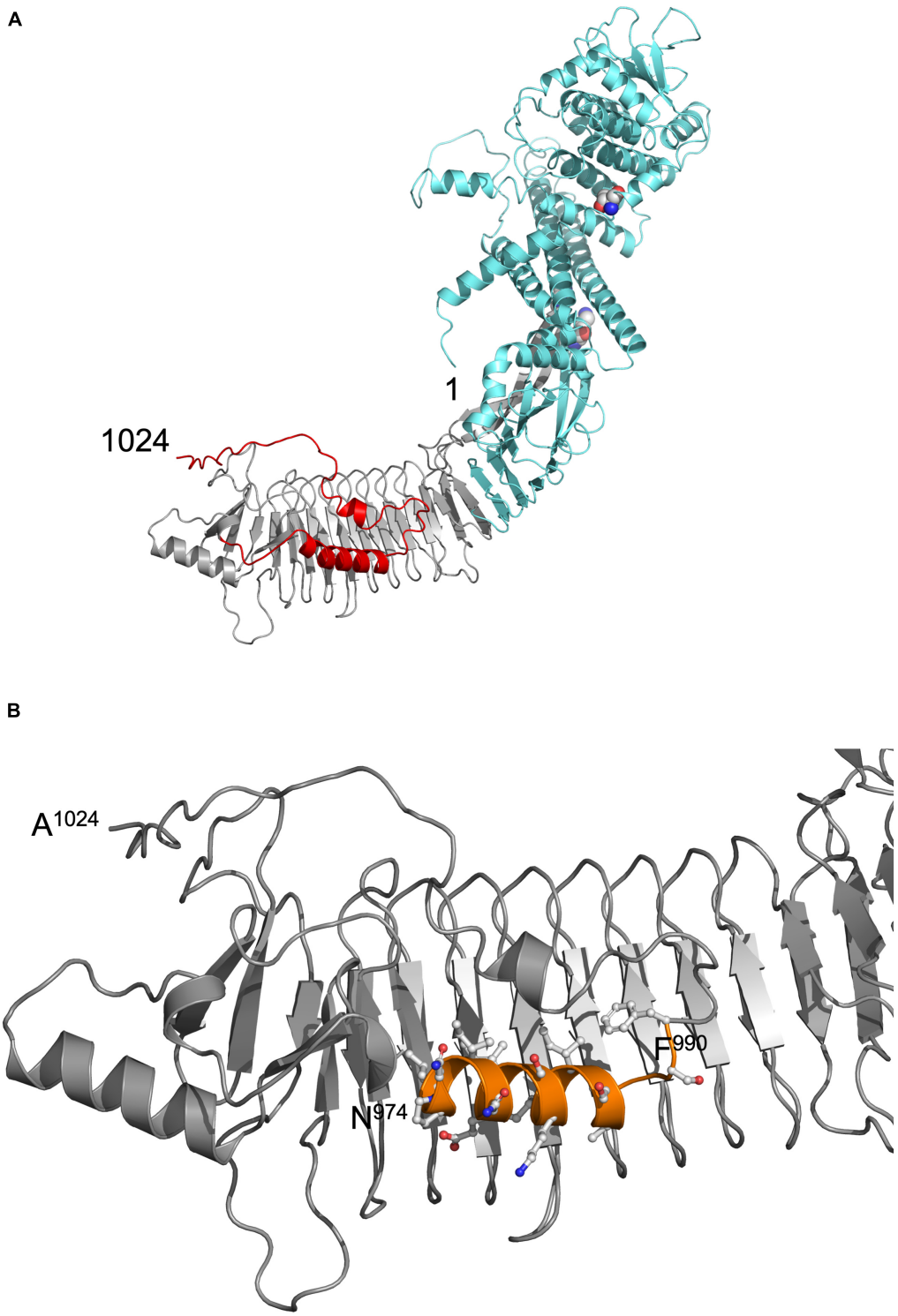

FIGURE 1 | (A) Model of pro-HlyA predicted by AlphaFold (Jumper et al., 2021). The N- and C-termini are indicated by numbers (1 and 1024, respectively). The secretion signal is highlighted in red, the RTX in gray and the N-terminal pore-forming domain in cyan. The two Lys residues (K564 and K690) that are acylated by HlyC prior to secretion are highlighted as spheres. **(B)** Zoom in into the C-terminal region of the structural model of folded pro-HlyA. The C-terminus (A^{1024}) as well as the positions of residues N^{974} and F^{990} are indicated. The amphipathic helix is shown in orange with the side chains in ball-and-sticks representation. Hydrophobic residues are clearly located on one side of the helix, while polar and charged residues are located on the opposite side. The Repeat in ToXins (RTX) domain, which adopts a β-roll structure even in the absence of Ca^{2+} ions, is oriented toward the back of the representation.

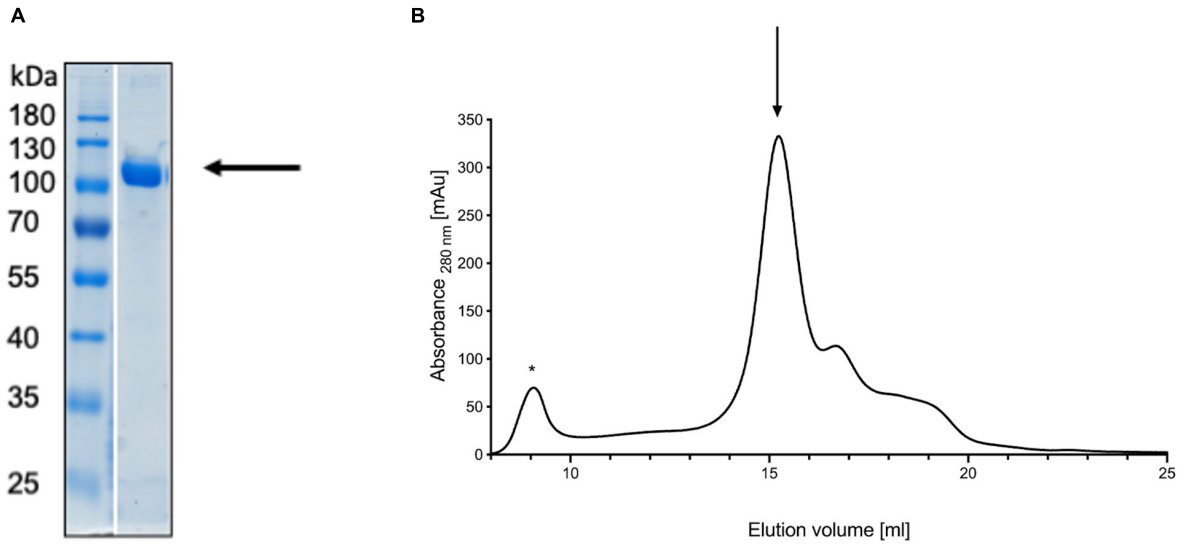

FIGURE 2 | Denaturing gel of refolded pro-HlyA (indicated by an arrow) **(A)** and the corresponding SEC chromatogram **(B)**. The void volume is indicated by an asterisk and the elution peak of pro-HlyA by an arrow. The SDS-PAGE gel was stained with Coomassie Brilliant Blue.

Illustration and Visualization

The amphipathic nature of a helix was visualized by a helical wheel projection using NetWheel (Mol et al., 2018). Protein and peptide structures were visualized using PyMOL.[2] In order to illustrate and identify hydrophobic surfaces the yrb-script was applied in PyMOL, which highlights carbon atoms that are not bound to oxygen or nitrogen in yellow, the charged oxygens of Glu and Asp residues in red, the charged nitrogens of Lys and Arg residues in blue, while all other atoms are white (Hagemans et al., 2015).

RESULTS

The structure of pro-HlyA is unknown and established homology modeling tools such as PHYRE2 (Kelley et al., 2015) were unable to model a complete structure of pro-HlyA. HlyA is acylated at two Lys residues (K564 and K690) in the cytosol of *E. coli* prior to secretion. Only its acylated version forms pores in the host membrane. Consequently, the non-acylated, inactive form is called pro-HlyA. Recent developments, resulting in the program AlphaFold (Jumper et al., 2021) allowed the modeling of the entire pro-HlyA monomer. Even in the absence of Ca^{2+} ions, the characteristic feature of RTX proteins, the β-roll of the GG-repeats (Linhartova et al., 2010) was completely modeled (**Figure 1A**).

To verify this model experimentally, we turned to small angle X-ray scattering (SAXS). Small angle X-ray scattering allows the study of proteins in solution and offers information about the oligomeric state. Wild type pro-HlyA, i.e., the non-acylated version of the protein, was expressed and purified from inclusion bodies (**Figure 2A**). As shown in **Figure 2B**, size exclusion chromatography indicated a broadly eluting sample, which was used for subsequent SAXS experiments.

We used size exclusion chromatography-coupled SAXS (SEC-SAXS) to separate different higher oligomeric species as well as aggregates from the sample. Analyzing different frames revealed an inhomogeneous distribution within the peak. Frames were subsequently merged using CHROMIX and the corresponding buffer frames were subtracted. The determined molecular weight for pro-HlyA was near to that of the calculated dimer (220.38 kDa), leading to the conclusion that the protein forms a dimer in solution (**Table 2**). Nevertheless, a monomer/dimer mixture was present in solution and an *ab initio* model for the pro-HlyA dimer (χ^2:1.19) was calculated using GASBORMX. SASREFMX and the AlphaFold monomer model were used to dock a dimer based on the SAXS data (χ^2:1.4). With the resulting dimer and the initial monomer, a content of 81.7% dimers and 18.2% monomers in the chosen frames using OLIGOMER was determined. The SAREFMX dimer model was superimposed with the calculated *ab initio* model of GASBORMX and the dimer interface was localized to the C-terminal part of the pro-HlyA protein (**Figure 3**).

The nature of the additional densities is highly speculative and might reflect the high flexibility of pro-HlyA. However, the good quality of the main part of the dimer model suggests that the overall structure of pro-HlyA is of high reliability. Most importantly, an amphipathic helix (**Figure 1B**) covering residues 975–987 within the secretion signal was present in the AlphaFold model.

In the early studies, random and directed mutagenesis methods were applied to the secretion signal of an N-terminally truncated construct of HlyA, called HlyA1 (residue 806–1024; 23 kDa) (Stanley et al., 1991; Kenny et al., 1992; Chervaux and Holland, 1996), which covers three GG-repeats of the RTX

[2]www.pymol.org

TABLE 2 | Overall small angle X-ray scattering (SAXS) Data of pro-HlyA.

SAXS Device	**BM29, ESRF Grenoble (Pernot et al., 2010, 2013)**
Data collection parameters	
Detector	PILATUS 1 M
Detector distance (m)	2.869
Beam size	700 μm × 700 μm
Wavelength (nm)	0.099
Sample environment	Quartz capillary,1 mm ø
s range (nm^{-1})‡	0.025–5.0
Exposure time per frame (s)	2
Sample	**pro-HlyA refolded**
Organism	*E. coli* UTI89
UniProt ID and range	P08715
Mode of measurement	Online SEC-SAXS
Temperature (°C)	10
Protein buffer	100 mM HEPES pH 8.0, 250 mM NaCl, 10 mM $CaCl_2$
SEC-Column	Superose 6 increase 10/300
Injection volume (μl)	110
Flowrate	0.5 ml/min
Protein concentrations	8.0 mg/ml
Structural parameters	
I(0) from *P(r)*	97.54
R_g [real-space from *P(r)*] (nm)	7.04
I(0) from Guinier fit	95.91
s-range for Guinier fit (nm^{-1})	0.080–0.187
R_g (from Guinier fit) (nm)	6.65
points from Guinier fit	4–27
D_{max} (nm)	25.26
POROD volume estimate (nm^3)	346.40
Molecular mass (kDa)	
From *I(0)*	n.d.
From Qp (Porod, 1951)	242.10
From MoW2 (Fischer et al., 2010)	204.90
From Vc (Rambo and Tainer, 2013)	195.01
Bayesian Inference (Hajizadeh et al., 2018)	208.00
From POROD	173.2–216.5
From sequence	110.19 (monomer) 220.38 (dimer)
Structure evaluation	
Gasbor MX fit χ^2	1.19
Sasref MX fit χ^2	1.4
Oligomer fit χ^2 (ratio)	1.32 (81.7% dimer/18.2% monomer)
Ambimeter score	2.525
Software	
ATSAS Software Version (Manalastas-Cantos et al., 2021)	3.0.4
Primary data reduction	CHROMIXS (Panjkovich and Svergun, 2017)/PRIMUS (Konarev et al., 2003)
Data processing	GNOM (Svergun, 1992)
Ab initio modeling	GASBORMX (Svergun et al., 2001; Petoukhov et al., 2012)
Rigid body modeling	SASREFMX (Petoukhov and Svergun, 2005; Petoukhov et al., 2012)
Mixture analysis	OLIGOMER (Konarev et al., 2003)
Superimposing	SUPCOMB (Kozin and Svergun, 2001)
Structure evaluation	AMBIMETER (Petoukhov and Svergun, 2015)
Model visualization	PyMOL (www.pymol.org)

‡$s = 4\pi sin(\theta)/\lambda$, 2θ – *scattering angle,* λ – *X-ray-wavelength, n.d. not determined.*

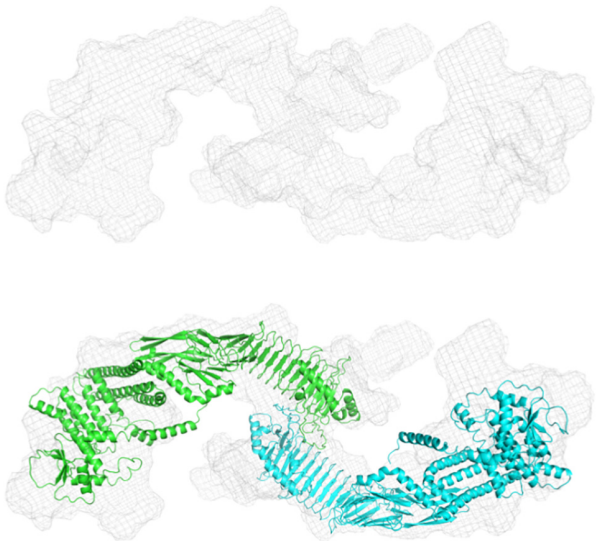

FIGURE 3 | *Ab initio* and rigid body modeling of refolded pro-HlyA. Upper panel: Volumetric envelope of the GASBORMX *ab initio* model. Lower panel: Overlay of the *ab initio* and the dimer model. The single monomers are colored in cyan and green.

domain as well as the secretion signal. These studies revealed that the secretion signal is relatively tolerant toward mutations; however, some mutations had drastic impacts on the amount of secreted HlyA1 and most of them clustered in a proposed amphipathic α-helix predicted between residue L973 and F990 (Koronakis et al., 1989). In light of the AlphaFold model and its fit to the SAXS envelope (**Figure 3**), we therefore re-investigated the mutational studies of this region (Chervaux and Holland, 1996). It is not expected that pro-HlyA will fold in the cytosol of *E. coli* (Bakkes et al., 2010) as the concentration of free Ca^{2+} is too low [approximately 300 nM (Jones et al., 1999)] to bind to the GG-repeats of the RTX domain and thereby inducing folding. However, secondary structure elements also exist in unfolded proteins as demonstrated by solid state NMR (Curtis-Fisk et al., 2008; Wasmer et al., 2009) making the presence of the amphipathic helix possible in the cytosol of *E. coli*.

We introduced all of these mutations and combinations thereof (Chervaux and Holland, 1996) as well as proline-substitutions into full length HlyA. In a first step, we explored their hemolytic activities (for HlyA) as well as their secretion rates (for non-acylated pro-HlyA). As pro-HlyA requires acylation of two internal lysine residues (K564 and K690) for hemolytic activity (Stanley et al., 1994), wild type and all mutants were activated by an *in vitro* acylation assay according to Thomas et al. (2014b). This allowed us to quantify their activity and, most importantly, normalize it to the amount of HlyA used in the hemoglobin release assay by measuring the absorption spectrum. Here, and in contrast to earlier work (Chervaux and Holland, 1996), normalization to the amount of active HlyA in the assay clearly demonstrated that none of the mutations affected the actual hemolytic activity of HlyA within experimental error (**Figure 4A**).

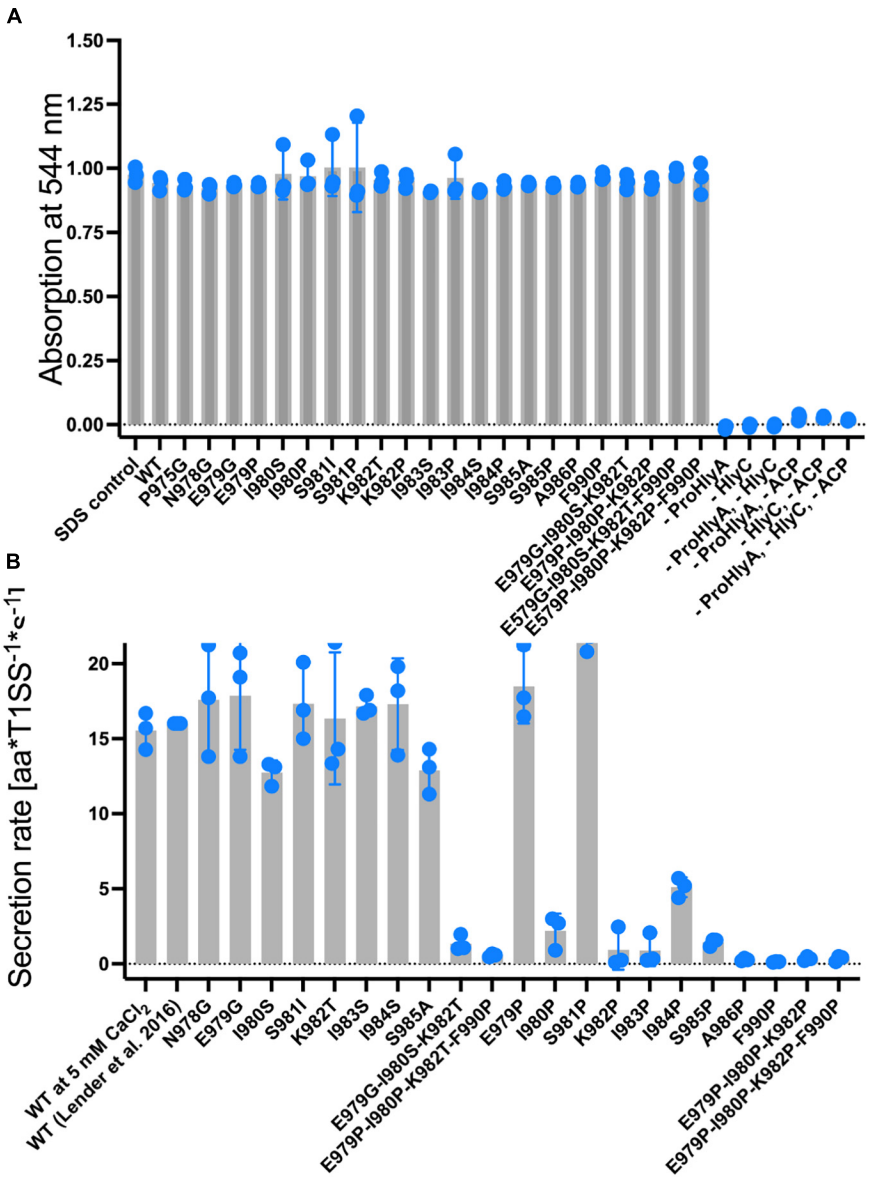

FIGURE 4 | (A) Normalized hemolytic activity of wild type HlyA (left bar), single, triple and quadruple mutations within the secretion signal. The lysis of erythrocytes was quantified by measuring the release of hemoglobin by absorption spectroscopy at 544 nm. Control measurements shown to the right of the quadruple mutations lacked HlyA (acylated form), the acylase HlyC, Acyl-carrier protein (ACP), or a combination of these, in the assay. These results demonstrated that lysis was only induced in the presence of acylated HlyA. HlyA is as efficient in hemoglobin release as an SDS incubation (Thomas et al., 2014b) (not shown). Individual assays were performed in at three biological independent experiments and shown as scatter dot plots. **(B)** Summary of the secretion rates of wild type pro-HlyA (left), single, triple and quadruple mutations within the putative secretion signal. The value "WT" was taken from Lenders et al. (2016). Data represent the average of three biologically independent experiments and are shown as scatter dot plots.

The hemolytic activity of all HlyA single point mutants, which were already investigated by Chervaux and Holland (1996), did not affect the hemolytic activity. We also created and included triple mutants since they are part of the predicted amphipathic α-helix to verify whether cumulative effects might be present. As shown in **Figure 4A**, no change in hemolytic activity was detected for these mutants. Based on the results of the hemolytic assay, we moved one step further and determined the secretion rates of all mutants according to Lenders et al. (2016) (**Figure 4B**).

In contrast to the hemolytic activity of acylated HlyA, the secretion rates of non-acylated pro-HlyA clearly showed a reduction in the rates for certain mutations. Wild type pro-HlyA was secreted at 14.3 ± 3.1 amino acids*T1SS^{-1}*s^{-1}, which is in the range of the reported value of 16.0 ± 1.3 amino acids*T1SS^{-1}*s^{-1} within experimental error (Lenders et al., 2016). All of the non-proline single point mutations displayed the same secretion rates as the wild type within standard error. The values ranged from 12.8 ± 2.0

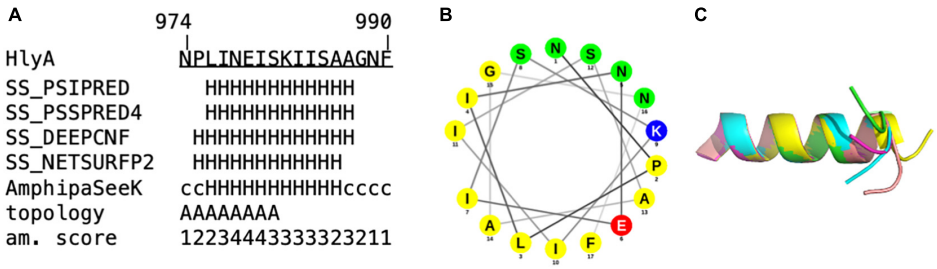

FIGURE 5 | *In silico* analysis of **(A)** amino acids 974 to 990 of the secretion signal of HlyA. H = α-helix, c = coiled coil. Predictions labeled with "SS" were obtained from Quick2D, that utilizes multiple prediction algorithms. Topology = predicted by AmphipaSeeK: "A" indicated those residues that are predicted to be inserted parallel into the membrane. Am. score = amphipathy score predicted by AmphipaSeeK with 1 = lowest amphipathy and 5 = highest amphipathy. **(B)** Helical wheel projection of residue 974–990 of HlyA. Non-polar residues are colored yellow, lysine blue, glutamate red and polar residues green. **(C)** Superimposition of five PEP-FOLD3 models of residue 974–990 of HlyA. The helix is similar in all five models with the C-terminal tail showing variability in orientation.

amino acids*T1SS^{-1}*s^{-1} (I980S) to 20.2 ± 2.1 amino acids amino acids*T1SS^{-1}*s^{-1} (E979G). In contrast, all single proline mutations, with the exception of E979P and S981P, displayed a clear reduction in the secretion rates. In the case of E979P and S981P, the rates were slightly higher than the rate of wild type pro-HlyA (19.5 ± 2.3 amino acids*T1SS^{-1}*s^{-1}) and (19.4 ± 3.4 amino acids*T1SS^{-1}*s^{-1}, respectively). For the triple (red bars in **Figure 4B**) and the quadruple (brown bars in **Figure 4B**) mutants, the secretion rates were close to the background.

Proline is known as a so-called helix breaker, due to its unique conformation and rigid rotation. Its preferred position in helices is at the N-terminus (Richardson and Richardson, 1988), but helices with proline in or close to the center are still possible (Kim and Kang, 1999). In order to correctly interpret the secretion rates of especially the proline mutants, secondary structure prediction tools (Sapay et al., 2006; Zimmermann et al., 2018) as well as peptide modeling with the tool PEP-FOLD3 (Thevenet et al., 2012) were employed. This was necessary as the algorithm implemented in AlphaFold was not trained on single mutants and is insensitive to single side chain changes (Jumper et al., 2021). Firstly, this analysis revealed that a putative amphipathic α-helix of HlyA is situated between residue P975 and A987 (**Figure 5**) in strong agreement with the structural model (**Figure 1B**). Alternatively, the prediction tools placed the α-helix between residues 975 and 987 or 974 and 986. Secondly, the mutants E979P and S981P, which showed secretion rates similar to the wild type within standard deviation (**Figure 3**), are still able to form an amphipathic α-helix. In contrast, mutants such as I980P and I984P, whose secretion rates were strongly reduced, showed much shorter helices in the predictions (**Figure 6**).

The secondary structure prediction tools predicted impairments of the amphipathic α-helix for almost all mutants that exhibited a reduced secretion rate. Four mutants were identified whose secretion rate was strongly reduced, but a helix was still predicted: F990P, which is not part of the amphipathic α-helix, K982P, S985P and A986P. However, their secretion rate phenotypes can be rationalized with the help of additional *in silico* tools.

The latter two mutations, S985P and A986P, showed a slightly shortened amphipathic α-helix in the predictions (**Figures 6E,G**) while A986 marks the end of the amphipathic α-helix in wild type pro-HlyA, followed by another Ala residue and a Gly residue. This region [(S)AAG] is therefore flexible, which is also reflected by the five different models from PEP-FOLD3 for wild type HlyA-amphipathic α-helix, where tails project in different directions (**Figure 5C**). This flexibility is most likely impaired when a proline residue is introduced at this position, which explains the observed reduced secretion rate. In addition to the reduced flexibility, the polarity of the polar side of the amphipathic α-helix is reduced for S985P, which is illustrated in the helical wheel projection (**Figure 6H**).

The mutant K982P also results in a change of polarity, correlating with a reduced secretion rate of 1.3 ± 0.8 aa T1SS^{-1}*s^{-1} (**Figure 6I**). However, the mutant K982T, which equally eliminates the positive charge at this position, shows wild type-like secretion (**Figure 4B**), showing that a positive charge at this position is not essential for efficient secretion. However, a proline at this position introduces a bend to the amphipathic α-helix as seen in the PEP-FOLD3 models (**Figure 6J**). The proline substitution at n-1 (S981P) also shows a bend of the amphipathic α-helix but no impairment of the secretion rate within experimental error (19.4 ± 3.4 aa T1SS^{-1}*s^{-1}) (**Figure 6J**). These two mutants were found to bend the amphipathic α-helix in opposite directions, with S981P resembling the wild type more than K982P (**Figure 6I**). This is in line with the secretion rates (**Figure 4B**) and further supports the hypothesis that the precise secondary structure of this motif is essential for secretion.

F990 is not part of the predicted amphipathic α-helix but highly susceptible to mutations and essential for secretion. In previous studies it has been demonstrated that a substitution of this residue to His, Cys, Ala, Ser, Ile, Asn or Pro strongly reduced the secretion of HlyA to <20% compared to wild type (Chervaux and Holland, 1996). The substitution to Tyr was least affected and allowed a secretion of approximately 35% compared to wild type protein (Chervaux and Holland, 1996). Interestingly, CyaA from *B. pertussis* also contains a Tyr residue at this position (Bumba et al., 2016).

Further support of the importance of the amphipathic α-helix comes from calculations of the hydrophobic moment (**Table 3**).

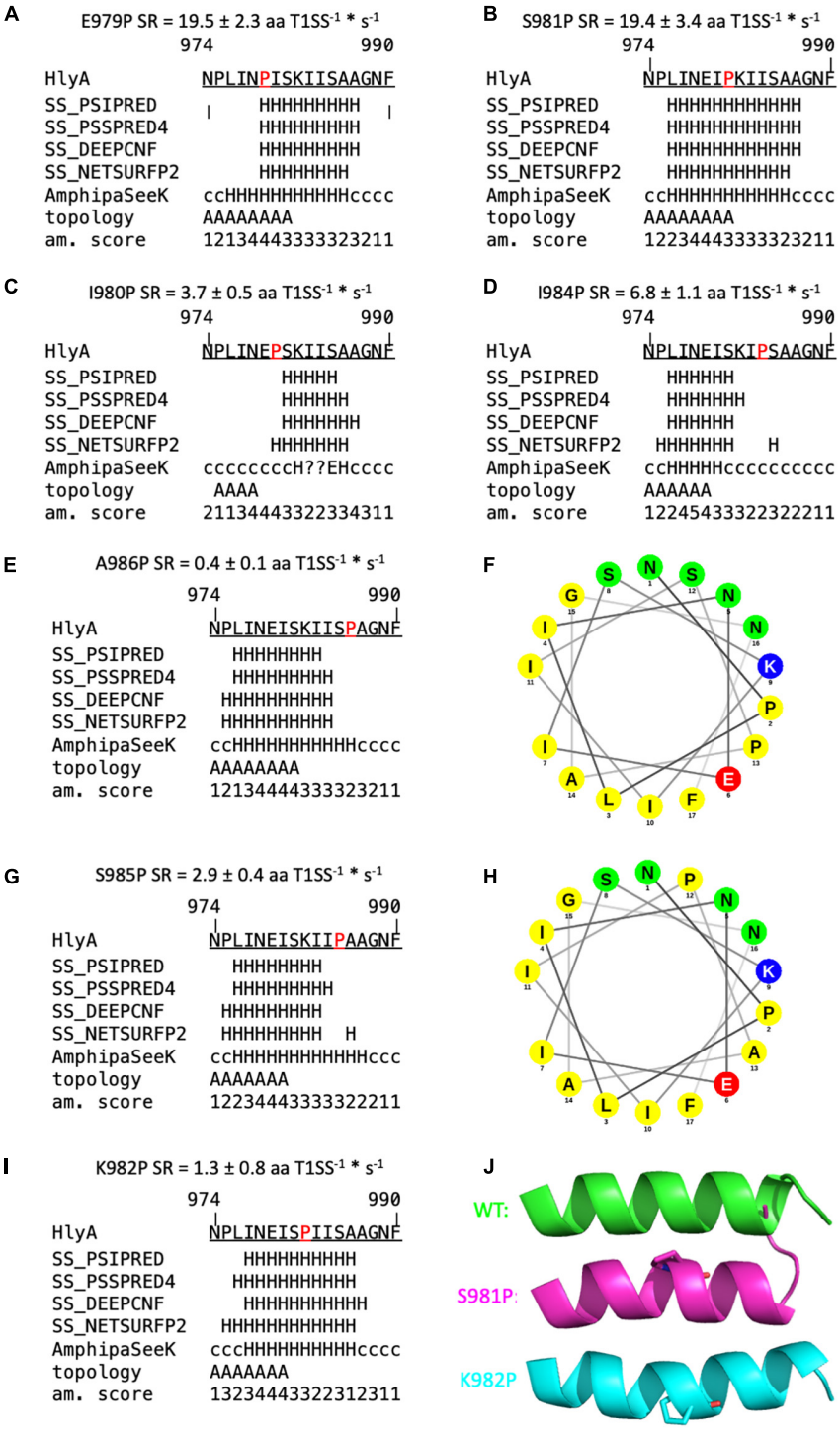

FIGURE 6 | Secondary structure predictions of mutants of the secretion signal of HlyA. Predictions labeled with "SS" are derived from Quick2D. Topology = predicted by AmphipaSeeK, "A" indicated those residues that are predicted to be inserted parallel into the membrane. Am. score = amphipathy score predicted by AmphipaSeeK with 1 = lowest amphipathy and 5 = highest amphipathy. H = α-helix, c = coiled coil, E = β-sheet, ? = no prediction. Mutated residues are marked in red. Secretion rate (SR) is given for each mutant as mean ± SD of three independent measurements. **(A,B)** Single proline mutations with SR similar to wild type pro-HlyA. **(C,D)** Single proline mutations with reduced SR compared to the wild type protein. **(F,H)** Helical wheel projection of A986P **(F)** and S985P **(H)**. Non-polar residues are colored yellow, lysine blue, glutamate red and polar residues green. Proline at position 985 reduces the polarity on the polar site of the amphipathic α-helix compared to wild type HlyA (**Figure 1B**). **(E,G,I)** Proline substitutions with drastically reduced SR. **(J)** Cartoon representation of PEP-FOLD3 models of wild type pro-HlyA (green), S981P (pink) and K982P (cyan). Mutated proline residues are shown as sticks. All models have an identical orientation for comparison. K982P and S981P bend the helix in opposite directions.

The hydrophobic moments decreases with decreasing secretion rates with the only exception being the I984P mutant. This dependence again highlights that the amphipathic α-helix plays an essential role during secretion.

At least five other RTX proteins can be secreted by the HlyBD-TolC system (**Figure 7**; Gygi et al., 1990; Highlander et al., 1990; Masure et al., 1990; Thompson and Sparling, 1993; Kuhnert et al., 2000). The structure of the C-terminus of one of these has been solved (CyaA), and also shows an amphipathic α-helix followed by an aromatic residue (Bumba et al., 2016). The secondary structures of the last 60 residues of the remaining four RTX proteins have been predicted with secondary structure prediction tools and all four show amphipathic α-helices in the N-terminus of their secretion signal followed by an aromatic residue (**Figure 7**). Taken together, the secretion rate phenotypes of the HlyA mutants in combination with their *in silico* analysis and the comparisons to heterologous substrates of the HlyBD-TolC system strongly support the presence of an amphipathic α-helix in the secretion signal and emphasize the importance of the correct secondary structure for secretion.

In summary, the data presented here including functional data, structural modeling and *in silico* analysis strongly point toward an essential role of an amphipathic α-helix covering amino acid residues 970-987 in the C-terminal secretion signal of HlyA.

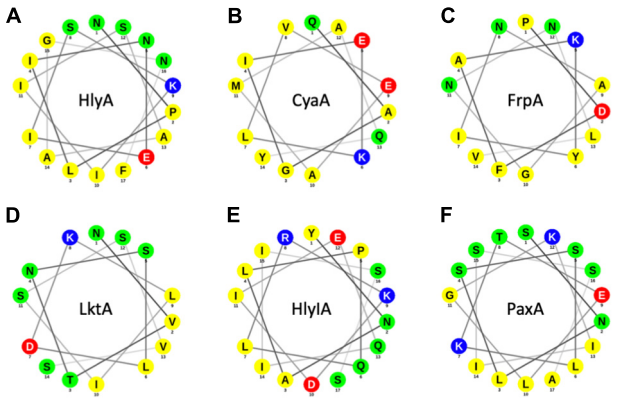

FIGURE 7 | Helical wheel projections of RTX proteins that can be secreted by the HlyBD-TolC apparatus. Helical wheels were drawn with NetWheel. Non-polar residues are shown in yellow, polar residues in green, basic residues in blue and acidic residues in red. Next to HlyA **(A)**, secretion by HlyBD-TolC has been shown for CyaA **(B)** by Masure et al. (1990), for FrpA **(C)** by Thompson and Sparling (1993), for LktA **(D)** by Highlander et al. (1990), for HlyIA **(E)** by Gygi et al. (1990) and for PaxA **(F)** by Kuhnert et al. (2000).

DISCUSSION

The AlphaFold algorithm (Jumper et al., 2021) correctly modeled the β-roll domain of pro-HlyA (**Figure 1A**) even in the absence of Ca^{2+} ions. Currently, ligands cannot be included, but the predicted β-roll of pro-HlyA aligns well with the corresponding regions of alkaline protease (Baumann et al., 1993) or block IV/V of the RTX domain of CyaA (Bumba et al., 2016), increasing the confidence in the model. Motivated by this three-dimensional model produced by AlphaFold (**Figure 1A**) that demonstrated the presence of an amphipathic α-helix in the secretion signal (**Figure 1B**), we re-examined the presence and role of this amphipathic α-helix for the secretion of pro-HlyA by its cognate T1SS.

TABLE 3 | Hydrophobic moments of the single side mutations of the predicted amphipathic α-helix.

Sequence	Calculated hydrophobic moment	Secretion rate [aa/T1SS*sec]
NPLINPISKIISAAGNF	0.519	19.5
NPLINEISKIISAAGNE	0.494	16
NPLINEIPKIISAAGNE	0.492	19.4
NPLINEISKIIPAAGNE	0.481	2.9
NPLINEISKIPSAAGNE	0.436	6.8
NPLINEPSKIISAAGNE	0.420	3.7
NPLINEISKIISPAGNE	0.41	0.4
NPLINEISPIISAAGNE	0.403	1.3

Hydrophobic moments were calculation using hmoment (https://www.bioinformatics.nl/cgi-bin/emboss/hmoment) employing standard settings. Mutants are arranged according to decreasing hydrophobic moments.

Small angle X-ray scattering (SAXS) data of pro-HlyA in solution were used to further improve the quality and accuracy of the model (**Figure 3**). One has to note that pro-HlyA in solution predominantly forms dimers (Thomas et al., 2014a), a fact that was also confirmed by SEC-SAXS and included in docking of the pro-HlyA model into the SAXS envelope (**Figure 3**). Without going into the details of the obtained model, the presence of an amphipathic α-helix (**Figure 1B**) was already proposed by Koronakis et al. (1989) with slight deviations in the exact position and length of the α-helix. Based on this agreement between theory and experiment, we analyzed the precise nature of the amphipathic α-helix signaling and its involvement in the secretion process of HlyA. We also tried to verify this structure by single particle cryo-EM. The C-terminal part, i.e., the RTX domain and the secretion signal, fitted well into the map. However, no density was observed for the N-terminal part indicating a high degree of flexibility and/or denaturation during grid preparation (not shown).

The hemolytic assay of HlyA and the mutants did not reveal any significant differences in activity (**Figure 4A**) as long as the proteins were used at identical concentrations. This is in contrast to mutations within the last six amino acids of HlyA (Jumpertz et al., 2010). Here, a reduced hemolytic activity was determined, which likely was due to impaired folding of the mutant protein. In the case of mutations within the amphipathic α-helix, folding and the resulting activity is apparently not influenced, pointing toward a role of these residues in an earlier step of the secretion process. Thus, steps taking place on the extracellular side are not impaired and we focused processes at the cytoplasmic side and measured the secretion rates per transporter of each mutant and compared it to the wild type protein (**Figure 4B**). All of the non-proline, single mutations within the amphipathic

α-helix showed no change in the secretion rate per transporter within experimental error. For the single proline mutations, the situation was more complex. Positions E979 and S981 were insensitive to mutations to proline, while positions I980, K982, I983, I984, S985, and A986 were very sensitive and showed drastic reductions of the secretion rate, some had secretion rates close to background values (**Figure 4B**). This was also true for position F990, which is not part of the amphipathic α-helix, but one of the few amino acids that were determined in mutational studies to be essential for efficient secretion (Chervaux and Holland, 1996; Holland et al., 2016). Since the most efficient secretion can be achieved by a substitution with another aromatic residue, π-π interactions can be assumed, that are disrupted in F990P. Vernon et al. provided an extensive study analyzing π-π interactions in different protein crystal structures (Vernon et al., 2018). Amongst other findings they show that Phe and Tyr have very similar preferences for the nature of their contacts, and that π-π stacking with non-aromatic residues is actually more common than aromatic-aromatic stacking. Furthermore, they identified Arg as the first or second most likely interaction partner for any given aromatic side chain (Vernon et al., 2018). Conserved Arg residues can be found, for example in the cytosolic domain (CD) of HlyD and could present an interaction partner to F990.

In summary, these results supported the notion that secretion rates as read-out for impaired secretion efficiency is a valid approach. The triple and quadruple mutants were also drastically impaired in their secretion rates. Importantly, the secretion rate of the triple mutant E979G/I980S/K982T, containing no proline residues, was also reduced close to background levels. This was in contrast to the single mutations, which displayed secretion rates identical to the wild type protein, suggesting an additive or even cooperative effect of these mutations in HlyA secretion that disrupted the predicted amphipathic α-helix. Since the AlphaFold algorithm was not trained to take single site mutations into account for accurate structure predictions (Jumper et al., 2021), we turned to an *in silico* analysis of the mutants. For wildtype pro-HlyA, a close match between the model and the prediction for the amphipathic α-helix using different programs was obtained (**Figure 5**). More importantly, however, was the analysis of the mutants. In all cases, in which the secretion was not impaired within experimental error, an amphipathic α-helix was predicted that resembled strongly the wild type. In contrast, in all cases that impaired the secretion rates, the length of the amphipathic α-helix was reduced (**Figures 6C,D**) or the bending of the amphipathic α-helix was inverted (**Figures 6I,J**). Thus, the correct length and bending direction are indispensable for efficient secretion of the substrate, which is also supported by the calculation of the hydrophobic moments of the mutants (**Table 3**).

Moving one step further, we also analyzed further RTX toxins, which have been secreted in the past using the HlyA T1SS (**Figure 7**). For CyaA, the structure of block IV/V of the RTX domain was determined by X-ray crystallography but the region of the amphipathic α-helix and the flanking aromatic residue (F990 in HlyA) is not resolved (Bumba et al., 2016). Consequently, we performed an *in silico* analysis of those five additional substrates. As shown in **Figure 7**, all five RTX proteins contained an amphipathic α-helix and a flanking aromatic residue. Obviously, five examples of substrates of sub-family 2 T1SS are not sufficient to make a real significant statement, but these results suggest that the 'amphipathic α-helix/aromatic residue' motif might be a general feature of sub-family 2 T1SS and also impose a sort of substrate selectivity. Overall, we propose that the presence and bending of the amphipathic α-helix combined with a C-terminally flanking aromatic residue triggers an early step in substrate secretion. Eventually it even constitutes the initial trigger to assemble the continues channel across the periplasm, through which HlyA is transported in one-step into the extracellular space.

DATA AVAILABILITY STATEMENT

The raw data supporting the conclusions of this article will be made available by the authors, without undue reservation. SAXS data were uploaded to the Small Angle Scattering Biological Data Bank (SASBDB) (Kikhney et al., 2020), with the accession codes SASDM67.

AUTHOR CONTRIBUTIONS

LS and SS conceived and directed this study. SP, KK, and IE conducted the expression and protein purification. SP performed the hemolytic assays. ML determined the secretion rates. JR generated the SAXS model of HlyA. OS and KK conducted the bioinformatic analyses. MM and BL performed the single particle cryo-EM experiments including data evaluation. OS, IE, KK, JR, SS, and LS wrote the manuscript. All authors read and approved the manuscript.

FUNDING

This work was supported by the Deutsche Forschungsgemeinschaft (DFG, CRC 1208 project A01 to LS) and the Manchot Graduate School "Molecules of Infections" to LS. The Center for Structural studies was funded by the DFG (Grant numbers 417919780 and INST 208/761-1 FUGG to SS). BL and MM were supported by ERC advanced award (742210).

ACKNOWLEDGMENTS

We are indebted to I. Barry Holland for a longstanding and fruitful collaboration. We acknowledge the European Synchrotron Radiation Facility for provision of synchrotron radiation facilities and we would like to thank Petra Pernot for assistance in using beamline BM29, as well as the whole EMBL Outstation Grenoble Team. We thank Iris Frey for support in cloning, and all members of the Institute of Biochemistry for the stimulating and helpful discussions.

REFERENCES

Bakkes, P. J., Jenewein, S., Smits, S. H., Holland, I. B., and Schmitt, L. (2010). The rate of folding dictates substrate secretion by the *Escherichia coli* hemolysin type 1 secretion system. *J. Biol. Chem.* 285, 40573–40580. doi: 10.1074/jbc.M110.173658

Baumann, U., Wu, S., Flaherty, K. M., and McKay, D. B. (1993). Three-dimensional structure of the alkaline protease of *Pseudomonas aeruginosa*: a two-domain protein with a calcium binding parallel beta roll motif. *EMBO J.* 12, 3357–3364. doi: 10.1002/j.1460-2075.1993.tb06009.x

Bumba, L., Masin, J., Macek, P., Wald, T., Motlova, L., Bibova, I., et al. (2016). Calcium-Driven folding of RTX domain beta-rolls ratchets translocation of RTX proteins through type i secretion ducts. *Mol. Cell* 62, 47–62. doi: 10.1016/j.molcel.2016.03.018

Chervaux, C., and Holland, I. B. (1996). Random and directed mutagenesis to elucidate the functional importance of helix II and F-989 in the C-terminal secretion signal of *Escherichia coli* hemolysin. *J. Bacteriol.* 178, 1232–1236. doi: 10.1128/jb.178.4.1232-1236.1996

Combet, C., Blanchet, C., Geourjon, C., and Deleage, G. (2000). NPS@: network protein sequence analysis. *Trends Biochem. Sci.* 25, 147–150. doi: 10.1016/s0968-0004(99)01540-6

Curtis-Fisk, J., Spencer, R. M., and Weliky, D. P. (2008). Native conformation at specific residues in recombinant inclusion body protein in whole cells determined with solid-state NMR spectroscopy. *J. Am. Chem. Soc.* 130, 12568–12569. doi: 10.1021/ja8039426

Felmlee, T., Pellett, S., and Welch, R. A. (1985). Nucleotide sequence of an *Escherichia coli* chromosomal hemolysin. *J. Bacteriol.* 163, 94–105.

Fischer, H., Neto, M. D., Napolitano, H. B., Polikarpov, I., and Craievich, A. F. (2010). Determination of the molecular weight of proteins in solution from a single small-angle X-ray scattering measurement on a relative scale. *J. Appl. Crystallogr.* 43, 101–109.

Gray, L., Mackman, N., Nicaud, J. M., and Holland, I. B. (1986). The carboxy-terminal region of haemolysin 2001 is required for secretion of the toxin from *Escherichia coli*. *Mol. Gen. Genet.* 205, 127–133. doi: 10.1007/BF02428042

Guinier, A. (1939). Small-angle X-ray diffraction: application to the study of ultramicroscopic phenomena. *Ann. Phys.* 12, 161–237.

Gygi, D., Nicolet, J., Frey, J., Cross, M., Koronakis, V., and Hughes, C. (1990). Isolation of the Actinobacillus pleuropneumoniae haemolysin gene and the activation and secretion of the prohaemolysin by the HlyC, HlyB and HlyD proteins of *Escherichia coli*. *Mol. Microbiol.* 4, 123–128. doi: 10.1111/j.1365-2958.1990.tb02021.x

Hagemans, D., Van Belzen, I. A., Moran Luengo, T., and Rudiger, S. G. (2015). A script to highlight hydrophobicity and charge on protein surfaces. *Front. Mol. Biosci.* 2:56. doi: 10.3389/fmolb.2015.00056

Hajizadeh, N. R., Franke, D., Jeffries, C. M., and Svergun, D. I. (2018). Consensus Bayesian assessment of protein molecular mass from solution X-ray scattering data. *Sci. Rep.* 8:7204. doi: 10.1038/s41598-018-25355-2

Highlander, S. K., Engler, M. J., and Weinstock, G. M. (1990). Secretion and expression of the Pasteurella haemolytica Leukotoxin. *J. Bacteriol.* 172, 2343–2350. doi: 10.1128/jb.172.5.2343-2350.1990

Holland, I. B., Peherstorfer, S., Kanonenberg, K., Lenders, M., Reimann, S., and Schmitt, L. (2016). Type I protein secretion-deceptively simple yet with a wide range of mechanistic variability across the family. *EcoSal Plus* 7, 1–46. doi: 10.1128/ecosalplus.ESP-0019-2015

Hui, D., and Ling, V. (2002). A combinatorial approach toward analyzing functional elements of the *Escherichia coli* hemolysin signal sequence. *Biochemistry* 41, 5333–5339. doi: 10.1021/bi011425g

Hui, D., Morden, C., Zhang, F., and Ling, V. (2000). Combinatorial analysis of the structural requirements of the *Escherichia coli* hemolysin signal sequence. *J. Biol. Chem.* 275, 2713–2720. doi: 10.1074/jbc.275.4.2713

Jarchau, T., Chakraborty, T., Garcia, F., and Goebel, W. (1994). Selection for transport competence of C-terminal polypeptides derived from *Escherichia coli* hemolysin: the shortest peptide capable of autonomous HlyB/HlyD-dependent secretion comprises the C-terminal 62 amino acids of HlyA. *Mol. Gen. Genet.* 245, 53–60. doi: 10.1007/BF00279750

Jones, H. E., Holland, I. B., Baker, H. L., and Campbell, A. K. (1999). Slow changes in cytosolic free Ca2+ in *Escherichia coli* highlight two putative influx mechanisms in response to changes in extracellular calcium. *Cell Calcium* 25, 265–274. doi: 10.1054/ceca.1999.0028

Jumper, J., Evans, R., Pritzel, A., Green, T., Figurnov, M., Ronneberger, O., et al. (2021). Highly accurate protein structure prediction with AlphaFold. *Nature* 596, 583–589. doi: 10.1038/s41586-021-03819-2

Jumpertz, T., Chervaux, C., Racher, K., Zouhair, M., Blight, M. A., Holland, I. B., et al. (2010). Mutations affecting the extreme C terminus of *Escherichia coli* haemolysin A reduce haemolytic activity by altering the folding of the toxin. *Microbiology* 156, 2495–2505. doi: 10.1099/mic.0.038562-0

Kanonenberg, K., Schwarz, C. K., and Schmitt, L. (2013). Type I secretion systems - a story of appendices. *Res. Microbiol.* 164, 596–604. doi: 10.1016/j.resmic.2013.03.011

Kelley, L. A., Mezulis, S., Yates, C. M., Wass, M. N., and Sternberg, M. J. (2015). The Phyre2 web portal for protein modeling, prediction and analysis. *Nat. Protoc.* 10, 845–858. doi: 10.1038/nprot.2015.053

Kenny, B., Chervaux, C., and Holland, I. B. (1994). Evidence that residues -15 to -46 of the haemolysin secretion signal are involved in early steps in secretion, leading to recognition of the translocator. *Mol. Microbiol.* 11, 99–109. doi: 10.1111/j.1365-2958.1994.tb00293.x

Kenny, B., Taylor, S., and Holland, I. B. (1992). Identification of individual amino acids required for secretion within the haemolysin (HlyA) C-terminal targeting region. *Mol. Microbiol.* 6, 1477–1489. doi: 10.1111/j.1365-2958.1992.tb00868.x

Kikhney, A. G., Borges, C. R., Molodenskiy, D. S., Jeffries, C. M., and Svergun, D. I. (2020). SASBDB: towards an automatically curated and validated repository for biological scattering data. *Protein Sci.* 29, 66–75. doi: 10.1002/pro.3731

Kim, M. K., and Kang, Y. K. (1999). Positional preference of proline in alpha-helices. *Protein Sci.* 8, 1492–1499. doi: 10.1110/ps.8.7.1492

Konarev, P. V., Volkov, V. V., Sokolova, A. V., Koch, M. H. J., and Svergun, D. I. (2003). PRIMUS: a Windows PC-based system for small-angle scattering data analysis. *J. Appl. Crystallogr.* 36, 1277–1282. doi: 10.1107/s0021889803012779

Koronakis, V., Koronakis, E., and Hughes, C. (1989). Isolation and analysis of the C-terminal signal directing export of *Escherichia coli* hemolysin protein across both bacterial membranes. *EMBO J.* 8, 595–605. doi: 10.1002/j.1460-2075.1989.tb03414.x

Kozin, M. B., and Svergun, D. I. (2001). Automated matching of high- and low-resolution structural models. *J. Appl. Crystallogr.* 34, 33–41. doi: 10.1107/s0021889800014126

Kuhnert, P., Heyberger-Meyer, B., Nicolet, J., and Frey, J. (2000). Characterization of PaxA and its operon: a cohemolytic RTX toxin determinant from pathogenic Pasteurella aerogenes. *Infect. immun.* 68, 6–12. doi: 10.1128/IAI.68.1.6-12.2000

Lamiable, A., Thevenet, P., Rey, J., Vavrusa, M., Derreumaux, P., and Tuffery, P. (2016). PEP-FOLD3: faster de novo structure prediction for linear peptides in solution and in complex. *Nucleic Acids Res.* 44, W449–W454. doi: 10.1093/nar/gkw329

Lenders, M. H., Beer, T., Smits, S. H., and Schmitt, L. (2016). *In vivo* quantification of the secretion rates of the hemolysin A Type I secretion system. *Sci. Rep.* 6:33275. doi: 10.1038/srep33275

Linhartova, I., Bumba, L., Masin, J., Basler, M., Osicka, R., Kamanova, J., et al. (2010). RTX proteins: a highly diverse family secreted by a common mechanism. *FEMS Microbiol. Rev.* 34, 1076–1112. doi: 10.1111/j.1574-6976.2010.00231.x

Mackman, N., Baker, K., Gray, L., Haigh, R., Nicaud, J. M., and Holland, I. B. (1987). Release of a chimeric protein into the medium from *Escherichia coli* using the C-terminal secretion signal of haemolysin. *EMBO J.* 6, 2835–2841.

Manalastas-Cantos, K., Konarev, P. V., Hajizadeh, N. R., Kikhney, A. G., Petoukhov, M. V., Molodenskiy, D. S., et al. (2021). ATSAS 3.0: expanded functionality and new tools for small-angle scattering data analysis. *J. Appl. Crystallogr.* 54, 343–355. doi: 10.1107/S1600576720013412

Masure, H. R., Au, D. C., Gross, M. K., Donovan, M. G., and Storm, D. R. (1990). Secretion of the Bordetella pertussis adenylate cyclase from *Escherichia coli* containing the hemolysin operon. *Biochemistry* 29, 140–145. doi: 10.1021/bi00453a017

Meier, R., Drepper, T., Svensson, V., Jaeger, K. E., and Baumann, U. (2007). A calcium-gated lid and a large beta-roll sandwich are revealed by the crystal structure of extracellular lipase from *Serratia marcescens*. *J. Biol. Chem.* 282, 31477–31483. doi: 10.1074/jbc.M704942200

Mol, A. R., Castro, M. S., and Fontes, W. (2018). NetWheels: a web application to create high quality peptide helical wheel and net projections. *bioRxiv* [Preprint]. doi: 10.1101/416347

Nicaud, J. M., Mackman, N., Gray, L., and Holland, I. B. (1986). The C-terminal, 23 kDa peptide of E. coli haemolysin 2001 contains all the information necessary for its secretion by the haemolysin (Hly) export machinery. *FEBS Lett.* 204, 331–335. doi: 10.1016/0014-5793(86)80838-9

Panjkovich, A., and Svergun, D. I. (2017). CHROMIXS: automatic and interactive analysis of chromatography-coupled small angle X-ray scattering data. *Bioinformatics* 34, 1944–1946. doi: 10.1093/bioinformatics/btx846

Pernot, P., Round, A., Barrett, R., De Maria Antolinos, A., Gobbo, A., Gordon, E., et al. (2013). Upgraded ESRF BM29 beamline for SAXS on macromolecules in solution. *J. Synchrotron Radiat.* 20, 660–664. doi: 10.1107/S0909049513010431

Pernot, P., Theveneau, P., Giraud, T., Fernandes, R. N., Nurizzo, D., Spruce, D., et al. (2010). New beamline dedicated to solution scattering from biological macromolecules at the ESRF. *J. Phys.* 247:012009. doi: 10.1088/1742-6596/247/1/012009

Petoukhov, M. V., Franke, D., Shkumatov, A. V., Tria, G., Kikhney, A. G., Gajda, M., et al. (2012). New developments in the ATSAS program package for small-angle scattering data analysis. *J. Appl. Crystallogr.* 45, 342–350. doi: 10.1107/S0021889812007662

Petoukhov, M. V., and Svergun, D. I. (2005). Global rigid body modeling of macromolecular complexes against small-angle scattering data. *Biophys. J.* 89, 1237–1250. doi: 10.1529/biophysj.105.064154

Petoukhov, M. V., and Svergun, D. I. (2015). Ambiguity assessment of small-angle scattering curves from monodisperse systems. *Acta Crystallogr. D Biol. Crystallogr.* 71, 1051–1058. doi: 10.1107/S1399004715002576

Porod, G. (1951). Die Röntgenkleinwinkelstreuung Von Dichtgepackten Kolloiden Systemen - 1 Teil. *Kolloid-Zeitschrift Zeitschrift Fur Polymere* 124, 83–114. doi: 10.1007/bf01512792

Rambo, R. P., and Tainer, J. A. (2013). Accurate assessment of mass, models and resolution by small-angle scattering. *Nature* 496, 477–481. doi: 10.1038/nature12070

Richardson, J. S., and Richardson, D. C. (1988). Amino acid preferences for specific locations at the ends of alpha helices. *Science* 240, 1648–1652. doi: 10.1126/science.3381086

Sanchez-Magraner, L., Viguera, A. R., Garcia-Pacios, M., Garcillan, M. P., Arrondo, J. L., de la Cruz, F., et al. (2007). The calcium-binding C-terminal domain of *Escherichia coli* alpha-hemolysin is a major determinant in the surface-active properties of the protein. *J. Biol. Chem.* 282, 11827–11835. doi: 10.1074/jbc.M700547200

Sapay, N., Guermeur, Y., and Deleage, G. (2006). Prediction of amphipathic in-plane membrane anchors in monotopic proteins using a SVM classifier. *BMC Bioinform.* 7:255. doi: 10.1186/1471-2105-7-255

Shen, Y., Maupetit, J., Derreumaux, P., and Tuffery, P. (2014). Improved PEP-FOLD approach for peptide and miniprotein structure prediction. *J. Chem. Theory Comput.* 10, 4745–4758. doi: 10.1021/ct500592m

Stanley, P., Koronakis, V., and Hughes, C. (1991). Mutational analysis supports a role for multiple structural features in the C-terminal secretion signal of *Escherichia coli* haemolysin. *Mol. Microbiol.* 5, 2391–2403. doi: 10.1111/j.1365-2958.1991.tb02085.x

Stanley, P., Packman, L. C., Koronakis, V., and Hughes, C. (1994). Fatty acylation of two internal lysine residues required for the toxic activity of *Escherichia coli* hemolysin. *Science* 266, 1992–1996. doi: 10.1126/science.7801126

Svergun, D. I. (1992). Determination of the regularization parameter in indirect-transform methods using perceptual criteria. *J. Appl. Crystallogr.* 25, 495–503. doi: 10.1107/s0021889892001663

Svergun, D. I., Petoukhov, M. V., and Koch, M. H. (2001). Determination of domain structure of proteins from X-ray solution scattering. *Biophys. J.* 80, 2946–2953. doi: 10.1016/S0006-3495(01)76260-1

Thevenet, P., Shen, Y., Maupetit, J., Guyon, F., Derreumaux, P., and Tuffery, P. (2012). PEP-FOLD: an updated de novo structure prediction server for both linear and disulfide bonded cyclic peptides. *Nucleic Acids Res.* 40, W288–W293. doi: 10.1093/nar/gks419

Thomas, S., Bakkes, P. J., Smits, S. H., and Schmitt, L. (2014a). Equilibrium folding of pro-HlyA from *Escherichia coli* reveals a stable calcium ion dependent folding intermediate. *Biochim. Biophys. Acta* 1844, 1500–1510. doi: 10.1016/j.bbapap.2014.05.006

Thomas, S., Smits, S. H., and Schmitt, L. (2014b). A simple *in vitro* acylation assay based on optimized HlyA and HlyC purification. *Anal. Biochem.* 464, 17–23. doi: 10.1016/j.ab.2014.07.001

Thompson, S. A., and Sparling, P. F. (1993). The RTX cytotoxin-related FrpA protein of *Neisseria meningitidis* is secreted extracellularly by meningococci and by HlyBD+ *Escherichia coli*. *Infect. immun.* 61, 2906–2911. doi: 10.1128/iai.61.7.2906-2911.1993

Vernon, R. M., Chong, P. A., Tsang, B., Kim, T. H., Bah, A., Farber, P., et al. (2018). Pi-Pi contacts are an overlooked protein feature relevant to phase separation. *Elife* 7:e31486. doi: 10.7554/eLife.31486

Wasmer, C., Benkemoun, L., Sabate, R., Steinmetz, M. O., Coulary-Salin, B., Wang, L., et al. (2009). Solid-state NMR spectroscopy reveals that E. coli inclusion bodies of HET-s(218-289) are amyloids. *Angew Chem. Int. Ed. Engl.* 48, 4858–4860. doi: 10.1002/anie.200806100

Welch, R. A. (2001). RTX toxin structure and function: a story of numerous anomalies and few analogies in toxin biology. *Curr. Topics Microbiol. Immunol.* 257, 85–111. doi: 10.1007/978-3-642-56508-3_5

Yin, Y., Zhang, F., Ling, V., and Arrowsmith, C. H. (1995). Structural analysis and comparison of the C-terminal transport signal domains of hemolysin A and leukotoxin A. *FEBS Lett.* 366, 1–5. doi: 10.1016/0014-5793(95)00454-h

Zimmermann, L., Stephens, A., Nam, S. Z., Rau, D., Kubler, J., Lozajic, M., et al. (2018). A Completely reimplemented mpi bioinformatics toolkit with a new hhpred server at its core. *J. Mol. Biol.* 430, 2237–2243. doi: 10.1016/j.jmb.2017.12.007

Conflict of Interest: The authors declare that the research was conducted in the absence of any commercial or financial relationships that could be construed as a potential conflict of interest.

Publisher's Note: All claims expressed in this article are solely those of the authors and do not necessarily represent those of their affiliated organizations, or those of the publisher, the editors and the reviewers. Any product that may be evaluated in this article, or claim that may be made by its manufacturer, is not guaranteed or endorsed by the publisher.

frontiers in Physiology

ORIGINAL RESEARCH
published: 28 February 2022
doi: 10.3389/fphys.2022.822509

Insights Into the Peroxisomal Protein Inventory of Zebrafish

Maki Kamoshita[1†‡], Rechal Kumar[1‡], Marco Anteghini[2,3], Markus Kunze[4], Markus Islinger[5], Vítor Martins dos Santos[2,3] and Michael Schrader[1]*

[1] College of Life and Environmental Sciences, Biosciences, University of Exeter, Exeter, United Kingdom, [2] LifeGlimmer GmbH, Berlin, Germany, [3] Systems and Synthetic Biology, Wageningen University & Research, Wageningen, Netherlands, [4] Center for Brain Research, Medical University of Vienna, Vienna, Austria, [5] Institute of Neuroanatomy, Mannheim Center for Translational Neuroscience, Medical Faculty Mannheim, Heidelberg University, Mannheim, Germany

OPEN ACCESS

Edited by:
Francisco F. De-Miguel, National Autonomous University of Mexico, Mexico

Reviewed by:
Andrés D. Klein, Universidad del Desarrollo, Chile
Araceli Del Arco, University of Castilla-La Mancha, Spain

***Correspondence:**
Michael Schrader
m.schrader@exeter.ac.uk

†Present address:
Maki Kamoshita, Department of Experimental Genome Research, Research Institute for Microbial Diseases, Osaka University, Osaka, Japan

‡These authors have contributed equally to this work

Specialty section:
This article was submitted to Membrane Physiology and Membrane Biophysics, a section of the journal Frontiers in Physiology

Received: 25 November 2021
Accepted: 07 February 2022
Published: 28 February 2022

Citation:
Kamoshita M, Kumar R, Anteghini M, Kunze M, Islinger M, Martins dos Santos V and Schrader M (2022) Insights Into the Peroxisomal Protein Inventory of Zebrafish. Front. Physiol. 13:822509. doi: 10.3389/fphys.2022.822509

Peroxisomes are ubiquitous, oxidative subcellular organelles with important functions in cellular lipid metabolism and redox homeostasis. Loss of peroxisomal functions causes severe disorders with developmental and neurological abnormalities. Zebrafish are emerging as an attractive vertebrate model to study peroxisomal disorders as well as cellular lipid metabolism. Here, we combined bioinformatics analyses with molecular cell biology and reveal the first comprehensive inventory of *Danio rerio* peroxisomal proteins, which we systematically compared with those of human peroxisomes. Through bioinformatics analysis of all PTS1-carrying proteins, we demonstrate that *D. rerio* lacks two well-known mammalian peroxisomal proteins (BAAT and ZADH2/PTGR3), but possesses a putative peroxisomal malate synthase (Mlsl) and verified differences in the presence of purine degrading enzymes. Furthermore, we revealed novel candidate peroxisomal proteins in *D. rerio,* whose function and localisation is discussed. Our findings confirm the suitability of zebrafish as a vertebrate model for peroxisome research and open possibilities for the study of novel peroxisomal candidate proteins in zebrafish and humans.

Keywords: peroxisomes, *Danio rerio*, proteome, lipid metabolism, organelle biogenesis, protein targeting, PTS1

INTRODUCTION

Peroxisomes represent ubiquitous, single-membrane bound subcellular compartments in eukaryotes. They are oxidative organelles with important functions in cellular lipid metabolism and redox homeostasis (Islinger et al., 2018). In mammals, peroxisomes perform a variety of essential metabolic functions including fatty acid α- and β-oxidation, degradation of D-amino acids, contribution to purine catabolism, and biosynthesis of ether lipids, polyunsaturated fatty acids and bile acids (Wanders and Waterham, 2006). Loss of peroxisomal functions causes severe disorders with developmental and neurological abnormalities, highlighting the importance of peroxisomes for human health. Loss of functional peroxisomes or enzyme deficiencies in humans result in an accumulation of undegraded molecules

Abbreviations: PEX, peroxin; PMP, peroxisomal membrane protein; PTS, peroxisomal targeting signal; TMD, transmembrane domain; VLCFA, very long chain fatty acids.

[e.g., very long chain fatty acids (VLCFA), bile acid intermediates, phytanic acid], while physiologically essential molecules (e.g., bile acids, plasmalogens, docosahexaenoic acid) become deficient. In addition to lipid metabolism, mammalian peroxisomes play a role in several non-lipid metabolic pathways such as purine, polyamine, glyoxylate, and amino acid metabolism. Due to their role in H_2O_2 metabolism and ROS homeostasis, peroxisomes have also been linked to cellular ageing and age-related disorders as well as cancer (Fransen et al., 2013; Islinger et al., 2018). Moreover, functions in cellular signalling and anti-viral defence have been revealed (Dixit et al., 2010; Lismont et al., 2019). However, the role of peroxisomes in the functioning of tissues and organs or during developmental processes remains largely unresolved.

The zebrafish (*Danio rerio*) is a popular vertebrate model organism for developmental biology and neurobiology due to its similarly to mammals. Advantages are the rapid development and short generation time, relatively low cost, ease of genetic manipulation and optical transparency of the developing fish, which in combination with novel imaging techniques allows the *in vivo* visualization of biological processes at the organism level (Dawes et al., 2020). In addition, zebrafish are used as a model to study lipid metabolism in lipid-related diseases (Hölttä-Vuori et al., 2010; Turchini et al., 2022). As peroxisomes are crucial for cellular lipid metabolism and developmental processes as well as neurological functions, zebrafish represent an attractive model to study peroxisome biology. In line with this, zebrafish has successfully been used as a model for adrenoleukodystrophy (ALD) (Strachan et al., 2017), a devastating disorder based on a defect in ABCD1, the peroxisomal transporter for VLCFA (Engelen et al., 2014). Very recently, a zebrafish model for Zellweger syndrome disorder (ZSD), a group of severe peroxisome biogenesis disorders caused by loss of peroxisome functions, has also been developed (Takashima et al., 2021).

Using diaminobenzidine (DAB)-cytochemistry for catalase, a classical peroxisomal marker, proxisomes were already visualised in the embryo and adult zebrafish by light- and electron microscopy (Braunbeck et al., 1990; Krysko et al., 2010). Similar to mammals and man, peroxisomes were most prominent in the liver, renal proximal tubules and the intestinal epithelium. Similarly to rodents, zebrafish hepatic peroxisomes respond to peroxisome proliferators with an increase in peroxisome number in liver when fish were exposed to fibrates or phthalate esters (Ortiz-Zarragoitia et al., 2006; Venkatachalam et al., 2012). In line with this, Peroxisome Proliferator-Activated Receptors (PPARs), nuclear hormone receptors, which regulate the expression of genes involved in lipid metabolism, have been identified in zebrafish (Den Broeder et al., 2015).

Peroxisomal matrix protein import is mediated by the peroxisomal import receptors PEX5 and PEX7, which bind to type-1 or type-2 peroxisomal targeting signals (PTS1 or PTS2) on cargo proteins in the cytosol. The PTS1 receptor PEX5 recognises a C-terminal tripeptide (SKL-type), whereas PEX7 recognises a nonapeptide within the N-terminus (Walter and Erdmann, 2019; Kunze, 2020). Several predictors have been developed to identify peroxisomal proteins, their PTS, and their sub-peroxisomal location (Kunze, 2018; Anteghini et al., 2021).

Despite growing interest, a comprehensive analyis of the *D. rerio* peroxisomal protein inventory and metabolic pathways associated with peroxisomes as well as of peroxisomal targeting signals is still missing. In this study, we combined bioinformatics analyses with molecular cell biology, and provide the first comprehensive inventory of peroxisomal proteins, their targeting signals and association with metabolic pathways in zebrafish. A comparison with *H. sapiens* gained new insights into the basic peroxisomal protein inventory shared among vertebrates and revealed novel candidate peroxisomal proteins and functions in *D. rerio*. We show that *D. rerio* peroxisomal functions do not vary considerably from those in humans confirming the suitability of zebrafish as a vertebrate model for peroxisome research. Our findings open possibilities for the study of novel peroxisomal candidate proteins in zebrafish and humans.

MATERIALS AND METHODS

Search for Potential Peroxisomal Proteins in *Danio rerio*

The *Danio rerio* proteome available on UniProt[1] was screened for proteins carrying a PTS1 at the very C-terminus using all possible combinations of residues found in PTS1 motifs (consensus) [ASCNPHTG]-[RKHQNSL]-[LMIVF] (Lametschwandtner et al., 1998; Neuberger et al., 2003; **Figure 1**). Among 46,848 proteins, we identified 2,638 proteins matching the pattern. We analysed the corresponding fasta sequences using the software TMHMM Server v. 2.0[2] (Krogh et al., 2001). The entries with defined topologies 'o' (out) or 'i' (in), without transmembrane helices, were kept as well as the entries with a ratio $\geq$ 0.9 between the expected number of amino acids in transmembrane helices and the expected number of amino acids in transmembrane helices in the first 60 amino acids of the protein (with transmembrane helices just in the signal peptide) resulting in 1,966 protein sequences (**Figure 1**). We executed locally WoLF PSORT (Package Command Line Version 0.2) (Horton et al., 2007) to obtain the predicted subcellular location of each specific protein. Entries with "ER" as possible subcellular localization were removed, resulting in 1,171 sequences. Thereafter, the identified proteins were further analysed by PTS1 predictor algorithms[3] (Neuberger et al., 2003; Schlüter et al., 2010) and sequences which produced no hit with the "metazoa" or "general" modus of the software were removed (**Figure 1**). For further validation selected sequences were screened for conservation of the potential PTS1 using BLAST2.0. Additionally, mitochondrial targeting was examined using Mitoprot2 (Claros and Vincens, 1996); and Predotar1.03 (Small et al., 2004); potential targeting to the secretory pathway was screened with TargetP1.1 (Emanuelsson et al., 2000). Peroxisomal targeting signal 2 (PTS2) was analysed by PTS2 prediction algorithms (Schlüter et al., 2007). Functions were attributed to the potential peroxisomal proteins with regard

[1] www.uniprot.org

[2] https://services.healthtech.dtu.dk/service.php?TMHMM-2.0

[3] https://mendel.imp.ac.at/pts1/

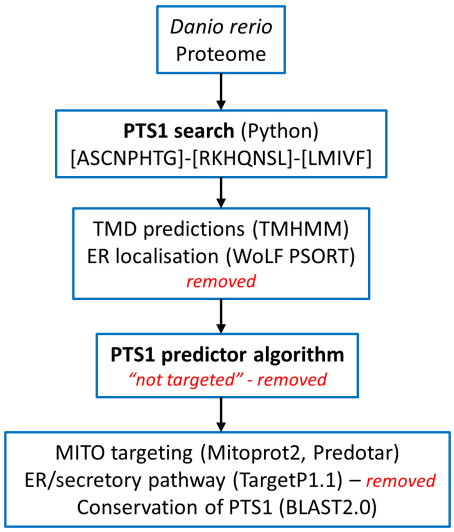

FIGURE 1 | Overview of the screening of the *Danio rerio* proteome to identify candidate proteins with a C-terminal peroxisomal targeting sequence (PTS1). See Materials and Methods for details.

to their homology to known proteins from other species and proteins were organised into specific metabolic pathways. The ZFIN zebrafish information network database[4] was screened for peroxisomal proteins (e.g., without a PTS1) including PMPs and peroxisome biogenesis factors (peroxins), by key word search and BLAST analysis. Furthermore, published data (Pub Med) was included (e.g., Jansen et al., 2021). Protein sequence alignment was performed by Clustal Omega (1.2.4) Multiple Sequence Alignment (Madeira et al., 2019).

Mammalian Cell Culture and Transfection

COS-7 (African green monkey kidney cells, CRL-1651; ATCC) and HEK293T (Human embryonic kidney 293T cells; ECACC) cells were maintained in Dulbecco's Modified Eagle's Medium (DMEM), high glucose (4.5 g/L) supplemented with 10% fetal bovine serum (FBS), 100 U/ml penicillin and 100 µg/ml streptomycin (all from Life Technologies) at 37°C with 5% CO2 and 95% humidity. COS-7 cells were transfected with DNA constructs either by incubation with diethylaminoethyl (DEAE)-dextran (Sigma-Aldrich) (Bonekamp et al., 2010) or Turbofect (Thermo Fisher Scientific) (**Supplementary Table S1**). For DEAE-transfection, 4 µg of plasmid DNA were mixed with 0.5 ml serum-free DMEM and 4 µg of DEAE–Dextran. The mixture was applied to a 60-mm dish of non-confluent cells after washing twice with PBS. After incubating 1.5 h at 37°C in a humidified incubator the DEAE–Dextran–DNA mixture was removed and 4 ml complete DMEM as well as 4 µl of chloroquine (Serva, Heidelberg, Germany) (60 mg/ml stock solution) were added. After 3 h the medium was changed to complete DMEM. For lipofection, 1 µg of DNA [0.1 µg EGFP-reporter plasmid and 0.9 µg vector DNA without EGFP (pcDNA3.1)] was premixed with 100 µl DMEM without supplements and 1.25 µl of Turbofect was added. After 15 min incubation at room temperature the mixture was dropped onto COS7 cells in 400 µl fresh complete DMEM medium (24-well plate). After 24 h cells were trypsinized and 50% of the cells were seeded on glass coverslips (24-well plate). Cells were processed 24-48 h after transfection for immunofluorescence microscopy.

Immunofluorescence and Microscopy

Cells grown on glass coverslips were fixed for 20 min with 4% para-formaldehyde in PBS, pH 7.4, permeabilised with 0.2% Triton X-100 (10 min), blocked with 1% BSA (10 min) and sequentially incubated with primary and secondary antibodies for 1 h in a humid chamber at room temperature (Bonekamp et al., 2013). Rabbit anti-PEX14 (1:1400) (Grant et al., 2013) (generated by D. Crane, Griffith University, Brisbane, Australia), anti-PMP70 (1:3000) (ABR, Golden, CO, United States), and mouse anti-Myc primary antibody (1:100) [Santa Cruz Biotechnology, Inc (9E10)] were used. Species-specific Alexa Fluor 488 (594) labelled secondary antibodies (1:500) (Thermo Fisher Scientific) and Cy3-labelled Donkey-anti-rabbit IgG (1:400) (Jackson Immuno Research Laboratories, West Grove, PA, United States) were applied. Microscopy analysis was performed using an Olympus IX81 microscope (Olympus Optical. Hamburg, Germany) equipped with an UPlanSApo 100 × /1.40 oil objective (Olympus) and a CoolSNAP HQ2 CCD camera. Digital images were taken and processed using VisiView software (Visitron Systems). Images were adjusted for contrast and brightness using MetaMorph 7 (Molecular Devices).

Molecular Cell Biology and Generation of Plasmids

For cloning of human genes, total RNA was extracted from HEK cells using Nucleo Spin RNA II kit (Macherey-Nagel- NZ74095550) and reverse transcribed into cDNA using SuperScript® II Reverse Transcriptase kit (Invitrogen/Fisher). N-terminally Myc-tagged expression constructs for human CDC5L (NM_001253.4) (Cell division cycle 5-like protein) (Myc-*Hs*CDC5L) and KCTD5 (NM_018992.4) (Potassium channel tetramerization domain-containing 5) (Myc-*Hs*KCTD5) were generated. Human CDC5L (Q99459) and KCTD5 (Q9NXV2) were amplified from HEK cDNA, and the PCR products inserted into pCMV-Tag-3 vector (Agilent Technologies, La Jolla, CA, United States) (**Supplementary Tables S1**, **S2**).

To test the functionality of putative PTS1 or PTS2 motifs, reporter proteins were used. For PTS1 motifs the plasmid EGFP-C3 (Clontech) was digested with *Bgl*II/*Hin*dIII and the respective oligonucleotides were inserted as described previously (Chong et al., 2019; **Supplementary Tables S1**, **S2**). This generated plasmids PTS1-*Dr*Urad DLHSIVLSDIQTKL, PTS1-*Dr*Meox2a DLHDSDQSSDHAHL, PTS1-*Dr*Cdc5l DLLMLDKQTLSSKI, PTS1-*Dr*Kctd5a DLKAKILQEQGSRM, and PTS1-*Hs*CDC5L DLLLEKETLKSKF. For PTS2 motifs the reporter plasmid PTS2-tester (Kunze et al., 2011) was digested with *Eco*RI and *Pst*I and the oligonucleotides (Oli_2982 and Oli_2983) were inserted to generate PTS2-*Dr*Urah RLQHIRGHI

[4]https://zfin.org/

(**Supplementary Tables S1**, **S2**). In-frame insertion of all constructs was verified by sequencing (Eurofins Genomics).

RESULTS AND DISCUSSION

The study of model organisms has greatly contributed to our understanding of peroxisome biology. Fungal model systems greatly contributed to the identification of peroxisome biogenesis factors (peroxins, PEX), and to the understanding of protein import and peroxisome functions. The fruitfly *Drosophila melanogaster* has also been established as a non-vertebrate model organism to study peroxisomes (Pridie et al., 2020). In addition, several mouse models have been developed to investigate the physiological role of peroxisomes and their impact on human disease (Van Veldhoven and Baes, 2013). The zebrafish *Danio rerio* is now developing as a promising vertebrate model to investigate peroxisome biology (Van Veldhoven and Baes, 2013), but a comprehensive analysis of the *D. rerio* peroxisomal protein inventory, metabolic pathways and protein targeting is lacking. To delineate the peroxisomal proteome of *D. rerio* as well as targeting information of candidate proteins, we performed a comprehensive bioinformatics analysis (**Figure 1**). For identification of proteins with a potential peroxisomal targeting signal, we screened the proteome of *D. rerio*[5] for proteins with a PTS1 or PTS2 sequence (PTS2 based on orthologous protein sequences). These are recognised by the matrix protein import receptors PEX5 and PEX7, respectively (**Figure 2**). The initial PTS1 search was performed with the broader consensus [ASCNPHTG]-[RKHQNSL]-[LMIVF] (Lametschwandtner et al., 1998; Neuberger et al., 2003) to also detect potential non-canonical C-terminal PTS1 sequences (and resulted in 2,638 proteins). We then determined potential ER targeting signals as well as the presence of transmembrane domains (TMD). Proteins with an ER signal peptide or TMD were excluded resulting in 1171 proteins. The identified candidate proteins were afterward analysed by PTS1 predictor algorithms, which consider 12 aa at the C-terminus. This approach resulted in a total of 371 candidate proteins with a potential PTS1 (**Supplementary Tables S3**, **S4**). Of those, 204 had a predicted weak targeting signal (twilight zone). We attributed functions to the candidate proteins based on homology to known proteins from other species and organised them into specific metabolic pathways. This was in part supported by literature and database search (ZFIN; PODB) (**Table 1** and **Supplementary Table S3**). Peroxisomal membrane proteins and peroxins were identified by key word and database search as well as BLAST analysis.

Comparison of the Classical Peroxisomal Protein Inventory Shared by Humans and Zebrafish

In the following, we present the results of our comprehensive analysis of the *D. rerio* peroxisomal protein inventory and metabolic pathways associated with peroxisomes. First, we present and discuss the "core" peroxisomal proteins involved in biogenesis, dynamics and metabolic pathways including fatty acid oxidation, ether lipid biosynthesis, purine catabolism and ROS metabolism. Furthermore, we link our analyses to recent publications on peroxisome research in zebrafish providing a timely overview.

Peroxin Proteins

Peroxins (encoded by PEX genes) represent proteins essential for the biogenesis of peroxisomes. They include PEX proteins required for peroxisomal matrix protein import, membrane biogenesis, and peroxisome proliferation. *D. rerio* encodes orthologues of all 14 human peroxins (**Figure 2** and **Supplementary Table S3**). They belong to the core of PEX proteins that are broadly conserved in most eukaryotes, including PEX3/16/19 (peroxisomal membrane protein sorting), PEX1/6, PEX2/10/12, PEX13/14, and PEX5/7 (matrix protein import) and proteins of the PEX11 family (peroxisome proliferation) (**Figure 2** and **Supplementary Table S3**). Overall, 37 peroxins have been identified in yeast, plants and animals (including functional orthologues). Being a vertebrate, *D. rerio* most closely reflects the situation in humans. Interestingly, *Dr*Pex3 possesses a predicted N-terminal mitochondrial targeting signal (MTS) (**Figure 2** and **Supplementary Table S3**). Potentially hidden N-terminal MTS are also found in human PEX3 and may explain its mistargeting to mitochondria in the absence of peroxisomes (Sugiura et al., 2017). Like *H. sapiens*, *D. rerio* encodes three isoforms of Pex11 (Pex11a, Pex11b, Pex11g), which in mammals are involved in the growth, division and proliferation of peroxisomes. In addition to the PTS1 receptor Pex5, two Pex5-related proteins (Pex5la; Pex5lb) are present in *D. rerio*. It should be noted that zebrafish often harbour two copies of many genes. This is due to a genome wide duplication event, which took place approx. 350 million years ago when the bony fishes diverged from the common ancestor with humans (Hölttä-Vuori et al., 2010). The duplicated genes often exhibit differential tissue expression patterns with partitioning of ancestral functions, rather than the evolution of completely new functions (Force et al., 1999). The Pex5-related proteins may represent paralogs of Pex5, which may no longer function in peroxisomal matrix protein import. PEX5-related proteins are found in other vertebrates; PEX5R/TRIP8b (tetratrico-peptide-repeat containing, Rab8b-interacting protein) is involved in the regulation of hyperpolarization-activated cyclic nucleotide-gated (HCN) channels in the mammalian central nervous system (Han et al., 2020). Although PEX5R can bind PTS1-containing proteins *in vitro* (Amery et al., 2001), there is currently no evidence for a role in peroxisome biogenesis as PEX5R does not complement loss of PEX5. The PTS1 receptor Pex5 of *D. rerio* contains several characteristic tetratricopeptide repeats (TPR) at the C-terminus involved in the interaction with the PTS1 cargo, and a disordered region at the N-terminus. The latter contains a PEX7-binding domain which is conserved in PEX5 proteins of several species (e.g., PEX5L, the long isoform in humans) (**Figure 2** and **Supplementary Figure S1**; Jansen et al., 2021) and enables function as a PEX7 co-receptor for PTS2

[5]https://www.uniprot.org/proteomes/UP000000437

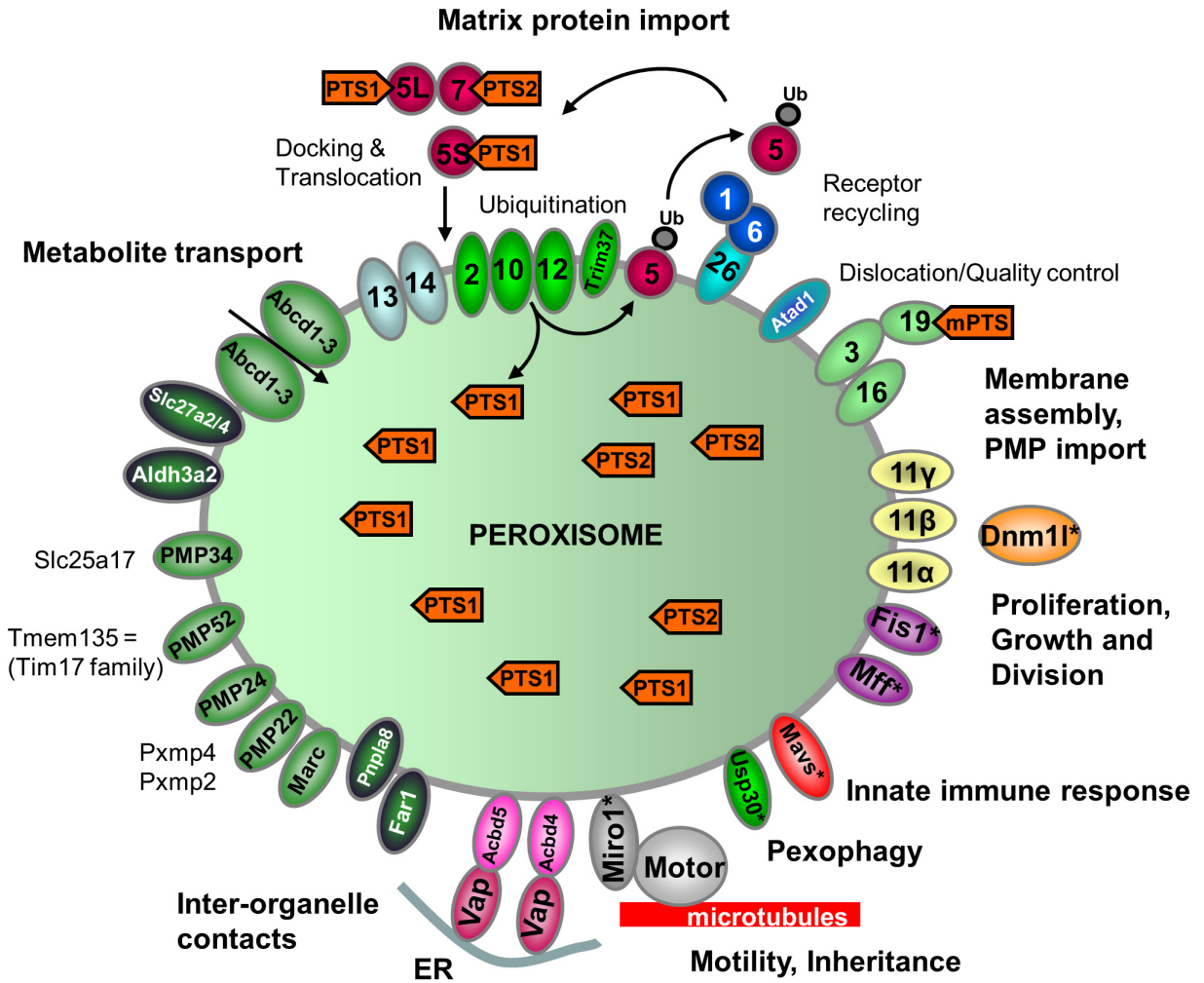

FIGURE 2 | Schematic overview of the predicted molecular machineries and *D. rerio* proteins localized at the membranes of peroxisomes in zebrafish. See text for further details. *Matrix protein import*: after synthesis on free ribosomes, cargo proteins containing the peroxisomal targeting signals PTS1 or PTS2 bind to the corresponding cytosolic receptors Pex5 (E7FGF7) or Pex7 (A8KBW8) (Pex-proteins are indicated as sole numbers) and form receptor–cargo complexes. The Pex7–cargo complex requires accessory factors for import (e.g., Pex5L, a long isoform of Pex5). Import is achieved by a complex set of integral or peripheral PMPs that form the matrix protein import machinery, which mediates docking of the cargo-bound import receptor at the peroxisomal membrane [Pex13 (Q6PFQ3), Pex14 (A0A2R8QMZ2)], cargo translocation into the matrix of the organelle by a dynamic translocon [Pex2 (E7F4V8), Pex10 (Q5XJ92), Pex12 (B0R157)], and export of the receptor back to the cytosol [Pex1 (A0A0R4IPF0), Pex6 (F1QMB0)]. Recycling of the receptor involves its ubiquitination (Ub) and extraction from the membrane by an AAA–ATPase complex (Pex1, Pex6). Pex6 binds to the membrane protein Pex26 (F1RBL0). *Membrane assembly and insertion of PMPs* (containing an mPTS) depend on Pex19 (F1R313), Pex3 (Q5RIV3), and Pex16 (F1RDG2). Pex19 functions as a cycling receptor/chaperone, which binds the PMPs in the cytosol and interacts with Pex3 at the peroxisomal membrane. *Proliferation, growth and division*: Pex11α (A3QJY9), Pex11β (Q0P453), and Pex11γ (Q4V8Z0) are involved in the regulation of peroxisome size and number (proliferation). Pex11β remodels the peroxisomal membrane and interacts with the membrane adaptors Mff (F1Q877; A8E7S0) and Fis1 (A0A2R8Q8G0), which recruit the dynamin 1-like fission GTPase Dnm1l to peroxisomes, which in mammals is activated by Pex11β. *Motility*: mammalian peroxisomes move along microtubules, and Miro/Rhot (Rhot1a, Q6NVC5; Rhot1b, A0A0R4IGX0; Rhot2, Q32LU1) serves as membrane adaptor for the microtubule-dependent motor proteins kinesin and dynein. *Tethering*: Acbd5 (E9QCH6; A5WV69) and Acbd4 (F1QA31) interact with ER-resident Vap (Vapb, Q6P2B0) to mediate peroxisome–ER contacts. *Metabolite transport*: uptake of fatty acids in *D. rerio* peroxisomes is mediated by ABC transporter proteins (Abcd1, F1RBC8; Abcd2, E7F973; Abcd3a, A0A0R4IRL4; Abcd3b, B0UY91). Other peroxisomal transporter and membrane proteins in zebrafish include (functions are in part unclear): PMP34 (Slc25a17) (A5D6T2), a peroxisomal CoA transporter; PMP52 (Tmem135) (A4QN71) and PMP24 (Pxmp4) (A0A2R8QFW3) belong to the Tim17 family of transporters; PMP22 (Pxmp2) (Q66HU7); Slc27a2/4 (F1QQC5, Q1ECW0; Q567D7), acyl-CoA synthetase long chain family member; Marc (A0A2R8PWS6), mitochondrial amidoxime reducing component; Atad1 (A0A2R8RM20, B2GP29), ATPase family AAA (ATPase associated with various cellular activities) domain-containing protein 1 with a potential role in dislocation/quality control of tail-anchored membrane proteins; Aldh3a2 (A0A2R8PW97, E9QH31), fatty aldehyde dehydrogenase; Far1/2 (A0A0R4ICF6/Q1L8Q4), fatty acyl-CoA reductase 1/2 (ether lipid biosynthesis); Mavs (F1REK4), mitochondrial antiviral signalling protein with a putative role in innate immune response; Trim37 (E7FBZ8), tripartite motif-containing protein 37, an E3 ubiquitin-protein ligase involved in Pex5 mediated peroxisomal matrix protein import; Usp30 (A2BGT0), ubiquitin-specific protease 30, a deubiquitinase involved in the turnover of peroxisomes; Pnpla8 (F1RE62), Patatin-like phospholipase domain-containing 8. Proteins with a potential dual localization to both peroxisomes and mitochondria are marked with an asterisk. Pex, peroxin; PMP, peroxisomal membrane protein (adapted from Islinger et al., 2018, but containing the zebrafish specific nomenclature).

TABLE 1 | Inventory of *Danio rerio* peroxisomal proteins and metabolic pathways in comparison to *H. sapiens*.

Function/pathway			Protein		Dr	Hs
Fatty acid activation			Very long-chain acyl CoA synthase (Slc27a2/Fatp2)			
			Very long-chain acyl CoA synthase (Slc27a4/Fatp4)			
FA-CoA transport			ABC transporter class D (Abcd1-3)			
			Acyl-CoA binding domain proteins (Acbd5, Acbd4)			
Lipid metabolism	Core enzymes	FA β-oxidation	Acyl-CoA oxidases (Acox)	Acox1		
				Acox2	–	
				Acox3		
				Acoxl		
			Acyl CoA dehydrogenase 11 (Acad11)			
			Bifunctional enzymes	Enoyl-CoA hydratase, hydroxyacyl-CoA dehydrogenase (Ehhadh) (L-BP)		
				Hydroxysteroid (17-beta) dehydrogenase 4 (Hsd17b4) (D-BP)		
			Thiolases	3-Ketoacyl-CoA thiolase/ Acetyl-CoA acyltransferase (Acaa1)	PTS2	PTS2
				Sterol carrier protein (Scp2)		
	Accessory enzymes	β-oxidation	Alpha-methylacyl-CoA racemase (Amacr)			
			Peroxisomal trans-2-enoyl-CoA reductase (Pecr)			
		Bile acid synthesis	Bile acid-CoA:amino acid N-acyltransferase (Baat)		–	
		α-oxidation	Phytanoyl-CoA 2-hydroxylase (Phyh)		PTS2	PTS2
			2-Hydroxyphytanoyl-CoA lyase (Hacl1)			
			Fatty aldehyde dehydrogenase (Aldh3a2)			
		Saturation PUFAS	2,4-dienoyl-CoA reductase (Decr2)			
			3,2-enoyl-CoA isomerase (Eci2)			
			Peroxisomal enoyl CoA hydratase 1 (Ech1)			
		FA-CoA deactivation/export	Peroxisomal acyl-CoA thioesterase (Acot8)			
			Acyl-CoA thioesterase (Acot4)		–	
			Peroxisomal carnitine O-octanoyltransferase (Crot)			
			Carnitine O-acetyltransferase (Crata)			
Ether lipid synthesis			Glycerone phosphate O-acyltransferase (Gnpat)			
			Alkyldihydroxyacetone phosphate synthase (Agps)		PTS2	PTS2
			Fatty acyl-CoA reductase (Far1/2)			
			Alkyldihydroxyacetone phosphate reductase (Dhrs7b)			
Glycolate/Glyoxylate metabolism			Hydroxyacid oxidase 1 (Hao1)			
			Hydroxyacid oxidase 2 (Hao2)			
			Hydroxyacid oxidase 3 (Hao3)		–	
			Malate synthase-like (Mlsl)			–
			Alanine-glyoxylate aminotransferase (Agxta)			
Amino acid catabolism			D-amino acid oxidase 1 (Dao1)			
			D-amino acid oxidase 2 (Dao2)			–
			D-amino acid oxidase 3 (Dao3)			–
			D-aspartate oxidase (Ddo)			
			3-hydroxy-3-methylglutaryl CoA lyase (Hmgcl)			
			Pipecolic acid oxidase (Pipox)			
Amine metabolism			Peroxisomal (poly)amine oxidase (Paox)			
Purine and pyrimidine metabolism			Urate oxidase (Uricase) (Uox)			–[1]
			Allantoicase (Allc)			–
			Urate (5-hydroxyiso-) hydrolase a (Uraha)		PTS2	–[1]
			Ureidoimidazoline decarboxylase (Urad)			–[1]
Oxygen metabolism/Oxidation redox equivalents			Catalase (Cat)			
			Epoxide hydrolase 2 (Ephx2)			
			Glutathione S-transferase kappa 1 (Gstk1)			
			Copper chaperone of SOD1 (Ccs)			
			Superoxide dismutase 1 (Sod1)			
			Peroxiredoxin 5 (Prdx5)			

(Continued)

TABLE 1 | (Continued)

Function/pathway	Protein	Dr	Hs
	Nitric oxide synthase 2 (Nos2)	■	■
Proteases	Insulin-degrading enzyme (Ide)	■	■
	Peroxisomal LON protease-like (Lonp2)	■	■
	Trypsin domain containing 1 (Tysnd1)	■	■
Carbohydrate metabolism	Glucose 6-phosphate dehydrogenase (G6pd)	■	■
	Isocitrate dehydrogenase (Idh)	■	■
	Peroxisomal malate dehydrogenase (Mdh)	■	■
	Lactate dehydrogenase B (LDHB)	■	■
	Glycerol-3-phosphate dehydrogenase 1 (Gpd1)	■	■
Cleavage of cofactors	Coenzyme A diphosphatase (Nudt7)	■	■
	Coenzyme A diphosphatase (Nudt19)	■	■
	NADH pyrophosphatase (Nudt12)	■	■
Retinoid metabolism	Short-chain alcohol dehydrogenase/Dehydrogenase/reductase SDR family member 4	■	■
L-Ascorbate synthesis	L-gulonolactone oxidase (Gulo)	–	–
Peroxisome division	Mitochondrial fission 1 (Fis1)	■	■
	Mitochondrial fission factor (Mff)	■	■
	Dynamin-like protein 1 (Dnm1l)	■	■
Peroxisome motility	Rhot1 (Miro1)	■	■
	Rhot2 (Miro2)	■	■
Misc. peroxisomal membrane proteins	Slc25a17 (PMP34) (CoA transporter in Dr)	■	■
	Pxmp2 (PMP22)	■	■
	Pxmp4 (PMP24)	■	■
	Tmem135 (PMP52)	■	■
	Mpv17/Mpv17-like	■	■
	Mitochondrial amidoxime reducing component (Marc/Mosc)	■	■
	Mitochondrial antiviral-signaling protein (Mavs)	■	■
	ATPase family AAA domain containing 1 (Atad1)	■	■
	Ubiquitin carboxyl-terminal hydrolase 30 (Usp30)	■	■
	Slc22a21 (Organic cation transporter)	■	■
	Tripartite motif-containing 37 (Trim37)	■	■
	Patatin-like phospholipase domain-containing 8 (Pnpla8)/Calcium-independent phospholipase A2γ	■	■
	Fibronectin type III domain containing 5 (Fndc5b)	■	■
Other proteins with PTS1 in Dr or Hs	Serine hydrolase-like protein (Serhl)	■	■
	Dehydrogenase/reductase (SDR family) member 4 (Dhrs4)	■	■
	Ubiquitin carboxyl-terminal hydrolase (Usp2 – short)	■	■
	Ubiquitin carboxyl-terminal hydrolase (Usp2 – long)	■	■
	Isochorismatase domain containing 1 (Isoc1)	■	■
	β-Lactamase-like protein 2 (Lactb2)	■	■
	Hydroxysteroid dehydrogenase-like 2 (Hsdl2)	■	■
	CoA synthase (coasy)	■	■
	Acyl-CoA thioesterase (Acot14)	■	–
	Acyl-CoA thioesterase (Acot15)	■	■
	Acyl-CoA thioesterase (Acot16)	■	–
	Acyl-CoA thioesterase (Acot17)	■	–
	Acyl-CoA thioesterase (Acot18)	■	–
	Acyl-CoA thioesterase (Acot20)	■	■
	Cell division cycle 5-like protein (Cdc5l)	■	■
	Potassium channel tetramerization domain-containing 5 (Kctd5)	■	■
	Kelch-like protein 41 (Klhl41b)	■	■
	Prostaglandin reductase 3 (ZADH2/PTGR3)	–[2]	■

Hs, H. sapiens; Dr, D. rerio.
□ *– absent/not identified.*
■ *– Protein present, peroxisomal and/or with a predicted PTS1/PTS2.*
■ *– Protein present without a confirmed PTS or peroxisomal localization.*
[1] *inactivation by pseudogenization.*
[2] *lost in Cypriniformes.*

import (Kunze, 2020). This indicates that Pex5 is required as a co-receptor for Pex7-mediated PTS2 import in *D. rerio*.

While Pex7 (and PTS2 cargo proteins) are present in *D. rerio*, other model organisms such as the nematode *C. elegans*, lack PEX7 and a PTS2 targeting pathway (Motley et al., 2000). A PTS2 import pathway is also lacking in the fruit fly *D. melanogaster*, but PEX7 is present (Pridie et al., 2020). *C. elegans* and *D. melanogaster* also appear to lack PEX26, the anchoring protein for PEX1/6, which is present in *D. rerio* and other vertebrates (Jansen et al., 2021). The AAA (ATPase associated with diverse cellular activities) ATPases PEX1 (Pex1, A0A0R4IPF0_DANRE) and PEX6 (Pex6, F1QMB0_DANRE) are required for PEX5 export from the peroxisomal membrane in order to recycle it back to the cytosol. Like in humans, *D. rerio* Pex26 is a tail-anchored membrane protein supposed to retain Pex1 and Pex6 at the membrane (**Figure 2** and **Supplementary Table S3**).

Very recently, a zebrafish model for Zellweger spectrum disorders, a group of severe peroxisome biogenesis disorders based on defects in PEX genes has been developed (Takashima et al., 2021). Disruption of the zebrafish *pex2* gene (encoding an E3 ubiquitin ligase with a zinc RING finger domain residing in the peroxisomal membrane, which is involved in matrix protein import/receptor recycling) caused phenotypes similar to human patients suffering from ZSD including locomotive defects, eating disabilities, liver abnormalities and early death (Takashima et al., 2021). Similar to the human disease, the ZS model fish also showed increased tissue levels of VLCFA and branched chain fatty acids as well as a reduction in ether phospholipids. Furthermore, mutant specific gene-expression changes, that might lead to the symptoms, were detected including a reduction in crystallin (lens), troponin, parvalbumin (muscle contraction), and fatty acid metabolic genes.

Proteins Involved in Peroxisome Division and Motility

In addition to PEX11 proteins, which are involved in membrane remodelling and growth/expansion of the peroxisomal membrane prior to division, the tail-anchored adaptor proteins FIS1 and MFF are required, which recruit the fission GTPase DRP1/DLP1 to the peroxisomal membrane (Schrader et al., 2016; **Figure 2**). Homologues of those proteins have been identified in *D. rerio* (Fis1, Mffa, Mffb, Dnm1l) (**Table 1** and **Supplementary Table S3**). Interestingly, they are shared with mitochondria and also mediate mitochondrial division. In addition, the orthologues of the tail-anchored adaptor proteins Miro1/2 (Rhot1a, Rhot1b, Rhot2) are present in *D. rerio*. In mammals they have been implicated in the recruitment of microtubule motor proteins (e.g., kinesin) to peroxisomes (and mitochondria) and regulation of organelle motility. The Miro-motor complex can exert pulling forces at the peroxisome membrane, which also contribute to membrane elongation/expansion and division (Castro et al., 2018; Covill-Cooke et al., 2021). Targeting of the tail-anchored membrane proteins to peroxisomes is mediated by a combination of biochemical properties of the TMD and tail region (TMD hydrophobicity; positive net charge of the tail) and depends on PEX19, the import receptor/chaperone for PMPs (Costello et al., 2017a; **Figure 2**). In addition to its role in matrix protein import, PEX14 may act as docking factor to microtubules via its N-terminal tubulin binding domain (aa 1-78) (Reuter et al., 2021), which is conserved between *H. sapiens* and *D. rerio*.

Peroxisomal Metabolism

Fatty Acid β-Oxidation

Peroxisomes fulfil important functions in cellular lipid metabolism, often in cooperation with other subcellular compartments such as mitochondria, ER and lipid droplets (Silva et al., 2020). The β-oxidation of fatty acids is an important and conserved peroxisomal pathway (see overview **Figure 3A**). Fatty acid β-oxidation is distributed between peroxisomes and mitochondria in animals and several fungi, but exclusively peroxisomal in yeast and plants. In line with this, we identified candidate genes coding for all the enzymes required for a peroxisomal and a mitochondrial fatty acid β-oxidation pathway in *D. rerio* (**Table 1** and **Supplementary Table S3**). Substrates for peroxisomal β-oxidation are VLCFA (>C22:0), branched chain fatty acids (e.g., pristanic acid), bile acid intermediates [such as di- and tri-hydroxycholestanoyl-CoA (DHCA, THCA)], poly-unsaturated fatty acid (e.g., docosahexaenoic acid), long chain dicarboxylic acids, 2-hydroxy fatty acids, and a number of prostanoids. Mitochondria on the other hand preferentially β-oxidise long chain, medium chain, and short chain fatty acids (C18 and shorter).

Fatty acid degradation is preceded by activation of fatty acids through conjugation to coenzyme A and subsequent import into peroxisomes by members of the ATP-binding cassette (ABC) transporter subfamily D (reviewed in Chornyi et al., 2020; **Figure 2**). The esterification of fatty acids into their corresponding CoA esters is catalysed by acyl-CoA synthetases, and is a requirement for import via the peroxisomal ABCD transporters as well as for fatty acid β-oxidation. In humans, the two very-long-chain acyl-CoA synthetases SLC27A2 (FATP2) and SLC27A4 (FATP4) have been partially localized to the peroxisomal membrane (reviewed in Chornyi et al., 2020). Both proteins are mainly involved in the activation of fatty acids rather than transport across membranes. Similar to human SLC27A2, the two *D. rerio* orthologues (Slc27a2a, Slc27a2b) have a non-canonical PTS1 (TRL, FRL, respectively) (**Table 1** and **Supplementary Table S3**). The *D. rerio* Slc27a4 also possesses a non-canonical PTS1 (QKL) (**Supplementary Table S3**). PTS1 signals normally mediate the targeting of matrix proteins, and it has not been demonstrated that PTS1 signals also target membrane proteins like SLC27A2 and SLC27A4. However, peroxisomal SLC27A2 is supposed to be a peripheral membrane protein facing the matrix (Smith et al., 2000), and splice variants of SLC27A4, a putative transmembrane protein, with and without TMD may exist. It is discussed whether hydrolysis of the CoA ester bond is required for ABCD transporter-mediated acyl-CoA transport into peroxisomes (reviewed in Chornyi et al., 2020). In such a scenario, acyl-CoA synthetases must also be present in the peroxisomal matrix, e.g., to re-activate the imported fatty acids prior to β-oxidation. We also identified a *D. rerio* acyl-CoA synthetase long chain family member 5 (Acsl5,

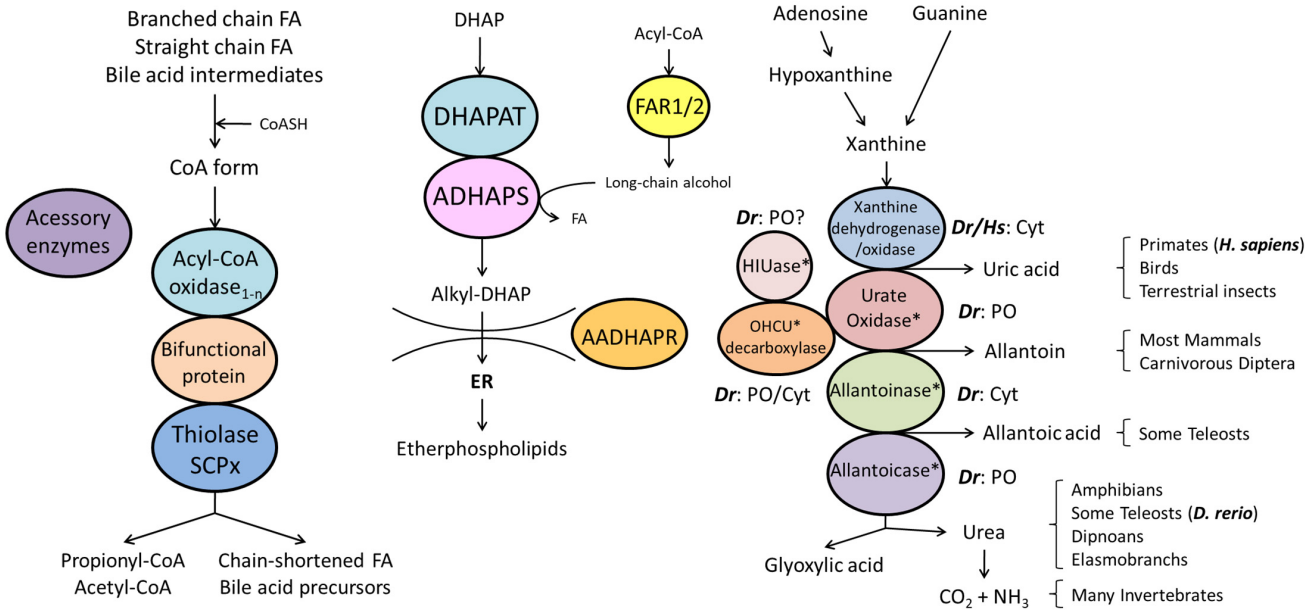

FIGURE 3 | Schematic representation of the pathways of fatty acid β-oxidation **(A)**, ether phospholipid synthesis **(B)** and purine catabolism **(C)** in peroxisomes. **(A)** Peroxisomes degrade fatty acids in four consecutive steps: (1) oxidation, (2) hydration, (3) dehydrogenation, and (4) thiolytic cleavage. Step 1 is performed by multiple acyl-CoA oxidases (1-n) with different substrate specificities. Steps 2 and 3 involve two bifunctional proteins (L-BP, D-BP) harbouring both enoyl-CoA hydratase and 3-hydroxy-acyl-CoA dehydrogenase activity. Step 4 requires different thiolases (e.g., ACAA1, SCPx). Peroxisomes have acquired a set of accessory enzymes (e.g., for fatty acid α-oxidation) to transform the acyl-CoA esters of those fatty acids (FA), which cannot directly enter the β-oxidation pathway (e.g., phytanic acid) (see text for details). **(B)** The first three steps of ether phospholipid synthesis take place in peroxisomes; synthesis continues in the endoplasmic reticulum (ER). **(C)** Enzymes involved in purine catabolism in different vertebrate groups and their excretion products. Note that the cellular localisation (cytosolic, peroxisomal) of these enzymes varies amongst vertebrate species. Xanthine oxidase is cytosolic (Cyt) in *H. sapiens* (*Hs*) and *D. rerio* (*Dr*). Urate oxidase, HIUase, OHCU decarboxylase, and allantoicase are supposed to localise to peroxisomes (PO) in *D. rerio*, but are absent in *H. sapiens* (asterisks) (see also **Table 1**). Allantoinase is cytosolic in *D. rerio*, but absent in *H. sapiens* (asterisks). AADHAPR, alkyl-dihydroxyacetone phosphate reductase; ADHAPS, alkyl-dihydroxyacetone phosphate synthase; DHAP, dihydroxyacetone phosphate; DHAPAT, dihydroxyacetone phosphate acyltransferase; FAR1/2, fatty acyl-CoA reductases 1/2; HIUase, 5-hydroxyisourate hydrolase; OHCU decarboxylase, 2-oxo-4-hydroxy-4-carboxy-5-ureidoimidazoline decarboxylase (adapted from Islinger et al., 2010).

F1RAK0_DANRE) with a weak PTS1 (ANM), which appears to be an N-terminal tail-anchored membrane protein localising to multiple organelles (**Supplementary Table S3**). Mammalian ACSL1, the most abundant acyl-CoA synthetase in liver, is according to numerous proteomics studies also supposed to be peroxisomal, and possesses a TMD at the N-terminus (Watkins and Ellis, 2012; Yifrach et al., 2018).

In *D. rerio* four transporters homologous to the mammalian peroxisomal transporters ABCD1 (Abcd1, F1RBC8_DANRE), ABCD2 (Abcd2, E7F973_DANRE), and ABCD3 (Abcd3a, A0A0R4IRL4_DANRE; Abcd3b, B0UY91_DANRE) were identified (**Figure 2**, **Table 1**, and **Supplementary Table S3**). Defects in human ABCD1, required for the uptake of very long-chain fatty acids (VLCFA) into peroxisomes, cause adrenoleukodystrophy (ALD), a devastating neurodegenerative disease with central and peripheral demyelination (Engelen et al., 2014). It has been shown that *D. rerio* Abcd1 is highly conserved at the amino acid level with human ABCD1, and during development is expressed in corresponding regions/tissues including the central nervous system (CNS) and adrenal glands (Strachan et al., 2017). A zebrafish model of ALD has recently been established that recapitulates key features of the human disease pathology. Similar to ALD patients, zebrafish *abcd1* mutants have elevated VLCFA levels, develop a motor impairment, and show reduced life expectancy. Furthermore, CNS development was disrupted, with reduced numbers of oligodendrocytes with altered patterning, hypomyelination, and increased apoptosis (Strachan et al., 2017). The zebrafish ALD model has been successfully used in a drug screen to identify compounds to alleviate lipid toxicity (Raas et al., 2021).

In mammals, ABCD1 and ABCD2 are involved in the transport of long and very long chain fatty acids, whereas ABCD3 is suggested to mediate the transport of branched chain acyl-CoA, the bile acid intermediates di- and tri-hydroxycholestanoyl-CoA (DHCA and THCA), and medium to long-chain acyl-CoA (Violante et al., 2019). Under normal conditions, the latter are preferentially degraded in mitochondria. ABCD3 defects have been linked to hepatosplenomegaly, a liver disease (Ferdinandusse et al., 2015). ABCD4 (Abcd4, K9M7F0_DANRE), the fourth member of the ABC subfamily D, is no longer considered a peroxisomal protein. It localises to the ER and lysosomes, and is involved in vitamin B12 transport with defects leading to vitamin B12-deficiency anaemia in man and zebrafish (Kawaguchi and Morita, 2016; Choi et al., 2019).

In addition to the ABC transporters, the acyl-CoA binding domain containing proteins Acbd5a, Acbd5b, and Acbd4 have been identified in *D. rerio* (**Figure 2**, **Table 1**, and **Supplementary Table S3**). Human ACBD5 is required for VLCFA-acyl-CoA import via ABCD1, and its loss results in a new peroxisomal disorder, ACBD5 deficiency, with accumulation of VLCFA and neurological abnormalities (Ferdinandusse et al., 2017; Yagita et al., 2017; Darwisch et al., 2020). Furthermore, in mammals ACBD5 and ACBD4 are involved in the tethering of peroxisomes to the ER and membrane contact site formation (Costello et al., 2017b,c; Hua et al., 2017). Like human ACBD4/5, the zebrafish proteins are also tail-anchored membrane proteins.

Similar to mitochondrial β-oxidation, the peroxisomal pathway degrades fatty acids in four consecutive steps, namely by (i) oxidation, (ii) hydration, (iii) dehydrogenation, and (iv) thiolytic cleavage (**Figure 3A**). The first step involves acyl-CoA oxidases (ACOX), and we identified three ACOX in *D. rerio*: Acox1 (F1R071_DANRE), Acox3 (F1QXK3_DANRE) and an ACOX-like protein (Acoxl, A0A2R8QDD9_DANRE; F1R4J4_DANRE) (**Table 1** and **Supplementary Table S3**). Alternative splicing isoforms of zebrafish Acox1 were described suggesting tissue-specific modulation of Acox1 activity (Morais et al., 2007). Acox1, Acox3 and Acoxl display canonical PTS1 (SKL, AKL, SKL), whereas the other Acoxl isoform (F1R4J4_DANRE) lacks a PTS1 or PTS2. Humans have four acyl-CoA oxidases (ACOX1, ACOX2, ACOX3, ACOXL/ACOX4), with ACOX1 preferentially degrading straight-chain fatty acids with different chain lengths, while ACOX2 is the only human acyl-CoA oxidase involved in bile acid biosynthesis, and both ACOX2 and ACOX3 are involved in the degradation of branched-chain fatty acids (Ferdinandusse et al., 2018). We noticed that for human ACOXL/ACOX4, which is not well studied (Van Veldhoven, 2010) similar to *D. rerio* Acoxl, a C-terminally extended isoform exists (Q9NUZ1-4), which possesses a PTS1 (AKL). If the other ACOXL/Acoxl isoforms lacking a PTS1 also localise to peroxisomes, e.g., in a complex with the PTS1-targeted isoforms, remains to be elucidated.

In animals, the second and third step is mediated by D- and L-bifunctional enzymes (D- and L-BP), which both function concomitantly as an enoyl-CoA hydratase and a 3-hydroxyacyl CoA dehydrogenase, but display different substrate specificity (**Figure 3A**). Both are present in *D. rerio* [Hsd17b4 (Dbp), Ehhadh (Lbp)] and contain a PTS1 (**Table 1** and **Supplementary Table S3**). Knockdown of Dbp in zebrafish resulted in defective craniofacial morphogenesis, growth retardation, and abnormal neuronal development similar to D-BP mutations in humans (Kim et al., 2014). Furthermore, the development of blood, blood vessels, and endoderm-derived organs (e.g., liver, pancreas) was impaired suggesting that zebrafish is a useful model to study the role of peroxisomes during vertebrate development (Kim et al., 2014).

In humans, two peroxisomal thiolases, 3-ketoacyl-CoA-thiolase 1 (pTH1, ACAA1) and SCPx (sterol carrier protein x; pTH2), can exert the last step. pTH1 metabolizes only straight chain fatty acids, whereas the branched chain fatty acids and bile acid precursors (pristanic acid, DHCA, and THCA) are solely cleaved by SCPx. Sterol carrier protein 2 (SCP2) is a second isoform from the same gene lacking the N-terminal thiolase domain. SCP2 is a multilocalised protein described in peroxisomes, the cytosol, the ER and potentially mitochondria as it harbours a putative MTS at its N-terminus. *D. rerio* possesses a 3-ketoacyl-CoA thiolase (Acaa1) carrying a PTS2 as well as two sterol carrier proteins (Scp2a, Scp2b) with a PTS1 (AKL) (**Table 1** and **Supplementary Table S3**). Scp2a represents the traditional SCPx including the thiolase domain (538aa), whereas Scp2b represents a shorter form (142aa) lacking the thiolase domain. The crystal structure of the zebrafish Scp2-thiolase was recently revealed (Kiema et al., 2019). Expression changes of *scp2a* and *acaa1*, as well as the β-oxidation genes *ehhadh* (L-BP), *hsd17b4* (D-BP), *acox1* and *acox3* were recently reported in a zebrafish model for *pex2* deficiency (Takashima et al., 2021).

The above mentioned proteins are involved in the β-oxidation of straight-chain saturated fatty acids and α-methyl branched-chain fatty acids with the methyl group in the (2S)-configuration (Wanders and Waterham, 2006). However, the β-oxidation of (2R)-methyl branched-chain FAs and unsaturated FAs requires auxiliary enzymes (**Table 1**). As direct oxidation of (2R)-methyl branched-chain fatty acids is not possible, the peroxisomal 2-methylacyl-CoA racemase (AMACR), which converts (2R)- into (2S) branched-chain acyl-CoAs, is required. The *D. rerio* 2-methylacyl-CoA racemase (Amacr) possesses a PTS1 (ARL) (**Supplementary Table S3**) and a potential N-terminal mitochondrial targeting signal (Amery et al., 2000).

Peroxisomes also contain enzymes to remove the double bonds in mono- and polyunsaturated fatty acids (Wanders and Waterham, 2006; Chornyi et al., 2020). Degradation of fatty acids with an internal double bond at an even-numbered position involves a state of two conjugated double bonds, which are subsequently processed by 2,4-dienoyl-CoA reductase (DECR2) and Δ3,Δ2-enoyl-CoA isomerase (PECI) before re-entering β-oxidation in the hydratase step. Both enzymes (Decr2, Eci2) are present in zebrafish both containing a PTS1 (**Table 1** and **Supplementary Table S3**). Like the human enzyme, the *D. rerio* Δ3,5, Δ2,4-dienoyl-CoA isomerase (Ech1) is likely involved in the processing of fatty acids with a double bond at an odd-numbered position, and possesses a canonical PTS1 (SKL) (**Table 1** and **Supplementary Table S3**). Furthermore, an additional gene encoding a potential enoyl-CoA isomerase/hydratase (zgc:101569, F1R2G5_DANRE) with a PTS1 (SKL) was identified (**Supplementary Table S3**).

After shortening of the fatty acid chains to medium chain fatty acyl-CoA by the peroxisomal β-oxidation pathway, the fatty acids are conjugated to carnitine, exit the peroxisomes, and undergo further β-oxidation in mitochondria (Houten et al., 2020). The *D. rerio* carnitine O-acetyltransferase a (Crata) displays a PTS1 (AKL), whereas the carnitine O-acetyltransferase b (Cratb) does not possess a PTS1. *D. rerio* carnitine octanoyltransferase (Crot) has a weak PTS1 (SQL) (**Table 1** and **Supplementary Table S3**). Crot is likely involved in the export of the medium chain fatty acids, whereas Crat is most probably involved in the export of the acetyl-CoA units generated by β -oxidation.

Alternatively, acyl-CoA products can be hydrolysed by acyl-CoA thioesterases (ACOTs) that generate a free carboxylate that can cross the peroxisomal membrane (Houten et al., 2020).

Similar to humans, *D. rerio* Acot8 contains a canonical PTS1 (SKL), whereas a homologue of *Hs*ACOT4 was not identified (**Table 1** and **Supplementary Table S3**). Interestingly, an orthologue of bile acid-CoA:amino acid N-acyltransferase (BAAT), which in humans converts choloyl-CoA and deoxycholoyl-CoA to taurine- or glycine-conjugated cholic acid, or deoxycholic acid, was not identified in *D. rerio* (**Table 1** and **Supplementary Table S3**). As Cypriniformes (including *D. rerio*) lack C24 bile acids (which are formed by side chain shortening in human peroxisomes), a peroxisomal contribution to bile acid synthesis in zebrafish is rather unlikely (Hagey et al., 2010). This is also supported by the absence of ACOX2, which in humans is involved in bile acid biosynthesis. Comparison with various other fish species demonstrate that BAAT is found in neither of these species (**Figure 4D**).

Mitochondrial β-oxidation relies on acyl-CoA dehydrogenases (ACADs). Interestingly, peroxisomes also harbour an acyl-CoA dehydrogenase, ACAD11 (Camões et al., 2015). Like the human ACAD11, the *D. rerio* Acad11 has a canonical PTS1 (AKL) (**Table 1** and **Supplementary Table S3**). If the enzyme contributes to the 1st step of peroxisomal β-oxidation is not known; however, this could circumvent generation of H_2O_2 by peroxisomal ACOX (Camões et al., 2015). A potential Acad11 isoform was also identified, which only contains the N-terminal aminoglycoside phosphotransferase (APH) domain (E9QBY4_DANRE) but lacks a PTS1. Fungi still contain independent enzymes with the APH and ACAD function, which appear to be fused during evolution. However, in fungi both individual enzymes possess a PTS1 (Camões et al., 2015).

Whereas a mitochondrial fatty acid β-oxidation pathway is absent in yeast and plants, which solely rely on the peroxisomal pathway, it is present in animals and many other fungi. Zebrafish also encodes a set of homologous enzymes of human mitochondrial β-oxidation, e.g., short-chain to very long-chain specific acyl-CoA dehydrogenases (Acadvl, F1Q8J4_DANRE; Acadl, A3KQR0_DANRE, Acadm, A2CG95_DANRE; Acads Q6AXI7_DANRE) for the initial dehydrogenation reaction of fatty acids, and enoyl-CoA hydratases (Hadhaa, A7YT47_DANRE; Echs1, Q7ZZ04_DANRE) for the 2nd step. Zebrafish candidates for the third and fourth reaction of mitochondrial β-oxidation are again Hadhaa or 3-hydroxyacyl-CoA dehydrogenase (Hadh, Q6DI22_DANRE) and the 3-ketoacyl-CoA thiolases (Hadhb, A0A2R8RRC9_DANRE; Acat1, Q6AZA0_DANRE) and acetyl-CoA acyltransferase 2 (Acaa2, B0S5C5_DANRE). Hence, fatty acid substrate spectra metabolized in peroxisomes or mitochondria seem to closely resemble the situation in human. This is also corroborated by the specific increase of very long chain fatty acids in zebrafish knockout models for peroxisomal disorders (Takashima et al., 2021).

Peroxisomal Fatty Acid Alpha-Oxidation

Our comprehensive analysis revealed candidate proteins for several other important metabolic pathways in *D. rerio* peroxisomes (**Table 1**). Due to a methyl group at position 3, 3-methyl branched-chain fatty acids such as phytanic acid cannot undergo β-oxidation directly. Peroxisomal α-oxidation is required to remove the last carbon atom generating a 2-methyl branched-chain fatty acid, which can be β-oxidised (Wanders and Waterham, 2006). *D. rerio* possesses a phytanoyl-CoA 2-hydroxylase (Phyh) carrying a PTS2 for hydroxylation of phytanoyl-CoA (**Table 1** and **Supplementary Table S3**). The generated 2-hydroxyphytanoyl-CoA is cleaved by 2-hydroxyacyl-CoA lyase (Hacl1) containing a PTS1 (SNL) to pristanal and formyl-CoA. Pristanal is oxidised to pristanic acid by a peroxisomal aldehyde dehydrogenase, which in humans is FALDH, a tail-anchored membrane protein with a peroxisomal and an ER-targeted isoform (Costello et al., 2017b). *D. rerio* possesses two homologous fatty aldehyde dehydrogenases (Aldh3a2a, Aldh3a2b), which are also tail-anchored membrane proteins (**Table 1** and **Supplementary Table S3**). However, their peroxisomal or ER localisation needs to be determined.

Biosynthesis of Ether Phospholipids

The biosynthesis of ether phospholipids (e.g., myelin sheath lipids and plasmalogens) is a characteristic feature of peroxisomes in animals, but supposed to be absent in plants and yeast (Dorninger et al., 2020). It requires metabolic cooperation of peroxisomes with the ER. The formation of the typical ether bond in ether phospholipids is catalysed by the peroxisomal enzyme alkyl-dihydroxyacetone phosphate synthase (alkyl-DHAP synthase) (**Figure 3B**). In *D. rerio*, this key enzyme (Agps) possesses a PTS2 (**Table 1** and **Supplementary Table S3**). Formation of the two substrates for alkyl-DHAP synthase, namely acyl-DHAP and a long chain alcohol, is catalysed by DHAP acyltransferase (DHAPAT) (*D. rerio* Gnpat) carrying a PTS1 (ARL), and FAR1 or FAR2, two different acyl-CoA reductases (**Table 1** and **Supplementary Table S3**). Like human FAR1, *D. rerio* Far1 (A0A0R4ICF6_DANRE) appears to be a tail-anchored membrane protein; however, a potential Far1 isoform without a TMD and a PTS1 (SRL) may exist (F1QSU9_DANRE) (**Supplementary Table S3**). An orthologue of human FAR2 was also identified (si:dkey-97m3.1, Q1L8Q4_DANRE), which appears to be a tail-anchored membrane protein as well (**Table 1** and **Supplementary Table S3**). The DHAP-backbone (precursor compound) is reduced by the enzyme acyl/alkyl-DHAP reductase (AADHAPR) encoded by *DHRS7B* (dehydrogenase/reductase SDR family member 7B) at the cytosolic face of the peroxisomal or ER membrane. The *D. rerio* Dhrs7b possesses an N-terminal TMD (**Table 1** and **Supplementary Table S3**).

Glycolate/Glyoxylate Metabolism and Detoxification

Furthermore, several enzymes involved in glycolate/glyoxylate metabolism and detoxification have been identified including hydroxyacid oxidase 1 and 2 (Hao1, Hao2) with a PTS1 (**Tables 1**, **2** and **Supplementary Table S3**). Humans express three 2-hydroxyacid oxidases (HAOX1-3) in a tissue-specific manner; an orthologue of HAOX3, which may have evolved from Hao2, was not found in zebrafish. These flavin-linked enzymes convert 2-hydroxy acids to 2-keto acids thereby reducing molecular oxygen to hydrogen peroxide. HAOX1 shows a preference for the two-carbon substrate, glycolate, but is also active on 2-hydroxy fatty acids, whereas HAOX2

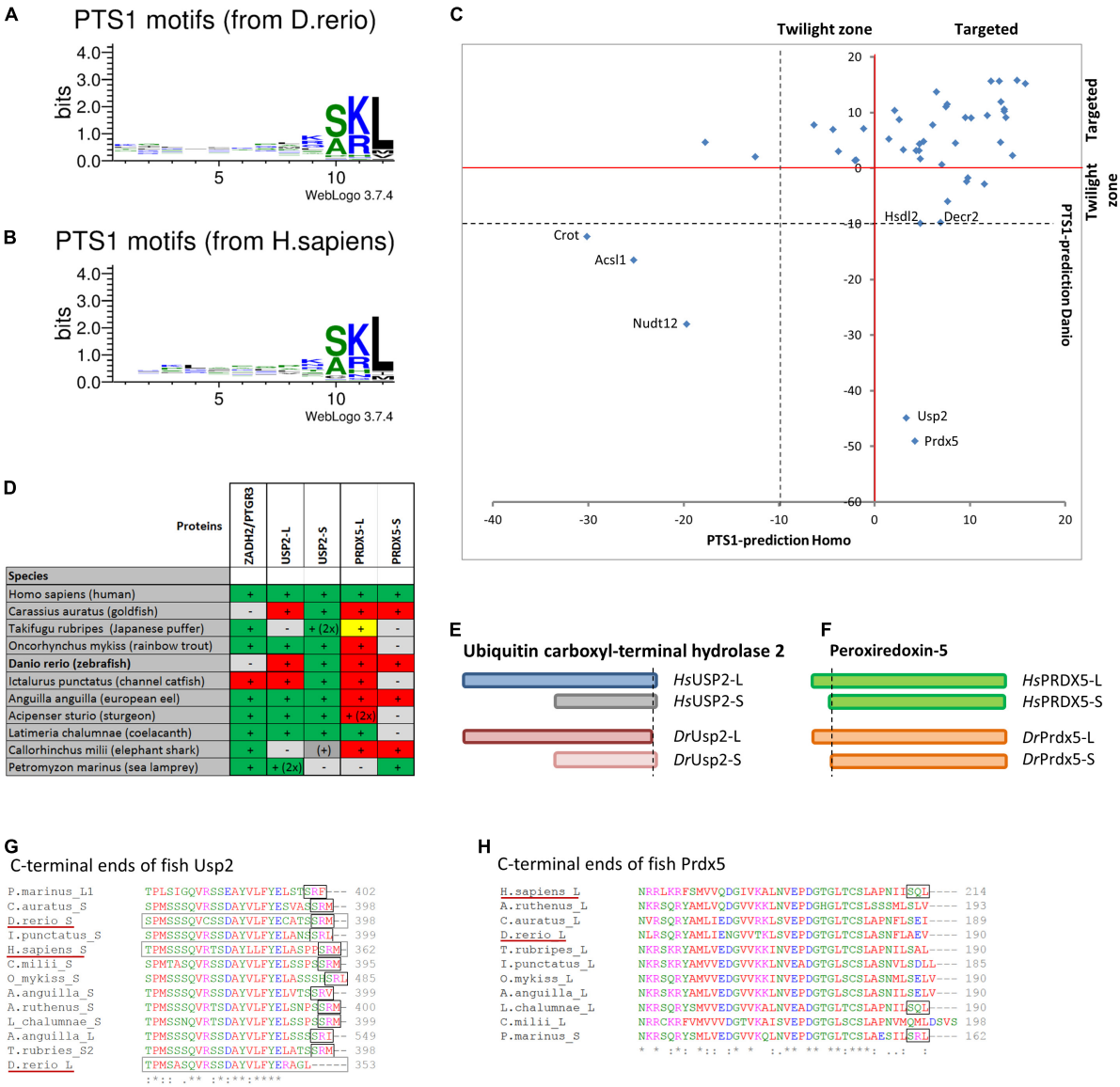

FIGURE 4 | Comparison of PTS1 motifs between *D. rerio* and *H. sapiens*: To depict the difference in the average abundance of amino acids at different positions of the PTS1 in fish **(A)** and humans **(B)**, we selected proteins from each species, which were predicted to harbour a PTS1 (Neuberger et al., 2003), and depicted them as WebLogo (http://weblogo.threeplusone.com/create.cgi). **(C)** A comparison of the numerical values of the PTS1-predictions for those proteins is plotted for *H. sapiens* (*x*-axis) and *D. rerio* (*y*-axis) and depicted relative to the threshold for the evaluation of targeted proteins (>0, red) or the "twilight zone" (–10 < x < 0, grey); proteins with negative prediction are highlighted. **(D)** Systematic overview of orthologous fish proteins, which were either not found in *D. rerio* (ZADH2/PTGR3) or lack a PTS1 (Usp-L, long isoform; Prdx-5). (+) or (–) indicate presence or absence of the protein; 2x indicates 2 variants; traditional PTS1 identified (green) or not found (red); non-canonical PTS1 (yellow). **(E)** Schematic representation of the two isoforms of ubiquitin carboxyl-terminal hydrolase 2 (USP2) in *H. sapiens* (blue) and *D. rerio* (red). No PTS1 was found in the long isoform of Usp2 (Usp2-L). **(F)** Schematic representation of the two isoforms of peroxiredoxin-5 (Prdx-5) in *H. sapiens* (green) and *D. rerio* (orange). The long variant harbours an additional mitochondrial targeting signal, whereas the C-terminal sequence is identical. **(G,H)** Sequence comparison of the C-terminal end of USP2 orthologues **(G)** and PRDX5-orthologues **(H)**. The loss of the PTS1 in Usp2-L is unique for *D. rerio*, whereas the PTS1 of human PRDX5 is found only in more ancient fish species.

displays a preference for 2-hydroxypalmitate, and HAOX3 for the medium chain substrate 2-hydroxyoctanoate. These findings suggest that HAOX1-3 are involved in the oxidation of 2-hydroxy fatty acids and may also contribute to fatty acid α-oxidation (Jones et al., 2000).

Zebrafish also contains a putative peroxisomal alanine:glyoxylate aminotransferase (AGT) (Agxta, F1QY24_DANRE) with a weak PTS1 (SRV), a key enzyme to prevent oxalate accumulation (**Table 1** and **Supplementary Table S3**). The peroxisomal AGT converts glyoxylate generated in peroxisomes (by HAOX1/glycolate oxidase) into glycine using alanine as the primary amino group donor (Wanders and Waterham, 2006). This prevents the conversion of glyoxylate into oxalate, which is toxic. AGT enzymatic activities associated

TABLE 2 | Candidate peroxisomal oxidases in zebrafish.

Name	Protein symbol	Uniprot ID	ROS/NOS	PTS1	Localisation (predicted)
Acyl-CoA oxidase 1	Acox1	F1R071_DANRE	H_2O_2	SKL	PO
Acyl-CoA oxidase 3	Acox3	F1QXK3_DANRE	H_2O_2	AKL	PO
Acyl-CoA oxidase-like	Acoxl	F1R4J4_DANRE	H_2O_2	–	PO?
L-α-Hydoxyacid oxidase 1	Hao1	Q7SXE5_DANRE	H_2O_2	SRI	PO
L-α-Hydoxyacid oxidase 2	Hao2	F1QCD8_DANRE	H_2O_2	SRL	PO
D-amino-acid oxidase 1	Dao1	Q4V981_DANRE	H_2O_2	SRL	PO
D-amino-acid oxidase 2	Dao2	Q6NY97_DANRE	H_2O_2	SRL	PO
D-amino-acid oxidase 3	Dao3	Q6P009_DANRE	H_2O_2	SRL	PO
D-aspartate oxidase	Ddo	A0A0R4IZE6_DANRE	H_2O_2	ARL	PO
L-Pipecolic acid oxidase	Pipox	A7MBQ2_DANRE	H_2O_2	SSL	PO
Polyamine oxidase	Paox	B8JJQ4_DANRE	H_2O_2	SKL	PO
Urate oxidase	Uox	Q6DG85_DANRE	H_2O_2	ARM	PO
Xanthine oxidase	Xdh	A0A2R8Q1T4_DANRE	H_2O_2, $NO^{\bullet}$, $O_2^{\bullet-}$	–	Cyt
L-gulonolactone oxidase (ascorbate synthesis)	Gulo	–	H_2O_2	–	absent

Inducible nitric oxide synthase (NOS2) ($NO^{\bullet}$, $O_2^{\bullet-}$) not listed (no PTS, Cyt, PO?).

with mitochondria are also required to utilize certain amino acids for gluconeogenesis. Interestingly, zebrafish encode another putative AGT (agxtb, Q6PHK4_DANRE) which lacks a PTS1 but possesses an N-terminal MTS. Mitochondrial AGT can transaminate alanine and serine to pyruvate and hydroxypyruvate for gluconeogenesis. The peroxisomal and/or mitochondrial localisation of AGT in animals reflects the organism's diet. Glyoxylate, as a metabolite of glycolate, is taken up by the consumption of plants, whereas protein-rich diets from animal sources deliver high quantities of amino acids such as glycine, alanine and serine. Therefore, AGT localises to mitochondria in many carnivores, to peroxisomes in herbivores, and to both organelles in omnivores (Danpure, 1997). In contrast to zebrafish, mammals contain only a single AGT gene, and dual localisation of AGT, e.g., in rat or marmoset is often mediated by alternative transcription/translation generating a PTS1 or MTS. In humans, AGT is exclusively peroxisomal; AGT deficiency results in primary hyperoxaluria, with accumulation and precipitation of oxalate in the liver and kidney, ultimately leading to kidney failure (Dindo et al., 2019). Hyperoxaluria type 1 can also be caused by a polymorphism (Pro11Leu) in the AGT gene in combination with the mutation Gly170Arg, which creates a MTS mislocalising the enzyme to mitochondria in homozygote patients (Leiper and Danpure, 1997). Furthermore, we identified a malate synthase-like protein (Mls1) with a PTS1 (ARL) in *D. rerio*, which is absent in *H. sapiens* (**Table 1** and **Supplementary Figure S3A**). The enzyme can convert glyoxylate and acetyl-CoA into malate.

Catabolism of D- and L-Amino Acids

Like mammals, zebrafish peroxisomes also appear to contain several enzymes involved in the catabolism of D- and L-amino acids. These include three putative D-amino acid oxidases (dao1-3) carrying a SRL, which oxidize the D-isomers of neutral and basic amino acids, as well as D-aspartate oxidase (Ddo), which oxidizes the D-isomers of acidic amino acids such as D-aspartate, D-glutamate, and N-methyl-D-aspartate that have important neuroregulatory functions in the central nervous system (**Tables 1**, **2** and **Supplementary Table S3**). Those enzymes generate the corresponding keto-acids, ammonia, and hydrogen peroxide (Wanders and Waterham, 2006). We also identified enzymes, which may be involved in the degradation of L-amino acids, e.g., leucine (Hmgcl, F1QTF0_DANRE) (**Table 1** and **Supplementary Table S3**). For human peroxisomal hydroxymethylglutaryl-CoA lyase (HMGCL), a role in the regulation of ketone body metabolism has been suggested (Arnedo et al., 2019). Furthermore, a *D. rerio* L-pipecolate oxidase (Pipox) with a weak PTS1 (SSL) was identified, which likely oxidizes L-pipecolate to Δ1-piperideine-6-carboxylate (Wanders and Waterham, 2006; **Tables 1**, **2** and **Supplementary Table S3**). The enzyme is present in human and primate peroxisomes but is mitochondrial in rabbit liver.

Polyamine Oxidation

Zebrafish also contain a candidate polyamine oxidase (Paox) with a canonical PTS1 (SKL), which in humans is involved in the degradation of spermine and spermidine (Wanders and Waterham, 2006; **Tables 1**, **2** and **Supplementary Table S3**). These natural polyamines are present in all eukaryotic cells and support essential functions in cell proliferation, differentiation and immune regulation, which requires tight control of their levels.

Purine Catabolism

Peroxisomes also harbour enzymes for purine catabolism. In fish, amphibians and many invertebrates purine degradation is catalysed by xanthine oxidase, urate oxidase, allantoinase, and allantoicase, which produce the metabolites uric acid, allantoin, allantoic acid and urea as well as ureidoglycolate (Islinger et al., 2010) (see overview **Figure 3C**). In freshwater fish such as zebrafish xanthine oxidase and allantoinase are cytosolic enzymes, whereas urate oxidase (Uox, Q6DG85_DANRE) and allantoicase (Allc, Q6DGA6) are peroxisomal containing a PTS1 (**Tables 1**, **2** and **Supplementary Table S3**; Hayashi et al., 1989).

The structure and activity of zebrafish urate oxidase was recently reported (Marchetti et al., 2016). Most mammals excrete allantoin and do not express allantoinase and allantoicase (**Figure 3C**). Furthermore, humans (as well as other primates, birds and reptiles) do not possess a functional uricase gene, thus excreting uric acid (Hayashi et al., 2000; Islinger et al., 2020). This makes humans susceptible to gout or urate kidney stones.

Other enzymes associated with urate degradation have recently been identified (Ramazzina et al., 2006; **Figure 3C**). In contrast to humans, zebrafish also possess a 5-hydroxyisourate hydrolase (Uraha) involved in the degradation of uric acid to (S)-allantoin (**Table 1** and **Supplementary Table S3**). Following urate oxidation to 5-hydroxyisourate (HIU), which is catalysed by urate oxidase, hydrolysis of HIU to 2-oxo-4-hydroxy-4-carboxy-5-ureidoimidazoline (OHCU) and subsequent decarboxylation of OHCU to (S)-allantoin are catalysed by HIUase and OHCU decarboxylase (Urad), respectively (**Table 1** and **Supplementary Table S3**). The structure of the *D. rerio* HIUase and OHCU decarboxylase has been revealed (Zanotti et al., 2006; Cendron et al., 2007). *D. rerio* Uraha contains a putative PTS2, which is also found in the amphibian or mammalian proteins (Ramazzina et al., 2006), whereas *D. rerio* Urad possesses a predicted weak PTS1 (TKL). Interestingly, inactivation by pseudogenization of the uricase gene (see above) and the HIUase and OHCU decarboxylase genes of the pathway occurred during hominoid evolution.

To verify the functionality of these targeting signals, we generated EGFP reporter proteins with the respective PTS2 or PTS1 sequence (PTS2-*Dr*Uraha; PTS1-*Dr*Urad). Expression in COS-7 cells revealed a predominantly cytoplasmic localisation of PTS1-*Dr*Urad; however, peroxisomes were also labelled confirming that the PTS1 (TKL) is weak but functional (**Supplementary Figure S2**). Surprisingly, PTS2-*Dr*Uraha was not targeted to peroxisomes suggesting that the PTS2 may not be functional in zebrafish (**Supplementary Figure S2**).

Oxygen and ROS Metabolism

Peroxisomes harbour a number of oxidases that reduce oxygen to hydrogen peroxide (**Table 2**), thus contributing to oxygen and ROS metabolism (Antonenkov et al., 2010). The H_2O_2 produced can be decomposed by several peroxisomal enzymes. The key enzyme is catalase, a heme-binding tetrameric enzyme, which can perform a catalytic ($2H_2O_2 \rightarrow O_2 + 2H_2O$) or peroxidatic reaction ($H_2O_2 + AH_2 \rightarrow A + 2H_2O$), in which the conversion of H_2O_2 to H_2O is coupled to the oxidation of a hydrogen donor (AH_2) (e.g., ethanol, methanol, formaldehyde, formate, nitrite). Like other organisms, *D. rerio* catalase (Cat) contains a non-canonical, less effective PTS1 (SKM), which is supposed to allow proper folding of the protein prior to peroxisomal import (Williams et al., 2012; **Table 1** and **Supplementary Table S3**). The peroxidatic reaction of catalase is exploited for diaminobenzidine (DAB) cytochemistry to specifically label peroxisomes for light- and electron microscopy (Fahimi, 2009), and has been successfully applied to identify peroxisomes in zebrafish tissues (Braunbeck et al., 1990; Krysko et al., 2010).

Xanthine oxidase, which generates superoxide anions, is likely not peroxisomal in zebrafish, and localises to the cytosol instead (**Table 2**). Superoxide radicals can be inactivated by superoxide dismutases. The presence of Cu/Zn-SOD and Mn-SOD activities in peroxisomes from mammals has been reported (Schrader and Fahimi, 2006). Cu/Zn-SOD1, which does not possess a PTS signal, is imported piggy-back into peroxisomes by its copper chaperone which carries a PTS1 (Islinger et al., 2009), but also localises to the cytosol, nucleus and mitochondria. A candidate copper chaperone for SOD is also present in zebrafish (Ccs, A0A0R4IHZ8_DANRE) showing a PTS1 (SHL), as well as superoxide dismutase (Sod1, O73872-SODC_DANRE) lacking a PTS1 (**Table 1** and **Supplementary Table S3**). By contrast, Mn-SOD (SOD2) has recently been reported to exclusively localize to mitochondria in mice and men (Karnati et al., 2013).

Peroxisomes also contain nitric oxide (NO) synthase activity. Zebrafish NO synthases (Nos2a, Nos2b) do not possess a PTS1, however, the molecular mechanism of NO synthase targeting is currently unclear, and the enzyme may present a source of superoxide radicals in peroxisomes (Fransen et al., 2012; **Table 1** and **Supplementary Table S3**).

Peroxiredoxins are a family of antioxidant proteins ubiquitously conserved in a wide variety of organisms ranging from bacteria to humans. In zebrafish, six peroxiredoxins (Prdx1-6) have been identified. Prdx1 is a highly abundant cytosolic thioredoxin-dependent peroxidase and appears to be more efficient at removing H_2O_2 and organic hydroperoxides. Prdx1 is important for vascular development in zebrafish (Huang et al., 2017), and has a stimulatory role in the initiation of adaptive humoral immunity (Liu et al., 2018). Different isoforms of human peroxiredoxin-5 exist which localise to the cytosol, mitochondria or peroxisomes. The peroxisomal isoform possesses a PTS1 (Yamashita et al., 1999), whereas the *D. rerio* Prdx5 (Prdx5, F1QCE3_DANRE) lacks a PTS1 or PTS2 (**Figure 4**, **Table 1**, and **Supplementary Table S3**). Thus, neither of the *D. rerio* Prdx1-6 appears to possess a PTS1.

Peroxisomes, in addition to mitochondria, also contain glutathione S-transferase kappa (GSTK1), which is supposed to catalyse the conjunction of xenobiotics and lipid peroxide products with glutathione for detoxification (Fransen et al., 2012). The peroxisomal localisation of GSTK1 depends on a PTS1 (Morel et al., 2004), which is also present in *D. rerio* Gstk1 (PTS1 AKM) (**Table 1** and **Supplementary Table S3**).

Finally, a candidate for *D. rerio* epoxide hydrolase 2 (Ephx2) with a PTS1 has been identified (**Table 1** and **Supplementary Table S3**). In mammals, EPHX2 localises to the cytosol and peroxisomes carrying a weak PTS1 (Mullen et al., 1999). The homodimeric enzyme is supposed to detoxify fatty-acid derived epoxides converting them to the corresponding dihydrothiols. Downregulation or inhibition of epoxide hydrolase in zebrafish impaired the development of the caudal vein plexus (Frömel et al., 2012).

Peroxisomal Proteases

We also identified *D. rerio* candidate proteins for the three peroxisomal proteases identified so far. Whereas insulin-degrading enzyme (Ide) may degrade oxidised proteins in peroxisomes, Lon protease homolog 2 (Lonp2) is an ATP-dependent protease that mediates the selective degradation of

matrix proteins damaged by oxidation (Bartoszewska et al., 2012) as well as sorting and processing of PTS1-containing proteins (Omi et al., 2008). Trypsin domain-containing 1 (Tysnd1) processes several PTS1-containing proteins, cleaves N-terminal presequences from PTS2-containing protein precursors, and proteolytic processing of β-oxidation enzymes (Kurochkin et al., 2007; Okumoto et al., 2011). All three *D. rerio* proteases possess a PTS1 (**Table 1** and **Supplementary Table S3**).

Carbohydrate Metabolism

Peroxisomes also contain enzymes involved in carbohydrate metabolism, for example the two pentose phosphate pathway enzymes, glucose-6-phosphate dehydrogenase and 6-phosphogluconate dehydrogenase (Wanders and Waterham, 2006). It is supposed that these enzymes provide intraperoxisomal NADPH from $NADP^+$, which is generated during beta-oxidation of unsaturated fatty acids by 2,4-dienoyl-CoA reductase (DECR2) and through conversion of phytenoyl-CoA into phytanoyl-CoA by trans-2-enoyl-CoA reductase (PECR). Whereas the candidate *D. rerio* glucose 6-phosphate dehydrogenase (G6pd) possesses a weak PTS1 (HKL), the candidate 6-phosphogluconate dehydrogenases (Pgd) do not possess a PTS1 (**Table 1** and **Supplementary Table S3**). Alternatively, intraperoxisomal NADPH can be regenerated by isocitrate dehydrogenase 1 (IDH1) in a peroxisomal 2-oxoglutarate/isocitrate NADP(H) redox shuttle (reviewed in Chornyi et al., 2020). The *D. rerio* Idh1 contains a PTS1 (PKL) indicating that this shuttle system also exists in zebrafish (**Table 1** and **Supplementary Table S3**).

NADH, which is produced from NAD^+ during peroxisomal α- and β-oxidation, may be reoxidised to NAD^+ by different NAD^+-dependent dehydrogenases, which have been reported to reside in human peroxisomes and may contribute to a NAD^+/NADH shuttle system: (i) lactate dehydrogenase B (LDHB), which converts pyruvate into lactate, (ii) malate dehydrogenase 1 (MDH1), which converts oxaloacetate into malate, and (iii) glycerol-3-phosphate dehydrogenase 1 (GPD1), which converts DHAP into G3P (reviewed in Chornyi et al., 2020). Human LDHA and LDHB both lack PTS signals, but for LDHB a translational read-through of the stop codon was reported to result in an alternative, C-terminally extended isoform with a PTS1 (Schueren et al., 2014). Similarly, MDH1 does not possess a PTS, but translational read-through to generate an extended isoform with a functional PTS1 has been reported (Hofhuis et al., 2016). Interestingly, an isoform of malate dehydrogenase 1Aa (Mdh1x, NP_001303854.1) carrying a PTS1 (SRL) was identified in zebrafish, which is generated by translational read through of the UGA stop codon to the downstream UAA termination codon generating a C-terminally extended isoform (Stiebler et al., 2014; **Table 1** and **Supplementary Table S3**). Whereas a Gpd1-based redox shuttle has been described in yeast (with *Sc*Gpd1 carrying a PTS2), it is unclear how mammalian Gpd1 targets peroxisomes as it lacks a PTS and does not show translational read-through (reviewed in Chornyi et al., 2020). *D. rerio* Gpd1 (Q567A1_DANRE; Q5XIZ6| GPD1L_DANRE) does not appear to possess a PTS2 or PTS1 signal. The same applies to the *D. rerio* lactate dehydrogenases (Ldhb), and it appears that translational readthrough and peroxisomal targeting of Ldhb is restricted to mammals (Hofhuis et al., 2016). Furthermore, the higher degree of conservation of MDH1 readthrough in comparison to LDHB readthrough co-evolved with the targeting signal strength of their respective PTS1. Thus, there is evidence for a peroxisomal oxaloacetate/malate NAD^+/NADH shuttle system in zebrafish, whereas the peroxisomal localisation of other NAD^+-dependent dehydrogenases and their role in a NAD^+/NADH shuttle system need to be elucidated.

Peroxisomal CoA Transporter

The import and export of small metabolites (such as pyruvate, lactate, oxaloacetate, malate, DHAP, G3P, isocitrate, and 2-oxoglutarate) is likely mediated by peroxisomal pore-forming proteins and transporters. *D. rerio* possesses two orthologues of the human peroxisomal transmembrane protein PMP34/SLC25A17 (Slc25a17, A5D6T2_DANRE; Slc25a17-like), which in zebrafish resulted from gene duplication and function as a peroxisomal CoA transporter (Kim et al., 2020; **Figure 2**, **Table 1**, and **Supplementary Table S3**). These members of the solute carrier protein family (SLC) exhibit six transmembrane domains, and have been shown to localise to peroxisomes in zebrafish embryos (Kim et al., 2020). Targeting of PMPs is mediated by the PMP import receptor/chaperone PEX19. Knockdown of Slc25a17 impaired development of multiple organs, including swim bladder, during zebrafish embryogenesis. Furthermore, the concentration of VLCFA was increased after Slc25a17 knockdown, whereas the concentration of plasmalogens was decreased supporting a role in lipid metabolism/cofactor transport (Kim et al., 2020).

CoA is an important co-factor in peroxisomal lipid metabolism, which is released during hydrolysis of acyl-CoA esters by the thioesterases (*see* section "Fatty acid β-oxidation"). It is re-used inside peroxisomes (e.g., for the activation of pristanic acid), or is degraded by one of the peroxisomal Nudix Hydrolases (NUDT). Orthologues of the human Nudix Hydrolases NUDT7 and NUDT19/RP2p, two CoA diphosphohydrolases that degrade CoA and acyl-CoAs to 3′,5′-ADP and 4′-(acyl)phosphopantetheine, are also present in zebrafish. *D. rerio* Nudt7 and Nudt19 have a canonical PTS1 (SKL), but the Nudt19 PTS1 signal appears to be weak and may allow targeting to other subcellular compartments (**Table 1** and **Supplementary Table S3**). In addition, the pyrophosphatase NUDT12, which mediates the degradation of NAD^+ and NADH, was reported to target human peroxisomes. However, the *D. rerio* Nudt12 does not possess a predicted PTS1 and may localise to the cytosol.

Peroxisomal Membrane Proteins

Orthologues of the human peroxisomal membrane proteins PXMP2 (PMP22), PXMP4 (PMP24) and PMP52 (TMEM135) were also identified in *D. rerio* (Pxmp2, Pxmp4, Tmem135) (**Figure 2**, **Table 1**, and **Supplementary Table S3**). PXMP2 is supposed to be a pore-forming protein; PXMP4 and TMEM135 belong to the Tim17 family and they may be involved in peroxisomal metabolite transport (reviewed

in Chornyi et al., 2020; Beasley et al., 2021). Furthermore, orthologues of human membrane proteins MPV17 and MPV17-like are present in zebrafish (Mpv17, Mpv17l, Mpv17l2), which belong to the Mpv/Pxmp2 family (**Figure 2**, **Table 1**, and **Supplementary Table S3**). Their peroxisomal localisation is controversial (Iida et al., 2006; Spinazzola et al., 2006; Weiher et al., 2016), and Mpv1 appears to be an inner mitochondrial membrane protein (Martorano et al., 2019). It possesses a weak predicted PTS1 (NKM), but as a multi-pass membrane protein, peroxisomal targeting would depend on Pex19. The two *D. rerio* Mpv17-like proteins are as well multi-pass membrane proteins.

Furthermore, only one orthologue of the human peroxisomal membrane proteins MARC1/2 is present in *D. rerio* (Marc1, Q66HU7_DANRE) (**Figure 2**, **Table 1**, and **Supplementary Table S3**), which is most likely due to a recent gene duplication in amniota after the separation from fish. MARC2, which has been identified in proteomics studies of mammalian peroxisomes, mediates the reduction of N-hydroxylated drugs in mitochondria (Havemeyer et al., 2006), but its peroxisomal function is unknown. Interestingly, MARC2 knockout mice exhibit lower body weight and are resistant to high-fat-diet induced obesity linking MARC2 function to the regulation of energy homeostasis (Rixen et al., 2019). If *D. rerio* Marc localises to peroxisomes needs to be determined. Other putative peroxisomal membrane proteins identified in *D. rerio* are the mitochondrial antiviral-signaling protein Mavs, a tail-anchored membrane protein, which in humans localises to mitochondria and peroxisomes (Dixit et al., 2010); the AAA-ATPase Msp1/Atad1, which dually localises to mitochondria and peroxisomes and is involved in the quality control of tail-anchored membrane proteins (Jiang, 2021); the deubiquitinase Usp30, which is regulating the turnover of peroxisomes by suppressing basal pexophagy (Marcassa et al., 2019; Riccio et al., 2019); the putative organic cation transporter Slc22a21, which may be involved in carnitine transport (reviewed in Chornyi et al., 2020), Trim37, an E3 ubiquitin-protein ligase involved in Pex5 mediated peroxisomal matrix protein import (Wang et al., 2017), and the phospholipase Pnpla8 (**Figure 2**, **Table 1**, and **Supplementary Table S3**). The latter has been show to localise to mitochondria and peroxisomes, where it may be involved in the maintenance of the organelle's membrane phospholipids, and possesses a canonical PTS1 (SKL) (Mancuso et al., 2004, 2007). Pnpla8 was suggested to peripherally associate to the inner leaflet of the peroxisome membrane after import into the peroxisomal matrix (Mancuso et al., 2000). Furthermore, Fibronectin type III domain containing 5, a putative single-pass transmembrane protein, containing a PTS1 (SKV) has been identified (G1K2P4_DANRE) (**Table 1** and **Supplementary Table S3**). Mouse Fndc5/PeP has been shown to target peroxisomes via its PTS1 in a Pex5-dependent manner (Ferrer-Martínez et al., 2002). Murine Fndc5 is also supposed to target the plasma membrane and contains an N-terminal signal peptide. Interestingly, N-terminally truncated isoforms lacking the signal peptide exist in zebrafish (G1K2P4_DANRE) and humans (Q8NAU1-4). If those isoforms target peroxisomes via their PTS1/PEX5 or mPTS/PEX19 remains to be elucidated.

L-gulonolactone oxidase, a single pass membrane protein, is the ultimate enzyme of hepatic ascorbate formation in ascorbate-synthesizing species. In mouse liver, it localises to the ER and peroxisomes (Braun et al., 1999). However, the enzyme is absent in teleost fish and also humans, who do not synthesize ascorbate (Fracalossi et al., 2001; **Tables 1**, **2** and **Supplementary Table S3**).

Analysis of Peroxisomal Targeting Signals

After annotation of the peroxisomal protein inventory of *D. rerio*, we analysed the peroxisomal targeting signals in more detail. We revealed that similar to other vertebrates/animals, the majority of the peroxisomal matrix proteins of *D. rerio* contain a PTS1, and only a few possess a PTS2 (**Table 1** and **Supplementary Table S3**). The latter include peroxisomal 3-ketoacyl-CoA thiolase (Acaa1), a protein exerting the last step of peroxisomal fatty acid β-oxidation (see above), phytanoyl-CoA 2-hydroxylase (Phyh), a key enzyme of peroxisomal fatty acid α-oxidation, and alkylglycerone-phosphate synthase (Agps), a key enzyme of peroxisomal ether phospholipid biosynthesis (**Table 1** and **Supplementary Table S3**). The human orthologues of these enzymes also possess a PTS2. Furthermore, urate (5-hydroxyiso-) hydrolase a (Uraha), an enzyme involved in urate catabolism, which is not expressed in humans, carries a putative PTS2 (Ramazzina et al., 2006), but may not target peroxisomes in zebrafish (**Supplementary Figure S2**). The zebrafish orthologues of other human proteins with a putative PTS2 (Kv channel-interacting protein 4 isoform 1; von Willebrand factor A domain-containing protein 8) do not possess a predicted PTS2.

To verify that the characteristic pattern of PTS1 motifs was conserved between fish and humans, we compiled the known human PTS1-carrying matrix proteins and their *D. rerio* orthologues and plotted the relative abundance of amino acids at each position of the PTS1 (**Figures 4A,B**). The patterns were very similar, and a direct comparison using SeqLogo[6] did also not suggest any substantial differences (**Supplementary Figure S3B**). To visualize the differences in the PTS1 motifs of all proteins included in this study, we plotted either the prediction of fish and human PTS1 sequences as x,y-plot (**Figure 4C**) to show differences on the population scale or compared them side-by-side (**Supplementary Figure S3A**). We found that in a number of proteins the PTS1 estimation changed from "targeted" to "twilight," reflecting a putative reduction in efficiency, whereas in several proteins a PTS1 was gained or lost. To investigate the loss of PTS1 signals in selected *D. rerio* proteins further, we also included other fish species in our analysis (**Figure 4** and **Supplementary Figure S3C**).

Overall, our analysis revealed that two well-known mammalian peroxisomal proteins, bile acid-CoA:amino acid N-acyltransferase (BAAT) and zinc binding alcohol dehydrogenase domain containing 2/prostaglandin reductase 3 (ZADH2/PTGR3) are absent in *D. rerio* (**Table 1**). A previous study revealed that mouse PTGR3 is a novel 15-oxoprostaglandin-Δ(13)-reductase with a critical role in the modulation of adipocyte differentiation through the regulation of PPARγ activity (Yu et al., 2013). Whereas BAAT appears to

[6]https://services.healthtech.dtu.dk/service.php?Seq2Logo-2.0

be absent in fish, ZADH2 is present in other fish species and possesses (with the exception of Siluriformes, a sister group of Cypriniformes) a conserved PTS1 (SKL), which is also present in the human protein (**Figure 4D** and **Supplementary Figure S3C**). These findings highlight specific alterations in Cypriniform evolution with respect to peroxisomal protein inventory and metabolic functions.

Peroxiredoxin 5 (Prdx5) has lost its PTS1 in *D. rerio* and in most teleost fish species, whereas human PRDX5 possesses a PTS1, which is also retained in more ancient fish species (**Figures 4D,F,H**) suggesting a subcellular relocation of an originally peroxisomal protein in teleosts. Ubiquitin carboxyl-terminal hydrolase 2 (Usp2) has also lost its PTS1 in *D. rerio*. This only applies to the long isoform, Usp2-L (XP_005157570.1), which contains a PTS1 in several other fish species and in *H. sapiens* USP2 (Gousseva and Baker, 2003; **Figures 4D,E,G**). The short isoform, Usp2-S (Usp2b, F1RDC7_DANRE), possesses a PTS1 in *D. rerio*, *H. sapiens* (USP2-S; NP_004196.4) and in most other fish species analysed (**Figures 4D,E,G**).

Other *D. rerio* proteins with a negative PTS1 score include Crot, Acsl1, and Nudt12 (**Figure 4C** and **Supplementary Figure S3A**). It should however be noted that the PTS1 signal of the human orthologues, the carnitine octanoyltransferase CROT and the acyl-CoA synthetase ACSL1, is unclear and that the pyrophosphatase NUDT12 has only a weak PTS1.

Peroxisomal proteins with a PTS1 only identified in *D. rerio*, but not in *H. sapiens*, include urate oxidase (Uox), which is involved in purine catabolism (see above) (**Figure 4C** and **Supplementary Figure S3A**). Due to differences in the secretion products of purine degradation, several other enzymes of this pathway are absent in *H. sapiens*, often through pseudogenization (**Figure 3C** and **Table 1**). Furthermore, a malate synthase-like protein (Mlsl, A0A0R4IAX5_DANRE) appears to be present in *D. rerio* peroxisomes, but is absent in *H. sapiens* (**Figure 4C**, **Table 1**, **Supplementary Figure S3A**, and **Supplementary Table S3**). Malate synthase is a key enzyme of the glyoxylate cycle required for carbohydrate synthesis from acetyl-CoA, which exists in fungi, plants and bacteria. Malate synthase-like genes have, however, also been identified in genomes from most fish, amphibiens and marsupials (Kondrashov et al., 2006). In fungi and plants, malate synthase is localized in peroxisomes. Animal malate synthase-like proteins are functionally not characterized and have a patchy distribution of predicted PTS1 sequences, which we found in teleost fish and marsupials, but not in amphibians, monotremata and cartilaginous fish. In some animals, the degradation pathway of purines can lead to the generation of glyoxylate through the cleavage of allantoic acid by allantoicase activity (Kunze and Hartig, 2013). A possible function of Mlsl may thus be to condense the glyoxylate derived from purine degradation with acetyl-CoA to provide the versatile metabolite malate.

Other PTS1 containing proteins have an altered targeting prediction. Compared to the human orthologues, *D. rerio* Agt, Decr2, Hsdl2, and Nudt19 have a less efficient predicted PTS1, whereas Gstk1, Dhrs4, Hsd17b4 (Dbp), and Serhl appear to have a more efficient PTS1 signal (**Table 1**, **Supplementary Figure S3A**, and **Supplementary Table S3**).

In summary, our results demonstrate that although the average properties of PTS1 motifs do not differ significantly between the species (**Figures 4A,B**), differences are observed at the level of the individual proteins as outlined above (**Figure 4C** and **Supplementary Figure S3A**).

Identification of Predicted Novel Peroxisomal Candidate Proteins in Zebrafish

Our prediction also contributed to the identification of potentially novel peroxisomal proteins in zebrafish and humans. Interestingly, in addition to Acot8 (**Table 1** and **Supplementary Table S3**), we found several PTS1-containing acyl-CoA thioesterases in *D. rerio* (Acot14-18, Acot20) (**Table 1** and **Supplementary Tables S3**, **S4**). ACOTs hydrolyze acyl-CoAs to the free fatty acid and CoA, and are important for the regulation of their intracellular levels. The identified Acots and their isoforms all carry a PTS1 (AKL; Acot20: SML), but may also localise to other compartments such as mitochondria, ER or the cytosol. (**Table 1** and **Supplementary Tables S3**, **S4**). Several human ACOTs as well contain a potential PTS1 sequence: *Hs*ACOT2 localises to mitochondria (Hunt et al., 2006), but its isoforms possess a PTS1 (SKV), and may thus target mitochondria and peroxisomes. However, the C-terminal sequence of *Hs*ACOT2 is identical to *Hs*ACOT1, which localises to the cytosol and does not target peroxisomes (Hunt et al., 2006). Of the human ACOTs, ACOT4 and ACOT8 have been localised to peroxisomes. *Hs*ACOT6 (Q3I5F7, A0A2R8Y7H3) possesses a predicted weak PTS1 (SKI) indicating that other human ACOT family members may also localise to peroxisomes. Remarkably, mice possess a gene cluster of six ACOT genes with three (ACOT3-5) localizing to peroxisomes (Hunt et al., 2006). When aligned with the mammalian sequences, zebrafish Acot20 appears to be most closely related to the human ACOTs 1–6, while zebrafish Acot 14-18 build a more independent sequence cluster. Apparently, multiple gene duplications and subsequent losses resulted in a complex pattern of the ACOT gene family in different animals.

We also identified an orthologue of human β-Lactamase-like protein 2 (LACTB2), a zinc-binding endoribonuclease, which has recently been localised to mitochondria (Levy et al., 2016). However, the enzyme has also been identified in proteomics studies of rat and human liver peroxisomes (Islinger et al., 2007; Gronemeyer et al., 2013). The *D. rerio* Lactb2 possesses a predicted PTS1 (SNL), as do humans (Q53H82; -AHL), whereas the rat orthologue encodes a mutation (Q561R9; -ASL) (**Table 1** and **Supplementary Table S3**). Myc-*Rn*LACTB2 did, however, not target peroxisomes when expressed in COS-7 cells, and remained in the cytosol (Camões et al., 2015). As proteins with both a mitochondrial and peroxisomal targeting signal exist (Costello et al., 2018), peroxisomal targeting of Lactb2 may depend on certain environmental conditions. Many of the proteins dually localized to peroxisomes and mitochondria are associated with fatty acid and ROS metabolism. A competitive recognition process between the peroxisomal and mitochondrial targeting machineries has been suggested. This may involve a

hierarchical targeting system where individual receptor proteins scan a nascent protein in chronological order (Neuberger et al., 2004; Kunze and Berger, 2015). Examples for such a hierarchical sorting are the human alanine-glyoxylate aminotransferase (AGT), where specific mutations in the N-terminus create an MTS (see above), and L-bifunctional protein (EHHADH), where N-terminal mutations result in a dual peroxisomal and mitochondrial localisation (Klootwijk et al., 2014). However, how the dual targeting is prioritized under physiological conditions, is largely unknown (see Costello et al., 2018 for a recent review on dual targeting to peroxisomes and mitochondria).

Surprisingly, we identified several nuclear proteins with a potential PTS1 in zebrafish including the nuclear pore complex protein Nup93, anaphase-promoting complex subunit 5 (Anapc5), cell division cycle 5-like protein (Cdc5l), bromodomain adjacent to zinc finger domain 1A (Baz1a), BRISC and BRCA1-A complex member 2 (Babam2), calcium/calmodulin-dependent protein kinase I (Camk1), mesenchyme homeobox 2 (Meox2), and potassium channel tetramerization domain-containing 5 (Kctd5) (**Supplementary Tables S4**, **S5**). To verify the functionality of the PTS1 encoded in the *D. rerio* proteins Meox2a (E7FEH1), Cdc5l (E9QIC1), and Kctd5 (Q6NYY3), we generated expression plasmids for EGFP variants extended by the last 12 amino acids of these proteins. When expressed in COS-7 cells, PTS1-Meox2a was not targeted to peroxisomes (**Supplementary Figure S2**), whereas PTS1-Cdc5l showed a clear peroxisomal localisation (**Figure 5**). In addition, PTS1-Kctd5 localised to peroxisomes, but also showed a strong cytoplasmic background (**Figure 5**). This is consistent with the PTS1 peroxisomal targeting prediction, which indicates "targeting" for Cdc5l, but "twilight zone" for Meox2a and Kctd5 (**Supplementary Tables S4**, **S5**). However, the potential weak Meox2a and Kctd5 PTS1 appear to be conserved in different vertebrate species (**Supplementary Table S5**).

Putative PTS1 signals were also found in the human orthologues with predicted targeting for *Hs*CDC5L (Q99459) and *Hs*KCTD5 (Q9NXV2) (**Supplementary Table S5**). To verify the functionality of the human PTS1-CDC5L, which slightly differs from the *D. rerio* PTS1, we also generated an EGFP fusion. The PTS1-CDC5L was clearly targeted to peroxisomes confirming the functionality of the human PTS1 signal (**Figure 5**).

To investigate peroxisomal targeting of the human nuclear candidates with a PTS1, we selected *Hs*KCTD5 (SRM) and *Hs*CDC5L (SKF) because of their targeting sequence and accessibility of the PTS1 within the C-terminus (based on protein structure prediction). Expression of N-terminally Myc-tagged CDC5L (Myc-CDC5L) in COS-7 cells resulted in nuclear targeting, however, co-localisation with the peroxisomal marker PEX14 was not observed (**Figure 6**). Myc-KCTD5 localised mainly to the cytosol, but a peroxisomal localisation was also not detected (**Figure 6**). Our findings indicate that the PTS1 of human CDC5L (and zebrafish Cdc5L) is functional; furthermore, the PTS1 sequences of some of the nuclear candidate proteins identified appear to be maintained across different vertebrate or mammalian species. Nevertheless, full-length CDC5L is not efficiently targeted to peroxisomes in our experimental setup. An explanation may be a hierarchy of targeting signals (Neuberger et al., 2004) with a functional NLS dominating over a PTS1 under standard conditions. However, targeting may be regulated by additional factors,

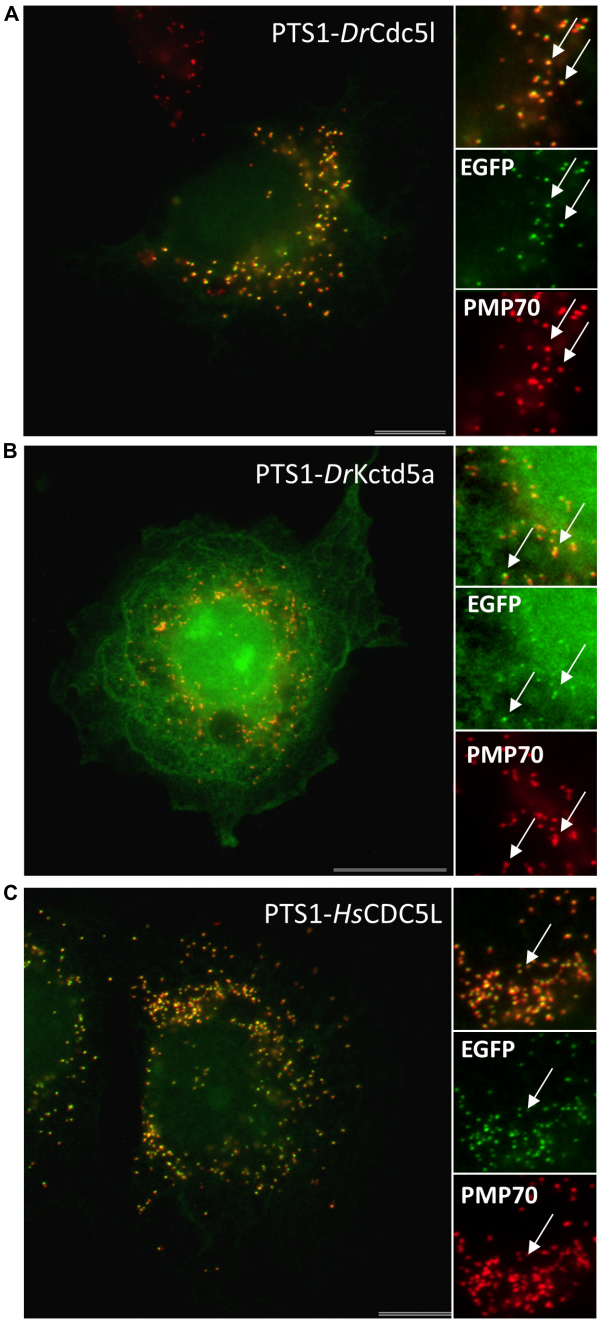

FIGURE 5 | Verification of PTS1 functionality for selected candidate proteins. COS-7 cells were transfected with an EGFP fusion protein containing the C-terminal putative PTS1 of *D. rerio* Cdc5l DLLMLDKQTLSSKI **(A)**, *D. rerio* Kctd5a DLKAKILQEQGSRM **(B)**, and *H. sapiens* CDC5L DLLLEKETLKSKF **(C)**. Cells were processed for immunofluorescence microscopy using anti-PMP70 (red) as a peroxisomal marker. White arrows highlight peroxisomes that are clearly detectable in both channels. Bars, 10 μm **(A,C)**, 20 μm **(B)**.

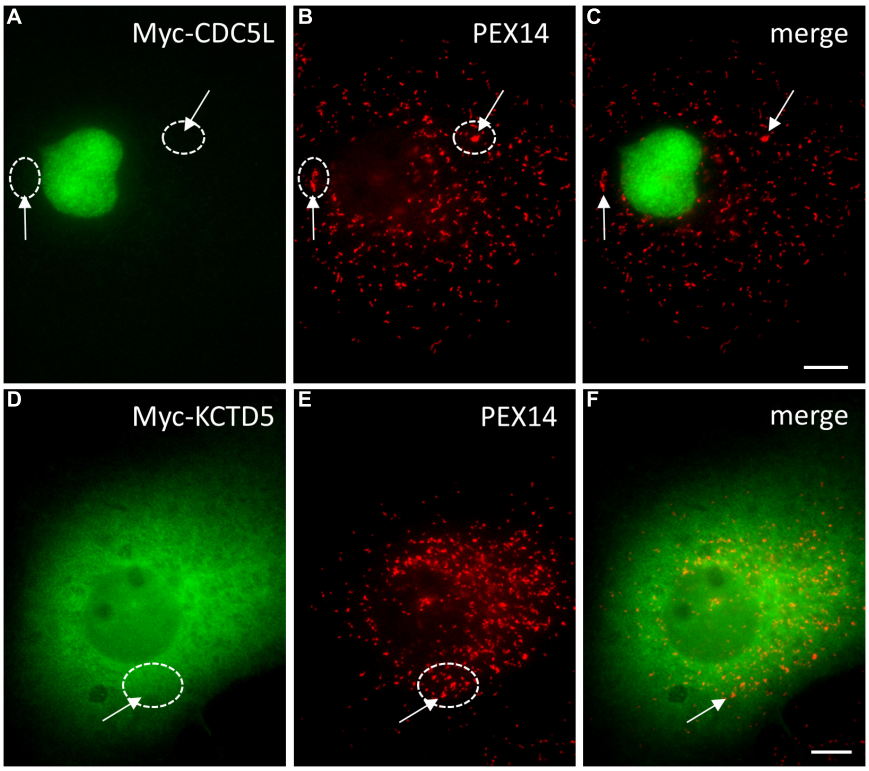

FIGURE 6 | Localisation of *Hs*CDC5L and *Hs*KCTD5 in COS-7 cells. COS-7 cells were transfected with Myc-CDC5L **(A–C)** or Myc-KCTD5 **(D–F)** and processed for immunofluorescence microscopy using anti-Myc and anti-PEX14 (peroxisomal marker) antibodies. Note that a peroxisomal localisation is not detected (arrows), even at large peroxisomal structures (circles). Bars, 10 μm.

which may be cell type-specific or are activated under certain physiological conditions. As recently described for the nuclear transcription factor FOXM1, which translocates into mitochondria to inhibit oxidative phosphorylation (Black et al., 2020), nuclear proteins could also target peroxisomes to coordinate nuclear regulation with peroxisomal metabolism. How this may be regulated under physiological conditions is currently unknown. Our findings may inspire further studies on nuclear-peroxisome communication, a research area, which is not well explored.

CONCLUSION

We reveal the first comprehensive inventory of *D. rerio* peroxisomal proteins, their targeting signals, association with peroxisomal metabolic pathways and comparison to human peroxisomes. Despite approx. 350 million years of coevolution, the protein inventories of human and zebrafish peroxisomes still appear to be largely identical implying a high degree of conservation in peroxisome metabolic functions. However, some critical changes in metabolic pathways need to be considered such as differences in purine degradation and bile acid synthesis. Our analysis confirms the suitability of zebrafish as a vertebrate model for peroxisome research and opens possibilities to study the functions of novel and established peroxisomal proteins in zebrafish in order to gain novel insights into the contribution of peroxisomes to human disorders.

DATA AVAILABILITY STATEMENT

The original contributions presented in the study are included in the article/**Supplementary Material**, further inquiries can be directed to the corresponding author/s.

AUTHOR CONTRIBUTIONS

MakK, RK, MA, MarK, and MI performed the experiments and analyzed the data. MS, MarK, MI, and VM conceived the project and analyzed the data. MS, MI, and MarK wrote the manuscript. All authors contributed to Methods.

FUNDING

This work was supported by the Biotechnology and Biological Sciences Research Council (BBSRC) (BB/T002255/1 and BB/R016844/1 to MS), and the European Union's H2020 Research and Innovation Programme under the Marie Skłodowska-Curie grant agreement no. 812968 PERICO (to MS and VM). RK and MA were supported by the Marie

Skłodowska-Curie grant agreement no. 812968 PERICO. MI was supported by the Deutsche Forschungsgemeinschaft, DFG, grant no. 397476530.

ACKNOWLEDGMENTS

We would like to acknowledge the support of T. A. Schrader and R. E. Carmichael (cell culture and molecular cloning).

SUPPLEMENTARY MATERIAL

The Supplementary Material for this article can be found online at: https://www.frontiersin.org/articles/10.3389/fphys.2022.822509/full#supplementary-material

Supplementary Figure S1 | Alignment of PEX5 N-terminus and comparison between selected vertebrate species.

Supplementary Figure S2 | Analysis of PTS1/PTS2 functionality for selected *D. rerio* candidate proteins.

Supplementary Figure S3 | Differences in the PTS1-evaluation for candidate proteins.

Supplementary Table S1 | Plasmids generated in this study.

Supplementary Table S2 | Oligonucleotides used in this study.

Supplementary Table S3 | *Danio rerio* theoretical peroxisomal protein inventory.

Supplementary Table S4 | *Danio rerio* predicted novel PTS1 proteins and PTS1 conservation in humans and goldfish.

Supplementary Table S5 | Selected putative *Danio rerio* nuclear proteins with a PTS1 and PTS1 conservation in vertebrate species.

REFERENCES

Amery, L., Fransen, M., De Nys, K., Mannaerts, G. P., and Van Veldhoven, P. P. (2000). Mitochondrial and peroxisomal targeting of 2-methylacyl-CoA racemase in humans. *J. Lipid Res.* 41, 1752–1759.

Amery, L., Sano, H., Mannaerts, G. P., Snider, J., Van Looy, J., Fransen, M., et al. (2001). Identification of PEX5p-related novel peroxisome-targeting signal 1 (PTS1)-binding proteins in mammals. *Biochem. J.* 357(Pt. 3), 635–646. doi: 10.1042/0264-6021:3570635

Anteghini, M., Martins dos Santos, V., and Saccenti, E. (2021). In-Pero: exploiting deep learning embeddings of protein sequences to predict the localisation of peroxisomal proteins. *Int. J. Mol. Sci.* 22:6409. doi: 10.3390/ijms22126409

Antonenkov, V. D., Grunau, S., Ohlmeier, S., and Hiltunen, J. K. (2010). Peroxisomes are oxidative organelles. *Antioxid. Redox Signal.* 13, 525–537. doi: 10.1089/ars.2009.2996

Arnedo, M., Latorre-Pellicer, A., Lucia-Campos, C., Gil-Salvador, M., Antońanzas-Peréz, R., Gómez-Puertas, P., et al. (2019). More than one HMG-CoA lyase: the classical mitochondrial enzyme plus the peroxisomal and the cytosolic ones. *Int. J. Mol. Sci.* 20:6124. doi: 10.3390/ijms20246124

Bartoszewska, M., Williams, C., Kikhney, A., Opaliński, Ł., van Roermund, C. W. T., de Boer, R., et al. (2012). Peroxisomal proteostasis involves a Lon family protein that functions as protease and chaperone. *J. Biol. Chem.* 287, 27380–27395. doi: 10.1074/jbc.M112.381566

Beasley, H. K., Rodman, T. A., Collins, G. V., Hinton, A. J., and Exil, V. (2021). TMEM135 is a novel regulator of mitochondrial dynamics and physiology with implications for human health conditions. *Cells* 10:1750. doi: 10.3390/cells10071750

Black, M., Arumugam, P., Shukla, S., Pradhan, A., Ustiyan, V., Milewski, D., et al. (2020). FOXM1 nuclear transcription factor translocates into mitochondria and inhibits oxidative phosphorylation. *Mol. Biol. Cell* 31, 1411–1424. doi: 10.1091/mbc.E19-07-0413

Bonekamp, N. A., Islinger, M., Lázaro, M. G., and Schrader, M. (2013). Cytochemical detection of peroxisomes and mitochondria. *Methods Mol. Biol. (Clifton, N.J.)* 931, 467–482. doi: 10.1007/978-1-62703-056-4_24

Bonekamp, N. A., Vormund, K., Jacob, R., and Schrader, M. (2010). Dynamin-like protein 1 at the Golgi complex: a novel component of the sorting/targeting machinery en route to the plasma membrane. *Exp. Cell Res.* 316, 3454–3467. doi: 10.1016/j.yexcr.2010.07.020

Braun, L., Mile, V., Schaff, Z., Csala, M., Kardon, T., Mandl, J., et al. (1999). Induction and peroxisomal appearance of gulonolactone oxidase upon clofibrate treatment in mouse liver. *FEBS Lett.* 458, 359–362. doi: 10.1016/s0014-5793(99)01184-9

Braunbeck, T., Görge, G., Storch, V., and Nagel, R. (1990). Hepatic steatosis in zebra fish (*Brachydanio rerio*) induced by long-term exposure to gamma-hexachlorocyclohexane. *Ecotoxicol. Environ. Saf.* 19, 355–374. doi: 10.1016/0147-6513(90)90036-5

Camões, F., Islinger, M., Guimarães, S. C., Kilaru, S., Schuster, M., Godinho, L. F., et al. (2015). New insights into the peroxisomal protein inventory: Acyl-CoA oxidases and -dehydrogenases are an ancient feature of peroxisomes. *Biochim. Biophys. Acta* 1853, 111–125. doi: 10.1016/j.bbamcr.2014.10.005

Castro, I. G., Richards, D. M., Metz, J., Costello, J. L., Passmore, J. B., Schrader, T. A., et al. (2018). A role for mitochondrial Rho GTPase 1 (MIRO1) in motility and membrane dynamics of peroxisomes. *Traffic (Copenhagen, Denmark)* 19, 229–242. doi: 10.1111/tra.12549

Cendron, L., Berni, R., Folli, C., Ramazzina, I., Percudani, R., and Zanotti, G. (2007). The structure of 2-oxo-4-hydroxy-4-carboxy-5-ureidoimidazoline decarboxylase provides insights into the mechanism of uric acid degradation. *J. Biol. Chem.* 282, 18182–18189. doi: 10.1074/jbc.M701297200

Choi, Y. M., Kim, Y.-I., Choi, J.-H., Bhandari, S., Nam, I.-K., Hong, K., et al. (2019). Loss of abcd4 in zebrafish leads to vitamin B(12)-deficiency anemia. *Biochem. Biophys. Res. Commun.* 514, 1264–1269. doi: 10.1016/j.bbrc.2019.05.099

Chong, C.-S., Kunze, M., Hochreiter, B., Krenn, M., Berger, J., and Maurer-Stroh, S. (2019). Rare human missense variants can affect the function of disease-relevant proteins by loss and gain of Peroxisomal targeting motifs. *Int. J. Mol. Sci.* 20:4609. doi: 10.3390/ijms20184609

Chornyi, S., IJlst, L., van Roermund, C. W. T., Wanders, R. J. A., and Waterham, H. R. (2020). Peroxisomal metabolite and cofactor transport in humans. *Front. Cell Dev. Biol.* 8:613892. doi: 10.3389/fcell.2020.613892

Claros, M. G., and Vincens, P. (1996). Computational method to predict mitochondrially imported proteins and their targeting sequences. *Eur. J. Biochem.* 241, 779–786. doi: 10.1111/j.1432-1033.1996.00779.x

Costello, J. L., Castro, I. G., Camões, F., Schrader, T. A., McNeall, D., Yang, J., et al. (2017a). Predicting the targeting of tail-anchored proteins to subcellular compartments in mammalian cells. *J. Cell Sci.* 130, 1675–1687. doi: 10.1242/jcs.200204

Costello, J. L., Castro, I. G., Hacker, C., Schrader, T. A., Metz, J., Zeuschner, D., et al. (2017b). ACBD5 and VAPB mediate membrane associations between peroxisomes and the ER. *J. Cell Biol.* 216, 331–342. doi: 10.1083/jcb.201607055

Costello, J. L., Castro, I. G., Schrader, T. A., Islinger, M., and Schrader, M. (2017c). Peroxisomal ACBD4 interacts with VAPB and promotes ER-peroxisome associations. *Cell Cycle (Georgetown, Tex.)* 16, 1039–1045. doi: 10.1080/15384101.2017.1314422

Costello, J. L., Passmore, J. B., Islinger, M., and Schrader, M. (2018). Multi-localized proteins: the peroxisome-mitochondria connection. *Sub Cell. Biochem.* 89, 383–415. doi: 10.1007/978-981-13-2233-4_17

Covill-Cooke, C., Toncheva, V. S., and Kittler, J. T. (2021). Regulation of peroxisomal trafficking and distribution. *Cell. Mol. Life Sci. CMLS* 78, 1929–1941. doi: 10.1007/s00018-020-03687-5

Danpure, C. J. (1997). Variable peroxisomal and mitochondrial targeting of alanine: glyoxylate aminotransferase in mammalian evolution and disease. *BioEssays* 19, 317–326. doi: 10.1002/bies.950190409

Darwisch, W., von Spangenberg, M., Lehmann, J., Singin, Ö., Deubert, G., Kühl, S., et al. (2020). Cerebellar and hepatic alterations in ACBD5-deficient mice are associated with unexpected, distinct alterations in cellular lipid homeostasis. *Commun. Biol.* 3:713. doi: 10.1038/s42003-020-01442-x

Dawes, M. L., Soeller, C., and Scholpp, S. (2020). Studying molecular interactions in the intact organism: fluorescence correlation spectroscopy in the living zebrafish embryo. *Histochem. Cell Biol.* 154, 507–519. doi: 10.1007/s00418-020-01930-5

Den Broeder, M. J., Kopylova, V. A., Kamminga, L. M., and Legler, J. (2015). Zebrafish as a model to study the role of peroxisome proliferating-activated receptors in adipogenesis and obesity. *PPAR Res.* 2015:358029. doi: 10.1155/2015/358029

Dindo, M., Conter, C., Oppici, E., Ceccarelli, V., Marinucci, L., and Cellini, B. (2019). Molecular basis of primary hyperoxaluria: clues to innovative treatments. *Urolithiasis* 47, 67–78. doi: 10.1007/s00240-018-1089-z

Dixit, E., Boulant, S., Zhang, Y., Lee, A. S. Y., Odendall, C., Shum, B., et al. (2010). Peroxisomes are signaling platforms for antiviral innate immunity. *Cell* 141, 668–681. doi: 10.1016/j.cell.2010.04.018

Dorninger, F., Forss-Petter, S., Wimmer, I., and Berger, J. (2020). Plasmalogens, platelet-activating factor and beyond – Ether lipids in signaling and neurodegeneration. *Neurobiol. Dis.* 145:105061. doi: 10.1016/j.nbd.2020.105061

Emanuelsson, O., Nielsen, H., Brunak, S., and von Heijne, G. (2000). Predicting subcellular localization of proteins based on their N-terminal amino acid sequence. *J. Mol. Biol.* 300, 1005–1016. doi: 10.1006/jmbi.2000.3903

Engelen, M., Kemp, S., and Poll-The, B.-T. (2014). X-linked adrenoleukodystrophy: pathogenesis and treatment. *Curr. Neurol. Neurosci. Rep.* 14:486. doi: 10.1007/s11910-014-0486-0

Fahimi, H. D. (2009). Peroxisomes: 40 years of histochemical staining, personal reminiscences. *Histochem. Cell Biol.* 131, 437–440. doi: 10.1007/s00418-009-0562-8

Ferdinandusse, S., Denis, S., van Roermund, C. W. T., Preece, M. A., Koster, J., Ebberink, M. S., et al. (2018). A novel case of ACOX2 deficiency leads to recognition of a third human peroxisomal acyl-CoA oxidase. *Biochim. Biophys. Acta Mol. Basis Dis.* 1864, 952–958. doi: 10.1016/j.bbadis.2017.12.032

Ferdinandusse, S., Falkenberg, K. D., Koster, J., Mooyer, P. A., Jones, R., van Roermund, C. W. T., et al. (2017). ACBD5 deficiency causes a defect in peroxisomal very long-chain fatty acid metabolism. *J. Med. Genet.* 54, 330–337. doi: 10.1136/jmedgenet-2016-104132

Ferdinandusse, S., Jimenez-Sanchez, G., Koster, J., Denis, S., Van Roermund, C. W., Silva-Zolezzi, I., et al. (2015). A novel bile acid biosynthesis defect due to a deficiency of peroxisomal ABCD3. *Hum. Mol. Genet.* 24, 361–370. doi: 10.1093/hmg/ddu448

Ferrer-Martínez, A., Ruiz-Lozano, P., and Chien, K. R. (2002). Mouse PeP: a novel peroxisomal protein linked to myoblast differentiation and development. *Dev. Dyn.* 224, 154–167. doi: 10.1002/dvdy.10099

Force, A., Lynch, M., Pickett, F. B., Amores, A., Yan, Y. L., and Postlethwait, J. (1999). Preservation of duplicate genes by complementary, degenerative mutations. *Genetics* 151, 1531–1545. doi: 10.1093/genetics/151.4.1531

Fracalossi, D. M., Allen, M. E., Yuyama, L. K., and Oftedal, O. T. (2001). Ascorbic acid biosynthesis in Amazonian fishes. *Aquaculture* 192, 321–332. doi: 10.1016/S0044-8486(00)00455-5

Fransen, M., Nordgren, M., Wang, B., and Apanasets, O. (2012). Role of peroxisomes in ROS/RNS-metabolism: implications for human disease. *Biochim. Biophys. Acta* 1822, 1363–1373. doi: 10.1016/j.bbadis.2011.12.001

Fransen, M., Nordgren, M., Wang, B., Apanasets, O., and Van Veldhoven, P. P. (2013). Aging, age-related diseases and peroxisomes. *Sub Cell. Biochem.* 69, 45–65. doi: 10.1007/978-94-007-6889-5_3

Frömel, T., Jungblut, B., Hu, J., Trouvain, C., Barbosa-Sicard, E., Popp, R., et al. (2012). Soluble epoxide hydrolase regulates hematopoietic progenitor cell function via generation of fatty acid diols. *Proc. Natl. Acad. Sci. U.S.A.* 109, 9995–10000. doi: 10.1073/pnas.1206493109

Gousseva, N., and Baker, R. T. (2003). Gene structure, alternate splicing, tissue distribution, cellular localization, and developmental expression pattern of mouse deubiquitinating enzyme isoforms Usp2-45 and Usp2-69. *Gene Expr.* 11, 163–179. doi: 10.3727/000000003108749053

Grant, P., Ahlemeyer, B., Karnati, S., Berg, T., Stelzig, I., Nenicu, A., et al. (2013). The biogenesis protein PEX14 is an optimal marker for the identification and localization of peroxisomes in different cell types, tissues, and species in morphological studies. *Histochem. Cell Biol.* 140, 423–442. doi: 10.1007/s00418-013-1133-6

Gronemeyer, T., Wiese, S., Ofman, R., Bunse, C., Pawlas, M., Hayen, H., et al. (2013). The proteome of human liver peroxisomes: identification of five new peroxisomal constituents by a label-free quantitative proteomics survey. *PLoS One* 8:e57395. doi: 10.1371/journal.pone.0057395

Hagey, L. R., Møller, P. R., Hofmann, A. F., and Krasowski, M. D. (2010). Diversity of bile salts in fish and amphibians: evolution of a complex biochemical pathway. *Physiol. Biochem. Zool.* 83, 308–321. doi: 10.1086/649966

Han, Y., Lyman, K. A., Foote, K. M., and Chetkovich, D. M. (2020). The structure and function of TRIP8b, an auxiliary subunit of hyperpolarization-activated cyclic-nucleotide gated channels. *Channels (Austin, Tex.)* 14, 110–122. doi: 10.1080/19336950.2020.1740501

Havemeyer, A., Bittner, F., Wollers, S., Mendel, R., Kunze, T., and Clement, B. (2006). Identification of the missing component in the mitochondrial benzamidoxime prodrug-converting system as a novel molybdenum enzyme. *J. Biol. Chem.* 281, 34796–34802. doi: 10.1074/jbc.M607697200

Hayashi, S., Fujiwara, S., and Noguchi, T. (1989). Degradation of uric acid in fish liver peroxisomes. Intraperoxisomal localization of hepatic allantoicase and purification of its peroxisomal membrane-bound form. *J. Biol. Chem.* 264, 3211–3215. doi: 10.1016/s0021-9258(18)94053-6

Hayashi, S., Fujiwara, S., and Noguchi, T. (2000). Evolution of urate-degrading enzymes in animal peroxisomes. *Cell Biochem. Biophys.* 32 Spring, 123–129. doi: 10.1385/cbb:32:1-3:123

Hofhuis, J., Schueren, F., Nötzel, C., Lingner, T., Gärtner, J., Jahn, O., et al. (2016). The functional readthrough extension of malate dehydrogenase reveals a modification of the genetic code. *Open Biol.* 6:160246. doi: 10.1098/rsob.160246

Hölttä-Vuori, M., Salo, V. T. V., Nyberg, L., Brackmann, C., Enejder, A., Panula, P., et al. (2010). Zebrafish: gaining popularity in lipid research. *Biochem. J.* 429, 235–242. doi: 10.1042/BJ20100293

Horton, P., Park, K.-J., Obayashi, T., Fujita, N., Harada, H., Adams-Collier, C. J., et al. (2007). WoLF PSORT: protein localization predictor. *Nucleic Acids Res.* 35, W585–W587. doi: 10.1093/nar/gkm259

Houten, S. M., Wanders, R. J. A., and Ranea-Robles, P. (2020). Metabolic interactions between peroxisomes and mitochondria with a special focus on acylcarnitine metabolism. *Biochim. Biophys. Acta Mol. Basis Dis.* 1866:165720. doi: 10.1016/j.bbadis.2020.165720

Hua, R., Cheng, D., Coyaud, É, Freeman, S., Di Pietro, E., Wang, Y., et al. (2017). VAPs and ACBD5 tether peroxisomes to the ER for peroxisome maintenance and lipid homeostasis. *J. Cell Biol.* 216, 367–377. doi: 10.1083/jcb.201608128

Huang, P.-C., Chiu, C.-C., Chang, H.-W., Wang, Y.-S., Syue, H.-H., Song, Y.-C., et al. (2017). Prdx1-encoded peroxiredoxin is important for vascular development in zebrafish. *FEBS Lett.* 591, 889–902. doi: 10.1002/1873-3468.12604

Hunt, M. C., Rautanen, A., Westin, M. A. K., Svensson, L. T., and Alexson, S. E. H. (2006). Analysis of the mouse and human acyl-CoA thioesterase (ACOT) gene clusters shows that convergent, functional evolution results in a reduced number of human peroxisomal ACOTs. *FASEB J.* 20, 1855–1864. doi: 10.1096/fj.06-6042com

Iida, R., Yasuda, T., Tsubota, E., Takatsuka, H., Matsuki, T., and Kishi, K. (2006). Human Mpv17-like protein is localized in peroxisomes and regulates expression of antioxidant enzymes. *Biochem. Biophys. Res. Commun.* 344, 948–954. doi: 10.1016/j.bbrc.2006.04.008

Islinger, M., Cardoso, M. J. R., and Schrader, M. (2010). Be different – the diversity of peroxisomes in the animal kingdom. *Biochim. Biophys. Acta* 1803, 881–897. doi: 10.1016/j.bbamcr.2010.03.013

Islinger, M., Costello, J. L., Kors, S., Soupene, E., Levine, T. P., Kuypers, F. A., et al. (2020). The diversity of ACBD proteins – From lipid binding to protein modulators and organelle tethers. *Biochim. Biophys. Acta Mol. Cell Res.* 1867:118675. doi: 10.1016/j.bbamcr.2020.118675

Islinger, M., Li, K. W., Seitz, J., Völkl, A., and Lüers, G. H. (2009). Hitchhiking of Cu/Zn superoxide dismutase to peroxisomes–evidence for a natural piggyback import mechanism in mammals. *Traffic (Copenhagen, Denmark)* 10, 1711–1721. doi: 10.1111/j.1600-0854.2009.00966.x

Islinger, M., Lüers, G. H., Li, K. W., Loos, M., and Völkl, A. (2007). Rat liver peroxisomes after fibrate treatment. A survey using quantitative mass spectrometry. *J. Biol. Chem.* 282, 23055–23069. doi: 10.1074/jbc.M610910200

Islinger, M., Voelkl, A., Fahimi, H. D., and Schrader, M. (2018). The peroxisome: an update on mysteries 2.0. *Histochem. Cell Biol.* 150, 443–471. doi: 10.1007/s00418-018-1722-5

Jansen, R. L. M., Santana-Molina, C., van den Noort, M., Devos, D. P., and van der Klei, I. J. (2021). Comparative genomics of peroxisome biogenesis proteins: making sense of the PEX proteins. *Front. Cell Dev. Biol.* 9:654163. doi: 10.3389/fcell.2021.654163

Jiang, H. (2021). Quality control pathways of tail-anchored proteins. *Biochim. Biophys. Acta Mol. Cell Res.* 1868:118922. doi: 10.1016/j.bbamcr.2020.118922

Jones, J. M., Morrell, J. C., and Gould, S. J. (2000). Identification and characterization of HAOX1, HAOX2, and HAOX3, three human peroxisomal

2-hydroxy acid oxidases. *J. Biol. Chem.* 275, 12590–12597. doi: 10.1074/jbc.275.17.12590

Karnati, S., Lüers, G., Pfreimer, S., and Baumgart-Vogt, E. (2013). Mammalian SOD2 is exclusively located in mitochondria and not present in peroxisomes. *Histochem. Cell Biol.* 140, 105–117. doi: 10.1007/s00418-013-1099-4

Kawaguchi, K., and Morita, M. (2016). ABC transporter subfamily D: distinct differences in behavior between ABCD1-3 and ABCD4 in subcellular localization, function, and human disease. *BioMed Res. Int.* 2016:6786245. doi: 10.1155/2016/6786245

Kiema, T.-R., Thapa, C. J., Laitaoja, M., Schmitz, W., Maksimainen, M. M., Fukao, T., et al. (2019). The peroxisomal zebrafish SCP2-thiolase (type-1) is a weak transient dimer as revealed by crystal structures and native mass spectrometry. *Biochem. J.* 476, 307–332. doi: 10.1042/BCJ20180788

Kim, Y.-I., Bhandari, S., Lee, J. N., Yoo, K.-W., Kim, S.-J., Oh, G.-S., et al. (2014). Developmental roles of D-bifunctional protein-A zebrafish model of peroxisome dysfunction. *Mol. Cells* 37, 74–80. doi: 10.14348/molcells.2014.2300

Kim, Y.-I., Nam, I.-K., Lee, D.-K., Bhandari, S., Charton, L., Kwak, S., et al. (2020). Slc25a17 acts as a peroxisomal coenzyme A transporter and regulates multiorgan development in zebrafish. *J. Cell. Physiol.* 235, 151–165. doi: 10.1002/jcp.28954

Klootwijk, E. D., Reichold, M., Helip-Wooley, A., Tolaymat, A., Broeker, C., Robinette, S. L., et al. (2014). Mistargeting of peroxisomal EHHADH and inherited renal Fanconi's syndrome. *New Engl. J. Med.* 370, 129–138. doi: 10.1056/NEJMoa1307581

Kondrashov, F. A., Koonin, E. V., Morgunov, I. G., Finogenova, T. V., and Kondrashova, M. N. (2006). Evolution of glyoxylate cycle enzymes in Metazoa: evidence of multiple horizontal transfer events and pseudogene formation. *Biol. Direct* 1:31. doi: 10.1186/1745-6150-1-31

Krogh, A., Larsson, B., von Heijne, G., and Sonnhammer, E. L. (2001). Predicting transmembrane protein topology with a hidden Markov model: application to complete genomes. *J. Mol. Biol.* 305, 567–580. doi: 10.1006/jmbi.2000.4315

Krysko, O., Stevens, M., Langenberg, T., Fransen, M., Espeel, M., and Baes, M. (2010). Peroxisomes in zebrafish: distribution pattern and knockdown studies. *Histochem. Cell Biol.* 134, 39–51. doi: 10.1007/s00418-010-0712-z

Kunze, M. (2018). Predicting peroxisomal targeting signals to elucidate the peroxisomal proteome of mammals. *Sub Cell. Biochem.* 89, 157–199. doi: 10.1007/978-981-13-2233-4_7

Kunze, M. (2020). The type-2 peroxisomal targeting signal. *Biochim. Biophys. Acta* 1867:118609. doi: 10.1016/j.bbamcr.2019.118609

Kunze, M., and Berger, J. (2015). The similarity between N-terminal targeting signals for protein import into different organelles and its evolutionary relevance. *Front. Physiol.* 6:259. doi: 10.3389/fphys.2015.00259

Kunze, M., and Hartig, A. (2013). Permeability of the peroxisomal membrane: lessons from the glyoxylate cycle. *Front. Physiol.* 4:204. doi: 10.3389/fphys.2013.00204

Kunze, M., Neuberger, G., Maurer-Stroh, S., Ma, J., Eck, T., Braverman, N., et al. (2011). Structural requirements for interaction of peroxisomal targeting signal 2 and its receptor PEX7. *J. Biol. Chem.* 286, 45048–45062. doi: 10.1074/jbc.M111.301853

Kurochkin, I. V., Mizuno, Y., Konagaya, A., Sakaki, Y., Schönbach, C., and Okazaki, Y. (2007). Novel peroxisomal protease Tysnd1 processes PTS1- and PTS2-containing enzymes involved in beta-oxidation of fatty acids. *EMBO J.* 26, 835–845. doi: 10.1038/sj.emboj.7601525

Lametschwandtner, G., Brocard, C., Fransen, M., Van Veldhoven, P., Berger, J., and Hartig, A. (1998). The difference in recognition of terminal tripeptides as peroxisomal targeting signal 1 between yeast and human is due to different affinities of their receptor Pex5p to the cognate signal and to residues adjacent to it. *J. Biol. Chem.* 273, 33635–33643. doi: 10.1074/jbc.273.50.33635

Leiper, J. M., and Danpure, C. J. (1997). A unique molecular basis for enzyme mistargeting in primary hyperoxaluria type 1. *Clin. Chim. Acta* 266, 39–50. doi: 10.1016/s0009-8981(97)00165-4

Levy, S., Allerston, C. K., Liveanu, V., Habib, M. R., Gileadi, O., and Schuster, G. (2016). Identification of LACTB2, a metallo-β-lactamase protein, as a human mitochondrial endoribonuclease. *Nucleic Acids Res.* 44, 1813–1832. doi: 10.1093/nar/gkw050

Lismont, C., Revenco, I., and Fransen, M. (2019). Peroxisomal hydrogen peroxide metabolism and signaling in health and disease. *Int. J. Mol. Sci.* 20:3673. doi: 10.3390/ijms20153673

Liu, G.-P., Xiang, L.-X., Shao, T., Lin, A.-F., and Shao, J.-Z. (2018). Stimulatory function of peroxiredoxin 1 in activating adaptive humoral immunity in a zebrafish model. *Dev. Comp. Immunol.* 84, 353–360. doi: 10.1016/j.dci.2018.03.004

Madeira, F., Park, Y. M., Lee, J., Buso, N., Gur, T., Madhusoodanan, N., et al. (2019). The EMBL-EBI search and sequence analysis tools APIs in 2019. *Nucleic Acids Res.* 47, W636–W641. doi: 10.1093/nar/gkz268

Mancuso, D. J., Han, X., Jenkins, C. M., Lehman, J. J., Sambandam, N., Sims, H. F., et al. (2007). Dramatic accumulation of triglycerides and precipitation of cardiac hemodynamic dysfunction during brief caloric restriction in transgenic myocardium expressing human calcium-independent phospholipase A2gamma. *J. Biol. Chem.* 282, 9216–9227. doi: 10.1074/jbc.M607307200

Mancuso, D. J., Jenkins, C. M., and Gross, R. W. (2000). The genomic organization, complete mRNA sequence, cloning, and expression of a novel human intracellular membrane-associated calcium-independent phospholipase A(2). *J. Biol. Chem.* 275, 9937–9945. doi: 10.1074/jbc.275.14.9937

Mancuso, D. J., Jenkins, C. M., Sims, H. F., Cohen, J. M., Yang, J., and Gross, R. W. (2004). Complex transcriptional and translational regulation of iPLAgamma resulting in multiple gene products containing dual competing sites for mitochondrial or peroxisomal localization. *Eur. J. Biochem.* 271, 4709–4724. doi: 10.1111/j.1432-1033.2004.04435.x

Marcassa, E., Kallinos, A., Jardine, J., Rusilowicz-Jones, E. V., Clague, M. J., and Urbé, S. (2019). New aspects of USP30 biology in the regulation of pexophagy. *Autophagy* 15, 1634–1637. doi: 10.1080/15548627.2019.1615304

Marchetti, M., Liuzzi, A., Fermi, B., Corsini, R., Folli, C., Speranzini, V., et al. (2016). Catalysis and structure of zebrafish urate oxidase provide insights into the origin of hyperuricemia in hominoids. *Sci. Rep.* 6:38302. doi: 10.1038/srep38302

Martorano, L., Peron, M., Laquatra, C., Lidron, E., Facchinello, N., Meneghetti, G., et al. (2019). The zebrafish orthologue of the human hepatocerebral disease gene MPV17 plays pleiotropic roles in mitochondria. *Dis. Model. Mech.* 12:dmm037226. doi: 10.1242/dmm.037226

Morais, S., Knoll-Gellida, A., André, M., Barthe, C., and Babin, P. J. (2007). Conserved expression of alternative splicing variants of peroxisomal acyl-CoA oxidase 1 in vertebrates and developmental and nutritional regulation in fish. *Physiol. Genomics* 28, 239–252. doi: 10.1152/physiolgenomics.00136.2006

Morel, F., Rauch, C., Petit, E., Piton, A., Theret, N., Coles, B., et al. (2004). Gene and protein characterization of the human glutathione S-transferase kappa and evidence for a peroxisomal localization. *J. Biol. Chem.* 279, 16246–16253. doi: 10.1074/jbc.M313357200

Motley, A. M., Hettema, E. H., Ketting, R., Plasterk, R., and Tabak, H. F. (2000). Caenorhabditis elegans has a single pathway to target matrix proteins to peroxisomes. *EMBO Rep.* 1, 40–46. doi: 10.1093/embo-reports/kvd010

Mullen, R. T., Trelease, R. N., Duerk, H., Arand, M., Hammock, B. D., Oesch, F., et al. (1999). Differential subcellular localization of endogenous and transfected soluble epoxide hydrolase in mammalian cells: evidence for isozyme variants. *FEBS Lett.* 445, 301–305. doi: 10.1016/s0014-5793(99)00142-8

Neuberger, G., Kunze, M., Eisenhaber, F., Berger, J., Hartig, A., and Brocard, C. (2004). Hidden localization motifs: naturally occurring peroxisomal targeting signals in non-peroxisomal proteins. *Genome Biol.* 5:R97. doi: 10.1186/gb-2004-5-12-r97

Neuberger, G., Maurer-Stroh, S., Eisenhaber, B., Hartig, A., and Eisenhaber, F. (2003). Prediction of peroxisomal targeting signal 1 containing proteins from amino acid sequence. *J. Mol. Biol.* 328, 581–592. doi: 10.1016/s0022-2836(03)00319-x

Okumoto, K., Kametani, Y., and Fujiki, Y. (2011). Two proteases, trypsin domain-containing 1 (Tysnd1) and peroxisomal lon protease (PsLon), cooperatively regulate fatty acid β-oxidation in peroxisomal matrix. *J. Biol. Chem.* 286, 44367–44379. doi: 10.1074/jbc.M111.285197

Omi, S., Nakata, R., Okamura-Ikeda, K., Konishi, H., and Taniguchi, H. (2008). Contribution of peroxisome-specific isoform of Lon protease in sorting PTS1 proteins to peroxisomes. *J. Biochem.* 143, 649–660. doi: 10.1093/jb/mvn020

Ortiz-Zarragoitia, M., Trant, J. M., and Cajaravillet, M. P. (2006). Effects of dibutylphthalate and ethynylestradiol on liver peroxisomes, reproduction, and development of zebrafish (*Danio rerio*). *Environ. Toxicol. Chem.* 25, 2394–2404. doi: 10.1897/05-456r.1

Pridie, C., Ueda, K., and Simmonds, A. J. (2020). Rosy beginnings: studying peroxisomes in *Drosophila*. *Front. Cell Dev. Biol.* 8:835. doi: 10.3389/fcell.2020.00835

Raas, Q., van de Beek, M.-C., Forss-Petter, S., Dijkstra, I. M., Deschiffart, A., Freshner, B. C., et al. (2021). Metabolic rerouting via SCD1 induction impacts X-linked adrenoleukodystrophy. *J. Clin. Invest.* 131:e142500. doi: 10.1172/JCI142500

Ramazzina, I., Folli, C., Secchi, A., Berni, R., and Percudani, R. (2006). Completing the uric acid degradation pathway through phylogenetic comparison of whole genomes. *Nat. Chem. Biol.* 2, 144–148. doi: 10.1038/nchembio768

Reuter, M., Kooshapur, H., Suda, J.-G., Gaussmann, S., Neuhaus, A., Brühl, L., et al. (2021). Competitive microtubule binding of PEX14 coordinates peroxisomal protein import and motility. *J. Mol. Biol.* 433:166765. doi: 10.1016/j.jmb.2020.166765

Riccio, V., Demers, N., Hua, R., Vissa, M., Cheng, D. T., Strilchuk, A. W., et al. (2019). Deubiquitinating enzyme USP30 maintains basal peroxisome abundance by regulating pexophagy. *J. Cell Biol.* 218, 798–807. doi: 10.1083/jcb.201804172

Rixen, S., Havemeyer, A., Tyl-Bielicka, A., Pysniak, K., Gajewska, M., Kulecka, M., et al. (2019). Mitochondrial amidoxime-reducing component 2 (MARC2) has a significant role in N-reductive activity and energy metabolism. *J. Biol. Chem.* 294, 17593–17602. doi: 10.1074/jbc.RA119.007606

Schlüter, A., Fourcade, S., Domènech-Estévez, E., Gabaldón, T., Huerta-Cepas, J., Berthommier, G., et al. (2007). PeroxisomeDB: a database for the peroxisomal proteome, functional genomics and disease. *Nucleic Acids Res.* 35, D815–D822. doi: 10.1093/nar/gkl935

Schlüter, A., Real-Chicharro, A., Gabaldón, T., Sánchez-Jiménez, F., and Pujol, A. (2010). PeroxisomeDB 2.0: an integrative view of the global peroxisomal metabolome. *Nucleic Acids Res.* 38, D800–D805. doi: 10.1093/nar/gkp935

Schrader, M., and Fahimi, H. D. (2006). Peroxisomes and oxidative stress. *Biochim. Biophys. Acta* 1763, 1755–1766. doi: 10.1016/j.bbamcr.2006.09.006

Schrader, M., Costello, J. L., Godinho, L. F., Azadi, A. S., and Islinger, M. (2016). Proliferation and fission of peroxisomes – An update. *Biochim. Biophys. Acta* 1863, 971–983. doi: 10.1016/j.bbamcr.2015.09.024

Schueren, F., Lingner, T., George, R., Hofhuis, J., Dickel, C., Gärtner, J., et al. (2014). Peroxisomal lactate dehydrogenase is generated by translational readthrough in mammals. *ELife* 3:e03640. doi: 10.7554/eLife.03640

Silva, B. S. C., DiGiovanni, L., Kumar, R., Carmichael, R. E., Kim, P. K., and Schrader, M. (2020). Maintaining social contacts: the physiological relevance of organelle interactions. *Biochim. Biophys. Acta Mol. Cell Res.* 1867:118800. doi: 10.1016/j.bbamcr.2020.118800

Small, I., Peeters, N., Legeai, F., and Lurin, C. (2004). Predotar: a tool for rapidly screening proteomes for N-terminal targeting sequences. *Proteomics* 4, 1581–1590. doi: 10.1002/pmic.200300776

Smith, B. T., Sengupta, T. K., and Singh, I. (2000). Intraperoxisomal localization of very-long-chain fatty acyl-CoA synthetase: implication in X-adrenoleukodystrophy. *Exp. Cell Res.* 254, 309–320. doi: 10.1006/excr.1999.4757

Spinazzola, A., Viscomi, C., Fernandez-Vizarra, E., Carrara, F., D'Adamo, P., Calvo, S., et al. (2006). MPV17 encodes an inner mitochondrial membrane protein and is mutated in infantile hepatic mitochondrial DNA depletion. *Nat. Genet.* 38, 570–575. doi: 10.1038/ng1765

Stiebler, A. C., Freitag, J., Schink, K. O., Stehlik, T., Tillmann, B. A. M., Ast, J., et al. (2014). Ribosomal readthrough at a short UGA stop codon context triggers dual localization of metabolic enzymes in Fungi and animals. *PLoS Genet.* 10:e1004685. doi: 10.1371/journal.pgen.1004685

Strachan, L. R., Stevenson, T. J., Freshner, B., Keefe, M. D., Miranda Bowles, D., and Bonkowsky, J. L. (2017). A zebrafish model of X-linked adrenoleukodystrophy recapitulates key disease features and demonstrates a developmental requirement for abcd1 in oligodendrocyte patterning and myelination. *Hum. Mol. Genet.* 26, 3600–3614. doi: 10.1093/hmg/ddx249

Sugiura, A., Mattie, S., Prudent, J., and McBride, H. M. (2017). Newly born peroxisomes are a hybrid of mitochondrial and ER-derived pre-peroxisomes. *Nature* 542, 251–254. doi: 10.1038/nature21375

Takashima, S., Takemoto, S., Toyoshi, K., Ohba, A., and Shimozawa, N. (2021). Zebrafish model of human Zellweger syndrome reveals organ-specific accumulation of distinct fatty acid species and widespread gene expression changes. *Mol. Genet. Metab.* 133, 307–323. doi: 10.1016/j.ymgme.2021.05.002

Turchini, G. M., Francis, D. S., Du, Z.-Y., Olsen, R. E., Ringø, E., and Tocher, D. R. (2022). "The lipids," in *Fish Nutrition*, Fourth Edn, eds R. W. Hardy and S. J. Kaushik (San Diego, CA: Academic Press), 303–468. doi: 10.1016/B978-0-12-819587-1.00003-3

Van Veldhoven, P. P. (2010). Biochemistry and genetics of inherited disorders of peroxisomal fatty acid metabolism. *J. Lipid Res.* 51, 2863–2895. doi: 10.1194/jlr.R005959

Van Veldhoven, P. P., and Baes, M. (2013). Peroxisome deficient invertebrate and vertebrate animal models. *Front. Physiol.* 4:335. doi: 10.3389/fphys.2013.00335

Venkatachalam, A. B., Lall, S. P., Denovan-Wright, E. M., and Wright, J. M. (2012). Tissue-specific differential induction of duplicated fatty acid-binding protein genes by the peroxisome proliferator, clofibrate, in zebrafish (*Danio rerio*). *BMC Evol. Biol.* 12:112. doi: 10.1186/1471-2148-12-112

Violante, S., Achetib, N., van Roermund, C. W. T., Hagen, J., Dodatko, T., Vaz, F. M., et al. (2019). Peroxisomes can oxidize medium- and long-chain fatty acids through a pathway involving ABCD3 and HSD17B4. *FASEB J.* 33, 4355–4364. doi: 10.1096/fj.201801498R

Walter, T., and Erdmann, R. (2019). Current advances in protein import into peroxisomes. *Protein J.* 38, 351–362. doi: 10.1007/s10930-019-09835-6

Wanders, R. J. A., and Waterham, H. R. (2006). Biochemistry of mammalian peroxisomes revisited. *Annu. Rev. Biochem.* 75, 295–332. doi: 10.1146/annurev.biochem.74.082803.133329

Wang, W., Xia, Z.-J., Farré, J.-C., and Subramani, S. (2017). TRIM37, a novel E3 ligase for PEX5-mediated peroxisomal matrix protein import. *J. Cell Biol.* 216, 2843–2858. doi: 10.1083/jcb.201611170

Watkins, P. A., and Ellis, J. M. (2012). Peroxisomal acyl-CoA synthetases. *Biochim. Biophys. Acta* 1822, 1411–1420. doi: 10.1016/j.bbadis.2012.02.010

Weiher, H., Pircher, H., Jansen-Dürr, P., Hegenbarth, S., Knolle, P., Grunau, S., et al. (2016). A monoclonal antibody raised against bacterially expressed MPV17 sequences shows peroxisomal, endosomal and lysosomal localisation in U2OS cells. *BMC Res. Notes* 9:128. doi: 10.1186/s13104-016-1939-0

Williams, C., Bener Aksam, E., Gunkel, K., Veenhuis, M., and van der Klei, I. J. (2012). The relevance of the non-canonical PTS1 of peroxisomal catalase. *Biochim. Biophys. Acta* 1823, 1133–1141. doi: 10.1016/j.bbamcr.2012.04.006

Yagita, Y., Shinohara, K., Abe, Y., Nakagawa, K., Al-Owain, M., Alkuraya, F. S., et al. (2017). Deficiency of a retinal dystrophy protein, Acyl-CoA binding domain-containing 5 (ACBD5), impairs peroxisomal β-oxidation of very-long-chain fatty acids. *J. Biol. Chem.* 292, 691–705. doi: 10.1074/jbc.M116.760090

Yamashita, H., Avraham, S., Jiang, S., London, R., Van Veldhoven, P. P., Subramani, S., et al. (1999). Characterization of human and murine PMP20 peroxisomal proteins that exhibit antioxidant activity in vitro. *J. Biol. Chem.* 274, 29897–29904. doi: 10.1074/jbc.274.42.29897

Yifrach, E., Fischer, S., Oeljeklaus, S., Schuldiner, M., Zalckvar, E., and Warscheid, B. (2018). Defining the mammalian peroxisomal proteome. *Subcell. Biochem.* 89, 47–66. doi: 10.1007/978-981-13-2233-4_2

Yu, Y. H., Chang, Y. C., Su, T. H., Nong, J. Y., Li, C. C., and Chuang, L. M. (2013). Prostaglandin reductase-3 negatively modulates adipogenesis through regulation of PPARγ activity. *J. Lipid Res.* 54, 2391–2399. doi: 10.1194/jlr.M037556

Zanotti, G., Cendron, L., Ramazzina, I., Folli, C., Percudani, R., and Berni, R. (2006). Structure of zebra fish HIUase: insights into evolution of an enzyme to a hormone transporter. *J. Mol. Biol.* 363, 1–9. doi: 10.1016/j.jmb.2006.07.079

Conflict of Interest: MA and VM were employed by company LifeGlimmer GmbH.

The remaining authors declare that the research was conducted in the absence of any commercial or financial relationships that could be construed as a potential conflict of interest.

Publisher's Note: All claims expressed in this article are solely those of the authors and do not necessarily represent those of their affiliated organizations, or those of the publisher, the editors and the reviewers. Any product that may be evaluated in this article, or claim that may be made by its manufacturer, is not guaranteed or endorsed by the publisher.

frontiers | Frontiers in Physiology

REVIEW
published: 11 July 2022
doi: 10.3389/fphys.2022.833540

Signal Peptide Features Determining the Substrate Specificities of Targeting and Translocation Components in Human ER Protein Import

Sven Lang[1], Duy Nguyen[2†], Pratiti Bhadra[2], Martin Jung[1], Volkhard Helms[2] and Richard Zimmermann[1]**

[1]Medical Biochemistry and Molecular Biology, Saarland University, Homburg, Germany, [2]Center for Bioinformatics, Saarland University, Saarbrücken, Germany

OPEN ACCESS

Edited by:
Andrey L. Karamyshev, Texas Tech University Health Sciences Center, United States

Reviewed by:
Johannes M. Herrmann, University of Kaiserslautern, Germany
Teresa M. Buck, University of Pittsburgh, United States

***Correspondence:**
Sven Lang
sven.lang@uni-saarland.de
Richard Zimmermann
richard.zimmermann@uks.eu

†Present address:
Duy Nguyen, Deutsches Krebsforschungszentrum (DKFZ), Heidelberg, Germany

Specialty section:
This article was submitted to Membrane Physiology and Membrane Biophysics, a section of the journal Frontiers in Physiology

Received: *11 December 2021*
Accepted: *17 May 2022*
Published: *11 July 2022*

Citation:
Lang S, Nguyen D, Bhadra P, Jung M, Helms V and Zimmermann R (2022) Signal Peptide Features Determining the Substrate Specificities of Targeting and Translocation Components in Human ER Protein Import. Front. Physiol. 13:833540. doi: 10.3389/fphys.2022.833540

In human cells, approximately 30% of all polypeptides enter the secretory pathway at the level of the endoplasmic reticulum (ER). This process involves cleavable amino-terminal signal peptides (SPs) or more or less amino-terminal transmembrane helices (TMHs), which serve as targeting determinants, at the level of the precursor polypeptides and a multitude of cytosolic and ER proteins, which facilitate their ER import. Alone or in combination SPs and TMHs guarantee the initial ER targeting as well as the subsequent membrane integration or translocation. Cytosolic SRP and SR, its receptor in the ER membrane, mediate cotranslational targeting of most nascent precursor polypeptide chains to the polypeptide-conducting Sec61 complex in the ER membrane. Alternatively, fully-synthesized precursor polypeptides and certain nascent precursor polypeptides are targeted to the ER membrane by either the PEX-, SND-, or TRC-pathway. Although these targeting pathways may have overlapping functions, the question arises how relevant this is under cellular conditions and which features of SPs and precursor polypeptides determine preference for a certain pathway. Irrespective of their targeting pathway(s), most precursor polypeptides are integrated into or translocated across the ER membrane via the Sec61 channel. For some precursor polypeptides specific Sec61 interaction partners have to support the gating of the channel to the open state, again raising the question why and when this is the case. Recent progress shed light on the client spectrum and specificities of some auxiliary components, including Sec62/Sec63, TRAM1 protein, and TRAP. To address the question which precursors use a certain pathway or component in intact human cells, i.e., under conditions of fast translation rates and molecular crowding, in the presence of competing precursors, different targeting organelles, and relevant stoichiometries of the involved components, siRNA-mediated depletion of single targeting or transport components in HeLa cells was combined with label-free quantitative proteomics and differential protein abundance analysis. Here, we present a summary of the experimental approach as well as the resulting differential protein abundance analyses and discuss their mechanistic implications in light of the available structural data.

Keywords: endoplasmic reticulum, protein targeting, protein translocation, signal peptides, Sec61 complex, human cells, siRNA-mediated depletion of single targeting or transport components, label-free quantitative proteomics in combination with differential protein abundance anlysis

1 INTRODUCTION

1.1 Protein Biogenesis at the Endoplasmic Reticulum

In analogy to the division of the human body into various organs, the nucleated human cell is divided into different compartments, the cell organelles. Organelles are surrounded and, thus, separated from the cytosol by phospholipid bilayers (**Figure 1A**). The vast majority of the roughly 30,000 types of polypeptides of human cells is synthesized in the cytosol. Therefore, the proteins of the various organelles have to be targeted to the specific organelles and, subsequently, inserted into or translocated across the organelle membrane(s). Protein import into the organelle network termed endoplasmic reticulum (ER) is the first step in the biogenesis of about one third of the different soluble and membrane proteins of human cells (Gemmer and Förster, 2020; O'Keefe et al., 2021a; Pool, 2022; Tirincsi et al., 2022a). The hallmarks of this process were first established about 70 years ago by Palade et al., who also described different ER morphologies, or -as these are termed today- domains (Palade and Porter, 1954; Palade, 1975). From their electron microscopic images these authors concluded that the ER represents a "continuous, tridimensional reticulum" consisting of "cisternae," which appear to communicate freely with the "tubules" (Palade and Porter, 1954; Palade, 1975). Furthermore, Palade et al. wrote that "although such cisternae may assume considerable breadth they seem to retain, in general, a depth of ~50 μm" and "the surface of the latter appears to be dotted with small, dense granules that cover them in part or in entirety" (Palade and Porter, 1954; Palade, 1975). Today, those original domains of the ER are referred to as rough sheets and smooth tubules, where rough and smooth refers to the presence or absence of the dense granules observed by Palade et al. (Palade and Porter, 1954; Palade, 1975), i.e., ribosomes or polysomes which are attached to the cytosolic ER surface (**Figure 1B**) (Shibata et al., 2006; Shibata et al., 2010; Westrate et al., 2015; Nixon-Abell at el., 2016; Valm et al., 2017).

Originally, the roughly 10,000 soluble and membrane proteins that first enter the ER in the course of their biogenesis were known to fulfill their functions in the membrane or lumen of the ER plus the nuclear envelope, or in one of the organelles of the pathways of endo- and exocytosis (i.e., ERGIC, Golgi apparatus, endosome, lysosome, trafficking vesicles), or at the cell surface as secretory- or plasma membrane-proteins. With the exception of resident proteins of the ER, most of the correctly folded and assembled proteins are transported to their functional location by trafficking vesicles, which bud from sub-domains of the tubular ER that are termed exit sites (ERES) (Raote et al., 2018; Raote et al., 2020). In recent years, however, an increasing number of membrane proteins destined to lipid droplets, peroxisomes or mitochondria was observed to be first targeted to and inserted into the ER membrane prior to their integration into budding lipid droplets or peroxisomes or prior to their delivery to mitochondria via the ER-SURF pathway (Hansen et al., 2018; Schrul and Schliebs, 2018; Jansen and Klei, 2019; Dhimann et al., 2020; Goodman, 2020; Koch et al., 2021; Lalier et al., 2021). Interestingly, the budding of lipid droplets and peroxisomes also occurs in sub-domains of the tubular ER, which may be spatially or physically related to ERES (see below) (Schrul and Kopito, 2016; Song et al., 2021; Zimmermann et al., 2021). Moreover, several cytosolic proteins are synthesized on ER-bound ribosomes (Seiser and Nicchitta, 2000; Potter et al., 2001; Pyhtila et al., 2008; Reid and Nicchitta, 2012; Calvin et al., 2014; Berkovits and Mayr, 2015; Ma and Mayr, 2018).

1.2 Endoplasmic Reticulum Targeting Mechanisms

Typically, protein import into the ER involves ER membrane targeting as the first step and insertion of nascent or fully-synthesized membrane proteins into or translocation of soluble precursor polypeptides across the ER membrane as the second step (**Figures 1C,D**). These two processes depend on cleavable amino-terminal signal peptides (SPs) or non-cleavable and more or less amino-terminal transmembrane helices (TMHs), which, by definition, both serve as import determinants in the precursor polypeptides (von Heijne, 1985; von Heijne, 1986; von Heijne and Gavel, 1988; Goder and Spiess, 2003; Goder et al., 2004; Hegde and Bernstein, 2006; Baker et al., 2017; Armenteros et al., 2019). In general, the Sec61 complex in the ER membrane represents the entry point for most of these precursor polypeptides into the organelle (**Figures 1**, **2**; **Table 1**) (Görlich et al., 1992b; Görlich and Rapoport, 1993; Hartmann et al., 1994; Simon and Blobel, 1991; Beckmann et al., 2001; Wirth et al., 2003; van den Berg et al., 2004; Pfeffer et al., 2012; Pfeffer et al., 2014; Pfeffer et al., 2015; Voorhees et al., 2014, Voorhees and Hegde, 2016). However, membrane insertion of some precursors of membrane proteins can be facilitated by alternative membrane protein insertases and components such as the ER membrane protein complex (EMC), TMCO1 complex, and WRB/CAML (Shurtleff et al., 2018; Chitwood et al., 2018; Pleiner et al., 2020; Bai et al., 2020; O'Donnell et al., 2020; Wang et al., 2016; Anghel et al., 2017; McGilvray et al., 2020). Notably, the latter has its main role in the membrane insertion of tail anchored (TA) membrane proteins (Borgese and Fasana, 2011; Yamamoto and Sakisaka, 2012; Borgese et al., 2019). Together with its cytosolic interaction partners, the latter can also facilitate targeting of precursor polypeptides to the Sec61 complex, as apparently do the SRP/SR-, PEX19/PEX3-, and SND-targeting pathways (**Figure 2**) (Meyer and Dobberstein, 1980a; Meyer and Dobberstein, 1980b; Gilmore et al., 1982a; Gilmore et al., 1982b; Tajima et al., 1986; Siegel and Walter, 1988; Ng et al., 1996; Egea et al., 2005; Gamerdinger et al., 2015; Aviram et al., 2016; Casson et al., 2017; Haßdenteufel et al., 2017; Haßdenteufel et al., 2018;

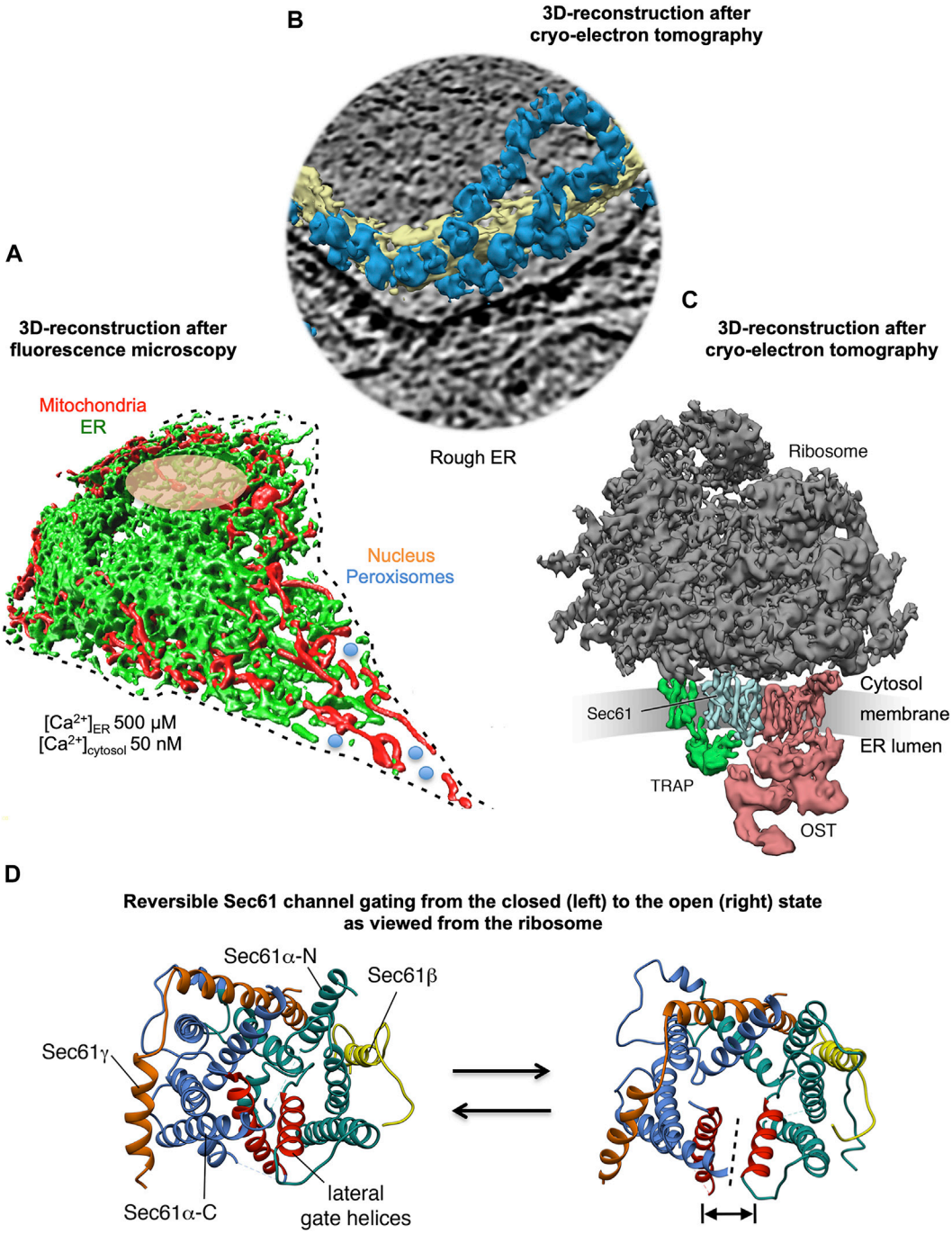

FIGURE 1 | 3D reconstructions of a nucleated mammalian cell, a section of rough ER, and a ribosome-bound Sec61 translocon. **(A)** 3D reconstruction after live cell fluorescence imaging, following import of GFP into the ER and of RFP into the mitochondria. The reconstruction was artificially complemented by a dashed line for the plasma membrane, by an orange ellipse for the nucleus, and by a couple of blue circles for peroxisomes. Typical concentrations of free Ca^{2+} are given for cytosol and ER in a resting cell. **(B)** 3D reconstruction of cellular rough ER after CET of a slice through the respective tomogram. ER membranes are shown in yellow, 80S ribosomes in blue. **(C)** 3D reconstruction of the native ribosome-translocon complex in rough microsomes. The membrane density was removed for better visibility of membrane integral parts of the translocon complex. TMHs in Sec61 complex, TRAP and OST can be distinguished. Helix 51 of an rRNA ES and ribosomal protein eL38 represent contacts of TRAPγ, but are hidden by other ribosomal densities. **(D)** The concept of reversible gating of the heterotrimeric Sec61 complex by SPs and allosteric effectors. The Sec61 channel is shown in its modeled closed (left) and open (right) conformational states, as viewed from the cytosol. These two states are suggested to be in a dynamic equilibrium with each other. The fully open state of the Sec61 channel allows the initial entry of precursor polypeptides from the cytosol into the ER lumen and ER membrane, respectively, and is experimentally observed as cleavage of SPs by signal peptidase on the lumenal side of the ER membrane. In addition, it allows the passive efflux of Ca^{2+} from the ER lumen into the cytosol and can be observed in live cell Ca^{2+} imaging in cytosol and ER lumen (Erdmann et al., 2011; Schäuble et al., 2012). Ca^{2+} efflux may also be possible in the expected transition state (not shown), which may be identical to the so-called primed state and is induced by ribosomes in cotranslational- and by Sec62/Sec63 in posttranslational-transport. The Figure and Figure legend were adapted from Sicking et al. (2021a).

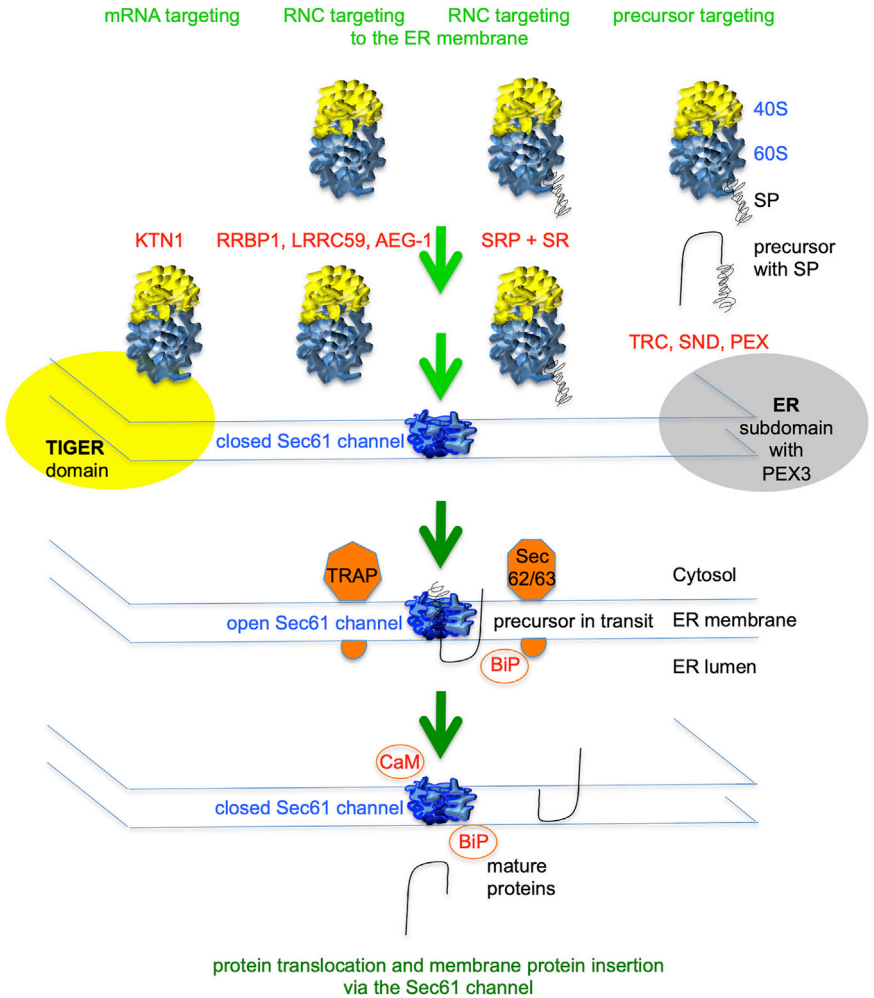

FIGURE 2 | Flow diagram for signal peptide-dependent import of precursor polypeptides into the human endoplasmic reticulum (ER). ER import of most precursor polypeptides involves the Sec61 channel in the ER membrane, which mediates membrane insertion of membrane proteins and translocation of soluble proteins with N-terminal signal peptides (SPs). Typically, SPs of nascent precursor polypeptides are cotranslationally targeted to the Sec61 complex in the ER membrane by SRP and its dimeric receptor in the ER membrane (SR). Others are targeted co- or posttranslationally by the TRC-, PEX19/PEX3- or hSnd2/hSnd3-pathway. Furthermore, there are components for mRNA- and/or RNC-targeting located in the ER membrane. Additional ER membrane proteins support Sec61 channel gating to the open state (TRAP or Sec62/Sec63) or membrane protein insertion, such as EMC (not shown). Channel gating to the closed state can be supported by cytosolic Ca^{2+}-CaM or BiP in the ER lumen (Erdmann et al., 2011; Schäuble et al., 2012). The green arrows symbolize progress of the import reaction. See **Table 1** for a complete list of proteins that are involved in ER protein import.

Haßdenteufel et al., 2019; Hsieh et al., 2020; Jomaa et al., 2021). Targeting of certain peroxisomal membrane proteins and some but not all hairpin membrane proteins of lipid droplets or the ER and their insertion into the ER membrane was found to involve cytosolic PEX19 and PEX3 in the ER membrane (Schrul and Kopito, 2016; Yamamoto and Sakisaka, 2018; Leznicki et al., 2021).

In addition, there is targeting of mRNAs to the Sec61 complex that depends on receptors for mRNAs (such as KTN1) (Ong et al., 2003; Ong et al., 2006), or receptors for ribosome nascent chain complexes, where the nascent polypeptide chains are not yet long enough to interact with SRP (such as RRBP1, LRRC59, and AEG-1) (**Figure 2**) (Savitz and Meyer, 1990; Tazawa et al., 1991; Ohsumi et al., 1993; Savitz and Meyer, 1993; Calvin et al., 2014; Hsu et al., 2018). In contrast to SRP/SR, these mRNA targeting mechanisms are nucleic acid based and may deliver essentially every kind of mRNA to the ER surface, including mRNAs coding for soluble proteins of the cytosol or the mitochondrial and peroxisomal matrix (Seiser and Nicchitta, 2000; Potter et al., 2001; Calvin et al., 2014; Berkovits and Mayr, 2015; Ma and Mayr, 2018). In the case that the mRNA codes for a cytosolic or matrix protein, the heterodimeric cytosolic protein nascent polypeptide-associated complex (NAC) can get access to the amino-terminus of the nascent polypeptide and trigger its release from Sec61 and the simultaneous release of the ribosome from the Sec61 complex (Wiedmann et al., 1994; Moeller et al., 1998; Gamerdinger et al., 2019; Hsieh et al., 2020). If the mRNA codes for a precursor

TABLE 1 | Protein transport components/*complexes,* associated proteins in HeLa cells and linked diseases.

Component/subunit	Abundance[a]	Location[b]	Linked Diseases
for ER targeting			
#LRRC59 (LRC59, p34)[c]	2480	ERM	
#RRBP1 (p180)	135	ERM	Hepatocellular Carcinoma, Colorectal Cancer
KTN1 (Kinectin 1)	263	ERM	
AEG-1 (LYRIC, MTDH)	575	ERM	
#*NAC*[d]		C	
- NAC α	1412		
- NAC β			
#*SRP*		C	
- SRP72	355		Aplasia, Myelodysplasia
- SRP68	197		
- SRP54	228		Neutropenia, Pancreas Insufficiency
- SRP19	33		
- SRP14	4295		
- SRP9	3436		
- 7SL RNA			
SRP receptor		ERM	
- SRα (docking protein)	249		
- SRβ	173		
Calmodulin	9428	C	
hSnd1	unknown		
Snd receptor		ERM	
- hSnd2 (TMEM208)	81		
- §hSnd3 (TMEM109)	49		
PEX19	80	C	Zellweger Syndrome
PEX3	103	ERM,PexM	Zellweger Syndrome
PEX16	9	ERM,PexM	Zellweger Syndrome
for ER targeting plus membrane integration			
#*Bag6 complex*		C	
- TRC35 (Get4)	171		CDG
- Ubl4A	177		
- Bag6 (Bat3)	133		Lung cancer
SGTA	549	C	Breast cancer, Lung cancer
TRC40 (Asna1, Get3)	381	C	CDG
TA receptor		ERM	
- CAML (CAMLG, Get2)	5		CDG
- WRB (CHD5, Get1)	4		Congenital Heart Disease
for ER membrane integration			
ERM protein complex		ERM	
- EMC1	124		Visual disorders
- EMC2	300		
- EMC3	270		
- EMC4	70		
- EMC5 (MMGT1)	35		
- EMC6 (TMEM93)	5		
- EMC7	247		
- EMC8	209		
- EMC9	1		
- EMC10	3		Developmental delay
#§*TMCO1 complex*		ERM	Glaucoma, Cerebrofaciothoracic Dysplasia
- TMCO1	2013		
- Nicalin	99		
- TMEM147	21		

(Continued on following page)

TABLE 1 | (*Continued*) Protein transport components/*complexes,* associated proteins in HeLa cells and linked diseases.

Component/subunit	Abundance[a]	Location[b]	Linked Diseases
- CCDC47 (Calumin)	193		
- NOMO	267		
PAT complex	193	ERM	
- PAT10 (Asterix)			
- CCDC47 (Calumin)			
for ER membrane integration plus translocation			
#§*Sec61 complex*		ERM	
- Sec61α1	139		Diabetes[e], CVID[f], TKD, Neutropenia
- Sec61β	456		PLD, Colorectal cancer
- Sec61γ	400		GBM, Hepatocellular carcinoma
#Sec62/Sec63		ERM	
- Sec62 (TLOC1)	26		Breast-, Prostate-, Cervix-, Lung-Cancer
- Sec63 (ERj2)	168		PLD, Colorectal cancer
#ERj1 (DNAJC1)	8	ERM	
#TRAM1	26	ERM	
TRAM2	40	ERM	
#*TRAP*		ERM	
- TRAPα ((SSR1)	568		
- TRAPβ (SSR2)			
- TRAPγ (SSR3)	1701		CDG, Hepatocellular Carcinoma
- TRAPδ (SSR4)	3212		CDG
#RAMP4 (SERP1)		ERM	
for folding plus assembly			
ER Chaperones			
- BiP (Grp78, HSPA5)	8253	ERL	HUS
- Calreticulin (CaBP3, ERp60)	14521	ERL	
- #Calnexin$_{palmitoylated}$	7278	ERM	
- ERj3 (DNAJB11)	1001	ERL	PKD
- ERj4 (DNAJB9)	12	ERL	
- ERj5 (DNAJC10)	43	ERL	
- ERj6 (DNAJC3, p58^{IPK})	237	ERL	Diabetes, Neurodegeneration
- ERj7 (DNAJC25)	10	ERM	Hyperinsulinismus, Allergic Asthma
- ERj8 (DNAJC16)	24	ERM	
- ERj9 (DNAJC22)		ERM	
- Grp94 (CaBP4, Hsp90B1)	4141	ERL	
- Grp170 (HYOU1)	923	ERL	
- Sil1 (BAP)	149	ERL	MSS
for covalent modification			
#*Oligosaccharyltransferase (OST-A)*		ERM	
- RibophorinI (Rpn1)	1956		
- RibophorinII (Rpn2)	527		
- OST48	273		CDG
- Dad1	464		
- OST4			
- TMEM258			
- Stt3A*	430		CDG
- DC2			
- Kcp2			
Oligosaccharyltransferase (OST-B)		ERM	
- RibophorinI (Rpn1)	1956		
- RibophorinII (Rpn2)	527		
- OST48	273		
- Dad1	464		CDG

(Continued on following page)

TABLE 1 | (*Continued*) Protein transport components/*complexes,* associated proteins in HeLa cells and linked diseases.

Component/subunit	Abundance[a]	Location[b]	Linked Diseases
- OST4			
- TMEM258			
- Stt3B*	150		CDG
- TUSC3			CDG
- MagT1	33		
Signal peptidase (SPC-A)		ERM	
- SPC12	2733		
- SPC18* (SEC11A)			
- SPC22/23	334		
- SPC25	94	ERM	
Signal peptidase (SPC-C)			
- SPC12	2733		
- SPC21* (SEC11C)			
- SPC22/23	334		
- SPC25	94		
GPI transamidase (GPI-T)		ERM	
- GPAA1	9		
- PIG-K	38		
- PIG-S	86		
- PIG-T	20		
- PIG-U	42		

[a]*Here, abundance refers to the concentration (nM) of the respective protein in HeLa cells, as reported by Hein et al. (2015).*
[b]*Localization refers to the functional intracellular localization(s) of the respective protein, i.e., C, Cytosol; ERL, ER lumen; ERM, ER membrane; PexM, Peroxisomal membrane.*
[c]*Alternative protein names are given in parentheses.*
[d]*Complexes are indicated by italics. Abbreviations for protein names: EMC, ER membrane (protein) complex; GET, Guided entry of tail-anchored proteins; GPI, Glycosylphosphatidylinositol; NAC, Nascent polypeptide-associated complex; OST, Oligosaccharyltransferase; SEC, (Protein involved in) secretion; SND, SRP-independent; SPC, signal peptidase; SR, SRP receptor; SRP, signal recognition particle; SSR, signal sequence receptor; TA, tail anchor; TMEM, Transmembrane (protein); TRAM, translocating chain-associating membrane (protein); TRAP, Translocon-associated protein; TRC, transmembrane recognition complex.*
[e]*Diabetes was linked to the particular protein in mouse.*
[f]*Abbreviation for diseases, i.e., CDG, Congenital disorder of glycosylation; CVID, Common variable immunodeficiency; GBM, Glioblastoma multiforme; HUS, Hemolytic-uremic syndrome; MSS, Marinesco-Sjögren syndrome; PKD, Polycystic kidney disease; PLD, Polycystic liver disease; TKD, tubulointerstitial kidney disease, as reported by Sicking et al. (2021a).*
**Indicates enzymatic activity.*
 # indicates ribosome association.
§Indicates ion channel activity.
We note that Calnexin, ERj1, Sec61ß, Sec63, SRα, TRAM1, and TRAPα were shown to be subject to phosphorylation.

polypeptide with SP or TMH, however, the latter may spontaneously interact with the Sec61 channel or the productive interaction may be facilitated by one of the protein targeting components.

In case of the SP- or TMH-dependent ER targeting, cotranslational ER targeting of nascent precursor polypeptides and their mRNAs is mediated by the cytosolic signal recognition particle (SRP) and its heterodimeric receptor in the ER membrane, i.e., SRP receptor or SR (**Table 1**) (Siegel and Walter, 1988; Ng et al., 1996; Egea et al., 2005; Gamerdinger et al., 2015; Hsieh et al., 2020; Jomaa et al., 2021; Meyer and Dobberstein, 1980a; Meyer and Dobberstein, 1980b; Gilmore et al., 1982a; Gilmore et al., 1982b; Tajima et al., 1986). Other binary targeting systems comprising a single ribosome-associating component and a heterodimeric membrane receptor may co- and posttranslationally direct precursor polypeptides to the Sec61 complex and were named TRC-, PEX19/PEX3-, and hSnd2/hSnd3-pathway (Borgese and Fasana, 2011; Yamamoto and Sakisaka, 2012; Borgese et al., 2019; Schrul and Kopito, 2016; Yamamoto and Sakisaka, 2018; Aviram et al., 2016; Casson et al., 2017; Haßdenteufel et al., 2017; Haßdenteufel et al., 2018; Haßdenteufel et al., 2019; Tirincsi et al., 2022b). Some hairpin and most TA membrane proteins depend on dedicated components and posttranslational pathways for their ER targeting and subsequent membrane insertion (**Figure 3**). The TRC-pathway (termed GET-pathway in yeast) handles TA proteins and the PEX3-dependent pathway some hairpin and certain peroxisomal membrane proteins (Borgese and Fasana, 2011; Yamamoto and Sakisaka, 2012; Borgese et al., 2019; Schrul and Kopito, 2016; Yamamoto and Sakisaka, 2018). In the case of the TRC-pathway, membrane targeting involves the Bag6 complex as well as additional cytosolic factors; in case of the PEX3-dependent pathway, membrane targeting involves cytosolic PEX19 (**Table 1**). Notably, these pathways are not strictly separated from each other, i.e., there are at least some precursor polypeptides, which can be targeted by more than one pathway. For example, certain small human presecretory proteins with a content of less than 100 amino acid residues, such as preproapelin, can be targeted to the Sec61 complex by the SRP-, SND- as well as the TRC-pathway (Haßdenteufel et al., 2017, 2018, and 2019). Likewise, some TA membrane proteins (such as Sec61ß and RAMP4) can be targeted to the membrane via the same three pathways (Casson et al., 2017). In addition, the Sec61ß coding mRNA can be targeted to the ER by

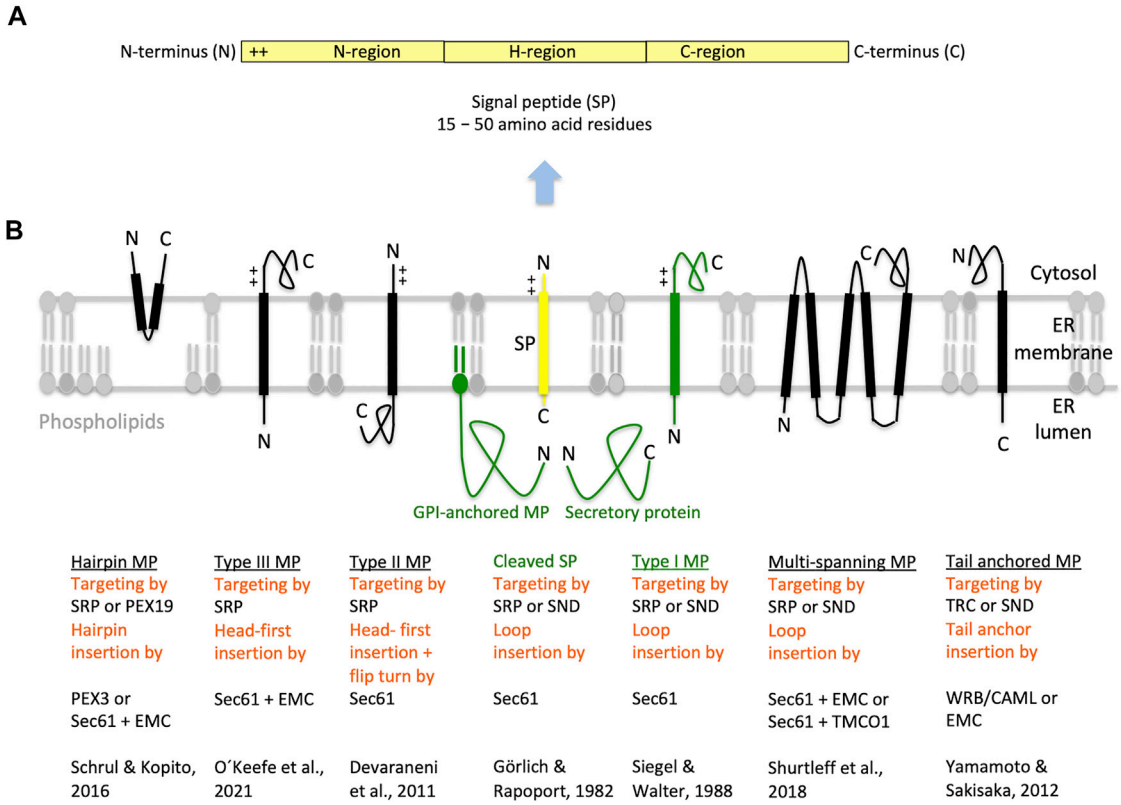

FIGURE 3 | Types of ER membrane proteins and their biogenesis. **(A,B)** The cartoons depict a signal peptide (SP) and six classes of ER membrane proteins (MP, underlined) with their particular membrane protein type and the respective mechanism of ER targeting and membrane insertion (both indicated below the cartoon in red). Cleavable SPs (in yellow) have a tripartite structure and facilitate ER import of secretory proteins (in green), glycosylphosphatidylinositol (GPI)-anchored- and single-spanning type I membrane proteins (in green). In addition, they may mediate ER import of certain multi-spanning membrane proteins, but not of hairpin, single-spanning type II or III, other multi-spanning and TA membrane proteins, which depend on transmembrane helices (TMHs) that serve as SPs and facilitate membrane targeting as well as insertion. Positively charged amino acid residues (+) play an important role in the orientation of membrane proteins and SPs in the membrane; typically, the orientation follows the positive inside rule. In the case of membrane proteins with amino-terminal TMHs, membrane insertion typically involves the same components and mechanisms, which deliver secretory proteins and GPI-anchored membrane proteins to the ER lumen. In certain cases, however, auxiliary membrane protein insertases, such as EMC or TMCO1 complex may be involved. Following their ER import, GPI-anchored membrane proteins become membrane anchored via their carboxy-termini by GPI-attachment. Some key references are given. The Figure and Figure legend were adapted from Sicking et al. (2021a). C, carboxy-terminus; N, amino-terminus.

an unknown mechanism (Cui et al., 2015). Thus there is redundancy in the targeting process, i.e., the targeting pathways have overlapping substrate specificities.

SPs for ER protein import, typically, comprise around 25 amino acid residues and have a tripartite structure with a positively charged amino-terminus (defined as N-region), a central hydrophobic region (defined as H-region), and a slightly polar carboxy-terminus (defined as C-region) (**Figure 3**) (von Heijne, 1985; Hegde and Bernstein, 2006). SPs have a dual function; they target presecretory proteins to the Sec61 complex and trigger the opening of an aqueous channel within the Sec61 complex for translocation of the polypeptide into the ER lumen (Görlich and Rapoport, 1993; Wirth et al., 2003; Dejgaard et al., 2010; Conti et al., 2015; Voorhees and Hegde, 2016). TMH are similar to SP in structure and function, except for the positioning of positively charged amino acid residues, which can be up- or downstream of the central hydrophobic region and determine the TMH orientation in the ER membrane, following the "positive inside rule" (Goder et al., 2004; Baker et al., 2017; Whitely et al., 2021).

1.3 Translocation Mechanisms

In human cells, the heterotrimeric Sec61 complex forms a large multicomponent system together with the ribosome and the oligomeric membrane proteins translocon-associated protein (TRAP) and oligosaccharyltransferase (OST), which catalyzes N-linked glycosylation (**Figure 1C**) (Pfeffer et al., 2012; Pfeffer et al., 2014; Pfeffer et al., 2015; Pfeffer et al., 2017; Mahamid et al., 2016). This super-complex or Sec61 translocon can insert into the membrane or translocate into the lumen a whole variety of topologically very different precursor polypeptides (type I-, type II-, type III-, TA and hairpin membrane proteins and soluble proteins, respectively) (**Figure 3**). Next, these precursors mature to membrane proteins with one or more hairpins or TMHs, as glycosylphosphatidylinositol- (GPI-) anchored membrane proteins, or soluble proteins in the ER lumen, such as ER-

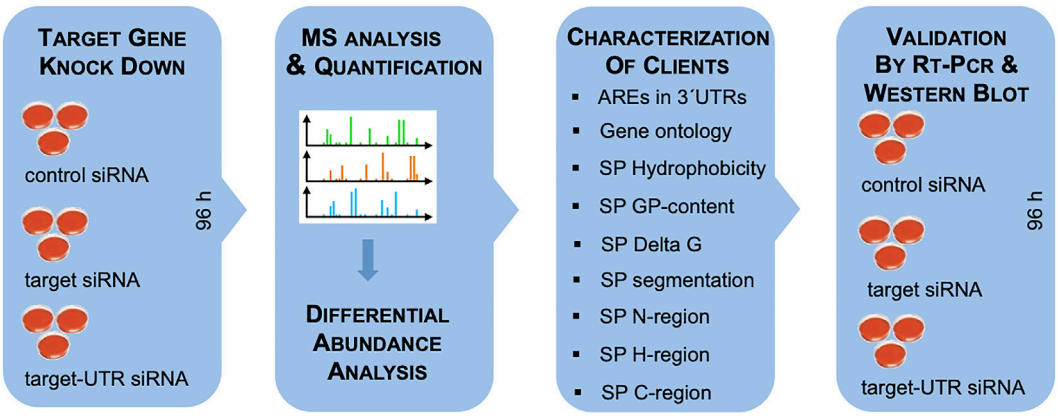

FIGURE 4 | Experimental strategy. The experimental strategy involved i) siRNA-mediated gene silencing using two different siRNAs for each target and one non-targeting (control) siRNA, respectively, with three replicates for each siRNA for 96 h; ii) label-free quantitative analysis of the total cellular proteome; iii) differential protein abundance analysis to identify negatively affected proteins (i.e., putative substrates or clients of the target) and positively affected proteins (i.e., putative compensatory mechanisms); iv) independent validation by western blot. For characterization of substrates, genes were screened for AU-rich elements (ATTTA motifs) in 3′UTRs using the AREsite2 database (http://rna.tbi.univie.ac.at/AREsite2/welcome) and SPs were analyzed for hydrophobicity according to Kyte and Doolittle, (1982) (https://www.bioinformatics.org/sms2/protein_gravy.html), GP-content (Nguyen et al., 2018), apparent Delta G for membrane insertion of TMHs (http://dgpred.cbr.su.se), or segmentation (https://phobius.sbc.su.se) in combination with characterization of the SP segments with the same tools as above.

lumenal or secretory proteins (Gemmer and Förster, 2020; O'Keefe et al., 2021a; Tirincsi et al., 2022a; Liaci and Förster, 2021). Typically, membrane insertion and translocation are facilitated by either a cleavable amino-terminal SP or the TMH of the nascent precursor polypeptide, which acts as a non-cleavable SP substitute. Cleavable SPs are removed from the precursor polypeptides in transit by one of the two signal peptidase complexes (SPCs), which have their catalytic sites in the ER lumen (Kalies et al., 1998; Chen et al., 2001; Liaci and Förster, 2021).

Thus, ER protein import involves three stages, i) co- or posttranslational targeting of the precursor to the heterotrimeric Sec61 complex in the ER membrane, ii) head-on ($N_{ER\ lumen\ or\ out}$-$C_{cytosol\ or\ in}$) or loop (N_{in}-C_{out}) insertion of the SP or TMH into the polypeptide-conducting Sec61 channel, and iii) completion of membrane insertion or translocation. Co- and posttranslational insertion of SP or TMH into the Sec61 channel and the simultaneous gating of the Sec61 channel to the open state occur either spontaneously or involve substrate-specific auxiliary components of the Sec61 channel (such as TRAP, Sec62/Sec63, TRAM1) (Wiedmann et al., 1987; Fons et al., 2003; Menetret et al., 2008; Sommer et al., 2013; Lang et al., 2012; Lakkaraju et al., 2012; Ziska et al., 2019; Görlich et al., 1992a; Voigt et al., 1996; Hegde et al., 1998; Sauri et al., 2007). Typically, the orientation of SP- and TMH in the Sec61 channel follows the positive inside rule (Goder et al., 2004; Baker et al., 2017), i.e. positively charged amino acid residues in the N-region support loop insertion (N_{in}-C_{out}) and positively charged residues downstream of the SP or TMH interfere with loop insertion and, therefore, favour head-on insertion (N_{out}-C_{in}) that can be followed by a "flip turn" (**Figure 3**) (Devaraneni et al., 2011).

Following the pioneering work by Blobel and Dobberstein (1975a) and Blobel and Dobberstein (1975b), ER protein import was studied in cell-free assays, which involve synthesis of a single precursor polypeptide in the presence of ER derived membrane vesicles or proteoliposomes and allow the conclusion of whether and how targeting and membrane insertion or translocation of a certain precursor can be facilitated by a certain component. Recently, more global approaches were employed, such as proximity-specific ribosome-profiling (Reid and Nicchitta, 2012; Calvin et al., 2014; Hsu et al., 2018; Shurtleff et al., 2018; Hannigan et al., 2020) and quantitative proteomics (Nguyen et al., 2018; Shurtleff et al., 2018; Tian et al., 2019; Klein et al., 2020; Schorr et al., 2020; Bhadra et al., 2021a; Zimmermann et al., 2021; Tirincsi et al., 2022b). We started to address the question which precursors use a certain pathway or component in intact human cells, i.e., under conditions of fast translation rates and in the presence of competing precursors. Typically, our approach employed siRNA-mediated depletion of single components in HeLa cells, label-free quantitative proteomic analysis, and differential protein abundance analysis to characterize client specificities of various components.

2 SUMMARY OF PREVIOUSLY REPORTED RESULTS FROM LABEL-FREE PROTEOMICS

2.1 A Proteomic Approach for the Analysis of Protein Import Into the Human Endoplasmic Reticulum

Our experimental approach was designed to identify substrates or clients of components, which are involved in targeting or translocation of precursor polypeptides into the human ER under cellular conditions, thereby setting it apart from experiments where single precursor proteins are studied one by one in either cell-free systems for synthesis of proteins and their import into ER-derived vesicles (rough microsomes) or

proteoliposomes, or the ER of semi-permeabilized cells, or under conditions where single precursor proteins are over-produced in cells. The approach represents a combination of siRNA-mediated knock down or CRISPR/Cas9-mediated knock-out of a certain protein targeting or translocation component in human cells (such as HeLa or HEK293 cells), label-free quantitative mass spectrometric (MS) analysis of the total cellular proteome, and differential protein abundance analysis for two different cell pools that had been treated with two different siRNAs, which target the same mRNA, compared to a pool of cells, which had been treated with a non-targeting siRNA (defined as negative control) (**Figure 4**). In the case of knock-out cells, only two cell pools were compared, a control cell line and the knock-out line; where available, deficient patient fibroblasts were analyzed (as in the case of Congenital disorders of glycosylation or Zellweger syndrome). The approach is based on the expectations that precursors polypeptides, destined to the ER, are degraded by the cytosolic proteasome upon interference with their ER import. Therefore, their cellular levels decrease compared to control cells, which is detected by quantitative MS in combination with subsequent differential protein abundance analysis (**Figure 4**). In several depletions (SEC61A, TRAPB, WRB, SRA) the absence of the target subunit, typically, caused degradation of the other subunit(s) of the complex or even other components of the same pathway, reminiscent of the "use it or loose it principle" of muscle physiology (Nguyen et al., 2018; Tirincsi et al., 2022b). Consistent with the starting expectation, the decrease of secretory pathway proteins was accompanied by an increase in ubiquitin-conjugating enzymes in the cytosol. Furthermore, in some cases the concomitant increase in other ER import components was observed, which may point to a possible functional, compensatory overlap between different pathways. Alternatively or additionally, we observed an increase in components for protein import into mitochondria, which appears to be an alternative to protein degradation in preventing aggregation of potentially dangerous polypeptides in the cytosol (Pfeiffer et al., 2013). All these phenomena were inversely correlated with the severity of the negative effect on secretory pathway proteins.

As a proof-of-principle, the approach was established for the Sec61 complex, which is necessary for or at least involved in the ER import of most precursor polypeptides (**Figures 1–3**; **Supplementary Table S1**) (Nguyen et al., 2018). In general, the timing of the experiment was optimized to seeding of the cells on day one with two consecutive siRNA transfections on the same and the following day and harvesting of the cells on day four (**Figure 4**). Alternatively, CRISPR/Cas9-treated knock-out cells and, in some cases, deficient patient fibroblasts were cultivated in parallel to the respective control cells for 96 h.

Typically, between 5,000 and 6,500 different proteins were quantified and statistically analyzed (**Supplementary Tables S1, S2**), including proteins with low and high cellular concentrations, which ranged from below 1 to almost 10,000 nM (Hein et al., 2015; Schorr et al., 2020; Bhadra et al., 2021a). For the control cells, Gene Ontology (GO) terms assigned the expected 26%–29% of proteins to organelles of the endocytic and exocytic pathways plus the extracellular space and plasma membrane (**Supplementary Tables S1, S2**). In the case of depletion or deficiency of an ER targeting or translocation component, GO terms assigned between 35% and 60% of the negatively affected proteins to organelles of the pathways of endocytosis and exocytosis plus cell surface, representing a more or less pronounced enrichment as compared to the total quantified proteome (**Supplementary Tables S1, S2**). Furthermore, similar enrichment of precursor proteins with SP, N-glycosylation, or membrane location was typically detected, and cytosolic proteins were under-represented among the negatively affected proteins (with the exception of KTN1 depletion, see below). Taken together, these results indicated that the precursors of these negatively proteins are substrates or clients of the respective component of interest.

As stated above, 30% of the total quantified proteome comprises ER protein import substrates. However, even in the case of Sec61 depletion, only 197 proteins with SP plus 98 with TMH, i.e., about 300 of the 6,000 quantified proteins or 5%, were negatively affected by the depletion (**Supplementary Table S1**). Thus, our experimental approach underestimates the number of different precursor polypeptides relying on this component by far. As expected, the numbers of negatively affected proteins were even lower for all the other translocation and targeting components since these components are expected to be precursor-specific, i.e., involved in import of only certain precursor polypeptides (Nguyen et al., 2018; Tian et al., 2019; Klein et al., 2020; Schorr et al., 2020; Bhadra et al., 2021a; Zimmermann et al., 2021; Tirincsi et al., 2022b). Obviously, this raises the question why we see only the tip of the iceberg in respect to clients. There are several contributing factors under conditions of siRNA-mediated knock-down: i) The depletion efficiency and its duration, which were optimized for minimal effects on cell growth and viability, was not high enough to cause significant accumulation and degradation of precursor proteins. Typically, the MS data suggested a depletion of close to 90% for the targeting or translocation component, which was confirmed by the validating western blot analysis. Thus the residual amount of the component of interest may have been sufficient to sustain the physiological functions of depleted proteins over the duration of the experiment. ii) As stated above, a certain function in ER protein import in human cells is compensated by other proteins or pathways. Except for the Sec61 complex, we actually expected that to be the case. iii) Some client proteins may have remained largely unaffected because they either have longer half-lives than the component of interest or may have a higher than average affinity for the component of interest. iv) Last but not least, some accumulating precursors may have stayed soluble in the cytosol, aggregated, or ended up in mitochondria where they were protected from degradation by the proteasome. Notably, we have observed mistargeting of certain precursors of secretory proteins into mitochondria in the absence of Sec61 function in human cells (Pfeiffer et al., 2013). Under knock-out conditions, the cells may also have adapted to the absence of a certain component, a phenomenon we observed to a certain extent even under siRNA-mediated depletion conditions in form of positively affected transport components (Nguyen et al., 2018;

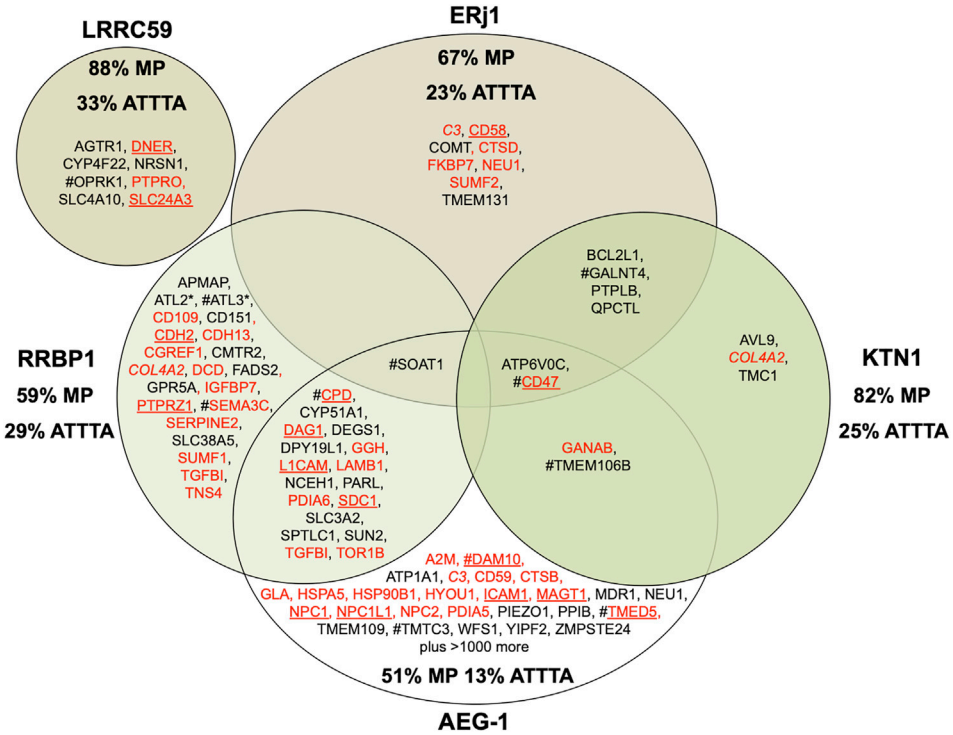

FIGURE 5 | Venn diagram for putative mRNA and RNC targeting components in the human ER membrane and their clients. The diagram summarizes precursors with SP (in red) or TMH (in black), which are destined to the secretory pathway and were negatively affected by the indicated depletion in HeLa cells (Bhadra et al., 2021) or were identified by mRNA crosslinking and ribosome proximity labeling, respectively (Hsu et al., 2018; Hannigan et al., 2020); membrane protein precursors with SP are underlined. All these precursor polypeptides are defined as potential clients or substrates of the respective component. The percentage of membrane proteins (MP) of the secretory pathway among the respective clients is indicated (%). For AEG-1 randomly selected examples of secretory pathway clients are shown and the % MP refers to the complete set of clients; for LRRC59 the secretory pathway representatives among the top twenty clients are shown and the % MP refers to these clients. COL4A2 is in italics to highlight that it was negatively affected by RRBP1 as well as KTN1 depletion. # highlights the presence of multiple ATTTA motifs in all mRNAs clients (i.e., ATTTA ≥ 10), which was tested for the top twenty clients in the case LRRC59 and for the complete set of clients in all other cases. Asterisks indicate hairpin proteins.

Tian et al., 2019; Klein et al., 2020; Schorr et al., 2020; Bhadra et al., 2021a; Zimmermann et al., 2021; Tirincsi et al., 2022b).

2.2 mRNA Targeting to the Human Endoplasmic Reticulum

As stated in the Introduction, there is SP- and, therefore, SRP-independent targeting of mRNAs or ribosome nascent chain complexes (RNCs) to the ER (**Figure 2**). According to pioneering biochemical and cell biological analysis by C. Nicchitta and coworkers, the synthesis of various types of polypeptides, such as cytosolic proteins, is initiated on 80S ribosomes or even 60S ribosomal subunits, which remain associated with the ER after termination of protein synthesis (Seiser and Nicchitta, 2000; Potter at al., 2001; Pyhtila et al., 2008; Reid and Nicchitta, 2012). As of today, the involved mRNA targeting appears to involve mRNA receptor proteins in the ER membrane, i.e., AEG-1 (Hsu et al., 2018), LRRC59 (Tazawa et al., 1991; Ohsumi et al., 1993; Hannigan et al., 2020), RRBP1 (Savitz and Meyer, 1990 and 1993; Bhadra et al., 2021a) and KTN1 1 (Ong et al., 2003; Ong et al., 2006; Bhadra et al., 2021a) (**Table 1**). Proximity-specific ribosome-profiling experiments, however, suggested ER-targeting of RNCs with nascent polypeptide chains, which are not sufficiently long to interact with SRP, play a more important role in mRNA targeting to the ER than direct targeting of mRNA to ER-associated ribosomes (Calvin et al., 2014). Notably, the first is translation-dependent, the latter is translation-independent (**Figure 2**). Insights into the possible specificities of these mRNA targeting reactions, however, are only beginning to accumulate (Hsu et al., 2018; Hannigan et al., 2020; Bhadra et al., 2021a). Until recently, there were just a couple of precursor polypeptides known to involve RRBP1 either as receptor for RNCs or mRNA, i.e., the SP-comprising precursors of the GPI-anchored membrane protein placental alkaline phosphatase (Cui et al., 2012; Cui et al., 2013), of certain Collagens (i.e., collagens Iα1 plus Iα2 and IIIγ) (Ueno et al., 2010) and of the ER-resident protein Calreticulin (Cui et al., 2012). More recent global data from mRNA crosslinking or ribosome proximity labeling in combination with transcriptome analysis, however, gave first glimpses of the substrate spectra of the two mRNA receptors AEG-1 (Hsu et al., 2018) and LRRC59 (Hannigan et al., 2020) (**Figure 5**).

We employed our MS approach to identify precursor polypeptides that may involve targeting of the corresponding mRNAs or RNCs by the two putative mRNA- or RNC-receptors

RRBP1 and KTN1 (Bhadra et al., 2021a). The approach suggested an additional collagen (i.e., COL4A2) and two ER-resident hairpin membrane proteins (i.e., ATL2 and ATL3) among the 39 negatively affected proteins as RRBP1 clients (**Figure 5**; **Supplementary Table S1**). For RRBP1, a role as RNC-receptor in the biogenesis of 22 precursors with SP (including six membrane protein precursors) plus 17 precursors with TMH, destined to the secretory pathway, was also supported by the positive effect on SRA and SRB as a consequence of RRBP1 depletion. For KTN1, in contrast, it turned out that not only proteins, destined to the ER (i.e., three precursors with cleavable SP –including one membrane protein- plus eight precursors with TMH), are degraded in the absence of KTN1 but also several cytosolic proteins, most notably cytoskeletal proteins and protein kinases (**Supplementary Table S1**, see below). The negative effect on ER protein import, however, is consistent with the idea that KTN1 can also play a role in the biogenesis of proteins, destined to the secretory pathway, as was suggested by the negative effect on the membrane protein precursor CD47 as well as the positive effect on RRBP1 (**Figure 5**). This view is consistent with our observation that crosslinking of native human microsomes and subsequent MS analysis observed among several intra-molecular crosslinks for KTN1 the intermolecular crosslink (peptide $_{42}$REQKLIPTK$_{52}$) to the translocon subunit TRAPγ (peptide $_{82}$FVLKHK$_{89}$) (Fan, L. and Jung, M., unpublished). Furthermore, the negative effect on CD47 suggested a function of KTN1 as the elusive ER-resident mRNA receptor in the so-called TIGER domain, which was proposed by C. Mayr to form a cytosolic micro-domain, which allows the enrichment of membrane protein-encoding mRNAs with multiple AU-rich elements (AREs, specifically ATTTA motifs) in their 3′ UTRs in the ER vicinity (Berkovits and Mayr, 2015; Ma and Mayr, 2018) (**Figure 2**). Thus, the key observation may be that KTN1 plays a role in targeting of certain mRNAs to ER subdomains. In the case of ERj1 (Dudek et al., 2002; Dudek et al., 2005; Blau et al., 2005; Benedix et al., 2010), another ER membrane protein that was proposed to interact with mRNAs or RNCs, the proteomic approach supports a function in cotranslational ER protein import rather than in ER targeting of mRNAs or RNCs (see below). Interestingly, when we compared our results with the published results from ribosome profiling experiments for the other two mRNA targeting components, we noticed that AEG-1 showed considerable overlap with clients of both KTN1 and RRBP1 while there was no overlap detected for LRRC59 (**Figure 5**) (Hsu et al., 2018; Hannigan et al., 2020). When the different putative clients were analyzed for ATTTA motifs, there were no general rules for mRNA recognition by these receptors emerging from the available data, with the possible exception of these motifs in the case of some KTN1- and RRBP1-clients (Bhadra et al., 2021a). The authors found that multiple ATTTA motifs (≥10) are present in the 3′ UTRs of mRNA clients of the different receptors to varying degrees, ranging from 13% to 33% (**Figure 5**). Thus, different motifs in the mRNAs appear to play a role.

In striking contrast to all other depletions of proteins that are involved in ER protein import, KTN1 depletion affected predominantly cytosolic proteins, i.e., their level increased from the average of 29% to 39%. In total, 21 cytosolic proteins were negatively affected, including two metabolic enzymes (GAPDH and GAPDHS), several protein kinases (OXSR1, PAK1, PDPK1, PDPK2 and ZAK), and various cytoskeletal proteins (Junction Plakoglobin, Myosin 11, Vinculin and Gamma-tubulin complex component 4). This raises the interesting question why cytosolic proteins should be degraded after their synthesis on free cytosolic ribosomes. We hypothesize that for the negatively affected cytoskeletal proteins it may be of importance to be synthesized and sequestered near their site of action rather than distributed throughout the cytosol, in particular for membrane interacting cytoskeletal proteins, such as Junction Plakoglobin and Vinculin, at adherens junctions between neighboring cells. In analogy, this may be true for certain protein kinases, such as OXSR1 (which is involved in regulating the actin cytoskeleton in response to environmental stress), PAK1 (which regulates cytoskeletal reorganization for cell motility and morphology), and PDPKs 1 and 2 (which are also located at cell junctions). Notably, multiple ATTTA motifs were also detected in the mRNAs of several cytosolic KTN1 clients (16% as compared to 31% of cytosolic clients of RRBP1, 43% for LRRC59, 13% for AEG-1, and 21% for ERj1) (Bhadra et al., 2021a).

On the basis of the data it was proposed that KTN1 may represent the mRNA-binding protein that resides in the ER membrane and is enriched in the TIGER domain in order to take over mRNAs from the cytosolic RNA-binding TIS11B and allow initiation of their translation by Sec61-associated ribosomes (**Figure 2**). If the mRNA codes for a membrane protein precursor with SP (such as CD47) or with an amino-terminal TMH, the nascent precursor begins to sample the Sec61 channel, which leads to spontaneous channel opening or the recruitment of auxiliary factors of the Sec61 channel. Since ERj1 was found to have overlapping substrate specificities with KTN1 in our proteomic studies, we suggest it to cooperate with KTN1 in allowing Sec61 channel opening when BiP is bound to ERj1′s J-domain (Dudek et al., 2002; Blau et al., 2005; Dudek et al., 2005; Benedix et al., 2010; Schäuble et al., 2012). Subsequently, the precursor is translocated into the ER or integrated into the ER membrane (CD47). If the mRNA codes for a cytosolic protein, however, sampling of the Sec61 channel remains unproductive and NAC gets access to the amino-terminus of the nascent polypeptide and causes its release from Sec61 and the concomitant release of the ribosome from Sec61 (Moeller et al., 1998). Next, synthesis of the cytosolic protein is completed and the protein is enriched in the TIGER domain to play its physiological role (Berkovits and Mayr, 2015; Ma and Mayr, 2018).

2.3 Precursor Polypeptide Targeting to the Human Endoplasmic Reticulum

2.3.1 SRP/SR

The signal hypothesis for targeting of nascent precursor polypeptides to the ER was put forward by G. Blobel et al. (Blobel, 1980). In later versions, it proposed that the amino-terminal SP of a nascent presecretory protein is recognized and bound by cytosolic SRP, which mediates a translational attenuation and facilitates association of the RNC-SRP

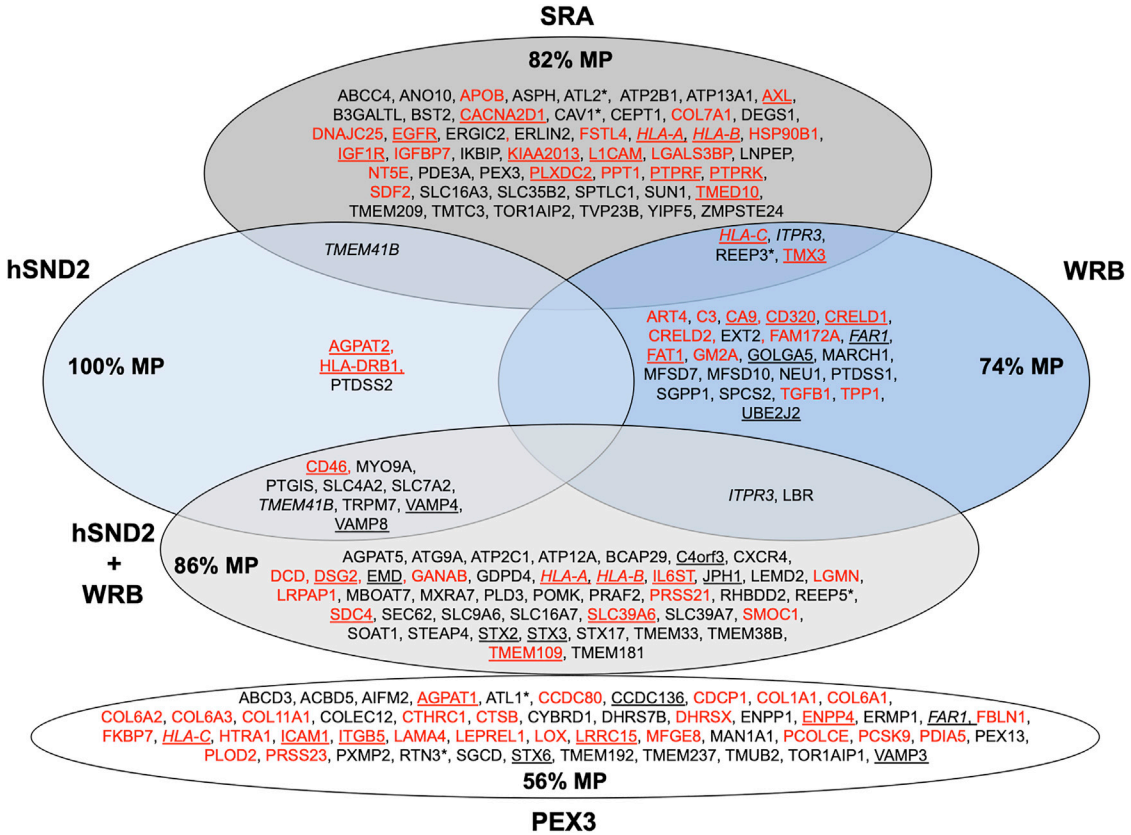

FIGURE 6 | Venn diagram for components for precursor targeting to the human ER membrane and their clients. The diagram summarizes precursors with SP (in red) or TMH (in black), which are destined to the secretory pathway and were negatively affected by the indicated depletion in HeLa cells (Tirincsi et al., 2022b) or by PEX3 depletion in HeLa cells and after PEX3 knock-out in Zellweger patient fibroblasts (Zimmermann et al., 2021); membrane protein precursors with SP are underlined, as are TMH proteins with TA. All these precursor polypeptides are defined as potential clients or substrates of the respective component or complex. The percentage of membrane proteins (MP) of the secretory pathway among the respective clients is indicated (%). HLA-C is in italics to highlight that it was negatively affected by PEX3 as well as SRA and WRB depletion, likewise are highlighted FAR1 and HLA-A, HLA-B, ITPR3 plus TMEM41B, respectively. Asterisks indicate hairpin proteins.

complex with the heterodimeric SRP receptor (SR), which is membrane-anchored via the β-subunit (Siegel and Walter, 1988; Ng et al., 1996; Egea et al., 2005; Gamerdinger et al., 2015; Hsieh et al., 2020; Meyer and Dobberstein, 1980a; Meyer and Dobberstein, 1980b; Gilmore et al., 1982a; Gilmore et al., 1982b; Tajima et al., 1986; Jomaa et al., 2021; Jomaa et al., 2022). The interaction of SRP with SR drives the mutual hydrolysis of bound GTP and leads to transfer of the RNC to the Sec61 complex (Halic and Beckmann, 2005, Halic et al., 2006; Jomaa et al., 2021). Thus, SRP represents a precursor as well as a mRNA targeting device (**Figure 2**). Comparative ribosome profiling experiments addressed functionality of the bacterial and yeast SRP *in vivo* (Chartron et al., 2016; Schibich et al., 2016; Costa et al., 2018) and demonstrated the strong preference of SRP for TMHs regardless of their position relative to the amino-terminus of the nascent polypeptide chain. Furthermore, they demonstrated the efficient ER targeting of precursors with just cleavable SPs in absence of SRP. Thereby, these studies stretch the versatility of SRP and reconciled two important considerations. First, the comparatively low abundance of SRP as compared to the abundance of translating ribosomes can be compensated by an mRNA targeting step, probably extending the time-window for the target recognition by SRP. Second, the crowded environment at the ribosomal tunnel exit can be eased by multiple iterations for SRP recognition without being limited to recognition of the SP or first TMH.

Late in the 1980s, characterization of precursor proteins with the ability for SRP-independent ER targeting, such as small presecretory proteins in mammalian cells and TA-membrane proteins in mammalian and yeast cells suggested alternative ER targeting machineries (Müller and Zimmermann, 1987; Schlenstedt and Zimmermann, 1987; Schlenstedt et al., 1990; Kutay et al., 1993; Ast et al., 2013). In the early 2000s, some small model presecretory proteins were shown to be targeted to the mammalian ER membrane in an SRP-independent fashion by their interaction with the cytosolic protein calcium-calmodulin and its putative association with the calcium-calmodulin (Ca^{2+}-CaM)-binding site in the cytosolic amino-terminus of the Sec61α

protein, possibly representing yet another targeting mechanism (Shao and Hegde, 2011; Schäuble et al., 2012). With respect to pathway interconnections, it is interesting to note that Ca^{2+}-CaM was found to inhibit rather than stimulate targeting of TA proteins to the ER membrane (Haßdenteufel et al., 2011).

Recently, we applied the proteomic strategy to identify precursor polypeptides that depend on SR for their targeting to the ER. Applying the established statistical analysis, we found that SRA depletion significantly affected the steady-state levels of 139 proteins: 133 negatively and 6 positively (**Figure 6**; **Supplementary Table S1**) (Tirincsi et al., 2022b). Among the negatively affected proteins, GO terms assigned 50% to organelles of the endocytic and exocytic pathways, thus representing a firm enrichment compared to the total quantified proteome (26%). Furthermore, we detected significant enrichment of precursor proteins with SP, N-glycosylated proteins, and membrane proteins. The negatively affected proteins included 24 proteins with cleavable SP, among them 14 membrane proteins plus 30 membrane proteins with TMH, including the ER hairpin membrane protein ATL2, many single-spanning membrane proteins and several multi-spanning membrane proteins, including the hairpin protein REEP3. Thus, the precursors of these negatively affected proteins with SP and TMH can be expected to be clients of the SRP and SR targeting pathway. When the SPs of SR-dependent precursor polypeptides were analyzed for hydrophobicity, GP content, and SP segmentation no significant distinguishing features were determined. Overall, SRP and SR clients showed a preference for cleavable SP (44%) or non-cleavable N-terminal targeting signals (77% of the remaining membrane protein clients) and an underrepresentation of TA, which is consistent with previous results from proximity-based ribosome profiling experiments (Chartron et al., 2016; Costa et al., 2018).

2.3.2 TRC

TA proteins are defined as single-spanning membrane proteins with a defining carboxy-terminal TMH (Kutay et al., 1993). Approximately 1% of the human protein-coding genome code for TA proteins. Not all of these, however, have a functional association with the secretory pathway (Borgese and Fasana, 2011; Borgese et al., 2019). TA proteins of the secretory pathway, such as the β- and γ-subunits of the Sec61 complex, the redox protein Cytochrome b_5, many apoptosis-associated proteins (including various Bcl family members) and many vesicular trafficking components (i.e., Syntaxins and VAMPs), have to be targeted to and inserted into the ER membrane (Borgese and Fasana, 2011; Borgese et al., 2019). Similar to SRP-mediated targeting, TA proteins are directed to the ER membrane via a heterodimeric ER membrane resident receptor complex, made up by WRB and CAML. The minimal cytosolic targeting machinery for TA proteins was termed TA receptor complex (TRC) in mammalian cells (**Table 1**). The cytosolic ATPase TRC40 binds the TA protein with its hydrophobic binding pocket and the WRB/CAML complex facilitates their efficient ER targeting. The WRB/CAML complex also facilitates the actual membrane insertion (Schuldiner et al., 2008; Yamamoto and Sakisaka, 2012; Borgese et al., 2019). Additionally, the TA targeting machinery includes a ribosome binding complex (comprising Bag6, Ubl4A, and TRC35), which acts upstream of TRC40 (Leznicki et al., 2010; Mariappan et al., 2010; Leznicki et al., 2011).

We applied our experimental strategy to identify precursor polypeptides that depend on WRB for their ER targeting (Tirincsi et al., 2022b). Applying the established statistical analysis, we found that WRB depletion significantly affected the steady-state levels of 296 proteins: 144 negatively and 152 positively (**Figure 6**; **Supplementary Table S1**). Among the negatively affected proteins, GO terms assigned 45% to organelles of the pathways of endocytosis and exocytosis. Some enrichment of precursor proteins with SP and membrane proteins was also detected. The identified precursors included 13 proteins with cleavable SP (including six membrane proteins) and 14 membrane proteins without SP, including the ER hairpin protein REEP3. When the SPs of WRB-dependent precursor polypeptides were analyzed for hydrophobicity, GP content, and SP segmentation, no significant distinguishing features were determined. However, when more WRB clients were identified under conditions of simultaneous depletion of WRB and hSnd2 (**Figure 6**) a preference of WRB for multispanning membrane proteins became visible and more WRB membrane protein clients were observed to have relatively more central and more carboxy-terminal TMH as compared to SRA dependent membrane proteins (Tirincsi et al., 2022b). Taken together, these results on the client spectrum of WRB point towards a more general targeting role of the TRC pathway than previously anticipated and may explain why pathogenic variants of TRC35 or TRC40 as well as CAML are linked to Congenital disorders of glycosylation in humans (Wilson et al., 2022). Notably, first hints towards this end already came from previous reports that small human presecretory proteins can be targeted to the ER of semi-permeabilized human cells by SR, WRB and hSnd2 (Haßdenteufel et al., 2018; Haßdenteufel et al., 2019) and that the cytosolic TRC pathway-component SGTA, which works upstream of Bag6, Ubl4A, and TRC35, is cotranslationally recruited to ribosomes, which synthesize a diverse range of membrane proteins, including those with cleavable SP (Leznicki and High, 2020).

2.3.3 SND

Although roughly one dozen genes coding for yeast TA proteins were characterized as essential, knock-out strains for the TA targeting components are viable, suggesting at least one further targeting route (Schuldiner et al., 2008). Indeed, in 2016 a high-throughput screening approach in yeast by M. Schuldiner and coworkers identified a novel targeting pathway, termed SRP-independent (SND) (Aviram et al., 2016). Three components of this pathway were identified and named Snd1, Snd2, and Snd3 (**Table 1**). Two hallmarks of the SND targeting pathway emerged. First, similar to the SRP and TA targeting pathways, precursor polypeptides were targeted via the combination of a cytosolic factor (named Snd1) and a heterodimeric receptor in the ER membrane (termed Snd2 and Snd3). Previously, Snd1 had already been described as a ribosome-binding protein. Second, the SND pathway showed a preference for substrates with a

central, rather than an amino- or a carboxy-terminal TMH. Furthermore, the SND pathway was able to provide an alternative targeting route for clients with a TMH at their amino- or carboxy-terminus (Aviram et al., 2016). Subsequent sequence comparisons identified the ER membrane protein TMEM208 as putative human Snd2 ortholog (named hSnd2) (Aviram et al., 2016). In experiments, combining siRNA-mediated gene silencing with protein transport into the ER of semi-permeabilized human cells in cell-free assays, hSnd2 appeared to have a similar function as its yeast ortholog (Casson et al., 2017; Haßdenteufel et al., 2017; Haßdenteufel et al., 2018), i.e., the TA membrane protein Cytochrome b_5 as well as some small presecretory proteins were targeted to the Sec61 complex in the mammalian cell-free assay. Briefly, the human hormone precursor proteins preproapelin and prestatherin can use Sec62 as well as SR for ER targeting in the cell-free assay. Interestingly, prestatherin preferred SRα over Sec62-mediated targeting, whereas preproapelin did the opposite, which was attributed to the higher hydrophobicity of the prestatherin SP (apparent ΔG −0.91 versus −0.19). Taken together with the observation that carboxy-terminal extension (by 187 amino acid residues) of preproapelin or prestatherin by the cytosolic protein DHFR leads to Sec62 independence, our data support the notion that small presecretory proteins use the SRP pathway for Sec61 targeting in human cells inefficiently, because the corresponding nascent chains are prone to be released from ribosomes before SRP can interact (Müller and Zimmermann, 1987; Schlenstedt and Zimmermann, 1987; Müller and Zimmermann, 1988; Schlenstedt et al., 1990; Lakkaraju et al., 2012; Haßdenteufel et al., 2018). Therefore, these precursors rely on alternative targeting pathways. In addition to SR and Sec62, co- and posttranslational targeting of preproapelin and prestatherin can also involve the TRC- and the SND-pathway, albeit with different efficiencies (Haßdenteufel et al., 2018). An ortholog of Snd1 has not yet been characterized in human cells. Recently, precursors of TRPC6 and various GPI-anchored proteins, such as CD55, CD59, and CD109 were added to the growing list of SND-clients (Talbot et al., 2019; Yang et al., 2021).

We applied the established proteomic strategy to identify precursor polypeptides that depend on hSnd2 for their targeting to the ER (Tirincsi et al., 2022b). Applying the established statistical analysis, we found that transient and partial hSnd2 depletion significantly affected the steady-state levels of 76 proteins: 43 negatively and 33 positively (**Figure 6**; **Supplementary Table S1**). Among the negatively affected proteins, GO terms assigned roughly 47% to organelles of the endocytic and exocytic pathways. We also detected a small enrichment of N-glycosylated proteins and a large one of membrane proteins. The negatively affected proteins included three proteins with cleavable SP (all being membrane proteins), and nine membrane proteins with TMH, including TA membrane proteins (such as Cytochrome b_5) plus single-spanning and multi-spanning membrane proteins (such as TRPM7), thus confirming previously observed classes of hSnd2 clients (TRPC6, Cytochrome b_5). Thus, there seems to be a preference of the human SND system for membrane protein precursors (**Figure 6**). When the SPs of hSnd2-dependent precursor polypeptides were analyzed for hydrophobicity, GP content, and segmentation, no significant distinguishing features were determined. However, when more hSnd2 clients were identified under conditions of simultaneous depletion of hSnd2 and WRB (**Figure 6**) a preference of hSnd2 for multispanning membrane proteins became visible and more hSnd2 membrane protein clients were found to have relatively more central or carboxy-terminal TMHs than SRA dependent membrane proteins (Tirincsi et al., 2022b), the latter two aspects being consistent with results for the yeast SND targeting pathway (Aviram et al., 2016). These observations are consistent with the fact that only little overlap between SRA clients and clients of the SND and TRC pathways was detected (**Figure 6**) and may explain why the latter two pathways can partially substitute for each other. In addition to SND clients, simultaneous depletion of hSnd2 and WRB negatively affected the ER membrane protein TMEM109, which was subsequently characterized as the hitherto elusive hSnd3 in experiments that were addressing its interaction with hSnd2 as well as its role in ER protein import (Tirincsi et al., 2022b).

2.3.4 PEX19/PEX3

Furthermore, recent work characterized the PEX19/PEX3-dependent pathway as a fourth pathway for targeting of precursor polypeptides to the ER (Schrul and Kopito, 2016; Yamamoto and Sakisaka, 2018). PEX3 was originally characterized as peroxisomal membrane protein, which cooperates with the cytosolic protein PEX19 in targeting of peroxisomal membrane proteins to pre-existent peroxisomes and in facilitating their membrane insertion (Erdmann et al., 1989; Hettema et al., 2000; Schmidt et al., 2012). As it turned out, however, PEX3 is also present in discrete subdomains of ER membranes and is involved in targeting of certain precursor proteins to ER membranes and most likely in their membrane insertion (Schrul and Kopito, 2016; Yamamoto and Sakisaka, 2018). These precursor proteins include membrane proteins, which either remain in the ER (the two-hairpin or reticulon-domain containing proteins ARL6IP1, RTN3A, RTN4C) or are pinched off in lipid droplets (such as the hairpin protein UBXD8) (Schrul and Kopito, 2016; Yamamoto and Sakisaka, 2018). These observations raised the question if this pathway, too, plays a more global role in protein targeting to the ER (Schrul and Schliebs, 2018; Jansen and Klei, 2019; Dhimann et al., 2020; Goodman, 2020).

Therefore, we addressed the client spectrum of PEX3 in ER protein targeting in human cells and asked if the PEX19/PEX3 pathway to the ER can also target precursor polypeptides to the Sec61 complex (Zimmermann et al., 2021). Here, the approach involved PEX3-depleted HeLa cells and chronically PEX3-deficient Zellweger patient fibroblasts (Schmidt et al., 2012). The negatively affected proteins found in the PEX3 knock-down or knock-out cells included seven peroxisomal membrane proteins and two hairpin proteins of the ER (ATL1, RTN3), thus confirming the two previously identified classes of PEX19/PEX3 clients for ER targeting in human cells (**Figure 6**; **Supplementary Table S1**). In addition, 18 membrane proteins (including TA proteins) and 28 proteins with SP (most

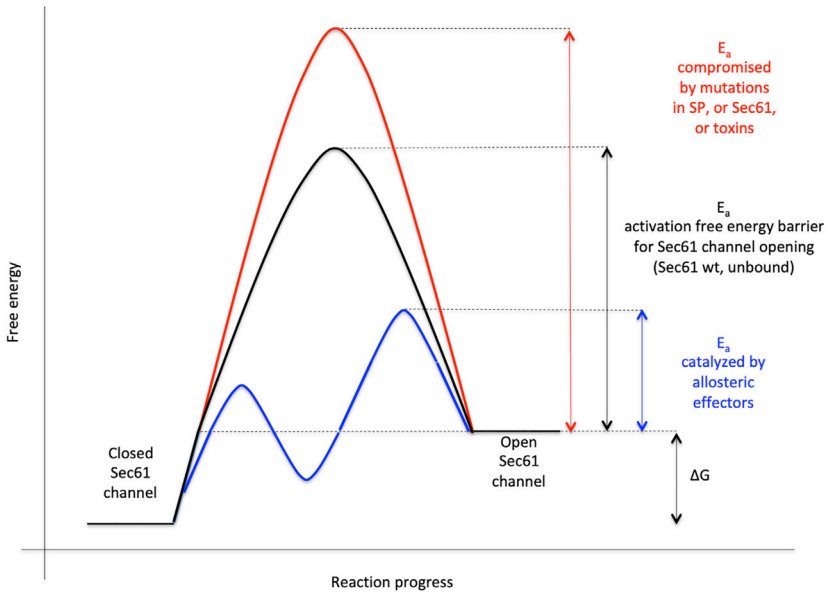

FIGURE 7 | Energetics and kinetics of Sec61 channel gating. In our view, the TRAP- or Sec62/Sec63 +/- BiP-mediated Sec61 channel gating is best visualized in analogy to an enzyme-catalysed reaction. Accordingly, TRAP, Sec62, Sec63 or BiP reduce the energetic barrier for full channel opening, which can apparently be reinforced by Sec61 channel inhibitors, such as cyclic heptadepsipeptides (such as CAM741) or certain eeyarestatins (such as ES24) (Pauwels et al., 2021; Pauwels et al., 2022). At least in the case of ES24, binding of the inhibitor within the channel pore arrests the channel in a partially open state, which may be identical with the primed state and is compatible with Ca^{2+}-efflux but not with full channel opening for protein translocation (Gamayun et al., 2019; Bhadra et al., 2021b). TRAP and BiP contribute to full channel opening by direct interaction with ER lumenal loops 5 and 7, respectively, of Sec61α (**Figure 1D**). *SEC61A1* mutations can increase the free energy barrier for channel opening *per se* (V67G, V85D and Q92R mutation) or indirectly, such as by interfering with BiP binding (Y344H mutation) (for recent reviews see Sicking et al., 2021a; Tirincsi et al., 2022a). Notably, all these effects are precursor specific because the amino-terminal SPs are either efficient or inefficient in driving Sec61 channel opening by themselves. Typical for an enzyme-catalysed reaction, BiP can also support efficient gating of the Sec61 channel to the closed state, i.e. the reverse reaction. The Figure and Figure legend were adapted from Sicking et al. (2021a).

notably 14 collagens plus collagen-related proteins as well as five membrane proteins) and belonging to the secretory pathway were negatively affected. The latter findings support the notion that PEX3 indeed represents a fourth pathway for targeting of precursor polypeptides to the Sec61 complex. Furthermore, it may suggest a hitherto unknown spatial or at least physical relationship between ER subdomains that are involved in ER shaping and the budding of peroxisomal precursor vesicles, large cargo vesicles, and lipid droplets. Thus in analogy to KTN1, the key observation may be that PEX3 plays a role in targeting of certain precursor polypeptides to Sec61 complexes in ER subdomains.

2.4 Translocation of Precursor Polypeptides Into the Human Endoplasmic Reticulum

2.4.1 Sec61 Complex

The heterotrimeric Sec61 complex provides an entry point for precursor polypeptides with SPs into the ER. In the course of co- and posttranslational membrane translocation, the SPs of precursor polypeptides first approach the Sec61 channel (Gumbart and Schulten, 2007; Lang et al., 2017; Lang et al., 2019; Bhadra and Helms, 2021). Subsequently, they begin to sample the cytosolic funnel of the Sec61 channel. According to molecular dynamics simulations, sampling in the Sec61 channel is affected by various properties of precursors or their mRNAs, i.e., deleterious charges, hydrophobicity, mature protein length, arrest peptides or poly-proline motifs in the precursor polypeptides and translation speed, which is dependent on pause sites, rare codons or hairpins in the mRNAs (Zhang and Miller, 2012). For productive SP insertion into and simultaneous full opening of the Sec61 channel, comparatively high hydrophobicity and, therefore, low apparent ΔG value for the H-region was found to be conducive (Gumbart and Schulten, 2007; Zhang and Miller, 2012; Bhadra and Helms, 2021). H-region hydrophobicity of the SP or TMH is supposed to be recognized by the hydrophobic patch formed by four residues of Sec61α TMHs 2 and 7, which line the lateral gate of the channel (Voorhees et al., 2014; Voorhees and Hegde, 2016).

In our opinion, gating of the Sec61 channel can best be described in analogy to an enzyme-catalyzed reaction where the precursor polypeptides with their SPs are the catalysts and the channel is their substrate (**Figures 1D**, **7**) (Haßdenteufel et al., 2018): Channel opening and closing represent two energetically un-favorable reversible reactions and the clients with or without support from auxiliary components or allosteric effectors (TRAP, Sec62/Sec63, see below) are the co-catalysts, which lower the activation energy for the required conformational transitions by binding to the Sec61 complex (Lang et al., 2017; Lang et al., 2019). Interestingly, there are SP mutations of certain precursor polypeptides, such as preproinsulin, preprorenin, as well as

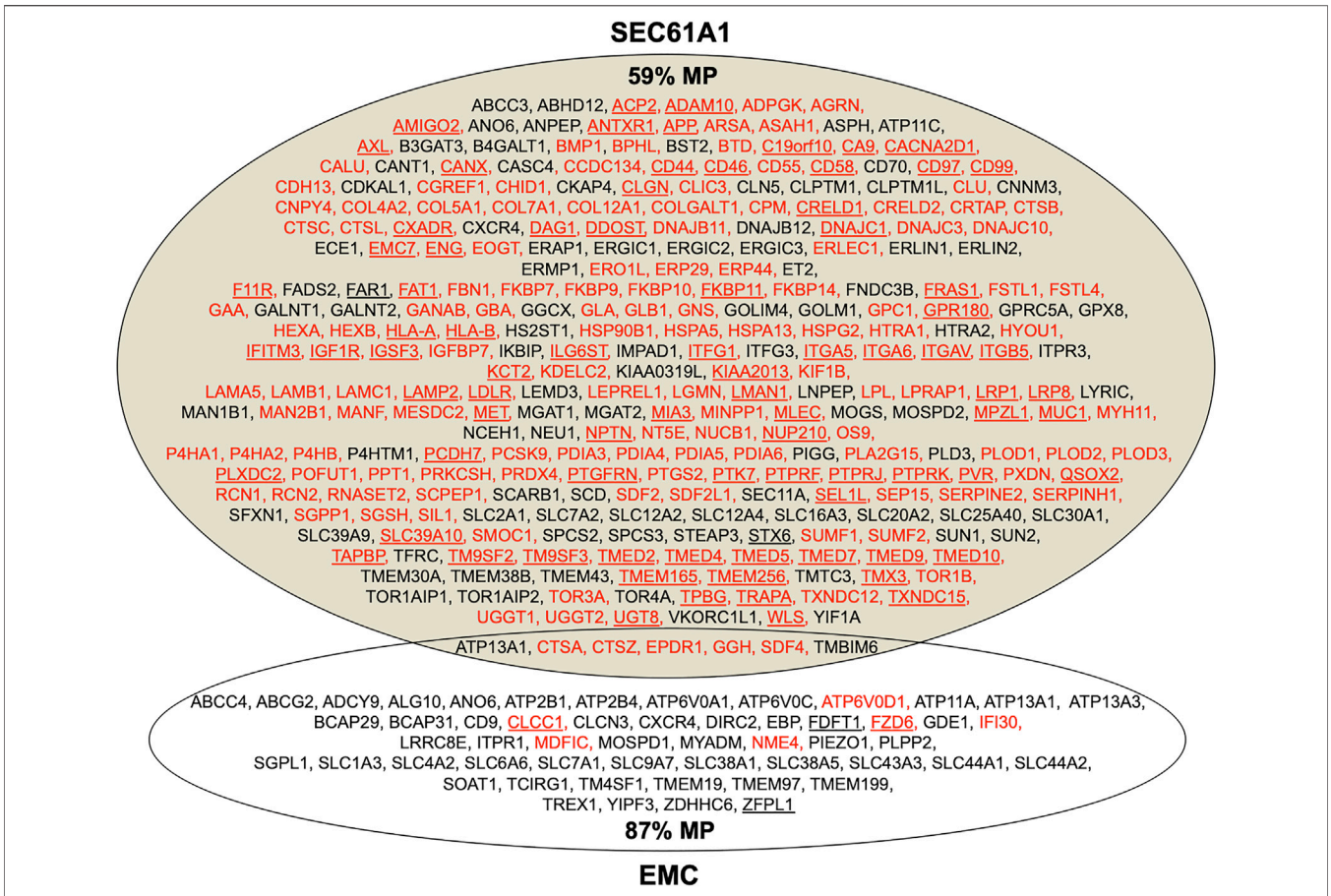

FIGURE 8 | Venn diagram for the Sec61 complex and ER membrane complex (EMC) in the human ER membrane and their clients. The diagram summarizes precursors with SP (in red) or TMH (in black), which are destined to the secretory pathway and were negatively affected by the indicated depletion; membrane protein precursors with SP are underlined, as are TMH proteins with TA. All these precursor polypeptides are defined as potential clients or substrates of the respective component or complex. The section for Sec61 summarizes the negatively affected proteins after the Sec61 depletion in HeLa cells (Nguyen et al., 2018); the section for EMC summarizes the negatively affected proteins after the EMC knock-out in HeLa cells (Shurtleff et al., 2018; Tian et al., 2019). The percentage of membrane proteins (MP) of the secretory pathway among the respective clients is indicated (%).

SEC61A1 mutations that can cause the same hereditary diseases, such as Diabetes mellitus and ADTKD (Lloyd et al., 2010; Guo et al., 2014; Bolar et al., 2016; Devuyst et al., 2019; Sicking et al., 2022). Again, this can best be described by an energy diagram for Sec61 channel gating (**Figure 7**). Accordingly, substitutions of crucial amino acids in either SPs or the pore-forming α-subunit of the Sec61 channel may increase the activation energy for Sec61 channel opening and, therefore, slow down ER import of the particular precursor polypeptide or a whole group of precursor polypeptides, which is particularly dependent on a certain amino acid residue in the Sec61 channel. Notably, *SEC61A1* mutations that cause ADTKD are discussed in the context of additional Sec61-channelopathies in more detail below in the Discussion and were recently reviewed by Sicking et al. (2021a).

As mentioned above, the depletion of Sec61α originally served as a proof-of-principle for the proteomic approach (**Figures 4**, **8**; **Supplementary Table S1**). Among the negatively affected proteins that included all three subunits of the Sec61 complex, GO terms assigned 61% to organelles of the pathways of endocytosis and exocytosis, thus representing a firm enrichment compared to the value for the total quantified proteome (26%) (Nguyen et al., 2018). Furthermore, significant enrichment of precursor proteins with SP (6.8-fold), N-glycosylated proteins (5.6-fold), and membrane proteins (3.0-fold) was detected for the negatively affected proteins (**Supplementary Table S1**). This suggests that the precursors of these negatively affected proteins, 198 with SP (including 80 membrane protein precursors) and 90 with TMH, represent clients of the Sec61 channel and, therefore, were degraded by the cytosolic proteasome upon Sec61 depletion (**Figure 8**). As also expected, the positively affected proteins included potential compensatory components, including the two subunits of the SRP receptor (Nguyen et al., 2018). When we analyzed the physicochemical properties of the SPs of the Sec61 clients, precursors with less-hydrophobic SPs were more strongly affected by Sec61 absence, i.e., over-represented in the negatively affected polypeptides, suggesting that precursor polypeptides with a higher SP hydrophobicity are more

efficient in Sec61 channel opening than those with lower hydrophobicity. Comparison of Sec61 clients with those of the membrane protein insertase EMC confirmed the preference of the latter for membrane protein precursors (**Figure 8**) (Shurtleff et al., 2018; Tian et al., 2019). However, the EMC data would also be consistent with the idea that EMC may also be able to facilitate Sec61 channel opening for precursors of soluble proteins with weak SPs, i.e., in analogy to TRAP and Sec62/Sec63 (see below).

2.4.2 Sec62/Sec63 Plus BiP

While the Sec61-complex mediates import of most precursor polypeptides into the ER, the Sec61-associated Sec62/Sec63 heterodimer supports ER protein import in a client-specific manner. Direct interaction between the Sec61 complex and Sec63 was demonstrated by co-immunoprecipitation as well as in living human cells (Tyedmers et al., 2000; Sicking et al., 2021b). Recently, four studies addressed the architecture of the posttranslationally acting translocon complex in yeast by cryo-electron microscopy (cryo-EM) (Itskanov and Park, 2019; Wu et al., 2019; Weng et al., 2021; Itskanov et al., 2021). This particular translocon represents a heptameric protein ensemble, termed the SEC complex (Deshaies et al., 1991). In the SEC complex the trimeric Sec61 complex is assembled with the tetrameric Sec62p/Sec63p complex. The latter comprises two essential, evolutionarily conserved subunits, the membrane proteins Sec62p and Sec63p, and two non-essential subunits, Sec71p and Sec72p. The data provided insights into the mechanism how the SEC complex allows gating of the Sec61 complex and supports ER protein import. Most informative were the observed interactions between Sec63p and the Sec61 complex, which include contacts in the cytosolic, membrane and lumenal domains. Strikingly, the cytosolic Brl domain of Sec63p contacts loops 6 and 8 of Sec61α, thereby blocking the ribosome binding site. Interestingly, as was structurally predicted for the interaction of the TRAPα/β subunits with the Sec61 complex (Pfeffer et al., 2017) and supported by Alphafold 2 (Jumper et al., 2021), the Brl domain of Sec63p represents a canonical beta-sandwich fold to allow an antigen-antibody-like binding to loop 6 of Sec61α. In the membrane, Sec63p (specifically TMH 3 of Sec63) contacts all three subunits of the Sec61 complex in the hinge region opposite of the lateral gate, including TMHs 5 and 1 of Sec61α as well the TMHs of Sec61β and Sec61γ (**Figure 1D**). Additionally, the short lumenal amino-terminus of Sec63p intercalates on the lumenal side of the channel between the hinge loop 5 of Sec61α and Sec61γ (Itskanov and Park, 2019; Wu et al., 2019; Itskanov et al., 2021; Weng et al., 2021). Apparently, binding of Sec62p/Sec63p to the Sec61 channel causes wide opening of the lateral gate (Van den Berg et al., 2004; Voorhees et al., 2014; Voorhees and Hegde, 2016). The functional implications for the SEC translocon as a consequence of gating by the Sec62p/Sec63p are that SP of many substrates are less hydrophobic and, therefore, have a lower chance to enter the lateral gate and trigger complete opening of the channel. Thus, in the SEC complex binding of the Sec62p/Sec63p induces a fully opened channel that readily accommodates even "weak" or inefficiently gating SPs (Ng et al., 1996; Trueman et al., 2011). Consistent with the concept of the Sec62p/Sec63p inducing wide opening of the lateral gate, yeast Sec62p was found to be able to aid in membrane topology of moderately hydrophobic signal anchor proteins, in particular single-spanning type II membrane proteins, which perform the energetically unfavorable 180° flip turn for correcting their initial type I orientation (Reithinger et al., 2013; Jung et al., 2014; Jung and Kim, 2021).

Similar to yeast, analyses of protein transport in mammalian cells showed a client-specific role of Sec62 in ER protein import. According to *in vitro* experiments with model proteins from insects (such as preprocecropin A) and humans (such as preproapelin and prestatherin), the ER import of presecretory proteins with a content of less than 100 amino acid residues (termed small precursor proteins) into the mammalian endoplasmic reticulum (ER) can occur posttranslationally (Schlenstedt et al., 1990; Shao and Hegde, 2011; Lakkaraju et al., 2012; Johnson et al., 2013; Haßdenteufel et al., 2018) and involves various targeting mechanisms (Haßdenteufel et al., 2018) as well as the ER-membrane proteins Sec62 and Sec63 (Lakkaraju et al., 2012; Lang et al., 2012; Johnson et al., 2013; Haßdenteufel et al., 2017, 2018, and 2019). In case of preprocecropin A, posttranslational ER import has been observed in intact human cells (Shao and Hegde, 2011) and Sec62-dependence of small human presecretory proteins was observed in intact human cells (Lakkaraju et al., 2012).

In contrast to yeast, however, the mammalian Sec62 protein apparently experienced a gain of function, i.e., it can interact with ribosomes near the ribosomal tunnel exit and can support cotranslational transport of certain clients, such as the precursors of ERj3- and prion-protein with 358 and 253 amino acid residues, repectively (Müller et al., 2010; Ziska et al., 2019; Schorr et al., 2020). Therefore, crosslinking experiments with stalled precursor polypeptides in transit through the mammalian translocon observed the dynamic recruitment of allosteric Sec61 channel effectors, such Sec62 (Conti et al., 2015). In contrast, the model precursor bovine preprolactin triggered Sec61 recruitment of accessory factors such as the allosteric effector TRAP and the auxiliary translocating chain-associating membrane (TRAM) protein. However, when ERj3- or prion-protein were used as model transport substrates the Sec62/Sec63 instead of TRAP and TRAM were recruited to the channel in order to allow translocation of substrates having a weak or inefficiently gating SP (Conti et al., 2015). In other studies, another dynamic transition of the translocon was observed for Sec62 and the SRP receptor. To allow cotranslational targeting the SR can displace Sec62 from the Sec61 complex, thereby switching the Sec61 channel from Sec62- to SRP-dependent translocation (Jadhav et al., 2015). According to the above mentioned crosslinking approach, however, SR and Sec62 can also act sequentially, namely after SRP-dependent targeting of precursors of ERj3- and prion-protein, Sec62 can displace SR from the Sec61 channel and -together with Sec63- support channel opening. Furthermore, Sec63 has to "take over" loops 6 and 8 of Sec61α from the ribosome. The cryo-EM structures of the yeast SEC complex may support the idea of a dynamic transition and flexibility of Sec62/Sec63. Both Sec62p and the ER lumenal J-domain of Sec63p could not be sufficiently resolved in the single particle

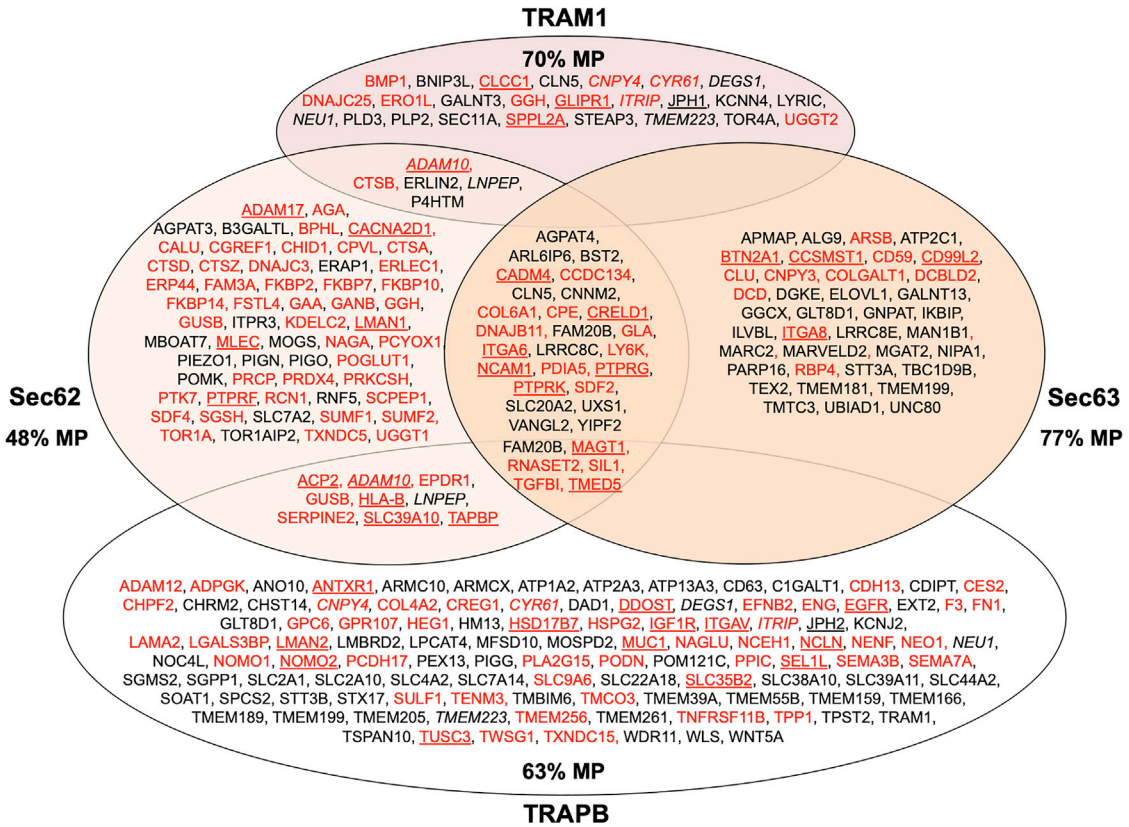

FIGURE 9 | Venn diagram for human ER protein translocation components and their clients. The diagram summarizes precursors with SP (in red) or TMH (in black), which are destined to the secretory pathway and were negatively affected by the indicated depletion; membrane protein precursors with SP are underlined, as are TMH proteins with TA. All these precursor polypeptides are defined as potential clients or substrates of the respective component or complex. The section for Sec62 and Sec63 summarizes the negatively affected proteins after the respective depletions in HeLa cells and the knock-outs in HEK293 cells, respectively (Schorr et al., 2020); the section for TRAM1 summarizes the negatively affected proteins after the TRAM1 depletion in HeLa cells (Klein et al., 2020); the section for TRAP summarizes the negatively affected proteins after the TRAPB depletion in HeLa cells and the TRAPD or TRAPG knock-outs in CDG patient fibroblasts (Nguyen et al., 2018). The percentage of membrane proteins (MP) of the secretory pathway among the respective clients is indicated (%). ADAM10, CNPY4, CYR61, ITRIP, LNPEP and TMEM223 are in italics to highlight that they were negatively affected by TRAM1 as well as TRAPB depletion.

analysis and this might have been due to their structural flexibility and dynamic assembly into the SEC translocon.

Notably, for the prion protein precursor, Sec62/Sec63-dependent ER-import has also been demonstrated in a genetic screen in human cells (Davis et al., 2015). Subsequent *in vitro* import assays, using a full-length prion protein precursor, demonstrated SRP-dependence and the fact that Sec63-dependence is not only due to the SP but also due to a polybasic motif, which is downstream of the SP in the mature region (Ziska et al., 2019) and was missing from the artificial prion protein construct in previous work (Rane et al., 2009; Davis et al., 2015). Furthermore, these *in vitro* import assays demonstrated that Sec63-dependence of the small preproapelin and the precursors of ERj3 and prion protein is related to gating of the Sec61 channel to the open state and coincides with BiP´s involvement, which was linked to the combination of a weak SP plus, in case of preproapelin ($_{37}$RRK) and the prion protein precursor ($_{1}$KKRPK), a positively charged cluster in the mature region (Haßdenteufel et al., 2018; Ziska et al., 2019). Notably, loss of Sec63 protein function in the liver of a subset of human patients with polycystic liver disease was also interpreted in light of a client specific function of Sec63 in ER protein import (Fedeles et al., 2011; Lang et al., 2012). Interestingly, Sec63-dependence of ERj3 import into the ER was indirectly confirmed in murine *SEC63* null cells, which were generated as an animal model for the human disease (Lang et al., 2012). These *SEC63*$^{-/-}$ cells lacked ERj3 while the levels of various other ER proteins were unchanged compared to murine *SEC63*$^{+/+}$ cells (Fedeles et al., 2011; Schorr et al., 2020).

With our proteomic approach, we determined the rules for engagement of Sec62/Sec63 in ER-import in intact human cells (Schorr et al., 2020). Applying the statistical analysis, we found that Sec62 depletion significantly affected the steady-state levels of 351 proteins: 155 negatively and 196 positively (**Figure 9**; **Supplementary Table S2**). The identified precursors included 18 proteins with cleavable SP and six proteins with TMH. The proteins positively affected by transient Sec62 depletion included both SRP- receptor subunits (SRPRA, SRPRB) and the TRAP ß-subunit (coded by the SSR2 gene). We assume that these short-term compensatory mechanisms may have

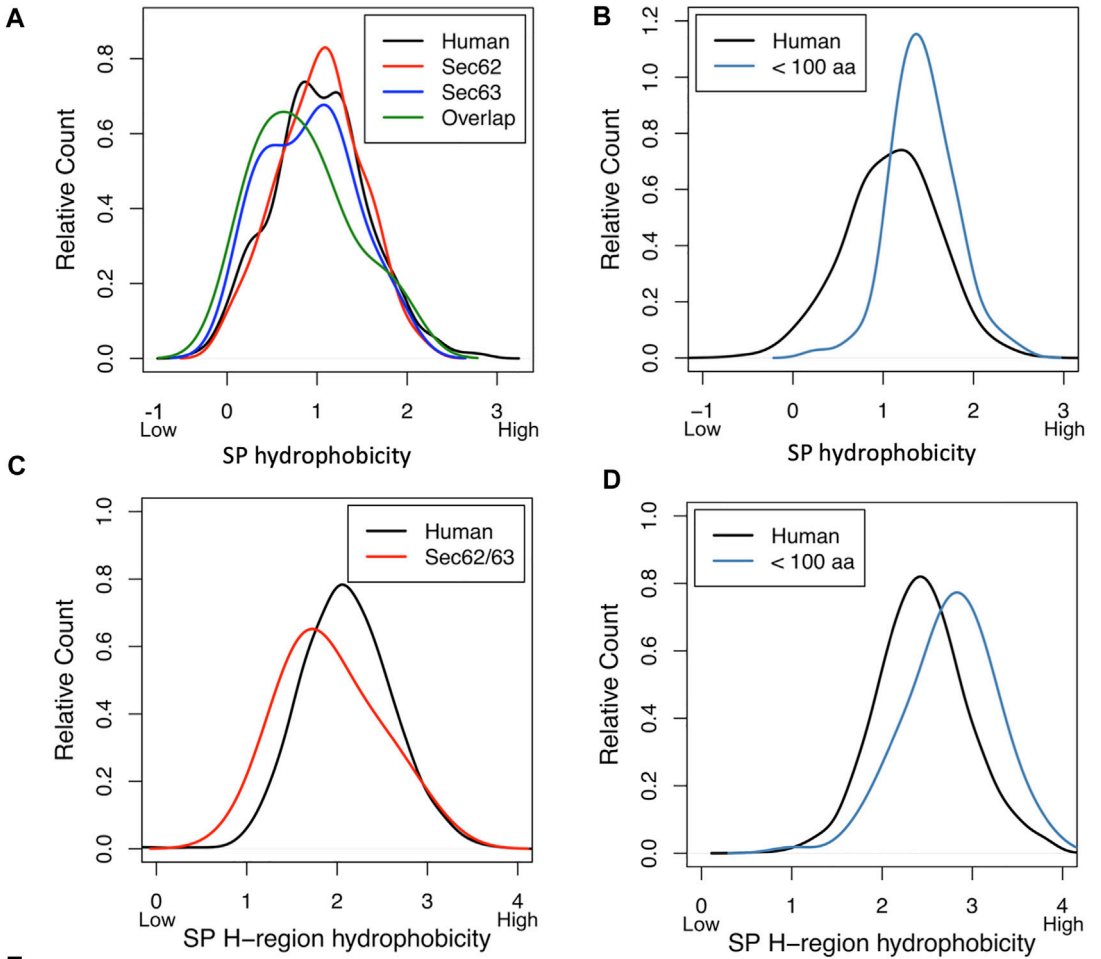

E

Precursor of	Hydrophobicity plot (Kyte-Doolittle)	Hydrophobicity Delta G	Nature & position of positively charged cluster
Statherin		2.2	
		-0.91	
Proapelin		1.5	$_{37}$RRK
		-0.19	
ERj3		1.6	$_{20}$KKAYRK
		1.00	
Prion protein		1.4	$_{1}$KKRPK
		0.63	

FIGURE 10 | Physicochemical properties of Sec62/Sec63 clients. **(A–C)** We used custom scripts to compute the hydrophobicity of SPs **(A,B)** and SP H-regions **(C,D)**, respectively. Hydrophobicity score was calculated as the averaged hydrophobicity of its amino acids according to the Kyte-Doolittle propensity scale. For the calculation of H-region hydrophobicity, each SP was subjected to segmentation using the prediction tool Phobius (https://phobius.sbc.su.se) and the H-region to the calculation according to Kyte-Doolittle. **(E)** Relevant properties of SPs (hydrophobicity and positively charged amino acid residues, respectively) and mature regions of four clients. Hydrophobicity scores were calculated according to the Kyte-Doolittle propensity scale and are displayed using the DNAstar software package. Apparent delta G values were determined with the ΔG_{app} predictor for TM helix insertion (http://dgpred.cbr.su.se). Clusters of positive charges in the respective mature region that were experimentally shown to contribute to Sec62/Sec63 dependence are indicated.

contributed to the comparatively low number of negatively affected proteins. The Sec63-depletion significantly affected the steady-state levels of 34 proteins: 21 negatively and 13 positively (**Figure 9**; **Supplementary Table S2**). The identified precursors included four proteins with cleavable SP and six proteins with TMH and only one of the proteins with SP had also been negatively affected by Sec62-depletion (TGFBI). Upon closer inspection of the potential overlap between Sec62 and Sec63 depletion in HeLa cells, four additional precursor polypeptides with SP were negatively affected by Sec63-depletion in HeLa cells, which, however, did not meet the significance threshold (ERj3 –coded by the DNAJB11 gene-, MAGT1, PDIA5, SDF2) (Schorr et al., 2020).

To identify additional substrates, we performed similar analyses after Sec62 or Sec63 knock-out, employing CRISPR/Cas9 treated HEK293 cells compared to HEK293 control cells (Fumagalli et al., 2017; Schorr et al., 2020). Here, we found that Sec62 deficiency significantly affected the steady-state levels of 329 proteins: 208 negatively and 121 positively (**Supplementary Table S2**). Of the negatively affected proteins, GO terms assigned ~48% to organelles of the endocytic and exocytic pathways. We also detected significant enrichment of proteins with SP (5.5-fold), N-glycosylated proteins (4.5-fold), and membrane proteins (1.8-fold). The identified precursors included 74 proteins with cleavable SP (including 19 membrane proteins) and 29 proteins with TMH. As expected (Conti et al., 2015), ERj3 was negatively affected. After Sec63 knock-out in HEK293 cells, we found that Sec63-deficiency significantly affected the steady-state levels of 302 proteins: 199 negatively and 103 positively (**Supplementary Table S2**). GO terms assigned ~37% of the negatively affected proteins to organelles of the endocytic and exocytic pathways. We also detected significant enrichment of proteins with SP (1.9-fold), N-glycosylated proteins (2.4-fold), and membrane proteins (1.8-fold). The identified precursors included 24 proteins with cleavable SP (including ten membrane proteins) and 38 proteins with TMH (**Figure 9**). Here, 22 precursor polypeptides were negatively affected by Sec62 as well as Sec63 deficiency, 11 each with SP (including six membrane proteins) and with TMH, all belonging to the secretory pathway (**Figure 9**). Upon closer inspection of the potential overlap between Sec62 and Sec63 in HEK293 cells, six additional precursor polypeptides with SP were negatively affected by Sec63-deficiency, which did not meet the significance threshold (MAGT1, PDIA5, RNASET2, SDF2, SIL1, TMED5) (Schorr et al., 2020). Interestingly, the analysis also identified 54 precursors with SP (including 11 membrane proteins) plus 17 precursors with TMH, which showed a requirement for Sec62 but not for Sec63, as well as 12 precursors with SP (including four membrane proteins) plus 26 precursors with TMH, which showed a requirement for Sec63 but not for Sec62, consistent with the previous observation *in vitro* that the two proteins can also support ER protein import independently of each other (Haßdenteufel et al., 2018). Notably, the overlap was probably underestimated since the analysis was done for mixed guide RNA clones in the case of Sec63, i.e., the cell pool did not represent a SEC63 knock-out (Schorr et al., 2020).

Along with confirming ERj3 as a client, 30 novel Sec62/Sec63-clients were identified under these in vivo-like conditions, 18 with SP (including eight membrane proteins) and 12 with TMH (**Figure 9**; **Supplementary Table S2**). These previously unknown substrates have in common less hydrophobic SPs with longer but less hydrophobic H-regions and lower C-region polarity (**Figures 10A,C**). Further analyses with four substrates, ERj3 in particular, revealed the combination of a weak SP and a translocation-disruptive positively charged cluster of amino acid residues within the mature part ($_{20}$KKAYRK) as decisive for the Sec62-/Sec63-requirement (**Figure 10E**) (Schorr et al., 2020). This is reminscent of preproapelin and prion protein import (Haßdenteufel et al., 2018; Ziska et al., 2019) and in all three cases these features were found to be responsible for an additional BiP-requirement and for sensitivity towards the Sec61 channel inhibitor CAM741. Thus, human Sec62/Sec63 may support Sec61 channel opening for precursor polypeptides with weak SPs by direct interaction with Sec61α and/or via recruitment of BiP and its interaction with the ER-lumenal loop 7 of Sec61α, which we supposed to lower the activation energy for channel opening (**Figure 7**).

2.4.3 ERj1 Plus BiP

ERj1 belongs to the class of ribosome-associated membrane proteins (RAMPs) (Dudek et al., 2002; Blau et al., 2005; Dudek et al., 2005; Benedix et al., 2010). However, its ribosome association, appears to be more dynamic as compared to the classical RAMPs, i.e., Sec61, TRAM and TRAP (Görlich et al., 1992b; Görlich and Rapoport, 1993). This was microscopically confirmed by fluorescence microscopy using fluorescently labeled antibodies against ERj1 in permeabilized MDCK cells (Snapp et al., 2004; Benedix et al., 2010). According to cryo-EM, the cytosolic domain of ERj1 binds at the ribosomal tunnel exit and involves expansion segment 27 (ES27) of the 28S rRNA (Blau et al., 2005). ERj1 was proposed to play a role in ER protein import as a possible functional homolog for Sec62/Sec63, combining the cytosolic ribosome binding activity of Sec62 with the ER lumenal Hsp40-type co-chaperone activity of Sec63 in one polypeptide (Dierks et al., 1996; Skowronek et al., 1999; Mayer et al., 2000; Tyedmers et al., 2000; Dudek et al., 2005; Tyedmers et al., 2005; Müller et al., 2010; Lang et al., 2012; Schäuble et al., 2012). Notably, human Sec62 was microscopically confirmed as RAMP, too, by fluorescence microscopy using fluorescently labeled antibodies against Sec62 in permeabilized MDCK cells (Snapp et al., 2004; Müller et al., 2010). Interestingly, the cytosolic domain of ERj1 is able to allosterically inhibit translation at the stage of initiation when its ER lumenal J-domain is not associated with BiP but allows translation when BiP is bound (Benedix et al., 2010). Thus, ERj1 would be perfectly able to allow initiation of protein synthesis of precursor polypeptides on ER bound ribosomes when BiP is available on the ER lumenal side of the membrane.

Employing the statistical analysis, we found that transient and partial ERj1 depletion significantly affected the steady-state levels of 172 proteins: 92 negatively and 80 positively (**Figure 5**; **Supplementary Table S2**) (Bhadra et al., 2021a). Of the

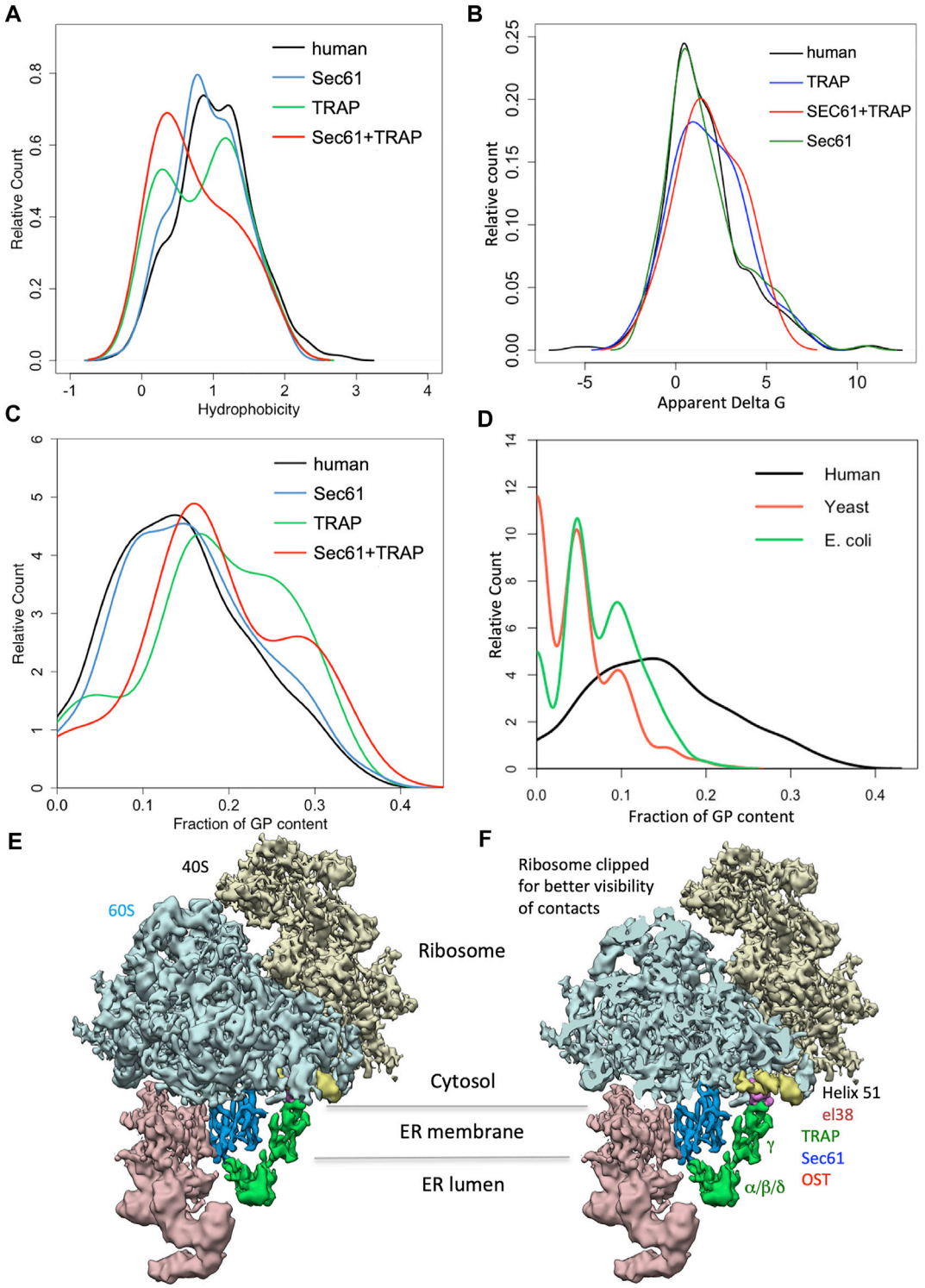

FIGURE 11 | Physicochemical properties of SPs of TRAP clients. **(A–C)** We used custom scripts to compute the hydrophobicity score **(A)**, apparent delta G **(B)**, and glycine/proline (GP) content **(C)** of SP sequences. Hydrophobicity score was calculated as the averaged hydrophobicity of its amino acids according to the well-known Kyte-Doolittle propensity scale. Apparent delta G values were determined with the ΔG_{app} predictor for TM helix insertion (http://dgpred.cbr.su.se). GP content was calculated as the total fraction of glycine and proline in the respective sequence. **(D)** We also used custom scripts to extract protein annotations for all human, *E. coli* and *S. cerevisiae* SPs from UniProtKB entries and to calculate their GP content. **(E,F)** Cartoon of unclipped **(E)** and clipped **(F)** 80S ribosome together with Sec61-complex and TRAP, and OST. Notably, without clipping eL38 and helix 51 is partially hidden.

negatively affected proteins, GO terms assigned almost 30% to organelles of the pathways of endocytosis and exocytosis. The identified precursors included seven proteins with cleavable SP, among them two membrane proteins, and eight membrane proteins with TMH and were discussed above in the context of KTN1-dependent mRNA targeting to the ER.

2.4.4 TRAP

Originally, TRAP was characterized as signal-sequence receptor (SSR) complex (Wiedmann et al., 1987). Furthermore, it had been crosslinked to nascent polypeptides at late translocation stages (Conti et al., 2015) and had been demonstrated to associate with Sec61 (Menetret et al., 2008; Dejgaard et al., 2010; Pfeffer et al., 2017). As mentioned in the Introduction, the ribosome-associated Sec61-complex and the TRAP form a stable stoichiometric super-complex called a translocon (Menetret et al., 2008; Bano-Polo et al., 2017; Pfeffer et al., 2017). *In vitro* transport studies showed that the TRAP stimulates protein translocation depending on the efficiency of the SP in transport initiation (Fons et al., 2003); Sec61 gating efficiency and TRAP dependence were inversely correlated. Recent studies in intact cells suggest that TRAP may also affect TMH topology (Sommer et al., 2013), reminiscent of Sec62/Sec63 in yeast (Reithinger et al., 2013; Jung et al., 2014).

To identify TRAP dependent precursors, we combined siRNA-mediated TRAP depletion in HeLa cells, label-free quantitative proteomics, differential protein abundance analysis, and statistical analysis. We found that TRAPβ depletion significantly affected the steady-state levels of 257 proteins: 180 negatively and 77 positively. Of the negatively affected proteins, GO terms assigned ~40% to organelles of the endocytotic and exocytotic pathways and included all four subunits of TRAP. We also detected significant enrichment of proteins with SP (3.3-fold), N-glycosylated proteins (2.7-fold), and membrane proteins (2.1-fold). The identified precursors included 38 proteins with cleavable SP and 22 proteins with TMH, and represented N-glycosylated proteins and non-glycosylated proteins (**Figure 9**; **Supplementary Table S2**). For TRAP deficient fibroblasts from patients with a Congenital disorder of glycosylation the steady-state levels of 318 proteins were altered: 279 negatively and 39 positively (**Supplementary Table S2**). Of the negatively affected proteins, GO terms assigned 36% to organelles of the pathways of endocytosis and exocytosis. The identified precursors included 34 proteins with cleavable SP and 41 proteins with TMH. Taken together, TRAP knock-down and knock-out identified 59 membrane proteins with TMH and 66 proteins with SP (including 20 membrane proteins), all belonging to the secretory pathway, as TRAP clients (**Figure 9**). Interestingly, six of the TRAP clients were found among the Sec62/Sec63 clients and nine among the Sec62 substrates, consistent with the view that these two allosteric Sec61 channel effectors have overlapping but non-identical functions.

The SP analysis of TRAP-substrates demonstrated an above-average glycine-plus-proline content (GP content) and below-average hydrophobicity as the key features (**Figures 11A–C**). Thus, the Sec61-associated TRAP supports protein translocation in a substrate-specific manner. We suggest that high GP content and low hydrophobicity extend the dwell time of SP at the cytosolic funnel of the Sec61 channel, and that TRAP can compensate this potential problem by stabilizing SP on the cytosolic surface and by aiding in Sec61 channel gating at the lumenal side. This raises the question of how TRAP relays the presence of an SP-bearing RNC to the Sec61 channel. In an attempt to interpret our findings at the structural level, i.e., in the context of the TRAP architecture, in which individual TRAP subunits were assigned positions within the overall density of human TRAP in native ER membranes by cryo-electron tomography (CET) (**Figures 11E,F**) (Pfeffer et al., 2017), the ER-lumenal domains of the TRAPαβ-subcomplex contact loop 5 in the hinge region between the amino- and carboxy-terminal halves of Sec61α and, thereby, mediate Sec61 channel opening by lowering the activation energy, required for channel opening (**Figure 7**). TRAPγ occupies a central position in human TRAP, contacting eL38 and short rRNA expansion segment (ES) on the ribosome, thus coordinating the other TRAP subunits with the ribosome and the additional translocon components, i.e. the Sec61-complex (contacted by TRAPαβ) and OST (contacted by TRAPδ). Previously, the ribosomal components uL24 and H59, both in vicinity to eL38 and TRAPγ, were observed to coordinate SP for SRP binding in the bacterial system (Jomaa et al., 2016). Assuming a similar SP position in the human system, the amino-terminal SP tip may consequently be close enough to interact with eL38 and the cytosolic domain of TRAPγ during the "hand-over" of the SP from SRP to Sec61 (**Figure 11E**). According to this hypothetical scenario, TRAP may support the insertion of SP into the Sec61 channel in the productive hairpin (rather than head-first) configuration.

2.4.5 TRAM1

TRAM (since the discovery of TRAM2 (Stefanonvic et al., 2004) termed TRAM1) represents an ER membrane protein with eight TMHs. It belongs to a protein family, characterized by the TLC (short for: TRAM/LAG1/CLN8) homology domain, which is supposed to bind ceramide or related sphingolipids (Klein et al., 2020). Similarly to TRAP, it was discovered by crosslinking of nascent presecretory proteins in the context of RNCs, but in contrast to TRAP early in their translocation into the ER (Görlich et al., 1992b; Görlich and Rapoport, 1993). Subsequently, it was described to interact with nascent membrane proteins in the course of their initial integration into the Sec61 channel (High et al., 1993; Mothes et al., 1994; Do et al., 1996; Voigt et al., 1996; Hegde et al., 1998; McCormick et al., 2003; Sadlish et al., 2005; Sauri et al., 2007). Actually, TRAM1 was one of the first proteins found to provide substrate-specific support for ER protein import (Görlich and Rapoport, 1993). Furthermore, it was observed that precursor proteins with short charged amino-terminal domains in their SPs require TRAM1 for efficient insertion into the lateral gate and that TRAM1 can regulate cytosolic extrusion of nascent chain domains into the gap between ribosome and translocon (Voigt et al., 1996; Hegde et al., 1998). In addition, it was concluded that precursors with shorter than average N-regions and shorter

H-regions in their SP require the help of TRAM1 for efficient insertion into the lateral gate.

By applying our unbiased proteomic approach, we identified 30 potential TRAM1 substrates that included 13 precursors with SP (including four membrane proteins) and 17 with TMH (**Figure 9**; **Supplementary Table S2**) (Klein et al., 2020). Comparing these precursors to those found for Sec61 and TRAP in similar experiments, did not point to a preference of TRAM1 for any particular type of precursor polypeptides. Furthermore, analysis of the physicochemical properties of SP and TMH of the TRAM1 substrates did not point to a specific feature, except for precursors with short N-regions in their SP. Notably, 27% of the TRAM1 substrates were also negatively affected by TRAP depletion (**Figure 9**). This is consistent with the co-localization of TRAM1 with Sec61 and TRAP (Görlich and Rapoport, 1993; Dejgaard et al., 2010). Considering the strong overlap in substrates of these two transport components and TRAM1's apparent lack of precursor preference may indicate that TRAM1 does not act as a receptor for SPs and TMHs. It may rather play a supportive role in ER protein import, such as making the phospholipid bilayer conducive for accepting SP and TMH in the vicinity of the lateral gate of the Sec61 channel. This interpretation is consistent with the above-mentioned prediction that TRAM1 may be able to bind sphingolipids (Klein et al., 2020).

3 DISCUSSION

In human cells, approximately 30% of all polypeptides enter the secretory pathway at the level of the ER. This process involves SPs or equivalent TMHs at the level of the precursor polypeptides and a multitude of cytosolic and ER proteins, which guarantee the initial ER targeting as well as the subsequent membrane integration or translocation (**Figure 2**). Cytosolic SRP and SR in the ER membrane mediate cotranslational targeting of most nascent precursor polypeptide chains to the polypeptide-conducting Sec61 complex in the ER membrane. Alternatively, nascent and fully-synthesized precursor polypeptides are targeted to the ER membrane by either the PEX3/19-, SND-, or TRC-pathway and mRNAs are targeted to the ER membrane by nucleic acid-based pathways. According to the classical *in vitro* studies for ER protein import, these targeting pathways may have overlapping functions, which raised the question how relevant this is under cellular conditions and which features of SPs and/or entire precursor polypeptides determine preference for a certain pathway under these conditions. Irrespective of their targeting pathway(s), most precursor polypeptides are integrated into or translocated across the ER membrane via the Sec61 channel. For some precursors Sec61 interaction partners have to support the gating of the channel, again raising the question why and when this is the case, i.e., what the client specificities of these auxiliary components are, i.e., Sec62/Sec63, TRAM1 protein, TRAP. In the course of the last 5 years, we combined siRNA-mediated depletion or knock-out of single targeting or transport components in human cells with label-free quantitative proteomics and differential protein abundance analysis to characterize client specificities of these components. Here, we present a summary of the clients, which were identified in the respective differential protein abundance analyses and highlight some of the lessons learned.

In mRNA targeting to the human ER, the putative receptors AEG-1 and RRBP1 show considerable overlap in their clients, which are directed towards the secretory pathway (**Figure 5**) (Hsu et al., 2018; Bhadra et al., 2021a). The results for KTN1 suggest a possible function of KTN1 (in possible cooperation with ERj1 and BiP) as the hitherto elusive ER membrane-resident mRNA receptor in the so-called TIGER domain, which may form a cytosolic micro-domain that enriches certain membrane protein- as well as cytoskeletal protein-encoding mRNAs with multiple AU-rich elements (AREs, specifically ATTTA motifs) in their 3′ UTRs in the vicinity of the ER (Berkovits and Mayr, 2015; Ma and Mayr, 2018; Bhadra et al., 2021a). Indeed multiple ATTTA motifs were found in the 3′ UTRs of several mRNAs and, therefore, appear to be one but certainly not the only distinguishing feature in this process.

In targeting of precursor polypeptides to the human ER, the results from the classical *in vitro* studies for ER protein import were confirmed, i.e. all four known targeting pathways were found to be able to target SPs and TMHs to the Sec61 complex in the ER membrane. When the respective SPs were analyzed with various analytical tools, no significant distinguishing features were determined. However, for the PEX3/PEX19-dependent pathway, which plays its major roles in targeting peroxisomal membrane proteins and certain hairpin membrane proteins of the ER and lipid droplets to a hitherto ill-defined ER subdomain (Schrul and Kopito, 2016; Yamamoto and Sakisaka, 2018), the analysis suggested that this subdomain may be physically or even spatially related to ER exit sites for large cargo vesicles, which are crucial for collagen secretion (Zimmermann et al., 2021). Therefore, various collagens as well as collagen-modifying enzymes and interacting proteins, most of them with SP, were found to be targeted to this subdomain by unknown features. We proposed that the defects in the biogenesis of certain collagens may contribute to the devastating effects of PEX3 deficiency in Zellweger patients. As expected, there were no TA membrane proteins found among the SRα clients and the SRP/SR-dependent pathway showed the expected preference for precursors with N-terminal SP or more amino-terminal TMH (Tirincsi et al., 2022b). In contrast to both the PEX3/PEX19- and SRP/SR-dependent pathways, TRC- and SND-dependent ER protein targeting showed a preference for multi-spanning membrane proteins as well as for membrane proteins with central or carboxy-terminal TMHs (Tirincsi et al., 2022b). These findings may explain why the latter two pathways can substitute for each other to a certain extent. Furthermore, they are consistent with the observations that there is a considerable overlap in clients between the latter two pathways and hardly any overlap with the other two pathways.

With respect to protein translocation into the human ER, precursors with less-hydrophobic SP were more strongly

affected by Sec61 depletion, i.e. over-represented among the negatively affected polypeptides (Nguyen et al., 2018). Thus, precursor polypeptides with a higher-than-average SP hydrophobicity appear to be more efficient in Sec61 channel opening than those with lower hydrophobicity, which may be linked to the characteristics of the hydrophobic patch formed by four residues of Sec61α TMHs 2 and 7 that line the lateral gate of the channel and are crucial for its opening (Voorhees et al., 2014; Voorhees and Hegde, 2016). In addition, SP hydrophobicity was observed to be crucial for the roles of the so-called allosteric effectors of the Sec61 channel, TRAP and Sec62/Sec63 plus BiP, in channel opening, thereby confirming conclusions from *in vitro* experiments and extending them to the cellular level. This may explain why the two auxiliary complexes share some substrates (**Figure 9**). For SPs having low overall hydrophobicity in combination with high glycine- plus proline-content, i.e. low alpha-helical propensity, full Sec61 channel opening in cotranslational transport was found to be supported by TRAP (Nguyen et al., 2018), a SP feature that had not been previously appreciated. Furthermore, to accommodate SPs with low H-region hydrophobicity, particularly in combination with detrimental features within the mature part, full Sec61 channel opening was observed to be supported by Sec62/Sec63 with or without BiP involvement (Ziska et al., 2019; Schorr et al., 2020). This raises the questions why this is the case and what the possible benefits are. To answer the second question first, we suggested that these features may allow differential regulation of ER protein import under different cellular conditions, for example by the known phosphorylation or Ca^{2+} binding of the respective transport components (**Table 1**). Sec63 and Sec62 were described to be subject to phosphorylation and Ca^{2+}-binding, respectively (Ampofo et al., 2013; Linxweiler et al., 2013). Thus, these modifications are candidates for Sec62/Sec63- and ER protein import-regulation, i.e. the different requirements of different precursors may provide a basis for dual intracellular location of proteins, such as ERj6 –coded by the DNAJC3 gene- (Shaffer et al., 2005; Oyamadori et al., 2006; Rutkowski et al., 2007; Petrova et al., 2008), a Sec62-client in HEK293 cells and in HeLa cells (Schorr et al., 2020). Furthermore, ERj1 was found to be subject to phosphorylation (Götz et al., 2009) and TRAPα was found to be subject to phosphorylation as well as Ca^{2+}-binding (Wada et al., 1991) and, therefore, may reciprocally respond to the same cellular conditions as compared to Sec62/Sec63. We are convinced that the detected variations in SP and TMH characteristics are responsible for the known precursor specific defects in various human diseases, termed Sec61-channelopathies (reviewed by Haßdenteufel et al., 2014; Sicking et al., 2021a), which include *SEC61A1*-linked Common variable immunodeficiency (Schubert et al., 2018), Neutropenia (Van Nieuwenhove et al., 2020) and Tubulointerstitial kidney disease (Bolar et al., 2016; Sicking et al., 2022), *SEC61B*- and *SEC63*-linked Polycystic liver disease (Fedeles et al., 2011; Lang et al., 2012; Besse et al., 2017), and *SSR*- as well as *CAML*-linked Congenital disorders of glycosylation (Pfeffer et al., 2017; Nguyen et al., 2018; Wilson et al., 2022) (**Table 1**).

To address the first question, it is noteworthy that higher than average overall hydrophobicity and higher than average H-region hydrophobicity seem to define "weak" or inefficiently gating SPs in the context of small precursor proteins (Haßdenteufel et al., 2019) (**Figures 10B,D**), which is in sharp contrast to the SP of precursor polypeptides in cotranslational translocation mentioned above (**Figures 10A,C**). Therefore, the question is how these contradictory findings can be reconciled. We suggest that both higher and lower than average SP hydrophobicity extends the dwell time of these SPs at the cytosolic funnel of the Sec61 channel, simply because their interactions with the hydrophobic patch are either too strong, i.e., disfavouring reversibility, or not strong enough to trigger spontaneous opening of the lateral gate and accompanying full channel opening, which may best be envisioned in the energy diagram for Sec61 channel gating (**Figure 7**). Therefore, these features were found to be responsible for the additional BiP-requirement in the case of the precursors of ERj3 (Schorr et al., 2020), prion protein (Ziska et al., 2019), and proapelin (Haßdenteufel et al., 2018), and the sensitivity towards the Sec61 channel inhibitor CAM741. This SP effect appears to be reinforced by clusters of positive charges downstream of the SP in co- and posttranslational translocation (**Figure 10E**) (Haßdenteufel et al., 2018; Ziska et al., 2019; Schorr et al., 2020). Therefore, allosteric Sec61 channel effectors have to bind to the channel, which supposedly lowers the activation energy for channel opening, in particular when aberrant SP hydrophobicity coincides with low SP helix propensity, as in the case of TRAP (Nguyen et al., 2018), or with deleterious features downstream of the SP in the mature region, as in the case of Sec62/Sec63 (Schorr et al., 2020). According to the available structural data, both accessory complexes, Sec62/Sec63 and TRAP, appear to act on the Sec61 channel on its lumenal side, i.e., in proximity to loop 5, which connects the amino- and carboxy-terminal halves of Sec61α. Thus, interaction of the accessory complexes with loop 5 might support the rigid body movement in the course of Sec61 channel opening. When BiP is involved in channel opening in addition to Sec62/Sec63, it is recruited to the Sec61 complex by Sec63, binds to ER lumenal loop 7 of Sec61α, and contributes to the lowering of the activation energy for channel opening (Schäuble et al., 2012; Haßdenteufel et al., 2018).

Considering the evolutionary conservation of the GP content of SPs encountered in TRAP-containing humans and TRAP-free organisms such as yeast and *E. coli* points to a much higher GP content in the former (**Figure 11D**). Thus, enabled by TRAP, the human Sec61 channel can manage SPs with a higher content of glycines and prolines, i.e., a lower helix propensity, compared to its homologous ancestors in yeast and bacteria. Such a scenario speaks in favor of a co-evolution of SPs and allosteric effectors of the Sec61 complex eventually allowing for a broader client spectrum and a more complex orchestration of protein transport.

AUTHOR CONTRIBUTIONS

SL, VH, and RZ designed the study and wrote the manuscript. All authors discussed the results and have read and agreed to the published version of the manuscript.

FUNDING

VH, SL, MJ, and RZ were supported by the Deutsche Forschungsgemeinschaft (DFG, German Research Foundation), with grants HE3875/15-1 to VH, ZI234/13-1 to RZ, IRTG1830 and SFB894 to SL, MJ, and RZ. Furthermore, the authors acknowledge support by the Deutsche Forschungsgemeinschaft (DFG, German Research Foundation) and Saarland University within the funding programme Open Access Publishing.

ACKNOWLEDGMENTS

The authors thank Bianca Schrul (Saarland University, Homburg, Germany), Johanna Dudek (Saarland University, Homburg, Germany), Stefan Pfeffer (ZMBH, Heidelberg, Germany), and Friedrich Förster (Utrecht University, Utrecht, Netherlands) for contributions to figures, fruitful collaborations, and stimulating discussion. Furthermore, they are grateful to Fan Liu (FMP, Berlin, Germany) for sharing her unpublished results.

SUPPLEMENTARY MATERIAL

The Supplementary Material for this article can be found online at: https://www.frontiersin.org/articles/10.3389/fphys.2022.833540/full#supplementary-material

REFERENCES

Armenteros, J. J. A., Salvatore, M., Emanuelsson, O., Winther, O., von Heijne, G., Elofsson, A., et al. (2019). Detecting Sequence Signals in Targeting Peptides Using Deep Learning. *Life Sci. Alliance* 2, e201900429. doi:10.26508/lsa.201900429

Ampofo, E., Welker, S., Jung, M., Müller, L., Greiner, M., Zimmermann, R., et al. (2013). CK2 Phosphorylation of Human Sec63 Regulates its Interaction with Sec62. *Biochimica Biophysica Acta (BBA) - General Subj.* 1830, 2938–2945. doi:10.1016/j.bbagen.2012.12.020

Anghel, S. A., McGilvray, P. T., Hegde, R. S., and Keenan, R. J. (2017). Identification of Oxa1 Homologs Operating in the Eukaryotic Endoplasmic Reticulum. *Cell. Rep.* 21, 3708–3716. doi:10.1016/j.celrep.2017.12.006

Ast, T., Cohen, G., and Schuldiner, M. (2013). A Network of Cytosolic Factors Targets SRP-independent Proteins to the Endoplasmic Reticulum. *Cell.* 152, 1134–1145. doi:10.1016/j.cell.2013.02.003

Aviram, N., Ast, T., Costa, E. A., Arakel, E. C., Chuartzman, S. G., Jan, C. H., et al. (2016). The SND Proteins Constitute an Alternative Targeting Route to the Endoplasmic Reticulum. *Nature* 540, 134–138. doi:10.1038/nature20169

Bai, L., You, Q., Feng, X., Kovach, A., and Li, H. (2020). Structure of the ER Membrane Complex, a Transmembrane-Domain Insertase. *Nature* 584, 475–478. doi:10.1038/s41586-020-2389-3

Baker, J. A., Wong, W.-C., Eisenhaber, B., Warwicker, J., and Eisenhaber, F. (2017). Charged Residues Next to Transmembrane Regions Revisited: "Positive-Inside Rule" Is Complemented by the "negative inside Depletion/outside Enrichment Rule". *BMC Biol.* 15, 66. doi:10.1186/s12915-017-0404-4

Bañó-Polo, M., Martínez-Garay, C. A., Grau, B., Martínez-Gil, L., and Mingarro, I. (2017). Membrane Insertion and Topology of the Translocon-Associated Protein (TRAP) Gamma Subunit. *Biochimica Biophysica Acta (BBA) - Biomembr.* 1859, 903–909. doi:10.1016/j.bbamem.2017.01.027

Beckmann, R., Spahn, C. M. T., Eswar, N., Helmers, J., Penczek, P. A., Sali, A., et al. (2001). Architecture of the Protein-Conducting Channel Associated with the Translating 80S Ribosome. *Cell.* 107, 361–372. doi:10.1016/s0092-8674(01)00541-4

Benedix, J., Lajoie, P., Jaiswal, H., Burgard, C., Greiner, M., Zimmermann, R., et al. (2010). BiP Modulates the Affinity of its Co-chaperone ERj1 for Ribosomes. *J. Biol. Chem.* 285, 36427–36433. doi:10.1074/jbc.M110.143263

Berkovits, B. D., and Mayr, C. (2015). Alternative 3′ UTRs Act as Scaffolds to Regulate Membrane Protein Localization. *Nature* 522, 363–367. doi:10.1038/nature14321

Besse, W., Dong, K., Choi, J., Punia, S., Fedeles, S. V., Choi, M., et al. (2017). Isolated Polycystic Liver Disease Genes Define Effectors of Polycystin-1 Function. *J. Clin. Invest.* 127, 1772–1785. doi:10.1172/JCI90129

Bhadra, P., Dos Santos, S., Gamayun, I., Pick, T., Neumann, C., Ogbechi, J., et al. (2021b). Mycolactone Enhances the Ca2+ Leak from Endoplasmic Reticulum by Trapping Sec61 Translocons in a Ca2+ Permeable State. *Biochem. J.* 478, 4005–4024. doi:10.1042/BCJ20210345

Bhadra, P., and Helms, V. (2021). Molecular Modeling of Signal Peptide Recognition by Eukaryotic Sec Complexes. *Ijms* 22, 10705. doi:10.3390/ijms221910705

Bhadra, P., Schorr, S., Lerner, M., Nguyen, D., Dudek, J., Förster, F., et al. (2021a). Quantitative Proteomics and Differential Protein Abundance Analysis after Depletion of Putative mRNA Receptors in the ER Membrane of Human Cells Identifies Novel Aspects of mRNA Targeting to the ER. *Molecules* 26, 3591. doi:10.3390/molecules26123591

Blau, M., Mullapudi, S., Becker, T., Dudek, J., Zimmermann, R., Penczek, P. A., et al. (2005). ERj1p Uses a Universal Ribosomal Adaptor Site to Coordinate the 80S Ribosome at the Membrane. *Nat. Struct. Mol. Biol.* 12, 1015–1016. doi:10.1038/nsmb998

Blobel, G., and Dobberstein, B. (1975b). Transfer of Proteins across Membranes. II. Reconstitution of Functional Rough Microsomes from Heterologous Components. *J. Cell. Biol.* 67, 852–862. doi:10.1083/jcb.67.3.852

Blobel, G., and Dobberstein, B. (1975a). Transfer of Proteins across Membranes. I. Presence of Proteolytically Processed and Unprocessed Nascent Immunoglobulin Light Chains on Membrane-Bound Ribosomes of Murine Myeloma. *J. Cell. Biol.* 67, 835–851. doi:10.1083/jcb.67.3.835

Blobel, G. (1980). Intracellular Protein Topogenesis. *Proc. Natl. Acad. Sci. U.S.A.* 77, 1496–1500. doi:10.1073/pnas.77.3.1496

Bolar, N. A., Golzio, C., Živná, M., Hayot, G., Van Hemelrijk, C., Schepers, D., et al. (2016). Heterozygous Loss-Of-Function SEC61A1 Mutations Cause Autosomal-Dominant Tubulo-Interstitial and Glomerulocystic Kidney Disease with Anemia. *Am. J. Hum. Genet.* 299, 174–187. doi:10.1016/j.ajhg.2016.05.028

Borgese, N., Coy-Vergara, J., Colombo, S. F., and Schwappach, B. (2019). The Ways of Tails: the GET Pathway and More. *Protein J.* 38, 289–305. doi:10.1007/s10930-019-09845-4

Borgese, N., and Fasana, E. (2011). Targeting Pathways of C-Tail-Anchored Proteins. *Biochimica Biophysica Acta (BBA) - Biomembr.* 1808, 937–946. doi:10.1016/j.bbamem.2010.07.010

Casson, J., McKenna, M., Haßdenteufel, S., Aviram, N., Zimmerman, R., and High, S. (2017). Multiple Pathways Facilitate the Biogenesis of Mammalian Tail-Anchored Proteins. *J. Cell. Sci.* 130, 3851–3861. doi:10.1242/jcs.207829

Chartron, J. W., Hunt, K. C. L., and Frydman, J. (2016). Cotranslational Signal-independent SRP Preloading during Membrane Targeting. *Nature* 536, 224–228. doi:10.1038/nature19309

Chen, X., VanValkenburgh, C., Liang, H., Fang, H., and Green, N. (2001). Signal Peptidase and Oligosaccharyltransferase Interact in a Sequential and Dependent Manner within the Endoplasmic Reticulum. *J. Biol. Chem.* 276, 2411–2416. doi:10.1074/jbc.m007723200

Chitwood, P. J., Juszkiewicz, S., Guna, A., Shao, S., and Hegde, R. S. (2018). EMC Is Required to Initiate Accurate Membrane Protein Topogenesis. *Cell.* 175, 1507–1519. doi:10.1016/j.cell.2018.10.009

Conti, B. J., Devaraneni, P. K., Yang, Z., David, L. L., and Skach, W. R. (2015). Cotranslational Stabilization of Sec62/63 within the ER Sec61 Translocon Is Controlled by Distinct Substrate-Driven Translocation Events. *Mol. Cell.* 58, 269–283. doi:10.1016/j.molcel.2015.02.018

Costa, E. A., Subramanian, K., Nunnari, J., and Weissman, J. S. (2018). Defining the Physiological Role of SRP in Protein-Targeting Efficiency and Specificity. *Science* 359, 689–692. doi:10.1126/science.aar3607

Cox, J., Hein, M. Y., Luber, C. A., Paron, I., Nagaraj, N., and Mann, M. (2014). Accurate Proteome-wide Label-free Quantification by Delayed Normalization and Maximal Peptide Ratio Extraction, Termed MaxLFQ. *Mol. Cell. Proteomics* 13, 2513–2526. doi:10.1074/mcp.M113.031591

Cox, J., and Mann, M. (2008). MaxQuant Enables High Peptide Identification Rates, Individualized p.p.b.-range Mass Accuracies and Proteome-wide Protein Quantification. *Nat. Biotechnol.* 26, 1367–1372. doi:10.1038/nbt.1511

Cui, X. A., Zhang, H., and Palazzo, A. F. (2012). p180 Promotes the Ribosome-independent Localization of a Subset of mRNA to the Endoplasmic Reticulum. *PLoS Biol.* 10, e1001336. doi:10.1371/journal.pbio.1001336

Cui, X. A., Zhang, Y., Hong, S. J., and Palazzo, A. F. (2013). Identification of a Region within the Placental Alkaline Phosphatase mRNA that Mediates P180-dependent Targeting to the Endoplasmic Reticulum. *J. Biol. Chem.* 288, 29633–29641. doi:10.1074/jbc.M113.482505

Cui, X. A., Zhang, H., Ilan, L., Liu, A. X., Kharchuk, I., and Palazzo, A. F. (2015). mRNA Encoding Sec61beta, a Tail-Anchored Protein, is Localized on the Endoplasmic Reticulum. *J. Cell Sci.* 128, 3398–3410. doi:10.1242/jcs.168583

Davis, E. M., Kim, J., Menasche, B. L., Sheppard, J., Liu, X., Tan, A.-C., et al. (2015). Comparative Haploid Genetic Screens Reveal Divergent Pathways in the Biogenesis and Trafficking of Glycophosphatidylinositol-Anchored Proteins. *Cell. Rep.* 11, 1727–1736. doi:10.1016/j.celrep.2015.05.026

Dejgaard, K., Theberge, J.-F., Heath-Engel, H., Chevet, E., Tremblay, M. L., and Thomas, D. Y. (2010). Organization of the Sec61 Translocon, Studied by High Resolution Native Electrophoresis. *J. Proteome Res.* 9, 1763–1771. doi:10.1021/pr900900x

Deshaies, R. J., Sanders, S. L., Feldheim, D. A., and Schekman, R. (1991). Assembly of Yeast Sec Proteins Involved in Translocation into the Endoplasmic Reticulum into a Membrane-Bound Multisubunit Complex. *Nature* 349, 806–808. doi:10.1038/349806a0

Devaraneni, P. K., Conti, B., Matsumura, Y., Yang, Z., Johnson, A. E., and Skach, W. R. (2011). Stepwise Insertion and Inversion of a Type II Signal Anchor Sequence in the Ribosome-Sec61 Translocon Complex. *Cell.* 146, 134–147. doi:10.1016/j.cell.2011.06.004

Devuyst, O., Olinger, E., Weber, S., Eckardt, K.-U., Kmoch, S., Rampoldi, L., et al. (2019). Autosomal Dominant Tubulointerstitial Kidney Disease. *Nat. Rev. Dis. Prim.* 5, 60. doi:10.1038/s41572-019-0109-9

Dhiman, R., Caesar, S., Thiam, A. R., and Schrul, B. (2020). Mechanisms of Protein Targeting to Lipid Droplets: A Unified Cell Biological and Biophysical Perspective. *Seminars Cell. & Dev. Biol.* 108, 4–13. doi:10.1016/j.semcdb.2020.03.004

Dierks, T., Volkmer, J., Schlenstedt, G., Jung, C., Sandholzer, U., Zachmann, K., et al. (1996). A Microsomal ATP-Binding Protein Involved in Efficient Protein Transport into the Mammalian Endoplasmic Reticulum. *EMBO J.* 15, 6931–6942. doi:10.1002/j.1460-2075.1996.tb01085.x

Do, H., Falcone, D., Lin, J., Andrews, D. W., and Johnson, A. E. (1996). The Cotranslational Integration of Membrane Proteins into the Phospholipid Bilayer Is a Multistep Process. *Cell.* 85, 369–378. doi:10.1016/s0092-8674(00)81115-0

Dudek, J., Greiner, M., Müller, A., Hendershot, L. M., Kopsch, K., Nastainczyk, W., et al. (2005). ERj1p Has a Basic Role in Protein Biogenesis at the Endoplasmic Reticulum. *Nat. Struct. Mol. Biol.* 12, 1008–1014. doi:10.1038/nsmb1007

Dudek, J., Volkmer, J., Bies, C., Guth, S., Müller, A., Lerner, M., et al. (2002). A Novel Type of Co-chaperone Mediates Transmembrane Recruitment of DnaK-like Chaperones to Ribosomes. *EMBO J.* 21, 2958–2967. doi:10.1093/emboj/cdf315

Eden, E., Navon, R., Steinfeld, I., Lipson, D., and Yakhini, Z. (2009). Gorilla: a Tool for Discovery and Visualization of Enriched GO Terms in Ranked Gene Lists. *BMC Bioinforma.* 10, 48. doi:10.1186/1471-2105-10-48

Egea, P. F., Stroud, R. M., and Walter, P. (2005). Targeting Proteins to Membranes: Structure of the Signal Recognition Particle. *Curr. Opin. Struct. Biol.* 15, 213–220. doi:10.1016/j.sbi.2005.03.007

Erdmann, F., Schäuble, N., Lang, S., Jung, M., Honigmann, A., Ahmad, M., et al. (2011). Interaction of Calmodulin with Sec61α Limits Ca2+leakage from the Endoplasmic Reticulumα Limits Ca^{2+} Leakage from the Endoplasmic Reticulum. *EMBO J.* 30, 17–31. doi:10.1038/emboj.2010.284

Erdmann, R., Veenhuis, M., Mertens, D., and Kunau, W. H. (1989). Isolation of Peroxisome-Deficient Mutants of *Saccharomyces cerevisiae*. *Proc. Natl. Acad. Sci. U.S.A.* 86, 5419–5423. doi:10.1073/pnas.86.14.5419

Fedeles, S. V., Tian, X., Gallagher, A.-R., Mitobe, M., Nishio, S., Lee, S. H., et al. (2011). A Genetic Interaction Network of Five Genes for Human Polycystic Kidney and Liver Diseases Defines Polycystin-1 as the Central Determinant of Cyst Formation. *Nat. Genet.* 43, 639–647. doi:10.1038/ng.860

Fons, R. D., Bogert, B. A., and Hegde, R. S. (2003). Substrate-specific Function of the Translocon-Associated Protein Complex during Translocation across the ER Membrane. *J. Cell. Biol.* 160, 529–539. doi:10.1083/jcb.200210095

Fumagalli, F., Noack, J., Bergmann, T. J., Cebollero, E., Pisoni, G. B., Fasana, E., et al. (2017). Translocon Component Sec62 Acts in Endoplasmic Reticulum Turnover during Stress Recovery. *Nat. Cell. Biol.* 18, 1173–1184.

Gamayun, I., O'Keefe, S., Pick, T., Klein, M.-C., Nguyen, D., McKibbin, C., et al. (2019). Eeyarestatin Compounds Selectively Enhance Sec61-Mediated Ca2+ Leakage from the Endoplasmic Reticulum. *Cell. Chem. Biol.* 26, 571–583. doi:10.1016/j.chembiol.2019.01.010

Gamerdinger, M., Hanebuth, M. A., Frickey, T., and Deuerling, E. (2015). The Principle of Antagonism Ensures Protein Targeting Specificity at the Endoplasmic Reticulum. *Science* 348, 201–207. doi:10.1126/science.aaa5335

Gamerdinger, M., Kobayashi, K., Wallisch, A., Kreft, S. G., Sailer, C., Schlömer, R., et al. (2019). Early Scanning of Nascent Polypeptides inside the Ribosomal Tunnel by NAC. *Mol. Cell.* 75, 996–1006. doi:10.1016/j.molcel.2019.06.030

Gemmer, M., and Förster, F. (2020). A Clearer Picture of the ER Translocon Complex. *J. Cell. Sci.* 133, jcs231340. doi:10.1242/jcs.231340

Gilmore, R., Blobel, G., and Walter, P. (1982a). Protein Translocation across the Endoplasmic Reticulum. I. Detection in the Microsomal Membrane of a Receptor for the Signal Recognition Particle. *J. Cell. Biol.* 95, 463–469. doi:10.1083/jcb.95.2.463

Gilmore, R., Walter, P., and Blobel, G. (1982b). Protein Translocation across the Endoplasmic Reticulum. II. Isolation and Characterization of the Signal Recognition Particle Receptor. *J. Cell. Biol.* 95, 470–477. doi:10.1083/jcb.95.2.470

Goder, V., Junne, T., and Spiess, M. (2004). Sec61p Contributes to Signal Sequence Orientation According to the Positive-Inside Rule. *MBoC* 15, 1470–1478. doi:10.1091/mbc.e03-08-0599

Goder, V., and Spiess, M. (2003). Molecular Mechanism of Signal Sequence Orientation in the Endoplasmic Reticulum. *EMBO J.* 22, 3645–3653. doi:10.1093/emboj/cdg361

Goodman, J. M. (2020). Building the Lipid Droplet Assembly Complex. *J. Cell. Biol.* 219, e202006025. doi:10.1083/jcb.202006025

Görlich, D., Hartmann, E., Prehn, S., and Rapoport, T. A. (1992a). A Protein of the Endoplasmic Reticulum Involved Early in Polypeptide Translocation. *Nature* 357, 47–52. doi:10.1038/357047a0

Görlich, D., Prehn, S., Hartmann, E., Kalies, K.-U., and Rapoport, T. A. (1992b). A Mammalian Homolog of SEC61p and SECYp Is Associated with Ribosomes and Nascent Polypeptides during Translocation. *Cell.* 71, 489–503. doi:10.1016/0092-8674(92)90517-g

Görlich, D., and Rapoport, T. A. (1993). Protein Translocation into Proteoliposomes Reconstituted from Purified Components of the Endoplasmic Reticulum Membrane. *Cell.* 75, 615–630. doi:10.1016/0092-8674(93)90483-7

Götz, C., Müller, A., Montenarh, M., Zimmermann, R., and Dudek, J. (2009). The ER-Membrane-Resident Hsp40 ERj1 Is a Novel Substrate for Protein Kinase CK2. *Biochem. Biophysical Res. Commun.* 388, 637–642. doi:10.1016/j.bbrc.2009.07.146

Gumbart, J., and Schulten, K. (2007). Structural Determinants of Lateral Gate Opening in the Protein Translocon. *Biochemistry* 46, 11147–11157. doi:10.1021/bi700835d

Guo, H., Xiong, Y., Witkowski, P., Cui, J., Wang, L.-j., Sun, J., et al. (2014). Inefficient Translocation of Preproinsulin Contributes to Pancreatic β Cell Failure and Late-Onset Diabetes. *J. Biol. Chem.* 289, 16290–16302. doi:10.1074/jbc.m114.562355

Halic, M., and Beckmann, R. (2005). The Signal Recognition Particle and its Interactions during Protein Targeting. *Curr. Opin. Struct. Biol.* 15, 116–125. doi:10.1016/j.sbi.2005.01.013

Halic, M., Blau, M., Becker, T., Mielke, T., Pool, M. R., Wild, K., et al. (2006). Following the Signal Sequence from Ribosomal Tunnel Exit to Signal Recognition Particle. *Nature* 444, 507–511. doi:10.1038/nature05326

Hannigan, M. M., Hoffman, A. M., Thompson, J. W., Zheng, T., and Nicchitta, C. V. (2020). Quantitative Proteomics Links the LRRC59 Interactome to mRNA Translation on the ER Membrane. *Mol. Cell. Proteom.* 19, 1826–1849. doi:10.1074/mcp.RA120.002228

Hansen, K. G., Aviram, N., Laborenz, J., Bibi, C., Meyer, M., Spang, A., et al. (2018). An ER Surface Retrieval Pathway Safeguards the Import of Mitochondrial Membrane Proteins in Yeast. *Science* 361, 1118–1122. doi:10.1126/science.aar8174

Hartmann, E., Sommer, T., Prehn, S., Görlich, D., Jentsch, S., and Rapoport, T. A. (1994). Evolutionary Conservation of Components of the Protein Translocation Complex. *Nature* 367, 654–657. doi:10.1038/367654a0

Haßdenteufel, S., Johnson, N., Paton, A. W., Paton, J. C., High, S., and Zimmermann, R. (2018). Chaperone-mediated Sec61 Channel Gating during ER Import of Small Precursor Proteins Overcomes Sec61 Inhibitor-Reinforced Energy Barrier. *Cell. Rep.* 23, 1373–1386. doi:10.1016/j.celrep.2018.03.122

Haßdenteufel, S., Klein, M.-C., Melnyk, A., and Zimmermann, R. (2014). Protein Transport into the Human ER and Related Diseases, Sec61-Channelopathies. *Biochem. Cell. Biol.* 92, 499–509. doi:10.1139/bcb-2014-0043

Haßdenteufel, S., Nguyen, D., Helms, V., Lang, S., and Zimmermann, R. (2019). ER Import of Small Human Presecretory Proteins: Components and Mechanisms. *FEBS Lett.* 593, 2506–2524. doi:10.1002/1873-3468.13542

Haßdenteufel, S., Schäuble, N., Cassella, P., Leznicki, P., Müller, A., High, S., et al. (2011). Ca2+-calmodulin Inhibits Tail-Anchored Protein Insertion into the Mammalian Endoplasmic Reticulum Membrane. *FEBS Lett.* 585, 3485–3490. doi:10.1016/j.febslet.2011.10.008

Haßdenteufel, S., Sicking, M., Schorr, S., Aviram, N., Fecher-Trost, C., Schuldiner, M., et al. (2017). hSnd2 Protein Represents an Alternative Targeting Factor to the Endoplasmic Reticulum in Human Cells. *FEBS Lett.* 591, 3211–3224. doi:10.1002/1873-3468.12831

Hegde, R. S., and Bernstein, H. D. (2006). The Surprising Complexity of Signal Sequences. *Trends Biochem. Sci.* 31, 563–571. doi:10.1016/j.tibs.2006.08.004

Hegde, R. S., Voigt, S., Rapoport, T. A., and Lingappa, V. R. (1998). TRAM Regulates the Exposure of Nascent Secretory Proteins to the Cytosol during Translocation into the Endoplasmic Reticulum. *Cell.* 92, 621–631. doi:10.1016/S0092-8674(00)81130-7

Hein, M. Y., Hubner, N. C., Poser, I., Cox, J., Nagaraj, N., Toyoda, Y., et al. (2015). A Human Interactome in Three Quantitative Dimensions Organized by Stoichiometries and Abundances. *Cell.* 163, 712–723. doi:10.1016/j.cell.2015.09.053

Hettema, E. H., Girzalsky, W., van den Berg, M., Erdmann, R., and Distel, B. (2000). *Saccharomyces cerevisiae* Pex3p and Pex19p Are Required for Proper Localization and Stability of Peroxisomal Membrane Proteins. *EMBO J.* 19, 223–233. doi:10.1093/emboj/19.2.223

High, S., Martoglio, B., Görlich, D., Andersen, S. S., Ashford, A. J., Giner, A., et al. (1993). Site-specific Photocross-Linking Reveals that Sec61p and TRAM Contact Different Regions of a Membrane-Inserted Signal Sequence. *J. Biol. Chem.* 268, 26745–26751. doi:10.1016/s0021-9258(19)74376-2

Hoffman, A. M., Chen, Q., Zheng, T., and Nicchitta, C. V. (2019). Heterogeneous Translational Landscape of the Endoplasmic Reticulum Revealed by Ribosome Proximity Labeling and Transcriptome Analysis. *J. Biol. Chem.* 294, 8942–8958. doi:10.1074/jbc.RA119.007996

Hsieh, H.-H., Lee, J. H., Chandrasekar, S., and Shan, S.-o. (2020). A Ribosome-Associated Chaperone Enables Substrate Triage in a Cotranslational Protein Targeting Complex. *Nat. Commun.* 11, 5840. doi:10.1038/s41467-020-19548-5

Hsieh, H.-H., and Shan, S.-o. (2022). Fidelity of Cotranslational Protein Targeting to the Endoplasmic Reticulum. *Ijms* 23, 281. doi:10.3390/ijms23010281

Hsu, J. C.-C., Reid, D. W., Hoffman, A. M., Sarkar, D., and Nicchitta, C. V. (2018). Oncoprotein AEG-1 Is an Endoplasmic Reticulum RNA-Binding Protein Whose Interactome Is Enriched in Organelle Resident Protein-Encoding mRNAs. *RNA* 24, 688–703. doi:10.1261/rna.063313.117

Itskanov, S., Kuo, K. M., Gumbart, J. C., and Park, E. (2021). Stepwise Gating of the Sec61 Protein-Conducting Channel by Sec63 and Sec62. *Nat. Struct. Mol. Biol.* 28, 162–172. doi:10.1038/s41594-020-00541-x

Itskanov, S., and Park, E. (2019). Structure of the Posttranslational Sec Protein-Translocation Channel Complex from Yeast. *Science* 363, 84–87. doi:10.1126/science.aav6740

Jadhav, B., McKenna, M., Johnson, N., High, S., Sinning, I., and Pool, M. R. (2015). Mammalian SRP Receptor Switches the Sec61 Translocase from Sec62 to SRP-dependent Translocation. *Nat. Commun.* 6, 10133. doi:10.1038/ncomms10133

Jagannathan, S., Hsu, J. C., Reid, D. W., Chen, Q., Thompson, W. J., Moseley, A. M., et al. (2014). Multifunctional Roles for the Protein Translocation Machinery in RNA Anchoring to the Endoplasmic Reticulum. *J. Biol. Chem.* 289, 25907–25924. doi:10.1074/jbc.M114.580688

Jan, C. H., Williams, C. C., and Weissman, J. S. (2014). Principles of ER Cotranslational Translocation Revealed by Proximity-specific Ribosome Profiling. *Science* 346, 1257521. doi:10.1126/science.1257521

Jansen, R. L. M., and Klei, I. J. (2019). The Peroxisome Biogenesis Factors Pex3 and Pex19: Multitasking Proteins with Disputed Functions. *FEBS Lett.* 593, 457–474. doi:10.1002/1873-3468.13340

Johnson, N., Haßdenteufel, S., Theis, M., Paton, A. W., Paton, J. C., Zimmermann, R., et al. (2013). The Signal Sequence Influences Post-Translational ER Translocation at Distinct Stages. *PLoS ONE* 8, e75394. doi:10.1371/journal.pone.0075394

Jomaa, A., Boehringer, D., Leibundgut, M., and Ban, N. (2016). Structures of the *E. coli* Translating Ribosome with SRP and its Receptor and with the Translocon. *Nat. Commun.* 7, 10471. doi:10.1038/ncomms10471

Jomaa, A., Eitzinger, S., Zhu, Z., Chandrasekar, S., Kobayashi, K., Shan, S.-o., et al. (2021). Molecular Mechanism of Cargo Recognition and Handover by the Mammalian Signal Recognition Particle. *Cell. Rep.* 36, 109350. doi:10.1016/j.celrep.2021.109350

Jomaa, A., Gamerdinger, M., Hsieh, H.-H., Wallisch, A., Chandrasekaran, V., Ulusoy, Z., et al. (2022). Mechanism of Signal Sequence Handover from NAC to SRP on Ribosomes during ER-Protein Targeting. *Science* 375, 839–844. doi:10.1126/science.abl6459

Jumper, J., Evans, R., Pritzel, A., Green, T., Figurnov, M., Ronneberger, O., et al. (2021). Highly Accurate Protein Structure Prediction with AlphaFold. *Nature* 596, 583–589. doi:10.1038/s41586-021-03819-2

Jung, S.-j., and Kim, H. (2021). Emerging View on the Molecular Functions of Sec62 and Sec63 in Protein Translocation. *Ijms* 22, 12757. doi:10.3390/ijms222312757

Jung, S. J., Kim, J. E., Reithinger, J. H., and Kim, H. (2014). The Sec62-Sec63 Translocon Facilitates Translocation of the C-Terminus of Membrane Proteins. *J. Cell. Sci.* 127, 4270–4278. doi:10.1242/jcs.153650

Kalies, K.-U., Rapoport, T. A., and Hartmann, E. (1998). The β Subunit of the Sec61 Complex Facilitates Cotranslational Protein Transport and Interacts with the Signal Peptidase during Translocation. *J. Cell. Biol.* 141, 887–894. doi:10.1083/jcb.141.4.887

Klein, M.-C., Lerner, M., Nguyen, D., Pfeffer, S., Dudek, J., Förster, F., et al. (2020). TRAM1 Protein May Support ER Protein Import by Modulating the Phospholipid Bilayer Near the Lateral Gate of the Sec61-Channel. *Channels* 14, 28–44. doi:10.1080/19336950.2020.1724759

Koch, C., Schuldiner, M., and Herrmann, J. M. (2021). ER-SURF: Riding the Endoplasmic Reticulum Surface to Mitochondria. *Ijms* 22, 9655. doi:10.3390/ijms22179655

Kutay, U., Hartmann, E., and Rapoport, T. (1993). A Class of Membrane Proteins with a C-Terminal Anchor. *Trends Cell. Biol.* 3, 72–75. doi:10.1016/0962-8924(93)90066-a

Kyte, J., and Doolittle, R. F. (1982). A Simple Method for Displaying the Hydrophobic Character of a Protein. *J. Mol. Biol.* 157, 105–132.

Lakkaraju, A. K. K., Thankappan, R., Mary, C., Garrison, J. L., Taunton, J., and Strub, K. (2012). Efficient Secretion of Small Proteins in Mammalian Cells Relies on Sec62-dependent Posttranslational Translocation. *MBoC* 23, 2712–2722. doi:10.1091/mbc.E12-03-0228

Lalier, L., Mignard, V., Joalland, M.-P., Lanoé, D., Cartron, P.-F., Manon, S., et al. (2021). TOM20-mediated Transfer of Bcl2 from ER to MAM and Mitochondria upon Induction of Apoptosis. *Cell. Death Dis.* 12, 182. doi:10.1038/s41419-021-03471-8

Lang, S., Benedix, J., Fedeles, S. V., Schorr, S., Schirra, C., Schäuble, N., et al. (2012). Differential Effects of Sec61α-, Sec62- and Sec63-Depletion on Transport of Polypeptides into the Endoplasmic Reticulum of Mammalian Cellsα-, Sec62 and Sec63-Depletion on Transport of Polypeptides into the Endoplasmic

Reticulum of Mammalian Cells. *J. Cell. Sci.* 125, 1958–1969. doi:10.1242/jcs.096727

Lang, S., Nguyen, D., Pfeffer, S., Förster, F., Helms, V., and Zimmermann, R. (2019). "Functions and Mechanisms of the Human Ribosome-Translocon Complex," in *Macromolecular Protein Complexes II: Structure and Function*. Editors J.R Harris and J. Marles-Wrigth, 93, 83–141. Subcell. Biochem. doi:10.1007/978-3-030-28151-9_4

Lang, S., Pfeffer, S., Lee, P.-H., Cavalié, A., Helms, V., Förster, F., et al. (2017). An Update on Sec61 Channel Functions, Mechanisms, and Related Diseases. *Front. Physiol.* 8, 887. doi:10.3389/fphys.2017.00887

Leznicki, P., Clancy, A., Schwappach, B., and High, S. (2010). Bat3 Promotes the Membrane Integration of Tail-Anchored Proteins. *J. Cell. Sci.* 123, 2170–2178. doi:10.1242/jcs.066738

Leznicki, P., and High, S. (2020). SGTA Associates with Nascent Membrane Protein Precursors. *EMBO Rep.* 21, e48835. doi:10.15252/embr.201948835

Leznicki, P., Schneider, H. O., Harvey, J. V., Shi, W. Q., and High, S. (2021). Co-translational Biogenesis of Lipid Droplet Integral Membrane Proteins. *J. Cell. Sci.* 135, jcs.259220. doi:10.1242/jcs.259220

Leznicki, P., Warwicker, J., and High, S. (2011). A Biochemical Analysis of the Constraints of Tail-Anchored Protein Biogenesis. *Biochem. J.* 436, 719–727. doi:10.1042/bj20101737

Liaci, A. M., and Förster, F. (2021). Take Me Home, Protein Roads: Structural Insights into Signal Peptide Interactions during ER Translocation. *Ijms* 22, 11871. doi:10.3390/ijms222111871

Liaci, A. M., Steigenberger, B., Telles de Souza, P. C., Tamara, S., Gröllers-Mulderij, M., Ogrissek, P., et al. (2021). Structure of the Human Signal Peptidase Complex Reveals the Determinants for Signal Peptide Cleavage. *Mol. Cell.* 81, 3934–3948. doi:10.1016/j.molcel.2021.07.031

Linxweiler, M., Schorr, S., Schäuble, N., Jung, M., Linxweiler, J., Langer, F., et al. (2013). Targeting Cell Migration and the Endoplasmic Reticulum Stress Response with Calmodulin Antagonists: a Clinically Tested Small Molecule Phenocopy of SEC62 Gene Silencing in Human Tumor Cells. *BMC Cancer* 13, 574. doi:10.1186/1471-2407-13-574

Lloyd, D. J., Wheeler, M. C., and Gekakis, N. (2010). A Point Mutation in Sec61α1 Leads to Diabetes and Hepatosteatosis in Mice. *Diabetes* 59, 460–470. doi:10.2337/db08-1362

Ma, W., and Mayr, C. (2018). A Membraneless Organelle Associated with the Endoplasmic Reticulum Enables 3′UTR-Mediated Protein-Protein Interactions. *Cell.* 175, 1492–1506. doi:10.1016/j.cell.2018.10.007

Mahamid, J., Pfeffer, S., Schaffer, M., Villa, E., Danev, R., Kuhn Cuellar, L., et al. (2016). Visualizing the Molecular Sociology at the HeLa Cell Nuclear Periphery. *Science* 351, 969–972. doi:10.1126/science.aad8857

Mariappan, M., Li, X., Stefanovic, S., Sharma, A., Mateja, A., Keenan, R. J., et al. (2010). A Ribosome-Associating Factor Chaperones Tail-Anchored Membrane Proteins. *Nature* 466, 1120–1124. doi:10.1038/nature09296

Mayer, H.-A., Grau, H., Kraft, R., Prehn, S., Kalies, K.-U., and Hartmann, E. (2000). Mammalian Sec61 Is Associated with Sec62 and Sec63. *J. Biol. Chem.* 275, 14550–14557.

Mayerhofer, P. U., Bañó-Polo, M., Mingarro, I., and Johnson, A. E. (2016). Human Peroxin PEX3 Is Co-translationally Integrated into the ER and Exits the ER in Budding Vesicles. *Traffic* 17, 117–130. doi:10.1111/tra.12350

McCormick, P. J., Miao, Y., Shao, Y., Lin, J., and Johnson, A. E. (2003). Cotranslational Protein Integration into the ER Membrane Is Mediated by the Binding of Nascent Chains to Translocon Proteins. *Mol. Cell.* 12, 329–341. doi:10.1016/s1097-2765(03)00304-6

McGilvray, P. T., Anghel, S. A., Sundaram, A., Zhong, F., Trnka, M. J., Fuller, J. R., et al. (2020). An ER Translocon for Multi-Pass Membrane Protein Biogenesis. *eLife* 9, e56889. doi:10.7554/eLife.56889

Ménétret, J.-F., Hegde, R. S., Aguiar, M., Gygi, S. P., Park, E., Rapoport, T. A., et al. (2008). Single Copies of Sec61 and TRAP Associate with a Nontranslating Mammalian Ribosome. *Structure* 16, 1126–1137. doi:10.1016/j.str.2008.05.003

Meyer, D. I., and Dobberstein, B. (1980a). A Membrane Component Essential for Vectorial Translocation of Nascent Proteins across the Endoplasmic Reticulum: Requirements for its Extraction and Reassociation with the Membrane. *J. Cell. Biol.* 87, 498–502. doi:10.1083/jcb.87.2.498

Meyer, D. I., and Dobberstein, B. (1980b). Identification and Characterization of a Membrane Component Essential for the Translocation of Nascent Proteins across the Membrane of the Endoplasmic Reticulum. *J. Cell. Biol.* 87, 503–508. doi:10.1083/jcb.87.2.503

Möller, I., Jung, M., Beatrix, B., Levy, R., Kreibich, G., Zimmermann, R., et al. (1998). A General Mechanism for Regulation of Access to the Translocon: Competition for a Membrane Attachment Site on Ribosomes. *Proc. Natl. Acad. Sci. U.S.A.* 95, 13425–13430. doi:10.1073/pnas.95.23.13425

Mothes, W., Prehn, S., and Rapoport, T. A. (1994). Systematic Probing of the Environment of a Translocating Secretory Protein during Translocation through the ER Membrane. *EMBO J.* 13, 3973–3982. doi:10.1002/j.1460-2075.1994.tb06713.x

Müller, G., and Zimmermann, R. (1988). Import of Honeybee Prepromelittin into the Endoplasmic Reticulum: Energy Requirements for Membrane Insertion. *EMBO J.* 7, 639–648. doi:10.1002/j.1460-2075.1988.tb02858.x

Müller, G., and Zimmermann, R. (1987). Import of Honeybee Prepromelittin into the Endoplasmic Reticulum: Structural Basis for Independence of SRP and Docking Protein. *EMBO J.* 6, 2099–2107. doi:10.1002/j.1460-2075.1987.tb02476.x

Müller, L., de Escauriaza, M. D., Lajoie, P., Theis, M., Jung, M., Müller, A., et al. (2010). Evolutionary Gain of Function for the ER Membrane Protein Sec62 from Yeast to Humans. *MBoC* 21, 691–703. doi:10.1091/mbc.e09-08-0730

Ng, D. T., Brown, J. D., and Walter, P. (1996). Signal Sequences Specify the Targeting Route to the Endoplasmic Reticulum Membrane. *J. Cell. Biol.* 134, 269–278. doi:10.1083/jcb.134.2.269

Nguyen, D., Stutz, R., Schorr, S., Lang, S., Pfeffer, S., Freeze, H. H., et al. (2018). Proteomics Reveals Signal Peptide Features Determining the Client Specificity in Human TRAP-dependent ER Protein Import. *Nat. Commun.* 9, 37639. doi:10.1038/s41467-018-06188-z

Nixon-Abell, J., Obara, C. J., Weigel, A. V., Li, D., Legant, W. R., Xu, C. S., et al. (2016). Increased Spatiotemporal Resolution Reveals Highly Dynamic Dense Tubular Matrices in the Peripheral ER. *Science* 354, aaf3928. doi:10.1126/science.aaf3928

O'Donnell, J. P., Phillips, B. P., Yagita, Y., Juszkiewicz, S., Wagner, A., Malinverni, D., et al. (2020). The Architecture of EMC Reveals a Path for Membrane Protein Insertion. *eLife* 9, e57887. doi:10.7554/eLife.57887

Ohsumi, T., Ichimura, T., Sugano, H., Omata, S., Isobe, T., and Kuwano, R. (1993). Ribosome-binding Protein P34 Is a Member of the Leucine-Rich-Repeat-Protein Superfamily. *Biochem. J.* 294, 465–472. doi:10.1042/bj2940465

O'Keefe, S., Pool, M. R., and High, S. (2021a). Membrane Protein Biogenesis at the ER: the Highways and Byways. *FEBS J.* Advance online publication. doi:10.1111/febs.15905

O'Keefe, S., Zong, G., Duah, K. B., Andrews, L. E., Shi, W. Q., and High, S. (2021b). An Alternative Pathway for Membrane Protein Biogenesis at the Endoplasmic Reticulum. *Commun. Biol.* 4, 828. doi:10.1038/s42003-021-02363-z

Ong, L.-L., Er, C. P. N., Ho, A., Aung, M. T., and Yu, H. (2003). Kinectin Anchors the Translation Elongation Factor-1δ to the Endoplasmic Reticulum. *J. Biol. Chem.* 278, 32115–32123. doi:10.1074/jbc.M210917200

Ong, L.-L., Lin, P.-C., Zhang, X., Chia, S.-M., and Yu, H. (2006). Kinectin-dependent Assembly of Translation Elongation Factor-1 Complex on Endoplasmic Reticulum Regulates Protein Synthesis. *J. Biol. Chem.* 281, 33621–33634. doi:10.1074/jbc.M607555200

Oyadomari, S., Yun, C., Fisher, E. A., Kreglinger, N., Kreibich, G., Oyadomari, M., et al. (2006). Cotranslocational Degradation Protects the Stressed Endoplasmic Reticulum from Protein Overload. *Cell.* 126, 727–739. doi:10.1016/j.cell.2006.06.051

Palade, G. E., and Porter, K. R. (1954). Studies on the Endoplasmic Reticulum. *J. Exp. Med.* 100, 641–656. doi:10.1084/jem.100.6.641

Palade, G. (1975). Intracellular Aspects of the Process of Protein Synthesis. *Science* 189, 347–358. doi:10.1126/science.1096303

Pauwels, E., Provinciael, B., Camps, A., Hartmann, E., and Vermeire, K. (2022). Reduced DNAJC3 Expression Affects Protein Translocation across the ER Membrane and Attenuates the Down-Modulating Effect of the Translocation Inhibitor Cyclotriazadisulfonamide. *Ijms* 23, 584. doi:10.3390/ijms23020584

Pauwels, E., Schülein, R., and Vermeire, K. (2021). Inhibitors of the Sec61 Complex and Novel High Throughput Screening Strategies to Target the Protein Translocation Pathway. *Ijms* 22, 12007. doi:10.3390/ijms222112007

Petrova, K., Oyadomari, S., Hendershot, L. M., and Ron, D. (2008). Regulated Association of Misfolded Endoplasmic Reticulum Lumenal Proteins with P58/DNAJc3. *EMBO J.* 27, 2862–2872. doi:10.1038/emboj.2008.199

Pfeffer, S., Brandt, F., Hrabe, T., Lang, S., Eibauer, M., Zimmermann, R., et al. (2012). Structure and 3D Arrangement of Endoplasmic Reticulum Membrane-Associated Ribosomes. *Structure* 20, 1508–1518. doi:10.1016/j.str.2012.06.010

Pfeffer, S., Burbaum, L., Unverdorben, P., Pech, M., Chen, Y., Zimmermann, R., et al. (2015). Structure of the Native Sec61 Protein-Conducting Channel. *Nat. Commun.* 6, 8403. doi:10.1038/ncomms9403

Pfeffer, S., Dudek, J., Gogala, M., Schorr, S., Linxweiler, J., Lang, S., et al. (2014). Structure of the Mammalian Oligosaccharyl-Transferase Complex in the Native ER Protein Translocon. *Nat. Commun.* 5, 3072. doi:10.1038/ncomms4072

Pfeffer, S., Dudek, J., Schaffer, M., Ng, B. G., Albert, S., Plitzko, J. M., et al. (2017). Dissecting the Molecular Organization of the Translocon-Associated Protein Complex. *Nat. Commun.* 8, 14516. doi:10.1038/ncomms14516

Pfeiffer, N. V., Dirndorfer, D., Lang, S., Resenberger, U. K., Restelli, L. M., Hemion, C., et al. (2013). Structural Features within the Nascent Chain Regulate Alternative Targeting of Secretory Proteins to Mitochondria. *EMBO J.* 32, 1036–1051. doi:10.1038/emboj.2013.46

Pleiner, T., Tomaleri, G. P., Januszyk, K., Inglis, A. J., Hazu, M., and Voorhees, R. M. (2020). Structural Basis for Membrane Insertion by the Human ER Membrane Protein Complex. *Science* 369, 433–436. doi:10.1126/science.abb5008

Pool, M. R. (2022). Targeting of Proteins for Translocation at the Endoplasmic Reticulum. *Ijms* 23, 3773. doi:10.3390/ijms23073773

Potter, M. D., Seiser, R. M., and Nicchitta, C. V. (2001). Ribosome Exchange Revisited: a Mechanism for Translation-Coupled Ribosome Detachment from the ER Membrane. *Trends Cell. Biol.* 11, 112–115. doi:10.1016/s0962-8924(00)01905-x

Pyhtila, B., Zheng, T., Lager, P. J., Keene, J. D., Reedy, M. C., and Nicchitta, C. V. (2008). Signal Sequence- and Translation-independent mRNA Localization to the Endoplasmic Reticulum. *RNA* 14, 445–453. doi:10.1261/rna.721108

Rane, N. S., Kang, S. W., Chakrabarti, O., Feigenbaum, L., and Hegde, R. S. (2008). Reduced Translocation of Nascent Prion Protein During ER Stress Contributes to Neurodegeneration. *Dev Cell.* 15 (3), 359–370. doi:10.1016/j.devcel.2008.06.015

Raote, I., Ernst, A. M., Campelo, F., Rothman, J. E., Pincet, F., and Malhotra, V. (2020). TANGO1 Membrane Helices Create a Lipid Diffusion Barrier at Curved Membranes. *eLIFE* 9, e57822. doi:10.7554/eLIFE.57822

Raote, I., Ortega-Bellido, M., Santos, A. J., Foresti, O., Zhang, C., Garcia-Parajo, M. F., et al. (2018). TANGO1 Builds a Machine for Collagen Export by Recruiting and Spatially Organizing COPII, Tethers and Membranes. *eLIFE* 7, e32723. doi:10.7554/eLIFE.32723

Reid, D. W., and Nicchitta, C. V. (2012). Primary Role for Endoplasmic Reticulum-Bound Ribosomes in Cellular Translation Identified by Ribosome Profiling. *J. Biol. Chem.* 287, 5518–5527. doi:10.1074/jbc.M111.312280

Reithinger, J. H., Kim, J. E. H., and Kim, H. (2013). Sec62 Protein Mediates Membrane Insertion and Orientation of Moderately Hydrophobic Signal Anchor Proteins in the Endoplasmic Reticulum (ER). *J. Biol. Chem.* 288, 18058–18067. doi:10.1074/jbc.M113.473009

Rutkowski, D. T., Kang, S.-W., Goodman, A. G., Garrison, J. L., Taunton, J., Katze, M. G., et al. (2007). The Role of p58IPK in Protecting the Stressed Endoplasmic Reticulum. *MBoC* 18, 3681–3691. doi:10.1091/mbc.e07-03-0272

Sadlish, H., Pitonzo, D., Johnson, A. E., and Skach, W. R. (2005). Sequential Triage of Transmembrane Segments by Sec61α during Biogenesis of a Native Multispanning Membrane Protein. *Nat. Struct. Mol. Biol.* 12, 870–878. doi:10.1038/nsmb994

Saurí, A., McCormick, P. J., Johnson, A. E., and Mingarro, I. (2007). Sec61α and TRAM Are Sequentially Adjacent to a Nascent Viral Membrane Protein during its ER Integration. *J. Mol. Biol.* 366, 366–374. doi:10.1016/j.jmb.2006.11.052

Savitz, A. J., and Meyer, D. I. (1993). 180-kD Ribosome Receptor Is Essential for Both Ribosome Binding and Protein Translocation. *J. Cell. Biol.* 120, 853–863. doi:10.1083/jcb.120.4.853

Savitz, A. J., and Meyer, D. I. (1990). Identification of a Ribosome Receptor in the Rough Endoplasmic Reticulum. *Nature* 346, 540–544. doi:10.1038/346540a0

Schäuble, N., Lang, S., Jung, M., Cappel, S., Schorr, S., Ulucan, Ö., et al. (2012). BiP-mediated Closing of the Sec61 Channel Limits Ca2+leakage from the ER. *EMBO J.* 31, 3282–3296. doi:10.1038/emboj.2012.189

Schibich, D., Gloge, F., Pöhner, I., Björkholm, P., Wade, R. C., von Heijne, G., et al. (2016). Global Profiling of SRP Interaction with Nascent Polypeptides. *Nature* 536, 219–223. doi:10.1038/nature19070

Schlenstedt, G., Gudmundsson, G. H., Boman, H. G., and Zimmermann, R. (1990). A Large Presecretory Protein Translocates Both Cotranslationally, Using Signal Recognition Particle and Ribosome, and Post-translationally, without These Ribonucleoparticles, when Synthesized in the Presence of Mammalian Microsomes. *J. Biol. Chem.* 265, 13960–13968. doi:10.1016/s0021-9258(18)77442-5

Schlenstedt, G., and Zimmermann, R. (1987). Import of Frog Prepropeptide GLa into Microsomes Requires ATP but Does Not Involve Docking Protein or Ribosomes. *EMBO J.* 6, 699–703. doi:10.1002/j.1460-2075.1987.tb04810.x

Schmidt, F., Dietrich, D., Eylenstein, R., Groemping, Y., Stehle, T., and Dodt, G. (2012). The Role of Conserved PEX3 Regions in PEX19-Binding and Peroxisome Biogenesis. *Traffic* 13, 1244–1260. doi:10.1111/j.1600-0854-2012.01380.x10.1111/j.1600-0854.2012.01380.x

Schorr, S., Klein, M.-C., Gamayun, I., Melnyk, A., Jung, M., Schäuble, N., et al. (2015). Co-chaperone Specificity in Gating of the Polypeptide Conducting Channel in the Membrane of the Human Endoplasmic Reticulum. *J. Biol. Chem.* 290, 18621–18635. doi:10.1074/jbc.M115.636639

Schorr, S., Nguyen, D., Haßdenteufel, S., Nagaraj, N., Cavalié, A., Greiner, M., et al. (2020). Identification of Signal Peptide Features for Substrate Specificity in Human Sec62/Sec63-dependent ER Protein Import. *Febs J.* 287, 4612–4640. doi:10.1111/febs.15274

Schrul, B., and Kopito, R. R. (2016). Peroxin-dependent Targeting of a Lipid-Droplet-Destined Membrane Protein to ER Subdomains. *Nat. Cell. Biol.* 18, 740–751. doi:10.1038/ncb3373

Schrul, B., and Schliebs, W. (2018). Intracellular Communication between Lipid Droplets and Peroxisomes: the Janus Face of PEX19. *Biol. Chem.* 399, 741–749. doi:10.1515/hsz-2018-0125

Schubert, D., Klein, M.-C., Hassdenteufel, S., Caballero-Oteyza, A., Yang, L., Proietti, M., et al. (2018). Plasma Cell Deficiency in Human Subjects with Heterozygous Mutations in Sec61 Translocon Alpha 1 Subunit (SEC61A1). *J. Allergy Clin. Immunol.* 141, 1427–1438. doi:10.1016/j.jaci.2017.06.042

Schuldiner, M., Metz, J., Schmid, V., Denic, V., Rakwalska, M., Schmitt, H. D., et al. (2008). The GET Complex Mediates Insertion of Tail-Anchored Proteins into the ER Membrane. *Cell.* 134, 634–645. doi:10.1016/j.cell.2008.06.025

Seiser, R. M., and Nicchitta, C. V. (2000). The Fate of Membrane-Bound Ribosomes Following the Termination of Protein Synthesis. *J. Biol. Chem.* 275, 33820–33827. doi:10.1074/jbc.M004462200

Shaffer, K. L., Sharma, A., Snapp, E. L., and Hegde, R. S. (2005). Regulation of Protein Compartmentalization Expands the Diversity of Protein Function. *Dev. Cell.* 9, 545–554. doi:10.1016/j.devcel.2005.09.001

Shao, S., and Hegde, R. S. (2011). A Calmodulin-dependent Translocation Pathway for Small Secretory Proteins. *Cell.* 147, 1576–1588. doi:10.1016/j.cell.2011.11.048

Shibata, Y., Shemesh, T., Prinz, W. A., Palazzo, A. F., Kozlov, M. M., and Rapoport, T. A. (2010). Mechanisms Determining the Morphology of the Peripheral ER. *Cell.* 143, 774–788. doi:10.1016/j.cell.2010.11.007

Shibata, Y., Voeltz, G. K., and Rapoport, T. A. (2006). Rough Sheets and Smooth Tubules. *Cell.* 126, 435–439. doi:10.1016/j.cell.2006.07.019

Shurtleff, M. J., Itzhak, D. N., Hussmann, J. A., Schirle Oakdale, N. T., Costa, E. A., Jonikas, M., et al. (2018). The ER Membrane Protein Complex Interacts Cotranslationally to Enable Biogenesis of Multipass Membrane Proteins. *eLife* 7, e37018. doi:10.7554/eLife.37018

Sicking, M., Jung, M., and Lang, S. (2021b). Lights, Camera, Interaction: Studying Protein-Protein Interactions of the ER Protein Translocase in Living Cells. *Ijms* 22, 10358. doi:10.3390/ijms221910358

Sicking, M., Lang, S., Bochen, F., Roos, A., Drenth, J. P. H., Zakaria, M., et al. (2021a). Complexity and Specificity of Sec61-Channelopathies: Human Diseases Affecting Gating of the Sec61 Complex. *Cells* 10, 1036. doi:10.3390/cells10051036

Sicking, M., Živná, M., Bhadra, P., Barešová, V., Tirincsi, A., Hadzibeganovic, D., et al. (2022). Phenylbutyrate Rescues the Transport Defect of the Sec61α Mutations V67G and T185A for Renin. *Life Sci. Alliance* 5, e202101150. doi:10.26508/lsa.202101150

Siegel, V., and Walter, P. (1988). Functional Dissection of the Signal Recognition Particle. *Trends biochem. Sci.* 13, 314–316. doi:10.1016/0968-0004(88)90127-2

Simon, S. M., and Blobel, G. (1991). A Protein-Conducting Channel in the Endoplasmic Reticulum. *Cell.* 65, 371–380. doi:10.1016/0092-8674(91)90455-8

Skowronek, M. H., Rotter, M., and Haas, I. G. (1999). Molecular Characterization of a Novel Mammalian DnaJ-like Sec63p Homolog. *Biol. Chem.* 380, 1133–1138. doi:10.1515/bc.1999.142

Snapp, E. L., Reinhart, G. A., Bogert, B. A., Lippincott-Schwartz, J., and Hegde, R. S. (2004). The Organization of Engaged and Quiescent Translocons in the Endoplasmic Reticulum of Mammalian Cells. *J. Cell. Biol.* 164, 997–1007. doi:10.1083/jcb.200312079

Sommer, N., Junne, T., Kalies, K.-U., Spiess, M., and Hartmann, E. (2013). TRAP Assists Membrane Protein Topogenesis at the Mammalian ER Membrane. *Biochimica Biophysica Acta (BBA) - Mol. Cell. Res.* 1833, 3104–3111. doi:10.1016/j.bbamcr.2013.08.018

Song, J., Mizrak, A., Lee, C.-W., Cicconet, M., Li, Z. W., Lu, C.-H., et al. (2021). Identification of Two Pathways Mediating Protein Targeting from ER to Lipid Droplets. *bioRxiv*. doi:10.1101/2021.09.14.460330

Stefanonvic, B., Stefanovic, L., Schnabl, B., Bataller, R., and Brenner, D. A. (2004). TRAM2 Protein Interacts With Endoplasmic Reticulum Ca2+ Pump Serca2b and is Necessary for Collagen Type I Synthesis. *Mol. Cell. Biol.* 24 (3), 1758–1768.

Tajima, S., Lauffer, L., Rath, V. L., and Walter, P. (1986). The Signal Recognition Particle Receptor Is a Complex that Contains Two Distinct Polypeptide Chains. *J. Cell. Biol.* 103, 1167–1178. doi:10.1083/jcb.103.4.1167

Talbot, B. E., Vandorpe, D. H., Stotter, B. R., Alper, S. L., and Schlondorff, J. (2019). Transmembrane Insertases and N-Glycosylation Crtically Determine Synthesis, Trafficking, and Activity of the Nonselective Cation Channel TRPC6. *J. Biol. Chem.* 294, 12655–12669. doi:10.1074/jbc.RA119.008299

Tazawa, S., Unuma, M., Tondokoro, N., Asano, Y., Ohsumi, T., Ichimura, T., et al. (1991). Identification of a Membrane Protein Responsible for Ribosome Binding in Rough Microsomal Membranes. *J. Biochem.* 109, 89–98.

Tian, S., Wu, Q., Zhou, B., Choi, M. Y., Ding, B., Yang, W., et al. (2019). Proteomic Analysis Indentifies Membrane Proteins Dependent on the ER Membrane Protein Complex. *Cell. Rep.* 28, 2517–2526. doi:10.1016/j.celrep.2019.08.006

Tirincsi, A., O`Keefe, S., Nguyen, D., Sicking, M., Dudek, J., Förster, F., et al. (2022b). Proteomics Identifies Substrates and a Novel Component in hSND2-dependent ER Protein Targeting. *bioRxiv*. preprint. doi:10.1101/2022.04.27.489649

Tirincsi, A., Sicking, M., Hadzibeganovic, D., Haßdenteufel, S., and Lang, S. (2022a). The Molecular Biodiversity of Protein Targeting and Protein Transport Related to the Mammalian Endoplasmic Reticulum. *Int. J. Mol. Sci.* 23, 143. doi:10.3390/ijms23010143

Trueman, S. F., Mandon, E. C., and Gilmore, R. (2011). Translocation Channel Gating Kinetics Balances Protein Translocation Efficiency with Signal Sequence Recognition Fidelity. *Mol. Biol. Cell.* 22, 2983–2993. doi:10.1091/mbc.E11-01-0070

Tyanova, S., Temu, T., Sinitcyn, P., Carlson, A., Hein, M. Y., Geiger, T., et al. (2016). The Perseus Computational Platform for Comprehensive Analysis of Proteomics Data. *Nat. Meth* 13, 731–740. doi:10.1038/nmeth.3901

Tyedmers, J., Lerner, M., Bies, C., Dudek, J., Skowronek, M. H., Haas, I. G., et al. (2000). Homologs of the Yeast Sec Complex Subunits Sec62p and Sec63p Are Abundant Proteins in Dog Pancreas Microsomes. *Proc. Natl. Acad. Sci. U. S. A.* 97, 7214–7219. doi:10.1073/pnas.97.13.7214

Tyedmers, J., Lerner, M., Wiedmann, M., Volkmer, J., and Zimmermann, R. (2005). Polypeptide Chain Binding Proteins Mediate Completion of Cotranslational Protein Translocation into the Mammalian Endoplasmic Reticulum. *EMBO Rep.* 4, 505–510. doi:10.1038/sj.embor.embor826

Ueno, T., Kaneko, K., Sata, T., Hattori, S., and Ogawa-Goto, K. (2011). Regulation of Polysome Assembly on the Endoplasmic Reticulum by a Coiled-Coil Protein, P180. *Nucleic Acids Res.* 40, 3006–3017. doi:10.1093/nar/gkr1197

Ueno, T., Tanaka, K., Kaneko, K., Taga, Y., Sata, T., Irie, S., et al. (2010). Enhancement of Procollagen Biosynthesis by P180 through Augmented Ribosome Association on the Endoplasmic Reticulum in Response to Stimulated Secretion. *J. Biol. Chem.* 285, 29942–29950. doi:10.1074/jbc.M109.094607

Valm, A. M., Cohen, S., Legant, W. R., Melunis, J., Hershberg, U., Wait, E., et al. (2017). Applying Systems-Level Spectral Imaging and Analysis to Reveal the Organelle Interactome. *Nature* 546, 162–167. doi:10.1038/nature22369

Van den Berg, B., Clemons, W. M., Collinson, I., Modis, Y., Hartmann, E., Harrison, S. C., et al. (2004). X-ray Structure of a Protein-Conducting Channel. *Nature* 427, 36–44. doi:10.1038/nature02218

Van Nieuwenhove, E., Barber, J., Smeets, E., Neumann, J., Willemsen, M., Pasciuto, E., et al. (2020). Defective Sec61α1 Underlies a Novel Cause of Autosomal Dominant Severe Congenital Neutropenia. *J. Allergy Clin. Immunol.* 146, 1180–1192. doi:10.1016/j.jaci.2020.03.034

Voigt, F., Zhang, H., Cui, X. A., Triebold, D., Liu, A. X., Eglinger, J., et al. (2017). Single-molecule Quantification of Translation-dependent Association of mRNAs with the Endoplasmic Reticulum. *Cell. Rep.* 21, 3740–3753. doi:10.1016/j.celrep.2017.12.008

Voigt, S., Jungnickel, B., Hartmann, E., and Rapoport, T. A. (1996). Signal Sequence-dependent Function of the TRAM Protein during Early Phases of Protein Transport across the Endoplasmic Reticulum Membrane. *J. Cell. Biol.* 134, 25–35. doi:10.1083/jcb.134.1.25

von Heijne, G., and Gavel, Y. (1988). Topogenic Signals in Integral Membrane Proteins. *Eur. J. Biochem.* 174, 671–678. doi:10.1111/j.1432-1033.1988.tb14150.x

von Heijne, G. (1985). Signal Sequences. *J. Mol. Biol.* 184, 99–105. doi:10.1016/0022-2836(85)90046-4

von Heijne, G. (1986). Towards a Comparative Anatomy of N-Terminal Topogenic Protein Sequences. *J. Mol. Biol.* 189, 239–242. doi:10.1016/0022-2836(86)90394-3

Voorhees, R. M., and Hegde, R. S. (2016). Structure of the Sec61 Channel Opened by a Signal Peptide. *Science* 351, 88–91. doi:10.1126/science.aad4992

Voorhees, R. M., Fernández, I. S., Scheres, S. H. W., and Hegde, R. S. (2014). Structure of the Mammalian Ribosome-Sec61 Complex to 3.4 Å Resolution. *Cell.* 157, 1632–1643. doi:10.1016/j.cell.2014.05.024

Wada, I., Rindress, D., Cameron, P. H., Ou, W.-J., Doherty, J. J., Louvard, D., et al. (1991). SSR α and Associated Calnexin Are Major Calcium Binding Proteins of the Endoplasmic Reticulum Membrane. *J. Biol. Chem.* 266, 19599–19610. doi:10.1016/s0021-9258(18)55036-5

Wang, Q.-C., Zheng, Q., Tan, H., Zhang, B., Li, X., Yang, Y., et al. (2016). TMCO1 Is an ER Ca^{2+} Load-Activated Ca^{2+} Channel. *Cell.* 165, 1454–1466. doi:10.1016/j.cell.2016.04.051

Weng, T.-H., Steinchen, W., Beatrix, B., Berninghausen, O., Becker, T., Bange, G., et al. (2021). Architecture of the Active Post-translational SEC Translocon. *EMBO J.* 40, e105643. doi:10.15252/embj.2020105643

Westrate, L. M., Lee, J. E., Prinz, W. A., and Voeltz, G. K. (2015). Form Follows Function: The Importance of Endoplasmic Reticulum Shape. *Annu. Rev. Biochem.* 84, 791–811. doi:10.1146/annurev-biochem-072711-163501

Whitely, P., Grau, B., Gumbart, J. C., Martinez-Gil, L., and Mingarro, I. (2021). Folding and Insertion of Transmembrane Helices at the ER. *Int. J. Mol. Sci.* 22, 9655. doi:10.3390/ijms22179655

Wiedmann, B., Saki, H., Davis, T. A., and Wiedmann, M. (1994). A Protein Complex Required for Signal-sequence-specific Sorting and Translocation. *Nature* 370, 434–440. doi:10.1038/370434a0

Wiedmann, M., Kurzchalia, T. V., Hartmann, E., and Rapoport, T. A. (1987). A Signal Sequence Receptor in the Endoplasmic Reticulum Membrane. *Nature* 328, 830–833. doi:10.1038/328830a0

Wilson, M. P., Durin, Z., Unal, Ö., Ng, B. G., Marrecau, T., Keldermans, L., et al. (2022). CAMLG-CDG: a Novel Congenital Disorder of Glycosylation Linked to Defective Membrane Trafficking. *Hum. Mol. Genet.* Advance online publication. doi:10.1093/hmg/ddac055

Wirth, A., Jung, M., Bies, C., Frien, M., Tyedmers, J., Zimmermann, R., et al. (2003). The Sec61p Complex Is a Dynamic Precursor Activated Channel. *Mol. Cell.* 12, 261–268. doi:10.1016/s1097-2756(03)00281-110.1016/s1097-2765(03)00283-1

Wu, X., Cabanos, C., and Rapoport, T. A. (2019). Structure of the Post-translational Protein Translocation Machinery of the ER Membrane. *Nature* 566, 136–139. doi:10.1038/s41586-018-0856-x

Yamamoto, Y., and Sakisaka, T. (2012). Molecular Machinery for Insertion of Tail-Anchored Membrane Proteins into the Endoplasmic Reticulum Membrane in Mammalian Cells. *Mol. Cell.* 48, 387–397. doi:10.1016/j.molcel.2012.08.028

Yamamoto, Y., and Sakisaka, T. (2018). The Peroxisome Biogenesis Factors Posttranslationally Target Reticulon Homology-Domain Containing Proteins

to the Endoplasmic Reticulum Membrane. *Sci. Rep.* 8, 2322. doi:10.1038/s41598-018-20797-0

Yang, J., Hirata, T., Liu, Yi-S., Guo, X.-Y., Gao, X.-D., Kinoshita, T., et al. (2021). Human SND2 Mediates ER Targeting of GPI-Anchored Proteins with Low Hydrophobic GPI Attachment Signals. *FEBS Lett.* 595, 1542–1558. doi:10.1002/1873-3468.14083

Zhang, B., and Miller, T. F., III (2012). Long-timescale Dynamics and Regulation of Sec-Facilitated Protein Translocation. *Cell. Rep.* 2, 927–937. doi:10.1016/j.celrep.2012.08.039

Zimmermann, R., Lang, S., Lerner, M., Förster, F., Nguyen, D., Helms, V., et al. (2021). Quantitative Proteomics and Differential Protein Abundance Ananalysis after Depletion of PEX3 from Human Cells Identifies Additional Aspects of Protein Targeting Tot He ER. *Int. J. Mol. Sci.* 22, 13028. doi:10.3390/ijms222313028

Ziska, A., Tatzelt, J., Dudek, J., Paton, A. W., Paton, J. C., Zimmermann, R., et al. (2019). The Signal Peptide Plus a Cluster of Positive Charges in Prion Protein Dictate Chaperone-Mediated Sec61-Channel Gating. *Biol. Open* 8, bio040691. doi:10.1242/bio.040691

Conflict of Interest: The authors declare that the research was conducted in the absence of any commercial or financial relationships that could be construed as a potential conflict of interest.

Publisher's Note: All claims expressed in this article are solely those of the authors and do not necessarily represent those of their affiliated organizations, or those of the publisher, the editors and the reviewers. Any product that may be evaluated in this article, or claim that may be made by its manufacturer, is not guaranteed or endorsed by the publisher.

frontiers | Frontiers in Physiology

REVIEW
published: 26 July 2022
doi: 10.3389/fphys.2022.933153

Bacterial Signal Peptides- Navigating the Journey of Proteins

*Sharbani Kaushik, Haoze He and Ross E. Dalbey**

Department of Chemistry and Biochemistry, The Ohio State University, Columbus, OH, United States

In 1971, Blobel proposed the first statement of the Signal Hypothesis which suggested that proteins have amino-terminal sequences that dictate their export and localization in the cell. A cytosolic binding factor was predicted, and later the protein conducting channel was discovered that was proposed in 1975 to align with the large ribosomal tunnel. The 1975 Signal Hypothesis also predicted that proteins targeted to different intracellular membranes would possess distinct signals and integral membrane proteins contained uncleaved signal sequences which initiate translocation of the polypeptide chain. This review summarizes the central role that the signal peptides play as address codes for proteins, their decisive role as targeting factors for delivery to the membrane and their function to activate the translocation machinery for export and membrane protein insertion. After shedding light on the navigation of proteins, the importance of removal of signal peptide and their degradation are addressed. Furthermore, the emerging work on signal peptidases as novel targets for antibiotic development is described.

Keywords: SecYEG translocase, SecA, signal peptide, protein transport, YidC, Tat pathway, signal peptidase, antibiotic targets

OPEN ACCESS

Edited by:
Inhwan Hwang,
Pohang University of Science and Technology, South Korea

Reviewed by:
Dong Wook Lee,
Chonnam National University, South Korea
Zhengyi Xu,
Northeast Normal University, China

****Correspondence:***
Ross E. Dalbey
dalbey@chemistry.ohio-state.edu

Specialty section:
This article was submitted to Membrane Physiology and Membrane Biophysics, a section of the journal Frontiers in Physiology

Received: *30 April 2022*
Accepted: *21 June 2022*
Published: *26 July 2022*

Citation:
Kaushik S, He H and Dalbey RE (2022) Bacterial Signal Peptides- Navigating the Journey of Proteins. Front. Physiol. 13:933153. doi: 10.3389/fphys.2022.933153

1 INTRODUCTION

The transport of proteins across cell membranes is fundamentally significant to many biological processes. Protein export also finds a special interest in biotechnology for production of hormones/enzymes and recombinant proteins, in laboratory techniques and disease diagnosis. Considerable progress has been made during the last several decades in understanding the characteristics of the folded state of substrates during translocation in the cytosol, membrane targeting, the structure and function of translocation devices, the insertion of membrane proteins into the lipid bilayer, and the role of energy in protein export. Insight into these fundamental concepts is highly appreciated and anticipated by scientists in the protein export field.

Protein integration and transport across the membranes are ubiquitous in every organism. Typically, these proteins are synthesized with a stretch of amino acids called the "signal peptide" that can be recognized by the cytosolic proteins for sorting and then targeting to the membrane. After being transferred to the translocation machinery, the proteins are membrane inserted or translocated across the membrane. In the final step, the signal peptide is proteolytically removed from the exported protein by signal peptidase.

The signal peptide plays center stage in this export process with a myriad of functions (Hegde and Bernstein, 2006). The signal peptides can bind to chaperones to prevent premature folding of the protein in the cytosol. In addition to slowing down the folding of a mature domain of a preprotein, signal peptides act as a zip code for sorting the proteins from the cytosol to the membrane. Finally, the signal peptide activates the translocation machinery, initiating the translocation process.

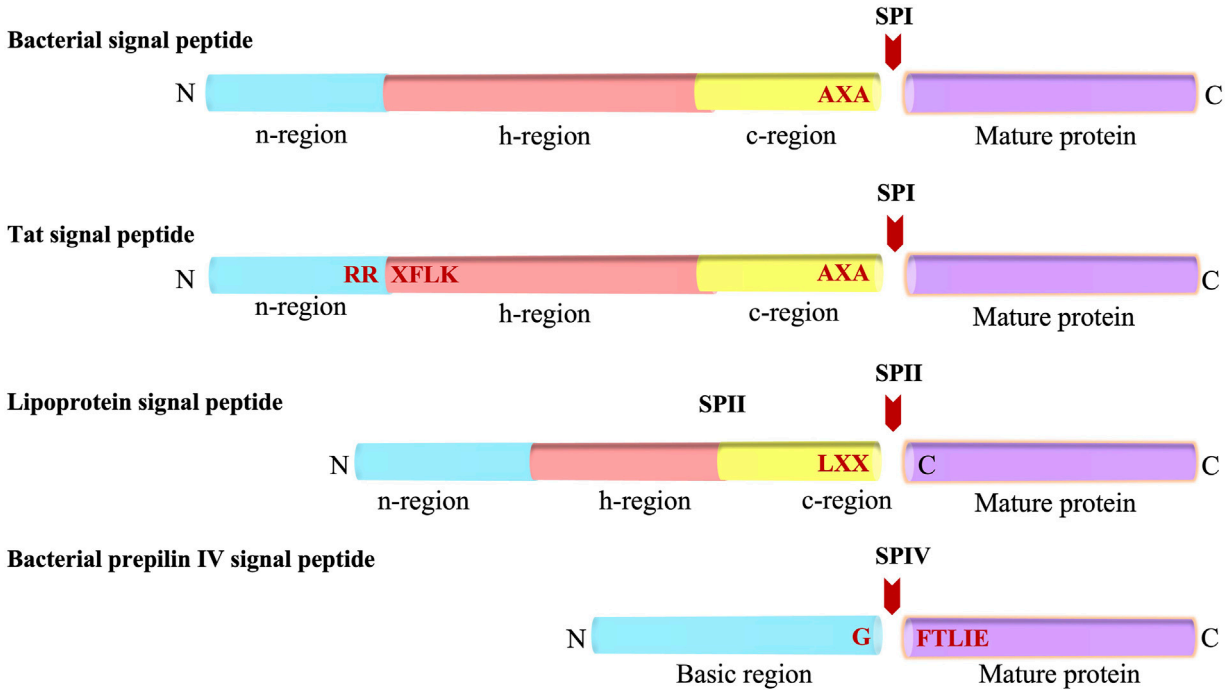

FIGURE 1 | Bacterial Signal peptides. Schematic representations of the Sec-type signal peptide, the twin-arginine (Tat) signal peptide, the lipoprotein signal peptide, and the prepilin signal peptide. The various regions of the signal peptides (n, h, c and basic regions) are indicated. The SP cleavage site is represented with a red arrow. N and C indicates amino and carboxyl-terminus, respectively.

This review highlights the function of signal peptides in Gram-negative bacteria in protein sorting and targeting to the inner membrane, and translocation across the membrane and insertion. After navigating the journey of proteins, their removal and degradation are discussed. Furthermore, the potential of the signal peptidases (endopeptidases which remove signal peptides) as antibacterial targets will be covered.

2 SIGNAL PEPTIDES

Most exported proteins in bacteria are transported across the inner membrane by the general secretion (Sec) pathway or the Twin arginine translocation (Tat) system or the simple membrane protein insertase YidC [reviewed in (Crane and Randall, 2017; Frain et al., 2019; Shanmugam and Dalbey, 2019; Oswald et al., 2021)]. The targeting of the preproteins to these pathways are dependent on the pathway selective for the respective signal peptide. These are the Sec signal peptide, the lipoprotein signal peptide, the Tat signal peptide and the prepilin signal peptide. Below we describe the properties of each of these signal peptides.

The Sec signal peptide targets the protein to the Sec machinery and is composed of three regions (**Figure 1**) (von Heijne and Abrahmsèn, 1989; Perlman and Halvorson, 1983; von Heijne, 1986a): 1) a positively charged N-terminal region (n), 2) a central hydrophobic region (h) and, 3) a rather polar C-terminal region which contains small amino acid residues at positions -1 and -3 (with respect to the cleavage site). Additionally, a helix breaking residue is often found at the -4 to -6 positions of the C-terminal region (von Heijne, 1986a). Genetic and mutagenesis studies have shown that the apolar region of the signal peptide is essential for the function of a cleavable signal peptide (Emr et al., 1978; Bassford and Beckwith, 1979; Michaelis and Beckwith, 1982). Moreover, the basic amino terminus can be important for making translocation more efficient (Vlasuk et al., 1983; Iino et al., 1987).

Similar to the Sec signal peptide, the lipoprotein signal peptide which is processed by signal peptidase 2 (SPase II, lipoprotein signal peptidase) has a positively charged n region and a hydrophobic central region (h region) (**Figure 1**). The main difference between Sec and lipoprotein signal sequences is that the c region of the lipoprotein contains the lipobox motif comprised of Leu-Ala/Ser-Gly/Ala-Cysteine at the −3 to +1 position (Sankaran and Wu, 1994). The lipobox motif is a structural determinant for lipid modification of the strictly conserved Cys at the +1 position of the mature domain that gets modified by diacylglyceride. The glyceride fatty acid lipid is attached by a preprolipoprotein diacylglycerol transferase (Lgt), prior to cleavage by SPase II (Sankaran and Wu, 1994). In Gram-negative and some Gram-positive bacteria, most lipoproteins are further modified by an acyl chain by N-acyl transferase (Lnt) after SPase II cleavage (Gupta and Wu, 1991). Analysis of the signal sequences have shown that the h regions are shorter for lipoprotein signal peptides as compared to that

present in the Sec signal peptides (Klein et al., 1988; von Heijne, 1989; Tjalsma et al., 2000).

The Tat signal peptide targets proteins to the Tat machinery and has a tripartite arrangement similar to the Sec signal peptide (**Figure 1**). It was initially discovered in chloroplast in exported proteins transported into the thylakoid lumen independently of ATP hydrolysis. Later, Berks and others observed it in cofactor containing periplasmic proteins of bacteria (Chaddock et al., 1995; Berks, 1996; Bogsch et al., 1998; Sargent et al., 1998; Weiner et al., 1998). The "Tat" signal peptide takes its name from the invariant and essential twin arginines in the n-region of the signal peptide. The motif for Tat signal peptides is RRXFLK where X can be any residue and F, L and K are quite commonly found. Mutagenesis of the twin arginines even to a lysine pair can abolish or significantly reduce transport although single mutations of the arginines are largely tolerated (Stanley et al., 2000; Buchanan et al., 2001; DeLisa et al., 2002). Typically, the Tat signal peptides are longer than the Sec signal peptides, and the h-region is less hydrophobic than that present in the Sec signal peptides (Cristobal et al., 1999). Moreover, there is often a basic residue in the c-region that functions as a Sec avoidance sequence (Bogsch et al., 1997). While most of the Tat preproteins are processed by signal peptidase 1 (SPase I) (Lüke et al., 2009), some contain a lipobox and are therefore processed by SPase II.

A specialized signal peptide called the prepilin signal peptide is found on the type 4 pilus proteins. Similar to the Sec and most lipoprotein signal peptides, it targets the protein to the Sec machinery. Type 4 substrates are found on the surface of many Gram-negative bacteria such as *Pseudomonas aeruginosa* and *Neisseria gonorrhoeae*. Pilin subunits allow the bacteria to stick to the surface of the host epithelial cells during infection. The prepilin signal peptide is unique as it is cleaved at the border of the n-h region (Strom and Lory, 1993; Mattick, 2002). The processing is carried out by prepilin signal peptidase, which recognizes the GFTLIE motif and cleaves after the glycine (Nunn and Lory, 1991). After cleavage, the prepilin signal peptidase methylates the amino terminus of the mature pilin (Strom et al., 1993). This generates N-methylphenylalanine as the first amino acid of the mature pilin.

In addition to these cleavable signal peptides, uncleaved signal peptides containing a longer hydrophobic stretch target proteins to the translocation machinery but remain as a membrane anchor sequence. These uncleavable signal peptides are found in membrane proteins which span the bacterial inner membrane as an α-helix. These domains are enriched in hydrophobic residues such as Ala, Ile, Leu, and Val but mostly void of charged residues (von Heijne, 2006). The uncleaved signals can span the membrane in different orientations, dictated by the positive inside rule (von Heijne, 1986b; von Heijne, 1999). If there are positive charges preceding the hydrophobic stretch, then the transmembrane (TM) segment is oriented with the C-terminus facing the periplasm whereas if the hydrophobic stretches are followed by positively charged residues, then the amino-terminus of the TM segment is localized to the cytoplasm. The positive inside rule is based on the finding that the membrane proteins have cytoplasmic loops that are enriched in positively charged residues (Lys, Arg) as compared to the periplasmic/translocated loops (von Heijne, 1986b).

2.1 Signal Peptide Targeting to the Membrane

Targeting of exported and membrane proteins is initiated early on after the amino terminus of the nascent protein emerges from the ribosomal exit channel (**Figure 2**). The targeting pathway is decided by the interaction of the nascent protein with the ribosome-bound chaperones and targeting factors such as the Trigger Factor (TF) (Hoffmann et al., 2010; Castanié-Cornet et al., 2014), the signal recognition particle (SRP) (Grudnik et al., 2009; Akopian et al., 2013; Saraogi and Shan, 2014) and SecA (the ATPase motor of the Sec translocation machinery) in some cases (Kusters and Driessen, 2011; Chatzi et al., 2014). These chaperones and targeting factors facilitate the localization to the inner membrane of bacteria.

In Gram-negative bacteria, the exported proteins are typically targeted to the Sec complex or the Tat translocase by the post-translational mechanism (**Figure 2**). Exported proteins which employ the Sec pathway contain moderately hydrophobic signal sequences and are transported through the Sec channel in a largely unfolded state. In contrast, the Tat substrates are translocated in the folded state after release of the protein from the ribosome and hence post-translational. Typically, the integral membrane proteins are targeted co-translationally either to the Sec machinery or the YidC insertase as soon as the hydrophobic TM segment emerges from the ribosomal tunnel.

2.1.1 Targeting of Exported Proteins

2.1.1.1 Sec Proteins

In the post-translational pathway, the TF is bound to the ribosome over the exit channel shielding the nascent chains from proteases (**Figure 2**) (Ferbitz et al., 2004). The ribosome-bound TF provides a protective environment preventing the premature folding and aggregation of the growing protein chain. Ribosome profiling studies have shown that the TF binds to the nascent chain only after approximately 100 amino acids are synthesized and play a role for the biogenesis of many β-barrel outer membrane proteins (Oh et al., 2011). After the protein is released from the ribosome, some proteins can form a complex with SecB (Kumamoto and Francetić, 1993), a dedicated molecular chaperone for export in bacteria. SecB is a tetramer (Xu et al., 2000) and how it keeps proteins in a non-native loosely-folded form (Randall and Hardy, 1986) is an intriguing mechanistic question. Recently, a state-of-the-art NMR study revealed that an unfolded preprotein wraps around the SecB. This is achieved by binding to the long hydrophobic grooves of SecB that run around the tetramer (Huang et al., 2016). The SecB delivers the preprotein to SecA bound to SecYEG at the membrane (Hartl et al., 1990). The targeting of the preprotein to SecA is achieved by SecA acting as a receptor that binds the signal peptide (Gelis et al., 2007) and the chaperone SecB (Zhou and Xu, 2003).

In an alternative scenario, cytosolic SecA can interact with the nascent chains emerging from the ribosome (**Figure 2**).

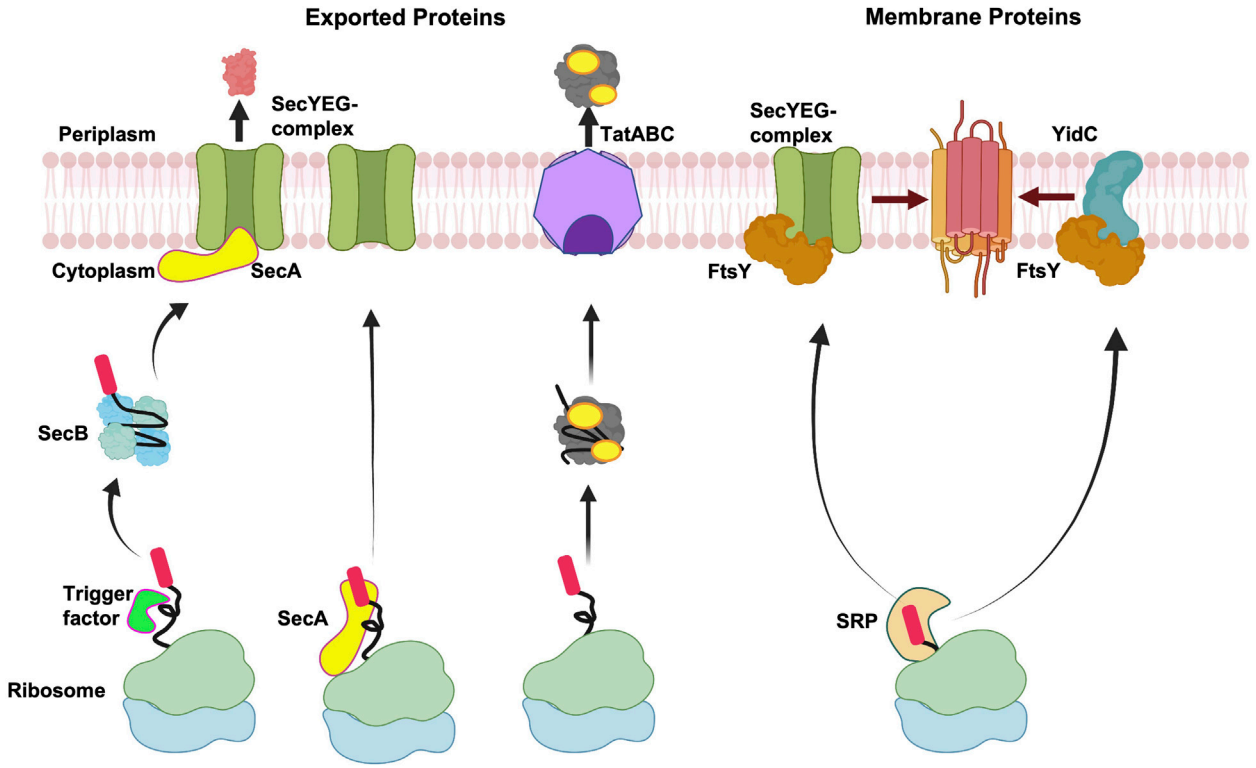

FIGURE 2 | Membrane targeting pathways. Overview of targeting of exported proteins and membrane proteins. After exported proteins are released from the ribosome, Sec-dependent proteins can be stabilized by the molecular chaperone SecB in an unfolded state and then targeted to SecA at the membrane, followed by translocation by the SecYEG complex. Alternatively, SecA can interact with the ribosome bound nascent chain and target the exported protein to the SecYEG complex. In case of Tat complex, the proteins fold in the cytoplasm before being exported by the Tat complex. In the event of co-translational targeting, the nascent membrane proteins form a complex with SRP, which target proteins to FtsY (SRP receptor) for membrane insertion either by the SecYEG complex or the YidC insertase. Created with BioRender.com.

Indeed, previous studies had suggested that SecA interacts with the nascent chains (Chun and Randall, 1994; Karamyshev and Johnson, 2005). In more recent studies, SecA was shown to interact with the ribosome near the ribosome exit channel (Huber et al., 2011). The binding of SecA to the ribosome is mediated by the ribosomal protein, L23. This interaction is important since mutations in L23 perturb SecA ribosome binding, significantly affecting the post-translational export of proteins *in vivo* (Huber et al., 2011). The isolation of mRNAs that copurify with SecA revealed that they encode both Sec exported and membrane proteins (Huber et al., 2017). The interaction of SecA with the nascent protein chains occurs only when the chains are longer than 110 residues. The interaction of SecA with the nascent chains is not dependent on TF or SecB. Notably, the authors found that SecB interaction with the nascent chains depended on SecA being bound to the nascent chains, suggesting that SecA interacts with a subset of SecB dependent substrates co-translationally (Huber et al., 2017). The emerging data suggests that SecA bound nascent chains can target proteins directly to the SecYEG complex or with the help of SecB (**Figure 2**). However, it is uncertain if the interaction of SecA with all SecA-dependent substrates occurs co-translationally.

In some cases, the preprotein is released from the ribosome with the TF still bound (not shown in **Figure 2**). *In vitro,* TF has been shown to form a stable 1 to 1 complex with proOmpA (Crooke et al., 1988), making proOmpA translocation competent. The TF functions as a holdase and foldase to bind its substrate in an unfolded state (Hoffmann et al., 2010). Saio et al. (2014) characterized the binding of the TF to the unfolded precursor of alkaline phosphatase (pre-PhoA) by NMR. With the help of multiple binding pockets, the TF engages with the nascent polypeptide and shields the emerging hydrophobic regions of pre-PhoA in solvent to prevent it from premature folding and aggregation. De Geyter et al. (2020) showed that the TF is a genuine export chaperone. Notably, they revealed that the TF bound preprotein can associate with the SecB, which then recruits SecA through its C-tail and promotes the transfer of the preprotein to SecA.

2.1.1.2 Tat Proteins

A different post-translational mechanism is used for targeting of Tat proteins to the inner membrane (**Figure 2**). These Tat proteins need to be folded in the cytoplasm prior to their translocation across the membrane (Palmer and Stansfeld, 2020). Many of the known substrates of the Tat pathway in

bacteria bind a variety of redox cofactors, including molybdopterin centers and FeS cluster. There are specialized chaperones termed REMP (redox enzyme maturation proteins) to mediate cofactor insertion and proof reading (Turner et al., 2004; Robinson et al., 2011). For example, TorD is a REMP for TorA that encodes Trimethylamine-N-Oxide Reductase. TorD facilitates cofactor insertion and protects the TorA signal peptide from proteases (Ilbert et al., 2003) enabling the TorA to be delivered correctly to the Tat translocase (Jack et al., 2004). Another REMP is the DmsD that is involved in the biogenesis of dimethyl sulphoxide (DMSO) reductase (DmsA) (Ray et al., 2003). DmsD associates with the DmsA signal peptide (Oresnik et al., 2001) and also interacts with the molecular chaperones DnaK, DnaJ, GroE, GroEL, and TF (Li et al., 20101804; Castanié-Cornet et al., 2014). Finally, NapD is a REMP for the nitrate reductase complex localized in the periplasmic space. NapD binds to the Tat signal peptide of NapA (Maillard et al., 2007) and is involved in the insertion of the molybdenum cofactor.

2.1.2 Targeting of Membrane Proteins

For integral membrane proteins the hydrophobic segments in the nascent proteins interact with SRP at the ribosome exit channel and are sorted away from exported proteins that contain less hydrophobic sequences (**Figure 2**) (Lee and Bernstein, 2001). The inference for this comes from ribosome profiling studies examining the mRNAs that are bound to SRP engaged ribosome nascent chains (Schibich et al., 2016). The study revealed 87% of the SRP interactors are membrane proteins and only 6% are periplasmic/outer membrane proteins (Schibich et al., 2016). SRP can scan the ribosome with low affinity even before the nascent chain reaches the exit tunnel and interacts with the ribosomal binding proteins L23 and L29. This is called the stand-by mode (Holtkamp et al., 2012). When the nascent chain of 30–35 amino acids length reaches the exit site, SRP forms a high affinity complex with the translating ribosome and signal peptide (Bornemann et al., 2008; Holtkamp et al., 2012). Soon after forming this high affinity complex, the nascent chain is delivered to its receptor at the membrane (**Figure 2**, right side) to form a quaternary complex. The receptor FtsY (in prokaryotes) then transfers the ribosome nascent chain to the SecYEG complex by a mechanism involving the catalysis of GTPases.

The SRP has also been shown to target membrane proteins to the YidC insertase (Welte et al., 2012) (**Figure 2**). For example, MscL (Facey et al., 2007) and the tail anchored proteins SciP, DjlC, and Flk require both YidC and SRP for membrane protein insertion (Pross et al., 2016; Peschke et al., 2018). Ffh and FtsY can be crosslinked to the cytoplasmic loop of YidC, suggesting that the SRP-YidC nascent chains are targeted to FtsY that is in proximity to the YidC cytoplasmic loop (Petriman et al., 2018). The YidC cytoplasmic loop C2 and the C-tail of YidC binds to the ribosome supporting YidC activity (Geng et al., 2015).

Although the classical model predicts that SRP binds to the TM segment when it is exposed out of the ribosome exit channel, SRP can also interact with the hydrophobic regions that are not a part of the TM segment in some cases. Pross and Kuhn (2020) proved that there are two hydrophobic segments in the amino-terminal part of the C-tailed anchored protein SciP, which are recognized by SRP allowing it to target SciP to YidC . Additionally, in contrast to the classical view, ribosome profiling studies showed that 29% of the SRP interactors skipped interaction with the first TM segment of the membrane protein but were bound to C-terminal TM segments (Schibich et al., 2016). The SRP prefers to bind to ribosomes exposing ~12-17 amino acids enriched in hydrophobic and/or aromatic residues (Ile, Leu, Val, Met, Phe, Tyr, Typ) (Schibich et al., 2016).

In another variation, certain membrane proteins with internal TM segment can be co-translationally targeted to the membrane by SecA (Wang et al., 2017). SecA binds to the ribosome near the exit channel where it can recognize certain membrane proteins. SecA interacts with high specificity with nascent RodZ chains containing a TM segment far from the amino-terminus and targets the protein to the inner membrane (Wang et al., 2017). Previously, Rawat et al. (2015) had shown that SecA drives TM insertion and that Ffh and FtsY were not involved. SecA is sufficient for membrane targeting of RodZ both *in vivo* and *in vitro* (Wang et al., 2017). Interestingly, Knüpffer et al. (2019) found that SecA, just like SRP, deeply inserts into the exit tunnel of the ribosome to make contact with the intra-tunnel loop of L23 (Knüpffer et al., 2019). When the nascent chain is synthesized, SecA withdraws from the tunnel and the SecA bound to the L23 ribosome protein recruits the nascent TM segment. It is intriguing that the SecA amino-terminal amphipathic helix and the ribosomal L23 protein bind the nascent chain TM segment with the TM segment clustered in between, as revealed by Cro-EM studies (Wang et al., 2019). The SecA ribosome nascent chain complex is then targeted to the SecYEG complex, which repositions SecA on the ribosome, allowing the TM segment containing the nascent chain to be handed over to the SecYEG.

2.2 Crossing the Membrane

Once the signal peptide has navigated the transported protein to the membrane, it promotes interaction with the translocation machineries (see below). A vast majority of proteins are translocated by the SecYEG/SecDF system (**Figure 3C**) and SecA (Oliver and Beckwith, 1981; Crane and Randall, 2017; Tsirigotaki et al., 2017; Cranford-Smith and Huber, 2018), whereas the Tat machinery is involved in the export of around 30 proteins in *E. coli* (Berks, 2015; Palmer and Stansfeld, 2020) (**Figure 3A**). As mentioned before, the Tat machinery is radically distinct from the SecA/SecYEG/SecDF system as it can export fully folded proteins.

The SecYEG/SecDF/YidC translocase (**Figure 3C**) plays the principal role for placing membrane proteins in the lipid bilayer with the correct topology (Cymer et al., 2015). Additionally, it functions to translocate hydrophilic domains of membrane proteins across the membrane and allows the hydrophobic regions to integrate into the lipid bilayer. The YidC insertase on its own or in cooperation with the Sec translocase can insert membrane proteins (Kiefer and Kuhn, 2018) (**Figures 3B,C**). The Tat machinery can act as insertase for the membrane proteins with C-terminal TM segments (Palmer and Stansfeld, 2020).

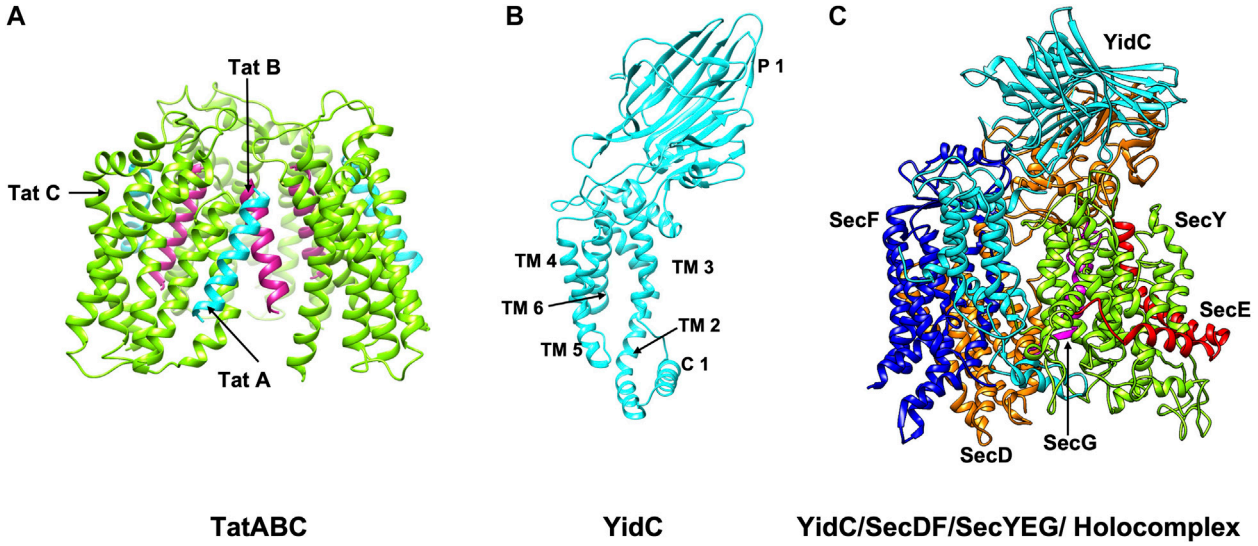

FIGURE 3 | The structures/models of the bacterial export and insertion machineries. Export of proteins across the membrane are catalyzed by **(A)** the Tat complex (resting complex shown) in a folded state (left side) (Habersetzer et al., 2017) or **(C)** by SecYEG/SecDF/YidC [adapted from Botte et al. (2016) PDB: 5MG3] energized by the SecA motor ATPase (not shown) in an unfolded state. TatA, TatB and TatC is shown in cyan, magenta and green, respectively. SecY, SecE, and SecG is shown in green, red, and magenta; SecD, SecF and YidC are shown in orange, blue and cyan. Membrane protein integration is catalyzed by the SecYEG/SecDF/YidC **(C)** complex or by the YidC insertase **(B)** [adapted from Kumazaki et al. (2014b) PDB: 3WVF]. The view is in the plane of the membrane with the periplasmic face at the top and the cytoplasmic face at the bottom.

2.2.1 Protein Translocation Across the Membrane

2.2.1.1 SecYEG/SecA Translocase

SecA plays a crucial role for the export process both as a receptor and molecular motor (Cranford-Smith and Huber, 2018). The preprotein binds with high affinity to SecA/SecYEG but not to SecYEG (Hartl et al., 1990). SecA is also necessary for the translocation of proteins across the inner membrane (Oliver and Beckwith, 1981).

The structure of the SecYEβ protein-conducting channel, comprised of three subunits, was solved from *Methanococcus jannashii* in 2004 (van den Berg et al., 2004). SecY is the main channel forming unit that has a classic hourglass structure where TM 1–5 and TM 6–10 form two symmetric bundles held together by a linker (**Figure 4A**). The second subunit, SecE forms a clamp around SecY by wrapping around the two sides *via* its TM segment and cytoplasmic tail to stabilize the complex (**Figure 4A**). The SecE in *E. coli* is a 14 kDa essential 3TM protein. Sec61β (SecG of *E. coli*) is located on the third side of SecY (**Figure 4A**). Both SecY and SecE are evolutionarily conserved in bacteria, archaea and eukaryotes while SecG is not conserved in the three domains of life (Hartmann et al., 1994; Pohlschröder et al., 1997).

There is a pore ring with a diameter of 4—6 Å (**Figure 4B**) at the center of the SecY channel (van den Berg et al., 2004). The pore ring is formed by 6 hydrophobic aliphatic residues and expands to accommodate the polypeptide chain during translocation (Bonardi et al., 2011). A short helix TM 2a termed as the "plug" keeps the pore closed (**Figure 4C**). The plug functions to maintain the integrity and preserve the permeability barrier of the membrane (Li et al., 2007). It has been shown that deleting the plug domain does not result in a major defect in protein export. However, channel experiments have shown that deletions of the plug compromise the membrane permeability of the channel as there are fluctuations between the open and closed state of the translocon (Li et al., 2007). This suggests that when the plug is present, the channel is stabilized in the closed state. Finally, on the front side of the channel, is the lateral gate (comprised of the TM 2a and TM 7) (**Figure 4D**) that can open sideways to allow signal peptides or TM segments to exit the channel (van den Berg et al., 2004).

The peripheral subunit of the Sec complex is SecA which docks onto the SecYEG channel. It utilizes the energy from both ATP binding as well as ATP hydrolysis to drive the transport of unfolded proteins across the Sec channel. Structurally, SecA contains multiple domains with two ATP binding domains (NBD-1 and NBD-2) (Hunt et al., 2002), the HSD (helical scaffold domain), a preprotein crosslinking domain (PPXD) (Hunt et al., 2002), a helical wing domain (HWD), and a carboxyl-terminal linker domain (CTL) (**Figure 5A**). The HSD domain also has the central helix and the 2 helix finger (2HF) (Zimmer et al., 2006) or the regulator of ATPase (IRA1) (Karamanou et al., 1999) subdomains. PPXD and the 2HF have been implicated in binding the signal peptide and the mature region of the preprotein (Kourtz and Oliver, 2000; Papanikou et al., 2005; Musial-Siwek et al., 2007).

The crystal structures of the SecA-SecYEG complexes with and without substrate have shed light on how SecA moves the substrate polypeptide through the channel (Zimmer et al., 2008;

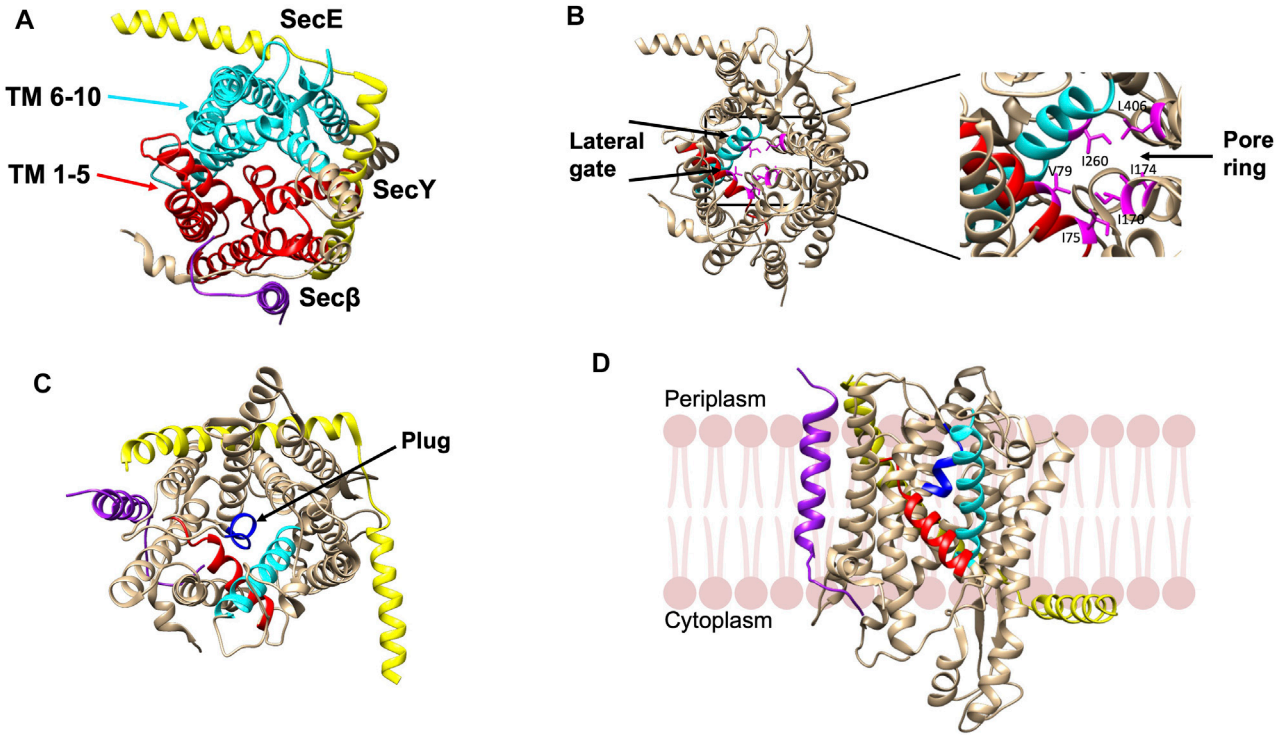

FIGURE 4 | Crystal structure of the SecYEβ complex in the resting state from *Methanocaldococcus jannaschii* [adapted from van den Berg et al. (2004) PDB: 1RHZ] **(A)**. TM1-5 (red) and TM6-10 (cyan) are the halves of SecY. SecE and Sec61β are in yellow and purple, respectively. **(B)** The pore ring comprised of six residues (pink) and lateral gate (TM2b in red and TM7 in cyan) are highlighted. **(C)** The plug helix located above the pore ring is indicated in dark blue. **(D)** The SecYEβ complex from *Thermus thermophiles* (PDB: 5AWW). The lateral gate region comprised of TM2b (red) and TM7 (blue) is the site where the signal peptide or TM segments of membrane proteins exit the channel upon opening of the gate. The SecYEβ structures in **(A–C)** are shown perpendicular to the membrane.

Li et al., 2016; Ma et al., 2019). In the crystal structure of the SecA–SecYEG complex, a single SecA protein is bound to a single SecYEG protomer creating a groove for the passage of the preprotein (Zimmer et al., 2008). A clamp region can be observed at the interface of PPXD and NBD-2 domains (**Figure 5A**). Based on the crosslinking studies, the clamp has been proposed to bind the preprotein (Bauer and Rapoport, 2009). The 2HF region of SecA (**Figure 6A**) may push the preprotein into the channel (Bauer and Rapoport, 2009). Interestingly, while an NMR study (Gelis et al., 2007) showed the signal peptide was bound to a SecA groove formed at the interface of the 2HF and the PPXD (**Figure 5B**), it is possible that it would move from this region to align more parallel to the 2HF, such that it could be pushed into the channel. Indeed, based on the FRET, mutagenesis and genetic studies, Oliver and coworkers proposed a model where the signal peptide binds parallel to the 2HF (**Figure 5C**) (Grady et al., 2012).

To examine the structure of the SecY channel during active SecA-dependent translocation, X-ray crystallography was used to solve a substrate engaged SecA-SecYE complex (**Figure 6A**). The substrate sequence, which included the OmpA signal sequence and a short mature region, was inserted at the end of the 2HF of SecA (Li et al., 2016). The structure suggested that the signal peptide moved into the lateral gate facing the lipid bilayer and the mature region inserted into the channel as a loop, displacing the plug. Thus, the interaction of the signal sequence with the lateral gate induces conformational changes and movements of the plug domain. This leads the way for the substrate to move up the pore ring towards the periplasm by repeated ATP binding and hydrolysis events moving roughly 20–25 amino acids into the translocon in each step.

More recently, in order to gain insight into the path of a translocating polypeptide through SecA, another substrate engaged SecA-SecYE was solved in an active transition state of ATP hydrolysis with ADPBeFx bound (**Figure 6B**) (Ma et al., 2019). The SecA/SecYE translocation intermediate with SecA locked in an ATP bound state was generated using a substrate fusion protein consisting of the proOmpA signal sequence, a linker region, and a folded GFP. In order to stabilize the complex, a cysteine was added after the signal sequence to form a disufide bond to the cysteine introduced at the SecY plug. The protein was then reconstituted into nanodiscs and solved by cryo-EM with a resolution of about 3.5 Å. Tracing the substrate within the SecA-SecYE complex confirmed that in addition to the polypeptide being in proximity to the SecA 2HF, it also interacts with the SecA clamp region via a short β-strand. It also showed that the signal sequence forms a helix that is positioned in a groove outside the lateral gate of the SecY channel.

There are several models that have been proposed to account for the role of ATP energy in energizing SecA/SecYEG in protein

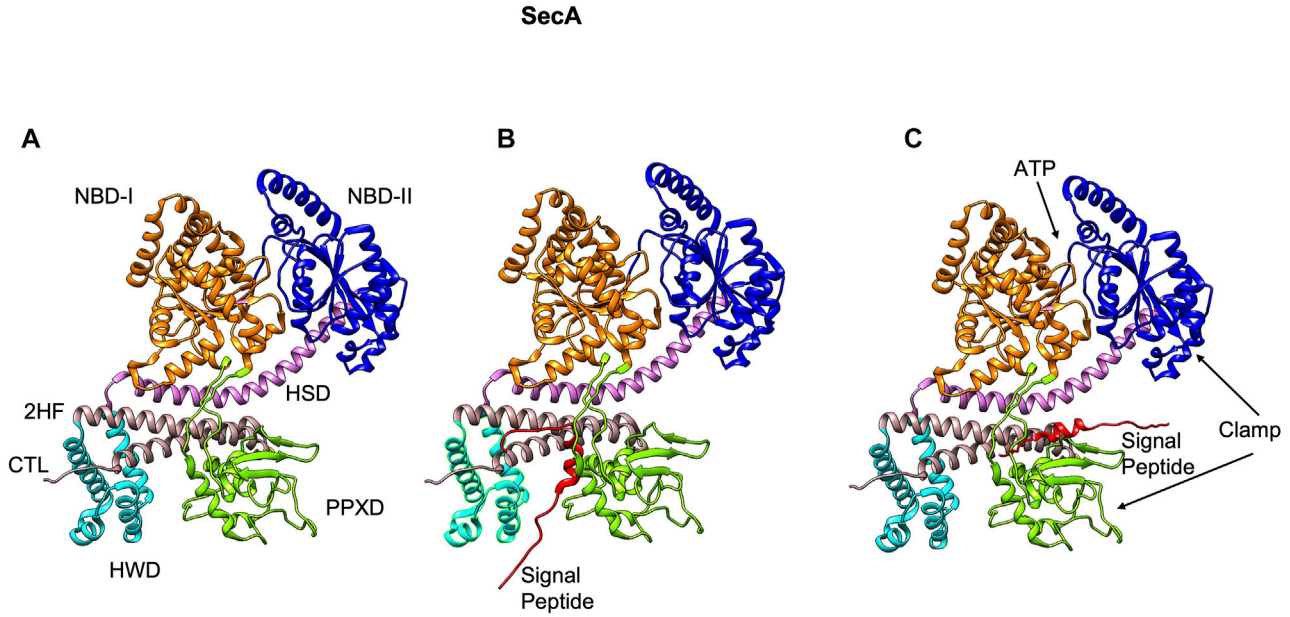

FIGURE 5 | The NMR structure of SecA from *E. coli* [adapted from Gelis et al. (2007) PDB: 2VDA]. **(A)** The various domains of SecA are highlighted (without the signal peptide). The nucleotide binding domains I (orange) and II (blue), the central helix subdomain of helical scaffold domain (HSD in purple), the preprotein crosslinking domain (PPXD green), the helical wing domain (HWD cyan), and the observed carboxyl-terminal linker domain (CTL). Also highlighted is the 2-helix finger (2HF tan) within the HSD domain. **(B)** The signal peptide (red) binds roughly perpendicular to 2HF based on NMR studies (Gelis et al., 2007). **(C)** The signal peptide is modeled parallel to the 2HF of the *E. coli* SecA NMR structure based on FRET, mutagenesis and genetic studies (Grady et al., 2012).

transport, including (Hegde and Bernstein, 2006) power stroke, (Oswald et al., 2021), Brownian ratchet, (Frain et al., 2019), push and slide, and other mechanisms. According to the power stroke model, the SecA ATP hydrolysis causes conformational changes that result in mechanical pushing of the polypeptide chain through the SecYEG channel. Indeed, a large segment of SecA was proposed to move through the SecYEG channel to the periplasmic region in order to translocate the polypeptide to the trans side of the membrane (Ulbrandt et al., 1992; Economou and Wickner, 1994). Later versions of the power stroke model proposed that the 2HF, which is positioned at the entrance of the SecYEG channel, functions as a piston to push the polypeptide through the membrane. This rationale comes from the fact that the SecA 2HF interacts with the preprotein during protein translocation (Erlandson et al., 2008). Upon ATP binding, the 2HF undergoes a large conformational change that pushes the protein substrate chain into the SecY channel (Catipovic et al., 2019). After the 2HF releases the polypeptide substrate of the preprotein, the finger resets to its original position (Catipovic et al., 2019). This cycle of conformational changes occur multiple times until the polypeptide is translocated through the channel.

In a Brownian ratchet mechanism, the movement of a protein chain occurs *via* diffusion through the channel. SecA would mediate SecYEG channel opening thereby enabling the preprotein to diffuse through the SecYEG pore. The evidence for this action was presented in a model by Allen et al. (2016). The authors demonstrated that the SecYEG gate is wide open when ATP is bound to SecA and slightly open with ADP bound to SecA. The slightly open channel allows protein substrate regions with small side chains to slide through the pore, but larger side chains would require the pore to open. Interestingly, the SecYEG channel and the SecA 2HF are able to detect the presence of a protein chain which results in nucleotide exchange, allowing ATP to replace ADP. The binding of ATP to SecA leads to opening of the SecYEG channel through which the chain crosses by diffusion. Backsliding of the polypeptide chain is prevented by closure of the channel. More recently, ATP-driven translocation through the SecYEG channel was shown to be indirectly coupled to ATP hydrolysis providing further support to the Brownian ratchet model (Allen et al., 2020).

A push and slide mechanism combines the power strokes and the passive diffusion models. Bauer et al. (2014) found that certain protein chains can slide passively through the SecYEG channel without ATP hydrolysis. Passive sliding of the polypeptide chain takes place after the preprotein is released by the 2HF and SecA has bound to ADP. Under these conditions, the clamp region between PPXD domain and NBD-2 domain is open and cannot bind the mature domain. The polypeptide chain can passively slide in either direction. Power stroke would occur again after the binding of ATP to SecA. During the power stroke, segments of the polypeptide chain move deep into the SecY channel (Catipovic and Rapoport, 2020) as the SecA 2HF moves into the channel. Prior to the retraction of the 2HF to the original position, the SecA captures and tightens its clamp region around the mature domain of the preprotein substrate, thus preventing back sliding of the polypeptide chain (Catipovic et al., 2019). This tightening enables the forward translocation of the chain to

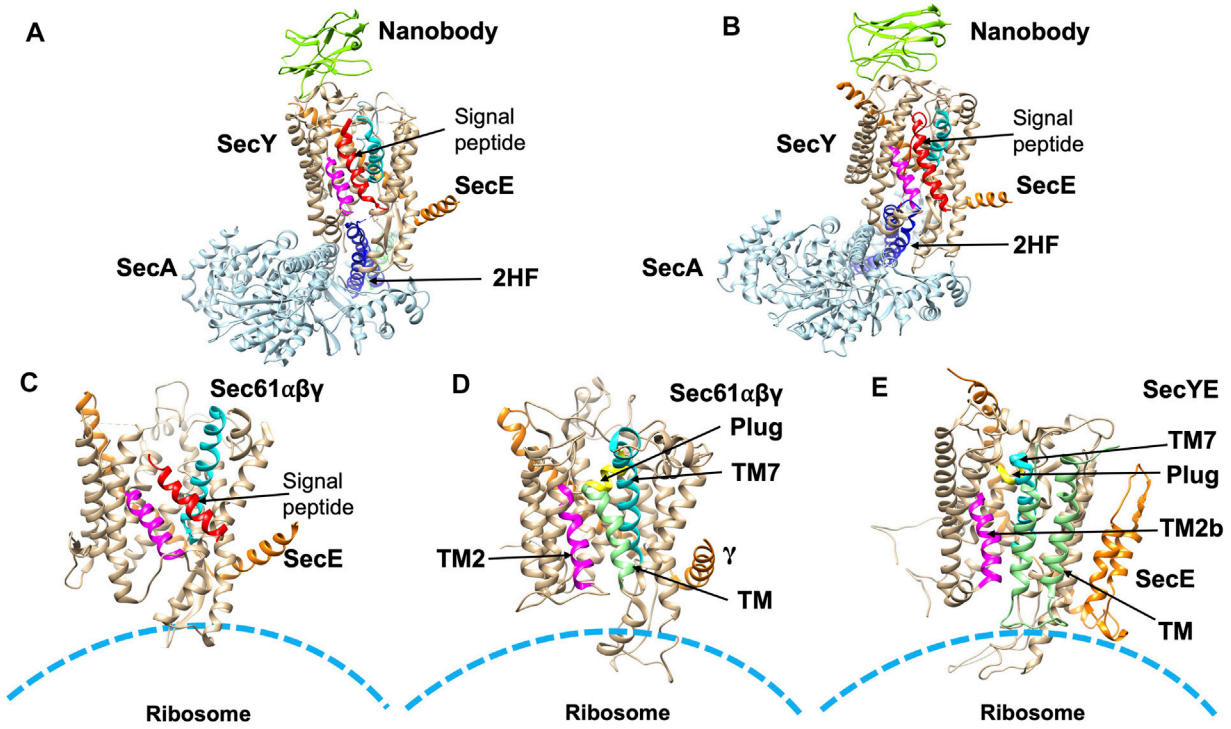

FIGURE 6 | Structures of substrate engaged SecYE or Sec61 complexes. **(A)** Crystal structure of SecYE-SecA [adapted from Li et al. (2016) PDB: 5EUL] with a portion of the preprotein (comprised of the OmpA signal sequence and a few residues in the mature region) fused into the 2HF (navy blue) by insertion between 741 and 744 of SecA. SecA (in light blue) was from *B. subtilis* and SecYE was from *Geobacillus thermodenitrificans*. Nanobody (chartreuse) bound to the periplasmic side of SecY (tan). **(B)** CryoEM structure of SecYEG-SecA complexed with a proOmpA sfGFP [adapted from Ma et al. (2019) PDB: 6ITC] fusion protein. The structure was performed with SecYE in a lipid nanodisc. An anti-GFP nanobody was inserted at the C-terminus of SecA to recognize and stabilize the fused sfGFP of the substrate. In addition, a disulfide was created between a cysteine at position 8 in the early mature region of the proOmpA GFP fusion protein and a cysteine placed in the plug domain of SecY. Finally, a SecY nanobody that recognizes the periplasmic SecY region was added to stabilize the complex. SecA was from *B. subtilis* and SecYE was from *Geobacillus thermodenitrificans*. The nanobody is shown in green in **(A,B)**. **(C)** CryoEM structure [adapted from Voorhees and Hegde, 2016 PDB: 3JC2] in detergent of the canine ribosome Sec61 channel engaged with the N-terminal 86-amino acid preprolactin region. **(D)** CryoEM structure [adapted from Gogala et al. (2014) PDB: 4CG6] of the canine Sec61 channel engaged with a hydrophobic TM segment (light green) of a leader peptidase (lep) arrested intermediate. The TM segment was modeled within the opened TM2/TM7 lateral gate. **(E)** CryoEM structure (adapted from Bischoff et al. (2014) PDB: 5ABB) of a stalled *E. coli* ribosome SecYE complex engaged with proteorhodopsin (TM indicated in light green). TM2 and TM7 of the lateral gate are shown in magneta and cyan, respectively in **(A–E)**. The signal peptide (red) is indicated in **(A–C)**. The plug helix is indicated in yellow in **(D,E)**.

be maintained. The clamp closure occurs before or during SecA ATP hydrolysis and that the 2HF resets all the way when the clamp is closed. Otherwise, as the 2HF resets, and moves away from the channel it would drag the polypeptide with it (Catipovic et al., 2019; Catipovic and Rapoport, 2020). One baffling fact is that the immobilization of the 2HF to SecYEG do not inhibit translocation (Whitehouse et al., 2012).

In addition to the energy of ATP binding and hydrolysis, the proton motive force (pmf) can also contribute to the translocation of preproteins across the SecYEG channel membrane (Date et al., 1980; Zimmermann and Wickner, 1983). SecD and SecF, which have 6 TM segments and a large periplasmic domain, are required for pmf stimulation of protein translocation (Arkowitz and Wickner, 1994). One model proposes that SecDF assists in translocation by binding the preprotein once it emerges from SecY and prevents back sliding (Tsukazaki et al., 2011). Then it swivels its head domain to translocate about 25 amino acids across the membrane with the help of the pmf. Therefore, SecDF functions in the pulling of preproteins across the membrane, and the release of preproteins from the SecYEG complex after complete translocation.

2.2.1.2 Tat Translocase

The Tat machinery exports fully folded proteins of different sizes. It is comprised of TatA, TatB, and TatC (Tat complex) in *E. coli* and TatAC in *B. subtilis* (Jongbloed et al., 2004; Berks, 2015; Palmer and Stansfeld, 2020). The Tat components in *E. coli* are assembled on the cytoplasmic membrane as a TatBC complex and a cytoplasmic TatA pool. Interestingly, TatC membrane insertion is a SecYEG and YidC dependent event (Welte et al., 2012; Zhu et al., 2012). After forming the TatBC complex, the TatA oligomers are recruited to the TatBC complex in a pmf dependent event before substrate translocation. The recognition

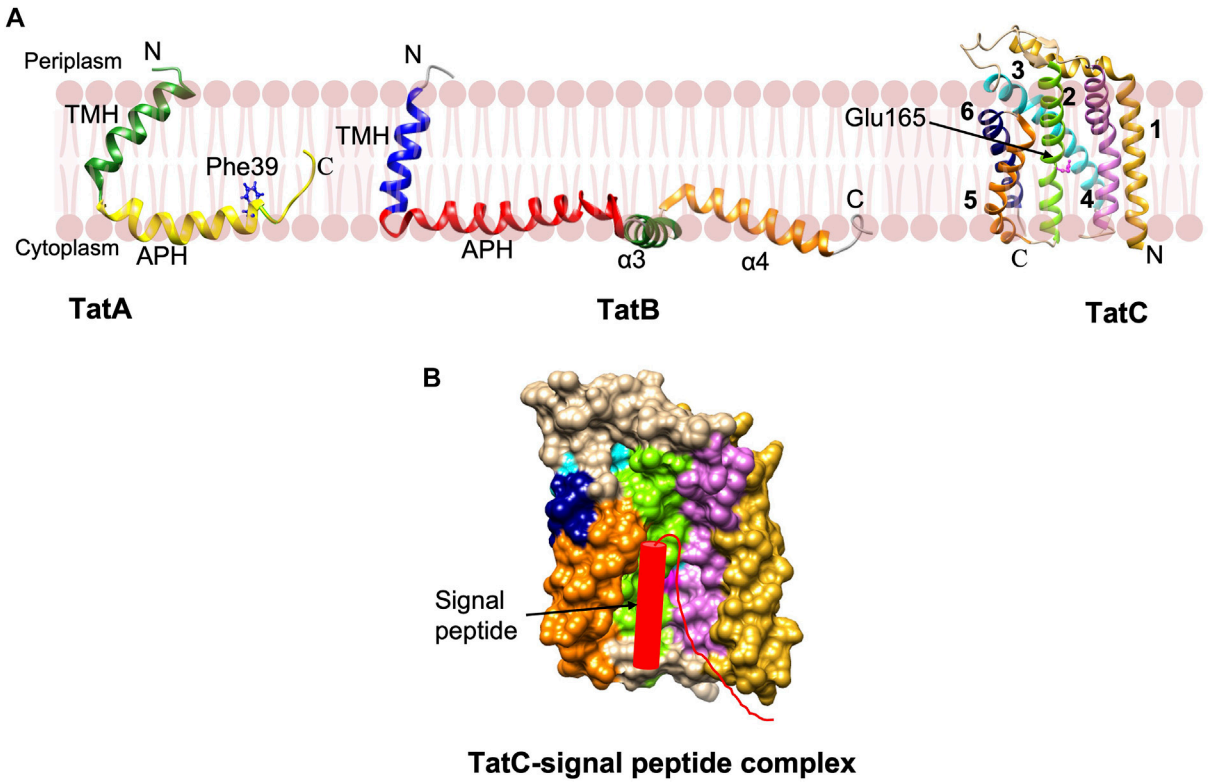

FIGURE 7 | The Tat complex components and a model of TatC-signal peptide complex. **(A)** The single span TatA (PDB: 2MN7) and TatB (PDB: 2MI2) proteins were determined by NMR (Rodriguez et al., 2013; Zhang et al., 2014). The structure of 6 membrane spanning TatC [adapted from Rollauer et al. (2012) PDB: 4B4A] was solved by X-ray crystallography (Rollauer et al., 2012; Ramasamy et al., 2013). **(B)** The model of TatC binding with the Tat signal peptide in the groove adapted from Ramasamy et al. (2013). Only signal peptide and early mature region of the preprotein are indicated.

of the twin arginine motif by a conserved patch on TatC (Palmer and Stansfeld, 2020) initiates the architectural reorganization of the active complex assembly. The low stability, size and transient nature of the active complex presents a daunting challenge to identify the precise assembled active complex needed for Tat translocation.

The Tat components TatA and TatB have similar features each possessing a small periplasmic N-terminal region, a single short TM helix (TMH) followed by an amphipathic helix (APH), and a cytoplasmic domain. TatA is assumed to form the translocation complex with the substrate as it is capable of forming oligomeric rings of different sizes (Gohlke et al., 2005). TatB functions with TatC as a receptor to bind Tat substrates (Cline and Mori, 2001; Behrendt and Brüser, 2014). TatB and TatC form a 1:1 complex and have an oligomeric structure with a size range of 360–700 kDa (Bolhuis et al., 2001).

In the resting state, the TatBC receptor complex most likely has some TatA associated and recent studies suggest there are three to four copies each of TatA, TatB and TatC in a ratio of 1:1:1 (Bolhuis et al., 2001; Alcock et al., 2016; Habersetzer et al., 2017). Based primarily on crosslinking studies it has been proposed recently that in the resting state, this TatABC complex is organized such that TatB binds to the TatC TM5 and TatA binds to the TatC TM6. Upon activation of the complex by substrate addition, TatA and TatB switch positions which may be triggered by the substrate with the signal peptide moving further into the membrane interior (Habersetzer et al., 2017).

NMR studies reveal that TatA and TatB proteins possess a short α-helical TM segment followed by the amphipathic helix (APH) (**Figure 7A**) (Rodriguez et al., 2013; Zhang et al., 2014). TatA forms oligomeric rings with variable number of TatA molecules (Rodriguez et al., 2013). Interestingly, structural studies and molecular dynamic (MD) simulations predict that the TatA structure causes significant thinning of the membrane due to its short TM segments (Rodriguez et al., 2013). This may be true with TatB as well since it has a short TM segment. The structure of the 6-membrane spanning TatC from *Aquifex aeolicus* revealed that the protein has a "cup hand" or "glove-like structure" (**Figure 7B**), where TatC assembles into a concave structure that can accommodate a TM segment of TatB or the neighboring TatC (Rollauer et al., 2012; Ramasamy et al., 2013). Remarkably, the TatC surface has an ionizable Glu165 side chain that is expected to be buried in the hydrophobic interior of the bilayer. MD simulations show that the TatC has a hydrated cavity facing the cytosol with the conserved Glu/Gln at this position inside the membrane. This hydrophilic cavity and the short TM segments 5 and 6, cause thinning of the membrane.

Export by the Tat pathway begins by the recognition of the Tat signal peptide of the preprotein substrate by TatC within the TatBC complex. TatC recognizes the RR motif via its N-terminal domain and a cytoplasmic loop 1 (**Figure 7B**) (Alami et al., 2003; Gérard and Cline, 2006). Subsequently, insertion of the signal sequence into the interior of the membrane takes place by contacting the periplasmic side of TatA. Following the substrate insertion into the TatBC complex, the oligomeric TatA complex is formed in a step that requires a TM pmf. An oligomeric complex of TatA facilitates the translocation of the folded substrate. TatA protomers are predicted to form oligomeric ring-like pores of varying diameters in the cytoplasmic membrane, permitting the movement of fully-folded proteins into the periplasm (Lausberg et al., 2012).

The precise mechanism of translocation is still debatable, but we will discuss the two main hypotheses documented in literature. The trap door model postulates that the amphipathic helix (APH) domain of TatA flips into the lipid bilayer with the help of membrane potential on contact with the substrate carrying the TatA interactive motif (Patel et al., 2014). Initially, TatA oligomers self-arrange to form a pore of ~8.5–13 nm in diameter to accommodate the folded protein (Frain et al., 2019). The APH of the TatA oligomers at the cytoplasmic face mirrors a "trap door" that regulates the transient channel for translocation of the substrate. This would essentially depend on the flexible hinge (the conserved Gly residue) between the APH and TMH (Frain et al., 2019). When the APH swings up to align with the TMH, the polar residues may interact with the hydrophilic protein to be translocated and thus the folded protein is promoted across the formfitting passive conduit.

The second model proposed a weakening of the lipid bilayer when TatA oligomerizes with its polar N-tail destabilizing the membrane, allowing translocation of the Tat substrate (Brüser and Sanders, 2003). This model where transient bilayer disruptions occur, is gaining more support with the NMR structure of TatA and suggests that the TatA topology may not be as flexible as predicted by the trap door model. MD simulations reveal the phospholipids are highly distorted and the membrane thickness is dramatically shortened (Rodriguez et al., 2013). It is believed that the thinning of the membrane is due to the short TatA TM segment and the presence of the conserved glutamine in the oligomer. However, this model does not clarify what drives the translocation of the substrate across the membrane.

2.3 The Insertion of Proteins Into the Membrane

The insertion of proteins in their proper conformation and orientation into the lipid bilayer is crucial for the functional integrity of the membrane proteins [for recent reviews see (Cymer et al., 2015; Tsirigotaki et al., 2017; Hegde and Keenan, 2021)].

2.3.1 SecYEG/YidC

For membrane protein topogenesis, the nascent membrane protein chain is presumed to be driven across the membrane utilizing the GTP hydrolysis energy from protein synthesis. This is possible because the ribosome binds to the SecYEG complex and may form a single aqueous conduit that stretches across most of the inner membrane.

As the membrane protein enters the SecYEG channel, the hydrophobic TM sequence or signal peptide may first enter the hydrophilic channel and then exit the lateral gate (van den Berg et al., 2004) or it can slide into the membrane via the lateral gate by thermodynamically partitioning between the lipid and the aqueous pore (Cymer et al., 2015). Rather than the sequence of amino acids of the TM segment, the overall hydrophobic character of the segment is important for insertion into the membrane (Hessa et al., 2005; Hessa et al., 2007). The hydrophobic stretch can stabilize the open lateral gate (Zhang and Miller, 2010).

As seen with the substrate engaged SecYEG/SecA complex, the ribosome bound-Sec translocon showed the signal peptide in the lateral gate region. A cryoEM structure of the canine ribosome Sec61 translocon engaged with a preprolactin substrate revealed the signal peptide in the lateral gate (**Figure 6C**) (Voorhees and Hegde, 2016). The pore region of the channel would allow the polar polypeptide chains to be translocated to the trans side of the membrane (Erlandson et al., 2008). After translocation, a simple membrane protein with 1 TM segment would completely exit the channel and partition into the lipid bilayer.

Similarly, the lateral gate accommodates the TM segment of the ribosome bound membrane protein inserting into the Sec61 complex, as revealed by cryo-EM study (**Figure 6D**) (Gogala et al., 2014). Notably, another cryo-EM study of a nascent membrane protein-SecYE complex demonstrated that the first 2 TM α-helices of proteorhodopsin had exited the lateral gate to face the lipid with the N-terminus at the periphery of SecY (**Figure 6E**) (Bischoff et al., 2014). Kater et al. (2019) further elucidated that a partially inserted hydrophobic region can cause opening of the lateral gate.

SecA is always required for translocation of large loops and occasionally for small loops of membrane proteins (Kuhn, 1988; Andersson and von Heijne, 1993; Deitermann et al., 2005; Soman et al., 2014). However, the mechanism by which this task is carried out has not been elucidated, as the ribosome is expected to be already bound to the SecYEG complex when the membrane protein inserts co-translationally. In order to perform the translocation function by SecA, the ribosome should be dissociated partly or completely from the SecYEG. This illustrates the dynamic nature of the insertion process and the interplay of the various SecYEG binding partners.

An interesting method to study *in vivo* insertion and co-translational folding of membrane proteins is the application of translational arrest peptides to measure forces acting on a nascent protein during membrane insertion (Ismail et al., 2012; Sandhu et al., 2021). In this approach, the arrest peptide binds to the ribosomal tunnel and induces ribosomal stalling at a specific amino acid. SecYEG mediated membrane insertion and folding of a nascent chain is followed by examining the release of stalling and resumption of protein synthesis. This technique has been used to study the co-translational insertion of simple to complex proteins spanning the membrane ten times, showing that the surface helices and re-entrant loops that flank a TM segment can

either advance or delay membrane protein insertion (Nicolaus et al., 2021). Moreover, the results supported a sliding mechanism where the inserting TM segment moved into the membrane along the outer part of the lateral gate.

The mechanism of insertion of multispanning membrane proteins is complicated with most of the findings coming from studies of the endoplasmic reticulum (ER) membrane system (Cymer et al., 2015; Hegde and Keenan, 2021). In some cases, a TM segment is inserted into the translocase and then reoriented within the channel (Goder and Spiess, 2003). Remarkably, some TM segments of the membrane proteins such as the aquaporin 4 channel, exit the channel but apparently interact again at a later stage in membrane biogenesis, validating the dynamic nature of membrane protein biogenesis. The Sec machinery can handle the internal TM segments by various mechanisms. Some TM segments integrate into the lipid bilayer spontaneously (Heinrich et al., 2000), others integrate into the lipid bilayer only after the protein synthesis is terminated (Do et al., 1996; McCormick et al., 2003), some pairs of TM segments co-integrate into the membrane (Skach and Lingappa, 1993; Heinrich and Rapoport, 2003), while the rest can be stabilized by chaperones such as TRAM and YidC (Do et al., 1996; Heinrich et al., 2000; Beck et al., 2001; Urbanus et al., 2001; Nagamori et al., 2004).

SecYEG plays the primary role in membrane insertion in the plasma membrane in bacteria. The accessory component, YidC actively participates in membrane protein biogenesis for several different Sec dependent proteins (**Figures 2**, **3**). Substrates that require the synergistic action of both YidC and SecYEG for insertion include, subunit a and b of the F1Fo ATP synthase (Yi et al., 2004) and TatC of the twin arginine translocase (Welte et al., 2012; Zhu et al., 2012). Moreover, YidC can bind to the TM segment of membrane proteins after the TM segment exits the SecYEG channel (Urbanus et al., 2001). This case is exemplified by the TM segments of FtsQ and leader peptidase (Houben et al., 2004) which were shown to initially contact SecYEG followed by contact with YidC at a later stage during its translocation process. This latter finding implied that YidC may facilitate Sec substrates to partition into the bilayer and assist in the clearing the Sec channel of its substrates. Remarkably, in the case of CyoA (subunit of cytochrome bo3 oxidase), the amino-terminal domain is inserted by the sole action of the YidC insertase whereas the large C-terminal domain requires SecYEG operating with the SecA motor ATPase for insertion (Celebi et al., 2006; van Bloois et al., 2006; Kol et al., 2009).

Furthermore, YidC acts as a chaperone (Nagamori et al., 2004) and assembler of multi-TM complexes (Saller et al., 2012). Studies with LacY biogenesis showed that YidC acts in the late stages of membrane protein biogenesis and is crucial for the correct folding of the protein but nonessential for its insertion (Nagamori et al., 2004; Zhu et al., 2013). Wagner et al. (2008) discovered a similar trend with MalF, a subunit of the maltose binding complex. Upon YidC depletion, the stability of the complex was affected without compromising the insertion of the TM segments of MalF mediated by the SecYEG complex.

In order to perform these multi-functions, YidC must be located close to the SecYEG complex. Indeed, YidC, SecDF/YajC may associate with SecYEG to form a holo-translocon (Schulze et al., 2014). This has been validated by copurification of YidC with the SecYEG and SecDF/YajC. The purified complex is capable of inserting *in vitro* synthesized membrane proteins (Komar et al., 2016). A low-resolution structure of the holocomplex SecYEG/SecDFYidC revealed that the SecYEG-YidC interface is a lipid filled cavity (Martin et al., 2019). Although a YidC holocomplex can be isolated, YidC is capable of dynamic interaction with SecYEG. When YidC contacts SecYEG, it is in proximity to the lateral gate of SecYEG and can contact helices on either side of the lateral gate (TMs 2b, 3, 7 and 8) (Sachelaru et al., 2017). This contact is maintained even in the absence of SecDF. Furthermore, SecYEG contacts TM1 and cytosolic loop 1 of YidC (Petriman et al., 2018). The Sec lateral gate can contact the YidC TM3-TM5 region which forms the greasy slide (Steudle et al., 2021). Taken together, these studies suggest that the insertion of Sec-dependent protein substrates occurs at the interface of YidC/SecYEG.

2.3.2 YidC-Only Pathway

In addition to assisting SecYEG and acting as a chaperone for membrane insertion, YidC can also operate independently. Examples of the Sec-independent proteins include M13 phage coat protein (PC) and the Pf3 coat protein, which were earlier presumed to be inserted by an unassisted mechanism. Depletion of YidC resulted in the accumulation of these proteins in the cytoplasm (Samuelson et al., 2000; Chen et al., 2002; Serek et al., 2004). Moreover, crosslinking studies revealed that YidC interacts with the inserting Pf3 coat (Chen et al., 2002). Subunit c of F_1F_0 ATPase was shown to be dependent on YidC for membrane insertion both *in vivo* (Yi et al., 2003; van Bloois et al., 2004) and *in vitro* (Van Der Laan et al., 2004). Interestingly, YidC proteoliposomes were capable of forming the subunit c oligomer whereas the liposomes were not (Kol et al., 2006). The indispensable nature of YidC in cells is still speculative. One of the reasons may be attributed to the fact that YidC is required for the biogenesis of the respiratory complexes (van der Laan et al., 2003).

Other substrates for the YidC-only pathway are MscL (Mechanosensitive channel of large conductance), which inserts co-translationally (Facey et al., 2007) and the tail anchored membrane proteins TssL (SciP), DjlK, and Flk (Aschtgen et al., 2012; Pross et al., 2016; Peschke et al., 2018). In eukaryotes, the ER tail anchored membrane proteins with a high hydrophobic TM segment are inserted by the Get pathway while those proteins with low hydrophobic TM segment are inserted by the ER membrane protein complex (EMC) (Hegde and Keenan, 2021). Interestingly, Get1 and EMC3 of the Get complex and EMC, respectively, are YidC homologs found in the ER (Anghel et al., 2017; Chen and Dalbey, 2018; McDowell et al., 2021).

The common feature of substrates of the YidC only pathway is that they have a short translocated region (Hennon et al., 2015), suggesting that the YidC insertase has limited translocase activity. Indeed, if the polarity of the translocated domain exceeds a certain threshold by introduction of charged/polar residues, then YidC requires the assistance of the SecYEG complex, implying that YidC is incapable to translocate these substrates

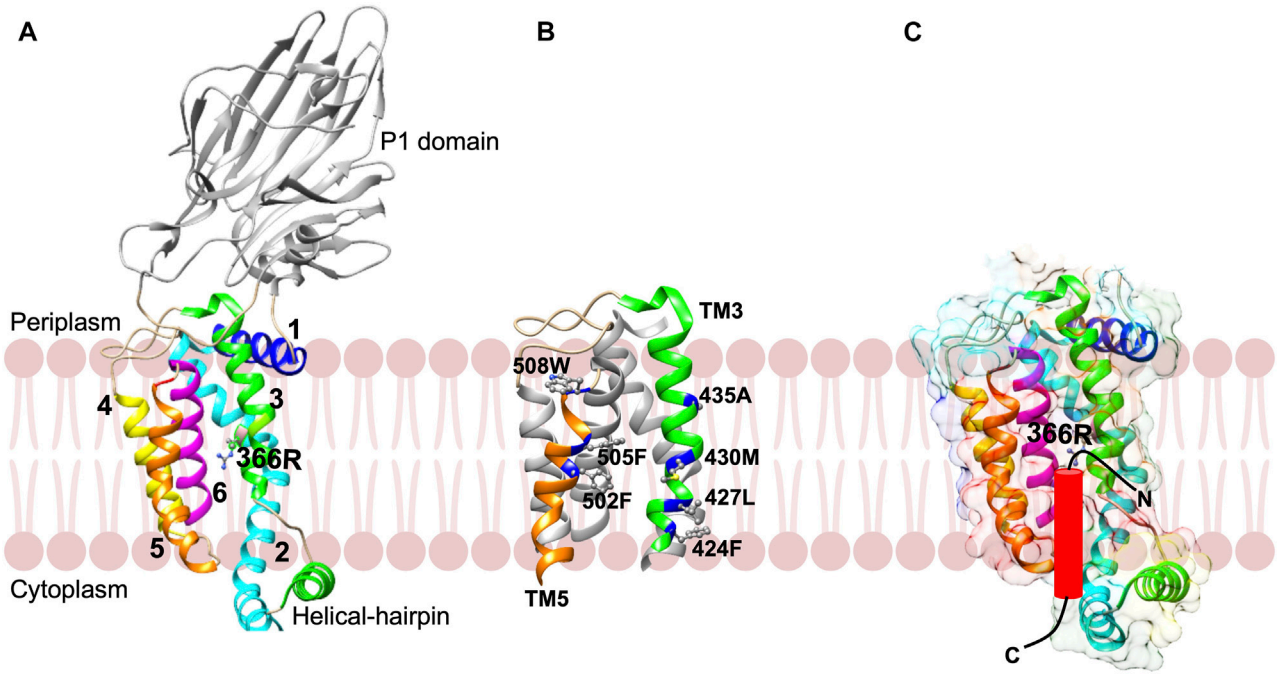

FIGURE 8 | The YidC insertase [adapted from Kumazaki et al. (2014b) PDB: 3WVF]. **(A)** The *E. coli* YidC has a large periplasmic domain, a coiled cytoplasmic domain, and a conserved core region comprising of 5 TM helices (TMs 2–6) that form a hydrophilic groove open to the cytoplasm and lipid bilayer. The hydrophilic groove has a strictly conserved arginine that helps to keep the region hydrated. **(B)** A close-up view of the greasy slide (TM3 and TM5) that contacts the TM region of YidC substrates during insertion. The residues that contact the substrate TM segment (s) are indicated in dark blue. **(C)** During membrane insertion of the Pf3 coat, the TM segment moves up the greasy slide with the N-tail region captured transiently in the hydrophilic groove. The periplasmic domain of YidC is omitted in **(B,C)**.

unaided (Soman et al., 2014; Hariharan et al., 2021). The switching from YidC-only pathway to the YidC/Sec pathway indicates that both the YidC and the SecYEG are surveying the polypeptide chain during the membrane insertion process. This is feasible by dynamic interaction of YidC with SecYEG (Sachelaru et al., 2017; Steudle et al., 2021) or, a certain portion of YidC is a part of the SecYEG/SecDFYajC/YidC holocomplex (Schulze et al., 2014).

Structural studies have shown that YidC is a monomer and contains a hydrophilic cavity within the 5 TM core region (**Figure 8**) (Kumazaki et al., 2014a; Kumazaki et al., 2014b). This aqueous groove with a conserved positively charged residue is open both to the cytoplasm and the lipid bilayer but closed from the periplasmic side. The existence of a hydrophilic groove located within the inner leaflet of the membrane was supported by *in vivo* solvent accessibility and MD simulation studies. The study also revealed that YidC shapes the membrane with significant membrane thinning around the protein (Chen et al., 2017). The presence of the hydrophilic groove in the membrane decreases the membrane crossing distance which would in turn reduce the energy cost of translocating a polypeptide chain. Wu and Rapoport (2021) have recently proposed that protein translocation through a locally thinned membrane is a new paradigm for lowering the energy cost for translocation.

Remarkably, the positively charged residue in the hydrophilic groove is essential for SpoIIIJ (YidC1) function in *B. subtilis*. It was proposed that the hydrophilic groove participates in an electrostatic step necessary to translocate the negatively charged N-terminal tail region of MifM across the membrane (Kumazaki et al., 2014a). However, the positive charge is not essential for the *E. coli* YidC (Chen et al., 2014). Rather, the positively charged residues plays a role in maintaining the hydrophilic microenvironment in the groove, which is necessary for the activity of YidC (Chen et al., 2022).

In addition to the hydrophilic groove, YidC has a cytoplasmic helical hairpin-like domain (**Figure 8A**) (Kumazaki et al., 2014a) which was predicted to be involved in the initial recruitment of the substrate. The arrangement of two antiparallel helices in the C1 region of EcYidC is rotated by 35° with respect to the core region, as compared to that in the BhYidC structure. Moreover, in both the structures the B factor for this region is high, demonstrating the flexibility of the C1 cytoplasmic loop region. Crosslinking studies of the essential C1 loop show contacts not only with the targeting proteins SRP and FtsY but also the Sec translocon (Geng et al., 2015; Petriman et al., 2018).

The mechanism of the substrate TM recognition by YidC is fascinating. Crosslinking studies have indicated that the TM3 of YidC contacts the TM domain of FtsQ, leader peptidase, subunit c of the F1FoATPase (Yu et al., 2008). Contacts are also observed with TM3 and TM5 of YidC to Pf3 coat and MscL (Klenner et al., 2008; Klenner and Kuhn, 2012). It has been proposed that the

substrate enters the YidC groove between these TM3 and TM5 segments, which constitutes a greasy slide where the TM segment moves across the membrane (**Figure 8B**). Kedrov et al. (2016), performed cryo-EM studies on a YidC-ribosome Foc nascent chain complex where YidC was reconstituted in nanodiscs. The study revealed that the Foc nascent chain was in proximity to TM3 facing the lipid region.

He et al. (2020) elucidated the pathway employed by the single spanning Pf3 coat to provide insight into the YidC insertion mechanism of simple membrane proteins (**Figure 8C**). The tracking of the Pf3 coat protein through YidC was obtained by "freezing" each step of the insertion process by creating translational arrested intermediates of different sizes and investigating them by thiol crosslinking (He et al., 2020). The results divulged that the TM segment of Pf3 moves up the YidC greasy slide during membrane insertion. After the TM reached the top of the slide, the N-tail transiently enters the YidC hydrophilic groove. In the next step, the N-tail is released from the groove and translocated across the periplasmic leaflet of the membrane.

2.3.3 TatC and TatC/SecYEG

The Tat substrates of *E. coli* include the five integral membrane proteins including HybO, FdnH, FdoH, HyaA and HybA (Hatzixanthis et al., 2003). The genes encode subunits of NiFe hydrogenase or formate dehydrogenase. They are encoded with a Tat signal peptide and possess a C-terminal TM segment that functions as a stop transfer domain. The recognition of these membrane proteins by the Tat complex is achieved by the interaction of the Tat signal peptide with the TatBC complex.

Although mechanistically different, surprisingly, in some bacteria, cooperation is observed between the Tat and the Sec pathway for the insertion and assembly of polytopic membrane proteins (Keller et al., 2012). The first evidence for this was from the analysis of the iron-sulfur membrane bound Rieske proteins from Gram-positive actinobacteria that has 3 TM segments. While the first 2 TM segments are inserted by the SecYEG translocase, the third TM segment, which is preceded by a Tat motif was inserted by the Tat system. To understand the mechanism of insertion further and to decipher the handover process from Sec to Tat, the *S. coelicolor* Rieske protein, Sco2149 was examined (Tooke et al., 2017). The authors observed that a moderate hydrophobicity of the TM3 segment and the presence of several C-terminal positively charged residues promote the release of the TM3 from the SecYEG apparatus. This further allows the Tat TM segment to engage with the Tat translocase and stimulate translocation across the membrane. Other examples of the dual participation by Sec/Tat machineries targeting membrane proteins include the five spanning membrane proteins *S. coelicolor* Molybdenum cofactor protein Sco3746, and the delta proteobacterium MLMS-1 FeS containing polyferredoxin. In these cases, the first 4 TM segments are inserted by the SecYEG complex, and the Tat system inserts the last TM segment and translocates the folded C-terminal domain. In each case, the fifth TM segment has moderate hydrophobicity and an amino terminal Tat RR-motif (Tooke et al., 2017).

2.4 Removal of the Signal Peptide and Degradation

The last step in the translocation pathway is the removal of the signal peptide. This allows the exported proteins to be released from the membrane so that they can continue their journey to the periplasm, outer membrane or to the extracellular medium. The removed signal peptides are degraded by enzymes having signal peptide hydrolase activity.

Signal peptidases cleave off the signal peptides and play crucial roles as endopeptidases with clear cut substrate specificities (Paetzel, 2019). Type I signal peptidase (SPase I; also known as leader peptidase) processes the majority of preproteins while Type II signal peptidases (SPase II; also known as lipoprotein signal peptidase) process lipoprotein precursors (Paetzel, 2014).

2.4.1 Signal Peptidase I

The first signal peptidase to be characterized was *E. coli* signal peptidase I (SPase I). It was overproduced and purified to homogeneity (Wolfe et al., 1982). The purified protease in detergent was shown to cleave a wide variety of preproteins, including eukaryotic secretory preproteins (Watts et al., 1983). Similarly, the eukaryotic signal peptidase can cleave bacterial preproteins, demonstrating that the cleavage specificity is evolutionarily conserved (Watts et al., 1983). Subsequently, the *E. coli* protease enzyme was shown to be localized to the inner membrane with its catalytic domain facing the periplasmic space (Wolfe et al., 1983). Moreover, it was shown to be an essential enzyme for the bacteria (Date, 1983).

Signal peptidases are indispensable for the secretion process. Disruption of the signal peptide processing prevents the preproteins from arriving to their correct destination in the cell (Dalbey and Wickner, 1985). Under decreased SPase I activity in a depletion strain, the accumulated preproteins were translocated but were anchored to the inner membrane by the uncleaved signal peptide. Therefore, the function of signal peptidase is to release the exported protein from the membrane by removing the signal peptide so that they proceed to their destination. It is now established that SPase I processes the majority of non-lipoproteins that are exported by the Sec pathway or by the Tat pathway (Lüke et al., 2009).

To understand how SPase cleaves and binds substrates at the active site, the structure of the *E. coli* signal peptidase periplasmic domain (Δ2-75) (Tschantz et al., 1995) was solved to high resolution of 1.9 Å (Paetzel et al., 1998) (**Figure 9A**). The catalytic serine (Ser 91) was covalently attached to the cleaved β-lactam inhibitor and the lysine 146 amino group was within hydrogen bond distance. This corroborates with the mutagenesis studies displaying the indispensable mechanism of active Ser and Lys dyad for catalysis (Sung and Dalbey, 1992; Tschantz et al., 1993; Paetzel et al., 1997) (**Figure 9A**) in contrast to the canonical Ser-His-Asp mechanism (Paetzel and Dalbey, 1997).

Intensive analysis of the structure of the active site region with the inhibitor (Paetzel et al., 1998) and a signal peptide

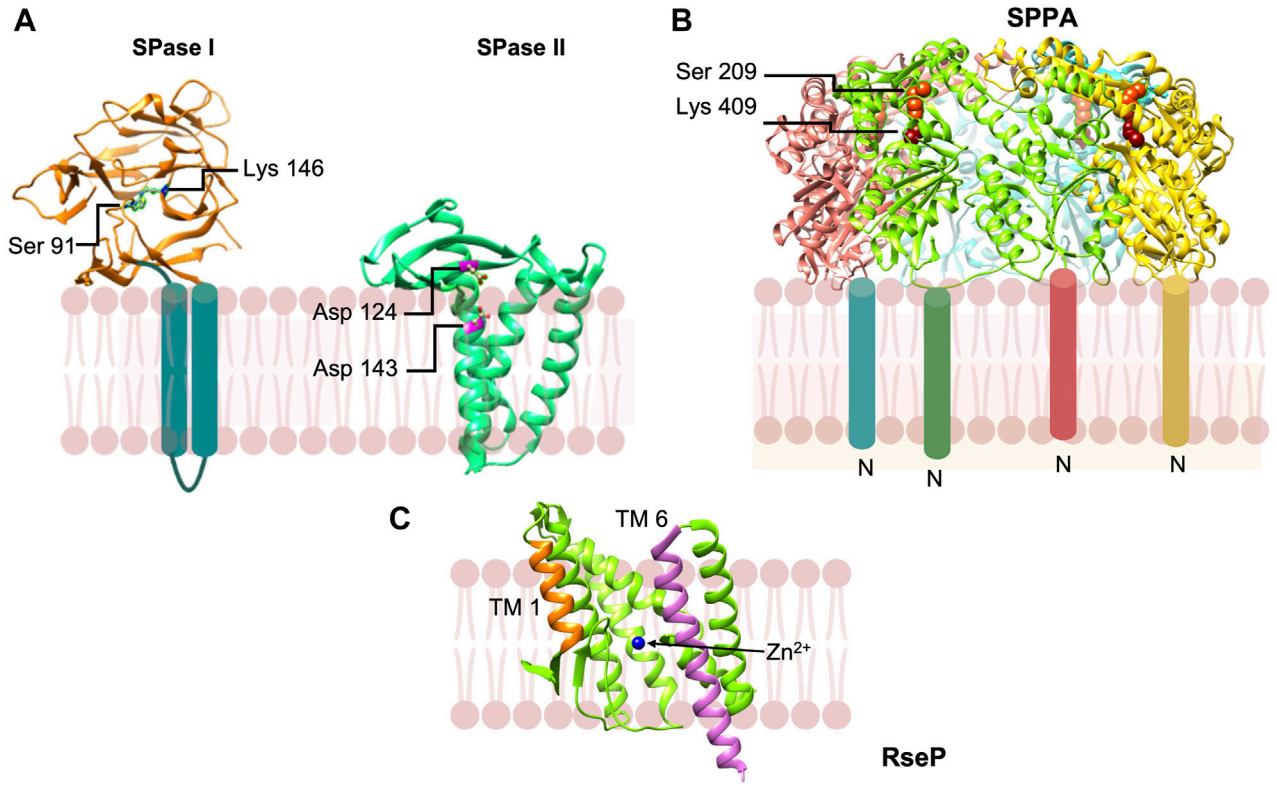

FIGURE 9 | Peptidases involved in the removal of signal peptides and their degradation. **(A)** Signal peptidase 1 [adapted from Paetzel et al. (2004) PDB: 1T7D] is a novel Ser-Lys protease that cleaves the preprotein at the membrane surface on the periplasmic side. Signal peptidase 2 [adapted from Vogeley et al. (2016) PDB: 5DIR] is an aspartic acid protease that cleaves a diacyl glyceride modified preproteins within the plane of the membrane. **(B)** SppA [adapted from Kim et al. (2008) PDB: 3BF0] is a tetrameric protein that degrades signal peptides which are released from the membrane into the periplasmic space. SppA employs a Ser-Lys dyad and is anchored to the membrane by an amino terminal TM segment. **(C)** RseP signal peptide peptidase [from *Methanocaldococcus jannaschii* adapted from Feng et al. (2007) PDB: 3B4R] in open state. Both water molecules and peptide substrates reach the active site containing Zn^{2+} ion (blue) during its open state.

modeled into the binding site of the apo enzyme (Paetzel et al., 2002) revealed the binding pockets at the S1 and S3 positions that account for the "-3 and -1" or "Ala-X-Ala" rule for processing based on conserved residues in preproteins (Heijne, 1983). The S1 pocket is quite small and the S3 pocket is slightly bigger, fitting well with the known substrate specificity. The -2, -4 and -5 residues are solvent exposed, consistent with almost any residue found at these positions. The substrate binding pocket was further supported by the structure of the *S. aureus* SPase I (SpsB) with a portion of the signal peptide and the early mature region sequence binding to the active site (Ting et al., 2016).

2.4.2 Signal Peptidase II

As mentioned earlier, the substrate for signal peptidase II (SPase II) is a diacylglycerol modified prolipoprotein (Tokunaga et al., 1982). Following cleavage and further maturation, the bacterial lipoproteins possess a N-acyl diacylglycerylcysteine at the N-terminal end of the protein, which serves to anchor lipoproteins to the inner membrane or the outer membrane.

The gene for SPase II (lsp) was cloned by the Mizushima and the Wu labs independently (Tokunaga et al., 1983; Yamagata et al., 1983). The SPase protein spans the membrane four times with the protein ends facing the cytoplasm. The initial evidence of this peptidase as an aspartic protease was the fact that it was inhibited by pepstatin (Dev and Ray, 1984). Also, in *B. subtilis*, several aspartic acid residues located at the ends of the TM segments were shown to be important for activity (Tjalsma et al., 1999).

The structure of SPase II from *Pseudomonas aeruginosa* in complex with the inhibitor globomycin solved to 2.8 Å provided evidence that SPase II was an aspartic acid protease (**Figure 9**) (Vogeley et al., 2016). Along with mutagenesis studies, the work revealed that Asp 124 and Asp 143 comprise a catalytic dyad (**Figure 9A**). Interestingly, the aspartic residues are located within the predicted membrane region confirming that SPase catalyzes intramembrane proteolysis. These findings validate the fact that lipoprotein signal peptides typically have short hydrophobic regions. Caffrey and coworkers proposed a model for how SPase II binds the preprotein and carries out catalysis

(Vogeley et al., 2016). The signal peptide helix of the preprotein enters the SPase II active region via TM segments 2 and 4, and then binds to the protein to position the preprotein lipobox residues analogous to the Leu-Ile-Ser tripeptide of the globomycin inhibitor. The signal peptide region immediately following the Leu residue in the lipobox is in an extended conformation with the Gly-Cys scissile bond positioned in proximity to the Asp catalytic dyad Asp124 and Asp143. The mature domain of the preprotein is located in the periplasmic region.

2.4.3 Signal Peptide Degradation

The final step "in the life and death of signal peptides (see ref von Heijne, 1998)" is their degradation. Degradation of the signal peptides is important because in many cases they can be toxic to the cell or interfere with protein export (Wickner et al., 1987; Bolhuis et al., 1999). The first protease discovered to possess signal peptide hydrolase activity was SppA (or protease IV), which was shown to degrade the lipoprotein signal peptide (Hussain et al., 1982). SppA is an inner protein that forms a tetrameric structure (Hussain et al., 1982; Ichihara et al., 1984). The catalytic domain of SppA containing the active site Ser-Lys dyad (**Figure 9B**) (Kim et al., 2008; Wang et al., 2008) is found within the periplasmic region at a large distance from the membrane indicating that the signal peptide is released from the membrane prior to its degradation (Kim et al., 2008). Apparently, SppA would cleave a wide variety of signal peptides that are released into the periplasmic space. Other proteases such as oligopeptidase A would hydrolyze signal peptides that are released into the cytoplasm (Novak et al., 1986).

The bacterial RseP, like signal peptide peptidase in eukaryotes (Lyko et al., 1995; Brown and Goldstein, 1997; Weihofen et al., 2002), can catalyze cleavage of membrane spanning signal peptides (Saito et al., 2011). RseP is a site-2 protease that can cleave within TM segments of membrane proteins as well (Akiyama et al., 2004). It is a zinc metalloprotease (**Figure 9C**). The active site is in an aqueous environment close to the cytoplasmic surface of the membrane. It binds zinc and has an essential catalytic glutamic acid. Saito et al. (2011) showed that RseP is capable of degrading a number of signal peptides from a wide variety of preproteins such as OmpA, M13 procoat, LivJ, LivK, PhoA, TolC, SecM, suggesting that it significantly contributes to signal peptide degradation in *E. coli*. This group of proteases is fascinating since they catalyze proteolysis within the membrane.

3 TARGETING THE SIGNAL PEPTIDE PROTEASES AS ANTIBIOTIC TARGET

Signal peptidase I and II are attractive antibacterial drug targets (Paetzel et al., 2000; Rao et al., 2014; Craney and Romesberg, 2015; El Arnaout and Soulimane, 2019; Upert et al., 2021). SPase I is conserved in bacterial pathogens and has a novel active site architecture (Ser-Lys dyad) that can be targeted. Its active site location on the periplasmic side of the membrane makes it readily accessible (Smith and Romesberg, 2012). SPase II presents as another target candidate as lipoprotein signal peptidases are absent in the eukaryotic organism. The reduced efficacy of the existing antibiotics and the emergence of drug-resistant bacterial pathogens has led to the urgent demand for new treatments. This warrants the study of novel antibacterial targets such as SPase I and SPase II.

3.1 SPase I as Antibiotic Target

Various companies have centered on SPase I as an antibacterial target including Smithkline Beecham pharmaceuticals (now GlaxoSmithKline), Merck, Eli Lilly and Genentech. Some of the first inhibitors were the β-lactams, including clavams, thioclavams, penem carboxylate C6 Substituted esters, and allyl (5S,6S)-6-[R)-acetoxyethyl]penem-3-carboxylate (**Figure 10A**) and (5S)-tricyclic penem (Black and Bruton, 1998). Some of the peptide inhibitors such as, α-ketoamide peptides and decanoyl-PTANA-aldehyde (**Figure 10C**) were effective (Bruton et al., 2003; Buzder-Lantos et al., 2009).

Another promising class of inhibitors are the natural products Krisynomycin and Arylomycins. They are produced in *Streptomyces* by the non-ribosomal peptide synthesis. The Arylomycin family includes Arylomycin A and B (Höltzel et al., 2002; Schimana et al., 2002), and Arylomycin C (a lipoglycopeptide) (Kulanthaivel et al., 2004) discovered in the beginning of the 21st century. More recently, Arylomycin D was discovered (see below). Arylomycin D and its derivative M131, as well as Krisynomycin displayed significant antibacterial activity against the methicillin resistant *S. aureus* (MRSA) (Therien et al., 2012; Tan et al., 2020). Romesberg and others have developed a total synthesis of Arylomycin A2 (Roberts et al., 2007), Arylomycins B2 (Dufour et al., 2010; Roberts et al., 2011), Arylomycin C (Liu et al., 2011) and members of the Arylomycin D class (Therien et al., 2012; Tan et al., 2020).

Noteworthy, Smith and Romesberg (2012) proposed that Arylomycins may represent a class of latent antibiotics whose activity can be masked by mutations in the SPase I protease which otherwise would have rendered them susceptible. While Arylomycins normally have a narrow spectrum of antibiotic activity (**Figure 10B**), these antibiotics have the potential to have a much broader spectrum antibiotic activity against both Gram-positive and Gram-negative bacteria. Romesberg and coworkers initially investigated *Staphylococcus epidermidis* that was sensitive to Arylomycin A and isolated resistant strains which had mutations in SPase I (Ser to Pro changes at position 29). Intriguingly, the analogous Pro mutations in SPases that occurred during evolution, accounted for the natural resistance that is observed in *E. coli*, *P. aeruginosa*, and *S. aureus*. Strikingly, they found that a wide variety of bacteria that lacked this Pro substitution were sensitive to Arylomycin.

To gain insight into how to improve the potency of Ayrlomycin the structure of the *E. coli* SPase-Arylomycin complex was solved (Paetzel et al., 2004). Paetzel and coworkers revealed that the carboxylate of Arylomycin was bound to the catalytic serine, and the penultimate alanine of the inhibitor was localized within the S3 pocket. The structure also shows that residue 84 of *E. coli* SPase that confers resistance to the antibiotic is positioned near the amino-terminal part of the Arylomycin lipopeptide. A proline at the 84 position prevents the

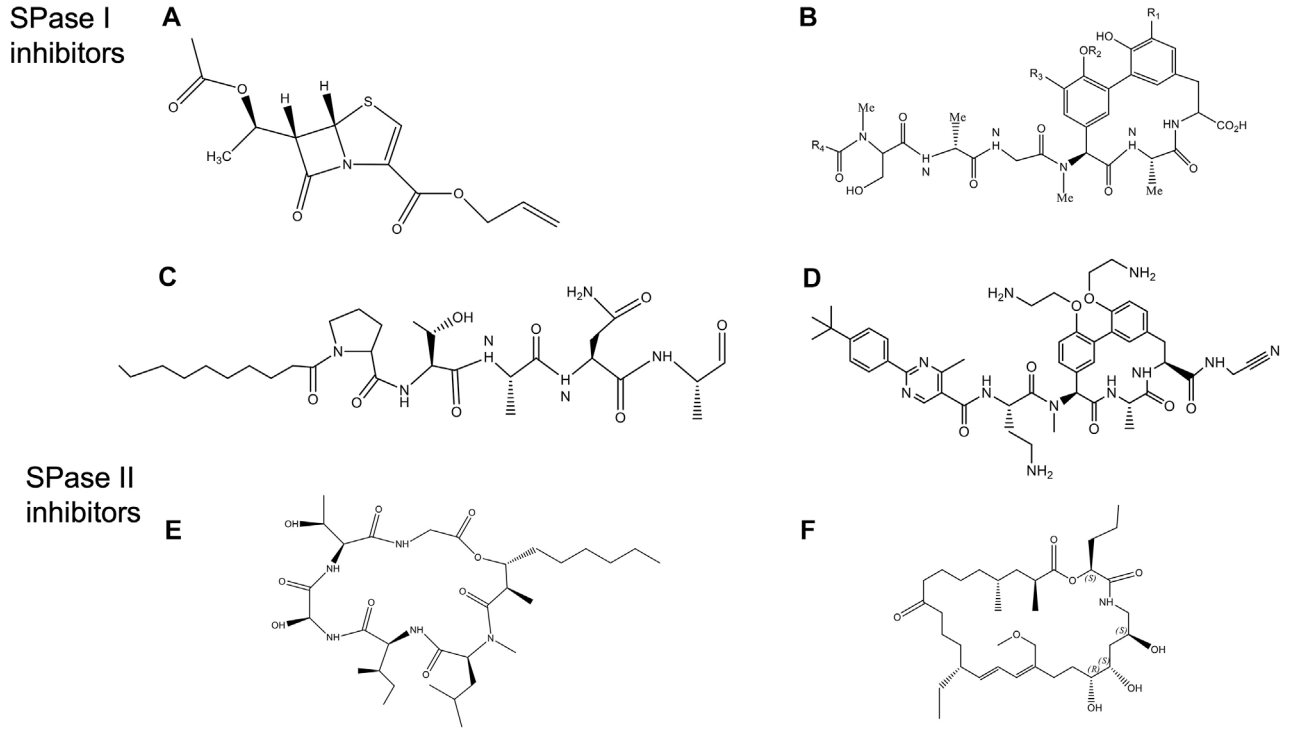

FIGURE 10 | Structures of Signal peptidase inhibitors (Rao et al., 2014). **(A)** allyl (5S,6S)-6 [(R)-acetoxyethyl]-penem-3-carboxylate. **(B)** Arylomycin A. **(C)** Decanoyl PTANA aldehyde. **(D)** GO775, an optimized arylomycin. **(E)** Globomycin. **(F)** Myxovirescin.

donation of one potential hydrogen bond from the backbone amide group on the β-strand 1 of SPase I to the carbonyl oxygen of the fatty acid of arylomycin. The presence of this extra H bond interaction would presumably increase the affinity of arylomycin to the SPase I proteins, making the bacteria more susceptible to the antibiotic.

A potential breakthrough in the antibiotic field by scientists at Genentech was the production of G0775, which represents a new class of Gram-negative antibiotics, that targets SPase I (**Figure 10D**) (Smith et al., 2018). This optimized arylomycin had several modifications including a replacement for the natural aliphatic tail, modification of the phenol groups of the tripeptide ring, and the introduction of an electrophilic warhead at the C-terminal carboxylate. GO775 was 500 times more potent than the arylomycin A-C16 against *E. coli* and *K. pneumoniae* which was normally not inhibited by arylomycin. It also had a potent activity against other pathogens. Additionally, it was effective in treating mice that were infected with Gram-negative bacterial pathogens, without any toxic impact on the mammalian cells. Intriguingly, the electrophilic warhead that was expected to covalently modify the active site serine instead modified the catalytic base lysine, by a novel mechanism. High affinity interaction between the target protein and the inhibitor made G0775 extremely active against multidrug resistant bacteria.

3.2 SPase II as Antibiotic Target

SPase II has been an attractive antibiotic target since the natural products globomycin (**Figure 10E**) and myxovirescin (**Figure 10F**) have been shown to have antibacterial activity (Inukai et al., 1978a; Inukai et al., 1978b; Nakajima et al., 1978; Xiao et al., 2012). Globomycin is a cyclic depsipeptide produced in *Streptomyces*. Myxovirescin is a secondary metabolite with a 28-membered macrocyclic lactone that is made in *myxobacteria*. Inhibition of SPase II is lethal in all Gram-negative bacteria.

Quite surprisingly, the structures of the *S. aureus* SPase II in complex with either globomycin or myxovirescin (Olatunji et al., 2020) revealed that the mode of inhibition is similar despite the two antibiotics interacting mostly with the protein on opposite sides of the substrate binding pocket. While both inhibitors bind to the catalytic Asp dyad with the hydroxyl group wedging in between (the β-hydroxy group of serine residue of globomycin and a 6 OH group from myxovirescin), most of the remaining parts of the molecule were on opposite sides of the substrate binding region. The interaction of the OH with the aspartic acid behaved like a non-cleavable tetrahedral analog (Olatunji et al., 2020). The hydroxyl groups of the antibiotics inhibited the enzyme by targeting the catalytic dyad aspartic acid residues.

To identify new inhibitors of SPase II, a high throughput screen was performed (Kitamura et al., 2018) where 646,275 molecules were analyzed using a SPase II FRET substrate assay. To validate their assay, they showed globomycin inhibited SPase II with an IC50 of 1.2 nM. Myxovirescin had a comparable or even better IC50. After identifying the best molecules from this initial screening, further optimization of the compound by medicinal chemistry resulted in an inhibitor of IC50 of 99 nM.

Although this was a potent SPase II inhibitor, it did not accrue antibacterial activity in *E. coli* unless it was used in combination with polymyxin B nonapeptide, which made the outer membrane more permeable to compounds.

More recently, the structure of Globomycin was optimized to improve its antibacterial activity against *E. coli* (Garland et al., 2020) and its permeability across the outer membrane. Taking advantage of the SPase-globomycin structure, modifications were made to alter the lipophilic side chains, the n-hexyl group, and the backbone to introduce a salt-bridge that interacted with the SPase II catalytic aspartic residues. Several compounds were obtained that had increased potency against several Gram-negative pathogens.

4 SUMMARY AND OUTLOOK

In conclusion, the signal peptide plays a universal central role in protein export in the three kingdoms of life. It orchestrates the sorting of proteins from the cytosol to the membrane. After targeting the protein to the membrane by binding to the receptor, the signal peptide activates the translocase such that the preprotein can make its way to the other side of the membrane.

Activation of the SecYEG channel occurs by binding of the signal peptide to the lateral gate, leading to a conformational change in the channel. Thus, signal peptide binding unlocks the Sec channel for translocation. In case of the Tat translocation machinery, the signal peptide provides the signal for the assembly of an oligomeric Tat translocase capable of transporting fully folded protein substrates. The key to triggering this process is the twin arginines within the signal peptide that binds to the TatBC receptor which switches on the Tat assembly process.

The final step in the translocation process is the removal of the signal peptide and its degradation. The hydrophobic region of the signal peptide positions the cleavage site for proteolysis by signal peptidases. After having served its purpose of protein navigation, the signal peptide is degraded by signal peptide hydrolases.

Owing to the decisive role the signal peptidases play in protein transport process, they have been appreciated recently as novel targets for antibiotics. The proteins so inhibited are involved in an array of bacterial fundamental processes essential for growth and viability of the bacteria/pathogen. The recent studies present Arylomycin and its derivatives such as G0775 as promising candidates for translation into new medicine to treat multidrug resistant pathogens. These compounds and the next generation of synthetic analogs will hopefully prove to be successful antibiotics to combat bacterial infections.

Yet, much remains to be discovered in the protein targeting and export field even 50 years after the Signal Hypothesis was proposed by Günter Blobel. Snapshots of the machineries engaged in substrate translocation are expected to provide new mechanistic insight into the processes of translocation dynamics and orientations of polytopic membrane proteins. Protein export has entered an exciting chapter, and more is anticipated in the days to come.

AUTHOR CONTRIBUTIONS

SK, HH, and RD all contributed to writing the paper.

FUNDING

This research is supported by a grant from National Science Foundation Grant MCB-1052033.

ACKNOWLEDGMENTS

I would like to thank Andreas Kuhn for valuable comments on the paper. In addition, I would like to thank Tracy Palmer for providing the coordinates of the TatABC model in the resting state.

REFERENCES

Akiyama, Y., Kanehara, K., and Ito, K. (2004). RseP (YaeL), an *Escherichia coli* RIP Protease, Cleaves Transmembrane Sequences. *Embo J.* 23, 4434–4442. doi:10.1038/sj.emboj.7600449

Akopian, D., Shen, K., Zhang, X., and Shan, S.-o. (2013). Signal Recognition Particle: An Essential Protein-Targeting Machine. *Annu. Rev. Biochem.* 82, 693–721. doi:10.1146/annurev-biochem-072711-164732

Alami, M., Lüke, I., Deitermann, S., Eisner, G., Koch, H.-G., Brunner, J., et al. (2003). Differential Interactions between a Twin-Arginine Signal Peptide and its Translocase in *Escherichia coli*. *Mol. Cell* 12, 937–946. doi:10.1016/s1097-2765(03)00398-8

Alcock, F., Stansfeld, P. J., Basit, H., Habersetzer, J., Baker, M. A., Palmer, T., et al. (2016). Assembling the Tat Protein Translocase. *Elife* 5, e20718. doi:10.7554/eLife.20718

Allen, W. J., Corey, R. A., Oatley, P., Sessions, R. B., Baldwin, S. A., Radford, S. E., et al. (2016). Two-Way Communication between SecY and SecA Suggests a Brownian Ratchet Mechanism for Protein Translocation. *Elife* 5, e15598. doi:10.7554/eLife.15598

Allen, W. J., Watkins, D. W., Dillingham, M. S., and Collinson, I. (2020). Refined Measurement of SecA-Driven Protein Secretion Reveals that Translocation Is Indirectly Coupled to ATP Turnover. *Proc. Natl. Acad. Sci. U.S.A.* 117, 31808–31816. doi:10.1073/pnas.2010906117

Andersson, H., and von Heijne, G. (1993). Sec Dependent and Sec Independent Assembly of *E. coli* Inner Membrane Proteins: The Topological Rules Depend on Chain Length. *EMBO J.* 12, 683–691. doi:10.1002/j.1460-2075.1993.tb05702.x

Anghel, S. A., McGilvray, P. T., Hegde, R. S., and Keenan, R. J. (2017). Identification of Oxa1 Homologs Operating in the Eukaryotic Endoplasmic Reticulum. *Cell Rep.* 21, 3708–3716. doi:10.1016/j.celrep.2017.12.006

Arkowitz, R. A., and Wickner, W. (1994). SecD and SecF Are Required for the Proton Electrochemical Gradient Stimulation of Preprotein Translocation. *EMBO J.* 13, 954–963. doi:10.1002/j.1460-2075.1994.tb06340.x

Aschtgen, M. S., Zoued, A., Lloubès, R., Journet, L., and Cascales, E. (2012). The C-Tail Anchored TssL Subunit, an Essential Protein of the Enteroaggregative *Escherichia coli* Sci-1 Type VI Secretion System, Is Inserted by YidC. *Microbiologyopen* 1, 71–82. doi:10.1002/mbo3.9

Bassford, P., and Beckwith, J. (1979). *Escherichia coli* Mutants Accumulating the Precursor of a Secreted Protein in the Cytoplasm. *Nature* 277, 538–541. doi:10.1038/277538a0

Bauer, B. W., and Rapoport, T. A. (2009). Mapping Polypeptide Interactions of the SecA ATPase during Translocation. *Proc. Natl. Acad. Sci. U. S. A.* 106, 20800–20805. doi:10.1073/pnas.0910550106

Bauer, B. W., Shemesh, T., Chen, Y., and Rapoport, T. A. (2014). A "Push and Slide" Mechanism Allows Sequence-Insensitive Translocation of Secretory Proteins by the SecA ATPase. *Cell* 157, 1416–1429. doi:10.1016/j.cell.2014.03.063

Beck, K., Eisner, G., Trescher, D., Dalbey, R. E., Brunner, J., and Müller, M. (2001). YidC, an Assembly Site for Polytopic *Escherichia coli* Membrane Proteins Located in Immediate Proximity to the SecYE Translocon and Lipids. *EMBO Rep.* 2, 709–714. doi:10.1093/embo-reports/kve154

Behrendt, J., and Brüser, T. (2014). The TatBC Complex of the Tat Protein Translocase in *Escherichia coli* and its Transition to the Substrate-Bound TatABC Complex. *Biochemistry* 53, 2344–2354. doi:10.1021/bi500169s

Berks, B. C. (1996). A Common Export Pathway for Proteins Binding Complex Redox Cofactors? *Mol. Microbiol.* 22, 393–404. doi:10.1046/j.1365-2958.1996.00114.x

Berks, B. C. (2015). The Twin-Arginine Protein Translocation Pathway. *Annu. Rev. Biochem.* 84, 843–864. doi:10.1146/annurev-biochem-060614-034251

Bischoff, L., Wickles, S., Berninghausen, O., van der Sluis, E. O., and Beckmann, R. (2014). Visualization of a Polytopic Membrane Protein during SecY-Mediated Membrane Insertion. *Nat. Commun.* 5, 4103. doi:10.1038/ncomms5103

Black, M. T., and Bruton, G. (1998). Inhibitors of Bacterial Signal Peptidases. *Curr. Pharm. Des.* 4, 133–154.

Bogsch, E., Brink, S., and Robinson, C. (1997). Pathway Specificity for a ΔpH-dependent Precursor Thylakoid Lumen Protein Is Governed by a 'Sec-Avoidance' Motif in the Transfer Peptide and a 'Sec-Incompatible' Mature Protein. *Embo J.* 16, 3851–3859. doi:10.1093/emboj/16.13.3851

Bogsch, E. G., Sargent, F., Stanley, N. R., Berks, B. C., Robinson, C., and Palmer, T. (1998). An Essential Component of a Novel Bacterial Protein Export System with Homologues in Plastids and Mitochondria. *J. Biol. Chem.* 273, 18003–18006. doi:10.1074/jbc.273.29.18003

Bolhuis, A., Mathers, J. E., Thomas, J. D., Barrett, C. M. L., and Robinson, C. (2001). TatB and TatC Form a Functional and Structural Unit of the Twin-Arginine Translocase from *Escherichia coli*. *J. Biol. Chem.* 276, 20213–20219. doi:10.1074/jbc.m100682200

Bolhuis, A., Matzen, A., Hyyryläinen, H.-L., Kontinen, V. P., Meima, R., Chapuis, J., et al. (1999). Signal Peptide Peptidase- and ClpP-like Proteins of Bacillus Subtilis Required for Efficient Translocation and Processing of Secretory Proteins. *J. Biol. Chem.* 274, 24585–24592. doi:10.1074/jbc.274.35.24585

Bonardi, F., Halza, E., Walko, M., Du Plessis, F., Nouwen, N., Feringa, B. L., et al. (2011). Probing the SecYEG Translocation Pore Size with Preproteins Conjugated with Sizable Rigid Spherical Molecules. *Proc. Natl. Acad. Sci. U. S. A.* 108, 7775–7780. doi:10.1073/pnas.1101705108

Bornemann, T., Jöckel, J., Rodnina, M. V., and Wintermeyer, W. (2008). Signal Sequence-independent Membrane Targeting of Ribosomes Containing Short Nascent Peptides within the Exit Tunnel. *Nat. Struct. Mol. Biol.* 15, 494–499. doi:10.1038/nsmb.1402

Botte, M., Zaccai, N. R., Nijeholt, J. L., Martin, R., Knoops, K., Papai, G., et al. (2016). A Central Cavity Within the Holo-Translocon Suggests a Mechanism for Membrane Protein Insertion. *Sci. Rep.* 6, 38399.

Brown, M. S., and Goldstein, J. L. (1997). The SREBP Pathway: Regulation of Cholesterol Metabolism by Proteolysis of a Membrane-Bound Transcription Factor. *Cell* 89, 331–340. doi:10.1016/s0092-8674(00)80213-5

Brüser, T., and Sanders, C. (2003). An Alternative Model of the Twin Arginine Translocation System. *Microbiol. Res.* 158, 7–17. doi:10.1078/0944-5013-00176

Bruton, G., Huxley, A., O'Hanlon, P., Orlek, B., Eggleston, D., Humphries, J., et al. (2003). Lipopeptide Substrates for SpsB, the *Staphylococcus aureus* Type I Signal Peptidase: Design, Conformation and Conversion to α-ketoamide Inhibitors. *Eur. J. Med. Chem.* 38, 351–356. doi:10.1016/s0223-5234(03)00040-0

Buchanan, G., Sargent, F., Berks, B., and Palmer, T. (2001). A Genetic Screen for Suppressors of *Escherichia coli* Tat Signal Peptide Mutations Establishes a Critical Role for the Second Arginine within the Twin-Arginine Motif. *Archives Microbiol.* 177, 107–112. doi:10.1007/s00203-001-0366-2

Buzder-Lantos, P., Bockstael, K., Anné, J., and Herdewijn, P. (2009). Substrate Based Peptide Aldehyde Inhibits Bacterial Type I Signal Peptidase. *Bioorg. Med. Chem. Lett.* 19, 2880–2883. doi:10.1016/j.bmcl.2009.03.064

Castanié-Cornet, M.-P., Bruel, N., and Genevaux, P. (2014). Chaperone Networking Facilitates Protein Targeting to the Bacterial Cytoplasmic Membrane. *Biochimica Biophysica Acta (BBA) - Mol. Cell Res.* 1843, 1442–1456. doi:10.1016/j.bbamcr.2013.11.007

Catipovic, M. A., Bauer, B. W., Loparo, J. J., and Rapoport, T. A. (2019). Protein Translocation by the SecA ATPase Occurs by a Power-Stroke Mechanism. *EMBO J.* 38, e101140. doi:10.15252/embj.2018101140

Catipovic, M. A., and Rapoport, T. A. (2020). Protease Protection Assays Show Polypeptide Movement into the SecY Channel by Power Strokes of the SecA ATPase. *EMBO Rep.* 21, e50905. doi:10.15252/embr.202050905

Celebi, N., Yi, L., J. Facey, S., Kuhn, A., and Dalbey, R. E. (2006). Membrane Biogenesis of Subunit II of Cytochrome Bo Oxidase: Contrasting Requirements for Insertion of N-Terminal and C-Terminal Domains. *J. Mol. Biol.* 357, 1428–1436. doi:10.1016/j.jmb.2006.01.030

Chaddock, A. M., Mant, A., Karnauchov, I., Brink, S., Herrmann, R. G., Klösgen, R. B., et al. (1995). A New Type of Signal Peptide: Central Role of a Twin-Arginine Motif in Transfer Signals for the Delta pH-dependent Thylakoidal Protein Translocase. *EMBO J.* 14, 2715–2722. doi:10.1002/j.1460-2075.1995.tb07272.x

Chatzi, K. E., Sardis, M. F., Economou, A., and Karamanou, S. (2014). SecA-mediated Targeting and Translocation of Secretory Proteins. *Biochimica Biophysica Acta (BBA) - Mol. Cell Res.* 1843, 1466–1474. doi:10.1016/j.bbamcr.2014.02.014

Chen, M., Samuelson, J. C., Jiang, F., Muller, M., Kuhn, A., and Dalbey, R. E. (2002). Direct Interaction of YidC with the Sec-independent Pf3 Coat Protein during its Membrane Protein Insertion. *J. Biol. Chem.* 277, 7670–7675. doi:10.1074/jbc.m110644200

Chen, Y., Capponi, S., Zhu, L., Gellenbeck, P., Freites, J. A., White, S. H., et al. (2017). YidC Insertase of *Escherichia coli*: Water Accessibility and Membrane Shaping. *Structure* 25, 1403–1414. e1403. doi:10.1016/j.str.2017.07.008

Chen, Y., and Dalbey, R. E. (2018). Oxa1 Superfamily: New Members Found in the ER. *Trends Biochem. Sci.* 43, 151–153. doi:10.1016/j.tibs.2017.12.005

Chen, Y., Soman, R., Shanmugam, S. K., Kuhn, A., and Dalbey, R. E. (2014). The Role of the Strictly Conserved Positively Charged Residue Differs Among the Gram-Positive, Gram-Negative, and Chloroplast YidC Homologs. *J. Biol. Chem.* 289, 35656–35667. doi:10.1074/jbc.m114.595082

Chen, Y., Sotomayor, M., Capponi, S., Hariharan, B., Sahu, I. D., Haase, M., et al. (2022). A Hydrophilic Microenvironment in the Substrate-Translocating Groove of the YidC Membrane Insertase Is Essential for Enzyme Function. *J. Biol. Chem.* 298, 101690. doi:10.1016/j.jbc.2022.101690

Chun, S. Y., and Randall, L. L. (1994). *In Vivo* studies of the Role of SecA during Protein Export in *Escherichia coli*. *J. Bacteriol.* 176, 4197–4203. doi:10.1128/jb.176.14.4197-4203.1994

Cline, K., and Mori, H. (2001). Thylakoid ΔpH-dependent Precursor Proteins Bind to a cpTatC-Hcf106 Complex before Tha4-dependent Transport. *J. Cell Biol.* 154, 719–730. doi:10.1083/jcb.200105149

Crane, J. M., and Randall, L. L. (2017). The Sec System: Protein Export in *Escherichia coli*. *EcoSal Plus* 7, 1. doi:10.1128/ecosalplus.ESP-0002-2017

Craney, A., and Romesberg, F. E. (2015). The Inhibition of Type I Bacterial Signal Peptidase: Biological Consequences and Therapeutic Potential. *Bioorg. Med. Chem. Lett.* 25, 4761–4766. doi:10.1016/j.bmcl.2015.07.072

Cranford-Smith, T., and Huber, D. (2018). The Way Is the Goal: How SecA Transports Proteins across the Cytoplasmic Membrane in Bacteria. *FEMS Microbiol. Lett.* 365, fny093. doi:10.1093/femsle/fny093

Cristobal, S., de Gier, J. W., Nielsen, H., and von Heijne, G. (1999). Competition between Sec- and TAT-dependent Protein Translocation in *Escherichia coli*. *Embo J.* 18, 2982–2990. doi:10.1093/emboj/18.11.2982

Crooke, E., Guthrie, B., Lecker, S., Lill, R., and Wickner, W. (1988). ProOmpA Is Stabilized for Membrane Translocation by Either Purified *E. coli* Trigger Factor or Canine Signal Recognition Particle. *Cell* 54, 1003–1011. doi:10.1016/0092-8674(88)90115-8

Cymer, F., von Heijne, G., and White, S. H. (2015). Mechanisms of Integral Membrane Protein Insertion and Folding. *J. Mol. Biol.* 427, 999–1022. doi:10.1016/j.jmb.2014.09.014

Dalbey, R. E., and Wickner, W. (1985). Leader Peptidase Catalyzes the Release of Exported Proteins from the Outer Surface of the *Escherichia coli* Plasma Membrane. *J. Biol. Chem.* 260, 15925–15931. doi:10.1016/s0021-9258(17)36347-0

Date, T. (1983). Demonstration by a Novel Genetic Technique that Leader Peptidase Is an Essential Enzyme of *Escherichia coli*. *J. Bacteriol.* 154, 76–83. doi:10.1128/jb.154.1.76-83.1983

Date, T., Goodman, J. M., and Wickner, W. T. (1980). Procoat, the Precursor of M13 Coat Protein, Requires an Electrochemical Potential for Membrane Insertion. *Proc. Natl. Acad. Sci. U.S.A.* 77, 4669–4673. doi:10.1073/pnas.77.8.4669

De Geyter, J., Portaliou, A. G., Srinivasu, B., Krishnamurthy, S., Economou, A., and Karamanou, S. (2020). Trigger Factor Is a Bona Fide Secretory Pathway Chaperone that Interacts with SecB and the Translocase. *EMBO Rep.* 21, e49054. doi:10.15252/embr.201949054

Deitermann, S., Sprie, G. S., and Koch, H.-G. (2005). A Dual Function for SecA in the Assembly of Single Spanning Membrane Proteins in *Escherichia coli*. *J. Biol. Chem.* 280, 39077–39085. doi:10.1074/jbc.m509647200

DeLisa, M. P., Samuelson, P., Palmer, T., and Georgiou, G. (2002). Genetic Analysis of the Twin Arginine Translocator Secretion Pathway in Bacteria. *J. Biol. Chem.* 277, 29825–29831. doi:10.1074/jbc.m201956200

Dev, I. K., and Ray, P. H. (1984). Rapid Assay and Purification of a Unique Signal Peptidase that Processes the Prolipoprotein from *Escherichia coli* B. *J. Biol. Chem.* 259, 11114–11120. doi:10.1016/s0021-9258(18)90629-0

Do, H., Falcone, D., Lin, J., Andrews, D. W., and Johnson, A. E. (1996). The Cotranslational Integration of Membrane Proteins into the Phospholipid Bilayer Is a Multistep Process. *Cell* 85, 369–378. doi:10.1016/s0092-8674(00)81115-0

Dufour, J., Neuville, L., and Zhu, J. (2010). Intramolecular Suzuki-Miyaura Reaction for the Total Synthesis of Signal Peptidase Inhibitors, Arylomycins A2 and B2. *Chem. Eur. J.* 16, 10523–10534. doi:10.1002/chem.201000924

Economou, A., and Wickner, W. (1994). SecA Promotes Preprotein Translocation by Undergoing ATP-Driven Cycles of Membrane Insertion and Deinsertion. *Cell* 78, 835–843. doi:10.1016/s0092-8674(94)90582-7

El Arnaout, T., and Soulimane, T. (2019). Targeting Lipoprotein Biogenesis: Considerations towards Antimicrobials. *Trends Biochem. Sci.* 44, 701–715. doi:10.1016/j.tibs.2019.03.007

Emr, S. D., Schwartz, M., and Silhavy, T. J. (1978). Mutations Altering the Cellular Localization of the Phage Lambda Receptor, an *Escherichia coli* Outer Membrane Protein. *Proc. Natl. Acad. Sci. U.S.A.* 75, 5802–5806. doi:10.1073/pnas.75.12.5802

Erlandson, K. J., Miller, S. B. M., Nam, Y., Osborne, A. R., Zimmer, J., and Rapoport, T. A. (2008). A Role for the Two-Helix Finger of the SecA ATPase in Protein Translocation. *Nature* 455, 984–987. doi:10.1038/nature07439

Facey, S. J., Neugebauer, S. A., Krauss, S., and Kuhn, A. (2007). The Mechanosensitive Channel Protein MscL Is Targeted by the SRP to the Novel YidC Membrane Insertion Pathway of *Escherichia coli*. *J. Mol. Biol.* 365, 995–1004. doi:10.1016/j.jmb.2006.10.083

Feng, L., Yan, H., Wu, Z., Yan, N., Wang, Z., Jeffrey, P. D., et al. (2007). Structure of a Site-2 Protease Family Intramembrane Metalloprotease. *Science* 318, 1608–1612.

Ferbitz, L., Maier, T., Patzelt, H., Bukau, B., Deuerling, E., and Ban, N. (2004). Trigger Factor in Complex with the Ribosome Forms a Molecular Cradle for Nascent Proteins. *Nature* 431, 590–596. doi:10.1038/nature02899

Frain, K. M., Robinson, C., and van Dijl, J. M. (2019). Transport of Folded Proteins by the Tat System. *Protein J.* 38, 377–388. doi:10.1007/s10930-019-09859-y

Garland, K., Pantua, H., Braun, M.-G., Burdick, D. J., Castanedo, G. M., Chen, Y.-C., et al. (2020). Optimization of Globomycin Analogs as Novel Gram-Negative Antibiotics. *Bioorg. Med. Chem. Lett.* 30, 127419. doi:10.1016/j.bmcl.2020.127419

Gelis, I., Bonvin, A. M. J. J., Keramisanou, D., Koukaki, M., Gouridis, G., Karamanou, S., et al. (2007). Structural Basis for Signal-Sequence Recognition by the Translocase Motor SecA as Determined by NMR. *Cell* 131, 756–769. doi:10.1016/j.cell.2007.09.039

Geng, Y., Kedrov, A., Caumanns, J. J., Crevenna, A. H., Lamb, D. C., Beckmann, R., et al. (2015). Role of the Cytosolic Loop C2 and the C Terminus of YidC in Ribosome Binding and Insertion Activity. *J. Biol. Chem.* 290, 17250–17261. doi:10.1074/jbc.m115.650309

Gérard, F., and Cline, K. (2006). Efficient Twin Arginine Translocation (Tat) Pathway Transport of a Precursor Protein Covalently Anchored to its Initial cpTatC Binding Site. *J. Biol. Chem.* 281, 6130–6135. doi:10.1074/jbc.m512733200

Goder, V., and Spiess, M. (2003). Molecular Mechanism of Signal Sequence Orientation in the Endoplasmic Reticulum. *EMBO J.* 22, 3645–3653. doi:10.1093/emboj/cdg361

Gogala, M., Becker, T., Beatrix, B., Armache, J.-P., Barrio-Garcia, C., Berninghausen, O., et al. (2014). Structures of the Sec61 Complex Engaged in Nascent Peptide Translocation or Membrane Insertion. *Nature* 506, 107–110. doi:10.1038/nature12950

Gohlke, U., Pullan, L., McDevitt, C. A., Porcelli, I., de Leeuw, E., Palmer, T., et al. (2005). The TatA Component of the Twin-Arginine Protein Transport System Forms Channel Complexes of Variable Diameter. *Proc. Natl. Acad. Sci. U.S.A.* 102, 10482–10486. doi:10.1073/pnas.0503558102

Grady, L. M., Michtavy, J., and Oliver, D. B. (2012). Characterization of the *Escherichia coli* SecA Signal Peptide-Binding Site. *J. Bacteriol.* 194, 307–316. doi:10.1128/jb.06150-11

Grudnik, P., Bange, G., and Sinning, I. (2009). Protein Targeting by the Signal Recognition Particle. *Biol. Chem.* 390, 775–782. doi:10.1515/bc.2009.102

Gupta, S. D., and Wu, H. C. (1991). Identification and Subcellular Localization of apolipoproteinN-Acyltransferase inEscherichia Coli. *FEMS Microbiol. Lett.* 78, 37–42. doi:10.1111/j.1574-6968.1991.tb04413.x

Habersetzer, J., Moore, K., Cherry, J., Buchanan, G., Stansfeld, P. J., and Palmer, T. (2017). Substrate-triggered Position Switching of TatA and TatB during Tat Transport in *Escherichia coli*. *Open Biol.* 7, 170091. doi:10.1098/rsob.170091

Hariharan, B., Pross, E., Soman, R., Kaushik, S., Kuhn, A., and Dalbey, R. E. (2021). Polarity/charge as a Determinant of Translocase Requirements for Membrane Protein Insertion. *Biochimica Biophysica Acta (BBA) - Biomembr.* 1863, 183502. doi:10.1016/j.bbamem.2020.183502

Hartl, F.-U., Lecker, S., Schiebel, E., Hendrick, J. P., and Wickner, W. (1990). The Binding Cascade of SecB to SecA to SecYE Mediates Preprotein Targeting to the *E. coli* Plasma Membrane. *Cell* 63, 269–279. doi:10.1016/0092-8674(90)90160-g

Hartmann, E., Sommer, T., Prehn, S., Görlich, D., Jentsch, S., and Rapoport, T. A. (1994). Evolutionary Conservation of Components of the Protein Translocation Complex. *Nature* 367, 654–657. doi:10.1038/367654a0

Hatzixanthis, K., Palmer, T., and Sargent, F. (2003). A Subset of Bacterial Inner Membrane Proteins Integrated by the Twin-Arginine Translocase. *Mol. Microbiol.* 49, 1377–1390. doi:10.1046/j.1365-2958.2003.03642.x

He, H., Kuhn, A., and Dalbey, R. E. (2020). Tracking the Stepwise Movement of a Membrane-Inserting Protein *In Vivo*. *J. Mol. Biol.* 432, 484–496. doi:10.1016/j.jmb.2019.10.010

Hegde, R. S., and Bernstein, H. D. (2006). The Surprising Complexity of Signal Sequences. *Trends Biochem. Sci.* 31, 563–571. doi:10.1016/j.tibs.2006.08.004

Hegde, R. S., and Keenan, R. J. (2021). The Mechanisms of Integral Membrane Protein Biogenesis. *Nat. Rev. Mol. Cell Biol.* 23 (2), 107–124. doi:10.1038/s41580-021-00413-2

Heijne, G. (1983). Patterns of Amino Acids Near Signal-Sequence Cleavage Sites. *Eur. J. Biochem.* 133, 17–21. doi:10.1111/j.1432-1033.1983.tb07424.x

Heinrich, S. U., Mothes, W., Brunner, J., and Rapoport, T. A. (2000). The Sec61p Complex Mediates the Integration of a Membrane Protein by Allowing Lipid Partitioning of the Transmembrane Domain. *Cell* 102, 233–244. doi:10.1016/s0092-8674(00)00028-3

Heinrich, S. U., and Rapoport, T. A. (2003). Cooperation of Transmembrane Segments during the Integration of a Double-Spanning Protein into the ER Membrane. *EMBO J.* 22, 3654–3663. doi:10.1093/emboj/cdg346

Hennon, S. W., Soman, R., Zhu, L., and Dalbey, R. E. (2015). YidC/Alb3/Oxa1 Family of Insertases. *J. Biol. Chem.* 290, 14866–14874. doi:10.1074/jbc.r115.638171

Hessa, T., Kim, H., Bihlmaier, K., Lundin, C., Boekel, J., Andersson, H., et al. (2005). Recognition of Transmembrane Helices by the Endoplasmic Reticulum Translocon. *Nature* 433, 377–381. doi:10.1038/nature03216

Hessa, T., Meindl-Beinker, N. M., Bernsel, A., Kim, H., Sato, Y., Lerch-Bader, M., et al. (2007). Molecular Code for Transmembrane-Helix Recognition by the Sec61 Translocon. *Nature* 450, 1026–1030. doi:10.1038/nature06387

Hoffmann, A., Bukau, B., and Kramer, G. (2010). Structure and Function of the Molecular Chaperone Trigger Factor. *Biochimica Biophysica Acta (BBA) - Mol. Cell Res.* 1803, 650–661. doi:10.1016/j.bbamcr.2010.01.017

Holtkamp, W., Lee, S., Bornemann, T., Senyushkina, T., Rodnina, M. V., and Wintermeyer, W. (2012). Dynamic Switch of the Signal Recognition Particle

from Scanning to Targeting. *Nat. Struct. Mol. Biol.* 19, 1332–1337. doi:10.1038/nsmb.2421

Höltzel, A., Schmid, D. G., Nicholson, G. J., Stevanovic, S., Schimana, J., Gebhardt, K., et al. (2002). Arylomycins A and B, New Biaryl-Bridged Lipopeptide Antibiotics Produced by Streptomyces Sp. Tue 6075. II. Structure Elucidation. *J. Antibiot.* 55, 571–577. doi:10.7164/antibiotics.55.571

Houben, E. N. G., ten Hagen-Jongman, C. M., Brunner, J., Oudega, B., and Luirink, J. (2004). The Two Membrane Segments of Leader Peptidase Partition One by One into the Lipid Bilayer via a Sec/YidC Interface. *EMBO Rep.* 5, 970–975. doi:10.1038/sj.embor.7400261

Huang, C., Rossi, P., Saio, T., and Kalodimos, C. G. (2016). Structural Basis for the Antifolding Activity of a Molecular Chaperone. *Nature* 537, 202–206. doi:10.1038/nature18965

Huber, D., Jamshad, M., Hanmer, R., Schibich, D., Döring, K., Marcomini, I., et al. (2017). SecA Cotranslationally Interacts with Nascent Substrate Proteins *In Vivo*. *J. Bacteriol.* 199, e00622–16. doi:10.1128/JB.00622-16

Huber, D., Rajagopalan, N., Preissler, S., Rocco, M. A., Merz, F., Kramer, G., et al. (2011). SecA Interacts with Ribosomes in Order to Facilitate Posttranslational Translocation in Bacteria. *Mol. Cell* 41, 343–353. doi:10.1016/j.molcel.2010.12.028

Hunt, J. F., Weinkauf, S., Henry, L., Fak, J. J., McNicholas, P., Oliver, D. B., et al. (2002). Nucleotide Control of Interdomain Interactions in the Conformational Reaction Cycle of SecA. *Science* 297, 2018–2026. doi:10.1126/science.1074424

Hussain, M., Ichihara, S., and Mizushima, S. (1982). Mechanism of Signal Peptide Cleavage in the Biosynthesis of the Major Lipoprotein of the *Escherichia coli* Outer Membrane. *J. Biol. Chem.* 257, 5177–5182. doi:10.1016/s0021-9258(18)34652-0

Ichihara, S., Beppu, N., and Mizushima, S. (1984). Protease IV, a Cytoplasmic Membrane Protein of *Escherichia coli*, Has Signal Peptide Peptidase Activity. *J. Biol. Chem.* 259, 9853–9857. doi:10.1016/s0021-9258(17)42778-5

Iino, T., Takahashi, M., and Sako, T. (1987). Role of Amino-Terminal Positive Charge on Signal Peptide in Staphylokinase Export across the Cytoplasmic Membrane of *Escherichia coli*. *J. Biol. Chem.* 262, 7412–7417. doi:10.1016/s0021-9258(18)48252-x

Ilbert, M., Méjean, V., Giudici-Orticoni, M.-T., Samama, J.-P., and Iobbi-Nivol, C. (2003). Involvement of a Mate Chaperone (TorD) in the Maturation Pathway of Molybdoenzyme TorA. *J. Biol. Chem.* 278, 28787–28792. doi:10.1074/jbc.m302730200

Inukai, M., Nakajima, M., Osawa, M., Haneishi, T., and Arai, M. (1978). Globomycin, a New Peptide Antibiotic with Spheroplast-Forming Activity. II. Isolation and Physico-Chemical and Biological Characterization. *J. Antibiot.* 31, 421–425. doi:10.7164/antibiotics.31.421

Inukai, M., Takeuchi, M., Shimizu, K., and Arai, M. (1978). Mechanism of Action of Globomycin. *J. Antibiot.* 31, 1203–1205. doi:10.7164/antibiotics.31.1203

Ismail, N., Hedman, R., Schiller, N., and von Heijne, G. (2012). A Biphasic Pulling Force Acts on Transmembrane Helices during Translocon-Mediated Membrane Integration. *Nat. Struct. Mol. Biol.* 19, 1018–1022. doi:10.1038/nsmb.2376

Jack, R. L., Buchanan, G., Dubini, A., Hatzixanthis, K., Palmer, T., and Sargent, F. (2004). Coordinating Assembly and Export of Complex Bacterial Proteins. *Embo J.* 23, 3962–3972. doi:10.1038/sj.emboj.7600409

Jongbloed, J. D. H., Grieger, U., Antelmann, H., Hecker, M., Nijland, R., Bron, S., et al. (2004). Two Minimal Tat Translocases in Bacillus. *Mol. Microbiol.* 54, 1319–1325. doi:10.1111/j.1365-2958.2004.04341.x

Karamanou, S., Vrontou, E., Sianidis, G., Baud, C., Roos, T., Kuhn, A., et al. (1999). A Molecular Switch in SecA Protein Couples ATP Hydrolysis to Protein Translocation. *Mol. Microbiol.* 34, 1133–1145. doi:10.1046/j.1365-2958.1999.01686.x

Karamyshev, A. L., and Johnson, A. E. (2005). Selective SecA Association with Signal Sequences in Ribosome-Bound Nascent Chains. *J. Biol. Chem.* 280, 37930–37940. doi:10.1074/jbc.m509100200

Kater, L., Frieg, B., Berninghausen, O., Gohlke, H., Beckmann, R., and Kedrov, A. (2019). Partially Inserted Nascent Chain Unzips the Lateral Gate of the Sec Translocon. *EMBO Rep.* 20, e48191. doi:10.15252/embr.201948191

Kedrov, A., Wickles, S., Crevenna, A. H., van der Sluis, E. O., Buschauer, R., Berninghausen, O., et al. (2016). Structural Dynamics of the YidC:Ribosome Complex during Membrane Protein Biogenesis. *Cell Rep.* 17, 2943–2954. doi:10.1016/j.celrep.2016.11.059

Keller, R., de Keyzer, J., Driessen, A. J. M., and Palmer, T. (2012). Co-operation between Different Targeting Pathways during Integration of a Membrane Protein. *J. Cell Biol.* 199, 303–315. doi:10.1083/jcb.201204149

Kiefer, D., and Kuhn, A. (2018). YidC-mediated Membrane Insertion. *FEMS Microbiol. Lett.* 365, 1. doi:10.1093/femsle/fny106

Kim, A. C., Oliver, D. C., and Paetzel, M. (2008). Crystal Structure of a Bacterial Signal Peptide Peptidase. *J. Mol. Biol.* 376, 352–366. doi:10.1016/j.jmb.2007.11.080

Kitamura, S., Owensby, A., Wall, D., and Wolan, D. W. (2018). Lipoprotein Signal Peptidase Inhibitors with Antibiotic Properties Identified through Design of a Robust *In Vitro* HT Platform. *Cell Chem. Biol.* 25, 301–308. e312. doi:10.1016/j.chembiol.2017.12.011

Klein, P., Somorjai, R. L., and Lau, P. C. K. (1988). Distinctive Properties of Signal Sequences from Bacterial Lipoproteins. *Protein Eng. Des. Sel.* 2, 15–20. doi:10.1093/protein/2.1.15

Klenner, C., and Kuhn, A. (2012). Dynamic Disulfide Scanning of the Membrane-Inserting Pf3 Coat Protein Reveals Multiple YidC Substrate Contacts. *J. Biol. Chem.* 287, 3769–3776. doi:10.1074/jbc.m111.307223

Klenner, C., Yuan, J., Dalbey, R. E., and Kuhn, A. (2008). The Pf3 Coat Protein Contacts TM1 and TM3 of YidC during Membrane Biogenesis. *FEBS Lett.* 582, 3967–3972. doi:10.1016/j.febslet.2008.10.044

Knüpffer, L., Fehrenbach, C., Denks, K., Erichsen, V., Petriman, N. A., and Koch, H. G. (2019). Molecular Mimicry of SecA and Signal Recognition Particle Binding to the Bacterial Ribosome. *mBio* 10, 1. doi:10.1128/mBio.01317-19

Kol, S., Majczak, W., Heerlien, R., van der Berg, J. P., Nouwen, N., and Driessen, A. J. M. (2009). Subunit a of the F1F0 ATP Synthase Requires YidC and SecYEG for Membrane Insertion. *J. Mol. Biol.* 390, 893–901. doi:10.1016/j.jmb.2009.05.074

Kol, S., Turrell, B. R., de Keyzer, J., van der Laan, M., Nouwen, N., and Driessen, A. J. M. (2006). YidC-mediated Membrane Insertion of Assembly Mutants of Subunit C of the F1F0 ATPase. *J. Biol. Chem.* 281, 29762–29768. doi:10.1074/jbc.m605317200

Komar, J., Alvira, S., Schulze, R. J., Martin, R., Lycklama a Nijeholt, J. A., Lee, S. C., et al. (2016). Membrane Protein Insertion and Assembly by the Bacterial Holo-Translocon SecYEG-SecDF-YajC-YidC. *Biochem. J.* 473, 3341–3354. doi:10.1042/bcj20160545

Kourtz, L., and Oliver, D. (2000). Tyr-326 Plays a Critical Role in Controlling SecA-Preprotein Interaction. *Mol. Microbiol.* 37, 1342–1356. doi:10.1046/j.1365-2958.2000.02078.x

Kuhn, A. (1988). Alterations in the Extracellular Domain of M13 Procoat Protein Make its Membrane Insertion Dependent on secA and secY. *Eur. J. Biochem.* 177, 267–271. doi:10.1111/j.1432-1033.1988.tb14371.x

Kulanthaivel, P., Kreuzman, A. J., Strege, M. A., Belvo, M. D., Smitka, T. A., Clemens, M., et al. (2004a). Novel Lipoglycopeptides as Inhibitors of Bacterial Signal Peptidase I. *J. Biol. Chem.* 279, 36250–36258. doi:10.1074/jbc.m405884200

Kumamoto, C. A., and Francetić, O. (1993). Highly Selective Binding of Nascent Polypeptides by an *Escherichia coli* Chaperone Protein *In Vivo*. *J. Bacteriol.* 175, 2184–2188. doi:10.1128/jb.175.8.2184-2188.1993

Kumazaki, K., Chiba, S., Takemoto, M., Furukawa, A., Nishiyama, K.-i., Sugano, Y., et al. (2014a). Structural Basis of Sec-independent Membrane Protein Insertion by YidC. *Nature* 509, 516–520. doi:10.1038/nature13167

Kumazaki, K., Kishimoto, T., Furukawa, A., Mori, H., Tanaka, Y., Dohmae, N., et al. (2014b). Crystal Structure of *Escherichia coli* YidC, a Membrane Protein Chaperone and Insertase. *Sci. Rep.* 4, 7299. doi:10.1038/srep07299

Kusters, I., and Driessen, A. J. M. (2011). SecA, a Remarkable Nanomachine. *Cell. Mol. Life Sci.* 68, 2053–2066. doi:10.1007/s00018-011-0681-y

Lausberg, F., Fleckenstein, S., Kreutzenbeck, P., Fröbel, J., Rose, P., Müller, M., et al. (2012). Genetic Evidence for a Tight Cooperation of TatB and TatC during Productive Recognition of Twin-Arginine (Tat) Signal Peptides in *Escherichia coli*. *PloS one* 7, e39867. doi:10.1371/journal.pone.0039867

Lee, H. C., and Bernstein, H. D. (2001). The Targeting Pathway of *Escherichia coli* Presecretory and Integral Membrane Proteins Is Specified by the Hydrophobicity of the Targeting Signal. *Proc. Natl. Acad. Sci. U.S.A.* 98, 3471–3476. doi:10.1073/pnas.051484198

Li, H., Chang, L., Howell, J. M., and Turner, R. J. (2010). DmsD, a Tat System Specific Chaperone, Interacts with Other General Chaperones and Proteins

Involved in the Molybdenum Cofactor Biosynthesis. *Biochimica Biophysica Acta (BBA) - Proteins Proteomics* 1804, 1301–1309. doi:10.1016/j.bbapap.2010.01.022

Li, L., Park, E., Ling, J., Ingram, J., Ploegh, H., and Rapoport, T. A. (2016). Crystal Structure of a Substrate-Engaged SecY Protein-Translocation Channel. *Nature* 531, 395–399. doi:10.1038/nature17163

Li, W., Schulman, S., Boyd, D., Erlandson, K., Beckwith, J., and Rapoport, T. A. (2007). The Plug Domain of the SecY Protein Stabilizes the Closed State of the Translocation Channel and Maintains a Membrane Seal. *Mol. Cell* 26, 511–521. doi:10.1016/j.molcel.2007.05.002

Liu, J., Luo, C., Smith, P. A., Chin, J. K., Page, M. G. P., Paetzel, M., et al. (2011). Synthesis and Characterization of the Arylomycin Lipoglycopeptide Antibiotics and the Crystallographic Analysis of Their Complex with Signal Peptidase. *J. Am. Chem. Soc.* 133, 17869–17877. doi:10.1021/ja207318n

Lüke, I., Handford, J. I., Palmer, T., and Sargent, F. (2009). Proteolytic Processing of *Escherichia coli* Twin-Arginine Signal Peptides by LepB. *Arch. Microbiol.* 191, 919–925. doi:10.1007/s00203-009-0516-5

Lyko, F., Martoglio, B., Jungnickel, B., Rapoport, T. A., and Dobberstein, B. (1995). Signal Sequence Processing in Rough Microsomes. *J. Biol. Chem.* 270, 19873–19878. doi:10.1074/jbc.270.34.19873

Ma, C., Wu, X., Sun, D., Park, E., Catipovic, M. A., Rapoport, T. A., et al. (2019). Structure of the Substrate-Engaged SecA-SecY Protein Translocation Machine. *Nat. Commun.* 10, 2872. doi:10.1038/s41467-019-10918-2

Maillard, J., Spronk, C. A. E. M., Buchanan, G., Lyall, V., Richardson, D. J., Palmer, T., et al. (2007). Structural Diversity in Twin-Arginine Signal Peptide-Binding Proteins. *Proc. Natl. Acad. Sci. U.S.A.* 104, 15641–15646. doi:10.1073/pnas.0703967104

Martin, R., Larsen, A. H., Corey, R. A., Midtgaard, S. R., Frielinghaus, H., Schaffitzel, C., et al. (2019). Structure and Dynamics of the Central Lipid Pool and Proteins of the Bacterial Holo-Translocon. *Biophysical J.* 116, 1931–1940. doi:10.1016/j.bpj.2019.04.002

Mattick, J. S. (2002). Type IV Pili and Twitching Motility. *Annu. Rev. Microbiol.* 56, 289–314. doi:10.1146/annurev.micro.56.012302.160938

McCormick, P. J., Miao, Y., Shao, Y., Lin, J., and Johnson, A. E. (2003). Cotranslational Protein Integration into the ER Membrane Is Mediated by the Binding of Nascent Chains to Translocon Proteins. *Mol. Cell* 12, 329–341. doi:10.1016/s1097-2765(03)00304-6

McDowell, M. A., Heimes, M., and Sinning, I. (2021). Structural and Molecular Mechanisms for Membrane Protein Biogenesis by the Oxa1 Superfamily. *Nat. Struct. Mol. Biol.* 28, 234–239. doi:10.1038/s41594-021-00567-9

Michaelis, S., and Beckwith, J. (1982). Mechanism of Incorporation of Cell Envelope Proteins in *Escherichia coli*. *Annu. Rev. Microbiol.* 36, 435–465. doi:10.1146/annurev.mi.36.100182.002251

Musial-Siwek, M., Rusch, S. L., and Kendall, D. A. (2007). Selective Photoaffinity Labeling Identifies the Signal Peptide Binding Domain on SecA. *J. Mol. Biol.* 365, 637–648. doi:10.1016/j.jmb.2006.10.027

Nagamori, S., Smirnova, I. N., and Kaback, H. R. (2004). Role of YidC in Folding of Polytopic Membrane Proteins. *J. Cell Biol.* 165, 53–62. doi:10.1083/jcb.200402067

Nakajima, M., Inukai, M., Haneishi, T., Terahara, A., Arai, M., Kinoshita, T., et al. (1978). Globomycin, a New Peptide Antibiotic with Spheroplast-Forming Activity. III. Structural Determination of Globomycin. *J. Antibiot.* 31, 426–432. doi:10.7164/antibiotics.31.426

Nicolaus, F., Metola, A., Mermans, D., Liljenström, A., Krč, A., Abdullahi, S. M., et al. (2021). Residue-by-residue Analysis of Cotranslational Membrane Protein Integration *In Vivo*. *Elife* 10, e64302. doi:10.7554/eLife.64302

Novak, P., Ray, P. H., and Dev, I. K. (1986). Localization and Purification of Two Enzymes from *Escherichia coli* Capable of Hydrolyzing a Signal Peptide. *J. Biol. Chem.* 261, 420–427. doi:10.1016/s0021-9258(17)42489-6

Nunn, D. N., and Lory, S. (1991). Product of the *Pseudomonas aeruginosa* Gene pilD Is a Prepilin Leader Peptidase. *Proc. Natl. Acad. Sci. U.S.A.* 88, 3281–3285. doi:10.1073/pnas.88.8.3281

Oh, E., Becker, A. H., Sandikci, A., Huber, D., Chaba, R., Gloge, F., et al. (2011). Selective Ribosome Profiling Reveals the Cotranslational Chaperone Action of Trigger Factor *In Vivo*. *Cell* 147, 1295–1308. doi:10.1016/j.cell.2011.10.044

Olatunji, S., Yu, X., Bailey, J., Huang, C.-Y., Zapotoczna, M., Bowen, K., et al. (2020). Structures of Lipoprotein Signal Peptidase II from *Staphylococcus aureus* Complexed with Antibiotics Globomycin and Myxovirescin. *Nat. Commun.* 11, 140. doi:10.1038/s41467-019-13724-y

Oliver, D. B., and Beckwith, J. (1981). *E. coli* Mutant Pleiotropically Defective in the Export of Secreted Proteins. *Cell* 25, 765–772. doi:10.1016/0092-8674(81)90184-7

Oresnik, I. J., Ladner, C. L., and Turner, R. J. (2001). Identification of a Twin-Arginine Leader-Binding Protein. *Mol. Microbiol.* 40, 323–331. doi:10.1046/j.1365-2958.2001.02391.x

Oswald, J., Njenga, R., Natriashvili, A., Sarmah, P., and Koch, H.-G. (2021). The Dynamic SecYEG Translocon. *Front. Mol. Biosci.* 8, 664241. doi:10.3389/fmolb.2021.664241

Paetzel, M. (2019). Bacterial Signal Peptidases. *Subcell. Biochem.* 92, 187–219. doi:10.1007/978-3-030-18768-2_7

Paetzel, M., and Dalbey, R. E. (1997). Catalytic Hydroxyl/amine Dyads within Serine Proteases. *Trends Biochem. Sci.* 22, 28–31. doi:10.1016/s0968-0004(96)10065-7

Paetzel, M., Dalbey, R. E., and Strynadka, N. C. J. (2002). Crystal Structure of a Bacterial Signal Peptidase Apoenzyme. *J. Biol. Chem.* 277, 9512–9519. doi:10.1074/jbc.m110983200

Paetzel, M., Dalbey, R. E., and Strynadka, N. C. J. (1998). Crystal Structure of a Bacterial Signal Peptidase in Complex with a β-lactam Inhibitor. *Nature* 396, 186–190. doi:10.1038/24196

Paetzel, M., Dalbey, R. E., and Strynadka, N. C. J. (2000). The Structure and Mechanism of Bacterial Type I Signal Peptidases. *Pharmacol. Ther.* 87, 27–49. doi:10.1016/s0163-7258(00)00064-4

Paetzel, M., Goodall, J. J., Kania, M., Dalbey, R. E., and Page, M. G. P. (2004). Crystallographic and Biophysical Analysis of a Bacterial Signal Peptidase in Complex with a Lipopeptide-Based Inhibitor. *J. Biol. Chem.* 279, 30781–30790. doi:10.1074/jbc.m401686200

Paetzel, M. (2014). Structure and Mechanism of *Escherichia coli* Type I Signal Peptidase. *Biochimica Biophysica Acta (BBA) - Mol. Cell Res.* 1843, 1497–1508. doi:10.1016/j.bbamcr.2013.12.003

Paetzel, M., Strynadka, N. C. J., Tschantz, W. R., Casareno, R., Bullinger, P. R., and Dalbey, R. E. (1997). Use of Site-Directed Chemical Modification to Study an Essential Lysine in *Escherichia coli* Leader Peptidase. *J. Biol. Chem.* 272, 9994–10003. doi:10.1074/jbc.272.15.9994

Palmer, T., and Stansfeld, P. J. (2020). Targeting of Proteins to the Twin-arginine Translocation Pathway. *Mol. Microbiol.* 113, 861–871. doi:10.1111/mmi.14461

Papanikou, E., Karamanou, S., Baud, C., Frank, M., Sianidis, G., Keramisanou, D., et al. (2005). Identification of the Preprotein Binding Domain of SecA. *J. Biol. Chem.* 280, 43209–43217. doi:10.1074/jbc.m509990200

Patel, R., Smith, S. M., and Robinson, C. (2014). Protein Transport by the Bacterial Tat Pathway. *Biochimica Biophysica Acta (BBA) - Mol. Cell Res.* 1843, 1620–1628. doi:10.1016/j.bbamcr.2014.02.013

Perlman, D., and Halvorson, H. O. (1983). A Putative Signal Peptidase Recognition Site and Sequence in Eukaryotic and Prokaryotic Signal Peptides. *J. Mol. Biol.* 167, 391–409. doi:10.1016/s0022-2836(83)80341-6

Peschke, M., Le Goff, M., Koningstein, G. M., Karyolaimos, A., de Gier, J.-W., van Ulsen, P., et al. (2018). SRP, FtsY, DnaK and YidC Are Required for the Biogenesis of the *E. coli* Tail-Anchored Membrane Proteins DjlC and Flk. *J. Mol. Biol.* 430, 389–403. doi:10.1016/j.jmb.2017.12.004

Petriman, N.-A., Jauss, B., Hufnagel, A., Franz, L., Sachelaru, I., Drepper, F., et al. (2018). The Interaction Network of the YidC Insertase with the SecYEG Translocon, SRP and the SRP Receptor FtsY. *Sci. Rep.* 8, 578. doi:10.1038/s41598-017-19019-w

Pohlschröder, M., Prinz, W. A., Hartmann, E., and Beckwith, J. (1997). Protein Translocation in the Three Domains of Life: Variations on a Theme. *Cell* 91, 563–566. doi:10.1016/s0092-8674(00)80443-2

Pross, E., and Kuhn, A. (2020). Two Signal Recognition Particle Sequences Are Present in the Amino-Terminal Domain of the C-Tailed Protein SciP. *J. Bacteriol.* 203, e00312–20. doi:10.1128/JB.00312-20

Pross, E., Soussoula, L., Seitl, I., Lupo, D., and Kuhn, A. (2016). Membrane Targeting and Insertion of the C-Tail Protein SciP. *J. Mol. Biol.* 428, 4218–4227. doi:10.1016/j.jmb.2016.09.001

Ramasamy, S., Abrol, R., Suloway, C. J. M., and Clemons, W. M., Jr. (2013). The Glove-like Structure of the Conserved Membrane Protein TatC Provides

Insight into Signal Sequence Recognition in Twin-Arginine Translocation. *Structure* 21, 777–788. doi:10.1016/j.str.2013.03.004

Randall, L. L., and Hardy, S. J. S. (1986). Correlation of Competence for Export with Lack of Tertiary Structure of the Mature Species: a Study *In Vivo* of Maltose-Binding Protein in *E. coli*. *Cell* 46, 921–928. doi:10.1016/0092-8674(86)90074-7

Rao, S., De Waelheyns, E., Economou, A., and Anné, J. (2014). Antibiotic Targeting of the Bacterial Secretory Pathway. *Biochimica Biophysica Acta (BBA) - Mol. Cell Res.* 1843, 1762–1783. doi:10.1016/j.bbamcr.2014.02.004

Rawat, S., Zhu, L., Lindner, E., Dalbey, R. E., and White, S. H. (2015). SecA Drives Transmembrane Insertion of RodZ, an Unusual Single-Span Membrane Protein. *J. Mol. Biol.* 427, 1023–1037. doi:10.1016/j.jmb.2014.05.005

Ray, N., Oates, J., Turner, R. J., and Robinson, C. (2003). DmsD Is Required for the Biogenesis of DMSO Reductase inEscherichia Colibut Not for the Interaction of the DmsA Signal Peptide with the Tat Apparatus. *FEBS Lett.* 534, 156–160. doi:10.1016/s0014-5793(02)03839-5

Roberts, T. C., Smith, P. A., Cirz, R. T., and Romesberg, F. E. (2007). Structural and Initial Biological Analysis of Synthetic Arylomycin A2. *J. Am. Chem. Soc.* 129, 15830–15838. doi:10.1021/ja073340u

Roberts, T. C., Smith, P. A., and Romesberg, F. E. (2011). Synthesis and Biological Characterization of Arylomycin B Antibiotics. *J. Nat. Prod.* 74, 956–961. doi:10.1021/np200163g

Robinson, C., Matos, C. F. R. O., Beck, D., Ren, C., Lawrence, J., Vasisht, N., et al. (2011). Transport and Proofreading of Proteins by the Twin-Arginine Translocation (Tat) System in Bacteria. *Biochimica Biophysica Acta (BBA) - Biomembr.* 1808, 876–884. doi:10.1016/j.bbamem.2010.11.023

Rodriguez, F., Rouse, S. L., Tait, C. E., Harmer, J., De Riso, A., Timmel, C. R., et al. (2013). Structural Model for the Protein-Translocating Element of the Twin-Arginine Transport System. *Proc. Natl. Acad. Sci. U. S. A.* 110, E1092–E1101. doi:10.1073/pnas.1219486110

Rollauer, S. E., Tarry, M. J., Graham, J. E., Jääskeläinen, M., Jäger, F., Johnson, S., et al. (2012). Structure of the TatC Core of the Twin-Arginine Protein Transport System. *Nature* 492, 210–214. doi:10.1038/nature11683

Sachelaru, I., Winter, L., Knyazev, D. G., Zimmermann, M., Vogt, A., Kuttner, R., et al. (2017). YidC and SecYEG Form a Heterotetrameric Protein Translocation Channel. *Sci. Rep.* 7, 101. doi:10.1038/s41598-017-00109-8

Saio, T., Guan, X., Rossi, P., Economou, A., and Kalodimos, C. G. (2014). Structural Basis for Protein Antiaggregation Activity of the Trigger Factor Chaperone. *Science* 344, 1250494. doi:10.1126/science.1250494

Saito, A., Hizukuri, Y., Matsuo, E.-i., Chiba, S., Mori, H., Nishimura, O., et al. (2011). Post-Liberation Cleavage of Signal Peptides Is Catalyzed by the Site-2 Protease (S2P) in Bacteria. *Proc. Natl. Acad. Sci. U.S.A.* 108, 13740–13745. doi:10.1073/pnas.1108376108

Saller, M. J., Wu, Z. C., de Keyzer, J., and Driessen, A. J. M. (2012). The YidC/Oxa1/Alb3 Protein Family: Common Principles and Distinct Features. *Biol. Chem.* 393, 1279–1290. doi:10.1515/hsz-2012-0199

Samuelson, J. C., Chen, M., Jiang, F., Möller, I., Wiedmann, M., Kuhn, A., et al. (2000). YidC Mediates Membrane Protein Insertion in Bacteria. *Nature* 406, 637–641. doi:10.1038/35020586

Sandhu, H., Hedman, R., Cymer, F., Kudva, R., Ismail, N., and von Heijne, G. (2021). Cotranslational Translocation and Folding of a Periplasmic Protein Domain in *Escherichia coli*. *J. Mol. Biol.* 433, 167047. doi:10.1016/j.jmb.2021.167047

Sankaran, K., and Wu, H. C. (1994). Lipid Modification of Bacterial Prolipoprotein. Transfer of Diacylglyceryl Moiety from Phosphatidylglycerol. *J. Biol. Chem.* 269, 19701–19706. doi:10.1016/s0021-9258(17)32077-x

Saraogi, I., and Shan, S.-o. (2014). Co-translational Protein Targeting to the Bacterial Membrane. *Biochimica Biophysica Acta (BBA) - Mol. Cell Res.* 1843, 1433–1441. doi:10.1016/j.bbamcr.2013.10.013

Sargent, F., Bogsch, E. G., Stanley, N. R., Wexler, M., Robinson, C., Berks, B. C., et al. (1998). Overlapping Functions of Components of a Bacterial Sec-independent Protein Export Pathway. *Embo J.* 17, 3640–3650. doi:10.1093/emboj/17.13.3640

Schibich, D., Gloge, F., Pöhner, I., Björkholm, P., Wade, R. C., von Heijne, G., et al. (2016). Global Profiling of SRP Interaction with Nascent Polypeptides. *Nature* 536, 219–223. doi:10.1038/nature19070

Schimana, J., Gebhardt, K., Hölztzel, A., Schmid, D. G., Süssmuth, R., Müller, J., et al. (2002). Arylomycins A and B, New Biaryl-Bridged Lipopeptide Antibiotics Produced by Streptomyces Sp. Tue 6075. I. Taxonomy, Fermentation, Isolation and Biological Activities. *J. Antibiot.* 55, 565–570. doi:10.7164/antibiotics.55.565

Schulze, R. J., Komar, J., Botte, M., Allen, W. J., Whitehouse, S., Gold, V. A. M., et al. (2014). Membrane Protein Insertion and Proton-motive-force-dependent Secretion through the Bacterial Holo-Translocon SecYEG-SecDF-YajC-YidC. *Proc. Natl. Acad. Sci. U.S.A.* 111, 4844–4849. doi:10.1073/pnas.1315901111

Serek, J., Bauer-Manz, G., Struhalla, G., van den Berg, L., Kiefer, D., Dalbey, R., et al. (2004). *Escherichia coli* YidC Is a Membrane Insertase for Sec-independent Proteins. *EMBO J.* 23, 294–301. doi:10.1038/sj.emboj.7600063

Shanmugam, S. K., and Dalbey, R. E. (2019). The Conserved Role of YidC in Membrane Protein Biogenesis. *Microbiol. Spectr.* 7, 1. doi:10.1128/microbiolspec.PSIB-0014-2018

Skach, W. R., and Lingappa, V. R. (1993). Amino-terminal Assembly of Human P-Glycoprotein at the Endoplasmic Reticulum Is Directed by Cooperative Actions of Two Internal Sequences. *J. Biol. Chem.* 268, 23552–23561. doi:10.1016/s0021-9258(19)49498-2

Smith, P. A., Koehler, M. F. T., Girgis, H. S., Yan, D., Chen, Y., Chen, Y., et al. (2018). Optimized Arylomycins Are a New Class of Gram-Negative Antibiotics. *Nature* 561, 189–194. doi:10.1038/s41586-018-0483-6

Smith, P. A., and Romesberg, F. E. (2012). Mechanism of Action of the Arylomycin Antibiotics and Effects of Signal Peptidase I Inhibition. *Antimicrob. Agents Chemother.* 56, 5054–5060. doi:10.1128/aac.00785-12

Soman, R., Yuan, J., Kuhn, A., and Dalbey, R. E. (2014). Polarity and Charge of the Periplasmic Loop Determine the YidC and Sec Translocase Requirement for the M13 Procoat Lep Protein. *J. Biol. Chem.* 289, 1023–1032. doi:10.1074/jbc.m113.522250

Stanley, N. R., Palmer, T., and Berks, B. C. (2000). The Twin Arginine Consensus Motif of Tat Signal Peptides Is Involved in Sec-independent Protein Targeting in *Escherichia coli*. *J. Biol. Chem.* 275, 11591–11596. doi:10.1074/jbc.275.16.11591

Steudle, A., Spann, D., Pross, E., Shanmugam, S. K., Dalbey, R. E., and Kuhn, A. (2021). Molecular Communication of the Membrane Insertase YidC with Translocase SecYEG Affects Client Proteins. *Sci. Rep.* 11, 3940. doi:10.1038/s41598-021-83224-x

Strom, M. S., and Lory, S. (1993). Structure-function and Biogenesis of the Type IV Pili. *Annu. Rev. Microbiol.* 47, 565–596. doi:10.1146/annurev.mi.47.100193.003025

Strom, M. S., Nunn, D. N., and Lory, S. (1993). A Single Bifunctional Enzyme, PilD, Catalyzes Cleavage and N-Methylation of Proteins Belonging to the Type IV Pilin Family. *Proc. Natl. Acad. Sci. U.S.A.* 90, 2404–2408. doi:10.1073/pnas.90.6.2404

Sung, M., and Dalbey, R. E. (1992). Identification of Potential Active-Site Residues in the *Escherichia coli* Leader Peptidase. *J. Biol. Chem.* 267, 13154–13159. doi:10.1016/s0021-9258(18)42186-2

Tan, Y. X., Peters, D. S., Walsh, S. I., Holcomb, M., Santos-Martins, D., Forli, S., et al. (2020). Initial Analysis of the Arylomycin D Antibiotics. *J. Nat. Prod.* 83, 2112–2121. doi:10.1021/acs.jnatprod.9b01174

Therien, A. G., Huber, J. L., Wilson, K. E., Beaulieu, P., Caron, A., Claveau, D., et al. (2012). Broadening the Spectrum of β-Lactam Antibiotics through Inhibition of Signal Peptidase Type I. *Antimicrob. Agents Chemother.* 56, 4662–4670. doi:10.1128/aac.00726-12

Ting, Y. T., Harris, P. W. R., Batot, G., Brimble, M. A., Baker, E. N., and Young, P. G. (2016). Peptide Binding to a Bacterial Signal Peptidase Visualized by Peptide Tethering and Carrier-Driven Crystallization. *Int. Union Crystallogr. J.* 3, 10–19. doi:10.1107/s2052252515019971

Tjalsma, H., Zanen, G., Bron, S., and van Dijl, J. M. (2000). "The Eubacterial Lipoprotein-specific (Type II) Signal Peptidases," in *The Enzymes (Co- and Posttranslational Proteolysis Of Proteins)*. Editors R. E. Dalbey and D. S. Sigman. third edition (London, UK): Academic Press), 3–26. XXII.

Tjalsma, H., Zanen, G., Venema, G., Bron, S., and van Dijl, J. M. (1999). The Potential Active Site of the Lipoprotein-specific (Type II) Signal Peptidase of Bacillus Subtilis. *J. Biol. Chem.* 274, 28191–28197. doi:10.1074/jbc.274.40.28191

Tokunaga, M., Loranger, J. M., and Wu, H. C. (1983). Isolation and Characterization of an *Escherichia coli* Clone Overproducing Prolipoprotein Signal Peptidase. *J. Biol. Chem.* 258, 12102–12105. doi:10.1016/s0021-9258(17)44136-6

Tokunaga, M., Tokunaga, H., and Wu, H. C. (1982). Post-Translational Modification and Processing of *Escherichia coli* Prolipoprotein *In Vitro*. *Proc. Natl. Acad. Sci. U.S.A.* 79, 2255–2259. doi:10.1073/pnas.79.7.2255

Tooke, F. J., Babot, M., Chandra, G., Buchanan, G., and Palmer, T. (2017). A Unifying Mechanism for the Biogenesis of Membrane Proteins Co-operatively Integrated by the Sec and Tat Pathways. *Elife* 6, e26577. doi:10.7554/eLife.26577

Tschantz, W., Paetzel, M., Cao, G., Suciu, D., Inouye, M., and Dalbey, R. E. (1995). Characterization of a Soluble, Catalytically Active Form of *Escherichia coli* Leader Peptidase: Requirement of Detergent or Phospholipid for Optimal Activity. *Biochemistry* 34, 3935–3941. doi:10.1021/bi00012a010

Tschantz, W. R., Sung, M., Delgado-Partin, V. M., and Dalbey, R. E. (1993). A Serine and a Lysine Residue Implicated in the Catalytic Mechanism of the *Escherichia coli* Leader Peptidase. *J. Biol. Chem.* 268, 27349–27354. doi:10.1016/s0021-9258(19)74256-2

Tsirigotaki, A., De Geyter, J., Šoštaric´, N., Economou, A., and Karamanou, S. (2017). Protein Export through the Bacterial Sec Pathway. *Nat. Rev. Microbiol.* 15, 21–36. doi:10.1038/nrmicro.2016.161

Tsukazaki, T., Mori, H., Echizen, Y., Ishitani, R., Fukai, S., Tanaka, T., et al. (2011). Structure and Function of a Membrane Component SecDF that Enhances Protein Export. *Nature* 474, 235–238. doi:10.1038/nature09980

Turner, R. J., Papish, A. L., and Sargent, F. (2004). Sequence Analysis of Bacterial Redox Enzyme Maturation Proteins (REMPs). *Can. J. Microbiol.* 50, 225–238. doi:10.1139/w03-117

Ulbrandt, N. D., London, E., and Oliver, D. B. (1992). Deep Penetration of a Portion of *Escherichia coli* SecA Protein into Model Membranes Is Promoted by Anionic Phospholipids and by Partial Unfolding. *J. Biol. Chem.* 267, 15184–15192. doi:10.1016/s0021-9258(18)42163-1

Upert, G., Luther, A., Obrecht, D., and Ermert, P. (2021). Emerging Peptide Antibiotics with Therapeutic Potential. *Med. Drug Discov.* 9, 100078. doi:10.1016/j.medidd.2020.100078

Urbanus, M. L., Scotti, P. A., Fröderberg, L., Sääf, A., de Gier, J. W. L., Brunner, J., et al. (2001). Sec-dependent Membrane Protein Insertion: Sequential Interaction of Nascent FtsQ with SecY and YidC. *EMBO Rep.* 2, 524–529. doi:10.1093/embo-reports/kve108

van Bloois, E., Haan, G.-J., de Gier, J.-W., Oudega, B., and Luirink, J. (2006). Distinct Requirements for Translocation of the N-Tail and C-Tail of the *Escherichia coli* Inner Membrane Protein CyoA. *J. Biol. Chem.* 281, 10002–10009. doi:10.1074/jbc.m511357200

van Bloois, E., Jan Haan, G., de Gier, J.-W., Oudega, B., and Luirink, J. (2004). F1F0ATP Synthase Subunit C Is Targeted by the SRP to YidC in the E. Coli Inner Membrane. *FEBS Lett.* 576, 97–100. doi:10.1016/j.febslet.2004.08.069

van den Berg, B., Clemons, W. M., Collinson, I., Modis, Y., Hartmann, E., Harrison, S. C., et al. (2004). X-Ray Structure of a Protein-Conducting Channel. *Nature* 427, 36–44. doi:10.1038/nature02218

Van Der Laan, M., Bechtluft, P., Kol, S., Nouwen, N., and Driessen, A. J. M. (2004). F1F0 ATP Synthase Subunit C Is a Substrate of the Novel YidC Pathway for Membrane Protein Biogenesis. *J. Cell Biol.* 165, 213–222. doi:10.1083/jcb.200402100

van der Laan, M., Urbanus, M. L., ten Hagen-Jongman, C. M., Nouwen, N., Oudega, B., Harms, N., et al. (2003). A Conserved Function of YidC in the Biogenesis of Respiratory Chain Complexes. *Proc. Natl. Acad. Sci. U.S.A.* 100, 5801–5806. doi:10.1073/pnas.0636761100

Vlasuk, G. P., Inouye, S., Ito, H., Itakura, K., and Inouye, M. (1983). Effects of the Complete Removal of Basic Amino Acid Residues from the Signal Peptide on Secretion of Lipoprotein in *Escherichia coli*. *J. Biol. Chem.* 258, 7141–7148. doi:10.1016/s0021-9258(18)32343-3

Vogeley, L., El Arnaout, T., Bailey, J., Stansfeld, P. J., Boland, C., and Caffrey, M. (2016). Structural Basis of Lipoprotein Signal Peptidase II Action and Inhibition by the Antibiotic Globomycin. *Science* 351, 876–880. doi:10.1126/science.aad3747

von Heijne, G. (1998). Life and Death of a Signal Peptide. *Nature* 396 (111), 111–113. doi:10.1038/24036

von Heijne, G. (1986). A New Method for Predicting Signal Sequence Cleavage Sites. *Nucl. Acids Res.* 14, 4683–4690. doi:10.1093/nar/14.11.4683

von Heijne, G., and Abrahmsèn, L. (1989). Species-specific Variation in Signal Peptide Design Implications for Protein Secretion in Foreign Hosts. *FEBS Lett.* 244, 439–446. doi:10.1016/0014-5793(89)80579-4

von Heijne, G. (2006). Membrane-protein Topology. *Nat. Rev. Mol. Cell Biol.* 7, 909–918. doi:10.1038/nrm2063

von Heijne, G. (1999). Recent Advances in the Understanding of Membrane Protein Assembly and Structure. *Quart. Rev. Biophys.* 32, 285–307. doi:10.1017/s0033583500003541

von Heijne, G. (1986). The Distribution of Positively Charged Residues in Bacterial Inner Membrane Proteins Correlates with the Trans-membrane Topology. *EMBO J.* 5, 3021–3027. doi:10.1002/j.1460-2075.1986.tb04601.x

von Heijne, G. (1989). The Structure of Signal Peptides from Bacterial Lipoproteins. *Protein Eng. Des. Sel.* 2, 531–534. doi:10.1093/protein/2.7.531

Voorhees, R. M., and Hegde, R. S. (2016). Structure of the Sec61 Channel Opened by a Signal Sequence. *Science* 351, 88–91. doi:10.1126/science.aad4992

Wagner, S., Pop, O., Haan, G.-J., Baars, L., Koningstein, G., Klepsch, M. M., et al. (2008). Biogenesis of MalF and the MalFGK2 Maltose Transport Complex in *Escherichia coli* Requires YidC. *J. Biol. Chem.* 283, 17881–17890. doi:10.1074/jbc.m801481200

Wang, P., Shim, E., Cravatt, B., Jacobsen, R., Schoeniger, J., Kim, A. C., et al. (2008). *Escherichia coli* Signal Peptide Peptidase A Is a Serine-Lysine Protease with a Lysine Recruited to the Nonconserved Amino-Terminal Domain in the S49 Protease Family. *Biochemistry* 47, 6361–6369. doi:10.1021/bi800657p

Wang, S., Jomaa, A., Jaskolowski, M., Yang, C.-I., Ban, N., and Shan, S.-o. (2019). The Molecular Mechanism of Cotranslational Membrane Protein Recognition and Targeting by SecA. *Nat. Struct. Mol. Biol.* 26, 919–929. doi:10.1038/s41594-019-0297-8

Wang, S., Yang, C.-I., and Shan, S.-o. (2017). SecA Mediates Cotranslational Targeting and Translocation of an Inner Membrane Protein. *J. Cell Biol.* 216, 3639–3653. doi:10.1083/jcb.201704036

Watts, C., Wickner, W., and Zimmermann, R. (1983). M13 Procoat and a Pre-immunoglobulin Share Processing Specificity but Use Different Membrane Receptor Mechanisms. *Proc. Natl. Acad. Sci. U.S.A.* 80, 2809–2813. doi:10.1073/pnas.80.10.2809

Weihofen, A., Binns, K., Lemberg, M. K., Ashman, K., and Martoglio, B. (2002). Identification of Signal Peptide Peptidase, a Presenilin-type Aspartic Protease. *Science* 296, 2215–2218. doi:10.1126/science.1070925

Weiner, J. H., Bilous, P. T., Shaw, G. M., Lubitz, S. P., Frost, L., Thomas, G. H., et al. (1998). A Novel and Ubiquitous System for Membrane Targeting and Secretion of Cofactor-Containing Proteins. *Cell* 93, 93–101. doi:10.1016/s0092-8674(00)81149-6

Welte, T., Kudva, R., Kuhn, P., Sturm, L., Braig, D., Müller, M., et al. (2012). Promiscuous Targeting of Polytopic Membrane Proteins to SecYEG or YidC by the Escherichia Coli Signal Recognition Particle. *MBoC* 23, 464–479. doi:10.1091/mbc.e11-07-0590

Whitehouse, S., Gold, V. A. M., Robson, A., Allen, W. J., Sessions, R. B., and Collinson, I. (2012). Mobility of the SecA 2-Helix-Finger Is Not Essential for Polypeptide Translocation via the SecYEG Complex. *J. Cell Biol.* 199, 919–929. doi:10.1083/jcb.201205191

Wickner, W., Moore, K., Dibb, N., Geissert, D., and Rice, M. (1987). Inhibition of Purified *Escherichia coli* Leader Peptidase by the Leader (Signal) Peptide of Bacteriophage M13 Procoat. *J. Bacteriol.* 169, 3821–3822. doi:10.1128/jb.169.8.3821-3822.1987

Wolfe, P. B., Silver, P., and Wickner, W. (1982). The Isolation of Homogeneous Leader Peptidase from a Strain of *Escherichia coli* Which Overproduces the Enzyme. *J. Biol. Chem.* 257, 7898–7902. doi:10.1016/s0021-9258(18)34466-1

Wolfe, P. B., Zwizinski, C., and Wickner, W. (1983). [3] Purification and Characterization of Leader Peptidase from *Escherichia coli*. *Methods Enzymol.* 97, 40–46. doi:10.1016/0076-6879(83)97116-1

Wu, X., and Rapoport, T. A. (2021). Translocation of Proteins through a Distorted Lipid Bilayer. *Trends Cell Biol.* 31, 473–484. doi:10.1016/j.tcb.2021.01.002

Xiao, Y., Gerth, K., Müller, R., and Wall, D. (2012). Myxobacterium-produced Antibiotic TA (Myxovirescin) Inhibits Type II Signal Peptidase. *Antimicrob. Agents Chemother.* 56, 2014–2021. doi:10.1128/aac.06148-11

Xu, Z., Knafels, J. D., and Yoshino, K. (2000). Crystal Structure of the Bacterial Protein Export Chaperone secB. *Nat. Struct. Biol.* 7, 1172–1177. doi:10.1038/82040

Yamagata, H., Daishima, K., and Mizushima, S. (1983). Cloning and Expression of a Gene Coding for the Prolipoprotein Signal Peptidase of *Escherichia coli*. *FEBS Lett.* 158, 301–304. doi:10.1016/0014-5793(83)80600-0

Yi, L., Celebi, N., Chen, M., and Dalbey, R. E. (2004). Sec/SRP Requirements and Energetics of Membrane Insertion of Subunits a, B, and C of the *Escherichia coli*

F1F0 ATP Synthase. *J. Biol. Chem.* 279, 39260–39267. doi:10.1074/jbc.m405490200

Yi, L., Jiang, F., Chen, M., Cain, B., Bolhuis, A., and Dalbey, R. E. (2003). YidC Is Strictly Required for Membrane Insertion of Subunits a and C of the F1F0ATP Synthase and SecE of the SecYEG Translocase. *Biochemistry* 42, 10537–10544. doi:10.1021/bi034309h

Yu, Z., Koningstein, G., Pop, A., and Luirink, J. (2008). The Conserved Third Transmembrane Segment of YidC Contacts Nascent *Escherichia coli* Inner Membrane Proteins. *J. Biol. Chem.* 283, 34635–34642. doi:10.1074/jbc.m804344200

Zhang, B., and Miller, T. F., 3rd. (2010). Hydrophobically Stabilized Open State for the Lateral Gate of the Sec Translocon. *Proc. Natl. Acad. Sci. U.S.A.* 107, 5399–5404. doi:10.1073/pnas.0914752107

Zhang, L., Liu, L., Maltsev, S., Lorigan, G. A., and Dabney-Smith, C. (2014). Investigating the Interaction between Peptides of the Amphipathic Helix of Hcf106 and the Phospholipid Bilayer by Solid-State NMR Spectroscopy. *Biochimica Biophysica Acta (BBA) - Biomembr.* 1838, 413–418. doi:10.1016/j.bbamem.2013.10.007

Zhou, J., and Xu, Z. (2003). Structural Determinants of SecB Recognition by SecA in Bacterial Protein Translocation. *Nat. Struct. Mol. Biol.* 10, 942–947. doi:10.1038/nsb980

Zhu, L., Kaback, H. R., and Dalbey, R. E. (2013). YidC Protein, a Molecular Chaperone for LacY Protein Folding via the SecYEG Protein Machinery. *J. Biol. Chem.* 288, 28180–28194. doi:10.1074/jbc.m113.491613

Zhu, L., Klenner, C., Kuhn, A., and Dalbey, R. E. (2012). Both YidC and SecYEG Are Required for Translocation of the Periplasmic Loops 1 and 2 of the Multispanning Membrane Protein TatC. *J. Mol. Biol.* 424, 354–367. doi:10.1016/j.jmb.2012.09.026

Zimmer, J., Li, W., and Rapoport, T. A. (2006). A Novel Dimer Interface and Conformational Changes Revealed by an X-Ray Structure of B. Subtilis SecA. *J. Mol. Biol.* 364, 259–265. doi:10.1016/j.jmb.2006.08.044

Zimmer, J., Nam, Y., and Rapoport, T. A. (2008). Structure of a Complex of the ATPase SecA and the Protein-Translocation Channel. *Nature* 455, 936–943. doi:10.1038/nature07335

Zimmermann, R., and Wickner, W. (1983). Energetics and Intermediates of the Assembly of Protein OmpA into the Outer Membrane of *Escherichia coli*. *J. Biol. Chem.* 258, 3920–3925. doi:10.1016/s0021-9258(18)32755-8

Conflict of Interest: The authors declare that the research was conducted in the absence of any commercial or financial relationships that could be construed as a potential conflict of interest.

Publisher's Note: All claims expressed in this article are solely those of the authors and do not necessarily represent those of their affiliated organizations, or those of the publisher, the editors and the reviewers. Any product that may be evaluated in this article, or claim that may be made by its manufacturer, is not guaranteed or endorsed by the publisher.

frontiers | Frontiers in Microbiology

TYPE Original Research
PUBLISHED 25 October 2022
DOI 10.3389/fmicb.2022.1017352

OPEN ACCESS

EDITED BY
Anastassios Economou,
KU Leuven, Belgium

REVIEWED BY
José Ascención Martínez-Álvarez,
University of Guanajuato, Mexico
Yongcai Li,
Gansu Agricultural University, China

*CORRESPONDENCE
Jiaoyu Wang
wangjiaoyu78@sina.com
Ling Li
liling-06@163.com

SPECIALTY SECTION
This article was submitted to Microbial Physiology and Metabolism, a section of the journal Frontiers in Microbiology

RECEIVED 11 August 2022
ACCEPTED 28 September 2022
PUBLISHED 25 October 2022

CITATION
Lu Z, Guo J, Li Q, Han Y, Zhang Z, Hao Z, Wang Y, Sun G, Wang J and Li L (2022) Monitoring peroxisome dynamics using enhanced green fluorescent protein labeling in *Alternaria alternata*. *Front. Microbiol.* 13:1017352. doi: 10.3389/fmicb.2022.1017352

Monitoring peroxisome dynamics using enhanced green fluorescent protein labeling in *Alternaria alternata*

Ziqi Lu[1,2], Jian Guo[3], Qiang Li[1], Yatao Han[1], Zhen Zhang[2], Zhongna Hao[2], Yanli Wang[2], Guochang Sun[2], Jiaoyu Wang[2]* and Ling Li[1]*

[1]The Key Laboratory for Quality Improvement of Agricultural Products of Zhejiang Province, College of Advanced Agricultural Sciences, Zhejiang Agriculture and Forestry University, Hangzhou, China, [2]State Key Laboratory for Managing Biotic and Chemical Threats to the Quality and Safety of Agro-Products, Institute of Plant Protection and Microbiology, Zhejiang Academy of Agricultural Sciences, Hangzhou, China, [3]College of Food and Health (College of Modern Food Industry), Zhejiang Agriculture and Forestry University, Hangzhou, China

Brown leaf spot on tobacco is a serious fungal disease caused by *Alternaria alternata*. Peroxisomes are organelles playing an important role in the development and infection of plant pathogenic fungi. But, until now, there is no report on the peroxisome dynamics during the conidia germination of *A. alternata*. To evaluate the roles of peroxisome in the development of the fungus, in the present work, an enhanced green fluorescent protein (eGFP) cassette tagged with peroxisome targeting signal 2 (PTS2) was integrated into *A. alternata* to label the organelles, and an eGFP cassette carrying a nuclear located signal (NLS) was performed parallelly. The transformants containing the fusions emitted fluorescence in punctate patterns. The fluorescence of eGFP-PTS2 was distributed exactly in the peroxisomes while those of eGFP-NLS were located in the nucleus. Typical *Aa*GB transformants were selected to be investigated for the peroxisome dynamics. The results showed that during spore germination, the number of peroxisomes in the spores decreased gradually, but increased in the germ tubes. In addition, when the transformants were cultured on lipid media, the numbers of peroxisomes increased significantly, and in a larger portion, present in striped shapes. These findings give some clues for understanding the peroxisomal functions in the development of *A. alternata*.

KEYWORDS

***Alternaria alternata*, eGFP-PTS2, peroxisome, dynamic analysis, lipid**

Introduction

Tobacco (*Nicotiana tabacum* L.) is an annual or perennial herbaceous plant of *Solanaceae* and an important cash crop with leaves of high commercial value. Both the planting area and the output of tobacco in China rank first in the world (Huang et al., 2021). Brown spot is one of the most severe diseases of tobacco caused by *Alternaria alternata* (Fr.) Keissler (Main, 1969; Dobhal and Monga, 1991), during the growing season, especially the mature stage (Zhang et al., 2011). The typical symptom of the disease on tobacco leaves is brown necrotic spots surrounded by yellowish-green halos. The disease normally causes broken leaves, and even affects the color and thickness of the baked leaves, resulting in the huge economic loss (Jenning et al., 2002; Slavov et al., 2004; Yakimova et al., 2009; Chen et al., 2017). During the process of infection, *A. alternata* forms a special infection structure called appressorium, a specialized differentiated structure that can firmly attach to the leaves (Hatzipapas et al., 2002; Wang, 2019).

The reactive oxygen species (ROSs) formed in host cells is the main barrier to fungal invasion and establishment of parasitism (Barna et al., 2003). The pathogens have to suppress the ROSs for successful infection. The enzymes required in ROSs degradation are distributed in peroxisomes in large portions. It was proved that pathogens generated an increased number of peroxisomes in response to the oxidative stress generated by the host (Chen et al., 2017). The metabolic reactions in the peroxisomes and the genes involved in peroxisomal biogenesis were demonstrated related to the pathogenicity of plant fungal pathogens. Peroxisomes plays important roles in hyphal growth, conidiation, conidial germination, and development of infection structures (Ramos-Pamplona and Naqvi, 2006; Kubo et al., 2015; Li et al., 2017; Chen et al., 2018; Wang et al., 2019; Falter and Reumann, 2022). The peroxisomal dynamic in *A. alternata* during infection is helpful for a better understanding of the pathogenesis of the fungus. However, there is a little knowledge on this topic (Pliego et al., 2009; Wang et al., 2015). Fluorescent proteins are widely used to assess gene expression and monitor the proteins' cellular or subcellular distribution (Yang et al., 2018). To date, three fluorescent proteins [enhanced green fluorescent protein (eGFP), red fluorescent protein (RFP), and yellow fluorescent protein (YFP)] have been mainly used in fungi (Straube et al., 2005).

In the present work, we used a fusion of eGFP with PTS2, driven under the promoter of *MPG1* gene (MGG_10315) from *Magnaporthe oryzae*, to monitor the peroxisomes in *A. alternata*. Using the *Agrobacterium tumefaciens*-mediated transformation (*At*MT), the eGFP-PTS2 was integrated and expressed stably in the transformants. The dynamic changes of peroxisomes in the spore germination of *A. alternata* were observed by fluorescence confocal microscopy. Meanwhile, we marked the nucleus of *A. alternata* using an eGFP version tagged with a nuclear located signal (NLS) and compared the relative locations of the nucleus and peroxisomes in the spores. These results provide a framework for the study of the pathogenic mechanisms and organelles biology of *A. alternata*.

Materials and methods

Fungal species and culture medium

We isolated *A. alternata* wild-type strain C15 from leaves with typical symptoms of tobacco brown spots and stored the strain in our laboratory. The wild-type strain and all transformants were cultured on a complete medium (CM) at 28°C for 3–10 days. The strain of *A. tumefaciens* used was *AGL1*. YEB agar and liquid medium were prepared as described by Holsters et al. (1978). YEB containing 50 μg/ml kanamycin, 34 μg/ml rifampicin, and 50 μg/ml ampicillin was used to culture *A. tumefaciens*. Induction medium (IM) (solid) was used to co-culture *A. alternata* and *A. tumefaciens* (Michielse et al., 2008). CM plates containing 50 μg/mL hygromycin B (Roche, Mannheim, Germany) was used to screen the transformants. The wild-type and transformants strains were inoculated on a minimal medium (MM) supplemented with 0.5% (v/v) Tween 80, 1% (v/v) olive oil, or 1% (v/v) glycerin, and cultured at 28°C for 7 days to compare the ability of the strains to utilize the carbon sources (Li et al., 2017).

Construction of fluorescent fusion vectors

p1300HMGB containing the *HPH* gene and eGFP-PTS2 (a PTS2-tagged eGFP), abbreviated as pHMGB in the present work, were used as peroxisome markers. To construct the pHMGB vector, we used p1300BMGB, a vector carrying the glufosinate-ammonium resistance gene (*BAR*), and eGFP-PTS2 with the promoter of *MPG1* gene (MGG_10315) from *M. oryzae* (abbreviated as pBMGB in present work) (Wang et al., 2008; Li et al., 2014). A 1.36 kb fragment of the *HPH* cassette was amplified using p1300-KO as the template and the primer pair *HPH*-Xh1/*HPH*-Xh2. We replaced the *BAR* gene in pBMGB with the *HPH* cassette using *Xho*I digestion to generate pHMGB. All the primers used are listed in **Table 1**. pHMGB was used to monitor the peroxisomes in *A. alternata*. pRp27GFP-NLS was generated by fusing a NLS fragment to the C terminus of eGFP, which was driven by a constitutive promoter from *M. oryzae* ribosomal protein 27 gene (RP27) in the binary vector pCAMBIA1300. All the vectors were transformed into *A. alternata*, respectively, using the *At*MT method (Rho et al., 2001).

Agrobacterium tumefaciens-mediated transformation of *Alternaria alternata*

AGL1 carrying pHMGB or pRp27GFP-NLS was spread on an LB agar plate containing kanamycin (50 mg/L) and incubated for 2 days at 28°C. A single colony was cultured in 5 mL of LB broth containing 50 mg/L kanamycin at 28°C with a shaking speed of 200 rpm for 48 h. Cells of 2 mL culture were then collected by centrifugation (5,000 × *g*) for 10 min, washed using *A. tumefaciens* induction medium (AIM, lipid) for 2 min, and then diluted, respectively, into OD_{600} about 0.6 in AIM supplemented in 200 mM acetosyringone (AS) and an AS-free AIM as a control. For transformation, 100 μL of *A. tumefaciens* cells were mixed with 100 μL 1 × 10^6 of *A. alternata* conidia, the mixture was spread on a sterilized nitrocellulose filter membrane (Pore size 0.45, Φ50 mm, Whatman, Sangon, Shanghai, China) overlaid on the surface of AIM agar plates and incubated for another 48 h at 23°C in the dark. After the incubation, the nitrocellulose filter membrane was cut with a sterilized knife into strips and transferred into selective CM plates containing 200 μg/mL hygromycin B, 200 μg/mL cefotaxime sodium, 200 μg/mL tetracycline hydrochloride and incubated for 5–7 days to selected the transformants. Thirteen selected hygromycin B-resistant transformants were verified by growing in a new selective CM plate for another 3–4 days at 28°C, together with the wild-type as a control.

Analysis of *Alternaria alternata* transformants

We used polymerase chain reaction (PCR) to amplify the *HPH* gene (with primers HPHCK1 and HPHCK2; **Table 1**). The amplified fragment of *HPH* was 1.0 kb long. We used a 50 μL reaction volume containing 2 μL Taq, 4 μL dNTP, 5 μL 10 × buffer, 35 μL ddH_2O, 2 μL forward primers, and 2 μL reverse primer. Our PCR reaction conditions were 5 min at 95°C; 35 cycles of 30 s at 95°C, 30 s at 55°C, and 90 s at 72°C; and 10 min at 72°C. PCR products were held at 4°C (Li et al., 2014).

Measurement of colony growth and spore production

The mycelia of the wild-type *A. alternata* strains and the 13 transformations were picked out and inoculated on a 9 cm CM culture medium, respectively, which was cultured at 28°C for 10 days under darkness. The experiment was repeated three times for each colony. Then, each plate was washed with 5 mL of sterile water, and the collected solution was filtered through three layers of lens paper. Collected spores were counted using a hemocytometer, and the conidia concentration and production were calculated.

TABLE 1 Hygromycin B amplification primer.

Primer	Sequence	Length
HPHCK1	TTCGCCCTTCCTCCCTTTATTTCA	1.0 kb
HPHCK2	GCTTCTGCGGGCGATTTGTGTACG	

Confocal microscopy and calcofluor white staining

We used a Leica SP2 confocal microscope (Leica, Germany) and a ZEISS LSM780 inverted confocal microscope (Zeiss, Germany) to examine transformant hyphae and spores. We used an excitation wavelength of 488 nm, and an emission wavelength of 520 nm. And we also observed the peroxisome situation of four mediums (MM, MM + 0.5% (v/v) Tween 80, MM + 1% (v/v) olive oil, or MM + 1% (v/v) glycerin) under confocal microscopy. Each treatment sets three replications with 20 conidia per replicate ($n = 60$).

The concentration of conidia solution of *A. alternata* was adjusted to 1 × 10^5 number/mL, and 20 μL of spore droplets were placed on both plastic coverslips and the onion epidermis and cultured under 28°C dark moisturizing conditions. Then, the spore solutions of 2, 4, 6, 8, 10, 12, 24, and 48 h were taken, respectively, and the dynamic changes of peroxisomes in the progress of spore germination and appressoria formation of *A. alternata* were observed by the fluorescence confocal microscopy. Each post-incubation hour set three replications. In addition, with 10 conidia, germ tube or appressoria per replicate were observed on plastic coverslips ($n = 30$).

Calcofluor white (CFW) staining using Fluorescent Brightener 28 (10 mg/ml, Sigma-Aldrich, Saint Louis, MO, USA) for the microscopy of mycelial branches was performed as described by Harris et al. (1994).

Results

Acquisition of pHMGB transformant in *Alternaria alternata*

The structures of pBMGB and pHMGB are shown in **Figure 1**. By the *At*MT method, we obtained 25 transformants for pHMGB. These transformants grew normally on the CM plates compared with the wild-type strain. After five successive subcultures without selection pressure, all 25 transformants were able to grow on selective CM but not the wild-type, indicating that all the obtained transformants are stable under our experimental conditions.

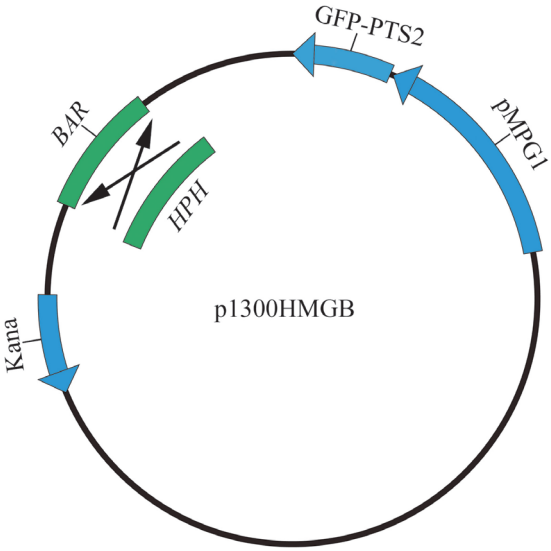

FIGURE 1
The structure of p1300HMGB.

Then, 13 transformants were randomly selected and confirmed by PCR amplification with the primers HPHCK1 (forward) and HPHCK2 (reverse). The hygromycin B gene can be amplified in transformants strains, but not in the wild-type strain C15. These results indicate that the pHMGB vector had been successfully inserted into the genome of the transformants (Figure 2).

Enhanced green fluorescent protein labeling of peroxisome and nucleus in *Alternaria alternata*

After the establishment of auxotrophic makers *via* the *At*MT, we were able to introduce a plasmid containing the maker gene hygromycin B and eGFP under the strong constitutive promoter *MPG1* or *Rp27*. Inspection of non-transformed *A. alternata* hyphae revealed strong auto-fluorescent in some compartments under a fluorescence microscope. In order to distinguish specific eGFP signals from such auto-fluorescent, eGFP was C-terminally tagged with PTS2 or a NLS from *A. alternata*. To quantify the transformation efficiency, we screened transformants microscopically. After 24 h incubation at 28°C in CM medium, 13 out of 25 eGFP-PTS2 transformants and 9 out of 14 eGFP-NLS transformants showed bright green fluorescence under a laser-scanning confocal microscope. However, no fluorescence was observed in the *A. alternata* wild-type strain C15 (control). We found the dots fluorescence are presented in hypha and spores of transformants. In *Aa*GB, green fluorescence is distributed in small green dots (0.2–1 μm in diameter) throughout the cell. We select a typical transformant *Aa*GB-1 to observe the dynamic of peroxisome in the progress of germination. The location and size of the small green dots are consistent with that of the peroxisome (Figure 3A). In eGFP-NLS transformants, they were visualized as spherical structures in the center of mycelia and conidial cell, where the cell nucleus is located (Figure 3B). These results indicate that the GFP fused with PTS2 or NLS is located in peroxisome or cell nucleus, respectively.

Peroxisomal dynamics of *Alternaria alternata* during spore germination and appressoria formation

To explore the role of peroxisome in spore germination and the infection process of *A. alternata*, we observed the dynamic changes in peroxisome by fluorescence confocal microscopy, placed on both plastic membrane and the onion epidermis at 0, 2, 4, 6, 8, 10, 12, and 24 h, respectively. The fluorescence in the eGFP-PTS2 transformants cells is punctate and mostly located throughout the cell at 0 h. During the elongation of the germ tube, the fluorescence intensity in the germ tube increased gradually. The number of peroxisomes in conidia, germ tubes, and appressoria was monitored within 24 h. The number of peroxisomes in the spore kept increasing before 6 hpi and decreased after 6 hpi, and increased continuously both in germ tube and appressoria (Figures 4A,B).

Calcofluor white can be combined with the cellulose and chitin of the fungal cell wall, so we can see the blue fluorescence under the fluorescence microscope. Using calcofluor white to stain the conidia solution of AaGB strain, which transformed the pHMGB into *A. alternata* at 2, 4, 6, 8, 10, and 12 h, we observe the structural dynamic changes in the conidia germination process (Figure 4C).

Peroxisomal response to lipid stress

To observe the effect of lipid on peroxisome, *Aa*GB is inoculated on MM, MM-C + olive, MM-C + glycerin, and MM-C + Tween culture medium, which are cultured for 7 days at 28°C and then observed by laser confocal fluorescence microscope (Figure 5A). The number of peroxisomes is increased in the conidia upon the strains cultured on the other three media compared to those on the MM media. On MM media, the number of peroxisomes is 20, and on the other three media, the numbers of peroxisome are 32, 30, and 38, respectively (Figure 5B). This result indicates that the addition of the appropriate amount of lipids to the medium promotes the division of peroxisomes, thus increasing the number of peroxisomes. In addition, the peroxisome exhibited a strip morphology on Tween media, while exhibiting a punctate pattern on other lipid media (Figure 5A).

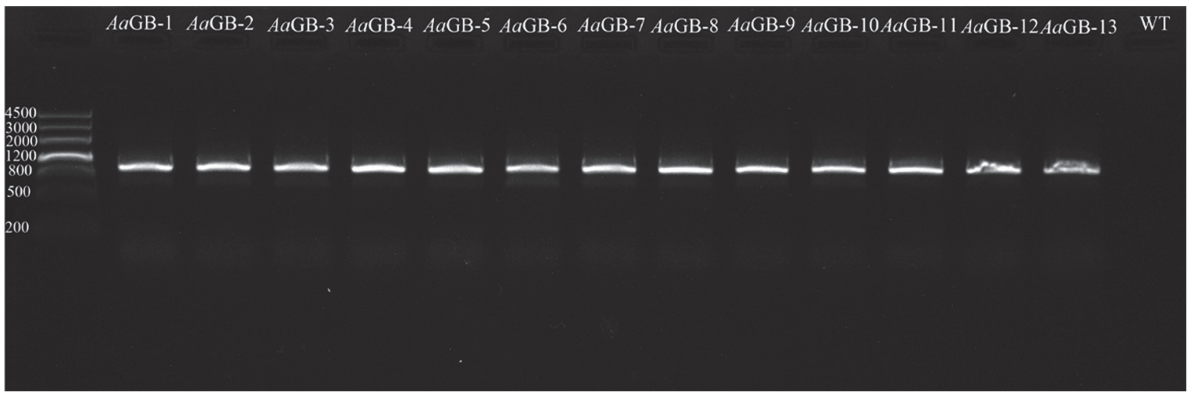

FIGURE 2
The result of transformants amplification hygromycin B by PCR.

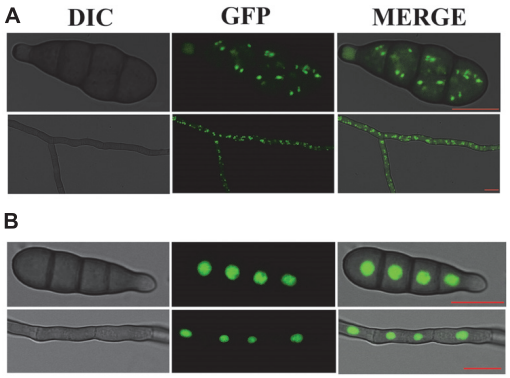

FIGURE 3
AaGB fluorescent labeling of the peroxisome with eGFP **(A)** and NLS fluorescent labeling of the nucleus with eGFP **(B)**, bar = 10 μm.

Discussion

Previous studies have shown that peroxisomes are involved in fungal growth, development, sporulation, invasion, and parasitizing of several pathogenic fungi (Kubo et al., 2015; Li et al., 2017; Wang et al., 2019; Falter and Reumann, 2022). Visualization of peroxisomes did not affect their functions or dynamics. It only required expression of the fusion gene encoding PTS1 or PTS2 added to the C- or N-terminus of GFP, respectively (Goto-Yamada et al., 2022). This also accords with our observations, which showed that there was no significant difference in growth morphology, appressorium formation, and spore production between transformants and WT strains (**Supplementary material**). Direct observation of peroxisomal dynamic in *A. alternata* facilitates the understanding of the pathogenesis of brown spot disease. Because it provides useful information about peroxisome dynamics, such as their morphology, number, size, intracellular distribution, direction of movement, and interactions with other subcellular components, which was difficult to obtain by traditional approaches. Moreover, the fusion gene of GFP with NLS can also be used to screen the genes related to plant disease resistance, elucidating the mechanism underlying the interaction between plants and pathogens (Geng et al., 2021).

The results of this study showed that the transformants successfully expressed the peroxisome or nucleus marker eGFP-PTS2 or NLS, respectively. To illustrate the dynamic of peroxisome during spore germination, the labeled peroxisomes were observed using a laser-scanning confocal microscope. As shown in **Figure 4B**, the number of peroxisomes in the spore first increased and then decreased after 6 h incubation, while the number of peroxisomes in the germ tube kept increasing. A possible explanation for this might be that there is a high rate of fatty acid degradation by peroxisomal β-oxidation to produce the energy needed for germination, reducing the amount of lipid droplets, and the number of peroxisomes located in close proximity to lipid droplets eventually decreased as well. In addition, peroxisomes tended to gather at spore septa. Similar results were obtained in other species such as *M. oryzae* (Wang et al., 2008) and *Fusarium graminearum* (Seong et al., 2008). Wang et al. (2008) found that the number of peroxisomes increased rapidly during the first 2-h of germination, and researched the maximum number at 2 h post-incubation (hpi). Then, the peroxisomes in spores transferred to the infant appressoria, and the number of peroxisomes in *M. oryzae* spore decreased (Wang et al., 2008). Interestingly, as described by Seong et al. (2008), peroxisomes also tended to be concentrated at spore septa, and the abundance of peroxisomes in the asexual spores of *F. graminearum* is correlated with a high number of lipid droplets in their vicinity, which disappear during germination. Peroxisomes are essential for the formation of fruiting bodies and the maturation and germination of spores. They facilitate the utilization of reserve

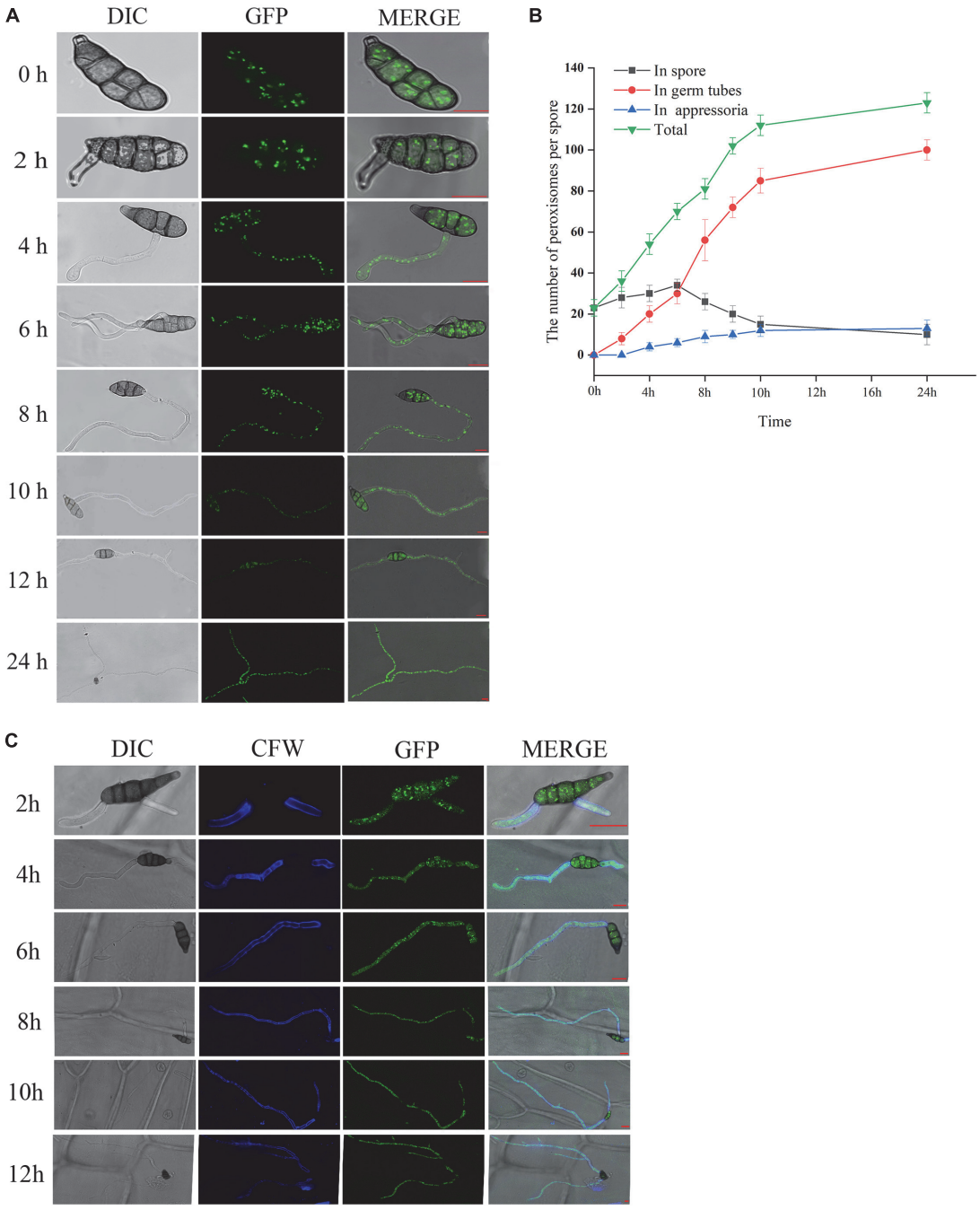

FIGURE 4
AaGB dynamic change of peroxisome by fluorescence confocal microscopy **(A)**, the number change of peroxisome **(B)**, and dynamic changes of the spore germination process by calcofluor **(C)**, bar = 10 μm.

compounds *via* fatty acid β-oxidation and the glyoxylate cycle, producing the energy, acetyl-CoA, and carbohydrates needed for the synthesis of cell wall polymers and turgor generation in infection structures (Peraza-Reyes and Berteaux-Lecellier, 2013; Falter and Reumann, 2022). In the rice blast fungus, lipid droplets are translocated through septa from the conidial cells to the appressorium. It is possible to hypothesize that peroxisomes are localized near the spore septa to facilitate fatty acid breakdown and energy mobilization at the site of need. As shown in **Figure 3**, the location and size of small green dots are consistent with that of the peroxisome, exhibiting an elliptic peroxisome morphology. In eGFP-NLS

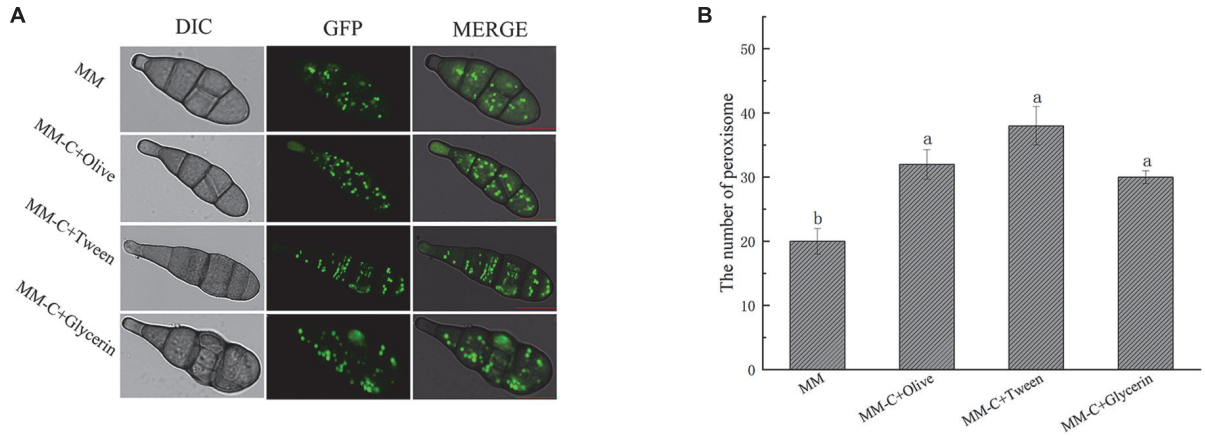

FIGURE 5
AaGB Lipid induced peroxisome fluorescence images **(A)** and changes of number **(B).** These images were filmed by laser confocal fluorescence microscope. AaGB is cultured for 7 days at 28°C, bar = 10 μm.

transformants, eGFP visualized round nuclei, consistent with previous studies (Escano et al., 2009; Shoji et al., 2010). RP27 from *M. oryzae* was used as a promoter to construct the NLS vector pck128 and localized in nuclei during interphase (Jones et al., 2016). To our knowledge, it is the first time that the promoter RP27, which is from *M. oryzae*, also worked in the vector pRp27GFP-NLS when transformed into *A. alternata*.

It is well-known that peroxisomes plays an important role in lipid metabolism. The results of the current study showed that the number of peroxisomes markedly increased in the strains grown on a fatty acid medium compared with those grown on a minimum medium. The finding reflects that of Imazaki et al. (2010) who also found that the number of peroxisomes increased in hyphal cells grown on oleic acid compared with those grown in a glucose medium. In addition, there was an interesting finding that the peroxisome exhibited strip morphology on Tween media compared with a punctate pattern on other lipid media. Peroxisomes multiply by growth and division from preexisting organelles. Peroxisome fission is preceded by the elongation of the peroxisome membrane *via* Pex11 family proteins (Navarro-Espíndola et al., 2020). The possible explanation for this discrepancy might be that peroxisome is in the process of being divided on Tween media, and division has been completed on other lipid media.

In conclusion, the results from our study confirmed that eGFP combined with PTS2 and NLS can be integrated into *A. alternata* to label organelles. Expressing N-terminal GFP-tagged proteins can be used to verify the organelle localization of some secondary metabolites' biosynthesis-related genes (Imazaki et al., 2010). Therefore, the labeling of fungal strains with fluorescent proteins is an effective way to elucidate the mechanisms underlying peroxisomal physiological activity in fungi and plants (Motley and Hettema, 2007; Goto-Yamada et al., 2022). The findings of this study have some important implications for future research, such as the co-localization of the nucleus and peroxisome using multi-color fluorescent proteins and the analysis of the gene involved in peroxisome assembly.

The colony morphology and conidiation of transformants

To observe the colony morphology difference of transformants compared with wild-type strain, mycelial blocks are incubated in CM plates for 10 days at 28°C under light conditions. The colonies were observed and photographed each day. As the number of days of incubation increased, the colonies became progressively larger and by the 10th day the colonies had grown to cover the entire plate. There were no significant differences in the colony morphology between the transformants and the wild-type strain (**Supplementary Figure 1A**). Colonies are irregularly rounded adaxially dark brown, loose and obvious ring tread. The edges are obvious, and peripheral yellow halo is narrow or not obvious. A dark brown or black mold can be seen at the center of the colony (**Supplementary Figure 1A**). Sporulation is an important condition to measure the viability of a strain. The conidia production of all the transformants are similar compared with the wild-type strain. Conidiation of wild-type are 1.85×10^8 cells/plate, and the transformants are from 1.73×10^8 to 2.16×10^8 cells/plate. Thus, it can be explained that the amount of sporulation of *At*MT gene transformed by *A. alternata* will not be affected basically (**Supplementary Figure 1B**).

The colony growth speed of transformants

To measure the growth speed and development of transformants strain, we choose one of the strains (*Aa*GB-1) to measure the colony diameters for 10 consecutive days. On the first day of culture, *Aa*GB-1 grew at a faster rate. On the 5th of culture, the growth diameter was nearly 6 cm (**Figures 4A,B**). In addition, the *Aa*GB-1 strains cover the whole 9 cm plate on the 9th day (**Supplementary Figures 2A,B**).

The conidia development progress of transformants

To observe conidia formation progress of transformations, we culture the *Aa*GB strains under 12 h light/12 h dark at 28°C for 5 consecutive days. The color of conidia is dark brown, which is formed by conidiophore and is borne singly or in bunches. With the increase in incubation time, the conidiophores will gradually elongate, branch, and form mycelium.

To observe the growth dynamic of conidia, the transformants strain are incubated in CM medium which is obliquely inserted into the cover glass at 25°C in the dark. The cultures are observed every 12 h from 0.5 to 5 days. During the first 2.5 days, the conidiophores continuously extend forward and branch. At the same time, only one conidium is formed at the apex of the branch, whose size and DNA contents increased. The conidia are inverted rod-shaped, with a transverse septum and longitudinal diaphragm on the surface, where the transverse septum is thicker and the number of transverse septa is mostly three. With the increase of culture time, the melanin production of conidiophores and conidia increased. New conidia constantly sprout from clusters of the old conidia, whose color is light in the initial period and melanin gradually deepens. Accordingly, the conidiophores branch continuously to give rise to clusters of conidia. At this point, a vast amount of conidia are produced, which are the main forms of infecting the host (**Supplementary Figure 3**).

The conidia germination and appressorial formation of transformants

The conidia of the transformants *Aa*GB were incubated on a plastic membrane to allow appressoria formation for 24 h. The spores gradually germinate and grow sprouting tubes at 28°C in dark conditions. The conidia can grow unilaterally out of the shoot tube and from multiple sides. Under light microscopy, the lengths of the bud tube are similar to these conidia and the rate of the conidia germination is about 30% at the first 2 h, there were already transverse compartments and longitudinal diaphragms within the conidia. The attachment cell is the spores of the pathogenic fungus that germinate and expand at the tip of the budding tube, forming a special morphological structure similar to a sucker. Appressoria are first formed at 4 h, and the rate is only about 3%. As the incubation time increases, the bud tube of spore germination gradually elongates as well as the rate of conidia germination and appressoria formation increased continuously. The rate of conidia germination is about 95% and appressoria formation is nearly 50% at 12 h. In addition, the rate of conidia germination and appressoria formation is raised slightly at 24 h compared to 12 h. At 24 h, the rate of germination and appressoria formation is at their highest, and the elongated budding tubes began to branch and continue to elongate (**Supplementary Figures 4A–C**).

Data availability statement

The original contributions presented in this study are included in the article/**Supplementary material**, further inquiries can be directed to the corresponding authors.

Author contributions

JW: conceptualization. LL, ZZ, and JG: data curation. ZL and QL: formal analysis. LL, JW, and GS: funding acquisition. ZL and YH: investigation. ZZ and JW: methodology. YW and GS: project administration. JG and ZZ: software. JW and GS: supervision. ZL, LL, and ZH: validation. LL and JG: writing—original draft. JW and LL: writing—review and editing. All authors contributed to the article and approved the submitted version.

Funding

We gratefully acknowledge the financial support provided by the National Natural Science Foundation of China (Grant Nos. 31900126 and 31701723), the Zhejiang Key Research and Development Program (Grant No. 2021C02010), the Fundamental Research Funds for the Provincial Universities of Zhejiang (Grant No. 2020YQ002), the Zhejiang Provincial Natural Science Foundation of China under (Grant No. LZ20C140001), the State Key Laboratory for Managing Biotic and Chemical Threats to the Quality and Safety of Argo-Products (Grant No. 2021DG700024-KF202110), and the Program of Innovative Entrepreneurship Training for Undergraduate of China (Grant No. 202110341006).

Acknowledgments

We thank Bo Dong for providing us with the pRp27GFP-NLS vector used in this study.

Conflict of interest

The authors declare that the research was conducted in the absence of any commercial or financial relationships that could be construed as a potential conflict of interest.

Publisher's note

All claims expressed in this article are solely those of the authors and do not necessarily represent those of their affiliated organizations, or those of the publisher, the editors and the reviewers. Any product that may be evaluated in this article, or claim that may be made by its manufacturer, is not guaranteed or endorsed by the publisher.

Supplementary material

The Supplementary Material for this article can be found online at: https://www.frontiersin.org/articles/10.3389/fmicb.2022.1017352/full#supplementary-material

SUPPLEMENTARY FIGURE 1
PHMGB-Aa transformant colonies and wild-type morphology **(A)** and their sporulation **(B)**. These colonies and wild-type were obtained by culturing in CM medium under dark conditions of 25°C for 7 days.

SUPPLEMENTARY FIGURE 2
AaGB colony growth morphology changes **(A)** and growth diameter of the colony **(B)**. Observed and recorded continuously for 10 days at 28°C under light conditions.

SUPPLEMENTARY FIGURE 3
AaGB transformant spore growth dynamic. The growth dynamics of spores in 5 days under 25°C light conditions were observed and recorded.

SUPPLEMENTARY FIGURE 4
Observation of the dynamics of AaGB conidial germination **(A)** and its germination rate **(B)**, appressorium formation rate **(C)**. Conidial germination dynamics were observed and germination rates were recorded after 48 h of continuous incubation at 28°C in the dark under moisturizing conditions, with attached cells being produced during spore germination. Adherent cell formation was observed continuously for 24 h at 28°C in the dark and the rate of formation was recorded, bar = 10 μm.

References

Barna, B., Fodor, J., Pogany, M., and Kiraly, Z. (2003). Role of reactive oxygen species and antioxidants in plant disease resistance. *Pest Manage. Sci.* 59, 459–464. doi: 10.1002/ps.706

Chen, J., Li, L. Y., Gao, M., Ma, G. H., Chen, G. K., and Yu, Q. T. (2017). Indoor screening and field trial of fungicides against tobacco brown spot. *Chin. Tob. Sci.* 38, 73–77.

Chen, Y., Zheng, S. Y., Ju, Z. Z., Zhang, C. Q., Tang, G. F., Wang, J., et al. (2018). Contribution of peroxisomal docking machinery to mycotoxin biosynthesis, pathogenicity and pexophagy in the plant pathogenic fungus *Fusarium graminearum*. *Environ. Microbiol.* 20, 3224–3245. doi: 10.1111/1462-2920.14291

Dobhal, V. K., and Monga, D. (1991). Genetic analysis of field resistance to brown spot caused by *Alternaria altemata* (FR.) Keisaler in *Nicotiana rustica* Linn. *Tob. Res.* 17, 11–15.

Escano, C. S., Juvvadi, P. R., Jin, F. J., Takahashi, T., Koyama, Y., Yamashita, S., et al. (2009). Disruption of the Ao pex11-1 gene involved in peroxisome proliferation leads to impaired woronin body formation in *Aspergillus oryzae*. *Eukaryot. Cell* 8, 296–305. doi: 10.1128/EC.00197-08

Falter, C., and Reumann, S. (2022). The essential role of fungal peroxisomes in plant infection. *Mol. Plant Pathol.* 23, 781–794. doi: 10.1111/mpp.13180

Geng, H. M., Zhang, Y. J., Li, J. X., Cui, Z. C., Wang, F., Wang, H. Y., et al. (2021). Genome-wide identification of NAC transcription factors with nuclear localization signal in wheat. *J. Hebei Agric. Univ.* 44, 9–16.

Goto-Yamada, S., Oikawa, K., Yamato, K. T., Kanai, M., Hikino, K., Nishimura, M., et al. (2022). Image-based analysis revealing the molecular mechanism of peroxisome dynamics in plants. *Front. Cell Dev. Biol.* 10:883491. doi: 10.3389/fcell.2022.883491

Harris, S. D., Morrell, J. L., and Hamer, J. E. (1994). Identification and characterization of *Aspergillus nidulans* mutants defective in cytokinesis. *Genetics* 136, 517–532. doi: 10.1093/genetics/136.2.517

Hatzipapas, P., Kalosak, K., Dara, A., and Christias, C. (2002). Spore germination and appressorium formation in the entomopathogenic *Alternaria alternata*. *Mycol. Res.* 106, 1349–1359. doi: 10.1017/S0953756202006792

Holsters, M., De Waele, D., Depicker, A., Messens, E., Van Montagu, M., and Schell, J. (1978). Transfection and transformation of *Agrobacterium tumefaciens*. *Mol. Gen. Genet.* 163, 181–187. doi: 10.1007/BF00267408

Huang, Y., Li, Z., Wang, H., Chen, Q., and Li, W. (2021). First report of leaf spot caused by *Nigrospora aurantiaca* in tobacco in China. *Plant Dis.* 105:1569. doi: 10.1094/PDIS-06-20-1201-PDN

Imazaki, A., Tanaka, A., Harimoto, Y., Yamamoto, M., Akimitsu, K., Park, P., et al. (2010). Contribution of peroxisomes to secondary metabolism and pathogenicity in the fungal plant pathogen *Alternaria alternata*. *Eukaryot. Cell* 9, 682–694. doi: 10.1128/EC.00369-09

Jenning, D. B., Daub, M. E., Pharr, D. M., and Williamson, J. D. (2002). Constitutive expression of a celery mannitol dehydrogenase in tobacco enhances resistance to the mannitol-secreting fungal pathogen *Alternaria alternata*. *Plant J.* 32, 41–49. doi: 10.1046/j.1365-313X.2001.01399.x

Jones, K., Jenkinson, C. B., Araújo, M. B., Zhu, J., Kim, R. Y., Kim, D. W., et al. (2016). Mitotic stopwatch for the blast fungus *Magnaporthe oryzae* during invasion of rice cells. *Fungal Genet. Biol.* 93, 46–49. doi: 10.1016/j.fgb.2016.06.002

Kubo, Y., Fujihara, N., Harata, K., Neumann, U., Robin, G. P., and Connell, R. O. (2015). *Colletotrichum orbiculare* FAM1 encodes a novel wogonin body-associated Pex22 peroxin required for appressorium-mediated plant infection. *mBio* 6, e01305–e01315. doi: 10.1128/mBio.01305-15

Li, L., Wang, J. Y., Chen, H. L., Chai, R. Y., Zhang, Z., Mao, X. Q., et al. (2017). Pex14/17, a filamentous fungus-specific peroxin, is required for the import of peroxisomal matrix proteins and full virulence of *Magnaporthe oryzae*. *Mol. Plant Pathol.* 18, 1238–1252. doi: 10.1111/mpp.12487

Li, L., Wang, J. Y., Zhang, Z., Wang, Y. L., Liu, M. X., Jiang, H., et al. (2014). MoPex19, which is essential for maintenance of peroxisomal structure and woronin bodies, is required for metabolism and development in the rice blast fungus. *PLoS One* 9:e85252. doi: 10.1371/journal.pone.0085252

Main, C. E. (1969). The tobacco brown spot lesion, a model to study halo formation. *Phytopathology* 59, 1040–1045.

Michielse, C. B., Hooykaas, P. J. J., van den Hondel, C. A. M. J. J., and Ram, A. F. J. (2008). Agrobacterium-mediated transformation of the filamentous fungus Aspergillus awamori. *Nature protocols* 3, 1671–1678. doi: 10.1038/nprot.2008.154

Motley, A. M., and Hettema, E. H. (2007). Yeast peroxisomes multiply by growth and division. *J. Cell Biol.* 178, 399–410. doi: 10.1083/jcb.200702167

Navarro-Espíndola, R., Suaste-Olmos, F., and Peraza-Reyes, L. (2020). Dynamic regulation of peroxisomes and mitochondria during fungal development. *J. Fungi* 6:302. doi: 10.3390/jof6040302

Peraza-Reyes, L., and Berteaux-Lecellier, V. (2013). Peroxisomes and sexual development in fungi. *Front. Physiol.* 4:244. doi: 10.3389/fphys.2013.00244

Pliego, C., Kanematsu, S., Ruano-Rosa, D., Vicente, A. D., López-Herrera, C., Cazorla, F. M., et al. (2009). GFP sheds light on the infection process of avocado roots by *Rosellinia necatrix*. *Fungal Genet. Biol.* 46, 137–145. doi: 10.1016/j.fgb.2008.11.009

Ramos-Pamplona, M., and Naqvi, N. I. (2006). Host invasion during rice-blast disease requires carnitine-dependent transport of peroxisomal acetyl-CoA. *Mol. Microbiol.* 61, 61–75. doi: 10.1111/j.1365-2958.2006.05194.x

Rho, H. S., Kang, S., and Lee, Y. H. (2001). Agrobacterium tumefaciens-mediated transformation of the plant pathogenic fungus, *Magnaporthe grisea*. *Mol. Cells* 12, 407–411.

Seong, K. Y., Zhao, X., Xu, J. R., Güldener, U., and Kistler, H. C. (2008). Conidial germination in the filamentous fungus *Fusarium graminearum*. *Fungal Genet. Biol.* 45, 389–399. doi: 10.1016/j.fgb.2007.09.002

Shoji, J. Y., Kikuma, T., Arioka, M., and Kitamoto, K. (2010). Macroautophagy-mediated degradation of whole nuclei in the filamentous fungus *Aspergillus oryzae*. *PLoS One* 5:e15650. doi: 10.1371/journal.pone.0015650

Slavov, S., Mayama, S., and Atanassov, A. (2004). Toxin production of *Alternaria alternata* tobacco pathotype. *Biotechnol. Biotechnol. Equip.* 18, 90–95. doi: 10.1080/13102818.2004.10817126

Straube, A., Weber, I., and Steinberg, G. (2005). A novel mechanism of nuclear envelope break-down in a fungus: Nuclear migration strips off the envelope. *EMBO J.* 24, 1674–1685. doi: 10.1038/sj.emboj.7600644

Wang, J. X. (2019). *Study on the function of virulence protein gene AIPev1 of ornamental tobacco brown spot disease*. MA thesis. Yunnan: Yunnan University.

Wang, J. Y., Li, L., Chai, R. Y., Qiu, H. P., Zhang, Z., Wang, Y. L., et al. (2019). Pex13 and Pex14, the key components of the peroxisomal docking complex, are required for peroxisome formation, host infection and pathogenicity-related morphogenesis in *Magnaporthe oryzae*. *Virulence* 10, 292–314. doi: 10.1080/21505594.2019.1598172

Wang, J. Y., Li, L., Zhang, Z., Qiu, H. P., Li, D. M., Fang, Y., et al. (2015). One of three pex11 family members is required for peroxisomal proliferation and full virulence of the rice blast fungus *Magnaporthe oryzae*. *PLoS One* 10:e0134249. doi: 10.1371/journal.pone.0134249

Wang, J. Y., Wu, X. Y., Zhang, Z., Du, X. F., Chai, R. Y., Liu, X. H., et al. (2008). Fluorescent co-localization of PTS1 and PTS2 and its application in analysis of the gene function and the peroxisomal dynamic in *Magnaporthe oryzae*. *J. Zhejiang Univ. Sci. B* 9, 802–810. doi: 10.1631/jzus.B0860001

Yakimova, E. T., Yordanova, Z. P., Slavov, S., Kapchina-Toteva, V. M., and Woltering, E. J. (2009). *Alternaria alternata* AT toxin induces programmed cell death in tobacco. *J. Phytopathol.* 157, 592–601. doi: 10.1111/j.1439-0434.2008.01535.x

Yang, X. M., Zhou, T. A. Y., and Shi, S. L. (2018). Establishment and nodular nitrogen fixation effect of green fluorescent labeled stains of alfalfa rhizobia. *Grassl. Turf* 38, 44–56.

Zhang, W. L., Zhai, Z. G., Xie, Y. J., and Li, G. Z. (2011). Research advance in tobacco brown spot. *Acta Agric. Jiangxi* 23, 118–120.

frontiers | Frontiers in Physiology

TYPE Review
PUBLISHED 01 June 2023
DOI 10.3389/fphys.2023.1213866

OPEN ACCESS

EDITED BY
Inhwan Hwang,
Pohang University of Science and Technology, Republic of Korea

REVIEWED BY
Dong Wook Lee,
Chonnam National University, Republic of Korea
Paul Jarvis,
University of Oxford, United Kingdom

*CORRESPONDENCE
Felix Kessler,
felix.kessler@unine.ch
Venkatasalam Shanmugabalaji,
shanmugabalaji.venkatasalam@unine.ch

†These authors have contributed equally to this work

RECEIVED 28 April 2023
ACCEPTED 22 May 2023
PUBLISHED 01 June 2023

CITATION
Ballabani G, Forough M, Kessler F and Shanmugabalaji V (2023), The journey of preproteins across the chloroplast membrane systems.
Front. Physiol. 14:1213866.
doi: 10.3389/fphys.2023.1213866

The journey of preproteins across the chloroplast membrane systems

Gent Ballabani†, Maryam Forough†, Felix Kessler* and Venkatasalam Shanmugabalaji*

Laboratory of Plant Physiology, Institute of Biology, University of Neuchâtel, Neuchâtel, Switzerland

The photosynthetic capacity of chloroplasts is vital for autotrophic growth in algae and plants. The origin of the chloroplast has been explained by the endosymbiotic theory that proposes the engulfment of a cyanobacterium by an ancestral eukaryotic cell followed by the transfer of many cyanobacterial genes to the host nucleus. As a result of the gene transfer, the now nuclear-encoded proteins acquired chloroplast targeting peptides (known as transit peptides; transit peptide) and are translated as preproteins in the cytosol. Transit peptides contain specific motifs and domains initially recognized by cytosolic factors followed by the chloroplast import components at the outer and inner envelope of the chloroplast membrane. Once the preprotein emerges on the stromal side of the chloroplast protein import machinery, the transit peptide is cleaved by stromal processing peptidase. In the case of thylakoid-localized proteins, cleavage of the transit peptides may expose a second targeting signal guiding the protein to the thylakoid lumen or allow insertion into the thylakoid membrane by internal sequence information. This review summarizes the common features of targeting sequences and describes their role in routing preproteins to and across the chloroplast envelope as well as the thylakoid membrane and lumen.

KEYWORDS

chloroplasts, preprotein, transit peptides, TOC-TIC, thylakoid

Introduction

The chloroplast is a member of the plastid organelle family known mostly for its photosynthetic activity though it does perform a vast array of other metabolic activities essential to plant survival, development, and stress responses (Jarvis and López-Juez, 2013). Plastids are the result of an endosymbiotic process that started over a billion years ago (Zimorski et al., 2014). Since that time, most plastid genes have either been lost or transferred to the nucleus (Timmis et al., 2004). Of the 2,000 plus chloroplast proteins only about 10% remain encoded by the chloroplast genome. The nuclear-encoded chloroplast preproteins contain an N-terminal transit peptide (TP). The TP can be compared to a molecular zip code of preproteins to be targeted to the chloroplast and imported via the chloroplast protein import machinery (Lee and Hwang, 2021).

The import mechanism involves multiple steps at different (sub-)organellar locations. Initially, the preprotein is guided through the cytosol accompanied by a chaperone complex until it is handed off at the outer envelope of the chloroplast where the transit peptide makes first contact with the TOC (Translocon at the Outer envelope of the Chloroplast) complex (Flores-Pérez and Jarvis, 2013). This involves the action of the two GTP-binding receptors TOC159 and TOC34. In a process that requires GTP and low concentrations of ATP

(0.1 mM), the preprotein is inserted across the large hybrid outer membrane protein-conducting channel that consists of the C-terminal ß-barrel membrane (M-) domain of TOC159 and that of TOC75 (Richardson et al., 2014; Schnell, 2019). At this stage already, the transit peptide is in contact with the intermembrane POTRA-domains of TOC75 and initiates contact with components of the TIC (translocon at the Inner envelope of the chloroplast) complex, namely, TIC22 and TIC20, however, without traversing the inner membrane (Kouranov et al., 1998). In the presence of high concentrations of ATP (> 1 mM) the preprotein crosses the TIC20 inner membrane protein-conducting channel and enters the chloroplast stroma assisted by ATP-dependent motor components (Richardson et al., 2018).

Once inside the stroma, the transit peptide is cleaved by the Stromal Processing Peptidase (SPP) (Richter and Lamppa, 1998). Many imported, mature proteins remain in the stroma and are folded with the help of chaperones. Some proteins, however, are targeted further to the thylakoid membrane or lumen. Thylakoid lumen targeted proteins possess bipartite targeting sequences consisting of a transit peptide followed by a thylakoid targeting signal that engages one of two pathways leading to the thylakoid lumen: The ΔpH-dependent TAT (twin arginine targeting) and SEC (secretory) pathways. However, the Signal Recognition Particle (SRP) pathway inserting proteins into the thylakoid membrane relies on targeting information residing within the mature sequence. Each of these pathways relies on a distinct set of protein components. Thylakoid targeting signals of preproteins are removed by a thylakoid processing peptidase (TPP) which promotes final assembly of the mature proteins leading to functional chloroplasts (Mori and Cline, 2001; Albiniak et al., 2012; Teixeira and Glaser, 2013).

Protein translocation into the chloroplast

The primary structures of transit peptides are highly diverse

"Signal Peptide" refers to an endoplasmic reticulum targeting sequence, "pre-sequence" to a mitochondrial one, and "transit peptide" is specific for chloroplast-targeted proteins (Bruce, 2000). In the late 1970s, after the signal hypothesis had been proposed, a study showed that *in vitro* translated Rubisco small unit (RbcS) protein had a higher molecular mass than mature RbcS in plant extracts. It was therefore considered a putative precursor (Dobberstein et al., 1977). The RbcS cDNA was cloned and revealed an N-terminal extension that was not present in the mature RbcS. It was identified as the chloroplast targeting sequence and coined "transit peptide" (Broglie et al., 1981; Coruzzi et al., 1983). Later studies demonstrated that the putative precursor of RbcS was transported into isolated chloroplasts and processed to its mature form (Highfield and Ellis, 1976; Chua and Schmidt, 1978). It has been proposed that transit peptides evolved from antimicrobial amphipathic peptides derived from host cells during endosymbiotic events, an intriguing hypothesis that is supported by experimental evidence (Caspari et al., 2023).

A motif study has shown that transit peptides contain three regions, a N-terminal region lacking charged amino acids, a central one containing hydroxylated amino acids and C-terminal one containing an arginine rich motif. This domain structure may be common to most preproteins (Karlin-Neumann and Tobin, 1986; von Heijne et al., 1989; Bruce, 2001). A later study, reporting extensive mutagenesis of the RbcS transit peptide, provided clues to the existence of FP/RK and MLM motifs in the transit peptide and their vital role in chloroplast protein import (Lee et al., 2006). Site-specific cross-linking experiments with the RbcS transit peptide, demonstrated that the FP/RK motif is important for interaction not only with components of the TOC complex, but also with the TIC20 component of the TIC complex (Richardson et al., 2018). In addition, FGLK is a transit peptide motif that has been characterized as being recurrent in transit peptides and playing an important role in the preprotein recognition by TOC34. The deletion of the FGLK sequence by mutagenesis prevented the preprotein from being translocated into the chloroplast (Chotewutmontri et al., 2012; Holbrook et al., 2016).

Based on a synthetic transit peptide, a study demonstrated that FGLK and FP/RK motifs are essential for RbcS transit peptide function and preprotein targeting of the chloroplast (Lee et al., 2015). Moderate hydrophobicity at the N-terminal region of the transit peptide is important for preprotein recognition, (Bhushan et al., 2006; Lee et al., 2006; Lee et al., 2008). Exchange of basic amino acids (N-terminal region) to acidic amino acids negatively affected preprotein import into chloroplasts (Razzak et al., 2017; Lee and Hwang, 2019). Twin-positive (positively charged amino acids) motifs in the TP appear to play a key role in preprotein import into old *versus* young chloroplasts (Teng et al., 2012). In addition, large scale *in silico* analysis and experimental evidence revealed that the twin-positive motif is important for preprotein import into leucoplasts (Chu et al., 2020).

The importance of proline residues in transit peptides has been demonstrated by comparing the import of preproteins containing proline-rich transit peptides with those lacking proline residues. The mutation of transit peptides by the replacement of prolines by alanines resulted in reduced efficiency of translocation into the chloroplast, specifically concerning transmembrane proteins and proteins prone to aggregation (Lee et al., 2018; Jeong et al., 2021). Proline is an amino acid that tends to disrupt the secondary structures of polypeptides (Guzzo, 1965). As preproteins are believed to be translocated across the TOC complex an unstructured transit peptide as described by the "perfect random coil hypothesis" may be advantageous to initiate the early stages of protein import (von Heijne and Nishikawa, 1991).

Energetics of translocation across at the chloroplast envelope membranes

The energy requirement of preprotein transport across the chloroplast envelopes was first analyzed in an *in vitro* import assay using isolated chloroplasts that were either light- or dark-adapted. The study showed that import into dark-adapted chloroplasts was compromised (Grossman et al., 1980). Exogenously added ATP rescued imports into dark-adapted chloroplasts, demonstrating that ATP was the primary energy

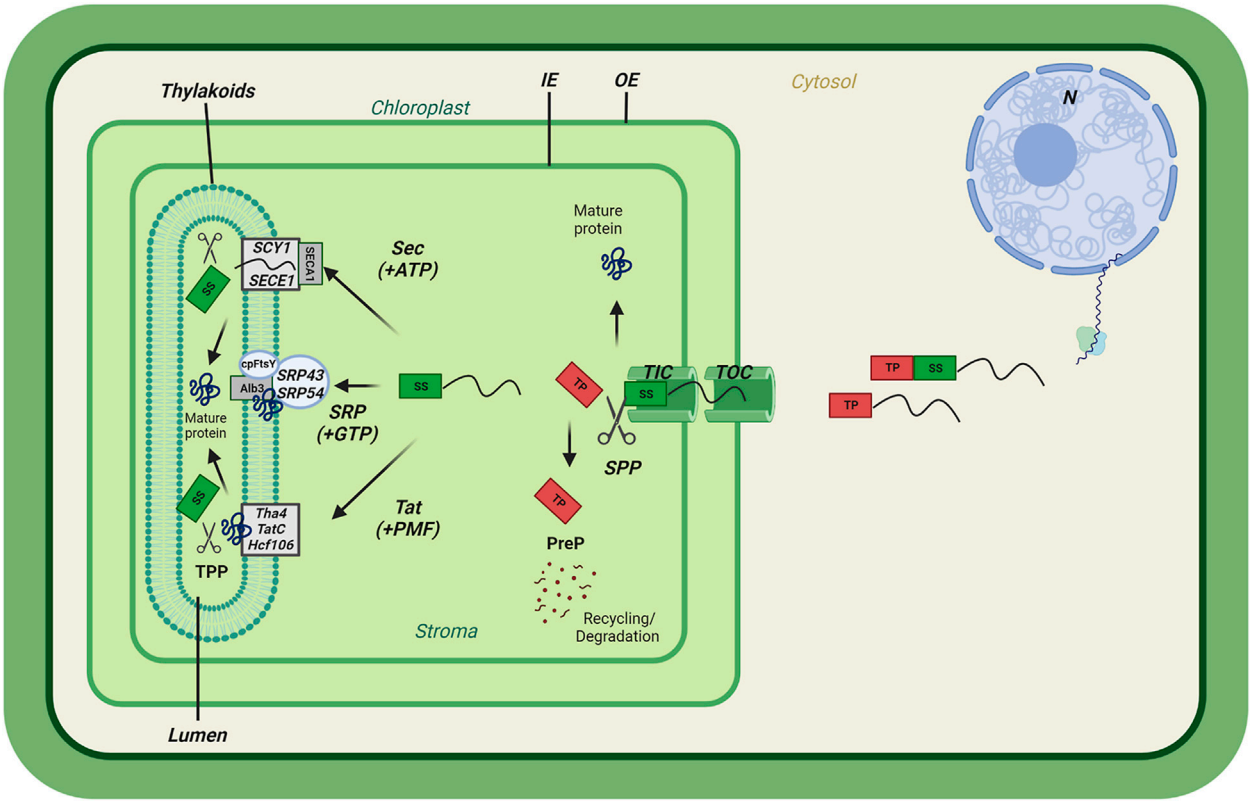

FIGURE 1
Preproteins translocation into chloroplast membrane systems. General scheme of chloroplast import of nuclear-encoded preproteins containing a transit peptide (TP) followed by a thylakoid Signal sequence (SS). Preprotein translocation passes through the Translocons at the Outer envelope (OE) of the Chloroplast (TOC) and the Inner envelope (IE) of the chloroplast (TIC). Upon entry, the transit peptide is cleaved by the Stromal Processing Peptidase (SPP) and processed by the PreP protease for recycling/degradation. The thylakoid-targeted proteins pass through either the Twin Arginine Transport (Tat) pathway requiring the Proton Motive Force (PMF), the Sec requiring ATP, or the Signal Recognition Particle (SRP) pathway. Upon thylakoid membrane insertion, the thylakoid signal sequence (SS) is cleaved by the Thylakoid Processing Peptidase (TPP), completing the final import step.

source (Cline et al., 1985). Later studies demonstrated that import of preproteins into chloroplasts was driven by the hydrolysis of ATP inside the chloroplast (Flügge and Hinz, 1986; Pain and Blobel, 1987; Theg et al., 1989). It was then revealed that distinct concentrations of ATP in different compartments defined separate steps of chloroplast protein import. Low concentrations of ATP (50–100 μM) were sufficient for preprotein binding to the surface of the chloroplast, whereas high concentrations of ATP (1 mM or more) were required for protein translocation across the chloroplast envelope (Olsen et al., 1989). The RbcS preprotein could be chemically crosslinked to chloroplast envelope component in an ATP-dependent manner (Perry and Keegstra, 1994).

The energetics findings were exploited to generate preprotein translocation intermediates and isolate the first components of the protein import machinery from isolated pea chloroplasts (Schnell and Blobel, 1993). In these experiments, recombinant preprotein of RbcS fused to two IgG-binding domains of *Staphylococcus aureus* ProteinA (resulting in pS-ProtA) was used as a tool. When incubated at low ATP concentrations, pS-ProtA is stably bound to isolated chloroplasts. pS-ProtA remained sensitive to exogenous protease and the transit peptide was not cleaved. This state defines the "early translocation intermediate". When incubated at high ATP concentrations, pS-ProtA was fully imported. However, its import could be arrested by chilling on ice. At this stage, pS-ProtA was both accessible to exogenous protease and the transit peptide partially cleaved resulting in mature S-ProtA. Thus, pS-ProtA and S-ProtA had traversed and were now spanning both the outer and inner envelope membrane. This state defines the "late translocation intermediate". It is important to note that the formation of both the "early" and "late" translocation intermediates critically depended on the presence of the transit peptide in pS-ProtA (Schnell and Blobel, 1993). The production of "early" and "late" translocation intermediates was upscaled from analytical to biochemical quantities allowing their isolation by IgG-affinity chromatography. The "early" translocation intermediate pS-ProtA was associated with three visible bands on a SDS-PAGE gel. These first three proteins were molecularly cloned and sequenced and are now known as TOC159, TOC75 and TOC34 (Kessler et al., 1994; Schnell et al., 1994). The three form the core of the TOC-complex as it is widely accepted today. In addition to the three core components of the TOC-complex, the "late" translocation intermediate pS-ProtA and S-ProtA associated with two more bands. One is known today as TIC110 while the second one, named IAP36 at the time, was never identified (Schnell et al., 1994). To this day, the role of TIC110 in

chloroplast protein import remains contested and is notably absent from algal protein import complexes (Ramundo et al., 2020).

Translocon complexes at the inner and outer chloroplast membranes

The large majority of chloroplast proteins are imported via the TOC-TIC complexes (Figure 1). The first components were identified in the beginning of 1990s as a result of studies on isolated pea chloroplasts and revealed three components of the outer and one at the inner envelope membranes (namely, Import intermediate Associated Proteins or Outer Envelope Protein), IAP/OEP34, IAP/OEP75, IAP/OEP86 and Inner Envelope Protein IAP100/IEP110 (Hirsch et al., 1994; Kessler et al., 1994; Perry and Keegstra, 1994; Schnell et al., 1994). These translocon components were renamed according to the TOC–TIC nomenclature as Toc34, Toc75, and Toc159 (for IAP/OEP86) and Tic110 (Schnell et al., 1997). The initial characterization revealed that TOC159 and TOC34 were homologous GTP-binding proteins exposed at the chloroplast surface. They were both sensitive to the addition of exogenous thermolysin protease fulfilling an important criterium for preprotein receptors at the chloroplast surface (Kessler et al., 1994). TOC75 was insensitive to exogenous thermolysin, bore homology to cyanobacterial ß-barrel solute channels related to the β-barrel assembly machinery A (BamA) family fulfilling criteria for a protein-conducting channel at the outer chloroplast membrane. TIC110 had two N-terminal alpha-helices and a large stromal domain suggesting that it may function as scaffold coordinating late translocation functions such as recruitment of chaperones for protein folding and assembly (Kessler and Blobel, 1996).

The presence of GTP-binding proteins in the TOC complex encouraged further energetics experimentation. Preprotein binding to chloroplasts does not only require low concentrations of ATP but also implicates GTP as non- and slowly-hydrolyzable GTP analogs inhibited import. These findings supported the importance of the role of TOC GTPase receptors (Olsen and Keegstra, 1992; Kessler et al., 1994). Apart from the irreversible energy-dependent interactions, the transit peptide is also reversibly bound to TOC159 and TOC75 in an energy-independent way as demonstrated by chemical cross-linking (Ma et al., 1996).

In Arabidopsis as well as other species, both of the GTP-binding TOCs are encoded by multigene families and consequently several isoforms of each have been discovered. The structure of TOC34 as well as those of its homologs consists of two main features, a N-terminal GTPase domain and a single C-terminal alpha-helical membrane-spanning domain followed by a short hydrophilic tail (Jarvis et al., 1998). TOC159 and its three homologs in Arabidopsis (atTOC120, −132, −90) possess a central GTPase (G-) domain, a C-terminal membrane-anchoring (M-) domain, and a N-terminal acidic (A-) domain at the N-terminus (Kubis et al., 2004). The M-domain has now been shown to take on a ß-barrel structure and associate with TOC75 to form a large hybrid channel at the outer chloroplast membrane (Jin et al., 2022; Liu et al., 2023). The A-domains in the four Arabidopsis isoforms of TOC159 are much more divergent than the G- and M-domains and appear to play a role in pre-protein specificity (Agne et al., 2010). It, however, is not clear how the various A-domains distinguish the transit peptides of different classes of preproteins (i.e., photosynthesis-associated *versus* house-keeping) (Bauer et al., 2000; Ivanova et al., 2004). TOC75 belongs to the BamA family with homologs in Gram-negative bacteria as well as mitochondria and plastids (Schleiff and Becker, 2011). Based on these similarities, TOC75 was proposed to function as the protein-conducting channel at the outer membrane of the chloroplast. TOC75 is encoded by a single orthologous gene in the genomes of all plant species sequenced so far. In addition to forming a ß-barrel channel, TOC75 has three N-terminal POTRA (polypeptide transport-associated) domains (Sánchez-Pulido et al., 2003; Srinivasan et al., 2023). The POTRA domain contributes to preprotein recognition and has chaperone-like activity to guide the incoming preprotein across the intermembrane space (Kouranov and Schnell, 1997; Paila et al., 2016; O'Neil et al., 2017).

At the inner envelope membrane, at least two models have been proposed for the TIC complex, the first consisting of the TIC20 (channel) TIC214 (plastid-encoded), TIC100, TIC56, TIC21 and TIC12 forming a 1 MDa complex (Kikuchi et al., 2013) the second consisting of TIC110 and TIC40. Currently, it is not clear whether the second complex functions together with or independently from the 1 MDa TIC complex in land plants. Cryo-EM structures of the Chlamydomonas TOC-TIC holocomplexes, however, did not contain homologs of TIC40 or TIC110 (Jin et al., 2022; Liu et al., 2023). In addition to the aforementioned components the intermembrane space component TIC236 constitutes a physical link between the TOC and TIC complexes (Chen et al., 2018). TIC22, another intermembrane space component, has been proposed to promote preprotein import across both envelope membranes and the intermembrane space besides its function as a chaperone (Kouranov et al., 1999). As preprotein import requires ATP, the existence of ATP-dependent motors has been proposed. However, the exact nature of such stromal import motor(s) is currently contested. On the one hand biochemical and genetic information provide support for a chaperone network consisting of cpHsp70, Hsp90C, and Hsp93) consuming the ATP and energizing translocation (Su and Li, 2010; Inoue et al., 2013; Huang et al., 2016). On the other hand, an alternative stromal motor has been proposed that consists of a 2-MDa ycf2/FtsH1 complex that also has predicted ATP hydrolysis activity (Kikuchi et al., 2018). However, the respective significance of the two proposed motor systems has not been evaluated so far, and neither of the two systems were observed in the currently available Cryo-EM structures (Jin et al., 2022; Liu et al., 2023).

Transit peptides are cleaved by stromal processing peptidase

Upon entry into the chloroplast stroma and possibly before complete translocation, the transit peptide is cleaved by Stromal Processing Peptidase (SPP) (Figure 1) (Richter and Lamppa, 2002; Richter and Lamppa, 2003). SPP is an M16 metallopeptidase carrying out a function comparable to that of the Mitochondrial Processing Peptidase (MPP), a metalloprotease, involved in the

maturation of nuclear encoded proteins imported into mitochondria (Pollock et al., 1988; Braun et al., 1992). SPP, cleaves at a semiconserved motif ((I/V)-X-(A/C)-↓-A (arrow marks cleavage site) at the C-terminus of the transit peptide (von Heijne et al., 1989). Thereby initiating the final steps of preprotein maturation. After transit peptide cleavage, these may include folding and/or assembly in the stroma or insertion into or translocation across the thylakoid membrane. SPP is an essential component of the import mechanism as demonstrated by the aborted seed phenotype observed in the *spp* homozygous knockout mutants (Trösch and Jarvis, 2011). Once cleaved, transit peptides are further degraded by presequence peptidases (PrePs) (Figure 1) (Ståhl et al., 2005).

Thylakoid membrane targeting sequences and alternative insertion pathway

The thylakoid membrane is home to the light reactions of photosynthesis. For thylakoid biogenesis, assembly of thylakoid luminal and integral membrane proteins is essential. For a considerable number of proteins, the journey therefore is not finished upon arrival inside the chloroplast. Cleavage of the transit peptide may expose a secondary targeting sequence that will engage one of at least two entry pathways to the thylakoids. Two routes exist for entering the thylakoid lumen: the twin-arginine translocase (TAT) that may accommodate folded proteins, or the SEC translocase for unfolded proteins (Figure 1) (Yuan et al., 1994; Mori et al., 1999). In addition, integral thylakoid membrane proteins require the signal recognition particle (SRP) pathway for alternative insertion (Figure 1) (Schünemann, 2007). Interestingly, all three pathways have been conserved from the cyanobacterial ancestor and exist in bacteria and, in the case of the SEC and SRP pathways, in animals to this day.

SEC translocation mechanism

The SEC pathway is well-known for its evolutionary conserved mechanism (Dalbey and Chen, 2004). In thylakoid targeting signals, the SEC-specific signal sequence has been described as containing three domains, a charged domain at the N-terminal part, a hydrophobic mid-section and C-terminal cleavage domain containing an A-x-A motif set for interaction with the thylakoid processing peptidase (TPP) (Hsu et al., 2011; Celedon and Cline, 2013). SEC1 is the SEC translocase at the thylakoid membrane (Fernandez, 2018). The SEC1 complex contains SCY1 and SECE1 thylakoid membrane protein channels associated with the stromal motor protein SECA1 (Nakai et al., 1994). Nuclear-encoded lumenal proteins are translocated in an unfolded form across the SEC translocase. The N-terminal part of the signal peptide interacts with SECA1 translocation motor and its ATPase activity provides the energy for translocation across the SCY1/SECE1 channel. Subsequently, the signal sequence is cleaved in the thylakoid lumen (Figure 1) (Albiniak et al., 2012). HSP90C may also assist the SEC1 translocation pathway in translocating thylakoid precursor proteins from the stroma to the lumen (Jiang et al., 2020). Surprisingly, a SEC2 translocase system also exists that is similar to SEC1, but SCY2 and SECE2 are inner envelope membrane protein channels using the stromal motor protein SECA2 (Skalitzky et al., 2011). The known examples of SEC2-dependent translocation of inner envelope proteins are TIC40 and FTSH12 (Li et al., 2017). However, the SEC2 translocase system is poorly understood compared to SEC1 due to a lack of studies.

TAT translocation mechanism

The Twin Arginine Transport (Tat) pathway is so called because the corresponding targeting sequences contain two neighbouring arginine residues (Cline et al., 1992). The TAT pathway is distinct from others in that it is able to transport fully folded protein across the thylakoid membrane and into the lumen. The TAT-specific signal sequence features are similar to those of SEC with the exception of the N-terminal part that contains the twin arginine (RR) motif. The RR motif is responsible for SEC avoidance response in thylakoid targeting (New et al., 2018). The Tat pathway is estimated to be responsible for the import of an estimated 50% of the thylakoid lumen proteins (Robinson and Bolhuis, 2004). The characteristic twin-arginine motif is essential for translocation and is disabled by mutation to other combinations of amino acids. The TAT pathway requires only the proton motive force (pmf) as energy source in order to achieve protein transport and has therefore also been called the ΔpH pathway (Mould and Robinson, 1991). Three proteins named TatC, Hcf106 and Tha4 form a complex that binds to the precursor protein's RRXFLK motif in the N-terminal part of the signal sequence in order to facilitate translocation (Figure 1). Liquid-liquid phase separation by Hcf106-ankyrin-repeat proteins (STT) interaction facilitates the TAT dependent translocation of the luminal proteins (Ouyang et al., 2020). Several models of translocation have been proposed for the plant TAT pathway. However, no proven model exists to date (New et al., 2018).

SRP

The chloroplast signal recognition particle (cpSRP) pathway, which is derived from prokaryotes and known as cpSRP pathway, targets and inserts abundant thylakoid membrane proteins, for example, light-harvesting chlorophyll-binding proteins (LHCPs) (Ziehe et al., 2018). Unlike SEC and TAT pathways, no conserved motif or domain is present at the N-terminal of the protein for thylakoid targeting. Several studies address LHCP recognition by the cpSRP pathway. The L18 motif (18 amino acids within the second and third transmembrane helices) of LHCP is crucial for recognition by cpSRP transit complex (Tu et al., 2000). Once nuclear-encoded LHCP is imported into the chloroplast via the TOC-TIC complex and processed by SPP, it forms the stromal transit complex together with cpSRP54 (GTPase) and cpSRP43 (Schuenemann et al., 1998). The cpSRP transit complex containing LHCP binds to cpSRP receptor cpFtsY (GTPase) (Kogata et al., 1999; Tu et al., 1999; Nguyen et al., 2011) and docks to Alb3 (insertase at thylakoid membrane) via cpSRP43, promoting precursor/LHCP insertion into thylakoid membrane (Figure 1) (Moore et al., 2000; Bals et al., 2010).

cpSRP43 has two distinct chaperone activities for i) LHCP insertion and ii) tetrapyrrole biosynthesis enzymes. The chaperone activity towards tetrapyrolle biosynthesis activity allows to coordinate LHCP insertion with chlorophyll biosynthesis and assembly into LHCP. Interestingly, cpSRP54 activates the cpSRP43 chaperone function towards LHCP insertion and inhibits the chaperone activity towards tetrapyrrole biosynthesis enzymes (Wang et al., 2018; Ji et al., 2021). However, except for LHCP, there is a lack of information about how the SRP targets are recognized by the components of the SRP pathway.

Thylakoid processing peptidase (TPP)

The thylakoid proteins are translocated into the thylakoid lumen by either the Sec or Tat pathways and, in a final step the N-terminal thylakoid targeting sequence is cleaved by Thylakoid Processing Peptidase (TPP) (Figure 1) (Hsu et al., 2011). TPP is a member of the membrane-bound proteases belonging to the type I signal peptidase (SPase I) family in both prokaryotes and eukaryotes. Plsp1 and Plsp2A/B are the two TPPs present in the thylakoids (Hsu et al., 2011). Plsp1 is known to be involved in the SEC and TAT dependent signal sequence cleavage and, surprisingly also, processing of TOC75 at the envelope membrane, suggesting that at least the Plsp1 protease is found not only in the thylakoid membrane but also in the envelopes. Plsp1 is essential for chloroplast biogenesis, its mutation resulting in a very pale green phenotype (Shipman and Inoue, 2009). Currently, the physiological and functional roles of Plsp2A/B in signal peptide processing are unclear.

Conclusion and future perspectives

In the last years, significant progress has been made with regard to the understanding of the molecular and mechanistic details of chloroplast import of nuclear-encoded proteins by the TOC-TIC complex. The recent cryo-EM structural studies reveal how the TOC-TIC components are arranged in detail and provide some information on the likely path of the preprotein and its transit peptide across the chloroplast envelope. It would now be highly interesting to study the cryo-EM structure of the TOC-TIC complex in association with a preprotein and its transit peptide to gain a complete understanding of the import process. Also, the recent cryo-EM structures failed to reveal the cytosolic GTPase domains of the TOC34 and −159 (Jin et al., 2022; Liu et al., 2023) that play a central role in transit peptide recognition. The GTPase domains should remain a key target in future structural work. Recent advances in the chloroplast transit peptide field reveal that specific motifs, i.e., the proline-rich motif, have vital roles in the preprotein interaction with the TOC-TIC translocon. However, fundamental knowledge concerning the recognition and distinction of transit peptides belonging to different classes of preproteins (i.e., photosynthesis-associated vs. nonphotosynthetic housekeeping) is still lacking. In the future, the identification and investigation of particular motifs playing essential roles in tissue- and plastid-specific protein import pathways are predicted to be important research questions. Last but not least, many questions regarding second targeting sequences and their role in processing and assembly of the all-important photosystems remain open and should be addressed in the future.

Author contributions

FK and VS conceived this review article. GB, MF, FK, and VS participated in the writing of the manuscript. GB prepared the figure. All authors contributed to the article and approved the submitted version.

Funding

This work was supported by the Swiss National Science Foundation (SNSF) grant 310030_208000 to FK.

Acknowledgments

We thank the BioRender program for the image.

Conflict of interest

The authors declare that the research was conducted in the absence of any commercial or financial relationships that could be construed as a potential conflict of interest.

Publisher's note

References

Agne, B., Andrès, C., Montandon, C., Christ, B., Ertan, A., Jung, F., et al. (2010). The acidic A-domain of Arabidopsis TOC159 occurs as a hyperphosphorylated protein. *Plant Physiol.* 153, 1016–1030. doi:10.1104/pp.110.158048

Albiniak, A. M., Baglieri, J., and Robinson, C. (2012). Targeting of lumenal proteins across the thylakoid membrane. *J. Exp. Bot.* 63, 1689–1698. doi:10.1093/jxb/err444

Bals, T., Dünschede, B., Funke, S., and Schünemann, D. (2010). Interplay between the cpSRP pathway components, the substrate LHCP and the translocase Alb3: An *in vivo* and *in vitro* study. *FEBS Lett.* 584, 4138–4144. doi:10.1016/j.febslet.2010.08.053

Bauer, J., Chen, K., Hiltbunner, A., Wehrli, E., Eugster, M., Schnell, D., et al. (2000). The major protein import receptor of plastids is essential for chloroplast biogenesis. *Nature* 403, 203–207. doi:10.1038/35003214

Bhushan, S., Kuhn, C., Berglund, A. K., Roth, C., and Glaser, E. (2006). The role of the N-terminal domain of chloroplast targeting peptides in organellar protein import and miss-sorting. *FEBS Lett.* 580, 3966–3972. doi:10.1016/j.febslet.2006.06.018

Braun, H. P., Emmermann, M., Kruft, V., and Schmitz, U. K. (1992). The general mitochondrial processing peptidase from potato is an integral part of cytochrome c

reductase of the respiratory chain. *Embo J.* 11, 3219–3227. doi:10.1002/j.1460-2075.1992.tb05399.x

Broglie, R., Bellemare, G., Bartlett, S. G., Chua, N. H., and Cashmore, A. R. (1981). Cloned DNA sequences complementary to mRNAs encoding precursors to the small subunit of ribulose-1,5-bisphosphate carboxylase and a chlorophyll a/b binding polypeptide. *Proc. Natl. Acad. Sci. U. S. A.* 78, 7304–7308. doi:10.1073/pnas.78.12.7304

Bruce, B. D. (2000). Chloroplast transit peptides: Structure, function and evolution. *Trends Cell Biol.* 10, 440–447. doi:10.1016/s0962-8924(00)01833-x

Bruce, B. D. (2001). The paradox of plastid transit peptides: Conservation of function despite divergence in primary structure. *Biochim. Biophys. Acta* 1541, 2–21. doi:10.1016/s0167-4889(01)00149-5

Caspari, O. D., Garrido, C., Law, C. O., Choquet, Y., Wollman, F. A., and Lafontaine, I. (2023). Converting antimicrobial into targeting peptides reveals key features governing protein import into mitochondria and chloroplasts. *Plant Commun.* 2023, 100555. doi:10.1016/j.xplc.2023.100555

Celedon, J. M., and Cline, K. (2013). Intra-plastid protein trafficking: How plant cells adapted prokaryotic mechanisms to the eukaryotic condition. *Biochim. Biophys. Acta* 1833, 341–351. doi:10.1016/j.bbamcr.2012.06.028

Chen, Y. L., Chen, L. J., Chu, C. C., Huang, P. K., Wen, J. R., and Li, H. M. (2018). TIC236 links the outer and inner membrane translocons of the chloroplast. *Nature* 564, 125–129. doi:10.1038/s41586-018-0713-y

Chotewutmontri, P., Reddick, L. E., Mcwilliams, D. R., Campbell, I. M., and Bruce, B. D. (2012). Differential transit peptide recognition during preprotein binding and translocation into flowering plant plastids. *Plant Cell* 24, 3040–3059. doi:10.1105/tpc.112.098327

Chu, C. C., Swamy, K., and Li, H. M. (2020). Tissue-specific regulation of plastid protein import via transit-peptide motifs. *Plant Cell* 32, 1204–1217. doi:10.1105/tpc.19.00702

Chua, N. H., and Schmidt, G. W. (1978). *In vitro* synthesis, transport, and assembly of ribulose 1,5-bisphosphate carboxylase subunits. *Basic Life Sci.* 11, 325–347. doi:10.1007/978-1-4684-8106-8_20

Cline, K., Ettinger, W. F., and Theg, S. M. (1992). Protein-specific energy requirements for protein transport across or into thylakoid membranes. Two lumenal proteins are transported in the absence of ATP. *J. Biol. Chem.* 267, 2688–2696. doi:10.1016/s0021-9258(18)45935-2

Cline, K., Werner-Washburne, M., Lubben, T. H., and Keegstra, K. (1985). Precursors to two nuclear-encoded chloroplast proteins bind to the outer envelope membrane before being imported into chloroplasts. *J. Biol. Chem.* 260, 3691–3696. doi:10.1016/s0021-9258(19)83678-5

Coruzzi, G., Broglie, R., Cashmore, A., and Chua, N. H. (1983). Nucleotide sequences of two pea cDNA clones encoding the small subunit of ribulose 1,5-bisphosphate carboxylase and the major chlorophyll a/b-binding thylakoid polypeptide. *J. Biol. Chem.* 258, 1399–1402. doi:10.1016/s0021-9258(18)32995-8

Dalbey, R. E., and Chen, M. (2004). Sec-translocase mediated membrane protein biogenesis. *Biochim. Biophys. Acta* 1694, 37–53. doi:10.1016/j.bbamcr.2004.03.009

Dobberstein, B., Blobel, G., and Chua, N. H. (1977). *In vitro* synthesis and processing of a putative precursor for the small subunit of ribulose-1,5-bisphosphate carboxylase of Chlamydomonas reinhardtii. *Proc. Natl. Acad. Sci. U. S. A.* 74, 1082–1085. doi:10.1073/pnas.74.3.1082

Fernandez, D. E. (2018). Two paths diverged in the stroma: Targeting to dual SEC translocase systems in chloroplasts. *Photosynth Res.* 138, 277–287. doi:10.1007/s11120-018-0541-9

Flores-Pérez, Ú., and Jarvis, P. (2013). Molecular chaperone involvement in chloroplast protein import. *Biochim. Biophys. Acta* 1833, 332–340. doi:10.1016/j.bbamcr.2012.03.019

Flügge, U. I., and Hinz, G. (1986). Energy dependence of protein translocation into chloroplasts. *Eur. J. Biochem.* 160, 563–570. doi:10.1111/j.1432-1033.1986.tb10075.x

Grossman, A. R., Bartlett, S. G., Schmidt, G. W., and Chua, N. H. (1980). Post-translational uptake of cytoplasmically synthesized proteins by intact chloroplasts *in vitro*. *Ann. N. Y. Acad. Sci.* 343, 266–274. doi:10.1111/j.1749-6632.1980.tb47257.x

Guzzo, A. V. (1965). The influence of amino-acid sequence on protein structure. *Biophys. J.* 5, 809–822. doi:10.1016/S0006-3495(65)86753-4

Highfield, P. E., and Ellis, R. J. (1976). Protein synthesis in chloroplasts. VII. Initiation of protein synthesis in isolated intact pea chloroplasts. *Biochim. Biophys. Acta* 447, 20–27. doi:10.1016/0005-2787(76)90091-5

Hirsch, S., Muckel, E., Heemeyer, F., Von Heijne, G., and Soll, J. (1994). A receptor component of the chloroplast protein translocation machinery. *Science* 266, 1989–1992. doi:10.1126/science.7801125

Holbrook, K., Subramanian, C., Chotewutmontri, P., Reddick, L. E., Wright, S., Zhang, H., et al. (2016). Functional analysis of semi-conserved transit peptide motifs and mechanistic implications in precursor targeting and recognition. *Mol. Plant* 9, 1286–1301. doi:10.1016/j.molp.2016.06.004

Hsu, S. C., Endow, J. K., Ruppel, N. J., Roston, R. L., Baldwin, A. J., and Inoue, K. (2011). Functional diversification of thylakoidal processing peptidases in *Arabidopsis thaliana*. *PLoS One* 6, e27258. doi:10.1371/journal.pone.0027258

Huang, P. K., Chan, P. T., Su, P. H., Chen, L. J., and Li, H. M. (2016). Chloroplast Hsp93 directly binds to transit peptides at an early stage of the preprotein import process. *Plant Physiol.* 170, 857–866. doi:10.1104/pp.15.01830

Inoue, H., Li, M., and Schnell, D. J. (2013). An essential role for chloroplast heat shock protein 90 (Hsp90C) in protein import into chloroplasts. *Proc. Natl. Acad. Sci. U. S. A.* 110, 3173–3178. doi:10.1073/pnas.1219229110

Ivanova, Y., Smith, M. D., Chen, K., and Schnell, D. J. (2004). Members of the Toc159 import receptor family represent distinct pathways for protein targeting to plastids. *Mol. Biol. Cell* 15, 3379–3392. doi:10.1091/mbc.e03-12-0923

Jarvis, P., Chen, L. J., Li, H., Peto, C. A., Fankhauser, C., and Chory, J. (1998). An Arabidopsis mutant defective in the plastid general protein import apparatus. *Science* 282, 100–103. doi:10.1126/science.282.5386.100

Jarvis, P., and López-Juez, E. (2013). Biogenesis and homeostasis of chloroplasts and other plastids. *Nat. Rev. Mol. Cell Biol.* 14, 787–802. doi:10.1038/nrm3702

Jeong, J., Hwang, I., and Lee, D. W. (2021). Functional organization of sequence motifs in diverse transit peptides of chloroplast proteins. *Front. Physiol.* 12, 795156. doi:10.3389/fphys.2021.795156

Ji, S., Siegel, A., Shan, S. O., Grimm, B., and Wang, P. (2021). Chloroplast SRP43 autonomously protects chlorophyll biosynthesis proteins against heat shock. *Nat. Plants* 7, 1420–1432. doi:10.1038/s41477-021-00994-y

Jiang, T., Mu, B., and Zhao, R. (2020). Plastid chaperone HSP90C guides precursor proteins to the SEC translocase for thylakoid transport. *J. Exp. Bot.* 71, 7073–7087. doi:10.1093/jxb/eraa399

Jin, Z., Wan, L., Zhang, Y., Li, X., Cao, Y., Liu, H., et al. (2022). Structure of a TOC-TIC supercomplex spanning two chloroplast envelope membranes. *Cell* 185, 4788–4800.e13. doi:10.1016/j.cell.2022.10.030

Karlin-Neumann, G. A., and Tobin, E. M. (1986). Transit peptides of nuclear-encoded chloroplast proteins share a common amino acid framework. *Embo J.* 5, 9–13. doi:10.1002/j.1460-2075.1986.tb04170.x

Kessler, F., and Blobel, G. (1996). Interaction of the protein import and folding machineries of the chloroplast. *Proc. Natl. Acad. Sci. U. S. A.* 93, 7684–7689. doi:10.1073/pnas.93.15.7684

Kessler, F., Blobel, G., Patel, H. A., and Schnell, D. J. (1994). Identification of two GTP-binding proteins in the chloroplast protein import machinery. *Science* 266, 1035–1039. doi:10.1126/science.7973656

Kikuchi, S., Asakura, Y., Imai, M., Nakahira, Y., Kotani, Y., Hashiguchi, Y., et al. (2018). A ycf2-FtsHi heteromeric AAA-ATPase complex is required for chloroplast protein import. *Plant Cell* 30, 2677–2703. doi:10.1105/tpc.18.00357

Kikuchi, S., Bédard, J., Hirano, M., Hirabayashi, Y., Oishi, M., Imai, M., et al. (2013). Uncovering the protein translocon at the chloroplast inner envelope membrane. *Science* 339, 571–574. doi:10.1126/science.1229262

Kogata, N., Nishio, K., Hirohashi, T., Kikuchi, S., and Nakai, M. (1999). Involvement of a chloroplast homologue of the signal recognition particle receptor protein, FtsY, in protein targeting to thylakoids. *FEBS Lett.* 447, 329–333. doi:10.1016/s0014-5793(99)00305-1

Kouranov, A., Chen, X., Fuks, B., and Schnell, D. J. (1998). Tic20 and Tic22 are new components of the protein import apparatus at the chloroplast inner envelope membrane. *J. Cell Biol.* 143, 991–1002. doi:10.1083/jcb.143.4.991

Kouranov, A., and Schnell, D. J. (1997). Analysis of the interactions of preproteins with the import machinery over the course of protein import into chloroplasts. *J. Cell Biol.* 139, 1677–1685. doi:10.1083/jcb.139.7.1677

Kouranov, A., Wang, H., and Schnell, D. J. (1999). Tic22 is targeted to the intermembrane space of chloroplasts by a novel pathway. *J. Biol. Chem.* 274, 25181–25186. doi:10.1074/jbc.274.35.25181

Kubis, S., Patel, R., Combe, J., Bédard, J., Kovacheva, S., Lilley, K., et al. (2004). Functional specialization amongst the Arabidopsis Toc159 family of chloroplast protein import receptors. *Plant Cell* 16, 2059–2077. doi:10.1105/tpc.104.023309

Lee, D. W., and Hwang, I. (2019). Protein import into chloroplasts via the Tic40-dependent and -independent pathways depends on the amino acid composition of the transit peptide. *Biochem. Biophys. Res. Commun.* 518, 66–71. doi:10.1016/j.bbrc.2019.08.009

Lee, D. W., and Hwang, I. (2021). Understanding the evolution of endosymbiotic organelles based on the targeting sequences of organellar proteins. *New Phytol.* 230, 924–930. doi:10.1111/nph.17167

Lee, D. W., Kim, J. K., Lee, S., Choi, S., Kim, S., and Hwang, I. (2008). Arabidopsis nuclear-encoded plastid transit peptides contain multiple sequence subgroups with distinctive chloroplast-targeting sequence motifs. *Plant Cell* 20, 1603–1622. doi:10.1105/tpc.108.060541

Lee, D. W., Lee, S., Lee, G. J., Lee, K. H., Kim, S., Cheong, G. W., et al. (2006). Functional characterization of sequence motifs in the transit peptide of Arabidopsis small subunit of rubisco. *Plant Physiol.* 140, 466–483. doi:10.1104/pp.105.074575

Lee, D. W., Woo, S., Geem, K. R., and Hwang, I. (2015). Sequence motifs in transit peptides act as independent functional units and can Be transferred to new sequence contexts. *Plant Physiol.* 169, 471–484. doi:10.1104/pp.15.00842

Lee, D. W., Yoo, Y. J., Razzak, M. A., and Hwang, I. (2018). Prolines in transit peptides are crucial for efficient preprotein translocation into chloroplasts. *Plant Physiol.* 176, 663–677. doi:10.1104/pp.17.01553

Li, Y., Martin, J. R., Aldama, G. A., Fernandez, D. E., and Cline, K. (2017). Identification of putative substrates of SEC2, a chloroplast inner envelope translocase. *Plant Physiol.* 173, 2121–2137. doi:10.1104/pp.17.00012

Liu, H., Li, A., Rochaix, J. D., and Liu, Z. (2023). Architecture of chloroplast TOC-TIC translocon supercomplex. *Nature* 615, 349–357. doi:10.1038/s41586-023-05744-y

Ma, Y., Kouranov, A., Lasala, S. E., and Schnell, D. J. (1996). Two components of the chloroplast protein import apparatus, IAP86 and IAP75, interact with the transit sequence during the recognition and translocation of precursor proteins at the outer envelope. *J. Cell Biol.* 134, 315–327. doi:10.1083/jcb.134.2.315

Moore, M., Harrison, M. S., Peterson, E. C., and Henry, R. (2000). Chloroplast Oxa1p homolog albino3 is required for post-translational integration of the light harvesting chlorophyll-binding protein into thylakoid membranes. *J. Biol. Chem.* 275, 1529–1532. doi:10.1074/jbc.275.3.1529

Mori, H., and Cline, K. (2001). Post-translational protein translocation into thylakoids by the Sec and DeltapH-dependent pathways. *Biochim. Biophys. Acta* 1541, 80–90. doi:10.1016/s0167-4889(01)00150-1

Mori, H., Summer, E. J., Ma, X., and Cline, K. (1999). Component specificity for the thylakoidal Sec and Delta pH-dependent protein transport pathways. *J. Cell Biol.* 146, 45–56. doi:10.1083/jcb.146.1.45

Mould, R. M., and Robinson, C. (1991). A proton gradient is required for the transport of two lumenal oxygen-evolving proteins across the thylakoid membrane. *J. Biol. Chem.* 266, 12189–12193. doi:10.1016/s0021-9258(18)98879-4

Nakai, M., Goto, A., Nohara, T., Sugita, D., and Endo, T. (1994). Identification of the SecA protein homolog in pea chloroplasts and its possible involvement in thylakoidal protein transport. *J. Biol. Chem.* 269, 31338–31341. doi:10.1016/s0021-9258(18)31698-3

New, C. P., Ma, Q., and Dabney-Smith, C. (2018). Routing of thylakoid lumen proteins by the chloroplast twin arginine transport pathway. *Photosynth Res.* 138, 289–301. doi:10.1007/s11120-018-0567-z

Nguyen, T. X., Chandrasekar, S., Neher, S., Walter, P., and Shan, S. O. (2011). Concerted complex assembly and GTPase activation in the chloroplast signal recognition particle. *Biochemistry* 50, 7208–7217. doi:10.1021/bi200742a

O'neil, P. K., Richardson, L. G. L., Paila, Y. D., Piszczek, G., Chakravarthy, S., Noinaj, N., et al. (2017). The POTRA domains of Toc75 exhibit chaperone-like function to facilitate import into chloroplasts. *Proc. Natl. Acad. Sci. U. S. A.* 114, E4868–e4876. doi:10.1073/pnas.1621179114

Olsen, L. J., and Keegstra, K. (1992). The binding of precursor proteins to chloroplasts requires nucleoside triphosphates in the intermembrane space. *J. Biol. Chem.* 267, 433–439. doi:10.1016/s0021-9258(18)48513-4

Olsen, L. J., Theg, S. M., Selman, B. R., and Keegstra, K. (1989). ATP is required for the binding of precursor proteins to chloroplasts. *J. Biol. Chem.* 264, 6724–6729. doi:10.1016/s0021-9258(18)83489-5

Ouyang, M., Li, X., Zhang, J., Feng, P., Pu, H., Kong, L., et al. (2020). Liquid-liquid phase transition drives intra-chloroplast cargo sorting. *Cell* 180, 1144–1159. doi:10.1016/j.cell.2020.02.045

Paila, Y. D., Richardson, L. G., Inoue, H., Parks, E. S., Mcmahon, J., Inoue, K., et al. (2016). Multi-functional roles for the polypeptide transport associated domains of Toc75 in chloroplast protein import. *Elife* 5, e12631. doi:10.7554/eLife.12631

Pain, D., and Blobel, G. (1987). Protein import into chloroplasts requires a chloroplast ATPase. *Proc. Natl. Acad. Sci. U. S. A.* 84, 3288–3292. doi:10.1073/pnas.84.10.3288

Perry, S. E., and Keegstra, K. (1994). Envelope membrane proteins that interact with chloroplastic precursor proteins. *Plant Cell* 6, 93–105. doi:10.1105/tpc.6.1.93

Pollock, R. A., Hartl, F. U., Cheng, M. Y., Ostermann, J., Horwich, A., and Neupert, W. (1988). The processing peptidase of yeast mitochondria: The two co-operating components MPP and PEP are structurally related. *Embo J.* 7, 3493–3500. doi:10.1002/j.1460-2075.1988.tb03225.x

Ramundo, S., Asakura, Y., Salomé, P. A., Strenkert, D., Boone, M., Mackinder, L. C. M., et al. (2020). Coexpressed subunits of dual genetic origin define a conserved supercomplex mediating essential protein import into chloroplasts. *Proc. Natl. Acad. Sci. U. S. A.* 117, 32739–32749. doi:10.1073/pnas.2014294117

Razzak, M. A., Lee, D. W., Yoo, Y. J., and Hwang, I. (2017). Evolution of rubisco complex small subunit transit peptides from algae to plants. *Sci. Rep.* 7, 9279. doi:10.1038/s41598-017-09473-x

Richardson, L. G. L., Small, E. L., Inoue, H., and Schnell, D. J. (2018). Molecular topology of the transit peptide during chloroplast protein import. *Plant Cell* 30, 1789–1806. doi:10.1105/tpc.18.00172

Richardson, L. G., Paila, Y. D., Siman, S. R., Chen, Y., Smith, M. D., and Schnell, D. J. (2014). Targeting and assembly of components of the TOC protein import complex at the chloroplast outer envelope membrane. *Front. Plant Sci.* 5, 269. doi:10.3389/fpls.2014.00269

Richter, S., and Lamppa, G. K. (1998). A chloroplast processing enzyme functions as the general stromal processing peptidase. *Proc. Natl. Acad. Sci. U. S. A.* 95, 7463–7468. doi:10.1073/pnas.95.13.7463

Richter, S., and Lamppa, G. K. (2002). Determinants for removal and degradation of transit peptides of chloroplast precursor proteins. *J. Biol. Chem.* 277, 43888–43894. doi:10.1074/jbc.M206020200

Richter, S., and Lamppa, G. K. (2003). Structural properties of the chloroplast stromal processing peptidase required for its function in transit peptide removal. *J. Biol. Chem.* 278, 39497–39502. doi:10.1074/jbc.M305729200

Robinson, C., and Bolhuis, A. (2004). Tat-dependent protein targeting in prokaryotes and chloroplasts. *Biochim. Biophys. Acta* 1694, 135–147. doi:10.1016/j.bbamcr.2004.03.010

Sánchez-Pulido, L., Devos, D., Genevrois, S., Vicente, M., and Valencia, A. (2003). Potra: A conserved domain in the FtsQ family and a class of beta-barrel outer membrane proteins. *Trends Biochem. Sci.* 28, 523–526. doi:10.1016/j.tibs.2003.08.003

Schleiff, E., and Becker, T. (2011). Common ground for protein translocation: Access control for mitochondria and chloroplasts. *Nat. Rev. Mol. Cell Biol.* 12, 48–59. doi:10.1038/nrm3027

Schnell, D. J. (2019). The TOC GTPase receptors: Regulators of the fidelity, specificity and substrate profiles of the general protein import machinery of chloroplasts. *Protein J.* 38, 343–350. doi:10.1007/s10930-019-09846-3

Schnell, D. J., and Blobel, G. (1993). Identification of intermediates in the pathway of protein import into chloroplasts and their localization to envelope contact sites. *J. Cell Biol.* 120, 103–115. doi:10.1083/jcb.120.1.103

Schnell, D. J., Blobel, G., Keegstra, K., Kessler, F., Ko, K., and Soll, J. (1997). A consensus nomenclature for the protein-import components of the chloroplast envelope. *Trends Cell Biol.* 7, 303–304. doi:10.1016/S0962-8924(97)01111-2

Schnell, D. J., Kessler, F., and Blobel, G. (1994). Isolation of components of the chloroplast protein import machinery. *Science* 266, 1007–1012. doi:10.1126/science.7973649

Schuenemann, D., Gupta, S., Persello-Cartieaux, F., Klimyuk, V. I., Jones, J. D., Nussaume, L., et al. (1998). A novel signal recognition particle targets light-harvesting proteins to the thylakoid membranes. *Proc. Natl. Acad. Sci. U. S. A.* 95, 10312–10316. doi:10.1073/pnas.95.17.10312

Schünemann, D. (2007). Mechanisms of protein import into thylakoids of chloroplasts. *Biol. Chem.* 388, 907–915. doi:10.1515/BC.2007.111

Shipman, R. L., and Inoue, K. (2009). Suborganellar localization of plastidic type I signal peptidase 1 depends on chloroplast development. *FEBS Lett.* 583, 938–942. doi:10.1016/j.febslet.2009.02.016

Skalitzky, C. A., Martin, J. R., Harwood, J. H., Beirne, J. J., Adamczyk, B. J., Heck, G. R., et al. (2011). Plastids contain a second sec translocase system with essential functions. *Plant Physiol.* 155, 354–369. doi:10.1104/pp.110.166546

Srinivasan, K., Erramilli, S. K., Chakravarthy, S., Gonzalez, A., Kossiakoff, A., and Noinaj, N. (2023). Characterization of synthetic antigen binding fragments targeting Toc75 for the isolation of TOC in A. thaliana and P. sativum. *Structure* 31, 595–606. doi:10.1016/j.str.2023.03.002

Ståhl, A., Nilsson, S., Lundberg, P., Bhushan, S., Biverståhl, H., Moberg, P., et al. (2005). Two novel targeting peptide degrading proteases, PrePs, in mitochondria and chloroplasts, so similar and still different. *J. Mol. Biol.* 349, 847–860. doi:10.1016/j.jmb.2005.04.023

Su, P. H., and Li, H. M. (2010). Stromal Hsp70 is important for protein translocation into pea and Arabidopsis chloroplasts. *Plant Cell* 22, 1516–1531. doi:10.1105/tpc.109.071415

Teixeira, P. F., and Glaser, E. (2013). Processing peptidases in mitochondria and chloroplasts. *Biochim. Biophys. Acta* 1833, 360–370. doi:10.1016/j.bbamcr.2012.03.012

Teng, Y. S., Chan, P. T., and Li, H. M. (2012). Differential age-dependent import regulation by signal peptides. *PLoS Biol.* 10, e1001416. doi:10.1371/journal.pbio.1001416

Theg, S. M., Bauerle, C., Olsen, L. J., Selman, B. R., and Keegstra, K. (1989). Internal ATP is the only energy requirement for the translocation of precursor proteins across chloroplastic membranes. *J. Biol. Chem.* 264, 6730–6736. doi:10.1016/s0021-9258(18)83490-1

Timmis, J. N., Ayliffe, M. A., Huang, C. Y., and Martin, W. (2004). Endosymbiotic gene transfer: Organelle genomes forge eukaryotic chromosomes. *Nat. Rev. Genet.* 5, 123–135. doi:10.1038/nrg1271

Trösch, R., and Jarvis, P. (2011). The stromal processing peptidase of chloroplasts is essential in Arabidopsis, with knockout mutations causing embryo arrest after the 16-cell stage. *PLoS One* 6, e23039. doi:10.1371/journal.pone.0023039

Tu, C. J., Peterson, E. C., Henry, R., and Hoffman, N. E. (2000). The L18 domain of light-harvesting chlorophyll proteins binds to chloroplast signal recognition particle 43. *J. Biol. Chem.* 275, 13187–13190. doi:10.1074/jbc.c000108200

Tu, C. J., Schuenemann, D., and Hoffman, N. E. (1999). Chloroplast FtsY, chloroplast signal recognition particle, and GTP are required to reconstitute the soluble phase of

light-harvesting chlorophyll protein transport into thylakoid membranes. *J. Biol. Chem.* 274, 27219–27224. doi:10.1074/jbc.274.38.27219

Von Heijne, G., and Nishikawa, K. (1991). Chloroplast transit peptides. The perfect random coil? *FEBS Lett.* 278, 1–3. doi:10.1016/0014-5793(91)80069-f

Von Heijne, G., Steppuhn, J., and Herrmann, R. G. (1989). Domain structure of mitochondrial and chloroplast targeting peptides. *Eur. J. Biochem.* 180, 535–545. doi:10.1111/j.1432-1033.1989.tb14679.x

Wang, P., Liang, F. C., Wittmann, D., Siegel, A., Shan, S. O., and Grimm, B. (2018). Chloroplast SRP43 acts as a chaperone for glutamyl-tRNA reductase, the rate-limiting enzyme in tetrapyrrole biosynthesis. *Proc. Natl. Acad. Sci. U. S. A.* 115, E3588–e3596. doi:10.1073/pnas.1719645115

Yuan, J., Henry, R., Mccaffery, M., and Cline, K. (1994). SecA homolog in protein transport within chloroplasts: Evidence for endosymbiont-derived sorting. *Science* 266, 796–798. doi:10.1126/science.7973633

Ziehe, D., Dünschede, B., and Schünemann, D. (2018). Molecular mechanism of SRP-dependent light-harvesting protein transport to the thylakoid membrane in plants. *Photosynth Res.* 138, 303–313. doi:10.1007/s11120-018-0544-6

Zimorski, V., Ku, C., Martin, W. F., and Gould, S. B. (2014). Endosymbiotic theory for organelle origins. *Curr. Opin. Microbiol.* 22, 38–48. doi:10.1016/j.mib.2014.09.008

frontiers | Frontiers in Cell and Developmental Biology

TYPE Opinion
PUBLISHED 06 June 2023
DOI 10.3389/fcell.2023.1198184

OPEN ACCESS

EDITED BY
Danilo Swann Matassa,
University of Naples Federico II, Italy

REVIEWED BY
Sharbani Kaushik,
The Ohio State University, United States

*CORRESPONDENCE
Zemfira N. Karamysheva,
zemfira.karamysheva@ttu.edu
Andrey L. Karamyshev,
andrey.karamyshev@ttuhsc.edu

RECEIVED 31 March 2023
ACCEPTED 26 May 2023
PUBLISHED 06 June 2023

CITATION
Karamysheva ZN and Karamyshev AL (2023), Aberrant protein targeting activates quality control on the ribosome. *Front. Cell Dev. Biol.* 11:1198184. doi: 10.3389/fcell.2023.1198184

Aberrant protein targeting activates quality control on the ribosome

Zemfira N. Karamysheva[1]* and Andrey L. Karamyshev[2]*

[1]Department of Biological Sciences, Texas Tech University, Lubbock, TX, United States, [2]Department of Cell Biology and Biochemistry, Texas Tech University Health Sciences Center, Lubbock, TX, United States

KEYWORDS

signal peptide, signal recognition particle (SRP), ribosome, disease, protein targeting and transport, protein sorting, protein quality control, RNA degradation

Introduction

Cells synthesize thousands of different proteins that should be delivered to different cellular compartments, integrated into membranes, or secreted outside of the cell to conduct their functions. Over 20 thousand genes are detected in a human genome including about 3,000 genes encoding secreted proteins and 5,500 genes encoding membrane proteins (Uhlen et al., 2015). Thus, about 40% of all proteins are transported through or integrated into cellular membranes. What happens to secretory/membrane proteins that are not able to be targeted to the endoplasmic reticulum (ER) because of the mutations in the signal peptides or defects in the protein transport machinery? These proteins are potentially harmful to cells if they are mislocalized. In this article we discuss secretory protein targeting, signal peptides interactions with transport machinery of the cells, defects in these processes, their possible implications in human diseases, and cellular mechanisms preventing synthesis of defective secretory proteins.

Signal peptides and protein targeting to ER

How cells distinguish secretory and membrane proteins from others to transport them? Many secreted proteins are synthesized with an extra N-terminal amino acid sequence called signal sequence or signal peptide that is removed (cleaved off) upon translocation of the proteins into ER lumen. These signal sequences are served as "tags" or "zip codes" to direct proteins to the ER for their further transport. Some membrane proteins also have cleavable signal peptides, while others use their first transmembrane spans for these purposes. Signal peptides from different secretory proteins do not have consensus of distinct amino acid sequences and they do not show significant amino acid homology. However, they have similar organization and three featured domains—N, H, and C (Figure 1A). The N is N-terminal portion of the signal peptides (1-5 amino acids), it often has one-two positively charged amino acids; H or hydrophobic core is presented by a region of 7-15 hydrophobic amino acids; and C region (3-7 amino acids) contains a site for signal peptidase (von Heijne, 1985; von Heijne, 1990). The signal peptide cleavage site is described by −3, −1 rule that provides restrictions of the amino acid residues in those positions of the signal peptide (von Heijne, 1983). Interestingly, signal peptides from different organisms (bacteria, yeast, mammals, etc.) have similar organization and features demonstrating universal concept for protein targeting signals.

Signal peptides are recognized by Signal Recognition Particle (SRP) (Hsieh and Shan, 2021; Kellogg et al., 2021). SRP dependent pathway is the major route for sorting of secreted

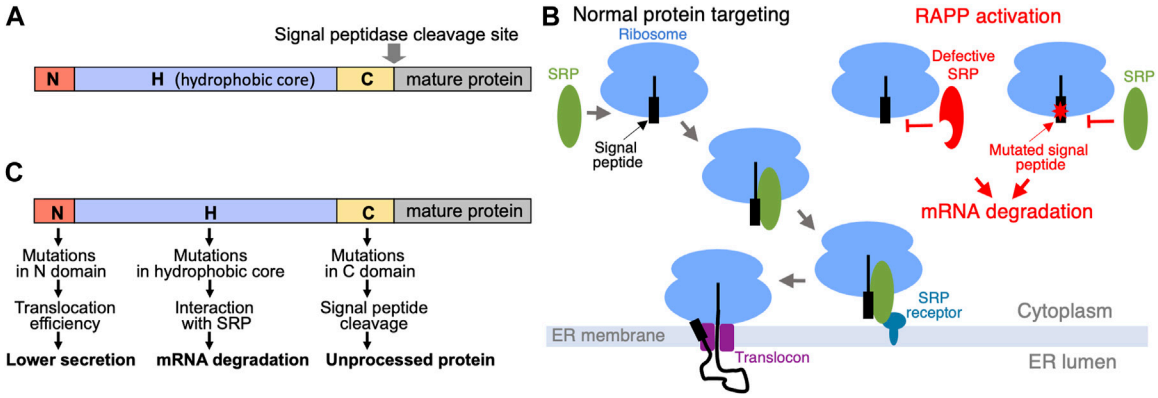

FIGURE 1
Signal peptides, protein targeting and its dysregulation. **(A)** Domain organization of signal peptides. **(B)** Scheme of SRP-dependent protein targeting in eukaryotes and Regulation of Aberrant Protein Production (RAPP) quality control on the ribosome. Under normal conditions SRP recognizes signal peptide and targets ribosomes to the SRP receptor in the ER membrane, and finally the secretory protein is translocated through the translocon to the ER lumen. However, when SRP is not able to recognize the signal peptide because of the mutations or because defects in the SRP itself, RAPP quality control is activated and the mRNAs are degraded. **(C)** Mutations in signal peptide domains affect different processes: mutations in the N domain affect efficiency of the protein translocation and secretion; mutations decreasing hydrophobicity of the H domain disrupt interaction with SRP, trigger RAPP protein quality control and lead to mRNA degradation of the mutated protein; mutations in the C domain may affect processing by a signal peptidase.

and membrane proteins in mammalian cells. SRP is a complex of six proteins (SRP9, SRP14, SRP19, SRP54, SRP68, SRP72) and one noncoding RNA (7SL RNA) in mammals. SRP plays a key point in selecting proteins for their targeting to the ER membrane. SRP recognizes signal peptides of secretory protein precursors or membrane spans of membrane proteins immediately after their appearance from the ribosome during translation. SRP54 subunit directly binds signal peptides during translation. This interaction leads to the SRP molecular rearrangement, temporal elongation arrest, targeting complex to the SRP receptor in the ER membrane, transferring it to the translocon, then SRP leaves the complex, translation resumes, and the polypeptide nascent chain is co-translationally translocated into ER lumen through the translocon (Figure 1B). Proteins translocated to ER are folded with participation of the ER chaperones, subjected to co- and post-translational modifications and transported further.

Aberrant signal peptides, defective SRPs, protein quality controls and human diseases

Mechanisms of protein targeting and transport are complex and, thus, many things can go wrong. It could be a problem with secretory protein itself because of genetic mutations or mistakes of transcription/translation, or issues with transport machinery because of defects in its components. Moreover, different stresses can affect proteins as well. These events can lead to protein mislocalization, misfolding and accumulation of insoluble protein aggregates that are potentially harmful. There are several cellular quality control mechanisms evolved to protect cells from these toxic species. They work at different levels and substrates, some of them are general and triggered by stress, others are specialized. Examples are responses to stress (unfolded protein response, UPR; ribosome-associated quality control, RQC, others), appearance of premature stop-codon mutations in mRNAs (nonsense mediated decay, NMD), mRNA truncations or ribosome stalling (no-go decay, NGD), or the absence of a natural stop codon (nonstop decay, NSD) (Brandman and Hegde, 2016; Shao and Hegde, 2016; Hetz and Papa, 2018; Joazeiro, 2019; Kurosaki et al., 2019; Sitron and Brandman, 2020; D'Orazio and Green, 2021). In addition, secretory and membrane proteins are controlled by a specific protein quality control on the ribosome termed Regulation of Aberrant Protein Production (RAPP) (Karamyshev et al., 2014; Karamyshev and Karamysheva, 2018). It senses signal peptide interactions with a targeting factor SRP and degrades the secretory protein mRNAs if these interactions are disrupted by mutations in a signal peptide or defects in SRP.

What mutations in signal sequences trigger RAPP? As mentioned above, the signal peptides have a domain organization. The domain structure of signal sequences reflects their functions. Thus, H region is crucial for binding with SRP54—deletions of hydrophobic amino acids from this area dramatically reduce interaction with SRP54, while alterations of charged amino acids in the N domain have only mild effect (Nilsson et al., 2015). Mutations in the signal peptide C region mostly affect processing (Karamyshev et al., 1998). However, impact of mutations in C region on SRP binding and protein transport have a minimal affect (Nilsson et al., 2015). Thus, hydrophobicity of the H domain is the major factor affecting SRP interaction with a signal peptide. Indeed, mutations decreasing hydrophobicity of the signal peptide in the preprolactin signal peptide H-region triggered degradation of the mutated protein mRNA (Karamyshev et al., 2014). Moreover, the effect of the mutations was graded—the mRNA degradation gradually increased with the severity of the mutations. Interestingly, depletion of the SRP54 subunit also triggers RAPP.

RAPP is a unique protein quality control—it co-translationally recognizes aberrant proteins at the ribosome and prevents their synthesis through specific mRNA degradation. It requires active translation. The RAPP response involves engagement of

AGO2 protein, specific chaperone network (HSPA1A, DNAJB1, HSP90AA1, others), ribosome rearrangement through exchange of the ribosomal protein RPS27 and RPS27L, and ribosome-associated ubiquitination (Karamyshev et al., 2014; Tikhonova et al., 2022). It is proposed that ribosome heterogeneity and specialization may play an important role in many cellular processes (Genuth and Barna, 2018a; Genuth and Barna, 2018b; Miller et al., 2023). Thus, exchange of ribosomal proteins during RAPP activation may be important for its molecular mechanism. It is also established that RAPP is a general pathway controlling many secretory and membrane proteins (Tikhonova et al., 2022). However, details of the molecular mechanism of RAPP are not well understood.

There are many diseases associated with the defects in protein targeting to ER. Generally, they can be divided into two large categories—disorders associated with defects in a targeting factor SRP, and diseases associated with mutations in specific secretory proteins. The first category includes defects in SRP protein subunits and 7SL RNA leading to very diverse disorders including cancer, autoimmunity, hematological, neurological, neurodegenerative, infectious, and other diseases (Kellogg et al., 2022). The molecular mechanisms of these disorders are diverse and they depend on the affected subunit. The loss of SRP54 as a result of autoimmune response or some mutations in SRP54 may induce the RAPP quality control. Some mutations may interfere with the efficiency of SRP interaction with SRP receptor, or with SRP complex formation. Several studies demonstrated that mutations in the G-domain of SRP54 are associated with neutropenia and Shwachman-Diamond syndrome (Carapito et al., 2017; Bellanne-Chantelot et al., 2018; Juaire et al., 2021). The second category of diseases is associated with mutations in secretory proteins. It is connected with a loss of expression or a change of processing of a single secretory protein. Among them are frontotemporal lobar degeneration (FTLD) connected with granulin haploinsufficiency, aspartylglucosaminuria caused by defects in aspartylglucosaminidase, Wolman disease associated with mutations in lipase A, and many others (Jarjanazi et al., 2008; Karamyshev et al., 2020). Molecular mechanisms of these diseases are associated with location of mutations in secretory proteins and their severity. We proposed that mutations in the signal peptide H-domain decreasing hydrophobicity induce RAPP, while mutations located in the C-region do not activate RAPP, but instead may inhibit processing (Tikhonova et al., 2019) (Figure 1C). Mutations in the signal peptide N-domain are unlikely to induce RAPP because this area is not important for interaction with SRP, but it may be important for secretion efficiency. Recently we elucidated that a pathological RAPP activation and mRNA degradation of the granulins with W7R and A9D mutations is a molecular mechanism of FTLD pathology for the patients bearing these mutations (Pinarbasi et al., 2018; Karamysheva et al., 2019). The similar conclusions were made for many other secretory proteins with mutations that are associated with a number of human diseases (Tikhonova et al., 2019). Thus, pathological RAPP activation may play a significant role in many human diseases. Interestingly, the RAPP pathway is also involved in some cases of the Parkinson's disease, however, the molecular basis of it is not clear yet (Hernandez et al., 2021).

Conclusion

The protein transport is one of the most important cellular processes. About 40% of all proteins in a cell are secretory and membrane proteins. Mutations in the hydrophobic core of the signal peptide or depletion of SRP54 subunit of the SRP complex lead to the RAPP activation and elimination of the secretory protein mRNA template. Activation of the RAPP pathway can cause a number of human diseases; however, many details of the RAPP mechanism remain unclear such as what components of mRNA degradation machinery are involved in the degradation process, and how changes in ribosome composition/modification contribute to RAPP. Therefore, understanding of the fine details of the molecular mechanism of the RAPP pathway is crucial for the development of new strategies for treatment multiple human diseases.

Author contributions

ZK and AK wrote, discussed, and edited the manuscript. All authors contributed to the article and approved the submitted version.

Funding

This work was supported by the National Institute of General Medical Sciences of the National Institutes of Health under award number R01GM135167 to AK. The content is solely the responsibility of the authors and does not necessarily represent the official views of the National Institutes of Health.

Conflict of interest

The authors declare that the research was conducted in the absence of any commercial or financial relationships that could be construed as a potential conflict of interest.

Publisher's note

References

Bellanne-Chantelot, C., Schmaltz-Panneau, B., Marty, C., Fenneteau, O., Callebaut, I., Clauin, S., et al. (2018). Mutations in the SRP54 gene cause severe congenital neutropenia as well as Shwachman-Diamond-like syndrome. *Blood* 132 (12), 1318–1331. doi:10.1182/blood-2017-12-820308

Brandman, O., and Hegde, R. S. (2016). Ribosome-associated protein quality control. *Nat. Struct. Mol. Biol.* 23 (1), 7–15. doi:10.1038/nsmb.3147

Carapito, R., Konantz, M., Paillard, C., Miao, Z., Pichot, A., Leduc, M. S., et al. (2017). Mutations in signal recognition particle SRP54 cause syndromic neutropenia with Shwachman-Diamond-like features. *J. Clin. Invest.* 127 (11), 4090–4103. doi:10.1172/JCI92876

D'Orazio, K. N., and Green, R. (2021). Ribosome states signal RNA quality control. *Mol. Cell.* 81 (7), 1372–1383. doi:10.1016/j.molcel.2021.02.022

Genuth, N. R., and Barna, M. (2018b). Heterogeneity and specialized functions of translation machinery: From genes to organisms. *Nat. Rev. Genet.* 19 (7), 431–452. doi:10.1038/s41576-018-0008-z

Genuth, N. R., and Barna, M. (2018a). The discovery of ribosome heterogeneity and its implications for gene regulation and organismal life. *Mol. Cell.* 71 (3), 364–374. doi:10.1016/j.molcel.2018.07.018

Hernandez, S. M., Tikhonova, E. B., Baca, K. R., Zhao, F., Zhu, X., and Karamyshev, A. L. (2021). Unexpected implication of SRP and AGO2 in Parkinson's disease: Involvement in alpha-synuclein biogenesis. *Cells* 10 (10), 2792. doi:10.3390/cells10102792

Hetz, C., and Papa, F. R. (2018). The unfolded protein response and cell fate control. *Mol. Cell.* 69 (2), 169–181. doi:10.1016/j.molcel.2017.06.017

Hsieh, H. H., and Shan, S. O. (2021). Fidelity of cotranslational protein targeting to the endoplasmic reticulum. *Int. J. Mol. Sci.* 23 (1), 281. doi:10.3390/ijms23010281

Jarjanazi, H., Savas, S., Pabalan, N., Dennis, J. W., and Ozcelik, H. (2008). Biological implications of SNPs in signal peptide domains of human proteins. *Proteins* 70 (2), 394–403. doi:10.1002/prot.21548

Joazeiro, C. A. P. (2019). Mechanisms and functions of ribosome-associated protein quality control. *Nat. Rev. Mol. Cell. Biol.* 20 (6), 368–383. doi:10.1038/s41580-019-0118-2

Juaire, K. D., Lapouge, K., Becker, M. M. M., Kotova, I., Michelhans, M., Carapito, R., et al. (2021). Structural and functional impact of SRP54 mutations causing severe congenital neutropenia. *Structure* 29 (1), 15–28.e7. doi:10.1016/j.str.2020.09.008

Karamyshev, A. L., Karamysheva, Z. N., Kajava, A. V., Ksenzenko, V. N., and Nesmeyanova, M. A. (1998). Processing of *Escherichia coli* alkaline phosphatase: Role of the primary structure of the signal peptide cleavage region. *J. Mol. Biol.* 277 (4), 859–870. doi:10.1006/jmbi.1997.1617

Karamyshev, A. L., and Karamysheva, Z. N. (2018). Lost in translation: Ribosome-associated mRNA and protein quality controls. *Front. Genet.* 9, 431. doi:10.3389/fgene.2018.00431

Karamyshev, A. L., Patrick, A. E., Karamysheva, Z. N., Griesemer, D. S., Hudson, H., Tjon-Kon-Sang, S., et al. (2014). Inefficient SRP interaction with a nascent chain triggers a mRNA quality control pathway. *Cell.* 156 (1-2), 146–157. doi:10.1016/j.cell.2013.12.017

Karamyshev, A. L., Tikhonova, E. B., and Karamysheva, Z. N. (2020). Translational control of secretory proteins in Health and disease. *Int. J. Mol. Sci.* 21 (7), 2538. doi:10.3390/ijms21072538

Karamysheva, Z. N., Tikhonova, E. B., and Karamyshev, A. L. (2019). Granulin in frontotemporal lobar degeneration: Molecular mechanisms of the disease. *Front. Neurosci.* 13, 395. doi:10.3389/fnins.2019.00395

Kellogg, M. K., Miller, S. C., Tikhonova, E. B., and Karamyshev, A. L. (2021). SRPassing Co-translational targeting: The role of the signal recognition particle in protein targeting and mRNA protection. *Int. J. Mol. Sci.* 22 (12), 6284. doi:10.3390/ijms22126284

Kellogg, M. K., Tikhonova, E. B., and Karamyshev, A. L. (2022). Signal recognition particle in human diseases. *Front. Genet.* 13, 898083. doi:10.3389/fgene.2022.898083

Kurosaki, T., Popp, M. W., and Maquat, L. E. (2019). Quality and quantity control of gene expression by nonsense-mediated mRNA decay. *Nat. Rev. Mol. Cell. Biol.* 20 (7), 406–420. doi:10.1038/s41580-019-0126-2

Miller, S. C., MacDonald, C. C., Kellogg, M. K., Karamysheva, Z. N., and Karamyshev, A. L. (2023). Specialized ribosomes in Health and disease. *Int. J. Mol. Sci.* 24 (7), 6334. doi:10.3390/ijms24076334

Nilsson, I., Lara, P., Hessa, T., Johnson, A. E., von Heijne, G., and Karamyshev, A. L. (2015). The code for directing proteins for translocation across ER membrane: SRP cotranslationally recognizes specific features of a signal sequence. *J. Mol. Biol.* 427 (6), 1191–1201. doi:10.1016/j.jmb.2014.06.014

Pinarbasi, E. S., Karamyshev, A. L., Tikhonova, E. B., Wu, I. H., Hudson, H., and Thomas, P. J. (2018). Pathogenic signal sequence mutations in progranulin disrupt SRP interactions required for mRNA stability. *Cell. Rep.* 23 (10), 2844–2851. doi:10.1016/j.celrep.2018.05.003

Shao, S., and Hegde, R. S. (2016). Target selection during protein quality control. *Trends Biochem. Sci.* 41 (2), 124–137. doi:10.1016/j.tibs.2015.10.007

Sitron, C. S., and Brandman, O. (2020). Detection and degradation of stalled nascent chains via ribosome-associated quality control. *Annu. Rev. Biochem.* 89, 417–442. doi:10.1146/annurev-biochem-013118-110729

Tikhonova, E. B., Gutierrez Guarnizo, S. A., Kellogg, M. K., Karamyshev, A., Dozmorov, I. M., Karamysheva, Z. N., et al. (2022). Defective human SRP induces protein quality control and triggers stress response. *J. Mol. Biol.* 434 (22), 167832. doi:10.1016/j.jmb.2022.167832

Tikhonova, E. B., Karamysheva, Z. N., von Heijne, G., and Karamyshev, A. L. (2019). Silencing of aberrant secretory protein expression by disease-associated mutations. *J. Mol. Biol.* 431 (14), 2567–2580. doi:10.1016/j.jmb.2019.05.011

Uhlen, M., Fagerberg, L., Hallstrom, B. M., Lindskog, C., Oksvold, P., Mardinoglu, A., et al. (2015). Proteomics. Tissue-based map of the human proteome. *Science* 347 (6220), 1260419. doi:10.1126/science.1260419

von Heijne, G. (1983). Patterns of amino acids near signal-sequence cleavage sites. *Eur. J. Biochem.* 133 (1), 17–21. doi:10.1111/j.1432-1033.1983.tb07424.x

von Heijne, G. (1985). Signal sequences, the limits of variation. *J. Mol. Biol.* 184 (1), 99–105. doi:10.1016/0022-2836(85)90046-4

von Heijne, G. (1990). The signal peptide. *J. Membr. Biol.* 115 (3), 195–201. doi:10.1007/bf01868635

frontiers | Frontiers in Cell and Developmental Biology

TYPE Original Research
PUBLISHED 17 August 2023
DOI 10.3389/fcell.2023.1213761

OPEN ACCESS

EDITED BY
Nathan Alder,
University of Connecticut, United States

REVIEWED BY
Dejana Mokranjac,
Ludwig Maximilian University of Munich, Germany
Richard Rachubinski,
University of Alberta, Canada

*CORRESPONDENCE
Ralf Erdmann,
ralf.erdmann@rub.de
Vishal C. Kalel,
vishal.kalel@rub.de

RECEIVED 28 April 2023
ACCEPTED 03 August 2023
PUBLISHED 17 August 2023

CITATION
Krishna CK, Schmidt N, Tippler BG, Schliebs W, Jung M, Winklhofer KF, Erdmann R and Kalel VC (2023), Molecular basis of the glycosomal targeting of PEX11 and its mislocalization to mitochondrion in trypanosomes. *Front. Cell Dev. Biol.* 11:1213761. doi: 10.3389/fcell.2023.1213761

Molecular basis of the glycosomal targeting of PEX11 and its mislocalization to mitochondrion in trypanosomes

Chethan K. Krishna[1], Nadine Schmidt[1], Bettina G. Tippler[1], Wolfgang Schliebs[1], Martin Jung[2], Konstanze F. Winklhofer[3], Ralf Erdmann[1]* and Vishal C. Kalel[1]*

[1]Department of Systems Biochemistry, Institute for Biochemistry and Pathobiochemistry, Faculty of Medicine, Ruhr University Bochum, Bochum, Germany, [2]Department of Medical Biochemistry and Molecular Biology, Saarland University, Homburg, Germany, [3]Department Molecular Cell Biology, Institute of Biochemistry and Pathobiochemistry, Faculty of Medicine, Ruhr University Bochum, Bochum, Germany

PEX19 binding sites are essential parts of the targeting signals of peroxisomal membrane proteins (mPTS). In this study, we characterized PEX19 binding sites of PEX11, the most abundant peroxisomal and glycosomal membrane protein from *Trypanosoma brucei* and *Saccharomyces cerevisiae*. *Tb*PEX11 contains two PEX19 binding sites, one close to the N-terminus (BS1) and a second in proximity to the first transmembrane domain (BS2). The N-terminal BS1 is highly conserved across different organisms and is required for maintenance of the steady-state concentration and efficient targeting to peroxisomes and glycosomes in both baker's yeast and *Trypanosoma brucei*. The second PEX19 binding site in *Tb*PEX11 is essential for its glycosomal localization. Deletion or mutations of the PEX19 binding sites in *Tb*PEX11 or *Sc*PEX11 results in mislocalization of the proteins to mitochondria. Bioinformatic analysis indicates that the N-terminal region of *Tb*PEX11 contains an amphiphilic helix and several putative TOM20 recognition motifs. We show that the extreme N-terminal region of *Tb*PEX11 contains a cryptic N-terminal signal that directs PEX11 to the mitochondrion if its glycosomal transport is blocked.

KEYWORDS

peroxisome, glycosome, peroxin, PEX19, PMP, mPTS, MTS

1 Introduction

Peroxisomes are single membrane bound organelles performing a wide range of functions (Rhodin, 1954; De Duve and Baudhuin, 1966). Glyoxysomes in plants, Woronin bodies in fungi, and glycosomes in trypanosomatid parasites are specialized forms of peroxisomes (Reichle and Alexander, 1965; Breidenbach and Beevers, 1967; Opperdoes and Borst, 1977). Peroxisomes can multiply by growth and division, or they can form *de novo* from pre-peroxisomal vesicles that are supposed to bud from the endoplasmic reticulum (Hoepfner et al., 2005; Motley and Hettema, 2007). Peroxisomes import matrix as well as membrane proteins post-translationally (Goldman Blobel, 1978; Lazarow and Fujiki, 1985; Sacksteder et al., 2000; Jones et al., 2004). The import depends on a machinery of Peroxins (PEX proteins) and requires the presence of peroxisomal targeting signals in the cargo

proteins (Gould et al., 1989; Swinkels et al., 1991; Faber et al., 1995). Biogenesis of peroxisomes requires two distinct machineries for protein targeting: The first is responsible for the formation of the peroxisomal membrane by the targeting and insertion of peroxisomal membrane proteins (PMPs), and the second machinery is responsible for the import of peroxisomal matrix proteins (reviewed in (Agrawal and Subramani, 2016)). The trafficking of proteins destined for the peroxisome matrix has been well studied. A striking feature is that peroxisomes can import folded, even oligomeric proteins (McNew andGoodman, 1994; Leon et al., 2006). Peroxisomal matrix proteins contain type 1 or type 2 peroxisomal targeting signals (PTS1/PTS2) at the extreme C-terminus or close to the N-terminus, respectively (Gould et al., 1989; Swinkels et al., 1991; Faber et al., 1995). Some proteins contain internal targeting signals (Galland et al., 2010) and some are transported by piggy-backing onto a PTS-containing protein (Islinger et al., 2009). The import of peroxisomal matrix proteins depends on cycling receptors that recognize peroxisomal proteins via their PTS in the cytosol and target them to a docking complex at the peroxisomal membrane. Import takes place through a transient pore or hydrogel-filled pore in an unknown fashion (Erdmann and Schliebs, 2005; Meinecke et al., 2016; Gao et al., 2022). The cargo-unloaded receptors are mono-ubiquitinated and released to the cytosol for another round of import in an ATP-dependent manner by the peroxisomal exportomer (Platta et al., 2004; Platta et al., 2005). The machinery that is responsible for the topogenesis of membrane proteins is distinct from the import machinery for matrix proteins (Reviewed in (Hasan et al., 2013; Mayerhofer, 2016)). Only three peroxins with a direct role in PMP targeting have been identified, namely, PEX3 (Hettema et al., 2000), PEX16 in mammals (South and Gould, 1999; Sacksteder et al., 2000), and PEX19 (Sacksteder et al., 2000) (Also reviewed in (Kalel and Erdmann, 2018)). In cells lacking any of these proteins, PMPs are either degraded or mistargeted to other subcellular compartments such as mitochondria, endoplasmic reticulum (ER), and membranes of unknown origin (Ghaedi et al., 2000; Hettema et al., 2000; Sacksteder et al., 2000). PMPs contain multiple binding sites (BSs) for the cytosolic receptor and chaperone PEX19 (Jones et al., 2004). These binding sites are essential for targeting of the PMPs to the peroxisomal membrane, as they can function as mPTS i.e., membrane peroxisome targeting signal (Halbach et al., 2005). The mPTS often comprises part of the transmembrane domains and a short adjacent sequence, which contains either a cluster of basic residues or a mixture of basic and hydrophobic amino acids (Marshall et al., 1996) (Reviewed in (Baerends et al., 2000; Murphy et al., 2003; Van Ael and Fransen, 2006)). Rottensteiner et al., developed PEX19 binding site prediction methodology using peptide arrays (Rottensteiner et al., 2004). Unlike PTS1 and PTS2 signals, which can be predicted more reliably (Kamoshita et al., 2022; Kunze, 2023), PEX19 BSs are comparatively degenerate and can be present multiple times in a PMP. Therefore, an efficient PEX19BS predictor is still needed. Nonetheless, PEX19 binding sites (BSs) have been identified in various yeast, human and parasite PMPs, which shows evolutionary conservation across eukaryotes (Rottensteiner et al., 2004; Saveria et al., 2007). In most eukaryotes, PEX19 harbors a farnesylation motif (CaaX box), and farnesylation has been shown to increase the binding efficiency of PMPs (Rucktaschel et al., 2009). However, trypanosomatid parasite PEX19 proteins lack such a CaaX motif (Banerjee et al., 2005).

PEX11 is an integral peroxisomal membrane protein with at least two predicted alpha-helical transmembrane domains and both termini facing the cytosol (Abe et al., 1998b; Lorenz et al., 1998; Anton et al., 2000; Bonekamp et al., 2013). In the yeast *Saccharomyces cerevisiae*, Pex11p, Pex25p, and Pex27p are the three members of the PEX11 protein family (Erdmann and Blobel, 1995; Rottensteiner et al., 2003; Tam et al., 2003). Similarly, mammals also encode three PEX11-family proteins namely, PEX11α, PEX11β, and PEX11γ (Li and Gould, 2002; Koch et al., 2010). In plants, there are five PEX11 homologs, for e. g., in *Arabidopsis thaliana At*PEX11a, -b, -c, -d, and -e (Lingard and Trelease, 2006). PEX11 family proteins are involved in the proliferation of peroxisome in yeasts, plants, and mammals (Erdmann and Blobel, 1995; Abe and Fujiki, 1998a; Schrader et al., 1998; Orth et al., 2007; Koch et al., 2010). Deletion of PEX11 in yeast has an effect on the β-oxidation of fatty acids, which can be due to defects in the transport of metabolites across the peroxisomal membrane (Sulter et al., 1993). PEX11β is widely expressed in mammalian tissues and it has a well-recognized function in the initial phase of peroxisomal fission when it remodels and elongates peroxisomal membranes (Delille et al., 2010; Yoshida et al., 2015; Schrader et al., 2016). The functions of PEX11α and PEX11γ are less clear (Schrader et al., 2016). Of the PEX11 proteins in mammals, only PEX11β deficiency was associated with the pathology of peroxisome biogenesis disorders (PBDs) (Li and Gould, 2002; Thoms and Gartner, 2012; Schrader et al., 2016).

In trypanosomes, three PEX11 family proteins are known, namely, PEX11, GIM5A and GIM5B (Lorenz et al., 1998; Maier et al., 2001; Voncken et al., 2003). Like in mammals, yeast, and plants, both N- and C-termini of *Tb*PEX11 are exposed to the cytosol (Lorenz et al., 1998). Overexpression of *Tb*PEX11 induces growth inhibition and transforms the globular glycosomes into long tubule clusters that occupy a large portion of the cytoplasm (Lorenz et al., 1998). Accordingly, *Tb*PEX11 appears to play a role in the proliferation of glycosomes in trypanosomes like its homologs in yeast and mammalian cells (van Roermund et al., 2000) (Reviewed in (Moyersoen et al., 2004)). PEX11 and both GIM5 proteins are essential for the survival of parasites (Lorenz et al., 1998; Voncken et al., 2003). At primary sequence level, PEX11 family proteins contain several conserved helices particularly in the N-terminal region (Lorenz et al., 1998; Opalinski et al., 2018). PEX19 binding sites have been identified in various glycosomal membrane proteins (Saveria et al., 2007), but not in *Tb*PEX11. Therefore, in this study, we characterized PEX19 binding sites of PEX11 from *Trypanosoma brucei* and *Saccharomyces cerevisiae*. *Tb*PEX11 contains two PEX19 binding sites, the N-terminal PEX19 binding site (BS1) in PEX11 is highly conserved across different organisms and is required for maintenance of the steady-state concentration as well as efficient targeting to peroxisomes and glycosomes in both baker's yeast and *T. brucei*. Deletion or mutations of the

TABLE 1 Strains and plasmids.

Sl no.	Expression in	Construct	Primer pair	Restriction sites	Cloned in vector
1	*E. coli*	GST-*Tb*PEX19	RE2926 - RE7038	BamHI/XhoI	pGEX4T-2
2	*E. coli*	GST-*Hs*PEX19	pAH5 Halbach et al. (2005)		
3	*S. cerevisiae*	GAL4 AD-*Sc*PEX14	Albertini et al. (1997)		
4	*S. cerevisiae*	GAL4 BD-*Sc*PEX17$_{167\text{-}199aa}$	Girzalsky et al. (2006)		
5	*S. cerevisiae*	GAL4 AD-*Tb*PEX19$_{1\text{-}285aa}$	RE3310 - RE3311 (pIA13, AG Erdmann)	SalI/NotI	pPC86
6	*S. cerevisiae*	GAL4 BD-*Tb*PEX11$_{1\text{-}218aa}$	RE7303 - RE7306	SalI/NotI	pPC97
7	*S. cerevisiae*	GAL4 BD-*Tb*PEX11$_{1\text{-}89aa}$	RE7303 - RE7305	SalI/NotI	pPC97
8	*S. cerevisiae*	GAL4 BD-*Tb*PEX11$_{90\text{-}218aa}$	RE7304 - RE7306	SalI/NotI	pPC97
9	*S. cerevisiae*	GAL4 BD-*Tb*PEX11$_{1\text{-}76aa}$	RE8882—RE8883	Quick change PCR	pPC97
10	*S. cerevisiae*	GAL4 BD-*Tb*PEX11$_{1\text{-}89aa}$ (S 25 D)	RE7713 - RE7714	Quick change PCR	pPC97
11	*S. cerevisiae*	GAL4 BD-*Tb*PEX11$_{1\text{-}89aa}$ (S 25 P)	RE7715 - RE7716	Quick change PCR	pPC97
12	*S. cerevisiae*	GAL4 BD-*Tb*PEX11$_{1\text{-}89aa}$ (L 31 P)	RE7717 - RE7718	Quick change PCR	pPC97
13	*S. cerevisiae*	GAL4 BD-*Tb*PEX11$_{1\text{-}89aa}$ (S 25 P, L 31 P)	RE7715 - RE7716, RE7717 - RE7718	Quick change PCR	pPC97
14	*S. cerevisiae*	GAL4 AD-*Hs*PEX19	RE7706 - RE7707	SalI/NotI	pPC86
15	*S. cerevisiae*	GAL4 BD-*Hs*PEX11$_{1\text{-}73aa}$	RE7843 - RE7844	SalI/NotI	pPC97
16	*S. cerevisiae*	GAL4 BD-*Hs*PEX11$_{1\text{-}73aa}$	RE7708 - RE7709	SalI/NotI	pPC97
17	*S. cerevisiae*	GAL4 BD-*Hs*PEX11$_{1\text{-}74aa}$	RE7845 - RE7846	SalI/NotI	pPC97
18	*S. cerevisiae*	*Sc*PEX11-GFP	Boutouja et al. (2019)		
19	*S. cerevisiae*	*Sc*PEX11 (L 35 P)-GFP	RE8063 - RE8064	Quick change PCR	pUG35
20	*T. brucei*	*Tb*PEX11-GFP	RE8070 - RE8071	BstBI/BamHI	pGN1
21	*T. brucei*	*Tb*PEX11$_{\Delta 13\text{-}35aa}$-GFP	RE8072 - RE8073	Quick change PCR	pGN1
22	*T. brucei*	*Tb*PEX11$_{\Delta 77\text{-}99aa}$-GFP	RE8074 - RE8075	Quick change PCR	pGN1
23	*T. brucei*	*Tb*PEX11$_{1\text{-}90aa}$-GFP	RE7378 - RE7379	ApaI/BamHI	pGN1
24	*T. brucei*	*Tb*PEX11$_{1\text{-}90aa\text{-}\Delta 13\text{-}35aa}$-GFP	RE8072 - RE8073	Quick change PCR	pGN1
25	*T. brucei*	*Tb*PEX11$_{1\text{-}90aa\text{-}\Delta 2\text{-}11aa}$-GFP	RE8096 - RE7379	BstBI/BamHI	pGN1

PEX19 binding site in *Tb*PEX11 (second PEX19 BS, i.e., BS2) or *Sc*PEX11 (single PEX19 BS) results in a mislocalization of the proteins to mitochondria. Trypanosomes contain multiple small glycosomes, but harbor a single mitochondrion (Tyler et al., 2001). We show that the extreme N-terminal region of *Tb*PEX11 contains a cryptic N-terminal signal that directs PEX11 to the mitochondrion if its glycosomal transport is blocked.

2 Materials and methods

2.1 Cloning

Escherichia coli, yeast, and *Trypanosoma* expression plasmid constructs and cloning strategies are listed in Table 1, and oligonucleotide sequences are listed in Table 2. Point mutations in *Sc*PEX11, *Tb*PEX11$_{1\text{-}89aa}$, and the gene fragment deletions (*Tb*PEX11$_{1\text{-}76aa}$ and *Tb*PEX11-GFP constructs) were generated by overlap extension PCR. Sequences of the constructs, mutations, and gene fragment deletions were verified for all constructs by automated Sanger sequencing.

2.2 Cell culture

2.2.1 *Trypanosoma*

Trypanosoma procyclic form (PCF) 29–13 cell line (co-expressing T7 RNAP and TetR) was used in this study. PCF cells were grown in SDM-79 medium supplemented with 10% FBS at 28°C (Brun and Schonenberger, 1979; Krishna et al., 2023). PCF cultures were maintained at 1 × 10^6–30 × 10^6 cells/mL. Transfections were performed with NotI-linearized plasmid constructs (pGN1-*Tb*PEX11 constructs), which was genomically integrated into the rRNA locus in the genome of cell line 29–13. Clones were selected using Blasticidin (10 μg/mL) as described previously (Kalel et al., 2015).

2.2.2 Yeast

S. cerevisiae wild-type strain BY4742 (for microscopy) and strain PCY2 (WT or Δ*pex19* for yeast two-hybrid assay) were grown in double dropout SD synthetic media as described in section 2.3 and 2.4.2. Yeast cells were transformed by the traditional Lithium-acetate method (Gietz and Woods, 2002).

2.2.3 *Escherichia coli*

Escherichia coli strain TOP10 was used for all plasmid amplifications and BL21 (DE3) strain was used for heterologous expression of recombinant GST-PEX19 fusion proteins. Liquid *E. coli* cultures were grown at 37°C under continuous shaking in LB medium containing the appropriate selective antibiotic (100 μg/mL Ampicillin).

2.3 Yeast two-hybrid analysis (Y2H)

Y2H studies were performed based on the Yeast protocols handbook (Clontech, Protocol No. PT3024-1, Version No. PR742227). Full length or various truncations of *Trypanosoma* or Human PEX11 were cloned in pPC97 vector containing GAL4-DNA Binding Domain (BD) and full-length *Trypanosoma* or human PEX19 were cloned in pPC86 vector containing GAL4-Activation domain (AD), as described in Table 1. Co-transformation of various two-hybrid plasmids i.e., BD and AD constructs were performed in WT PCY2 or Δ*pex19* PCY2 strain in case of *Hs*PEX19-*Hs*PEX11 constructs. The clones were selected on SD synthetic medium without tryptophan and leucine. A filter-based β-galactosidase assay and liquid culture assay using ONPG were performed in three replicates as described in the Yeast protocols handbook (Clontech).

2.4 Microscopy

2.4.1 *Trypanosoma*

Trypanosoma stable cell lines (Procyclic 29:13) encoding various tetracycline inducible PEX11-GFP constructs (full-length and mutants) were induced with 1 μg/mL tetracycline or treated with DMSO alone as negative control. Cells were sedimented and fixed by resuspension in 4% paraformaldehyde in PBS (phosphate-buffered saline, pH 7.4) at 4°C for 15 min. Fixed *Trypanosoma* cells were washed two times with PBS and stored at 4°C in a dark box. For imaging, fixed cells were immobilized on a glass slide (StarFrost 76 × 26 mm, Knittel Glass) pre-coated with 10% (v/v) of poly-L-lysine (Sigma-Aldrich) in water for 1 h at room temperature (RT). Further, the cell membranes were permeabilized with PBS containing 0.125% Triton X-100 and incubated for 10–15 min, followed by blocking with PBS containing 3% BSA, 0.25% Tween-20 for 1 h at RT. Rabbit α-Aldolase antibody (1:500 in blocking buffer) was used as glycosomal marker and incubated at RT for 1 h. Following 5 washes with PBS, anti-rabbit Alexa fluor 594 secondary antibodies (1:200 dilution) in PBS was applied and incubated for 30 min at RT in the dark. Further, the stained samples were washed, dried, and layered with anti-fading mounting medium, i.e., Mowiol with DAPI (4′,6-diamidino-2-phenylindole).

For mitochondrial staining, tetracycline-induced or uninduced (DMSO-treated) *Trypanosoma* cells were harvested and resuspended in the culture medium containing 75 nM MitoTracker® Deep Red and incubated for 5 min at 28°C. Following incubation, cells were washed with PBS twice and resuspended in the culture medium and further incubated for 30 min at 28°C. Subsequently, cells were fixed with 4% paraformaldehyde in PBS, and samples were prepared for microscopy as mentioned above.

Glycosome- or mitochondrion-stained cells were visualized and imaged with a Zeiss Elyra microscope and were analyzed using Zeiss Zen 3.2 software (blue edition). Both aldolase and MitoTracker which are markers for glycosome and mitochondrion respectively, are pseudo-colored to magenta for visualization.

2.4.2 Yeast

BY4742 yeast strain co-transformed with the plasmids encoding *Sc*PEX11-GFP (WT (Boutouja et al., 2019) and L_{35} to P mutant, with the endogenous promoter) and DsRed-SKL (as a peroxisomal reporter (Kuravi et al., 2006)) were grown overnight (16 h) with shaking in an SD synthetic medium without uracil and histidine. Next day the precultures were diluted to 0.1 OD_{600}/mL and were incubated under shaking until the cell density reached 0.6–0.8 OD_{600}/mL. After incubation, 1–2 mL cultures were harvested and washed with water. For mitochondrial staining, 5 mL of yeast cells, grown to a density of 0.6–0.8 OD_{600}/mL, expressing the *Sc*PEX11 constructs were stained with 150 nM MitoTracker™ Orange CMTMRos (Invitrogen) for 30 min with shaking in dark. Following incubation, 1–2 mL cultures were harvested and washed with water. All incubation steps were performed at 30°C. Yeast cells expressing various fluorescent proteins were directly visualized microscopically without fixation. Microscopy was performed with Carl Zeiss Microscope, using the Axiovision 4.6.3 software, and images were analyzed using Zen 3.2 (blue edition), a Carl Zeiss software. The DsRed-SKL, a peroxisomal reporter is pseudo-colored to magenta for visualization.

2.5 Peptide array

The immobilized peptides of 15-amino acids length, sequentially overlapping by 13 residues (2aa shift), representing the entire sequence of *Tb*PEX11 or the N-terminal domains of three human PEX11 isoforms were synthesized on a cellulose membrane as described previously (Hilpert et al., 2007; Neuhaus et al., 2014). The peptide array was first washed with ethanol for 10 min with gentle shaking followed by three washes with TBS (50 mM Tris, 137 mM NaCl, 2.7 mM KCl, adjusted to pH 8) for 10 min each. Further, the peptide array was incubated with a blocking buffer (TBS +3% BSA +0.05% Tween-20) for 2 h at room temperature (RT). The purified recombinant proteins GST-*Tb*PEX19, GST-*Hs*PEX19, or GST alone (10 mL of 1 μM solution prepared in blocking buffer) were incubated with the arrays for 1 h at 4°C. Then, the arrays were washed three times for 10 min at RT with TBS, and

TABLE 2 Oligonucleotides.

Primer	Sequence 5′to 3′
RE2926	GATCGGATCCATGTCTCATCCCGACAATGAC
RE3310	GATCGTCGACGATGTCTCATCCCGACAATGAC
RE3311	GATCGCGGCCGCCTACACTGATGGTTGCACATCG
RE7038	CCGCTCGAGTTACACTGATGGTTGCACATCGGCAAGTCC
RE7303	TGGACCGTCGACGATGTCTGAGTTCCAAAGGTTTGTT
RE7304	AATATAGTCGACTAAGTTCCTCCGCGTGCTGTGC
RE7305	AAGATAGCGGCCGCTTACAAGACCTCTTTCATGTTGAC
RE7306	AATAAGCGGCCGCCTATTTGATCTTGTTCCAGTTCAA
RE7378	AAGATAGGGCCCATGTCTGAGTTCCAAAGGTTTGTT
RE7379	AAATGGATCCGATCCGCTTCCCTTCAAGACCTCTTTCATGTTGAC
RE7706	AAGACGTCGACCATGGCCGCCGCTGAGGAAGGCTG
RE7707	AAGACGCGGCCGCTCACATGATCAGACACTGTTCA
RE7708	AAGATGTCGACAATGGACGCCTGGGTCCGCTTCAG
RE7709	AAGACGCGGCCGCTTATCTTTTGGCTGACTCAAGG
RE7713	GCCTTAAAGACACCATCAAATGCCTTTAGAATCTTGTCGCGGC
RE7714	GCCGCGACAAGATTCTAAAGGCATTTGATGGTGTCTTTAAGGC
RE7715	CTTAAAGACACCAGGAAATGCCTTTAGAATCTTGTCGCGG
RE7716	CCGCGACAAGATTCTAAAGGCATTTCCTGGTGTCTTTAAG
RE7717	GTGTCGAGGGAGCCAGGTGCCTTAAAGACAC
RE7718	GTGTCTTTAAGGCACCTGGCTCCCTCGACAC
RE7843	AGAAGTCGACAATGGACGCCTTCACCCGCTTCACC
RE7844	AAGAGCGGCCGCTTACTGCTCAGTTGCCTGTATAG
RE7845	AAGAAGTCGACAATGGCGTCGCTGAGCGGCCTGG
RE7846	AAGAGCGGCCGCTTATTGCTTAGTGTAGACAAACA
RE8063	CTGCTAAAAATCTTGCTGGATACTGCAGTAATCTGAGAACCTTTTCTCTGC
RE8064	GCAGAGAAAAGGTTCTCAGATTACTGCAGTATCCAGCAAGATTTTTAGCAG
RE8070	AAGAATTCGAAATGTCTGAGTTCCAAAGGTTTGTT
RE8071	AAGACGGATCCGATTTGATCTTGTTCCAGTTCAA
RE8072	TTCTTGAGACCTGTCAGAGCCGCTCAAG
RE8073	GACAGGTCTCAAGAAGCTTAACAAACCTTTGG
RE8074	TTCAGGATTATGTGCTCGGCGACAATG
RE8075	GCACATAATCCTGAATGGCATTCTGC
RE8096	AAGACTTCGAAATGGAGCAGACAGATGGCCGCGAC
RE8882	TTCAGGATTAAGCGGCCGCTAAGTAAG
RE8883	CCGCTTAATCCTGAATGGCATTCTGCATC

subsequently incubated with the anti-GST monoclonal antibody (Sigma, 1:2000) at RT for 1 h. Followed by three washes with TBS (10 min each), a secondary antibody (Horseradish peroxidase-coupled anti-mouse IgGs, 1:5,000 in blocking buffer) was applied, and the array was further incubated for 1 h at RT. After three washes with TBS, the array was scanned with chemiluminescence substrate (WesternBright Sirius) using Azure sapphire biomolecular imager.

2.6 Protein expression and purification, *in vitro* pull-downs and AlphaScreen binding assay

2.6.1 Protein expression and purification

The expression plasmids pGEX4T2, pGEX4T2-*Tb*PEX19 or pGEX4T1-*Hs*PEX19, encoding for GST, GST-*Tb*PEX19 or GST-*Hs*PEX19, respectively, were transformed into BL21 (DE3) *E. coli* strain. Single colonies were inoculated in LB medium containing ampicillin and incubated overnight with shaking at 37°C. On the following day, the cultures were reinoculated with 0.1 OD_{600}/mL and further incubated at 37°C with shaking, until the cell density reached 0.6 OD_{600}/mL. Protein expression was induced with 1 mM IPTG for 4 h at 30°C. Harvested cell pellets were stored at −20°C before use. For protein purification, *E. coli* cell pellets were resuspended in PBS with protease inhibitors (5 μg/mL Antipain, 2 μg/mL Aprotinin, 0.35 μg/mL Bestatin, 6 μg/mL Chymostatin, 2.5 μg/mL Leupeptin, 1 μg/mL Pepstatin, 0.1 mM PMSF, 25 μg/mL DNAse and 1 mM DTT). Cells were disrupted using EmulsiFlex and unbroken cells were removed by centrifugation at 4,500 rpm for 15 min (rotor SX4400, Beckman Coulter). The resulting supernatant (SN1) was subjected to a high-speed centrifugation at 14,000 rpm for 1 h (rotor SS-34, Thermo Scientific), which yielded supernatant 2 (SN2), a soluble fraction that included overexpressed proteins. Proteins were purified by affinity chromatography using Glutathione Agarose 4B beads (Macherey-Nagel). To this end, SN2 was incubated with the pre-equilibrated glutathione agarose beads for 2 h in a tube rotator. After collection of the flow-through, using a gravity flow column, the protein-bound beads were washed five times with PBS. Proteins were eluted with 10 mM reduced glutathione in 50 mM Tris-Cl (pH 8). The buffer of the eluted protein was exchanged to PBS using Amicon centrifugation tubes with molecular weight cut-off (MWCO) 10 kDa. The concentration of the proteins was determined by the Bradford method (Thermo, Coomassie Plus assay kit), and protein aliquots were stored at—80°C. All the purification steps were performed at 4°C.

2.6.2 *In vitro* pull-down

20 μL bed volume Glutathione Agarose 4B beads (Macherey-Nagel) were incubated with 200 μg of recombinantly purified GST and GST-*Tb*PEX19 proteins in separate tubes for 2 h at 4°C with gentle rotation. Following incubation, beads were washed with PBS to remove unbound proteins. Subsequently, 25 μg of C-terminally His_6-tagged synthetic peptides of crude grade, containing the corresponding *Tb*PEX19 binding regions in *Tb*PEX11 (BS1-BS3) were loaded to the respective tubes and were incubated for 2 h at 4°C with gentle rotation to allow binding of the peptides to GST-*Tb*PEX19 or control GST. Following washes with PBS, the bound proteins/peptides were eluted with 50 μL 10 mM reduced glutathione in 50 mM Tris (pH 8). The eluted samples were analyzed by SDS-PAGE followed by Coomassie staining and immunoblotting. The sequences of the *Tb*PEX11 peptides used for the pull-down are as follows, BS1: QTDGRDKILKAFSGVFKALGSLD-GS-His_6, BS2: CRAKGKVNMKEVLKFLRVLCNFL-GS-His_6 and BS3: VLDVVALYGALQKRASDPATS-GS-His_6.

2.6.3 AlphaScreen binding assay

N-terminal GST tagged *Tb*PEX19 and *Tb*PEX11 peptides with C-/N-terminal His_6 were used for the interaction study with the AlphaScreen system. The final reaction volume used for the study was 25 μL, which consist of 5 μL of each protein solution (30 nM for PEX19 and 300 nM of PEX11 peptides), 5 μL of buffer, and 5 μL of solution for each of the donor and acceptor beads (5 μg/mL). The above solutions were prepared in reaction buffer [0.5% BSA v/v, PBS (pH7.4)] on the day of the assay. Compounds were incubated with the proteins for 30 min at room temperature (RT). 5 μL of AlphaScreen Nickel-chelate acceptor beads (cat. no. 6760619C, PerkinElmer®) were added to the above mixture following 15 min incubation at RT. 5 μL AlphaScreen Glutathione donor beads (cat. no. 6765300, PerkinElmer®) were added to the mixture. The complete 25 μL reaction solutions were incubated for 45 min at RT in the dark, and Alpha signals were captured with Cytation 5 plate reader (BioTek®) with the gain value set at 180. All above concentrations mentioned for the AlphaScreen assays were final concentrations unless otherwise stated. The sequences of the *Tb*PEX11 peptides used for the AlphaScreen assay are as follows, BS1: QTDGRDKILKAFSGVFKALGSLD-GS-His_6, His_6-GS-QTDGRDKILKAFSGVFKALGSLD and BS2: CRAKGKVNMKEVLKFLRVLCNFL-GS-His_6. The binding assay were performed in three biological replicates, with 3 technical replicates each.

2.7 Immunoblotting

Proteins separated by SDS-PAGE were transferred on a nitrocellulose membrane with a pore size of 0.45 μm (Amersham Biosciences). Blotting was performed by using the MiniProtean III cell (BioRad) with blot transfer buffer (Dunn carbonate buffer) for 1 h with a constant current of 300 mA per chamber. Further, the membrane was blocked for 1 h at room temperature (RT), under constant swirling with 3% BSA in blot washing buffer (TBS with 0.05% Tween-20) to avoid nonspecific binding of antibodies. Then, the membrane was washed three times for 5 min at RT, and subsequently incubated with the primary antibodies in blot washing buffer at 4°C overnight. Following primary antibodies were used in this study: mouse anti-GFP (Sigma, 1:2,000), anti-GAL4 AD/-BD (Santa Cruz Biotechnology, 1:1,000) or anti-His_6 (Invitrogen, 1:2,000); rabbit anti-*Trypanosoma* Aldolase (1:20,000) or Enolase (1:20,000), and anti-Porin (*S. cerevisiae*, 1:10,000). After three washing steps, the corresponding secondary antibodies i.e., goat anti-rabbit IRDye 680 or goat anti-mouse IRDye 800CW (LI-COR Biosciences, both 1:15,000 in blot wash buffer) were applied, and the membrane was further incubated for 30 min at RT in the dark. Following three washes, immunoblots were scanned using the Li-Cor Odyssey 9120 Infrared Imaging System.

2.8 Statistical analysis

Microscopic data was collected from two independent *S. cerevisiae* or *T. brucei* cultures. Images were quantified using Pearson's correlation coefficient, which was calculated with colocalization tool of Zen 3.6 pro (blue edition). Statistical significances for colocalization studies were calculated using a one-way ANOVA (mixed) by Dunnett's multiple comparisons test (comparison with WT control) with each row representing matched or repeated measures. Statistical analysis for AlphaScreen

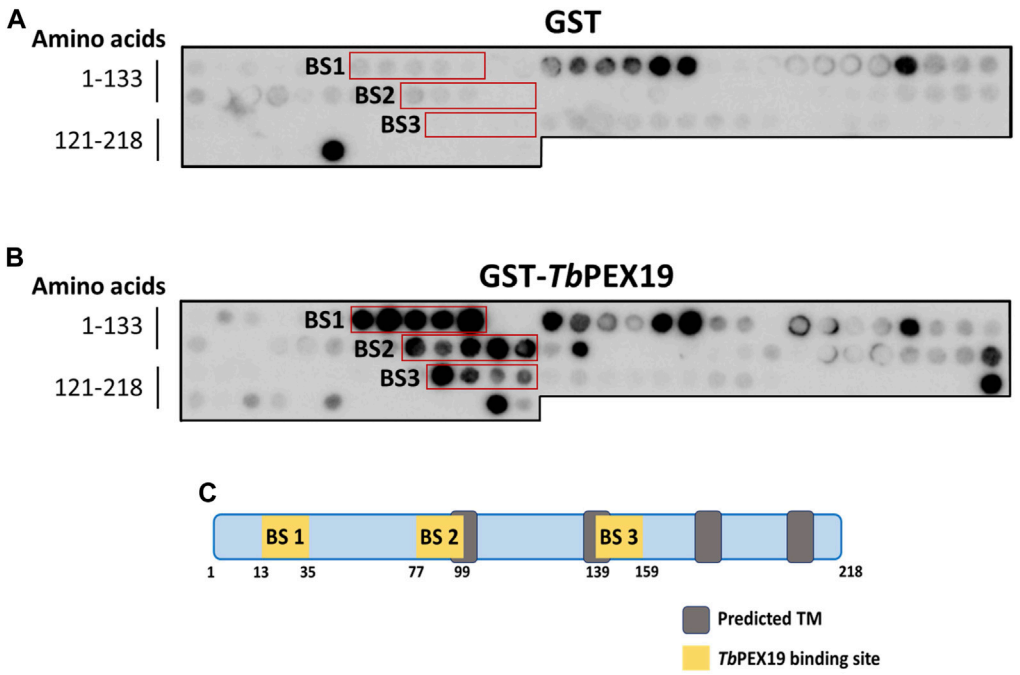

FIGURE 1
Identification of PEX19 binding sites in *Trypanosoma* PEX11 using synthetic peptide arrays. Synthetic 15-mer peptides with 2-amino acids shifts corresponding to the complete *Tb*PEX11 protein sequence were synthesized on cellulose membrane and probed with GST as negative control **(A)** or GST-*Tb*PEX19 **(B)**. Bound analyte was immuno-detected using primary antibodies against GST and horseradish peroxidase coupled secondary antibodies, followed by the signal detection using chemiluminescence. Three regions in *Tb*PEX11 showed clear and specific interaction with *Tb*PEX19 as compared to the GST control (red boxes, marked BS1-BS3). **(C)** Scheme of *Tb*PEX11 showing the identified binding regions in relation to transmembrane segments predicted using Phobius webtool (https://phobius.sbc.su.se/) (Supplementary Figure S2).

results was done using two-way ANOVA with Bonferroni's multiple comparison test (comparison with respective controls) with the values obtained from three independent biological replicates, each with three technical replicates.

3 Results

3.1 Identification and validation of PEX19 binding sites in *Trypanosoma brucei* PEX11

PEX19 acts as a cytosolic chaperone and receptor for the import of newly synthesized class 1 peroxisomal membrane proteins (PMPs), except the class II PMP i.e., PEX3, which can be imported independent of PEX19 (Sacksteder et al., 2000; Jones et al., 2004). PMPs contain multiple PEX19 binding sites, which are well characterized in yeast and humans. This includes the most abundant yeast PMP Pex11p and related PEX11-family proteins Pex25p and Pex27p (Rottensteiner et al., 2004; Halbach et al., 2005). In trypanosomatid parasites, PEX19 binding sites have been identified in various glycosomal membrane proteins as well as parasite specific PEX11 family proteins GIM5A/B (Saveria et al., 2007). However, the PEX19-binding sites (-BS) in parasite PEX11 remained uncharacterized. To identify these binding sites, we obtained synthetic peptide arrays, containing consecutive 15-amino acid peptides with two amino acid shifts, representing the entire sequence of *Tb*PEX11. Affinity purified recombinant GST-*Tb*PEX19 (Purification profile described in Supplementary Figure S1), or GST alone were incubated with the arrays and bound proteins were immuno-detected using monoclonal anti-GST antibodies. Immunodetection of at least three consecutive spots were considered as potential PEX19 binding sites (Rottensteiner et al., 2004). Comparison of control and test peptide arrays revealed the presence of three potential PEX19 binding sites (BS1-BS3) in *Tb*PEX11 (Figure 1). The topological prediction of transmembrane domains (TMDs) using Phobius webserver (Kall et al., 2007) indicates that *Tb*PEX11 contains four TMDs and an N-terminal extension of about 90 amino acids to the cytosol (Supplementary Figure S2). The first PEX19 binding site (BS1) is present close to the N-terminus of *Tb*PEX11 between amino acid (aa) residues 13–35, the second and third PEX19 binding sites are located between aa77-99 and aa139-159, respectively, in proximity of the first and second predicted transmembrane domains (Figure 1C). Both N- and C-termini of *Tb*PEX11 face the cytosol (Lorenz et al., 1998), which implies that the BS1 would remain exposed to the cytosol even after targeting and insertion of *Tb*PEX11 into the glycosomal membrane.

PEX19 binding motifs are conserved between peroxisomal proteins of yeast or mammals and trypanosomal glycosomal proteins (Saveria et al., 2007). Probing of the *Tb*PEX11 peptide array with GST-tagged recombinant human PEX19 also revealed a similar binding pattern (Supplementary Figure S3) as observed with *Tb*PEX19 (Figure 1). This further demonstrates the conservation of

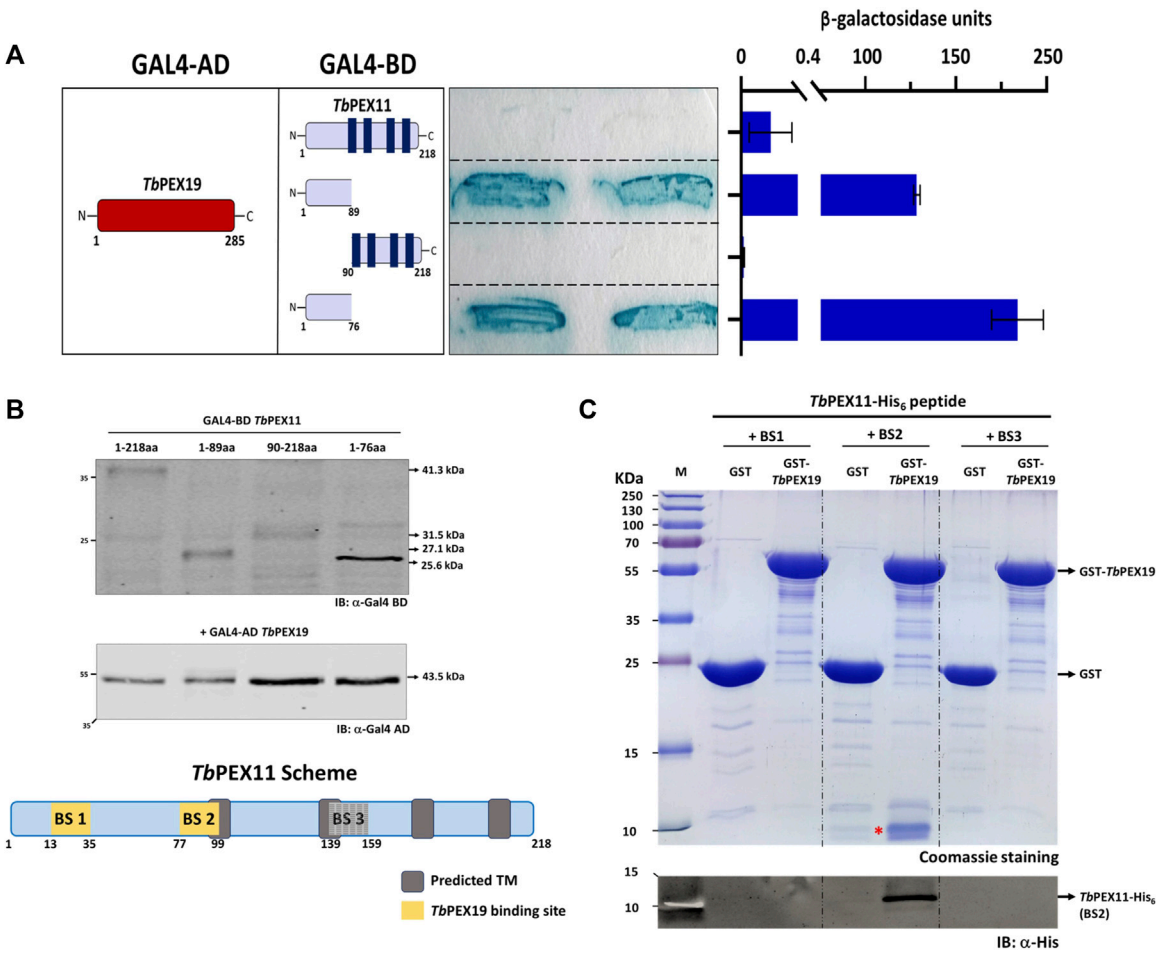

FIGURE 2
Validation of *Tb*PEX19 binding sites in *Tb*PEX11 **(A)** Yeast two-hybrid assay (Y2H): Full length *Tb*PEX19 and various *Tb*PEX11 constructs fused to the GAL4-activation domain (AD) or -binding domain (BD) as indicated (left panel) were co-transformed into PCY2 yeast strain and analyzed by Colony-lift filter assay (middle panel) and liquid ONPG assay (right panel). Both assays were done in three replicates and the β-galactosidase activity units shown are an average of the technical replicates with three different clones. Error bars represent mean with standard deviations. The soluble N-terminal fragments of *Tb*PEX11 comprising BS1 and partially BS2 (1–89) as well as a shorter fragment containing only BS1 (1–76) showed a clear interaction with full-length *Tb*PEX19. Full length *Tb*PEX11 showed a weaker interaction, while the PEX11-fragment (90–218), lacking the N-terminal PEX19 BSs, did not interact with *Tb*PEX19. The GAL4-AD fusion of *Tb*PEX19 and the various GAL4-BD fusions of *Tb*PEX11 were tested for autoactivation and no coloration of the filter was seen (not shown). **(B)** Expression of the GAL4-AD and -BD fusion proteins in the yeast two-hybrid (Y2H) assay was confirmed by immunoblotting with monoclonal antibodies against GAL4-AD and -BD as indicated. Arrow marks on the right correspond to the predicted molecular weights of the fusion proteins. The scheme at the bottom shows the modular structure of *Tb*PEX11, highlighting the identified putative *Tb*PEX19 binding regions. **(C)** *In vitro* pull-down of *Tb*PEX19 with His_6-tagged synthetic peptides of *Tb*PEX11 that correspond to the binding regions highlighted in the PEX11 scheme. Recombinant GST-*Tb*PEX19 or GST as negative control were pre-incubated with Glutathione agarose beads, followed by incubation with the C-terminally His_6-tagged synthetic peptides of *Tb*PEX11. After thorough washing, bound proteins were eluted with reduced glutathione and analyzed by SDS-PAGE and staining with Coomassie brilliant blue (upper panel). The peptide corresponding to BS2 (migrating at ~10 kDa and marked with a red asterisk) was pulled down with GST-*Tb*PEX19, which was also confirmed by immunoblotting using an anti-His monoclonal antibody (lower panel). The putative BS3 could not be validated by either of the assays, therefore it was not considered further and is shown as grey box in the scheme in **(B)**. AD: Activation domain, BD: Binding domain, ONPG: ortho-Nitrophenyl-ß-galactoside.

PEX19-BSs, which can be recognized by PEX19 from different organisms.

Binding of *Tb*PEX19 to the newly identified regions in *Tb*PEX11 were further investigated by yeast two-hybrid (Y2H) analysis and *in vitro* binding assays using pull-down and AlphaScreen. For the Y2H assay, GAL4-AD fusion of *Tb*PEX19 was used since the corresponding GAL4-BD fusions showed autoactivation (not shown). In addition to this, the corresponding GAL4-BD fused PEX11 constructs did not result in the auto activation when tested with GAL4-AD alone (not shown). Various *Tb*PEX11 constructs fused to GAL4-BD were tested for interaction with *Tb*PEX19 (Figure 2A). Full length *Tb*PEX11 showed only a very weak interaction with *Tb*PEX19. This could be due to the presence of several predicted transmembrane domains in *Tb*PEX11, which may hinder the translocation into the nucleus and activation of GAL-promoter. However, the N-terminal fragment of $TbPEX11_{1\text{-}89aa}$ that has been predicted to be soluble (Supplementary Figure S2) showed a clear

and strong interaction with the full length *Tb*PEX19, in both plate-based (sensitive) and liquid Y2H assays (quantitative) (Figure 2A). Construct that lacks the N-terminal domain but contains BS3 (*Tb*PEX11$_{90\text{-}218aa}$) did not interact with *Tb*PEX19. *Tb*PEX11$_{1\text{-}89}$ contains BS1 as well as partial BS2. We also tested a shorter construct that contains only BS1 (*Tb*PEX11$_{1\text{-}76}$), which still showed a strong interaction with *Tb*PEX19. Immunoblotting confirmed that all constructs are expressed in yeast at correct molecular weights (Figure 2B). Furthermore, we opted to introduce two mutations in *Trypanosoma* PEX11. The first mutation replaced serine 25, which is in the *Tb*PEX19 BS1 region, by aspartate to mimic phosphorylation (based on the post-translational modifications database). For the second mutation, we referred to a study in baker's yeast, which showed that replacing leucine at position 35 by proline results in the loss of interaction (Rottensteiner et al., 2004). We aligned the sequence with *Sc*PEX11 and chose the closest leucine residue (position 31) for replacement by proline. Mutation of serine$_{25}$ to aspartate i.e., phospho-mimicking did not affect the interaction, whereas mutation of serine$_{25}$ or leucine$_{31}$ individually and together to proline within BS1 in *Tb*PEX11$_{1\text{-}89}$ led to a reduced or complete abolishment of the interaction with *Tb*PEX19 (Supplementary Figure S4). Based on the peptide blot and the Y2H studies, it can be concluded that BS1 is a *bona fide* PEX19 binding motif.

As an alternative, we obtained C-terminally His$_6$-tagged synthetic peptides of *Tb*PEX11 corresponding to the three putative PEX19 binding sites. Affinity pull-down was performed with GST-*Tb*PEX19 or GST alone as negative control, which were bound to the glutathione affinity beads. Glutathione eluates of the *in vitro* pull-downs were analyzed by Coomassie staining as well as immunoblotting using anti-His$_6$ tag antibodies (Figure 2C; full profile of the pull-downs is shown in Supplementary Figure S5). The analysis shows that the synthetic peptide corresponding to BS2 (running at ~10 kDa) is efficiently retained with *Tb*PEX19 but not with GST alone. Similar binding of the BS2 representing peptide of *Tb*PEX11 was also observed with recombinant human GST-PEX19 (not shown). The synthetic peptides corresponding to BS1 and BS3 (both running at ~10 kDa) did not bind to recombinant GST-*Tb*PEX19 in this assay. The third putative PEX19 binding site (BS3) in *Tb*PEX11 that was identified in the peptide array analysis (Figure 1) could not be further validated by the methods employed here and was not considered further.

Finally, we analyzed the interaction of BS1 and BS2 with *Tb*PEX19 with the more sensitive AlphaScreen assay. This assay was performed using C-terminally His$_6$-tagged peptides that represent the *Tb*PEX11 binding sites with GST-*Tb*PEX19 or GST as negative control (Supplementary Figure S6). Again, the BS2 showed a clear interaction with *Tb*PEX19, while the BS1 did not interact. As the interacting BS1 containing region was N-terminally tagged in the Y2H assay (Figure 2A), we considered that the orientation of the tag might have an influence and therefore analyzed the interaction of an N-terminally tagged BS1-peptide, which indeed showed a significant interaction with *Tb*PEX19 (Supplementary Figure S6). Taken together this study identified two PEX19 binding sites in *Tb*PEX11 (BS1 and BS2).

3.2 Role of PEX19 binding sites in glycosomal targeting of *Tb*PEX11

We performed immunofluorescence microscopy analysis to assess the relevance of the newly identified PEX19 binding sites for the topogenesis of *Tb*PEX11. Tetracycline inducible stable cell lines of *Trypanosoma* were generated, which express C-terminally GFP-tagged full-length *Tb*PEX11 and variants lacking either BS1 or BS2. Glycosomal localization of the constructs was investigated by analysis of colocalization of the fluorescent GFP-fusions of *Tb*PEX11 with the glycosomal marker enzyme aldolase, which was monitored by immunofluorescence microscopy. Overexpressed *Tb*PEX11$_{WT}$-GFP colocalized with the glycosomal marker, indicative for its glycosomal localization (Figure 3A, upper panel). However, frequently glycosomes appeared to cluster, confirming an earlier study reporting that overexpression of *Tb*PEX11 results in clustering of glycosomes in bloodstream form of *T. brucei* (Lorenz et al., 1998). The GFP fluorescence of cells expressing both truncated *Tb*PEX11 variants was much weaker in comparison to the wild-type protein and clustering of glycosomes was not seen. This is explained by the decreased steady-state concentration of both truncated proteins, which is much lower in comparison to the full-length *Tb*PEX11 as indicated by the corresponding immunoblots. (Figure 3D). However, the fluorescence was bright enough to allow investigation of their subcellular localization. *Tb*PEX11 lacking BS1 (*Tb*PEX11$_{\triangle BS1}$-GFP) still showed a partial glycosomal localization (Figure 3A, Middle panel), while the *Tb*PEX11 variant lacking BS2 (*Tb*PEX11$_{\triangle BS2}$-GFP) was mislocalized, as indicated by the lacking colocalization with the glycosomal marker (Figure 3A, lower panel). Taken together this result demonstrated that deficiency in either BS1 or BS2 affects the steady-state concentration of *Tb*PEX11. Thus, binding of PEX19 to either of these sites might stabilize the protein. This is in agreement with studies in yeast, which showed that various PMPs, including PEX11, are unstable and their steady state levels are significantly reduced in PEX19-or PEX3-deficient cells (Hettema et al., 2000). In the absence of BS1, the remaining small amount of *Tb*PEX11 is still directed to glycosomes, while in the absence of BS2, PEX11 is mistargeted, indicating that BS2 is essential for glycosomal targeting of *Tb*PEX11.

In yeast, PEX11 mislocalizes to mitochondria in cells lacking peroxisomal membranes (Hettema et al., 2000; Mattiazzi Usaj et al., 2015). To assess whether mislocalized *Tb*PEX11 is targeted to mitochondria also in trypanosomes, mitochondrial staining was performed. Indeed, colocalization of the truncated *Tb*PEX11 with the MitoTracker indicated that *Tb*PEX11 lacking BS2 is mistargeted to the mitochondrion (Figure 3B, lower panel).

Multiple sequence alignment of the N-terminal region comprising BS1 of *Trypanosoma*, yeast, human, and plant PEX11 family proteins or isoforms indicates a high degree of sequence conservation, suggesting that the region corresponding to trypanosomal BS1 is conserved among PEX11 species (Figure 4A). To investigate the capacity of this region of human PEX11 proteins for PEX19 binding, we obtained synthetic peptide array of N-terminal soluble domains of all three human PEX11 isoforms (15mer peptides with 2-amino acids shifts). The arrays were probed with GST alone as a negative control, which showed little or no background (Figure 4B, upper panel). Probing

10.3389/fcell.2023.1213761

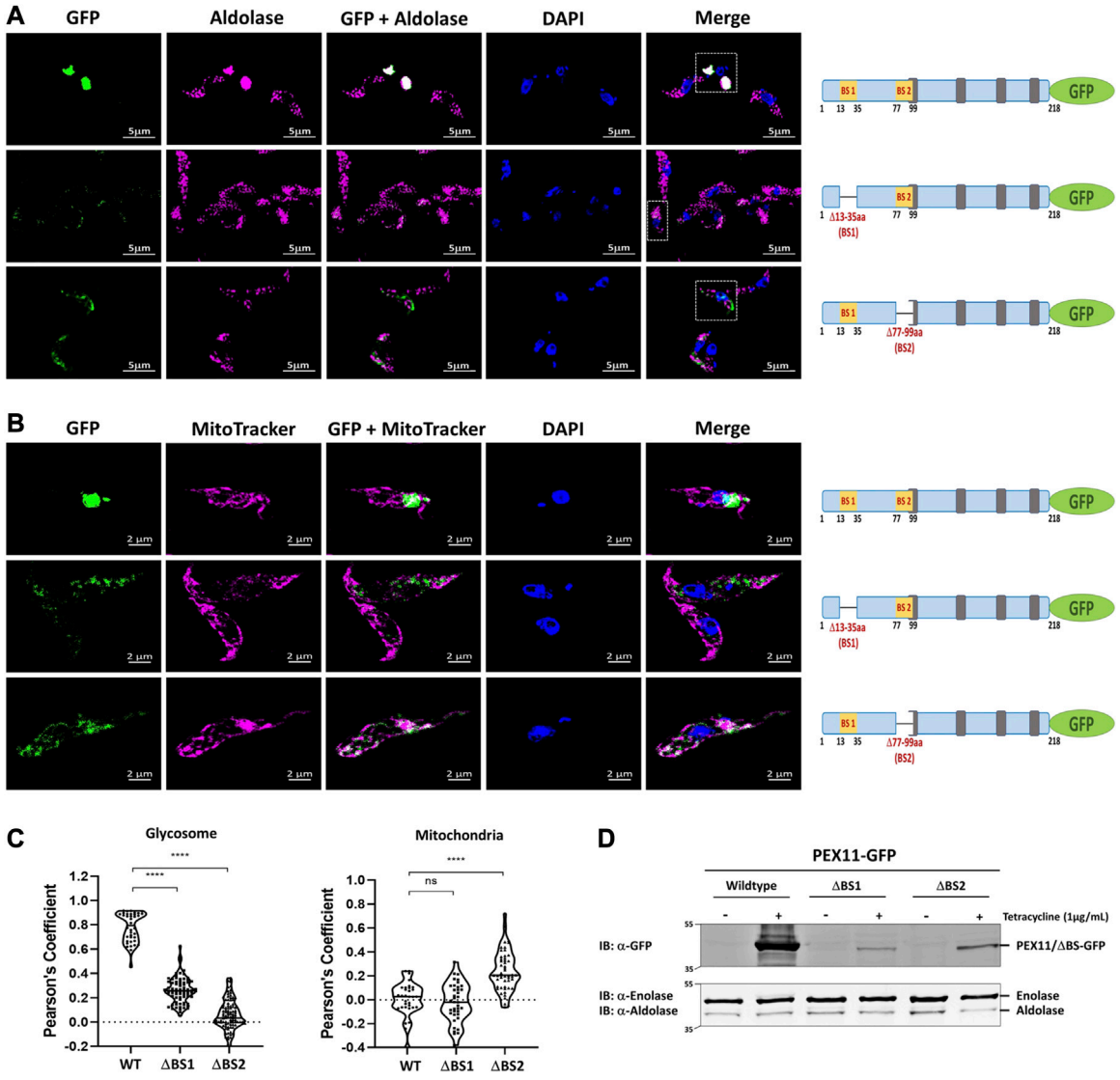

FIGURE 3
PEX19 binding sites are required for maintenance and essential for glycosomal targeting of *Tb*PEX11. **(A)** Binding site 2 (BS2) is required for glycosomal targeting of *Tb*PEX11. *Trypanosoma brucei* parasites (procyclic form) expressing tetracycline-induced and C-terminally GFP tagged *Tb*PEX11 constructs (wildtype or mutant proteins lacking PEX19 binding sites) were analyzed for localization of the GFP fusion proteins, the glycosomal marker aldolase, as well as the DAPI-stained nucleus and kinetoplast by fluorescence- or immunofluorescence microscopy. The GFP fusion of wildtype *Tb*PEX11 (upper panel) did colocalize with the glycosome marker aldolase (pseudo-colored to magenta). It is also evident that the overexpression of the full-length *Tb*PEX11 results in the clustering of glycosomes as previously reported (Lorenz et al., 1998). The mutant lacking the first PEX19 binding site (middle panel) partially colocalized with the glycosome marker aldolase. In this case, a clustering of glycosomes was not seen, most likely as the steady-state concentration of the truncated protein was much lower than the corresponding full-length *Tb*PEX11 (see below). PEX11-GFP harboring deletion of BS2 (Δ77-99aa) did not colocalize with the glycosomal marker aldolase (lower panel), but instead showed mislocalization to mitochondrion as demonstrated by colocalization with the mitochondrial marker MitoTracker (pseudo-colored to magenta) **(B)**. Scale bar—5 µm and –2 µm. Schematic representation of the various PEX11-GFP constructs is shown on the right. **(C)** Quantification of the colocalization to glycosomes (left) or mitochondrion (right). The Pearson's coefficient of colocalization to respective organelle is shown. Dots within the violin plot indicates individual Pearson correlation coefficient data points and the central line represents the median. Statistical significance were calculated by one-way ANOVA, with Dunnett's multiple comparisons test ($n \geq 35$ cells). ****, $p < 0.0001$; ns, not significant. **(D)** Analysis of the expression levels of PEX11-GFP (wildtype and mutants) upon tetracycline induction (+/–) by immunoblotting with anti-GFP antibodies. Cytosolic marker enolase and glycosomal marker aldolase served as the loading controls (lower panel). Wildtype *Tb*PEX11 expression was highly induced, resulting in a high steady-state concentration, while the steady-state concentration of both truncation mutants of *Tb*PEX11 were very low in comparison to the wildtype *Tb*PEX11, most likely due to an instability of the *Tb*PEX11 constructs lacking either of the PEX19 binding sites.

the array with GST-*Hs*PEX19 revealed that the peptides from PEX11γ did not bind PEX19, while PEX11α and PEX11β do contain potential PEX19-BS (Figure 4B, lower panel). To validate the interactions, Y2H analysis was performed to investigate the interaction of N-terminal domains of PEX11 isoforms and human PEX19 (Figure 4C). An interaction was seen only with PEX11β, in both the plate-based and the liquid assay. Immunoblot analysis of lysates of yeast cell used in Y2H shows that PEX11α and β were expressed, but not PEX11γ (Figure 4D).

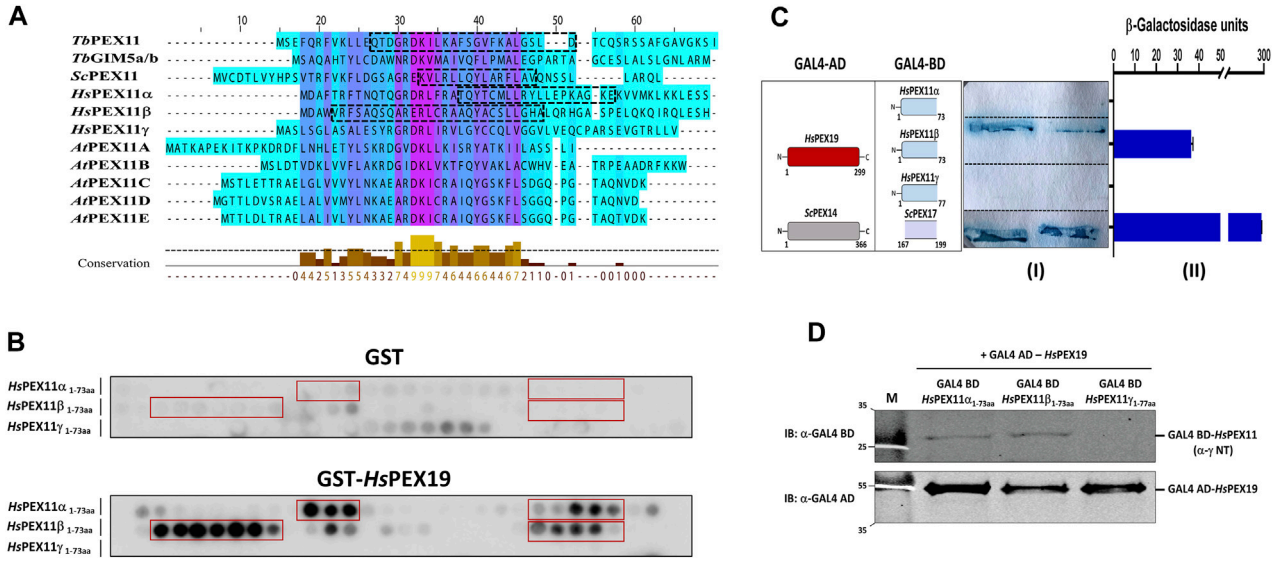

FIGURE 4
The N-terminal PEX19 binding site in PEX11 is conserved among species. **(A)** Multiple sequence alignment of N-terminal sequences of PEX11 proteins from parasites, baker's yeast, humans, and plants shows a high degree of conservation. The N-terminal PEX19 binding site (BS1) identified in *Trypanosoma brucei* is indicated by a black dotted box. The known PEX19 binding site from yeast and the newly identified PEX19 binding sites in humans are also indicated by black dotted boxes. **(B)** Identification of N-terminal PEX19 binding site in the human members of the PEX11 family. Synthetic 15-mer peptides with 2-amino acids shift of the N-terminal protein sequence of *Hs*PEX11 (α, β and γ) were synthesized on cellulose membrane and probed with GST as a negative control (upper panel) or GST-*Hs*PEX19 (lower panel). The bound analyte was immunodetected using primary antibodies against GST and horseradish peroxidase coupled secondary antibody. The signal was monitored using chemiluminescence. Binding regions in *Hs*PEX11 (α and β) showed clear interaction with *Hs*PEX19 (red boxes). **(C)** Validation of identified binding sites by Yeast two-hybrid analysis using Δ*pex19* PCY2 strain. Scheme of the cotransformed *Hs*PEX19 and *Hs*PEX11 (α, β and γ) N-terminal constructs is shown on the left. Colony lift filter assay (I) and liquid ONPG assay (II) were performed using full-length *Hs*PEX19 and different constructs of *Hs*PEX11 fused to GAL4-AD and -BD as indicated. The interaction of yeast PEX14-PEX17 served as a positive control. Both assays were performed in three replicates and the β-galactosidase activity units shown are an average of the technical replicates with three different clones. Error bars represents mean with standard deviations. Of the three members of the PEX11-family only the N-terminal fragment of *Hs*PEX11β showed a clear interaction with full-length *Hs*PEX19. **(D)** Expression of the GAL4-AD and -BD fused proteins were tested by immunoblotting using GAL4-AD and -BD with monoclonal antibodies. No expression of Gal BD-*Hs*PEX11γ N-terminal fragment was detected.

As PEX11γ was not expressed, no conclusion can be drawn from the negative result of the two-hybrid study. However, the results are clear in that PEX11β indeed does contain a PEX19 binding site in the region that corresponds to trypanosomal BS1.

In yeast, *Sc*PEX11 contains only one PEX19 binding site, spanning amino acids 27–41 (Rottensteiner et al., 2004), that is homologous to trypanosomal BS1. Mutational analysis of this binding site indicated that the L35P mutation completely abolished interaction with *Sc*PEX19 (Rottensteiner et al., 2004). Here we introduced this mutation into the full-length sequence of PEX11 fused to GFP and analyzed its subcellular localization in comparison to wild-type PEX11 by fluorescence microscopy (Figure 5A). As expected, the full-length PEX11-GFP is targeted to peroxisomes as indicated by its co-localization with the peroxisomal marker DsRed-SKL (Figure 5A, middle panel). The PEX11-GFP fusion harboring the L35P exchange, however, was partly mislocalized to tubular structures (Figure 5A, lower panel). We further performed staining of yeast cells that express $PEX11_{L35P}$-GFP together with a mitochondrial marker (MitoTracker) (Figure 5B, lower panel), confirming that the L35P mutant is mislocalized to mitochondria. Immunoblot analysis of cells shown in Figure 5A show that GFP-tagged wild-type PEX11 is stable, but the steady-state concentration of L35P mutant protein that cannot bind to PEX19 is very low in comparison (Figure 5D).

The data show that PEX11 from *Trypanosoma* and yeast as well as PEX11β from humans contain a conserved N-terminal region that can bind PEX19. This region, corresponding to BS1 in *Trypanosoma*, is required to maintain the steady-state concentration of PEX11 in all studied species, and at least for yeast, it is shown that it is also required for efficient targeting of PEX11 to peroxisomes.

3.3 Cryptic N-terminal targeting signal of trypanosomal PEX11

In the absence of PEX19, PMPs are mislocalized to the cytosol and rapidly degraded, or mislocalized to other membranes. For example, PEX3 localizes to the endoplasmic reticulum (Hoepfner et al., 2005) but many PMPs, including yeast PEX11 and PEX13, accumulate in mitochondria when peroxisomes are absent in the cell (Nuebel et al., 2021). PEX13 that is mislocalized to mitochondria can recruit functional docking and import peroxin complexes to mitochondria and also some peroxisomal matrix proteins (Nuebel et al., 2021). Peroxins also accumulate in mitochondria of Zellweger patient-derived cells leading to mitochondrial dysfunction (Nuebel et al., 2021). This can be rescued by overexpressing mitochondrial quality

10.3389/fcell.2023.1213761

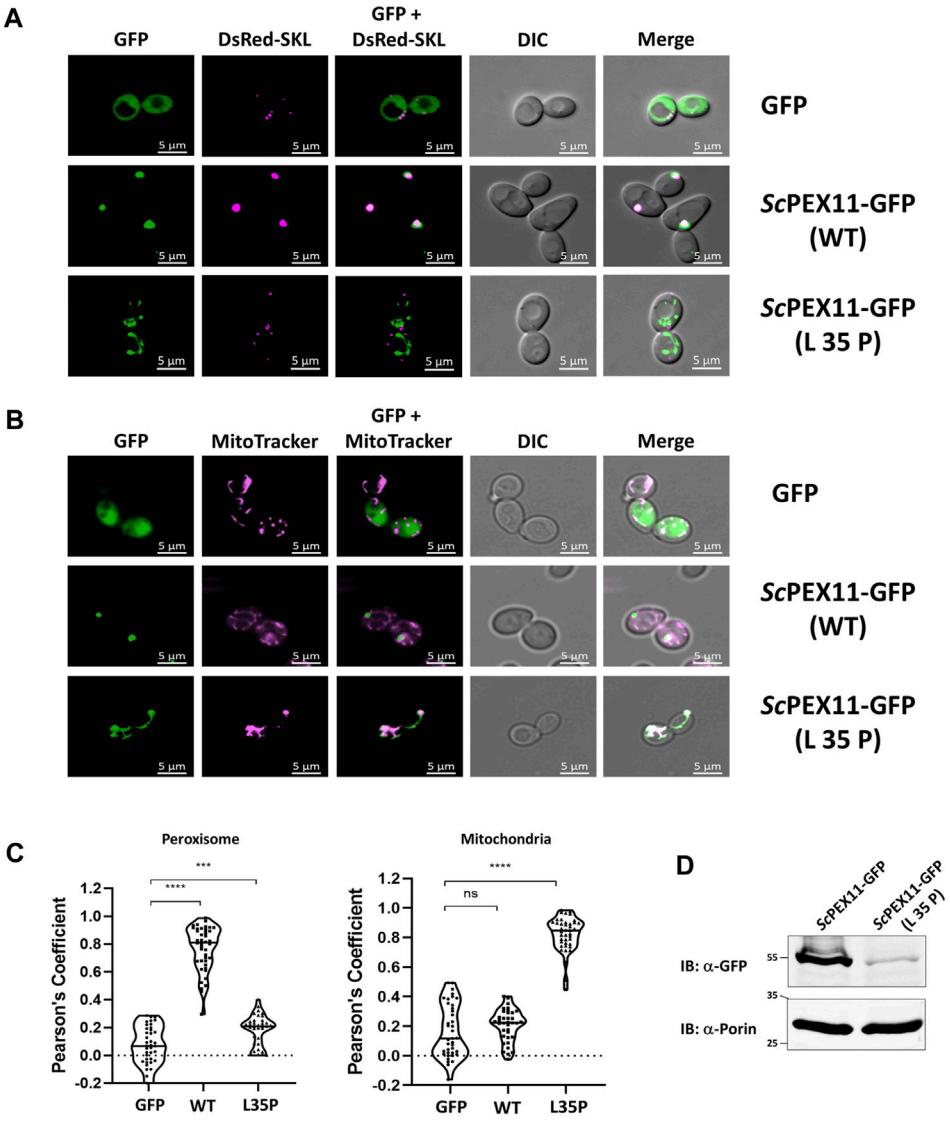

FIGURE 5
The N-terminal binding site for PEX19 is essential for peroxisomal localization of *Sc*PEX11. Plasmids expressing *Sc*PEX11-GFP (wildtype and L35P-mutant) or the peroxisomal marker protein DsRed-SKL were cotransformed in the BY4742 yeast strain. **(A)** Clones expressing GFP fusion proteins and the peroxisomal marker DsRed-SKL were grown on plates and visualized by fluorescence microscopy. Merged images reveal peroxisomal colocalization of *Sc*PEX11-GFP (wildtype) with DsRed-SKL (pseudo-colored to magenta), indicative for its peroxisomal localization. In contrast, the L35P exchange that is known to block PEX19 binding site result in mislocalization of *Sc*PEX11. **(B)** *Sc*PEX11-GFP with mutation L35P mislocalizes to mitochondria as demonstrated by its colocalization with MitoTracker (pseudo-colored to magenta). DIC–Differential Interference Contrast, Scale bar—5 µm. **(C)** Quantification of the colocalization of *Sc*PEX11-GFP to peroxisomes (left) or mitochondria (right). The Pearson's coefficient of colocalization to respective organelle is shown. Dots within the violin plot indicates individual Pearson correlation coefficient data points and the central line represents the median. Statistical significances were calculated by one-way ANOVA, with Dunnett's multiple comparisons test (n ≥ 35 cells). ****, $p < 0.0001$; ***, $p = 0.0003$; ns, not significant. **(D)** Expression of *Sc*PEX11-GFP (wildtype and L35P mutant) was tested by immunoblotting with anti-GFP antibody, which revealed that the steady-state concentration of the L35P is much lower than that of the corresponding wild-type protein. Porin served as the loading control.

control ATPase ATAD1. We showed that *Tb*PEX11-GFP lacking BS2 is mislocalized to mitochondrion in trypanosomes (Figure 3B, lower panel). However, glycosomal targeting also requires the presence of a transmembrane segment for correct targeting. Accordingly, the *Tb*PEX11 construct containing the first 90 amino acids fused to GFP that lacks the transmembrane domain (TMD) is also mistargeted to mitochondrion. This construct is used here as a control to investigate the requirement for the targeting of *Tb*PEX11 to mitochondria (Figure 6C, upper panel). Normally, mitochondrial proteins are targeted via N-terminal or internal mitochondrial targeting signals (Backes et al., 2018; Bykov et al., 2022), After mitochondrial import, the N-terminal targeting presequences of proteins are removed by mitochondrial processing peptidase (MPP) to allow the proper folding of the imported protein (Kunova et al., 2022). Here, we applied the Mitofates webtool to predict putative mitochondrial targeting signals in the N-terminal region of *Tb*PEX11 (Fukasawa et al., 2015). Although the tool does not identify the *Tb*PEX11-NTD as a classical mitochondrial presequence,

10.3389/fcell.2023.1213761

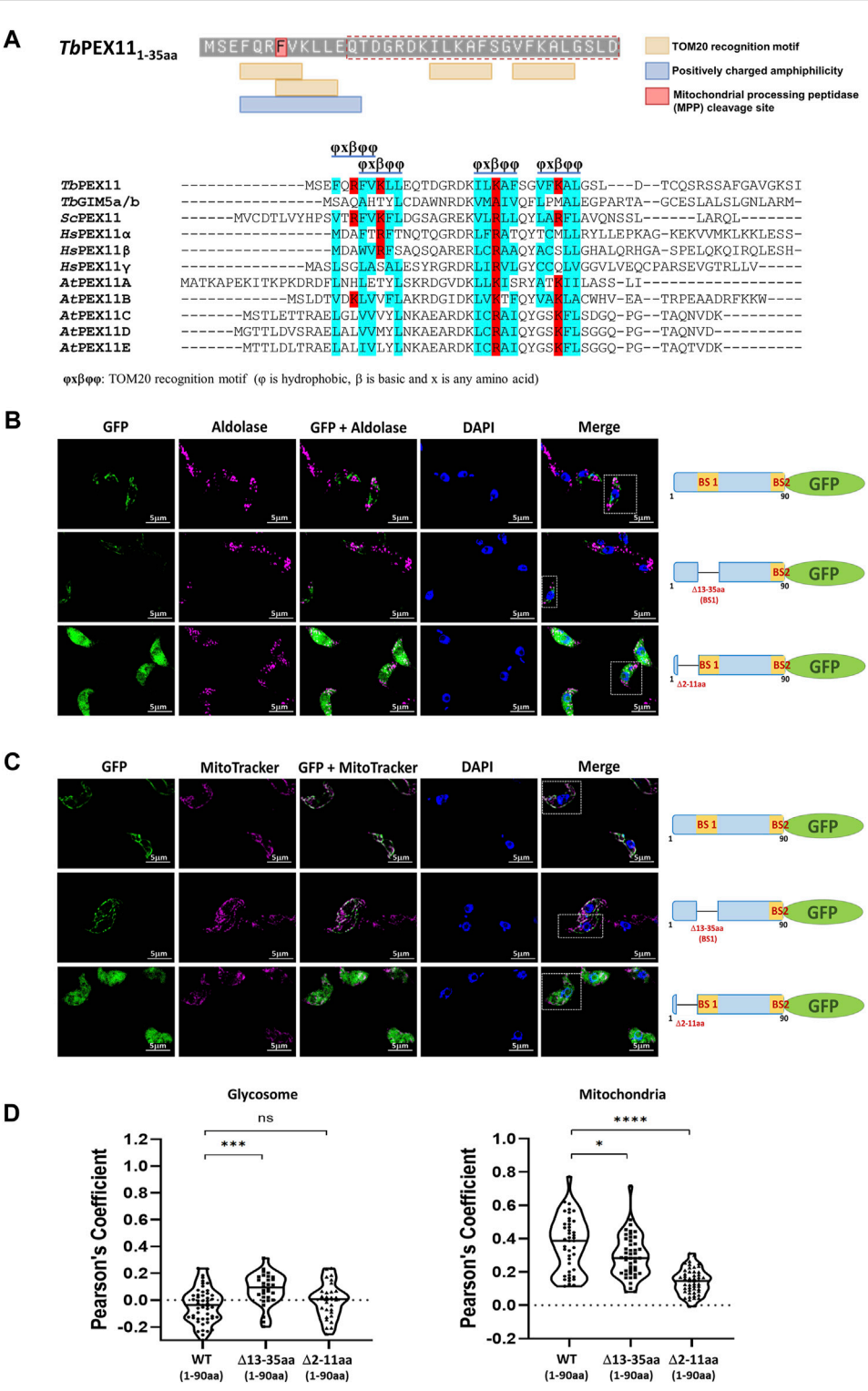

FIGURE 6
Cryptic signal at the N-terminus causes mitochondrial mislocalization of *Tb*PEX11. **(A)** Upper panel: Prediction of two overlapping putative TOM20 motifs with positively charged amphiphilicity within the N-terminal region *Tb*PEX11 and partially overlapping with the PEX19 binding site region (red dotted box). The residue highlighted in red indicates the presence of a mitochondrial processing peptidase (MPP) cleavage site. The presence of a predicted TOM20 recognition motif and positively charged amphiphilic region with MPP cleavage site were determined by Mitofates webtool (https://mitf.cbrc.pj.aist.go.jp/MitoFates/cgi-bin/top.cgi). Lower panel: Multiple sequence alignment of N-terminal sequences of PEX11 proteins from parasites, yeast, humans, and plants indicates the presence of conserved TOM20 motifs with positively charged (red) residues encased by hydrophobic (blue) amino acid residues. **(B)** Subcellular localization of the N-terminal domain of *Tb*PEX11 (1–90aa) fused to GFP with and without deletion of the PEX19-binding site 1 (Δ13-35aa) or deletion of a N-terminal putative TOM20 binding motif (Δ2-11aa) by fluorescence and immunofluorescence microscopy. The non-truncated fusion with and without PEX19 binding site 1 (BS1) did not co-localize with the glycosomal marker aldolase but was targeted to mitochondrion as shown below (upper and middle panel). The *Tb*PEX11-GFP lacking the TOM20 motif did mislocalize to the cytosol as

(*Continued*)

FIGURE 6 (Continued)
indicated by the overall cell labelling (lower panel). **(C)** The non-truncated fusion with and without PEX19 binding site 1 (BS1) localized to the mitochondrion, demonstrated by their colocalization with MitoTracker (upper and middle panel, respectively). The glycosomal marker aldolase (pseudo-colored to magenta) was labelled with the corresponding antibody, nuclei and kinetoplasts were stained with DAPI, and mitochondrion was visualized by MitoTracker (pseudo-colored to magenta). Scale bar—5 μm. **(D)** Quantification of the colocalization to glycosomes (left) or the mitochondrion (right). The Pearson's coefficient of colocalization to respective organelle is shown. Dots within the violin plot indicate individual Pearson correlation coefficient data points and the central line represents the median. Statistical significances were calculated by one-way ANOVA, with Dunnett's multiple comparisons test (n ≥ 35 cells). ****, $p < 0.0001$; ***, $p = 0.0001$; *, $p = 0.0262$; ns, not significant.

it predicts the presence of two tandem TOM20 recognition motifs and a positively charged amphiphilic region with mitochondrial processing peptidase (MPP) cleavage site (Figure 6A, upper panel). The putative TOM20 recognition motifs are in the N-terminal region of *Tb*PEX11 (4–31 aa), partially overlapping with the identified BS1-binding region for *Tb*PEX19 (13–35aa) (Figure 6A, upper panel). Further, we looked for the TOM20 motifs by performing multiple sequence alignment of N-terminal region of PEX11 across organisms (Figure 6A, lower panel), which also contains PEX19 binding site (BS) of yeast (Rottensteiner et al., 2004) and the identified PEX19-BS in *T. brucei* and human (this study). This alignment indicates the conservation of TOM20 motifs in the N-terminal region of PEX11, pointing to its role in mitochondrial mislocalization. To test the putative signal sequences for functionality, we analyzed the role of this region for mitochondrial and glycosomal targeting by fluorescence microscopy (Figure 6B). To this end, GFP tagged N-terminal 90 amino acid region of *Tb*PEX11, with or without BS1 (Δ13-35aa) was analyzed for co-localization with glycosomal marker aldolase (Figure 6B, upper and middle panel). Both fusion proteins were expressed and not targeted to glycosomes but mislocalized to mitochondrion as evident from co-staining with mitochondrial marker (Figure 6C). The expression of these constructs was confirmed by immunoblotting using α-GFP monoclonal antibody (Supplementary Figure S7). Finally, $TbPEX11_{NTD(1\text{-}90aa)}$-GFP lacking amino acid residues 2–11, which were predicted to contain TOM20 motifs and positively charged amphiphilicity was analyzed. Expression of this construct did result in a diffuse cytosolic labelling (Figures 6B,C, lower panels), indicating that deletion of this extreme N-terminal region prevented mitochondrial targeting of the fusion protein.

4 Discussion

Here we show that the glycosomal membrane protein *Tb*PEX11 contains two PEX19 binding sites in its N-terminal region, as shown by peptide array analysis, yeast two-hybrid studies, pull-down experiments, and AlphaScreen assays. PEX19 is a peroxisomal membrane protein (PMP) receptor and chaperone that stabilizes its cargo proteins and targets them to peroxisomes (Hettema et al., 2000; Sacksteder et al., 2000; Jones et al., 2004). PEX19 binding sites are distributed across the length of cargo proteins, including the C-terminus in case of tail-anchored (TA) proteins (Halbach et al., 2006). Apart from yeast Pex11p (aa 27–41), PEX19 binding sites close to the N-terminus were also found in yeast Pex3p (aa 28–42) and Pxa1p (aa 33–47) (Rottensteiner et al., 2004). Along this line, the N-terminal 95 residues of Pxa1p have recently been shown to be sufficient for targeting a reporter protein to peroxisomes. Interestingly, truncated Pxa1p lacking residues 1–95 still localized to peroxisomes but its targeting depended on the presence of its interaction partner Pxa2 (Jansen et al., 2023).

Eukaryotic organisms contain multiple proteins belonging to the PEX11 family. In yeast, Pex11p contains a single PEX19-BS near its N-terminus, while in the other *Sc*PEX11-family members, Pex25p and Pex27p, binding of PEX19 occurs far distal from the N-terminus (Rottensteiner et al., 2004). A recent study identified a classical PEX19-BS near the N-terminus of *Pichia pastoris* PEX11 (Zientara-Rytter et al., 2022). However, the study also showed that amphipathic helix 4 (H4) located in the C-terminal region of *Pp*PEX11, functions as a second, PEX19-independent mPTS, which is preserved among PEX11-family proteins (Zientara-Rytter et al., 2022). Thus, unlike most PMPs, PEX11 of *Pichia pastoris* can use two mechanisms of transport to peroxisomes, where only one of them depends on its direct interaction with PEX19, but the other does not. The presence of such a PEX19-independent targeting signal is not confirmed in our studies for PEX11 from *T. brucei* and *S. cerevisiae*, as N-terminal mutations or truncations of PEX19-binding sites BS1 or BS2 but not of the amphiphilic helix 4 did prevent efficient glycosomal or peroxisomal targeting of the proteins.

Our data indicate that the N-terminal binding site (BS1) for PEX19 is conserved among *Tb*PEX11 orthologues but not in PEX11-family member GIM5/B of *Trypanosoma* or *Leishmania* (Saveria et al., 2007). Our results also indicate differences within PEX11 isoforms in humans. All three isoforms, PEX11α, PEX11β, and PEX11γ show sequence similarities to the established PEX19 binding site BS1 in yeast and *T. brucei*, but only *Hs*PEX11β did bind human PEX19 (Figures 4B,C). PEX11β is a key factor in the regulation of peroxisome abundance in mammals (reviewed in (Schrader et al., 2016)). It functions as a membrane-remodeling protein that can deform and elongate the peroxisome membrane prior to fission (Delille et al., 2010; Yoshida et al., 2015). Accordingly, PEX11β is the functional counterpart of yeast and *T. brucei* PEX11 that are targeted to their destination in a PEX19-dependent manner and contribute to the morphogenesis of the peroxisomal membrane, which is required for subsequent fission. Overall, the N-terminal PEX11-binding sites for PEX19 are conserved among species. In this study, this is highlighted by the peptide array analysis of *Tb*PEX11, which revealed that human PEX19 binds to the same regions as trypanosomal PEX19 (Supplementary Figure S3).

In the absence of peroxisomes, many PMPs are unstable and degraded or mistargeted to other organelles such as ER and mitochondria. This is seen in yeast as well as in human cells derived from patients suffering from a Peroxisome Biogenesis Disorder (PBD) (Hettema et al., 2000; Nuebel et al., 2021). In yeast, PEX3 localizes to the ER (Toro et al., 2009), while several peroxins/PMPs including PEX13, PEX14, PEX17 (peroxisomal docking complex) as well as PEX11 and

PEX25 accumulated on mitochondria (Nuebel et al., 2021). Here we show that mislocalization to mitochondria is seen for *Tb*PEX11 lacking its second PEX19-BS and *Sc*PEX11 harboring mutation of its sole PEX19-binding site, (Figure 3B; 5B). Mitochondria have been described as emergency landing places for abandoned peroxins, which results in a partial reconstitution of the peroxisomal import machinery and routing of a substantial part of the peroxisomal proteome to mitochondria (Nuebel et al., 2021; Vogtle and Meisinger, 2021). The mislocalization of PMPs, especially peroxins, to mitochondria are supposed to be the cause for mitochondrial dysfunction in PBD patients (Hettema et al., 2000; Nuebel et al., 2021). Therefore, it is of interest to gain insight into why some PMPs mislocalize to this particular organelle. Mitochondrial targeting signals (MTS) have been extensively characterized across different organisms and consensus motifs can be predicted. Bioinformatic prediction indicated the presence of positively charged amphiphilicity in the extreme N-terminal Helix 1 and detected four TOM20 recognition motifs in NTD of *Tb*PEX11, out of which two tandem motifs coincide with the N-terminal PEX19-BS (Figure 6A). There is no obvious structural similarity between PEX19 and TOM20. The TOM20 recognizes motifs in cargo proteins via its TPR (tetratricopeptide repeat) domain, which is not present in PEX19. In our *in vitro* studies, PEX19 can directly interact with the PEX19-BSs, without the requirement of an additional cofactor. Surprisingly, the iMTS-Ls predictor also recognizes PEX19-BSs in *Tb* and *Sc*PEX11 as having Internal Matrix Targeting Signal-like Sequences (iMTSL) propensity (Supplementary Figure S8) (Schneider et al., 2021). How these signals that have primary sequence and potential structural similarities, are faithfully recognized by the correct receptor, and targeted to the correct location requires further investigation. The expression of *Tb*PEX11-NTD lacking N-terminal Helix 1 did not any more mistarget to the mitochondrion. This demonstrates that the N-terminal amphipathic helix at the extreme N-terminus of *Tb*PEX11 is essential for the mitochondrial mislocalization. This result indicates that *Tb*PEX11 harbors a cryptic mitochondrial targeting signal. Whether this is also true for human PEX11 and other PMPs, and involvement of TOM complex machinery requires further investigation.

4.1 What could be the role of a mitochondrial targeting signal of PEX11?

In mature glycosomes/peroxisomes of the wild type cells, *Tb*PEX11-NTD is exposed to the cytosol. In this case, the cryptic N-terminal signals may be masked by the oligomerization of PEX11. However, in newly formed glycosomes, which are importing PEX11, these signals may be still accessible to interact with the mitochondrial TOM machinery, and this may mediate glycosome-mitochondrion membrane contact site (MCS). Accordingly, association of *Sc*PEX11 with the mitochondrial TOM complex has been seen in two studies, i) 37-fold enrichment of *Sc*PEX11 in the SILAC based interactome of yeast TOM22 (Opalinski et al., 2018), and ii) interaction of *Sc*PEX11 with TOM22 in split-ubiquitin assay (Eckert and Johnsson, 2003). Recently, a nuclear membrane protein Cnm1 (Contact nucleus mitochondria 1) was shown to interact with TOM70, a component of the mitochondrial TOM (translocase of outer membrane) complex (Eisenberg-Bord et al., 2021). This interaction establishes nuclear-mitochondrial contact sites, which are regulated by phosphatidylcholine metabolism. Interestingly, Cnm1 harbors two predicted transmembrane domains close to the N-terminus, while C-terminal end contains internal mitochondrial targeting signal-like (iMTS-L) sequences, which are known to directly bind to TOM70 (Backes et al., 2018). Similarly, PEX11 localized to the glycosomal membrane could still associate with the mitochondrial preprotein import machinery to establish glycosome-mitochondrial contact. Interestingly, PEX11 of parasite *Entamoeba histolytica* shows dual localization to peroxisomes and mitosomes (Verner et al., 2021). In baker's yeast, PEX11 interacts with Mdm34, a component of the ER–mitochondria encounter structure (ERMES), and act as a peroxisome–mitochondria tether (Mattiazzi Usaj et al., 2015). It has been shown that a mutant form of Mdm34, a component of the ERMES, which impairs ERMES formation and diminishes its association with the peroxisomal membrane protein PEX11, also causes defects in pexophagy (Liu et al., 2018). Along this line, a role for ERMES complex proteins on regulating peroxisome abundance has been reported (Esposito et al., 2019).

We do not yet know whether the newly identified cryptic mitochondrial targeting signal of *Tb*PEX11 is of functional relevance. However, peroxisomes are not only metabolically linked to mitochondria but also share components of their division machinery (Schrader et al., 2015). These include the tail-anchored adaptor proteins FIS1 and MFF, which are dually targeted to both peroxisomes and mitochondria, where they recruit the fission GTPase DRP1 (also known as DNML1) to the organelle membrane (Schrader et al., 2022). In this context, it is interesting to note that targeting of PEX11β to mitochondria induces mitochondrial division in human cells. Accordingly, like PEX11β also *Tb*PEX11 might have the potential to modulate mitochondrial dynamics.

Data availability statement

The original contributions presented in the study are included in the article/Supplementary Material, further inquiries can be directed to the corresponding authors.

Author contributions

CK, VK, and RE conceived and planned the experiments. CK carried out the experiments. NS and KW contributed to the super-resolution fluorescence microscopy. BT performed the AlphaScreen assay. MJ synthesized the peptide array. CK, VK, and RE wrote the manuscript with support from WS. VK and RE supervised the project. All authors contributed to the article and approved the submitted version.

Funding

This project work has received funding from the European Union's Horizon 2020 research and innovation program under the Marie Skłodowska-Curie grant agreement No. 812968—PerICo (to CK, and RE). The work was supported by DFG grant FOR1905 to RE.

Acknowledgments

We thank Paul Michels for kindly providing various antibodies and Wolfgang Girzalsky for critical reading of the manuscript. We acknowledge support by the Open Access Publication Funds of the Ruhr-Universität Bochum.

Conflict of interest

The authors declare that the research was conducted in the absence of any commercial or financial relationships that could be construed as a potential conflict of interest.

Publisher's note

All claims expressed in this article are solely those of the authors and do not necessarily represent those of their affiliated organizations, or those of the publisher, the editors and the reviewers. Any product that may be evaluated in this article, or claim that may be made by its manufacturer, is not guaranteed or endorsed by the publisher.

Supplementary material

The Supplementary Material for this article can be found online at: https://www.frontiersin.org/articles/10.3389/fcell.2023.1213761/full#supplementary-material

References

Abe, I., and Fujiki, Y. (1998a). cDNA cloning and characterization of a constitutively expressed isoform of the human peroxin Pex11p. *Biochem. Biophys. Res. Commun.* 252 (2), 529–533. doi:10.1006/bbrc.1998.9684

Abe, I., Okumoto, K., Tamura, S., and Fujiki, Y. (1998b). Clofibrate-inducible, 28-kDa peroxisomal integral membrane protein is encoded by PEX11. *FEBS Lett.* 431 (3), 468–472. doi:10.1016/s0014-5793(98)00815-1

Agrawal, G., and Subramani, S. (2016). De novo peroxisome biogenesis: evolving concepts and conundrums. *Biochim. Biophys. Acta* 1863 (5), 892–901. doi:10.1016/j.bbamcr.2015.09.014

Albertini, M., Rehling, P., Erdmann, R., Girzalsky, W., Kiel, J. A., Veenhuis, M., et al. (1997). Pex14p, a peroxisomal membrane protein binding both receptors of the two PTS-dependent import pathways. *Cell* 89 (1), 83–92. doi:10.1016/s0092-8674(00)80185-3

Anton, M., Passreiter, M., Lay, D., Thai, T. P., Gorgas, K., and Just, W. W. (2000). ARF- and coatomer-mediated peroxisomal vesiculation. *Cell Biochem. Biophys.* 32 (1), 27–36. doi:10.1385/cbb:32:1-3:27

Breidenbach, R. W., and Beevers, H. (1967). Association of the glyoxylate cycle enzymes in a novel subcellular particle from castor bean endosperm. *Biochem. Biophys. Res. Commun.* 27 (4), 462–469. doi:10.1016/s0006-291x(67)80007-x

Backes, S., Hess, S., Boos, F., Woellhaf, M. W., Godel, S., Jung, M., et al. (2018). Tom70 enhances mitochondrial preprotein import efficiency by binding to internal targeting sequences. *J. Cell Biol.* 217 (4), 1369–1382. doi:10.1083/jcb.201708044

Baerends, R. J., Faber, K. N., Kiel, J. A., van der Klei, I. J., Harder, W., and Veenhuis, M. (2000). Sorting and function of peroxisomal membrane proteins. *FEMS Microbiol. Rev.* 24 (3), 291–301. doi:10.1111/j.1574-6976.2000.tb00543.x

Banerjee, S. K., Kessler, P. S., Saveria, T., and Parsons, M. (2005). Identification of trypanosomatid PEX19: functional characterization reveals impact on cell growth and glycosome size and number. *Mol. Biochem. Parasitol.* 142 (1), 47–55. doi:10.1016/j.molbiopara.2005.03.008

Bonekamp, N. A., Grille, S., Cardoso, M. J., Almeida, M., Aroso, M., Gomes, S., et al. (2013). Self-interaction of human Pex11pβ during peroxisomal growth and division. *PLoS One* 8 (1), e53424. doi:10.1371/journal.pone.0053424

Boutouja, F., Stiehm, C. M., Mastalski, T., Brinkmeier, R., Reidick, C., El Magraoui, F., et al. (2019). Vps10-mediated targeting of Pep4 determines the activity of the vacuole in a substrate-dependent manner. *Sci. Rep.* 9 (1), 10557. doi:10.1038/s41598-019-47184-7

Brun, R., and Schonenberger (1979). Cultivation and *in vitro* cloning or procyclic culture forms of Trypanosoma brucei in a semi-defined medium. Short communication. *Acta Trop.* 36 (3), 289–292.

Bykov, Y. S., Flohr, T., Boos, F., Zung, N., Herrmann, J. M., and Schuldiner, M. (2022). Widespread use of unconventional targeting signals in mitochondrial ribosome proteins. *EMBO J.* 41 (1), e109519. doi:10.15252/embj.2021109519

De Duve, C., and Baudhuin, P. (1966). Peroxisomes (microbodies and related particles). *Physiol. Rev.* 46 (2), 323–357. doi:10.1152/physrev.1966.46.2.323

Delille, H. K., Agricola, B., Guimaraes, S. C., Borta, H., Luers, G. H., Fransen, M., et al. (2010). Pex11pbeta-mediated growth and division of mammalian peroxisomes follows a maturation pathway. *J. Cell Sci.* 123 (16), 2750–2762. doi:10.1242/jcs.062109

Eckert, J. H., and Johnsson, N. (2003). Pex10p links the ubiquitin conjugating enzyme Pex4p to the protein import machinery of the peroxisome. *J. Cell Sci.* 116 (17), 3623–3634. doi:10.1242/jcs.00678

Eisenberg-Bord, M., Zung, N., Collado, J., Drwesh, L., Fenech, E. J., Fadel, A., et al. (2021). Cnm1 mediates nucleus-mitochondria contact site formation in response to phospholipid levels. *J. Cell Biol.* 220 (11), e202104100. doi:10.1083/jcb.202104100

Erdmann, R., and Blobel, G. (1995). Giant peroxisomes in oleic acid-induced *Saccharomyces cerevisiae* lacking the peroxisomal membrane protein Pmp27p. *J. Cell Biol.* 128 (4), 509–523. doi:10.1083/jcb.128.4.509

Erdmann, R., and Schliebs, W. (2005). Peroxisomal matrix protein import: the transient pore model. *Nat. Rev. Mol. Cell Biol.* 6 (9), 738–742. doi:10.1038/nrm1710

Esposito, M., Hermann-Le Denmat, S., and Delahodde, A. (2019). Contribution of ERMES subunits to mature peroxisome abundance. *PLoS One* 14 (3), e0214287. doi:10.1371/journal.pone.0214287

Faber, K. N., Keizer-Gunnink, I., Pluim, D., Harder, W., Ab, G., and Veenhuis, M. (1995). The N-terminus of amine oxidase of Hansenula polymorpha contains a peroxisomal targeting signal. *FEBS Lett.* 357 (2), 115–120. doi:10.1016/0014-5793(94)01317-t

Fukasawa, Y., Tsuji, J., Fu, S. C., Tomii, K., Horton, P., and Imai, K. (2015). MitoFates: improved prediction of mitochondrial targeting sequences and their cleavage sites. *Mol. Cell Proteomics* 14 (4), 1113–1126. doi:10.1074/mcp.M114.043083

Galland, N., de Walque, S., Voncken, F. G., Verlinde, C. L., and Michels, P. A. (2010). An internal sequence targets Trypanosoma brucei triosephosphate isomerase to glycosomes. *Mol. Biochem. Parasitol.* 171 (1), 45–49. doi:10.1016/j.molbiopara.2010.01.002

Gao, Y., Skowyra, M. L., Feng, P., and Rapoport, T. A. (2022). Protein import into peroxisomes occurs through a nuclear pore-like phase. *Science* 378 (6625), eadf3971. doi:10.1126/science.adf3971

Ghaedi, K., Tamura, S., Okumoto, K., Matsuzono, Y., and Fujiki, Y. (2000). The peroxin pex3p initiates membrane assembly in peroxisome biogenesis. *Mol. Biol. Cell* 11 (6), 2085–2102. doi:10.1091/mbc.11.6.2085

Gietz, R. D., and Woods, R. A. (2002). Transformation of yeast by lithium acetate/single-stranded carrier DNA/polyethylene glycol method. *Methods Enzymol.* 350, 87–96. doi:10.1016/s0076-6879(02)50957-5

Girzalsky, W., Hoffmann, L. S., Schemenewitz, A., Nolte, A., Kunau, W. H., and Erdmann, R. (2006). Pex19p-dependent targeting of Pex17p, a peripheral component of the peroxisomal protein import machinery. *J. Biol. Chem.* 281 (28), 19417–19425. doi:10.1074/jbc.M603344200

Goldman, B. M., and Blobel, G. (1978). Biogenesis of peroxisomes: intracellular site of synthesis of catalase and uricase. *Proc. Natl. Acad. Sci. U. S. A.* 75 (10), 5066–5070. doi:10.1073/pnas.75.10.5066

Gould, S. J., Keller, G. A., Hosken, N., Wilkinson, J., and Subramani, S. (1989). A conserved tripeptide sorts proteins to peroxisomes. *J. Cell Biol.* 108 (5), 1657–1664. doi:10.1083/jcb.108.5.1657

Halbach, A., Landgraf, C., Lorenzen, S., Rosenkranz, K., Volkmer-Engert, R., Erdmann, R., et al. (2006). Targeting of the tail-anchored peroxisomal membrane proteins PEX26 and PEX15 occurs through C-terminal PEX19-binding sites. *J. Cell Sci.* 119 (12), 2508–2517. doi:10.1242/jcs.02979

Halbach, A., Lorenzen, S., Landgraf, C., Volkmer-Engert, R., Erdmann, R., and Rottensteiner, H. (2005). Function of the PEX19-binding site of human adrenoleukodystrophy protein as targeting motif in man and yeast. PMP targeting is evolutionarily conserved. *J. Biol. Chem.* 280 (22), 21176–21182. doi:10.1074/jbc.M501750200

Hasan, S., Platta, H. W., and Erdmann, R. (2013). Import of proteins into the peroxisomal matrix. *Front. Physiol.* 4, 261. doi:10.3389/fphys.2013.00261

Hettema, E. H., Girzalsky, W., van Den Berg, M., Erdmann, R., and Distel, B. (2000). *Saccharomyces cerevisiae* pex3p and pex19p are required for proper localization and stability of peroxisomal membrane proteins. *EMBO J.* 19 (2), 223–233. doi:10.1093/emboj/19.2.223

Hilpert, K., Winkler, D. F., and Hancock, R. E. (2007). Peptide arrays on cellulose support: sPOT synthesis, a time and cost efficient method for synthesis of large numbers of peptides in a parallel and addressable fashion. *Nat. Protoc.* 2 (6), 1333–1349. doi:10.1038/nprot.2007.160

Hoepfner, D., Schildknegt, D., Braakman, I., Philippsen, P., and Tabak, H. F. (2005). Contribution of the endoplasmic reticulum to peroxisome formation. *Cell* 122 (1), 85–95. doi:10.1016/j.cell.2005.04.025

Islinger, M., Li, K. W., Seitz, J., Volkl, A., and Luers, G. H. (2009). Hitchhiking of Cu/Zn superoxide dismutase to peroxisomes--evidence for a natural piggyback import mechanism in mammals. *Traffic* 10 (11), 1711–1721. doi:10.1111/j.1600-0854.2009.00966.x

Jansen, R. L. M., van den Noort, M., Krikken, A. M., Bibi, C., Bohm, A., Schuldiner, M., et al. (2023). Novel targeting assay uncovers targeting information within peroxisomal ABC transporter Pxa1. *Biochim. Biophys. Acta Mol. Cell Res.* 1870 (5), 119471. doi:10.1016/j.bbamcr.2023.119471

Jones, J. M., Morrell, J. C., and Gould, S. J. (2004). PEX19 is a predominantly cytosolic chaperone and import receptor for class 1 peroxisomal membrane proteins. *J. Cell Biol.* 164 (1), 57–67. doi:10.1083/jcb.200304111

Kalel, V. C., and Erdmann, R. (2018). Unraveling of the structure and function of peroxisomal protein import machineries. *Subcell. Biochem.* 89, 299–321. doi:10.1007/978-981-13-2233-4_13

Kalel, V. C., Schliebs, W., and Erdmann, R. (2015). Identification and functional characterization of Trypanosoma brucei peroxin 16. *Biochim. Biophys. Acta* 1853 (10), 2326–2337. doi:10.1016/j.bbamcr.2015.05.024

Kall, L., Krogh, A., and Sonnhammer, E. L. (2007). Advantages of combined transmembrane topology and signal peptide prediction--the Phobius web server. *Nucleic Acids Res.* 35, W429–W432. Web Server issue). doi:10.1093/nar/gkm256

Kamoshita, M., Kumar, R., Anteghini, M., Kunze, M., Islinger, M., Martins Dos Santos, V., et al. (2022). Insights into the peroxisomal protein inventory of zebrafish. *Front. Physiol.* 13, 822509. doi:10.3389/fphys.2022.822509

Koch, J., Pranjic, K., Huber, A., Ellinger, A., Hartig, A., Kragler, F., et al. (2010). PEX11 family members are membrane elongation factors that coordinate peroxisome proliferation and maintenance. *J. Cell Sci.* 123 (19), 3389–3400. doi:10.1242/jcs.064907

Krishna, C. K., Franke, L., Erdmann, R., and Kalel, V. C. (2023). "Isolation of glycosomes from trypanosoma brucei," in *Peroxisomes: Methods and protocols*. Editor M. Schrader (New York, NY: Springer US), 33–45.

Kunova, N., Havalova, H., Ondrovicova, G., Stojkovicova, B., Bauer, J. A., Bauerova-Hlinkova, V., et al. (2022). Mitochondrial processing peptidases-structure, function and the role in human diseases. *Int. J. Mol. Sci.* 23 (3), 1297. doi:10.3390/ijms23031297

Kunze, M. (2023). Computational evaluation of peroxisomal targeting signals in metazoa. *Methods Mol. Biol.* 2643, 391–404. doi:10.1007/978-1-0716-3048-8_28

Kuravi, K., Nagotu, S., Krikken, A. M., Sjollema, K., Deckers, M., Erdmann, R., et al. (2006). Dynamin-related proteins Vps1p and Dnm1p control peroxisome abundance in *Saccharomyces cerevisiae*. *J. Cell Sci.* 119 (19), 3994–4001. doi:10.1242/jcs.03166

Lazarow, P. B., and Fujiki, Y. (1985). Biogenesis of peroxisomes. *Annu. Rev. Cell Biol.* 1, 489–530. doi:10.1146/annurev.cb.01.110185.002421

Leon, S., Goodman, J. M., and Subramani, S. (2006). Uniqueness of the mechanism of protein import into the peroxisome matrix: transport of folded, co-factor-bound and oligomeric proteins by shuttling receptors. *Biochim. Biophys. Acta* 1763 (12), 1552–1564. doi:10.1016/j.bbamcr.2006.08.037

Li, X., and Gould, S. J. (2002). PEX11 promotes peroxisome division independently of peroxisome metabolism. *J. Cell Biol.* 156 (4), 643–651. doi:10.1083/jcb.200112028

Lingard, M. J., and Trelease, R. N. (2006). Five Arabidopsis peroxin 11 homologs individually promote peroxisome elongation, duplication or aggregation. *J. Cell Sci.* 119 (9), 1961–1972. doi:10.1242/jcs.02904

Liu, X., Wen, X., and Klionsky, D. J. (2018). Endoplasmic reticulum–mitochondria contacts are required for pexophagy in *Saccharomyces cerevisiae*. *Contact* 2, 2158. *Thousand Oaks)* 2. doi:10.1177/2515256418821584

Lorenz, P., Maier, A. G., Baumgart, E., Erdmann, R., and Clayton, C. (1998). Elongation and clustering of glycosomes in Trypanosoma brucei overexpressing the glycosomal Pex11p. *EMBO J.* 17 (13), 3542–3555. doi:10.1093/emboj/17.13.3542

Maier, A., Lorenz, P., Voncken, F., and Clayton, C. (2001). An essential dimeric membrane protein of trypanosome glycosomes. *Mol. Microbiol.* 39 (6), 1443–1451. doi:10.1046/j.1365-2958.2001.02333.x

Marshall, P. A., Dyer, J. M., Quick, M. E., and Goodman, J. M. (1996). Redox-sensitive homodimerization of Pex11p: a proposed mechanism to regulate peroxisomal division. *J. Cell Biol.* 135 (1), 123–137. doi:10.1083/jcb.135.1.123

Mattiazzi Usaj, M., Brloznik, M., Kaferle, P., Zitnik, M., Wolinski, H., Leitner, F., et al. (2015). Genome-wide localization study of yeast Pex11 identifies peroxisome-mitochondria interactions through the ERMES complex. *J. Mol. Biol.* 427 (11), 2072–2087. doi:10.1016/j.jmb.2015.03.004

Mayerhofer, P. U. (2016). Targeting and insertion of peroxisomal membrane proteins: eR trafficking versus direct delivery to peroxisomes. *Biochim. Biophys. Acta* 1863 (5), 870–880. doi:10.1016/j.bbamcr.2015.09.021

McNew, J. A., and Goodman, J. M. (1994). An oligomeric protein is imported into peroxisomes *in vivo*. *J. Cell Biol.* 127 (5), 1245–1257. doi:10.1083/jcb.127.5.1245

Meinecke, M., Bartsch, P., and Wagner, R. (2016). Peroxisomal protein import pores. *Biochim. Biophys. Acta* 1863 (5), 821–827. doi:10.1016/j.bbamcr.2015.10.013

Motley, A. M., and Hettema, E. H. (2007). Yeast peroxisomes multiply by growth and division. *J. Cell Biol.* 178 (3), 399–410. doi:10.1083/jcb.200702167

Moyersoen, J., Choe, J., Fan, E., Hol, W. G., and Michels, P. A. (2004). Biogenesis of peroxisomes and glycosomes: trypanosomatid glycosome assembly is a promising new drug target. *FEMS Microbiol. Rev.* 28 (5), 603–643. doi:10.1016/j.femsre.2004.06.004

Murphy, M. A., Phillipson, B. A., Baker, A., and Mullen, R. T. (2003). Characterization of the targeting signal of the Arabidopsis 22-kD integral peroxisomal membrane protein. *Plant Physiol.* 133 (2), 813–828. doi:10.1104/pp.103.027870

Neuhaus, A., Kooshapur, H., Wolf, J., Meyer, N. H., Madl, T., Saidowsky, J., et al. (2014). A novel Pex14 protein-interacting site of human Pex5 is critical for matrix protein import into peroxisomes. *J. Biol. Chem.* 289 (1), 437–448. doi:10.1074/jbc.M113.499707

Nuebel, E., Morgan, J. T., Fogarty, S., Winter, J. M., Lettlova, S., Berg, J. A., et al. (2021). The biochemical basis of mitochondrial dysfunction in Zellweger Spectrum Disorder. *EMBO Rep.* 22 (10), e51991. doi:10.15252/embr.202051991

Opalinski, L., Song, J., Priesnitz, C., Wenz, L. S., Oeljeklaus, S., Warscheid, B., et al. (2018). Recruitment of cytosolic J-proteins by TOM receptors promotes mitochondrial protein biogenesis. *Cell Rep.* 25 (8), 2036–2043.e5. doi:10.1016/j.celrep.2018.10.083

Opperdoes, F. R., and Borst, P. (1977). Localization of nine glycolytic enzymes in a microbody-like organelle in trypanosoma brucei: the glycosome. *FEBS Lett.* 80 (2), 360–364. doi:10.1016/0014-5793(77)80476-6

Orth, T., Reumann, S., Zhang, X., Fan, J., Wenzel, D., Quan, S., et al. (2007). The PEROXIN11 protein family controls peroxisome proliferation in Arabidopsis. *Plant Cell* 19 (1), 333–350. doi:10.1105/tpc.106.045831

Platta, H. W., Girzalsky, W., and Erdmann, R. (2004). Ubiquitination of the peroxisomal import receptor Pex5p. *Biochem. J.* 384 (1), 37–45. doi:10.1042/BJ20040572

Platta, H. W., Grunau, S., Rosenkranz, K., Girzalsky, W., and Erdmann, R. (2005). Functional role of the AAA peroxins in dislocation of the cycling PTS1 receptor back to the cytosol. *Nat. Cell Biol.* 7 (8), 817–822. doi:10.1038/ncb1281

Reichle, R. E., and Alexander, J. V. (1965). Multiperforate septations, Woronin bodies, and septal plugs in Fusarium. *J. Cell Biol.* 24 (3), 489–496. doi:10.1083/jcb.24.3.489

Rhodin, J. (1954). "Correlation of ultrastructural organization: and function in normal and experimentally changed proximal convoluted tubule cells of the mouse kidney: an electron microscopic study," (Sweden: Dept. of Anatomy, Karolinska Institutet). PhD Thesis.

Rottensteiner, H., Kramer, A., Lorenzen, S., Stein, K., Landgraf, C., Volkmer-Engert, R., et al. (2004). Peroxisomal membrane proteins contain common Pex19p-binding sites that are an integral part of their targeting signals. *Mol. Biol. Cell* 15 (7), 3406–3417. doi:10.1091/mbc.e04-03-0188

Rottensteiner, H., Stein, K., Sonnenhol, E., and Erdmann, R. (2003). Conserved function of pex11p and the novel pex25p and pex27p in peroxisome biogenesis. *Mol. Biol. Cell* 14 (10), 4316–4328. doi:10.1091/mbc.e03-03-0153

Rucktaschel, R., Thoms, S., Sidorovitch, V., Halbach, A., Pechlivanis, M., Volkmer, R., et al. (2009). Farnesylation of pex19p is required for its structural integrity and function in peroxisome biogenesis. *J. Biol. Chem.* 284 (31), 20885–20896. doi:10.1074/jbc.M109.016584

Sacksteder, K. A., Jones, J. M., South, S. T., Li, X., Liu, Y., and Gould, S. J. (2000). PEX19 binds multiple peroxisomal membrane proteins, is predominantly cytoplasmic, and is required for peroxisome membrane synthesis. *J. Cell Biol.* 148 (5), 931–944. doi:10.1083/jcb.148.5.931

Saveria, T., Halbach, A., Erdmann, R., Volkmer-Engert, R., Landgraf, C., Rottensteiner, H., et al. (2007). Conservation of PEX19-binding motifs required for protein targeting to mammalian peroxisomal and trypanosome glycosomal membranes. *Eukaryot. Cell* 6 (8), 1439–1449. doi:10.1128/EC.00084-07

Schneider, K., Zimmer, D., Nielsen, H., Herrmann, J. M., and Muhlhaus, T. (2021). iMLP, a predictor for internal matrix targeting-like sequences in mitochondrial proteins. *Biol. Chem.* 402 (8), 937–943. doi:10.1515/hsz-2021-0185

Schrader, M., Costello, J., Godinho, L. F., and Islinger, M. (2015). Peroxisome-mitochondria interplay and disease. *J. Inherit. Metab. Dis.* 38 (4), 681–702. doi:10.1007/s10545-015-9819-7

Schrader, M., Costello, J. L., Godinho, L. F., Azadi, A. S., and Islinger, M. (2016). Proliferation and fission of peroxisomes - an update. *Biochim. Biophys. Acta* 1863 (5), 971–983. doi:10.1016/j.bbamcr.2015.09.024

Schrader, M., Reuber, B. E., Morrell, J. C., Jimenez-Sanchez, G., Obie, C., Stroh, T. A., et al. (1998). Expression of PEX11beta mediates peroxisome proliferation in the absence of extracellular stimuli. *J. Biol. Chem.* 273 (45), 29607–29614. doi:10.1074/jbc.273.45.29607

Schrader, T. A., Carmichael, R. E., Islinger, M., Costello, J. L., Hacker, C., Bonekamp, N. A., et al. (2022). PEX11β and FIS1 cooperate in peroxisome division independently of mitochondrial fission factor. *J. Cell Sci.* 135 (13), jcs259924. doi:10.1242/jcs.259924

South, S. T., and Gould, S. J. (1999). Peroxisome synthesis in the absence of preexisting peroxisomes. *J. Cell Biol.* 144 (2), 255–266. doi:10.1083/jcb.144.2.255

Sulter, G. J., Verheyden, K., Mannaerts, G., Harder, W., and Veenhuis, M. (1993). The *in vitro* permeability of yeast peroxisomal membranes is caused by a 31 kDa integral membrane protein. *Yeast* 9 (7), 733–742. doi:10.1002/yea.320090707

Swinkels, B. W., Gould, S. J., Bodnar, A. G., Rachubinski, R. A., and Subramani, S. (1991). A novel, cleavable peroxisomal targeting signal at the amino-terminus of the rat 3-ketoacyl-CoA thiolase. *EMBO J.* 10 (11), 3255–3262. doi:10.1002/j.1460-2075.1991.tb04889.x

Tam, Y. Y., Torres-Guzman, J. C., Vizeacoumar, F. J., Smith, J. J., Marelli, M., Aitchison, J. D., et al. (2003). Pex11-related proteins in peroxisome dynamics: a role for the novel peroxin Pex27p in controlling peroxisome size and number in *Saccharomyces cerevisiae*. *Mol. Biol. Cell* 14 (10), 4089–4102. doi:10.1091/mbc.e03-03-0150

Thoms, S., and Gartner, J. (2012). First PEX11β patient extends spectrum of peroxisomal biogenesis disorder phenotypes. *J. Med. Genet.* 49 (5), 314–316. doi:10.1136/jmedgenet-2012-100899

Toro, A. A., Araya, C. A., Cordova, G. J., Arredondo, C. A., Cardenas, H. G., Moreno, R. E., et al. (2009). Pex3p-dependent peroxisomal biogenesis initiates in the endoplasmic reticulum of human fibroblasts. *J. Cell Biochem.* 107 (6), 1083–1096. doi:10.1002/jcb.22210

Tyler, K. M., Matthews, K. R., and Gull, K. (2001). Anisomorphic cell division by African trypanosomes. *Protist* 152 (4), 367–378. doi:10.1078/1434-4610-00074

Van Ael, E., and Fransen, M. (2006). Targeting signals in peroxisomal membrane proteins. *Biochim. Biophys. Acta* 1763 (12), 1629–1638. doi:10.1016/j.bbamcr.2006.08.020

van Roermund, C. W., Tabak, H. F., van Den Berg, M., Wanders, R. J., and Hettema, E. H. (2000). Pex11p plays a primary role in medium-chain fatty acid oxidation, a process that affects peroxisome number and size in *Saccharomyces cerevisiae*. *J. Cell Biol.* 150 (3), 489–498. doi:10.1083/jcb.150.3.489

Verner, Z., Zarsky, V., Le, T., Narayanasamy, R. K., Rada, P., Rozbesky, D., et al. (2021). Anaerobic peroxisomes in Entamoeba histolytica metabolize myo-inositol. *PLoS Pathog.* 17 (11), e1010041. doi:10.1371/journal.ppat.1010041

Vogtle, F. N., and Meisinger, C. (2021). Mitochondria as emergency landing for abandoned peroxins. *EMBO Rep.* 22 (10), e53790. doi:10.15252/embr.202153790

Voncken, F., van Hellemond, J. J., Pfisterer, I., Maier, A., Hillmer, S., and Clayton, C. (2003). Depletion of GIM5 causes cellular fragility, a decreased glycosome number, and reduced levels of ether-linked phospholipids in trypanosomes. *J. Biol. Chem.* 278 (37), 35299–35310. doi:10.1074/jbc.M301811200

Yoshida, Y., Niwa, H., Honsho, M., Itoyama, A., and Fujiki, Y. (2015). Pex11mediates peroxisomal proliferation by promoting deformation of the lipid membrane. *Biol. Open* 4 (6), 710–721. doi:10.1242/bio.201410801

Zientara-Rytter, K. M., Mahalingam, S. S., Farre, J. C., Carolino, K., and Subramani, S. (2022). Recognition and chaperoning by Pex19, followed by trafficking and membrane insertion of the peroxisome proliferation protein, Pex11. *Cells* 11 (1), 157. doi:10.3390/cells11010157

frontiers | Frontiers in Cell and Developmental Biology

TYPE Review
PUBLISHED 18 September 2023
DOI 10.3389/fcell.2023.1243038

OPEN ACCESS

EDITED BY
Markus Kunze,
Medical University of Vienna, Austria

REVIEWED BY
Maite Montero-Hadjadje,
Université de Rouen, France
Matthew Seaman,
University of Cambridge, United Kingdom

*CORRESPONDENCE
Klementina Fon Tacer,
fontacer@ttu.edu

RECEIVED 20 June 2023
ACCEPTED 31 August 2023
PUBLISHED 18 September 2023

CITATION
Štepihar D, Florke Gee RR, Hoyos Sanchez MC and Fon Tacer K (2023), Cell-specific secretory granule sorting mechanisms: the role of MAGEL2 and retromer in hypothalamic regulated secretion.
Front. Cell Dev. Biol. 11:1243038.
doi: 10.3389/fcell.2023.1243038

Cell-specific secretory granule sorting mechanisms: the role of MAGEL2 and retromer in hypothalamic regulated secretion

Denis Štepihar[1,2,3], Rebecca R. Florke Gee[1,2], Maria Camila Hoyos Sanchez[1,2] and Klementina Fon Tacer[1,2]*

[1]School of Veterinary Medicine, Texas Tech University, Amarillo, TX, United States, [2]Texas Center for Comparative Cancer Research (TC3R), Amarillo, TX, United States, [3]Biotechnical Faculty, University of Ljubljana, Ljubljana, Slovenia

Intracellular protein trafficking and sorting are extremely arduous in endocrine and neuroendocrine cells, which synthesize and secrete on-demand substantial quantities of proteins. To ensure that neuroendocrine secretion operates correctly, each step in the secretion pathways is tightly regulated and coordinated both spatially and temporally. At the *trans*-Golgi network (TGN), intrinsic structural features of proteins and several sorting mechanisms and distinct signals direct newly synthesized proteins into proper membrane vesicles that enter either constitutive or regulated secretion pathways. Furthermore, this anterograde transport is counterbalanced by retrograde transport, which not only maintains membrane homeostasis but also recycles various proteins that function in the sorting of secretory cargo, formation of transport intermediates, or retrieval of resident proteins of secretory organelles. The retromer complex recycles proteins from the endocytic pathway back to the plasma membrane or TGN and was recently identified as a critical player in regulated secretion in the hypothalamus. Furthermore, melanoma antigen protein L2 (MAGEL2) was discovered to act as a tissue-specific regulator of the retromer-dependent endosomal protein recycling pathway and, by doing so, ensures proper secretory granule formation and maturation. MAGEL2 is a mammalian-specific and maternally imprinted gene implicated in Prader-Willi and Schaaf-Yang neurodevelopmental syndromes. In this review, we will briefly discuss the current understanding of the regulated secretion pathway, encompassing anterograde and retrograde traffic. Although our understanding of the retrograde trafficking and sorting in regulated secretion is not yet complete, we will review recent insights into the molecular role of MAGEL2 in hypothalamic neuroendocrine secretion and how its dysregulation contributes to the symptoms of Prader-Willi and Schaaf-Yang patients. Given that the activation of many secreted proteins occurs after they enter secretory granules, modulation of the sorting efficiency in a tissue-specific manner may represent an evolutionary adaptation to environmental cues.

Abbreviations: SG, secretory granule; ISG, immature secretory granule; SeV, secretory vesicle; SV, synaptic vesicle; PC, proprotein convertase; CPE, carboxypeptidase E; M6P, mannose-6-phosphate; MPR, mannose-6-phosphate receptor; RSPs, regulated secretory proteins; AP-1, adaptor protein 1; GGA, Golgi-localized, γ-ear containing, ARF-binding; CKII, casein kinase II; PWS, Prader-Willi syndrome; SYS, Schaaf-Yang syndrome.

KEYWORDS

secretory granule, MAGEL2, anterograde and retrograde protein sorting, retromer, neuroendocrine cells, WASH complex, Prader-Willi and Schaaf-Yang syndromes, hormones and neuropeptides

1 Introduction

Constitutive secretion or exocytosis occurs in all cell types and predominantly facilitates housekeeping functions, including protein insertion into the plasma membrane or secretion of extracellular matrix components, growth hormones, and plasma proteins. In contrast, regulated secretion facilitates the specialized function of excitable cells (i.e., neurons and endocrine and neuroendocrine cells) which is to synthesize, store, and secrete on-demand hormones, neuropeptides, and neurotransmitters. The fundamental pathway and the basic machinery for regulated and constitutive secretion are similar, but their regulation and sorting mechanisms differ (Palade, 1975; Gerber and Sudhof, 2002). Through a series of membrane-trafficking steps, secretory proteins are synthesized in the endoplasmic reticulum (ER) and transported in membrane vesicles via the Golgi network to the plasma membrane (Palade, 1975). Unlike the continuous release of secretory molecules in the constitutive pathway, neuropeptides and hormones in the regulated secretion pathway are accumulated and stored in secretory vesicles, referred to as secretory granules (SGs), until cells receive a signal for their release through fusion with the plasma membrane (Figure 1) (Kelly, 1985). Some secreted small molecules, like neurotransmitters, are synthesized in the cytosol and taken up into synaptic vesicles (SVs) just before exocytosis (Liu and Edwards, 1997; Kogel and Gerdes, 2010). While some neurons contain only SVs or SGs, hypothalamic neurons can contain both at the same time (Thureson-Klein, 1983; Burgoyne and Morgan, 2003). Since the nomenclature and abbreviation of vesicles in constitutive and regulated secretion are sometimes confusing, we will use the terms secretory vesicles (SeVs) for organelles in the constitutive secretion pathway and secretory granules and synaptic vesicles for those in the regulated secretion pathway.

Although the two principal pathways of regulated secretion share many components, they differ in the size of the vesicles [i.e., SGs are bigger (>100 nm in radius) than SVs (<25 nm)], mechanisms by which secretory vesicles are filled with secretory

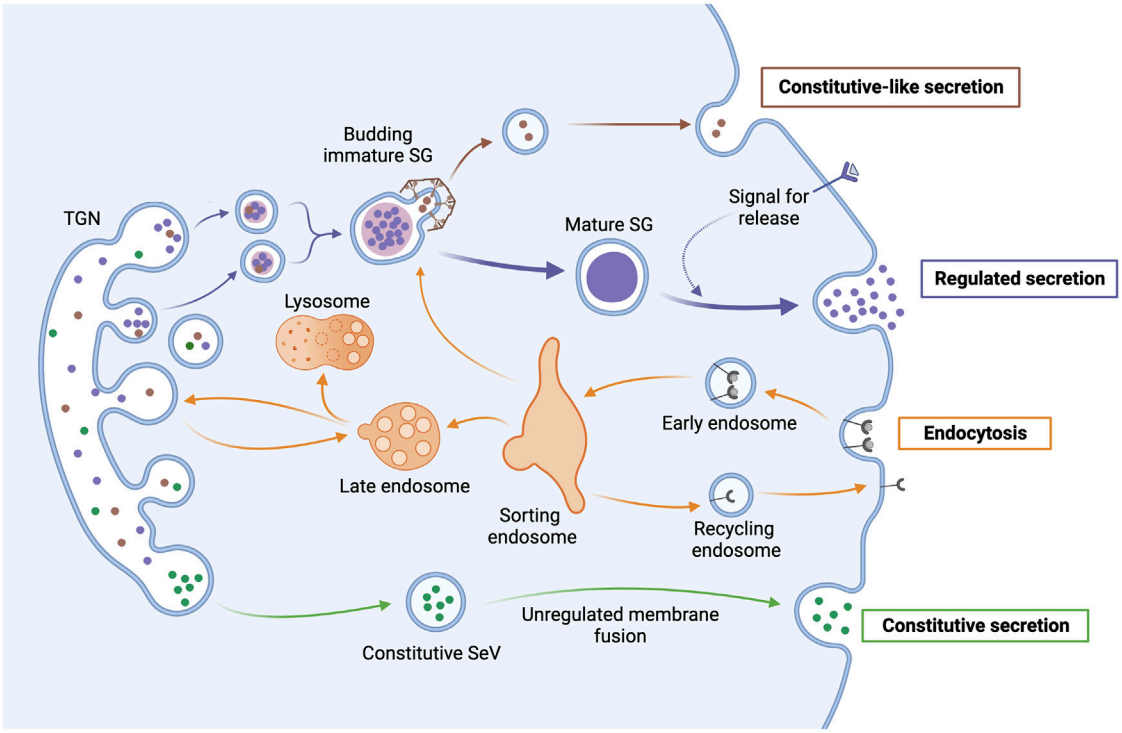

FIGURE 1
Anterograde and retrograde transport pathways in secretory cells. After protein synthesis in the ER, secretory proteins are sorted in the TGN through import signals, post-translational modifications, and other oligomeric associations. In the regulated secretion pathway, SGs go through a maturation process that includes fusion with other immature SGs and condensation of cargo proteins, as well as the removal of excess membrane and missorted cargo through the budding of clathrin-coated constitutive-like vesicles that may be secreted. Mature SGs accumulate near the plasma membrane until receiving a signal to undergo exocytosis and release their contents. In contrast, secretory vesicles (SeVs) in the constitutive secretion pathway continuously release their contents through unregulated membrane fusion. In retrograde transport, endocytosed material (e.g., receptors) are brought to a sorting endosome that directs endosomal material either back to the membrane in a recycling endosome, to immature SGs, to the lysosome for degradation, or to the TGN.

molecules, and how the vesicles recycle after exocytosis for a new round of secretion (Gerber and Sudhof, 2002). In Figure 1, we schematically depict the major pathways of anterograde and retrograde trafficking and use only SGs to represent regulated secretion as SVs are beyond the scope of this review. We will focus on the regulation and sorting of cargo and resident proteins of SGs and discuss the sorting mechanisms that direct cargo and resident proteins in the anterograde transport to SGs. Furthermore, we will discuss new insights into the regulation of retrograde trafficking and how it contributes to secretion in the hypothalamus. Recently, ubiquitination-mediated regulation of retromer and F-actin nucleation was found to be critical for the recycling of resident SG proteins and the neuroendocrine function of the hypothalamus. Ubiquitination is governed by Prader-Willi associated protein MAGEL2 in conjunction with E3 ubiquitin ligase TRIM27 and deubiquitinating enzyme USP7 (Hao et al., 2013; Hao et al., 2015; Chen et al., 2020).

2 Brief overview of the biogenesis, maturation, and anterograde transport of secretory granules

Regulated secretion of hormones and neuropeptides is a multistep, tightly regulated process, involving protein synthesis in the ER, protein sorting and packing into SGs at the *trans*-Golgi network (TGN), SG maturation during vesicle transport from the TGN to the plasma membrane, SG storage and accumulation near the plasma membrane, and ultimately, exocytosis to release SG cargo in response to a physiological stimulus (Figure 1). For more details on these steps beyond our summary below, please refer to the following: (Tooze, 1998; Chieregatti and Meldolesi, 2005; Kim et al., 2006; Wickner and Schekman, 2008; Kogel and Gerdes, 2010; Tanguy et al., 2016; Ma et al., 2021).

In a process similar to viral budding, nascent SGs start forming from the TGN by protein accumulation that leads to GTP-dependent membrane deformation (Tooze, 1998). Cholesterol facilitates membrane bending and SG scission by promoting negative membrane curvature and recruiting proteins, like the ubiquitously expressed mechano-GTPase dynamin-2 (Wang et al., 2000; Kim et al., 2006; Gonzalez-Jamett et al., 2013; Bhave et al., 2020). After leaving the TGN, the nascent or immature SGs (ISGs) undergo maturation while transported in a microtubule-dependent manner toward the plasma membrane and the F-actin-rich cell periphery (Figure 1) (Howell and Tyhurst, 1982; Rudolf et al., 2001; Ponnambalam and Baldwin, 2003).

During granule maturation, the content and membrane composition of granules undergo remodeling (Figure 2). Homotypic fusion of ISGs, which contributes to the increased size and density of mature granules, is mediated by several proteins, including NSF, α-SNAP, syntaxin 6, and synaptotagmin IV (Tooze et al., 1991; Urbe et al., 1998; Wendler et al., 2001; Ahras et al., 2006; Kogel and Gerdes, 2010). During maturation, the lumen of ISGs progressively acidifies through the activity of vacuolar-type H^+-ATPases (V-ATPases), which are integral membrane proteins in SGs (Figure 2) (Urbe et al., 1997; Jefferies et al., 2008). Besides enabling further condensation of soluble cargo, protein aggregation, and dense core formation, the acidic intragranular pH also activates PC1/3 and PC2 (Kogel and Gerdes, 2010). These proprotein convertases (PCs) and carboxypeptidase E (CPE) process most prohormones and neuropeptides into their mature, bioactive forms (Steiner, 1998). The maturation of ISGs also involves the removal of excess membranes and other proteins, including sortilin, carboxypeptidase D (CPD), syntaxin 6, VAMP-4, synaptotagmin IV, furin, and mannose-6-phosphate receptors (MPRs), which can be recycled back to the TGN by retrograde transport (Figures 1, 2, 4) (Klumperman et al., 1998; Varlamov et al., 1999; Eaton et al., 2000; Wendler et al., 2001; Ahras et al., 2006; Mitok et al., 2022). Mechanistically, ISGs contain coat protein patches of clathrin and AP-1 adaptor complex that mediate the budding of these proteins from ISGs into constitutive-like vesicles (Dittie et al., 1996; Dittie et al., 1997; Klumperman et al., 1998; Tooze, 1998; Eaton et al., 2000; Kakhlon et al., 2006). Overall, the process of maturation refines the composition of SGs and imparts responsiveness for regulated exocytosis (Burgoyne and Morgan, 2003; Kogel and Gerdes, 2010).

Mature SGs are stored near the membrane in the F-actin-rich cell cortex until receiving a stimulus for exocytosis. In contrast to constitutive secretion, exocytosis fusion is confined to specific sites within the plasma membrane of the polarized secreting cell and is temporally regulated by an extracellular secretion signal that increases the intracellular concentration of Ca^{2+} or cAMP (Meldolesi, 2002; Burgoyne and Morgan, 2003; Tanguy et al., 2016). Then, mature SGs undergo a series of ATP-dependent processes, such as priming, tethering, docking, and fusion to release their contents (Burgoyne and Morgan, 2003; Tanguy et al., 2016). These processes are mediated by several evolutionarily conserved proteins, including soluble N-ethylmaleimide-sensitive factor attachment protein receptors (SNAREs), NSF with adaptor proteins, Rab GTPases, SM (sec1/munc18-like) proteins, and synaptotagmins (Gerber and Sudhof, 2002; Burgoyne and Morgan, 2003; Wickner and Schekman, 2008). SNARE proteins enable the fusion of SGs with the plasma membrane through the formation of the SNARE complex, where v-SNARE (VAMP) on the SG membrane interacts with t-SNAREs (syntaxin 1 and SNAP-25) on the plasma membrane (Gerber and Sudhof, 2002; Burgoyne and Morgan, 2003). Synaptotagmins are calcium-binding proteins that act as calcium sensors and interact with both the granule and plasma membranes to trigger fusion and exocytosis (Sudhof, 2002).

Secretion is followed by rapid retrieval of the SG membrane and resident proteins through multiple endocytic pathways whose regulation is less understood but recently attracted our attention by the serendipitous discovery of the role of MAGEL2 in retromer-dependent retrograde transport (Chen et al., 2020). In the next section, we will describe the composition of SGs with a focus on the SG-unique resident proteins (i.e., granins, PCs, and CPE). Then, we will describe the current understanding of their sorting into the regulated secretion pathway at the TGN (i.e., anterograde transport) and their retrieval and sorting at the endosome (i.e., retrograde transport).

3 Secretory granule composition with a focus on SG-resident proteins

SGs are distinct organelles of endocrine and neuroendocrine cells with a lipid bilayer that encases a dense proteinaceous core to efficiently store hormones and neuropeptides in an osmotically inert

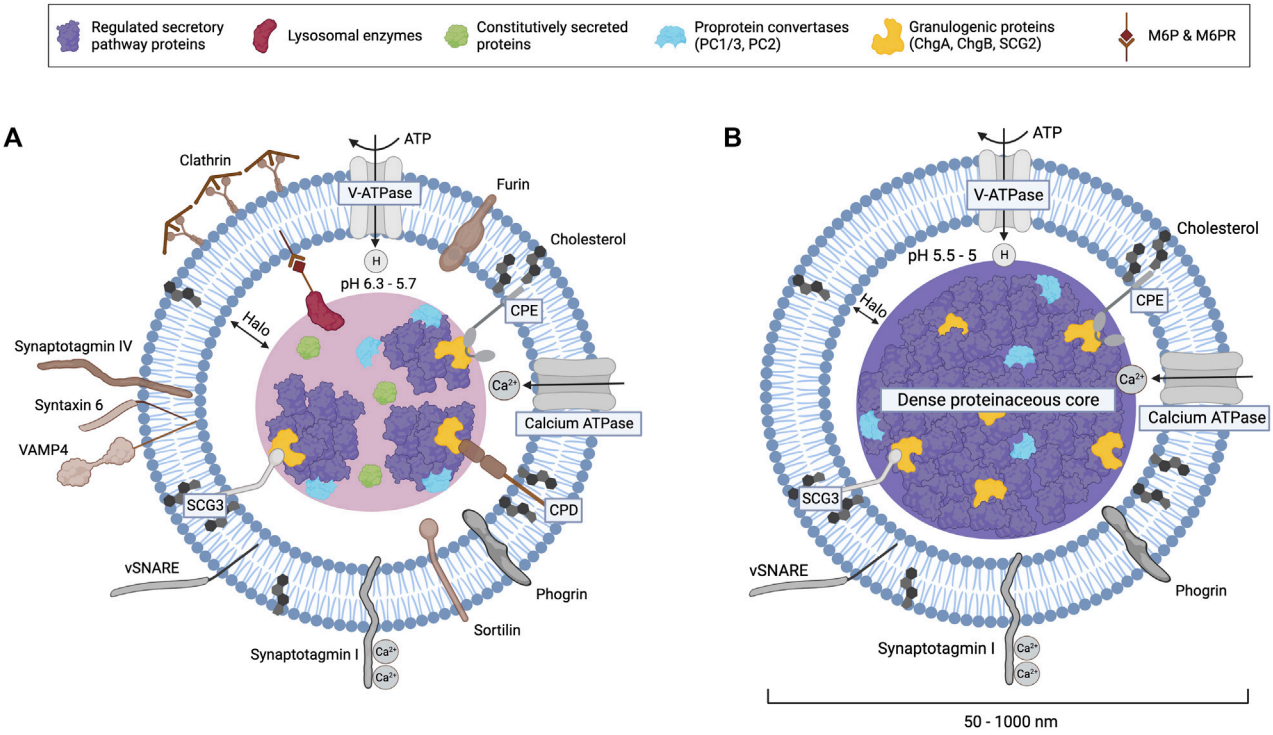

FIGURE 2
Components of immature **(A)** and mature **(B)** secretory granules. Lipid-raft-associated proteins like CPE, CPD, and secretogranin III interact with aggregates of regulated secretory pathway proteins and granulogenic proteins (e.g., granins like ChgA and ChgB) that form the dense proteinaceous core of mature SGs. Proton pumps increasingly acidify the SG lumen during maturation, which activates proprotein convertases and carboxypeptidases that process prohormones. The budding of clathrin-coated constitutive-like vesicles from immature SGs removes missorted constitutively secreted proteins and many other proteins shown in brown, including the peptidase furin, M6P-lysosomal enzymes bound to mannose-6-phosphate receptors (CI-M6PR or CD-M6PR), sortilin, synaptotagmin IV, VAMP4, and syntaxin 6. Calcium binding to synaptotagmin 1 stimulates exocytosis, which is mediated by v-SNARE proteins and other complexes. Mature SG size ranges from 50 nm in the sympathetic nervous system to 1,000 nm in pituitary mammotrophs or neurohypophyseal cells.

environment (Figure 2) (Burgess and Kelly, 1987). Compared to other biological membranes, SGs have a low protein-to-lipid ratio. Membrane proteins in SGs include transporters [e.g., V-ATPase, monoamine transporter, and peptidylglycine α-amidating monooxygenase enzyme (PAM)] and proteins that facilitate SG transport and exocytosis (e.g., VAMP and synaptotagmins) (Figure 2) (Thiele and Huttner, 1998b). The composition and size of SGs vary depending on cell type and maturation state (Hammel et al., 2010; Shitara et al., 2020). SGs contain several resident proteins, including PCs, CPE, and granins, that are required for the proper sorting of cargo proteins into ISGs at the TGN and the anterograde transport of SGs.

In neurons, SGs coexist with SVs that are filled locally with neurotransmitters, such as biogenic amines, at the presynaptic terminals and regenerated after exocytosis through the refilling of their cargo. However, the vesicles themselves are generated at the TGN (Burgoyne and Morgan, 2003). Though many proteins involved in regulated secretion are shared between vesicles and granules, some proteins are specific to SVs or SGs and facilitate their distinct functions of neurotransmitter or neuropeptide/hormone secretion, respectively (Gerber and Sudhof, 2002). SG-specific components are mainly enzymes and proteins that enable neuropeptide maturation and condensation during maturation for long-term storage. Importantly, protein recycling of many of these SG-resident proteins and granule membrane components is necessary for regulated secretion in the hypothalamus (Hurtley, 1993; Bittner et al., 2013; Chen et al., 2020).

3.1 Proprotein convertases (PCs)

Neuropeptide precursors packaged into SGs are cleaved into active peptides and hormones by SG-resident PCs. The PC family contains nine members: PC1/3, PC2, furin, PC4, PC5/6, PACE4, PC7, SKI-1/S1P, and PCSK9 (Seidah et al., 2013). PC1/3 and PC2 (proprotein convertase subtilisin/kexin type 1/3 and 2) are encoded by *PCSK1* and *PCSK2* genes and act as basic proprotein convertases that cleave after polybasic clusters (Seidah et al., 1991; Cendron et al., 2023). PC1/3 and PC2 are selectively expressed in endocrine and neuroendocrine cells, suggesting they are important in prohormone processing within SGs (Figure 3) (Halban and Irminger, 1994; Zhou et al., 1999). PC1/3 and PC2 process a plethora of prohormones, including pro-opiomelanocortin (POMC), neuropeptide Y (NPY), agouti-related peptide (AGRP), progrowth-hormone releasing hormone (GHRH), prothyrotropin-releasing hormone (TRH), proinsulin, and proglucagon (Paquet et al., 1996; Nillni, 2010;

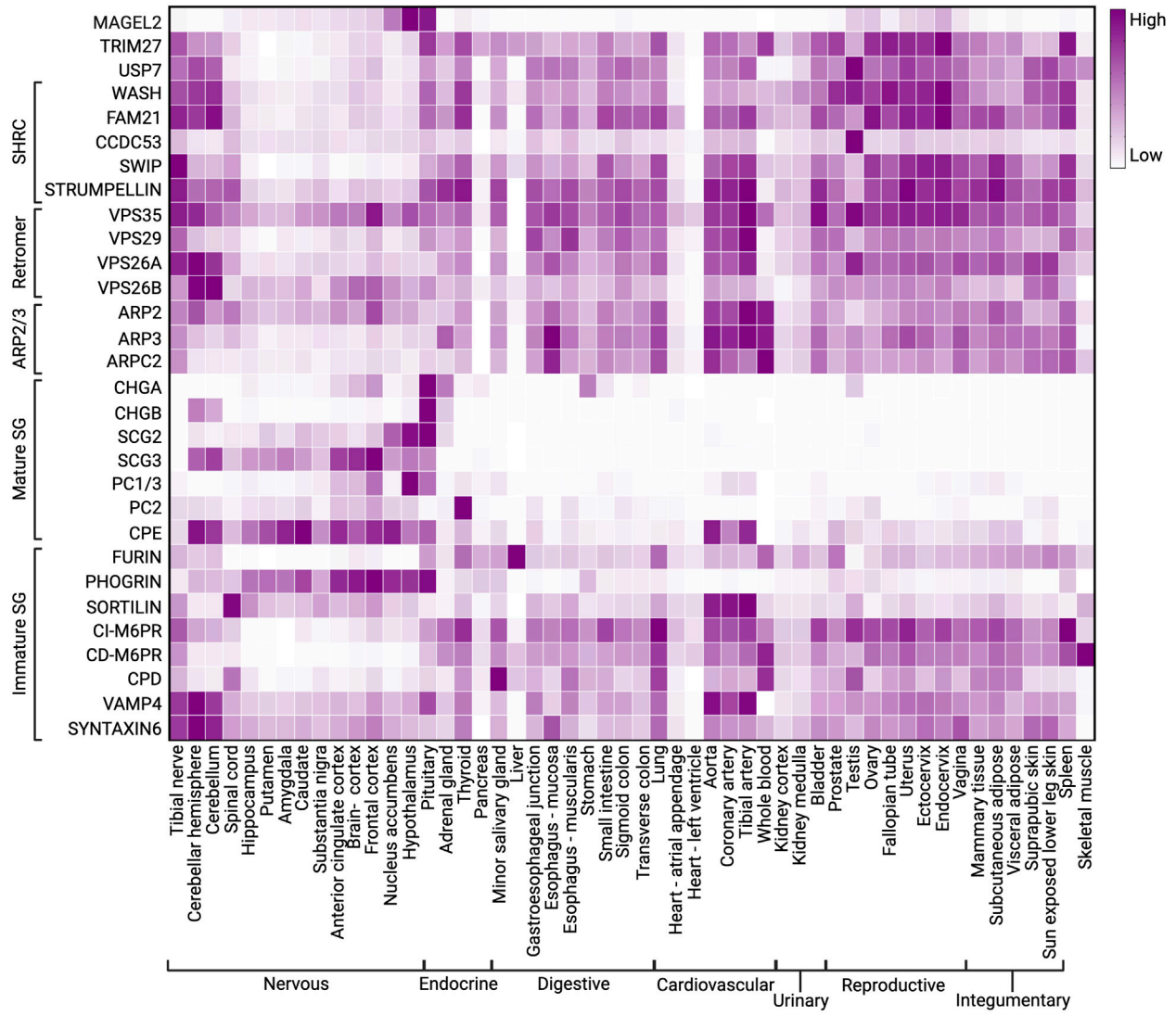

FIGURE 3
Heatmap showing expression of constitutive components of SGs, retromer, MUST, WASH, and ARP2/3 complexes. Data was extracted from GTEx on 05/24/2023.

Seidah, 2011; Cawley et al., 2016). Consequently, defects in PC1/3 or PC2 activity result in several endocrinopathies in both humans and rodents (Furuta et al., 1997; Jackson et al., 1997; Steiner, 1998; Zhu et al., 2002; Scamuffa et al., 2006; Mbikay et al., 2007; Anini et al., 2010; Creemers et al., 2012; Seidah and Prat, 2012).

3.2 Carboxypeptidase E (CPE)

After endoproteolytic cleavage by PC1/3 and/or PC2, the newly exposed C-terminal basic residues of prohormones are removed by CPE, another resident protein of SGs (Burgoyne and Morgan, 2003). CPE was first identified as enkephalin convertase and subsequently found to cleave the C-terminally extended basic residues from diverse peptide intermediates, including POMC and probrain-derived neurotrophic factor (BDNF) (Fricker and Snyder, 1982; Hook et al., 1982; Fricker, 1988; Lou et al., 2005). CPE is expressed primarily in endocrine tissues and specific areas of the central nervous system (Figure 3) (Fricker, 1988; Cawley et al., 2012; Ji et al., 2017). CPE differs from other carboxypeptidases in that its optimal pH is in the acidic range, consistent with its localization to acidic compartments of the TGN and to the dense core of SGs where prohormone processing occurs (Supattapone et al., 1984; Ji et al., 2017).

Like other proteins in the regulated secretory pathway, CPE is synthesized in the ER as a 476-amino acid precursor containing an N-terminal signal peptide that directs proCPE into the ER before its removal (Song and Fricker, 1995a). ProCPE is transported through the Golgi to SGs where the 17-amino acid "pro" region is cleaved after a penta-arginine sequence to generate mature membrane-bound CPE that is glycosylated at two N-linked glycosylation consensus sites, Asn139 and Asn390 (Song and Fricker, 1995a; Cawley et al., 2012; Ji et al., 2017). Within SGs, the membrane-

bound CPE can be further processed by cleavage of its C-terminal cytoplasmic tail to generate a soluble form of CPE that is enzymatically more active (Hook, 1985; Fricker and Devi, 1993).

In addition to its enzymatic function, CPE acts as the quintessential regulated secretory pathway sorting receptor for many prohormones (e.g., POMC, pro-BDNF, proenkephalin, proinsulin, and prophogrin). Under mildly acidic conditions and increasing calcium concentrations, CPE aggregates and binds SG cargo proteins through their prohormone sorting signals, such as those found in POMC (Song and Fricker, 1995b; Rindler, 1998; Zhang et al., 1999). CPE binding enables protein condensation and directs cargo proteins to SGs (Cawley et al., 2012). The C-terminus of CPE forms an amphipathic α-helix under acidic conditions that binds to lipid rafts in the TGN membrane and directs prohormones bound to CPE into nascent granules (Fricker et al., 1990; Dhanvantari and Loh, 2000; Dhanvantari et al., 2002; Zhang et al., 2003; Cawley et al., 2012). In a neutral environment (pH 7.2), CPE's C-terminus does not exhibit a helical secondary structure, preventing premature association with the membrane (Dhanvantari et al., 2002). Interestingly, CPE may only sort certain prohormones to the regulated secretory pathway, as CPE depletion did not affect sorting of chromogranin A (CHGA) (Cool et al., 1997; Normant and Loh, 1998; Ji et al., 2017).

3.3 The granin family

Chromogranins A and B (CHGB), secretogranins II and III (SCGII and SCGIII), and a few additional related proteins together comprise the granin family of water-soluble acidic glycoproteins (Bartolomucci et al., 2011). These granin proteins serve essential roles in the regulated secretory pathway, with the chromogranins comprising much of the SG matrix (O'Connor and Frigon, 1984; Borges et al., 2010), and, accordingly, are predominantly expressed in endocrine and neuroendocrine cells (Figure 3) (Day and Gorr, 2003; Dominguez et al., 2018). Like CPE and other SG resident proteins, granins are also synthesized at the rough ER, inserted into the ER cisternae via a signal peptide located at their N termini, and trafficked to the TGN via transport vesicles (Bartolomucci et al., 2011). Several biochemical properties that are critical for the function of granins include an acidic isoelectric point, Ca^{2+} binding, and thermostability (Yoo and Albanesi, 1991; Taupenot et al., 2003; Bartolomucci et al., 2011). Additionally, granins aggregate in an acidic environment (pH 5.5) with a millimolar concentration of calcium ions and, by doing so, induce granule formation (Chanat and Huttner, 1991; Parmer et al., 1993; Koshimizu et al., 2010). Granins are negatively charged, which may prevent premature aggregation, but a surplus of calcium ions and protons in the SG lumen may help neutralize the repulsive forces among the granin proteins to allow aggregation (Glombik and Gerdes, 2000). An alternative explanation proposed is that the pH gradient prompts interactions between negative and positive charges of cargo proteins, and then divalent ions may generate a chelate bridge between two negatively charged granins to permit aggregation (Ma et al., 2008; Zhang et al., 2010).

CHGA, the most well-studied granin family member, is a prohormone and a granulogenic factor in neuroendocrine tissues (Laguerre et al., 2020). While CHGA is mostly hydrophilic, its C- and N-termini contain hydrophobic and cell-specific evolutionarily conserved sequences necessary for sorting and granulogenesis (Yoo and Lewis, 1993; Cowley et al., 2000; Montero-Hadjadje et al., 2009; Elias et al., 2010). Cysteine residues within the amino terminus form an intramolecular disulfide loop to interact with the membrane (Parmer et al., 1993; Yoo, 1994; Kang and Yoo, 1997). The primary structure of CHGA contains several glutamic acid stretches that can interact with Ca^{2+}, leading to aggregation in specific environments, such as the TGN and SG (Parmer et al., 1993). CHGA may associate with membrane either directly by binding to specific lipids (e.g., phosphatidic acids enriched in TGN and SG membranes) (Carmon et al., 2020; Tanguy et al., 2020) or indirectly by interacting with SCGIII, which in turn binds to cholesterol-rich membranes and targets proteins to the regulated secretory pathway (Hosaka et al., 2004; Han et al., 2008).

Besides their granulogenic function, granins contribute to calcium homeostasis and many are also precursors of bioactive peptides that, upon further processing in ISGs, modulate different physiological processes, including pain pathways, inflammatory responses, metabolic and mood disorders, and blood pressure (Montero-Hadjadje et al., 2008). As an example, the CHGA-derived peptide pancreastatin, which was the first granin-derived peptide discovered, strongly inhibits glucose-induced insulin release (Tatemoto et al., 1986; Bartolomucci et al., 2011).

Even though the granin family is ubiquitously expressed in neuroendocrine tissues, individual proteins exhibit tissue specificity and redundancy (Figure 3). For example, the ablation of *Chga* and *Chgb* reduced the size and number of SGs in adrenal chromaffin cells, while SGs in mouse hippocampal neurons were unaffected (Dominguez et al., 2018). In addition, ablation of *Chga* upregulated the expression of Chgb and secretogranins II-VI in the adrenal medulla and other endocrine glands (Hendy et al., 2006). These data indicate that chromogranin-mediated dense core formation of SG is tissue-specific and that other granin family members may perform a similar function.

3.4 Mannose-6-phosphate receptors (MPRs)

MPRs facilitate the transport of soluble acid hydrolases from the TGN to the lysosome by binding to mannose-6-phosphate (M6P) modifications on the enzymes. There are two different MPRs, the larger cation-independent receptor (CI-MPR) and the smaller cation-dependent receptor (CD-MPR) that binds M6P more efficiently in the presence of divalent cations (Gary-Bobo et al., 2007). Besides binding to phosphomannosyl residues, the extracellular region of CI-MPR, also known as IGF2R, binds insulin-like growth factor (IGF)-II to facilitate its endocytosis and clearance by lysosomal degradation (Oka et al., 1985; Oshima et al., 1988; Schmidt et al., 1995; Brown et al., 2008). CI-M6PR also binds other ligands, such as retinoic acid, granzyme B, latent TGF-β, urokinase-type plasminogen activator receptor, and leukemia inhibitory factor, impacting a variety of biological pathways (Purchio et al., 1988; Kang et al., 1997; Blanchard et al., 1999; Godar et al., 1999; Veugelers et al., 2006).

CI-MPR is one of the most thoroughly studied proteins that is removed from ISGs and then recycled back to the TGN (Figures 1, 2, 4, 5) (Bonnemaison et al., 2013; Seaman, 2018). As SGs mature, the

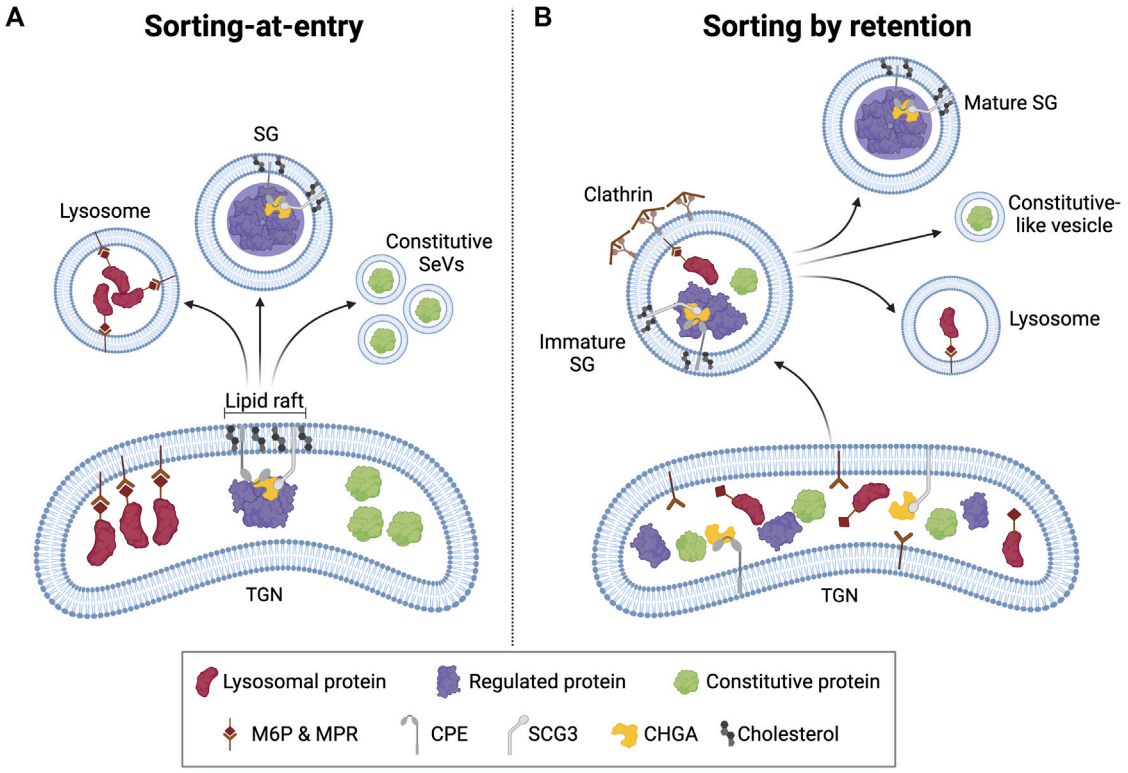

FIGURE 4
Proposed sorting models for secreted proteins. **(A)** In the "sorting for entry" model, secreted and lysosomal proteins are segregated by binding to specific receptors clustered in the TGN before granule formation. **(B)** In the "sorting by retention" model, secreted and lysosomal proteins enter nascent SGs, but the non-regulated secretory proteins are excluded from the maturing SG by budding, possibly mediated by clathrin.

concentration of MPRs declines by about 90% (Klumperman et al., 1998). MPRs are sorted from ISGs by binding to adaptor protein 1 (AP-1) and the Golgi-localized, γ-ear containing, ARF-binding (GGA) family of proteins in clathrin and syntaxin 6–positive vesicles that are delivered to endosomes (Figures 1, 2) (Klumperman et al., 1998; Coutinho et al., 2012). Then, the multiprotein retromer complex mediates the endosome-to-TGN retrieval of CI-MPR (Bonnemaison et al., 2013; Seaman, 2018). Retromer is critical for the recycling and reuse of MPRs in a new cycle of acid hydrolase transportation.

In the following sections, we discuss sorting into the regulated secretory pathway, as well as the retromer-dependent recycling of CI-MPR, potential retrograde trafficking targeting motifs, and finally, the tissue-specific role of MAGEL2 in the retromer-dependent recycling of mature and immature SG components.

4 Sorting compartments, mechanisms, and signals in the anterograde pathway of regulated secretion

Overall, the cellular life of regulated secretory proteins (RSPs) begins similarly to constitutive secretory proteins. An N-terminal signal sequence enables the signal recognition particle (SRP)-dependent co-translational translocation into the ER lumen. This signal sequence is then removed from the nascent protein, and the protein is post-translationally modified during anterograde transport through the Golgi to the TGN. The TGN serves as the main sorting station in the anterograde traffic of secretory proteins, and the sorting is fine-tuned during ISG maturation when the missorted proteins are removed by clathrin-coated vesicles (Figures 1, 2, 4) (Farquhar and Palade, 1998). The canonical targeting signals that direct proteins into the constitutive secretory pathway or to other cellular destinations (e.g., the plasma membrane, mitochondria, nucleus, and lysosomes), as well as the signals for ER or Golgi retention, are well established. In contrast, RSPs are not targeted to SGs by a common sorting motif but rather through intrinsic protein features and a variety of motifs that may synergize to increase granule-sorting efficiency (Glombik and Gerdes, 2000; Lacombe et al., 2005). As an example of multiple sorting signals being present on a single molecule, prothyrotropin-releasing hormone has two intermediates that are stored in different vesicles and secreted by different stimuli (Perello et al., 2008). Specific sorting signals that have been discovered on RSPs include linear amino acid sequences, conformation epitopes, polypeptides, and post-translational modifications (Thiele and Huttner, 1998b). The propensity of RSPs to aggregate contributes to their sequestration in the TGN, packaging into ISGs, and removal of mistargeted proteins from ISGs during maturation. Besides aggregation, association with distinct membrane lipids, sorting receptors, and adaptor proteins also facilitate the sorting of soluble RSPs to SGs (Thiele and Huttner, 1998b; Glombik and Gerdes, 2000; Kogel and Gerdes, 2010; Bonnemaison et al., 2013). These sorting signals and mechanisms can also be tissue- or cell-specific

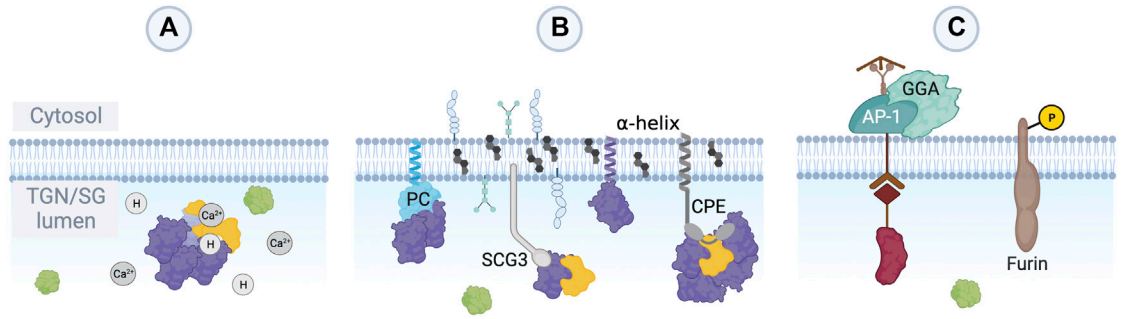

	Sorting mechanism	Sorting motifs/domains in RSPs	Sorting receptors, adaptors & effector proteins
Luminal side			
A	pH and cation-dependent aggregation	Soluble proteins Disulfide (CC) loops	Granins
B	Association with membrane lipids (directly or indirectly)	α-helices Di-basic processing sites Acidic motifs	SCG3 PCs CPE
Cytosolic side			
C	Interaction with sorting receptors and adaptor proteins	CPE binding motif AP-binding motif [YXXφ; (D/E)XXX(L/I)] GGA-binding motif (DXXLL	AP complexes ARFs GGAs
	Phosphorylation	Ser/Thr in acidic clusters	Casein kinase II (CK-II)

FIGURE 5
Sorting of proteins destined for the regulated secretory pathway occurs through various mechanisms, motifs, and adaptor proteins. **(A,B)** Within the lumen of the TGN and ISGs, sorting motifs within RSPs and interactions with other proteins facilitate aggregation and association with the membrane. **(C)** On the cytosolic side of the TGN/SG membrane, adaptor proteins recognize specific motifs in RSPs to help with sorting, and phosphorylation of some RSPs, like furin, enhances sorting.

(Chidgey, 1993; Marx et al., 1999; Cowley et al., 2000; Dikeakos and Reudelhuber, 2007).

4.1 Sorting models

For secreted proteins, there are two proposed sorting models that are not mutually exclusive, as supporting evidence suggests both models may occur in cells (Figure 4) (Dikeakos and Reudelhuber, 2007; Goronzy and Weyand, 2009). In the "sorting-at-entry" model, constitutively secreted proteins are segregated from regulated proteins by binding to specific receptors clustered in the TGN before granule formation (Figures 4, 5) (Chidgey, 1993). Initial aggregation of cargo proteins (e.g., granins and prohormones) in a mildly acidic pH (6.0–6.5) and cation-dependent manner excludes certain constitutive proteins. Then, the aggregates can bind to sorting receptors at the TGN membrane. One of the first sorting receptors proposed was CPE, which sorts POMC and proBDNF (Cool et al., 1997; Lou et al., 2005). SCGIII can also act as a sorting receptor, as SCGIII associates with cholesterol-sphingolipid-rich membrane microdomains (i.e., lipid rafts) in the TGN membrane and, by doing so, serves as a sorting receptor for CHGA in pituitary and pancreatic cells (Tooze, 1998; Hosaka et al., 2004; Park and Loh, 2008). Receptors are then recycled through vesicles budding off ISGs (Tooze, 1998).

In the "sorting by retention" model, both regulated and non-regulated proteins enter the nascent granule with the latter proteins excluded from the ISG by budding of clathrin-coated vesicles (Chidgey, 1993). In support of this model, lysosomal proteins have been found in immature SGs, which are then most likely excluded through binding to MPRs and budding of a constitutive-like vesicle. All evidence points to the conclusion that the best-fitting sorting model is reliant on the specific protein, its affinity for aggregation, the relative speed of its synthesis, and tissue or cell specificity (Tooze, 1998). As an example of cell specificity, the sorting domain in the C-terminus of PC2 is essential for sorting in Neuro2A cells (Assadi et al., 2004) but is not required in corticotrophic AtT-20 cells (Taylor et al., 1998; Lacombe et al., 2005). Similarly, the SG sorting of CHGA and CHGB requires an N-terminal domain in neuroendocrine PC12 cells but not in endocrine GH4C1 cells (Chanat et al., 1993); rather, a C-terminal region of CHGA was required for proper sorting in GH4C1 cells (Cowley et al., 2000). Different sorting domains on the same protein offer insights not only into targeting efficiency but also into the

possibility of targeting signal redundancy, which may offer protection from mutations and other damage.

4.2 Sorting mechanisms

Mechanistically, several processes contribute to sorting RSPs into the regulated secretory pathway. An intrinsic propensity to aggregate combined with Ca^{2+}-binding motifs underly one sorting mechanism–selective aggregation of a subset of soluble proteins in the TGN, excluding soluble non-aggregating proteins and giving rise to SGs (Figure 5). In this aggregation mechanism, only one or perhaps a small number of proteins need to interact with the membrane, as the other regulated proteins are targeted to the SG through protein-protein interactions mediated by helper proteins, like the granins. Accordingly, overexpression of CHGB led to more effective sorting into granules in cells (Natori and Huttner, 1996; Huh et al., 2003). Expression of granulogenic proteins (e.g., CHGA) in regulated secretory-deficient cells was sufficient to induce the formation of vesicles that resembled SGs (Kim et al., 2001; Huh et al., 2003; Beuret et al., 2004). However, aggregation alone is insufficient to target all RSPs to SGs (Quinn et al., 1991; Jutras et al., 2000), suggesting additional sorting mechanisms (Lacombe et al., 2005).

Association with lipid rafts is another sorting-at-entry mechanism used by several RSPs (Figure 5). Through insertion into lipid rafts, the transmembrane domains of several prohormone-processing enzymes, like PAM, mediate their own sorting into the regulated secretory pathway (Bell-Parikh et al., 2001). In addition, several sorting receptors in the TGN recruit and fasten SG-destined proteins to membrane sites where a nascent vesicle will bud (Park and Loh, 2008). For example, SCGIII, CPE, PC1/3, and PC2 have all been reported to associate with cholesterol- and sphingolipid-rich lipid rafts, which is crucial for their own targeting to the regulated secretory pathway (Dhanvantari and Loh, 2000; Jutras et al., 2000; Arnaoutova et al., 2003; Assadi et al., 2004; Hosaka et al., 2004; Dikeakos et al., 2009).

Besides interacting with sorting receptors, various cargo adaptors, such as adaptor protein (AP) complexes and monomeric GGA proteins, can help direct proteins into their appropriate transport carriers (Figure 5) (Robinson, 2004). The AP family includes five cytosolic heterotetrameric complexes, AP-1 to AP-5, that mediate sorting of transmembrane proteins on defined intracellular routes (Bonnemaison et al., 2013). AP-1, AP-3, and AP-4 are associated with the TGN, and AP-1 also removes material from ISGs (Bonnemaison et al., 2013; Guardia et al., 2018). AP-2 regulates clathrin-mediated endocytosis at the plasma membrane, and AP-5 facilitates the retrograde transport of proteins from endosomes to the TGN (Bonnemaison et al., 2013; Hirst et al., 2013; Guardia et al., 2018). The subunits of these AP complexes have several isoforms in mammals, suggesting evolutionary adaptation to finetune the process of regulated secretion, particularly in neurons that uniquely express two AP-3 subunits (Dell'Angelica et al., 1997; Boehm and Bonifacino, 2002; Bonifacino, 2014; Li et al., 2016; Guardia et al., 2018). GGA proteins act as monomeric clathrin adaptors (Bonifacino, 2004). Arf small G proteins in an active GTP-bound, membrane-associated state mediate the membrane recruitment of AP complexes and GGAs (Traub et al., 1993; Austin et al., 2000; Collins et al., 2003; Ren et al., 2013). Then, AP complexes can bind to the cytoplasmic tails of cargo proteins and recruit coat proteins (i.e., clathrin) and accessory proteins to drive vesicle formation (Bonnemaison et al., 2013; Tan and Gleeson, 2019). Upon the release of secretory vesicles from the TGN membrane, coat proteins are dissociated and recycled for additional rounds of vesicle formation (Tan and Gleeson, 2019).

4.3 Sorting domains and motifs

The motifs and domains on RSPs that are responsible for their proper sorting into SGs remain enigmatic and not uniform. In general, sorting signals facilitate the aggregation of cargo proteins or piggyback anchoring through association with membrane domains and other proteins (Figure 5).

Within the TGN lumen, proteins targeted to SGs tend to aggregate, not only promoting formation of the dense core of the SGs but also enabling their own sorting to the regulated secretion pathway (Figure 5) (Burgess and Kelly, 1987). Several motifs and domains within RSPs promote aggregation and sorting to SGs. In the case of CHGA, several glutamic acid repeats interact with Ca^{2+} and promote aggregation at the TGN and in SGs (Parmer et al., 1993). Small disulfide (CC) loops also act as SG sorting signals by promoting self-aggregation at the TGN (Reck et al., 2022). These CC loops are present frequently at the very N- or C-terminus of proteins or close to processing sites and thus potentially exposed (Reck et al., 2022). For example, in POMC, an N-terminal 13-residue CC loop is necessary and sufficient for granule sorting (Tam et al., 1993; Cool et al., 1995; Loh et al., 2002). Longer disulfide loops in CHGA and CHGB are also involved in their sorting to SGs (Kang and Yoo, 1997; Kromer et al., 1998; Glombik et al., 1999; Taupenot et al., 2002). In addition, di-basic processing sites and acidic motifs in prohormones were shown to promote granule sorting, likely via interaction with PCs or CPE (Brechler et al., 1996; Lou et al., 2005). The sorting signal motif for CPE recognition was first identified as two acidic residues and two aliphatic hydrophobic residues in POMC (Cool et al., 1995), and similar sorting motifs were subsequently found in proinsulin (Dhanvantari et al., 2003), BDNF (Lou et al., 2005), and proenkephalin (Normant and Loh, 1998; Cawley et al., 2016).

Amphipathic helices enable interaction with the granule membrane and are important for the incorporation of RSPs and enzymes, like PCs and CPE, into SGs. Besides a disulfide-bonded hydrophobic loop that interacts with SG membrane (Kang and Yoo, 1997), the N-terminal region of CHGA also contains an amphipathic α-helix that may be necessary for sorting CHGA/hormone aggregates into SGs (Thiele and Huttner, 1998a; Taupenot et al., 2002; Laguerre et al., 2020). Similarly, proglucagon is sorted by α-helices present in the mature hormone domains rather than in the typical prohormone domain (McGirr et al., 2013; Guizzetti et al., 2014). Tissue-specific processing of proglucagon by PCs yields glucagon in pancreatic α cells (Furuta et al., 2001) or glucagon-like peptide 1 (GLP-1) and GLP-2 in intestinal L cells and hypothalamic neurons (Dhanvantari et al., 1996; Damholt et al., 1999; Holt et al., 2019). Although each of these products contains α-helices, only the non-amphipathic, dipolar α-helices on glucagon and GLP-1 efficiently target them to the regulated secretory pathway (Guizzetti et al., 2014). In contrast, GLP-2 has a more uniform negative charge distribution

along the length of its α-helix (Guizzetti et al., 2014). PC1/3, PC2, and PC5/6A also contain α-helices in their C-termini that form electrostatic interactions and help sort proteins into the regulated secretion pathway (Assadi et al., 2004; Dikeakos et al., 2007b; Dikeakos et al., 2009). There seems to be no correlation between the helix length or the isoelectric point and sorting efficiency, but helices with a positive or negative charge and a hydrophobic segment seem the most effective in sorting (Dikeakos et al., 2007a), suggesting electrostatic interactions also play a role in aggregation, either inter- or intra-molecularly (Zhang et al., 2010). Indeed, Ma et al. (2008) identified four to five residues, two of which are charged, as the elementary sorting unit for protachykinin targeting to SGs. Clustering of these charged elementary units improved aggregation, leading to an additive and graduated effect that also improved sorting (Ma et al., 2008). In summary, charged amphipathic helices or non-amphipathic helices that have segregated charges and a hydrophobic patch are sufficient for targeting to secretory granules (Dikeakos et al., 2007a).

On the cytosolic side, specific motifs in the cytoplasmic domains of SG membrane proteins enable binding to adaptor proteins (Figure 5). The acidic-cluster-dileucine motif (DXXLL, where X is any amino acid) found in MPRs and sortilin, for example, is recognized by GGA proteins (Johnson and Kornfeld, 1992a; b; Chen et al., 1997; Nielsen et al., 2001; Puertollano et al., 2001). Serine and threonine residues embedded within cytosolic acidic clusters serve as substrates for casein kinase II (CKII) phosphorylation that enhances the sorting of proteins, like PAM, CI-MPR, and furin (Meresse et al., 1990; Jones et al., 1995; Chen et al., 1997; Steveson et al., 2001). In addition, VAMP4, phogrin, MPRs, and lysosomal proteins contain tyrosine-based (YXXΦ, where Φ is a bulky hydrophobic residue) and dileucine [(D/E)XXXL(L/I)] sorting motifs that are recognized by AP complexes (Glickman et al., 1989; Honing et al., 1997; Peden et al., 2001; Ghosh and Kornfeld, 2004; Torii et al., 2005; Wasmeier et al., 2005; Braulke and Bonifacino, 2009). These interactions between sorting motifs and adaptor proteins directs MPRs and their cargo proteins into TGN-derived, clathrin-coated vesicles that fuse with endosomes (Doray et al., 2002; Waguri et al., 2003; Braulke and Bonifacino, 2009).

In summary, several years of research uncovered how cells control the secretion of proteins and proposed two major models, sorting-at-entry and sorting by retention, to describe how proteins are sorted into the proper pathway at the TGN. Both models incorporate several sorting mechanisms that promote protein aggregation and binding to unique membrane lipids, leading to SG formation. After budding from the TGN, both constitutive and regulated secretory vesicles are transported to secretion sites at the plasma membrane via microtubule-based transport systems (Park and Loh, 2008).

4.4 Cytoskeletal filaments in the sorting and trafficking of regulated proteins

Kinesin, dynein, and myosin are molecular motors that transport SeVs and SGs along microtubule or actin tracks. In general, SeVs and SGs use the same type of microtubule motor, such as kinesin, for anterograde transport to the secretion sites, and cytoplasmic dynein for retrograde transport back to the cell body (van den Berg and Hoogenraad, 2012). Tight regulation of the transport machinery is critically important to ensure that proteins are picked up and delivered to the right place at the right time. At the end of microtubule-based transport, SGs are transferred to the actin cortex close to the plasma membrane with the help of myosin V and the F-actin motor proteins (Rose et al., 2003; Rudolf et al., 2003). Actin and myosin have established themselves as key players in regulated secretion by providing tracks to target SGs to fusion sites, actively squeezing cargoes from fused vesicles, and following fusion, retrieving excess membrane to maintain cell surface area and recycle several SG-resident proteins (Rudolf et al., 2003; Rojo Pulido et al., 2011; Li et al., 2018; Miklavc and Frick, 2020). Besides its role as the transport platform for myosin motors, F-actin acts as a physical barrier for SG exocytosis and is also involved in the regulation of sorting at the TGN (Park and Loh, 2008; Gutierrez and Villanueva, 2018). During SG biogenesis, F-actin is recruited to the budding granule by actin-related protein-2/3 (ARP2/3) and myosin 1b (Delestre-Delacour et al., 2017). ARP2/3 complex binds to actin and exerts an active role in SG formation through its nucleation and branching activities that provide a structural or force-generating scaffold (Goley and Welch, 2006). The nucleation core activity of ARP2/3 is activated by nucleation promoting factors, such as members of the Wiskott-Aldrich syndrome family (WASP, N-WASP, WAVE, and WASH proteins) (Welch and Mullins, 2002; Alekhina et al., 2017).

The fine-tuned control of actin polymerization on endosomes is fundamental for the retrieval and recycling of several cargoes (Puthenveedu et al., 2010; Simonetti and Cullen, 2019). Retrieval and recycling are orchestrated by several multi-protein complexes, including retromer, commander/CCC/retriever, sorting nexins, and the ARP2/3-activating WASH complex (Simonetti and Cullen, 2019; MacDonald et al., 2020; Placidi and Campa, 2021). Recently, MAGEL2 regulation of the WASH complex and ARP2/3 activation was shown to prevent lysosomal degradation of SG-resident proteins and enable the proper neuroendocrine function of the hypothalamus, suggesting a tissue-specific regulation of compensatory endocytosis in regulated secretion (Figure 6) (Chen et al., 2020). In the next paragraphs, we will briefly summarize retromer-dependent retrograde recycling and its regulation.

5 Endocytic recycling of proteins in the regulated secretory pathway

In the secretory pathway, the anterograde trafficking of membranes is compensated by the retrograde transport of lipids and proteins to maintain membrane homeostasis and recycle various proteins and lipids. Endocytic recycling contributes to membrane receptor abundance, cell resensitization, and downstream signaling (Sannerud et al., 2003; Lucas and Hierro, 2017). Protein recycling is also important in the regulated secretion of hormones and neuropeptides (Ferraro et al., 2005; Chen et al., 2020; Neuman et al., 2021).

Endocytosis, occurring through clathrin-dependent and -independent mechanisms, internalizes lipids and proteins from the plasma membrane into early/sorting endosomes (Cullen and Steinberg, 2018; MacDonald et al., 2020). From the sorting

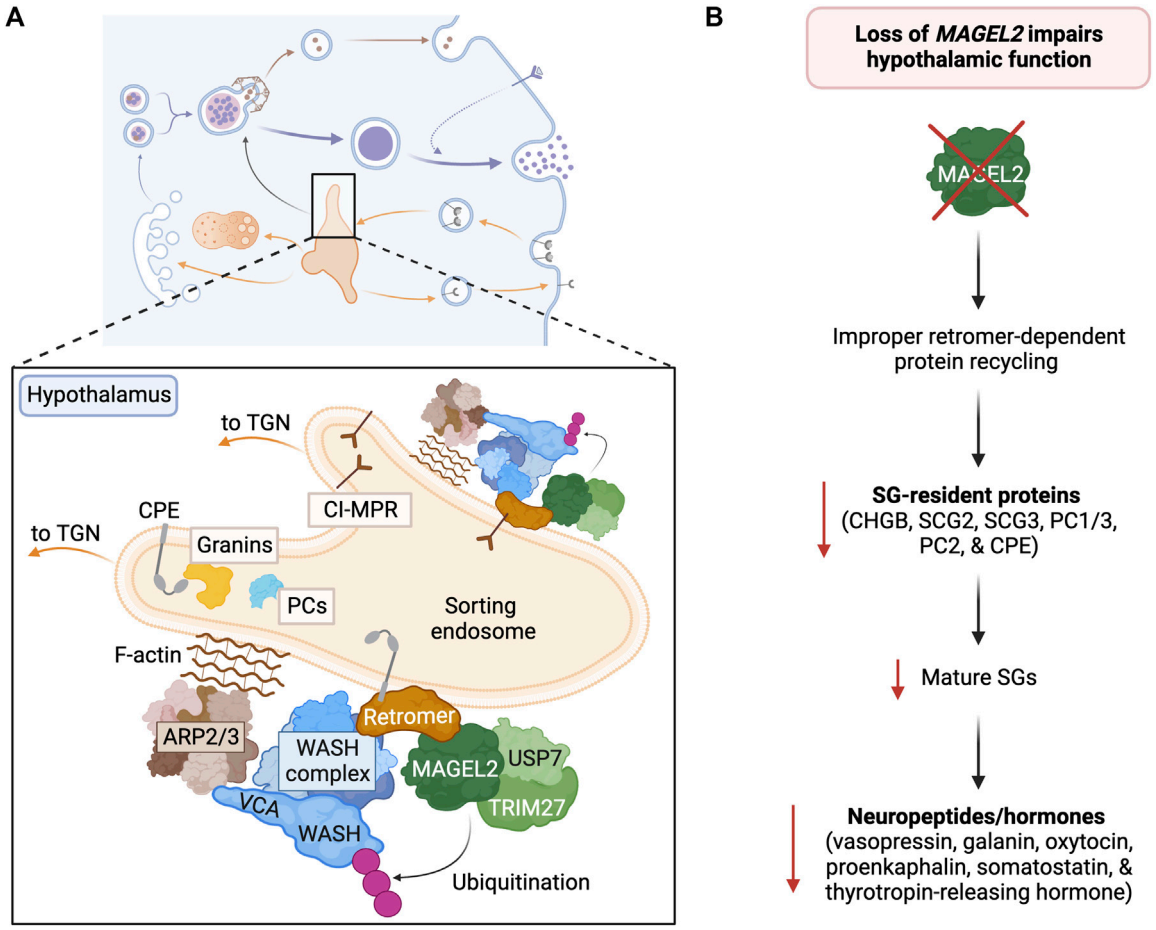

FIGURE 6
MAGEL2 functions in regulated secretion of the hypothalamus. **(A)** Within hypothalamic neurosecretory cells, MAGEL2 plays a critical role in the retromer-mediated transport of SG components (i.e., PC1/3, PC2, CHGA, CHGB, and CPE) and the lysosomal CI-MPR from the sorting endosome to the TGN. MAGEL2-TRIM27-mediated ubiquitination leads to WASH activation and actin nucleation. **(B)** The loss of *MAGEL2* leads to decreased abundance of SGs, SG-resident proteins, and neuropeptides in the hypothalamus, thus impairing hypothalamic neuroendocrine function.

endosome, cargo can be recycled back to the plasma membrane or retrograde trafficked to the TGN; both pathways prevent the lysosomal degradation of these recycled proteins (Chamberland and Ritter, 2017; Ma and Burd, 2020; Placidi and Campa, 2021). Ubiquitinated endosomal cargo is directed to lysosomes for degradation by ESCRT (endosomal sorting complex required for transport) complexes (Placidi and Campa, 2021).

Cargo recycling was historically thought of as a passive process, but the recent identification and characterization of specialized recycling complexes (i.e., retromer and commander/CCC/retriever complexes) that recognize specific signals in cytoplasmic domains of cargo proteins revealed the complexity of retrograde sorting machinery (Cullen and Steinberg, 2018; Singla et al., 2019; MacDonald et al., 2020; Placidi and Campa, 2021; Yong et al., 2022). The discovery that several transmembrane proteins, like CI-MPR and β2-adrenergic receptor, travel specific recycling routes first suggested the existence of active sorting to direct cargo into a non-degradative endosomal pathway to its correct cellular destination, such as the plasma membrane or TGN (Duncan and Kornfeld, 1988; Cao et al., 1999; MacDonald et al., 2020; Placidi and Campa, 2021). The subsequent discovery of the trimeric retromer complex (VPS26, VPS29, VPS35) (Arighi et al., 2004; Seaman, 2004), other retromer-like complexes (i.e., retriever) (McNally et al., 2017), and the WASH complex (composed of WASH, FAM21, CCDC53, SWIP/KIAA1033, and Strumpellin) (Derivery et al., 2009; Gomez and Billadeau, 2009; Harbour et al., 2010) confirmed that sequence-dependent recycling actively opposes degradation (Gershlick and Lucas, 2017; MacDonald et al., 2020; Placidi and Campa, 2021). The WASH complex is the major endosomal actin polymerization-promoting complex that stimulates the activity of the ubiquitously expressed ARP2/3 F-actin nucleation complex and the formation of branched actin patches (Derivery et al., 2009; Gomez and Billadeau, 2009; Liu et al., 2009; Seaman et al., 2013). As in anterograde transport, actin and regulation of its polymerization are key components of retrograde transport (Puthenveedu et al., 2010; Seaman et al., 2013; Simonetti and Cullen, 2019; Miklavc and Frick, 2020). Furthermore, the mammalian-specific MAGEL2 has emerged as a tissue-specific regulator of WASH activation and actin nucleation in the hypothalamus (Figure 6) (Chen et al., 2020).

More than 150 membrane proteins rely on the retromer complex for their localization on the cell surface (Steinberg et al., 2013), and neurons are particularly susceptible to any changes in endosomal trafficking due to their long axons and branched dendrites (Chamberland and Ritter, 2017). Retromer dysfunction has been linked to neurodegenerative diseases, such as Parkinson's disease, Alzheimer's disease, and frontotemporal lobar degeneration (Harrison et al., 2014; Seaman and Freeman, 2014; Reitz, 2018; Zhang et al., 2018). The loss of *MAGEL2* in neurons leads to aberrant endosomal protein trafficking and reduces the abundance of SG proteins, contributing to the etiology of Prader-Willi syndrome (PWS) (Chen et al., 2020). In addition to neuronal and neuroendocrine functions, several other physiological processes depend on retromer (Burd and Cullen, 2014). Furthermore, pathogens like *Chlamydia trachomatis* and *Legionella pneumophila* hijack the retromer complex for successful infection (Elwell et al., 2017; Elwell and Engel, 2018).

To summarize, the retrograde recycling of proteins is important for maintaining a plethora of physiological functions. The proper sorting of cargo proteins is critical for returning proteins to their proper place for reuse and preventing their lysosomal degradation. Retromer is at the very center of this retrograde sorting that happens at the early endosome, soon after the cargo is endocytosed.

5.1 Retromer evolution and function

Retromer is an evolutionarily conserved complex that regulates the retrograde pathway across all eukaryotes (Koumandou et al., 2011; McGough and Cullen, 2011; Chamberland and Ritter, 2017). In *Saccharomyces cerevisiae*, where retromer was first discovered, five vacuolar protein sorting (VPS) proteins compose the two retromer subcomplexes: the cargo-selective complex and the tubulation complex, both of which are conserved in higher eukaryotes (Seaman et al., 1998; Neuman et al., 2021). The cargo-selective complex is a trimer of Vps26, Vps29, and Vps35, which recruits cargo via an association between Vps35 and a sorting motif located within the cytoplasmic tail of cargo (Seaman et al., 1998). Retromer is recruited to the endosomal membrane by the sorting nexin (SNX) proteins Vps5 and Vps17 that form the tubulation complex and contain C-terminal Bin/amphysin/Rvs (BAR) domains that promote membrane tubulation and cargo vesicle formation (Horazdovsky et al., 1997; Nothwehr and Hindes, 1997; Seaman et al., 1998; Chamberland and Ritter, 2017).

Compared to the yeast retromer, the mammalian retromer is more complex and allows for more cargo specificity and transport regulation (Chen et al., 2019). In addition, the interactions between the retromer subcomplexes are more transitional and may not always occur in mammalian cells (Harbour and Seaman, 2011; Cullen and Steinberg, 2018). For example, both subcomplexes are needed to facilitate recycling of CI-MPR and other cargo in yeast cells (Yong et al., 2022), whereas the SNX-BAR dimer and not the VPS trimer is required for CI-MPR recycling in mammalian cells (Kvainickas et al., 2017; Simonetti et al., 2017), implying functional segregation of the two subcomplexes (Chamberland and Ritter, 2017). The acquisition of new binding partners in mammals that are not found in yeast provides further evidence of the functional divergence between the subcomplexes (Chamberland and Ritter, 2017). From now on in this manuscript, retromer will refer to the VPS26-VPS29-VPS35 heterotrimer core that is found in mammals (VPS26 has two isoforms in mammals).

The retromer complex serves as a hub for recruiting accessory proteins and complexes, such as receptor-mediated endocytosis-8 (RME-8) (Freeman et al., 2014), Eps15 homology domain-containing protein-1 (EHD1) (Gokool et al., 2007), TBC1D5 (Seaman et al., 2009), and the WASH complex (Kvainickas et al., 2017; Simonetti et al., 2017), that regulate retromer's role in endosomal trafficking and endosomal tubule dynamics (Harbour et al., 2010). For example, VPS35 binds to SNX3 and the GTPase Rab7, leading to membrane recruitment of retromer (Burd and Cullen, 2014; Harrison et al., 2014). While SNX3 directs retromer to early endosomes by binding to phosphatidylinositol 3-phosphate [PtdIns(3)P] (Harterink et al., 2011), Rab7-GTP recruits retromer to late endosomes (Rojas et al., 2008; Progida et al., 2010; Harrison et al., 2014). TBC1D5, which binds to VPS35 and VPS29, negatively regulates membrane recruitment of retromer by acting as a GTPase-activating protein for Rab7 (Seaman et al., 2009; Jia et al., 2016; Borg Distefano et al., 2018). Another important accessory protein is the WASH complex protein FAM21, which binds directly to VPS35 through its C-terminal repeats of the LFa motif (Gomez and Billadeau, 2009; Harbour et al., 2012; Jia et al., 2012; Helfer et al., 2013; Chen et al., 2019). WASH, which is regulated by MAGEL2 and USP7, then nucleates actin on the membrane (Hao et al., 2013; Hao et al., 2015; Florke Gee et al., 2020). The interaction between WASH and the Prader-Willi protein MAGEL2 will be discussed further in the last section.

5.2 Retromer and the sorting nexin protein family

Retromer functions as a coat complex that packages and delivers its cargo via tubular or vesicular structures to the TGN or plasma membrane (Lucas and Hierro, 2017; Wang et al., 2018). Vesicles coated with retromer are defined as retromer-coated endosomal tubular carriers (ETCs). Compared to other protein coats (i.e., clathrin, COPI, and COPII), ETCs are much more heterogeneous with a "loose" assembled coat, possibly an adaptation to different membrane curvatures (Chen et al., 2019). Retromer coat assembly depends on SNX proteins in mammals, as retromer does not possess intrinsic membrane-binding properties (Burd and Cullen, 2014; Chen et al., 2019). Different combinations of SNX proteins and retromer are important for recycling specific proteins (Gallon and Cullen, 2015; Chamberland and Ritter, 2017; Yong et al., 2022).

The SNX protein family expanded from 10 proteins in yeast to 33 in mammals and six of them (SNX1, SNX2, SNX3, SNX5, SNX6, and SNX27) were shown to associate with the retromer complex (Cullen, 2008; Burd and Cullen, 2014; Lucas and Hierro, 2017). SNX1 and SNX2 are Vps5 orthologs, and SNX5 and SNX6 are Vps17 orthologs (McGough and Cullen, 2011). All SNX proteins possess a Phox (PX) domain that binds to

phospholipids, in particular PtdIns(3)P, found in endosomes (Bugarcic et al., 2011; Chamberland and Ritter, 2017; Wang et al., 2018). SNX proteins are divided into subfamilies based on their domain architecture (Wang et al., 2018). SNX-PX subfamily members, like SNX3, only possess a PX domain. The SNX-FERM (4.1/ezrin/radixin/moesin) subfamily member SNX27 contains a FERM domain, which can bind to PtdIns(3)P and NPxY motifs, and a PDZ domain, which facilitates protein-protein interactions (Zhang et al., 2018). The SNX-BAR subfamily members contain a BAR domain that is capable of sensing and inducing membrane curvature (Burd and Cullen, 2014). The retromer-interacting proteins from the SNX-BAR subfamily include SNX1, SNX2, SNX5, and SNX6 (Lucas and Hierro, 2017). Although most SNX proteins associate with early endosome-enriched PtdIns(3)P, some also interact with late endosome-enriched phosphatidylinositol 3,5-phosphate [PtdIns(3,5)P]. SNX-PX-retromer and SNX-BAR-retromer mediate retrograde transport to the TGN, and SNX27-retromer mediates recycling to the plasma membrane through its PDZ domain (Temkin et al., 2011; Steinberg et al., 2013; Lucas and Hierro, 2017). Besides binding phosphatidylinositides, SNXs also play a central role in cargo recognition (Wang et al., 2018).

Retromer cargo selection is facilitated directly by VPS35 and VPS26 and/or by adaptor proteins, like SNXs, AP-1, and GGAs (Burd and Cullen, 2014; Cullen and Steinberg, 2018). The cargo proteins CI-MPR, sortilin, Wntless, and polymeric immunoglobulin (pIg) receptor possess a ΦX(L/M/V), where Φ is F/Y/W, consensus sequence that facilitates direct binding to SNX3-retromer (Verges et al., 2004; Seaman, 2007; Canuel et al., 2008; Harterink et al., 2011; Harrison et al., 2014; Lucas and Hierro, 2017; Cui et al., 2019; Yong et al., 2022). In general, at least a hydrophobic (F/W)L(M/V) motif that is commonly present in cargo proteins is needed for retromer-mediated sorting (Seaman, 2007; Cullen and Steinberg, 2018). This direct retromer interaction pathway is likely conserved in all eukaryotes. In contrast, metazoan-specific adaptor-dependent sorting allowed for the evolution of a plethora of sorting signals to finetune retrograde trafficking (Cullen and Steinberg, 2018). For example, a bipartite motif in VPS10, the functional homolog of CI-MPR in yeast, is needed for precise recognition by yeast retromer subunits Vps26 and Vps35 but not Vps17 (Suzuki et al., 2019). However, mammalian SNX5/SNX6 (yeast orthologs of Vps17) may function as the cargo-selecting module that recognizes a bipartite motif in CI-MPR and many other cargo proteins (Kvainickas et al., 2017; Simonetti et al., 2017; Simonetti et al., 2019; Yong et al., 2020). As another example, metazoan-specific SNX27 acts as an adaptor protein to select cargo through its FERM and PDZ domains (Cullen and Steinberg, 2018; Chen et al., 2019). Examples of SNX27 cargo containing a PDZ-binding motif [i.e., (S/T)xΦ] include β2-adrenergic receptor, parathyroid hormone receptor 1 (PTHR), α-amino-3-hydroxy-5-methyl-4-isoxazolepropionic acid (AMPA) receptor, and the N-methyl-D-aspartate (NMDA) receptor, which are all important in neuroendocrine tissues (Temkin et al., 2011; Steinberg et al., 2013; Lucas and Hierro, 2017). Some of these proteins, particularly their sorting motifs, must be phosphorylated to facilitate high-affinity binding to SNX27, suggesting additional complexity in regulation and finetuning of retrograde transport (Clairfeuille et al., 2016; Lucas and Hierro, 2017).

5.3 Retromer, the WASH complex, and F-actin in retrograde trafficking

An essential part of endosomal recycling is membrane remodeling, which is mediated by patches of branched F-actin, and requires membrane localization of the retromer, WASH, and ARP2/3 complexes (Fokin and Gautreau, 2021). Endosomal cargo proteins are recognized by specific combinations of retromer and SNXs (Gallon and Cullen, 2015; Chamberland and Ritter, 2017; Yong et al., 2022). SNX proteins localize the retromer complex to the membrane, and FAM21 binds to retromer's VPS35 to facilitate membrane localization of the WASH complex (Harbour et al., 2010; Bugarcic et al., 2011; Harbour et al., 2012; Jia et al., 2012; Helfer et al., 2013; Seaman and Freeman, 2014; Chamberland and Ritter, 2017). A recent study indicates that SWIP/KIAA1033 can also recruit the WASH complex to the endosomal membrane independently of the FAM21-VPS35 interaction (Dostal et al., 2023). The endosomal membrane recruitment of WASH complex may also be mediated through interaction with SNX27 (Temkin et al., 2011; Steinberg et al., 2013) or its own direct interaction with endosomal lipids (Derivery et al., 2009).

The WASH complex functions as the major actin nucleation-promoting factor in endosomal recycling and is required for the recycling of several proteins, including CI-MPR, glucose transporter 1 (GLUT1), α5β1 integrin, and major histocompatibility complex II (MHC II) (Gomez and Billadeau, 2009; Zech et al., 2011; Piotrowski et al., 2013; Graham et al., 2014; Dostal et al., 2023). WASH possesses a conserved C-terminal VCA (verprolin homologous or WASP-homology-2, connector, and acidic) domain that binds actin monomers and ARP2/3 to trigger actin filament nucleation (Linardopoulou et al., 2007; Duleh and Welch, 2010). More specifically, binding of ARP2/3 to WASH's VCA domain induces a conformational change in ARP2/3 that loads the first actin monomer and allows further actin polymerization through rapid ATP hydrolysis on ARP2 (Derivery et al., 2009; Padrick et al., 2011; Espinoza-Sanchez et al., 2018). Prior to actin nucleation, WASH's VCA domain is autoinhibited by intra- and intermolecular interactions (Hao et al., 2013). Small GTPases and PtdIns(4,5)P are some general regulators that may release VCA motif inhibition, but tissue-specific machinery, like the MUST complex (composed of MAGEL2, TRIM27 and USP7) might have evolved to enable better adaptation to specific environmental challenges (Figure 6) (Fon Tacer and Potts, 2017; Lee and Potts, 2017; Florke Gee et al., 2020).

The WASH complex promotes retromer trafficking by triggering actin polymerization via ARP2/3 complex recruitment and activation. Actin polymerization combined with the action of SNX-BAR proteins and motor proteins ultimately leads to the formation of tubular structures (Fokin and Gautreau, 2021). Subsequent actin polymerization and the activity of the dynein-dynactin complex leads to the fission of tubular vesicles that carry various cargo proteins to their final

destinations (Hunt et al., 2013; Wang et al., 2018; Fokin et al., 2021). This pathway is well-established for diverse constitutively secreted receptors; however, recent evidence suggests that essential SG membrane proteins and granins are recycled back to the TGN for nascent granule formation by retromer-dependent retrograde transport, though the mechanistic details and sorting motifs are still more or less unknown (Ferraro et al., 2005; Ma et al., 2020; Neuman et al., 2021). Interestingly, Prader-Willi mouse models with depletion of *Magel2* suggested that, in the hypothalamus, SG-resident proteins are the major targets of Magel2-retromer-dependent protein recycling (Figure 6) (Fon Tacer and Potts, 2017; Lee and Potts, 2017; Florke Gee et al., 2020).

6 MAGEL2 in regulated secretion of the hypothalamus

MAGEL2 is a mammalian-specific member of the melanoma antigen gene (MAGE) family that is specifically expressed in the brain and highly enriched in the hypothalamus (Figure 3) (Hao et al., 2015; Fon Tacer et al., 2019). Like many MAGE family proteins, MAGEL2 functions as a regulator of an E3 ubiquitin ligase (Doyle et al., 2010; Lee and Potts, 2017; Florke Gee et al., 2020). In particular, MAGEL2 interacts with the RING E3 ligase TRIM27 and VPS35 in the retromer complex, thus facilitating the localization of TRIM27 to retromer-positive endosomes (Figure 6A) (Hao et al., 2013). MAGEL2-TRIM27 promotes K63-linked polyubiquitination of WASH K220 (Hao et al., 2013). Unlike some other ubiquitin linkage types, K63-linked ubiquitination generally acts as a signaling event rather than targeting a protein for proteasomal degradation. Accordingly, MAGEL2-TRIM27-mediated ubiquitination leads to WASH activation and actin polymerization (Hao et al., 2013; Hao et al., 2015; Fon Tacer and Potts, 2017). The deubiquitinase USP7 forms a complex with MAGEL2-TRIM27 and preferentially cleaves K63-linked ubiquitin chains (Hao et al., 2015). Thus, USP7 fine-tunes F-actin levels in the endosome by counteracting TRIM27 activity and preventing the overactivation of WASH (Hao et al., 2015). Although retromer is the major player in endosomal retrieval and recycling, other similar complexes also recycle proteins (McNally and Cullen, 2018). Interestingly, the WASH complex can also associate with commander/CCC/retriever complex (Phillips-Krawczak et al., 2015; McNally et al., 2017; Chen et al., 2019); however, the role of MAGEL2 in activating WASH in association with this complex is not known and warrants future investigation. Furthermore, why WASH needs finetuning by MAGEL2 in the hypothalamic neurons is the subject of current research.

The hypothalamus is a region of the brain that integrates signals from different sensory inputs to maintain homeostasis by reacting and adapting to any changes or stressors in the environment. By controlling the autonomic nervous system via neurons linking it to both the parasympathetic and sympathetic systems, the hypothalamus regulates body temperature, hormones (e.g., thyrotropin-releasing hormone, gonadotropin-releasing hormone, somatostatin, and dopamine), and behavioral responses. Hormones released from hypothalamic neurons travel through the hypophyseal portal system to the pituitary gland, controlling the release of other hormones that regulate various endocrine glands and organs. By linking the nervous and endocrine systems, this hypothalamus-pituitary axis acts as a major control center in the body (Nillni, 2007). Intriguingly, the diverse functions of the MAGE protein family are unified in their physiological function of stress adaptation (Fon Tacer et al., 2019; Florke Gee et al., 2020). *MAGEL2* is uniquely expressed in the hypothalamus, and the molecular understanding of its function suggests its role as a tissue-specific regulator of the retrograde recycling of SG components and neuroendocrine function in the hypothalamus (Hao et al., 2015; Fon Tacer and Potts, 2017).

Given that the hypothalamus plays a key role in regulating many physiological processes, perturbations in the regulated secretion pathway lead to improper hypothalamic development and function that phenotypically manifests in syndromes, such as PWS and Schaaf-Yang syndrome (SYS) (Hoyos Sanchez et al., 2023). PWS is a complex neurogenetic disorder caused by paternal loss of the maternally imprinted 15q11-q13 chromosomal region (called the Prader-Willi region) that contains small nucleolar RNA genes and six protein-coding genes (*MKRN3*, *NDN*, *NPAP1*, *SNURF-SNRPN*, and *MAGEL2*) (Butler et al., 2019; Alves and Franco, 2020). While the loss of *MAGEL2* affects regulated secretion in the hypothalamus (Figure 6B), loss of the other Prader-Willi region genes also impacts the clinical presentation of PWS (Cassidy and Driscoll, 2009; Fon Tacer and Potts, 2017; Chen et al., 2020). Currently, PWS and SYS have no cure or effective therapy, and treatment focuses on managing the symptoms that arise from perturbations in the regulated secretion pathway and the dysregulation of crucial hypothalamic hormones (Alves and Franco, 2020; Hoyos Sanchez et al., 2023). Given that PWS is relatively common and affects 1 in 15,000 children, there is a pressing need to find better treatment options (Cassidy and Driscoll, 2009). The recent findings about MAGEL2's role in regulated secretion suggest that restoring this pathway may alleviate multiple symptoms of PWS and other similar neurodevelopmental disorders (Chen et al., 2020).

While the mechanisms of retrograde trafficking are extremely complex, cargo sorting at the endosomes culminates in ARP2/3 activation and, in turn, actin nucleation. Through facilitating the activation of WASH, MAGEL2 functions as a tissue-specific regulator of ARP2/3 activation in the hypothalamus (Hao et al., 2013; Hao et al., 2015). The loss of *MAGEL2* expression causes deficits in SG abundance and bioactive neuropeptide production, impacting hypothalamic neuroendocrine function and contributing to the clinical presentation of PWS (Figure 6B) (Chen et al., 2020; Hoyos Sanchez et al., 2023). In particular, reduced levels of the neuropeptides vasopressin, galanin, oxytocin, proenkephalin, somatostatin, and thyrotropin-releasing hormone and the SG components involved in their processing and release (i.e., CHGB, secretogranin II and III, PC1/3, PC2, and CPE) have been discovered in PWS mouse models and patient-derived neuronal cell models (Chen et al., 2020; Hoyos Sanchez et al., 2023).

7 Conclusion

Together, several decades of research provided important insights into the complexity of vesicle trafficking and protein

sorting in neuroendocrine cells. In the regulated secretory pathway, the anterograde transport is compensated by the retrograde movement of lipids and proteins to maintain membrane homeostasis and recycle various proteins. Intriguingly, the recycling of constitutive proteins of secretory granules (e.g., PCs, CPE, and granins) that enable hormone and neuropeptide maturation and cargo condensation, emerged as critical for proper hypothalamic secretion. Furthermore, actin polymerization at the site of protein sorting and vesicle budding controls retrograde transport and is regulated in a tissue-specific manner by WASH complex and MAGEL2 in the hypothalamus. Intriguingly, the diverse functions of the MAGE protein family are unified in their physiological function of stress adaptation. Given that *MAGEL2* is uniquely expressed in the hypothalamus, the molecular understanding of its function suggests its role to enable better and faster adaptation to an ever-changing environment. The loss of *MAGEL2* ultimately leads to insufficient F-actin nucleation and a decreased percentage of SG proteins recycled, which manifests in a perturbation of the hormonal secretion in patients with Prader-Willi and Schaaf-Yang syndromes. Further uncovering of the tissue-specific regulation of anterograde and retrograde transport thus offers potential therapeutic opportunities for patients.

Author contributions

Conceptualization: KFT, DŠ, RFG, and MH; writing—original draft preparation: DŠ, RFG, and KFT; writing—review and editing: RFG and KFT; supervision: KFT. All authors contributed to the article and approved the submitted version.

Funding

This work was supported by the Texas Tech University start-up (to KFT), Cancer Prevention and Research Institute of Texas Scholar Award RR200059 (to KFT), the Foundation for Prader–Willi Syndrome Research Grants 22-0321 and 23-0447 (to KFT). DŠ was the recipient of the 2022 American Slovenian Educational Foundation (ASEF) fellowship.

Acknowledgments

We thank members of the Fon Tacer laboratory for their advice and critical discussions. We apologize for our inability to discuss and reference all work in the field due to space limitations. Figures were created with BioRender (BioRender.com).

Conflict of interest

The authors declare that the research was conducted in the absence of any commercial or financial relationships that could be construed as a potential conflict of interest.

Publisher's note

References

Ahras, M., Otto, G. P., and Tooze, S. A. (2006). Synaptotagmin IV is necessary for the maturation of secretory granules in PC12 cells. *J. Cell. Biol.* 173, 241–251. doi:10.1083/jcb.200506163

Alekhina, O., Burstein, E., and Billadeau, D. D. (2017). Cellular functions of WASP family proteins at a glance. *J. Cell. Sci.* 130 (14), 2235–2241. doi:10.1242/jcs.199570

Alves, C., and Franco, R. R. (2020). Prader-willi syndrome: endocrine manifestations and management. *Arch. Endocrinol. Metab.* 64 (3), 223–234. doi:10.20945/2359-3997000000248

Anini, Y., Mayne, J., Gagnon, J., Sherbafi, J., Chen, A., Kaefer, N., et al. (2010). Genetic deficiency for proprotein convertase subtilisin/kexin type 2 in mice is associated with decreased adiposity and protection from dietary fat-induced body weight gain. *Int. J. Obes. (Lond)* 34 (11), 1599–1607. doi:10.1038/ijo.2010.90

Arighi, C. N., Hartnell, L. M., Aguilar, R. C., Haft, C. R., and Bonifacino, J. S. (2004). Role of the mammalian retromer in sorting of the cation-independent mannose 6-phosphate receptor. *J. Cell. Biol.* 165 (1), 123–133. doi:10.1083/jcb.200312055

Arnaoutova, I., Smith, A. M., Coates, L. C., Sharpe, J. C., Dhanvantari, S., Snell, C. R., et al. (2003). The prohormone processing enzyme PC3 is a lipid raft-associated transmembrane protein. *Biochemistry* 42 (35), 10445–10455. doi:10.1021/bi034277y

Assadi, M., Sharpe, J. C., Snell, C., and Loh, Y. P. (2004). The C-terminus of prohormone convertase 2 is sufficient and necessary for Raft association and sorting to the regulated secretory pathway. *Biochemistry* 43 (24), 7798–7807. doi:10.1021/bi036331g

Austin, C., Hinners, I., and Tooze, S. A. (2000). Direct and GTP-dependent interaction of ADP-ribosylation factor 1 with clathrin adaptor protein AP-1 on immature secretory granules. *J. Biol. Chem.* 275 (29), 21862–21869. doi:10.1074/jbc.M908875199

Bartolomucci, A., Possenti, R., Mahata, S. K., Fischer-Colbrie, R., Loh, Y. P., and Salton, S. R. (2011). The extended granin family: structure, function, and biomedical implications. *Endocr. Rev.* 32 (6), 755–797. doi:10.1210/er.2010-0027

Bell-Parikh, L. C., Eipper, B. A., and Mains, R. E. (2001). Response of an integral granule membrane protein to changes in pH. *J. Biol. Chem.* 276 (32), 29854–29863. doi:10.1074/jbc.M103936200

Beuret, N., Stettler, H., Renold, A., Rutishauser, J., and Spiess, M. (2004). Expression of regulated secretory proteins is sufficient to generate granule-like structures in constitutively secreting cells. *J. Biol. Chem.* 279 (19), 20242–20249. doi:10.1074/jbc.M310613200

Bhave, M., Mettlen, M., Wang, X., and Schmid, S. L. (2020). Early and nonredundant functions of dynamin isoforms in clathrin-mediated endocytosis. *Mol. Biol. Cell.* 31 (18), 2035–2047. doi:10.1091/mbc.E20-06-0363

Bittner, M. A., Aikman, R. L., and Holz, R. W. (2013). A nibbling mechanism for clathrin-mediated retrieval of secretory granule membrane after exocytosis. *J. Biol. Chem.* 288 (13), 9177–9188. doi:10.1074/jbc.M113.450361

Blanchard, F., Duplomb, L., Raher, S., Vusio, P., Hoflack, B., Jacques, Y., et al. (1999). Mannose 6-Phosphate/Insulin-like growth factor II receptor mediates internalization and degradation of leukemia inhibitory factor but not signal transduction. *J. Biol. Chem.* 274 (35), 24685–24693. doi:10.1074/jbc.274.35.24685

Boehm, M., and Bonifacino, J. S. (2002). Genetic analyses of adaptin function from yeast to mammals. *Gene* 286 (2), 175–186. doi:10.1016/s0378-1119(02)00422-5

Bonifacino, J. S. (2004). The GGA proteins: adaptors on the move. *Nat. Rev. Mol. Cell. Biol.* 5 (1), 23–32. doi:10.1038/nrm1279

Bonifacino, J. S. (2014). Adaptor proteins involved in polarized sorting. *J. Cell. Biol.* 204 (1), 7–17. doi:10.1083/jcb.201310021

Bonnemaison, M. L., Eipper, B. A., and Mains, R. E. (2013). Role of adaptor proteins in secretory granule biogenesis and maturation. *Front. Endocrinol. (Lausanne)* 4, 101. doi:10.3389/fendo.2013.00101

Borg Distefano, M., Hofstad Haugen, L., Wang, Y., Perdreau-Dahl, H., Kjos, I., Jia, D., et al. (2018). TBC1D5 controls the GTPase cycle of Rab7b. *J. Cell. Sci.* 131 (17). doi:10.1242/jcs.216630

Borges, R., Diaz-Vera, J., Dominguez, N., Arnau, M. R., and Machado, J. D. (2010). Chromogranins as regulators of exocytosis. *J. Neurochem.* 114 (2), 335–343. doi:10.1111/j.1471-4159.2010.06786.x

Braulke, T., and Bonifacino, J. S. (2009). Sorting of lysosomal proteins. *Biochim. Biophys. Acta* 1793 (4), 605–614. doi:10.1016/j.bbamcr.2008.10.016

Brechler, V., Chu, W. N., Baxter, J. D., Thibault, G., and Reudelhuber, T. L. (1996). A protease processing site is essential for prorenin sorting to the regulated secretory pathway. *J. Biol. Chem.* 271 (34), 20636–20640. doi:10.1074/jbc.271.34.20636

Brown, J., Delaine, C., Zaccheo, O. J., Siebold, C., Gilbert, R. J., van Boxel, G., et al. (2008). Structure and functional analysis of the IGF-II/IGF2R interaction. *EMBO J.* 27 (1), 265–276. doi:10.1038/sj.emboj.7601938

Bugarcic, A., Zhe, Y., Kerr, M. C., Griffin, J., Collins, B. M., and Teasdale, R. D. (2011). Vps26A and Vps26B subunits define distinct retromer complexes. *Traffic* 12 (12), 1759–1773. doi:10.1111/j.1600-0854.2011.01284.x

Burd, C., and Cullen, P. J. (2014). Retromer: A master conductor of endosome sorting. *Cold Spring Harb. Perspect. Biol.* 6 (2). doi:10.1101/cshperspect.a016774

Burgess, T. L., and Kelly, R. B. (1987). Constitutive and regulated secretion of proteins. *Annu. Rev. Cell. Biol.* 3, 243–293. doi:10.1146/annurev.cb.03.110187.001331

Burgoyne, R. D., and Morgan, A. (2003). Secretory granule exocytosis. *Physiol. Rev.* 83 (2), 581–632. doi:10.1152/physrev.00031.2002

Butler, M. G., Miller, J. L., and Forster, J. L. (2019). Prader-willi syndrome - clinical genetics, diagnosis and treatment approaches: an update. *Curr. Pediatr. Rev.* 15 (4), 207–244. doi:10.2174/1573396315666190716120925

Canuel, M., Lefrancois, S., Zeng, J., and Morales, C. R. (2008). AP-1 and retromer play opposite roles in the trafficking of sortilin between the Golgi apparatus and the lysosomes. *Biochem. Biophys. Res. Commun.* 366 (3), 724–730. doi:10.1016/j.bbrc.2007.12.015

Cao, T. T., Deacon, H. W., Reczek, D., Bretscher, A., and von Zastrow, M. (1999). A kinase-regulated PDZ-domain interaction controls endocytic sorting of the beta2-adrenergic receptor. *Nature* 401 (6750), 286–290. doi:10.1038/45816

Carmon, O., Laguerre, F., Riachy, L., Delestre-Delacour, C., Wang, Q., Tanguy, E., et al. (2020). Chromogranin A preferential interaction with Golgi phosphatidic acid induces membrane deformation and contributes to secretory granule biogenesis. *FASEB J.* 34 (5), 6769–6790. doi:10.1096/fj.202000074R

Cassidy, S. B., and Driscoll, D. J. (2009). Prader-Willi syndrome. *Eur. J. Hum. Genet.* 17 (1), 3–13. doi:10.1038/ejhg.2008.165

Cawley, N. X., Wetsel, W. C., Murthy, S. R., Park, J. J., Pacak, K., and Loh, Y. P. (2012). New roles of carboxypeptidase E in endocrine and neural function and cancer. *Endocr. Rev.* 33 (2), 216–253. doi:10.1210/er.2011-1039

Cawley, N. X., Li, Z., and Loh, Y. P. (2016). 60 years of POMC: biosynthesis, trafficking, and secretion of pro-opiomelanocortin-derived peptides. *J. Mol. Endocrinol.* 56 (4), T77–T97. doi:10.1530/JME-15-0323

Cendron, L., Rothenberger, S., Cassari, L., Dettin, M., and Pasquato, A. (2023). Proprotein convertases regulate trafficking and maturation of key proteins within the secretory pathway. *Adv. Protein Chem. Struct. Biol.* 133, 1–54. doi:10.1016/bs.apcsb.2022.10.001

Chamberland, J. P., and Ritter, B. (2017). Retromer revisited: evolving roles for retromer in endosomal sorting. *J. Cell. Biol.* 216 (11), 3433–3436. doi:10.1083/jcb.201708111

Chanat, E., and Huttner, W. B. (1991). Milieu-induced, selective aggregation of regulated secretory proteins in the trans-Golgi network. *J. Cell. Biol.* 115 (6), 1505–1519. doi:10.1083/jcb.115.6.1505

Chanat, E., Weiss, U., Huttner, W. B., and Tooze, S. A. (1993). Reduction of the disulfide bond of chromogranin B (secretogranin I) in the trans-Golgi network causes its missorting to the constitutive secretory pathways. *EMBO J.* 12 (5), 2159–2168. doi:10.1002/j.1460-2075.1993.tb05864.x

Chen, H. J., Yuan, J., and Lobel, P. (1997). Systematic mutational analysis of the cation-independent mannose 6-phosphate/insulin-like growth factor II receptor cytoplasmic domain. An acidic cluster containing a key aspartate is important for function in lysosomal enzyme sorting. *J. Biol. Chem.* 272 (11), 7003–7012. doi:10.1074/jbc.272.11.7003

Chen, K. E., Healy, M. D., and Collins, B. M. (2019). Towards a molecular understanding of endosomal trafficking by Retromer and Retriever. *Traffic* 20 (7), 465–478. doi:10.1111/tra.12649

Chen, H., Victor, A. K., Klein, J., Tacer, K. F., Tai, D. J., de Esch, C., et al. (2020). Loss of MAGEL2 in Prader-Willi syndrome leads to decreased secretory granule and neuropeptide production. *JCI Insight* 5 (17). doi:10.1172/jci.insight.138576

Chidgey, M. A. (1993). Protein targeting to dense-core secretory granules. *Bioessays* 15 (5), 317–321. doi:10.1002/bies.950150505

Chieregatti, E., and Meldolesi, J. (2005). Regulated exocytosis: new organelles for non-secretory purposes. *Nat. Rev. Mol. Cell. Biol.* 6 (2), 181–187. doi:10.1038/nrm1572

Clairfeuille, T., Mas, C., Chan, A. S., Yang, Z., Tello-Lafoz, M., Chandra, M., et al. (2016). A molecular code for endosomal recycling of phosphorylated cargos by the SNX27-retromer complex. *Nat. Struct. Mol. Biol.* 23 (10), 921–932. doi:10.1038/nsmb.3290

Collins, B. M., Watson, P. J., and Owen, D. J. (2003). The structure of the GGA1-GAT domain reveals the molecular basis for ARF binding and membrane association of GGAs. *Dev. Cell.* 4 (3), 321–332. doi:10.1016/s1534-5807(03)00037-6

Cool, D. R., and Loh, Y. P. (1998). Carboxypeptidase E is a sorting receptor for prohormones: binding and kinetic studies. *Mol. Cell. Endocrinol.* 139 (1-2), 7–13. doi:10.1016/s0303-7207(98)00081-1

Cool, D. R., Fenger, M., Snell, C. R., and Loh, Y. P. (1995). Identification of the sorting signal motif within pro-opiomelanocortin for the regulated secretory pathway. *J. Biol. Chem.* 270 (15), 8723–8729. doi:10.1074/jbc.270.15.8723

Cool, D. R., Normant, E., Shen, F., Chen, H. C., Pannell, L., Zhang, Y., et al. (1997). Carboxypeptidase E is a regulated secretory pathway sorting receptor: genetic obliteration leads to endocrine disorders in cpe(fat) mice. *Cell.* 88 (1), 73–83. doi:10.1016/s0092-8674(00)81860-7

Coutinho, M. F., Prata, M. J., and Alves, S. (2012). Mannose-6-phosphate pathway: A review on its role in lysosomal function and dysfunction. *Mol. Genet. Metab.* 105 (4), 542–550. doi:10.1016/j.ymgme.2011.12.012

Cowley, D. J., Moore, Y. R., Darling, D. S., Joyce, P. B., and Gorr, S. U. (2000). N- and C-terminal domains direct cell type-specific sorting of chromogranin A to secretory granules. *J. Biol. Chem.* 275 (11), 7743–7748. doi:10.1074/jbc.275.11.7743

Creemers, J. W., Choquet, H., Stijnen, P., Vatin, V., Pigeyre, M., Beckers, S., et al. (2012). Heterozygous mutations causing partial prohormone convertase 1 deficiency contribute to human obesity. *Diabetes* 61 (2), 383–390. doi:10.2337/db11-0305

Cui, Y., Carosi, J. M., Yang, Z., Ariotti, N., Kerr, M. C., Parton, R. G., et al. (2019). Retromer has a selective function in cargo sorting via endosome transport carriers. *J. Cell. Biol.* 218 (2), 615–631. doi:10.1083/jcb.201806153

Cullen, P. J., and Steinberg, F. (2018). To degrade or not to degrade: mechanisms and significance of endocytic recycling. *Nat. Rev. Mol. Cell. Biol.* 19 (11), 679–696. doi:10.1038/s41580-018-0053-7

Cullen, P. J. (2008). Endosomal sorting and signalling: an emerging role for sorting nexins. *Nat. Rev. Mol. Cell. Biol.* 9 (7), 574–582. doi:10.1038/nrm2427

Damholt, A. B., Buchan, A. M., Holst, J. J., and Kofod, H. (1999). Proglucagon processing profile in canine L cells expressing endogenous prohormone convertase 1/3 and prohormone convertase 2. *Endocrinology* 140 (10), 4800–4808. doi:10.1210/endo.140.10.7068

Day, R., and Gorr, S. U. (2003). Secretory granule biogenesis and chromogranin A: master gene, on/off switch or assembly factor? *Trends Endocrinol. Metab.* 14 (1), 10–13. doi:10.1016/s1043-2760(02)00011-5

Delestre-Delacour, C., Carmon, O., Laguerre, F., Estay-Ahumada, C., Courel, M., Elias, S., et al. (2017). Myosin 1b and F-actin are involved in the control of secretory granule biogenesis. *Sci. Rep.* 7 (1), 5172. doi:10.1038/s41598-017-05617-1

Dell'Angelica, E. C., Ohno, H., Ooi, C. E., Rabinovich, E., Roche, K. W., and Bonifacino, J. S. (1997). AP-3: an adaptor-like protein complex with ubiquitous expression. *EMBO J.* 16 (5), 917–928. doi:10.1093/emboj/16.5.917

Derivery, E., Sousa, C., Gautier, J. J., Lombard, B., Loew, D., and Gautreau, A. (2009). The Arp2/3 activator WASH controls the fission of endosomes through a large multiprotein complex. *Dev. Cell.* 17 (5), 712–723. doi:10.1016/j.devcel.2009.09.010

Dhanvantari, S., and Loh, Y. P. (2000). Lipid raft association of carboxypeptidase E is necessary for its function as a regulated secretory pathway sorting receptor. *J. Biol. Chem.* 275 (38), 29887–29893. doi:10.1074/jbc.M005364200

Dhanvantari, S., Seidah, N. G., and Brubaker, P. L. (1996). Role of prohormone convertases in the tissue-specific processing of proglucagon. *Mol. Endocrinol.* 10 (4), 342–355. doi:10.1210/mend.10.4.8721980

Dhanvantari, S., Arnaoutova, I., Snell, C. R., Steinbach, P. J., Hammond, K., Caputo, G. A., et al. (2002). Carboxypeptidase E, a prohormone sorting receptor, is anchored to secretory granules via a C-terminal transmembrane insertion. *Biochemistry* 41 (1), 52–60. doi:10.1021/bi015698n

Dhanvantari, S., Shen, F. S., Adams, T., Snell, C. R., Zhang, C., Mackin, R. B., et al. (2003). Disruption of a receptor-mediated mechanism for intracellular sorting of proinsulin in familial hyperproinsulinemia. *Mol. Endocrinol.* 17 (9), 1856–1867. doi:10.1210/me.2002-0380

Dikeakos, J. D., and Reudelhuber, T. L. (2007). Sending proteins to dense core secretory granules: still a lot to sort out. *J. Cell. Biol.* 177 (2), 191–196. doi:10.1083/jcb.200701024

Dikeakos, J. D., Lacombe, M. J., Mercure, C., Mireuta, M., and Reudelhuber, T. L. (2007a). A hydrophobic patch in a charged alpha-helix is sufficient to target proteins to dense core secretory granules. *J. Biol. Chem.* 282 (2), 1136–1143. doi:10.1074/jbc.M605718200

Dikeakos, J. D., Mercure, C., Lacombe, M. J., Seidah, N. G., and Reudelhuber, T. L. (2007b). PC1/3, PC2 and PC5/6A are targeted to dense core secretory granules by a common mechanism. *FEBS J.* 274 (16), 4094–4102. doi:10.1111/j.1742-4658.2007.05937.x

Dikeakos, J. D., Di Lello, P., Lacombe, M. J., Ghirlando, R., Legault, P., Reudelhuber, T. L., et al. (2009). Functional and structural characterization of a dense core secretory granule sorting domain from the PC1/3 protease. *Proc. Natl. Acad. Sci. U. S. A.* 106 (18), 7408–7413. doi:10.1073/pnas.0809576106

Dittie, A. S., Hajibagheri, N., and Tooze, S. A. (1996). The AP-1 adaptor complex binds to immature secretory granules from PC12 cells, and is regulated by ADP-ribosylation factor. *J. Cell. Biol.* 132 (4), 523–536. doi:10.1083/jcb.132.4.523

Dittie, A. S., Thomas, L., Thomas, G., and Tooze, S. A. (1997). Interaction of furin in immature secretory granules from neuroendocrine cells with the AP-1 adaptor complex is modulated by casein kinase II phosphorylation. *EMBO J.* 16 (16), 4859–4870. doi:10.1093/emboj/16.16.4859

Dominguez, N., van Weering, J. R. T., Borges, R., Toonen, R. F. G., and Verhage, M. (2018). Dense-core vesicle biogenesis and exocytosis in neurons lacking chromogranins A and B. *J. Neurochem.* 144 (3), 241–254. doi:10.1111/jnc.14263

Doray, B., Ghosh, P., Griffith, J., Geuze, H. J., and Kornfeld, S. (2002). Cooperation of GGAs and AP-1 in packaging MPRs at the trans-Golgi network. *Science* 297 (5587), 1700–1703. doi:10.1126/science.1075327

Dostal, V., Humhalova, T., Berankova, P., Pacalt, O., and Libusova, L. (2023). SWIP mediates retromer-independent membrane recruitment of the WASH complex. *Traffic* 24 (5), 216–230. doi:10.1111/tra.12884

Doyle, J. M., Gao, J., Wang, J., Yang, M., and Potts, P. R. (2010). MAGE-RING protein complexes comprise a family of E3 ubiquitin ligases. *Mol. Cell.* 39 (6), 963–974. doi:10.1016/j.molcel.2010.08.029

Duleh, S. N., and Welch, M. D. (2010). WASH and the Arp2/3 complex regulate endosome shape and trafficking. *Cytoskelet. Hob.* 67 (3), 193–206. doi:10.1002/cm.20437

Duncan, J. R., and Kornfeld, S. (1988). Intracellular movement of two mannose 6-phosphate receptors: return to the Golgi apparatus. *J. Cell. Biol.* 106 (3), 617–628. doi:10.1083/jcb.106.3.617

Eaton, B. A., Haugwitz, M., Lau, D., and Moore, H. P. (2000). Biogenesis of regulated exocytotic carriers in neuroendocrine cells. *J. Neurosci.* 20 (19), 7334–7344. doi:10.1523/JNEUROSCI.20-19-07334.2000

Elias, S., Delestre, C., Courel, M., Anouar, Y., and Montero-Hadjadje, M. (2010). Chromogranin A as a crucial factor in the sorting of peptide hormones to secretory granules. *Cell. Mol. Neurobiol.* 30 (8), 1189–1195. doi:10.1007/s10571-010-9595-8

Elwell, C., and Engel, J. (2018). Emerging role of retromer in modulating pathogen growth. *Trends Microbiol.* 26 (9), 769–780. doi:10.1016/j.tim.2018.04.001

Elwell, C. A., Czudnochowski, N., von Dollen, J., Johnson, J. R., Nakagawa, R., Mirrashidi, K., et al. (2017). Chlamydia interfere with an interaction between the mannose-6-phosphate receptor and sorting nexins to counteract host restriction. *Elife* 6. doi:10.7554/eLife.22709

Espinoza-Sanchez, S., Metskas, L. A., Chou, S. Z., Rhoades, E., and Pollard, T. D. (2018). Conformational changes in Arp2/3 complex induced by ATP, WASp-VCA, and actin filaments. *Proc. Natl. Acad. Sci. U. S. A.* 115 (37), E8642–E8651. doi:10.1073/pnas.1717594115

Farquhar, M. G., and Palade, G. E. (1998). The Golgi apparatus: 100 years of progress and controversy. *Trends Cell. Biol.* 8 (1), 2–10. doi:10.1016/s0962-8924(97)01187-2

Ferraro, F., Eipper, B. A., and Mains, R. E. (2005). Retrieval and reuse of pituitary secretory granule proteins. *J. Biol. Chem.* 280 (27), 25424–25435. doi:10.1074/jbc.M414156200

Florke Gee, R. R., Chen, H., Lee, A. K., Daly, C. A., Wilander, B. A., Fon Tacer, K., et al. (2020). Emerging roles of the MAGE protein family in stress response pathways. *J. Biol. Chem.* 295 (47), 16121–16155. doi:10.1074/jbc.REV120.008029

Fokin, A. I., and Gautreau, A. M. (2021). Assembly and activity of the WASH molecular machine: distinctive features at the crossroads of the actin and microtubule cytoskeletons. *Front. Cell. Dev. Biol.* 9, 658865. doi:10.3389/fcell.2021.658865

Fokin, A. I., David, V., Oguievetskaia, K., Derivery, E., Stone, C. E., Cao, L., et al. (2021). The Arp1/11 minifilament of dynactin primes the endosomal Arp2/3 complex. *Sci. Adv.* 7 (3). doi:10.1126/sciadv.abd5956

Fon Tacer, K., and Potts, P. R. (2017). Cellular and disease functions of the Prader-Willi Syndrome gene MAGEL2. *Biochem. J.* 474 (13), 2177–2190. doi:10.1042/BCJ20160616

Fon Tacer, K., Montoya, M. C., Oatley, M. J., Lord, T., Oatley, J. M., Klein, J., et al. (2019). MAGE cancer-testis antigens protect the mammalian germline under environmental stress. *Sci. Adv.* 5 (5), eaav4832. doi:10.1126/sciadv.aav4832

Freeman, C. L., Hesketh, G., and Seaman, M. N. (2014). RME-8 coordinates the activity of the WASH complex with the function of the retromer SNX dimer to control endosomal tubulation. *J. Cell. Sci.* 127 (9), 2053–2070. doi:10.1242/jcs.144659

Fricker, L. D., and Devi, L. (1993). Posttranslational processing of carboxypeptidase E, a neuropeptide-processing enzyme, in AtT-20 cells and bovine pituitary secretory granules. *J. Neurochem.* 61 (4), 1404–1415. doi:10.1111/j.1471-4159.1993.tb13634.x

Fricker, L. D., and Snyder, S. H. (1982). Enkephalin convertase: purification and characterization of a specific enkephalin-synthesizing carboxypeptidase localized to adrenal chromaffin granules. *Proc. Natl. Acad. Sci. U. S. A.* 79 (12), 3886–3890. doi:10.1073/pnas.79.12.3886

Fricker, L. D., Das, B., and Angeletti, R. H. (1990). Identification of the pH-dependent membrane anchor of carboxypeptidase E (EC 3.4.17.10). *J. Biol. Chem.* 265 (5), 2476–2482. doi:10.1016/S0021-9258(19)39824-2

Fricker, L. D. (1988). Carboxypeptidase E. *Annu. Rev. Physiol.* 50, 309–321. doi:10.1146/annurev.ph.50.030188.001521

Furuta, M., Yano, H., Zhou, A., Rouille, Y., Holst, J. J., Carroll, R., et al. (1997). Defective prohormone processing and altered pancreatic islet morphology in mice lacking active SPC2. *Proc. Natl. Acad. Sci. U. S. A.* 94 (13), 6646–6651. doi:10.1073/pnas.94.13.6646

Furuta, M., Zhou, A., Webb, G., Carroll, R., Ravazzola, M., Orci, L., et al. (2001). Severe defect in proglucagon processing in islet A-cells of prohormone convertase 2 null mice. *J. Biol. Chem.* 276 (29), 27197–27202. doi:10.1074/jbc.M103362200

Gallon, M., and Cullen, P. J. (2015). Retromer and sorting nexins in endosomal sorting. *Biochem. Soc. Trans.* 43 (1), 33–47. doi:10.1042/BST20140290

Gary-Bobo, M., Nirde, P., Jeanjean, A., Morere, A., and Garcia, M. (2007). Mannose 6-phosphate receptor targeting and its applications in human diseases. *Curr. Med. Chem.* 14 (28), 2945–2953. doi:10.2174/092986707782794005

Gerber, S. H., and Sudhof, T. C. (2002). Molecular determinants of regulated exocytosis. *Diabetes* 51 (1), S3–S11. doi:10.2337/diabetes.51.2007.s3

Gershlick, D. C., and Lucas, M. (2017). Endosomal trafficking: retromer and retriever are relatives in recycling. *Curr. Biol.* 27 (22), R1233–R1236. doi:10.1016/j.cub.2017.10.004

Ghosh, P., and Kornfeld, S. (2004). The cytoplasmic tail of the cation-independent mannose 6-phosphate receptor contains four binding sites for AP-1. *Arch. Biochem. Biophys.* 426 (2), 225–230. doi:10.1016/j.abb.2004.02.011

Glickman, J. N., Conibear, E., and Pearse, B. M. (1989). Specificity of binding of clathrin adaptors to signals on the mannose-6-phosphate/insulin-like growth factor II receptor. *EMBO J.* 8 (4), 1041–1047. doi:10.1002/j.1460-2075.1989.tb03471.x

Glombik, M. M., and Gerdes, H. H. (2000). Signal-mediated sorting of neuropeptides and prohormones: secretory granule biogenesis revisited. *Biochimie* 82 (4), 315–326. doi:10.1016/s0300-9084(00)00195-4

Glombik, M. M., Kromer, A., Salm, T., Huttner, W. B., and Gerdes, H. H. (1999). The disulfide-bonded loop of chromogranin B mediates membrane binding and directs sorting from the trans-Golgi network to secretory granules. *EMBO J.* 18 (4), 1059–1070. doi:10.1093/emboj/18.4.1059

Godar, S., Horejsi, V., Weidle, U. H., Binder, B. R., Hansmann, C., and Stockinger, H. (1999). M6P/IGFII-receptor complexes urokinase receptor and plasminogen for activation of transforming growth factor-beta1. *Eur. J. Immunol.* 29 (3), 1004–1013. doi:10.1002/(SICI)1521-4141(199903)29:03<1004:AID-IMMU1004>3.0.CO;2-Q

Gokool, S., Tattersall, D., and Seaman, M. N. J. (2007). EHD1 interacts with retromer to stabilize SNX1 tubules and facilitate endosome-to-Golgi retrieval. *Traffic* 8 (12), 1873–1886. doi:10.1111/j.1600-0854.2007.00652.x

Goley, E. D., and Welch, M. D. (2006). The ARP2/3 complex: an actin nucleator comes of age. *Nat. Rev. Mol. Cell. Biol.* 7 (10), 713–726. doi:10.1038/nrm2026

Gomez, T. S., and Billadeau, D. D. (2009). A FAM21-containing WASH complex regulates retromer-dependent sorting. *Dev. Cell.* 17 (5), 699–711. doi:10.1016/j.devcel.2009.09.009

Gonzalez-Jamett, A. M., Momboisse, F., Haro-Acuna, V., Bevilacqua, J. A., Caviedes, P., and Cardenas, A. M. (2013). Dynamin-2 function and dysfunction along the secretory pathway. *Front. Endocrinol. (Lausanne)* 4, 126. doi:10.3389/fendo.2013.00126

Goronzy, J. J., and Weyand, C. M. (2009). Developments in the scientific understanding of rheumatoid arthritis. *Arthritis Res. Ther.* 11 (5), 249. doi:10.1186/ar2758

Graham, D. B., Osborne, D. G., Piotrowski, J. T., Gomez, T. S., Gmyrek, G. B., Akilesh, H. M., et al. (2014). Dendritic cells utilize the evolutionarily conserved WASH and retromer complexes to promote MHCII recycling and helper T cell priming. *PLoS One* 9 (6), e98606. doi:10.1371/journal.pone.0098606

Guardia, C. M., De Pace, R., Mattera, R., and Bonifacino, J. S. (2018). Neuronal functions of adaptor complexes involved in protein sorting. *Curr. Opin. Neurobiol.* 51, 103–110. doi:10.1016/j.conb.2018.02.021

Guizzetti, L., McGirr, R., and Dhanvantari, S. (2014). Two dipolar alpha-helices within hormone-encoding regions of proglucagon are sorting signals to the regulated secretory pathway. *J. Biol. Chem.* 289 (21), 14968–14980. doi:10.1074/jbc.M114.563684

Gutierrez, L. M., and Villanueva, J. (2018). The role of F-actin in the transport and secretion of chromaffin granules: an historic perspective. *Pflugers Arch.* 470 (1), 181–186. doi:10.1007/s00424-017-2040-9

Halban, P. A., and Irminger, J. C. (1994). Sorting and processing of secretory proteins. *Biochem. J.* 299, 1–18. doi:10.1042/bj2990001

Hammel, I., Lagunoff, D., and Galli, S. J. (2010). Regulation of secretory granule size by the precise generation and fusion of unit granules. *J. Cell. Mol. Med.* 14 (7), 1904–1916. doi:10.1111/j.1582-4934.2010.01071.x

Han, L., Suda, M., Tsuzuki, K., Wang, R., Ohe, Y., Hirai, H., et al. (2008). A large form of secretogranin III functions as a sorting receptor for chromogranin A aggregates in PC12 cells. *Mol. Endocrinol.* 22 (8), 1935–1949. doi:10.1210/me.2008-0006

Hao, Y. H., Doyle, J. M., Ramanathan, S., Gomez, T. S., Jia, D., Xu, M., et al. (2013). Regulation of WASH-dependent actin polymerization and protein trafficking by ubiquitination. *Cell.* 152 (5), 1051–1064. doi:10.1016/j.cell.2013.01.051

Hao, Y. H., Fountain, M. D., Jr., Fon Tacer, K., Xia, F., Bi, W., Kang, S. H., et al. (2015). USP7 acts as a molecular rheostat to promote WASH-dependent endosomal protein recycling and is mutated in a human neurodevelopmental disorder. *Mol. Cell.* 59 (6), 956–969. doi:10.1016/j.molcel.2015.07.033

Harbour, M. E., and Seaman, M. N. (2011). Evolutionary variations of VPS29, and their implications for the heteropentameric model of retromer. *Commun. Integr. Biol.* 4 (5), 619–622. doi:10.4161/cib.4.5.16855

Harbour, M. E., Breusegem, S. Y., Antrobus, R., Freeman, C., Reid, E., and Seaman, M. N. (2010). The cargo-selective retromer complex is a recruiting hub for protein complexes that regulate endosomal tubule dynamics. *J. Cell. Sci.* 123 (21), 3703–3717. doi:10.1242/jcs.071472

Harbour, M. E., Breusegem, S. Y., and Seaman, M. N. (2012). Recruitment of the endosomal WASH complex is mediated by the extended 'tail' of Fam21 binding to the retromer protein Vps35. *Biochem. J.* 442 (1), 209–220. doi:10.1042/BJ20111761

Harrison, M. S., Hung, C. S., Liu, T. T., Christiano, R., Walther, T. C., and Burd, C. G. (2014). A mechanism for retromer endosomal coat complex assembly with cargo. *Proc. Natl. Acad. Sci. U. S. A.* 111 (1), 267–272. doi:10.1073/pnas.1316482111

Harterink, M., Port, F., Lorenowicz, M. J., McGough, I. J., Silhankova, M., Betist, M. C., et al. (2011). A SNX3-dependent retromer pathway mediates retrograde transport of the Wnt sorting receptor Wntless and is required for Wnt secretion. *Nat. Cell. Biol.* 13 (8), 914–923. doi:10.1038/ncb2281

Helfer, E., Harbour, M. E., Henriot, V., Lakisic, G., Sousa-Blin, C., Volceanov, L., et al. (2013). Endosomal recruitment of the WASH complex: active sequences and mutations impairing interaction with the retromer. *Biol. Cell.* 105 (5), 191–207. doi:10.1111/boc.201200038

Hendy, G. N., Li, T., Girard, M., Feldstein, R. C., Mulay, S., Desjardins, R., et al. (2006). Targeted ablation of the chromogranin a (Chga) gene: normal neuroendocrine dense-core secretory granules and increased expression of other granins. *Mol. Endocrinol.* 20 (8), 1935–1947. doi:10.1210/me.2005-0398

Hirst, J., Irving, C., and Borner, G. H. (2013). Adaptor protein complexes AP-4 and AP-5: new players in endosomal trafficking and progressive spastic paraplegia. *Traffic* 14 (2), 153–164. doi:10.1111/tra.12028

Holt, M. K., Richards, J. E., Cook, D. R., Brierley, D. I., Williams, D. L., Reimann, F., et al. (2019). Preproglucagon neurons in the nucleus of the solitary tract are the main source of brain GLP-1, mediate stress-induced hypophagia, and limit unusually large intakes of food. *Diabetes* 68 (1), 21–33. doi:10.2337/db18-0729

Honing, S., Sosa, M., Hille-Rehfeld, A., and von Figura, K. (1997). The 46-kDa mannose 6-phosphate receptor contains multiple binding sites for clathrin adaptors. *J. Biol. Chem.* 272 (32), 19884–19890. doi:10.1074/jbc.272.32.19884

Hook, V. Y., Eiden, L. E., and Brownstein, M. J. (1982). A carboxypeptidase processing enzyme for enkephalin precursors. *Nature* 295 (5847), 341–342. doi:10.1038/295341a0

Hook, V. Y. (1985). Differential distribution of carboxypeptidase-processing enzyme activity and immunoreactivity in membrane and soluble components of chromaffin granules. *J. Neurochem.* 45 (3), 987–989. doi:10.1111/j.1471-4159.1985.tb04094.x

Horazdovsky, B. F., Davies, B. A., Seaman, M. N., McLaughlin, S. A., Yoon, S., and Emr, S. D. (1997). A sorting nexin-1 homologue, Vps5p, forms a complex with Vps17p and is required for recycling the vacuolar protein-sorting receptor. *Mol. Biol. Cell.* 8 (8), 1529–1541. doi:10.1091/mbc.8.8.1529

Hoyos Sanchez, M. C., Bayat, T., Gee, R. R. F., and Fon Tacer, K. (2023). Hormonal imbalances in prader-willi and schaaf-yang syndromes imply the evolution of specific regulation of hypothalamic neuroendocrine function in mammals. *Int. J. Mol. Sci* 24 (17), 13109. doi:10.3390/ijms241713109

Hosaka, M., Suda, M., Sakai, Y., Izumi, T., Watanabe, T., and Takeuchi, T. (2004). Secretogranin III binds to cholesterol in the secretory granule membrane as an adapter for chromogranin A. *J. Biol. Chem.* 279 (5), 3627–3634. doi:10.1074/jbc.M310104200

Howell, S. L., and Tyhurst, M. (1982). Microtubules, microfilaments and insulin-secretion. *Diabetologia* 22 (5), 301–308. doi:10.1007/BF00253571

Huh, Y. H., Jeon, S. H., and Yoo, S. H. (2003). Chromogranin B-induced secretory granule biogenesis: comparison with the similar role of chromogranin A. *J. Biol. Chem.* 278 (42), 40581–40589. doi:10.1074/jbc.M304942200

Hunt, S. D., Townley, A. K., Danson, C. M., Cullen, P. J., and Stephens, D. J. (2013). Microtubule motors mediate endosomal sorting by maintaining functional domain organization. *J. Cell. Sci.* 126 (11), 2493–2501. doi:10.1242/jcs.122317

Hurtley, S. M. (1993). Recycling of a secretory granule membrane protein after stimulated secretion. *J. Cell. Sci.* 106 (2), 649–655. doi:10.1242/jcs.106.2.649

Jackson, R. S., Creemers, J. W., Ohagi, S., Raffin-Sanson, M. L., Sanders, L., Montague, C. T., et al. (1997). Obesity and impaired prohormone processing associated with mutations in the human prohormone convertase 1 gene. *Nat. Genet.* 16 (3), 303–306. doi:10.1038/ng0797-303

Jefferies, K. C., Cipriano, D. J., and Forgac, M. (2008). Function, structure and regulation of the vacuolar (H+)-ATPases. *Arch. Biochem. Biophys.* 476 (1), 33–42. doi:10.1016/j.abb.2008.03.025

Ji, L., Wu, H. T., Qin, X. Y., and Lan, R. (2017). Dissecting carboxypeptidase E: properties, functions and pathophysiological roles in disease. *Endocr. Connect.* 6 (4), R18–R38. doi:10.1530/EC-17-0020

Jia, D., Gomez, T. S., Billadeau, D. D., and Rosen, M. K. (2012). Multiple repeat elements within the FAM21 tail link the WASH actin regulatory complex to the retromer. *Mol. Biol. Cell.* 23 (12), 2352–2361. doi:10.1091/mbc.E11-12-1059

Jia, D., Zhang, J. S., Li, F., Wang, J., Deng, Z., White, M. A., et al. (2016). Structural and mechanistic insights into regulation of the retromer coat by TBC1d5. *Nat. Commun.* 7, 13305. doi:10.1038/ncomms13305

Johnson, K. F., and Kornfeld, S. (1992a). The cytoplasmic tail of the mannose 6-phosphate/insulin-like growth factor-II receptor has two signals for lysosomal enzyme sorting in the Golgi. *J. Cell. Biol.* 119 (2), 249–257. doi:10.1083/jcb.119.2.249

Johnson, K. F., and Kornfeld, S. (1992b). A His-Leu-Leu sequence near the carboxyl terminus of the cytoplasmic domain of the cation-dependent mannose 6-phosphate receptor is necessary for the lysosomal enzyme sorting function. *J. Biol. Chem.* 267 (24), 17110–17115. doi:10.1016/S0021-9258(18)41900-X

Jones, B. G., Thomas, L., Molloy, S. S., Thulin, C. D., Fry, M. D., Walsh, K. A., et al. (1995). Intracellular trafficking of furin is modulated by the phosphorylation state of a casein kinase II site in its cytoplasmic tail. *EMBO J.* 14 (23), 5869–5883. doi:10.1002/j.1460-2075.1995.tb00275.x

Jutras, I., Seidah, N. G., and Reudelhuber, T. L. (2000). A predicted alpha -helix mediates targeting of the proprotein convertase PC1 to the regulated secretory pathway. *J. Biol. Chem.* 275 (51), 40337–40343. doi:10.1074/jbc.M004757200

Kakhlon, O., Sakya, P., Larijani, B., Watson, R., and Tooze, S. A. (2006). GGA function is required for maturation of neuroendocrine secretory granules. *EMBO J.* 25 (8), 1590–1602. doi:10.1038/sj.emboj.7601067

Kang, Y. K., and Yoo, S. H. (1997). Identification of the secretory vesicle membrane binding region of chromogranin A. *FEBS Lett.* 404 (1), 87–90. doi:10.1016/s0014-5793(97)00099-9

Kang, J. X., Li, Y., and Leaf, A. (1997). Mannose-6-phosphate/insulin-like growth factor-II receptor is a receptor for retinoic acid. *Proc. Natl. Acad. Sci. U. S. A.* 94 (25), 13671–13676. doi:10.1073/pnas.94.25.13671

Kelly, R. B. (1985). Pathways of protein secretion in eukaryotes. *Science* 230 (4721), 25–32. doi:10.1126/science.2994224

Kim, T., Tao-Cheng, J. H., Eiden, L. E., and Loh, Y. P. (2001). Chromogranin A, an "on/off" switch controlling dense-core secretory granule biogenesis. *Cell.* 106 (4), 499–509. doi:10.1016/s0092-8674(01)00459-7

Kim, T., Gondre-Lewis, M. C., Arnaoutova, I., and Loh, Y. P. (2006). Dense-core secretory granule biogenesis. *Physiol. (Bethesda)* 21, 124–133. doi:10.1152/physiol.00043.2005

Klumperman, J., Kuliawat, R., Griffith, J. M., Geuze, H. J., and Arvan, P. (1998). Mannose 6-phosphate receptors are sorted from immature secretory granules via adaptor protein AP-1, clathrin, and syntaxin 6-positive vesicles. *J. Cell. Biol.* 141 (2), 359–371. doi:10.1083/jcb.141.2.359

Kogel, T., and Gerdes, H. H. (2010). Maturation of secretory granules. *Results Probl. Cell. Differ.* 50, 1–20. doi:10.1007/400_2009_31

Koshimizu, H., Kim, T., Cawley, N. X., and Loh, Y. P. (2010). Chromogranin A: A new proposal for trafficking, processing and induction of granule biogenesis. *Regul. Pept.* 160 (1-3), 153–159. doi:10.1016/j.regpep.2009.12.007

Koumandou, V. L., Klute, M. J., Herman, E. K., Nunez-Miguel, R., Dacks, J. B., and Field, M. C. (2011). Evolutionary reconstruction of the retromer complex and its function in Trypanosoma brucei. *J. Cell. Sci.* 124 (9), 1496–1509. doi:10.1242/jcs.081596

Kromer, A., Glombik, M. M., Huttner, W. B., and Gerdes, H. H. (1998). Essential role of the disulfide-bonded loop of chromogranin B for sorting to secretory granules is revealed by expression of a deletion mutant in the absence of endogenous granin synthesis. *J. Cell. Biol.* 140 (6), 1331–1346. doi:10.1083/jcb.140.6.1331

Kvainickas, A., Jimenez-Orgaz, A., Nagele, H., Hu, Z., Dengjel, J., and Steinberg, F. (2017). Cargo-selective SNX-BAR proteins mediate retromer trimer independent retrograde transport. *J. Cell. Biol.* 216 (11), 3677–3693. doi:10.1083/jcb.201702137

Lacombe, M. J., Mercure, C., Dikeakos, J. D., and Reudelhuber, T. L. (2005). Modulation of secretory granule-targeting efficiency by cis and trans compounding of sorting signals. *J. Biol. Chem.* 280 (6), 4803–4807. doi:10.1074/jbc.M408658200

Laguerre, F., Anouar, Y., and Montero-Hadjadje, M. (2020). Chromogranin A in the early steps of the neurosecretory pathway. *IUBMB Life* 72 (4), 524–532. doi:10.1002/iub.2218

Lee, A. K., and Potts, P. R. (2017). A comprehensive guide to the MAGE family of ubiquitin ligases. *J. Mol. Biol.* 429 (8), 1114–1142. doi:10.1016/j.jmb.2017.03.005

Li, P., Merrill, S. A., Jorgensen, E. M., and Shen, K. (2016). Two clathrin adaptor protein complexes instruct axon-dendrite polarity. *Neuron* 90 (3), 564–580. doi:10.1016/j.neuron.2016.04.020

Li, P., Bademosi, A. T., Luo, J., and Meunier, F. A. (2018). Actin remodeling in regulated exocytosis: toward a mesoscopic view. *Trends Cell. Biol.* 28 (9), 685–697. doi:10.1016/j.tcb.2018.04.004

Linardopoulou, E. V., Parghi, S. S., Friedman, C., Osborn, G. E., Parkhurst, S. M., and Trask, B. J. (2007). Human subtelomeric WASH genes encode a new subclass of the WASP family. *PLoS Genet.* 3 (12), e237. doi:10.1371/journal.pgen.0030237

Liu, Y., and Edwards, R. H. (1997). The role of vesicular transport proteins in synaptic transmission and neural degeneration. *Annu. Rev. Neurosci.* 20, 125–156. doi:10.1146/annurev.neuro.20.1.125

Liu, R., Abreu-Blanco, M. T., Barry, K. C., Linardopoulou, E. V., Osborn, G. E., and Parkhurst, S. M. (2009). Wash functions downstream of Rho and links linear and branched actin nucleation factors. *Development* 136 (16), 2849–2860. doi:10.1242/dev.035246

Loh, Y. P., Maldonado, A., Zhang, C., Tam, W. H., and Cawley, N. (2002). Mechanism of sorting proopiomelanocortin and proenkephalin to the regulated secretory pathway of neuroendocrine cells. *Ann. N. Y. Acad. Sci.* 971, 416–425. doi:10.1111/j.1749-6632.2002.tb04504.x

Lou, H., Kim, S. K., Zaitsev, E., Snell, C. R., Lu, B., and Loh, Y. P. (2005). Sorting and activity-dependent secretion of BDNF require interaction of a specific motif with the sorting receptor carboxypeptidase e. *Neuron* 45 (2), 245–255. doi:10.1016/j.neuron.2004.12.037

Lucas, M., and Hierro, A. (2017). Retromer. *Curr. Biol.* 27 (14), R687–R689. doi:10.1016/j.cub.2017.05.072

Ma, M., and Burd, C. G. (2020). Retrograde trafficking and plasma membrane recycling pathways of the budding yeast *Saccharomyces cerevisiae*. *Traffic* 21 (1), 45–59. doi:10.1111/tra.12693

Ma, G. Q., Wang, B., Wang, H. B., Wang, Q., and Bao, L. (2008). Short elements with charged amino acids form clusters to sort protachykinin into large dense-core vesicles. *Traffic* 9 (12), 2165–2179. doi:10.1111/j.1600-0854.2008.00836.x

Ma, C. J., Yang, Y., Kim, T., Chen, C. H., Polevoy, G., Vissa, M., et al. (2020). An early endosome-derived retrograde trafficking pathway promotes secretory granule maturation. *J. Cell. Biol.* 219 (3). doi:10.1083/jcb.201808017

Ma, C. J., Burgess, J., and Brill, J. A. (2021). Maturing secretory granules: where secretory and endocytic pathways converge. *Adv. Biol. Regul.* 80, 100807. doi:10.1016/j.jbior.2021.100807

MacDonald, E., Savage, B., and Zech, T. (2020). Connecting the dots: combined control of endocytic recycling and degradation. *Biochem. Soc. Trans.* 48 (6), 2377–2386. doi:10.1042/BST20180255

Marx, R., El Meskini, R., Johns, D. C., and Mains, R. E. (1999). Differences in the ways sympathetic neurons and endocrine cells process, store, and secrete exogenous neuropeptides and peptide-processing enzymes. *J. Neurosci.* 19 (19), 8300–8311. doi:10.1523/JNEUROSCI.19-19-08300.1999

Mbikay, M., Croissandeau, G., Sirois, F., Anini, Y., Mayne, J., Seidah, N. G., et al. (2007). A targeted deletion/insertion in the mouse Pcsk1 locus is associated with homozygous embryo preimplantation lethality, mutant allele preferential transmission and heterozygous female susceptibility to dietary fat. *Dev. Biol.* 306 (2), 584–598. doi:10.1016/j.ydbio.2007.03.523

McGirr, R., Guizzetti, L., and Dhanvantari, S. (2013). The sorting of proglucagon to secretory granules is mediated by carboxypeptidase E and intrinsic sorting signals. *J. Endocrinol.* 217 (2), 229–240. doi:10.1530/JOE-12-0468

McGough, I. J., and Cullen, P. J. (2011). Recent advances in retromer biology. *Traffic* 12 (8), 963–971. doi:10.1111/j.1600-0854.2011.01201.x

McNally, K. E., and Cullen, P. J. (2018). Endosomal retrieval of cargo: retromer is not alone. *Trends Cell. Biol.* 28 (10), 807–822. doi:10.1016/j.tcb.2018.06.005

McNally, K. E., Faulkner, R., Steinberg, F., Gallon, M., Ghai, R., Pim, D., et al. (2017). Retriever is a multiprotein complex for retromer-independent endosomal cargo recycling. *Nat. Cell. Biol.* 19 (10), 1214–1225. doi:10.1038/ncb3610

Meldolesi, J. (2002). Rapidly exchanging Ca(2+) stores: ubiquitous partners of surface channels in neurons. *News Physiol. Sci.* 17, 144–149. doi:10.1152/nips.01385.2002

Meresse, S., Ludwig, T., Frank, R., and Hoflack, B. (1990). Phosphorylation of the cytoplasmic domain of the bovine cation-independent mannose 6-phosphate receptor. Serines 2421 and 2492 are the targets of a casein kinase II associated to the Golgi-derived HAI adaptor complex. *J. Biol. Chem.* 265 (31), 18833–18842. doi:10.1016/S0021-9258(17)30589-6

Miklavc, P., and Frick, M. (2020). Actin and myosin in non-neuronal exocytosis. *Cells* 9 (6). doi:10.3390/cells9061455

Mitok, K. A., Keller, M. P., and Attie, A. D. (2022). Sorting through the extensive and confusing roles of sortilin in metabolic disease. *J. Lipid Res.* 63 (8), 100243. doi:10.1016/j.jlr.2022.100243

Montero-Hadjadje, M., Vaingankar, S., Elias, S., Tostivint, H., Mahata, S. K., and Anouar, Y. (2008). Chromogranins A and B and secretogranin II: evolutionary and functional aspects. *Acta Physiol. (Oxf)* 192 (2), 309–324. doi:10.1111/j.1748-1716.2007.01806.x

Montero-Hadjadje, M., Elias, S., Chevalier, L., Benard, M., Tanguy, Y., Turquier, V., et al. (2009). Chromogranin A promotes peptide hormone sorting to mobile granules in constitutively and regulated secreting cells: role of conserved N- and C-terminal peptides. *J. Biol. Chem.* 284 (18), 12420–12431. doi:10.1074/jbc.M805607200

Natori, S., and Huttner, W. B. (1996). Chromogranin B (secretogranin I) promotes sorting to the regulated secretory pathway of processing intermediates derived from a peptide hormone precursor. *Proc. Natl. Acad. Sci. U. S. A.* 93 (9), 4431–4436. doi:10.1073/pnas.93.9.4431

Neuman, S. D., Terry, E. L., Selegue, J. E., Cavanagh, A. T., and Bashirullah, A. (2021). Mistargeting of secretory cargo in retromer-deficient cells. *Dis. Model. Mech.* 14 (1). doi:10.1242/dmm.046417

Nielsen, M. S., Madsen, P., Christensen, E. I., Nykjaer, A., Gliemann, J., Kasper, D., et al. (2001). The sortilin cytoplasmic tail conveys Golgi-endosome transport and binds the VHS domain of the GGA2 sorting protein. *EMBO J.* 20 (9), 2180–2190. doi:10.1093/emboj/20.9.2180

Nillni, E. A. (2007). Regulation of prohormone convertases in hypothalamic neurons: implications for prothyrotropin-releasing hormone and proopiomelanocortin. *Endocrinology* 148 (9), 4191–4200. doi:10.1210/en.2007-0173

Nillni, E. A. (2010). Regulation of the hypothalamic thyrotropin releasing hormone (TRH) neuron by neuronal and peripheral inputs. *Front. Neuroendocrinol.* 31 (2), 134–156. doi:10.1016/j.yfrne.2010.01.001

Normant, E., and Loh, Y. P. (1998). Depletion of carboxypeptidase E, a regulated secretory pathway sorting receptor, causes misrouting and constitutive secretion of proinsulin and proenkephalin, but not chromogranin A. *Endocrinology* 139 (4), 2137–2145. doi:10.1210/endo.139.4.5951

Nothwehr, S. F., and Hindes, A. E. (1997). The yeast VPS5/GRD2 gene encodes a sorting nexin-1-like protein required for localizing membrane proteins to the late Golgi. *J. Cell. Sci.* 110 (9), 1063–1072. doi:10.1242/jcs.110.9.1063

O'Connor, D. T., and Frigon, R. P. (1984). Chromogranin A, the major catecholamine storage vesicle soluble protein. Multiple size forms, subcellular storage, and regional distribution in chromaffin and nervous tissue elucidated by radioimmunoassay. *J. Biol. Chem.* 259 (5), 3237–3247. doi:10.1016/S0021-9258(17)43286-8

Oka, Y., Rozek, L. M., and Czech, M. P. (1985). Direct demonstration of rapid insulin-like growth factor II Receptor internalization and recycling in rat adipocytes. Insulin stimulates 125I-insulin-like growth factor II degradation by modulating the IGF-II receptor recycling process. *J. Biol. Chem.* 260 (16), 9435–9442. doi:10.1016/S0021-9258(17)39385-7

Oshima, A., Nolan, C. M., Kyle, J. W., Grubb, J. H., and Sly, W. S. (1988). The human cation-independent mannose 6-phosphate receptor. Cloning and sequence of the full-length cDNA and expression of functional receptor in COS cells. *J. Biol. Chem.* 263 (5), 2553–2562. doi:10.1016/S0021-9258(18)69243-9

Padrick, S. B., Doolittle, L. K., Brautigam, C. A., King, D. S., and Rosen, M. K. (2011). Arp2/3 complex is bound and activated by two WASP proteins. *Proc. Natl. Acad. Sci. U. S. A.* 108 (33), E472–E479. doi:10.1073/pnas.1100236108

Palade, G. (1975). Intracellular aspects of the process of protein synthesis. *Science* 189 (4200), 347–358. doi:10.1126/science.1096303

Paquet, L., Zhou, A., Chang, E. Y., and Mains, R. E. (1996). Peptide biosynthetic processing: distinguishing prohormone convertases PC1 and PC2. *Mol. Cell. Endocrinol.* 120 (2), 161–168. doi:10.1016/0303-7207(96)03834-8

Park, J. J., and Loh, Y. P. (2008). How peptide hormone vesicles are transported to the secretion site for exocytosis. *Mol. Endocrinol.* 22 (12), 2583–2595. doi:10.1210/me.2008-0209

Parmer, R. J., Xi, X. P., Wu, H. J., Helman, L. J., and Petz, L. N. (1993). Secretory protein traffic. Chromogranin A contains a dominant targeting signal for the regulated pathway. *J. Clin. Invest.* 92 (2), 1042–1054. doi:10.1172/JCI116609

Peden, A. A., Park, G. Y., and Scheller, R. H. (2001). The Di-leucine motif of vesicle-associated membrane protein 4 is required for its localization and AP-1 binding. *J. Biol. Chem.* 276 (52), 49183–49187. doi:10.1074/jbc.M106646200

Perello, M., Stuart, R., and Nillni, E. A. (2008). Prothyrotropin-releasing hormone targets its processing products to different vesicles of the secretory pathway. *J. Biol. Chem.* 283 (29), 19936–19947. doi:10.1074/jbc.M800732200

Phillips-Krawczak, C. A., Singla, A., Starokadomskyy, P., Deng, Z., Osborne, D. G., Li, H., et al. (2015). COMMD1 is linked to the WASH complex and regulates endosomal trafficking of the copper transporter ATP7A. *Mol Biol Cell.* 26 (1), 91–103. doi:10.1091/mbc.E14-06-1073

Piotrowski, J. T., Gomez, T. S., Schoon, R. A., Mangalam, A. K., and Billadeau, D. D. (2013). WASH knockout T cells demonstrate defective receptor trafficking, proliferation, and effector function. *Mol. Cell. Biol.* 33 (5), 958–973. doi:10.1128/MCB.01288-12

Placidi, G., and Campa, C. C. (2021). Deliver on time or pay the fine: scheduling in membrane trafficking. *Int. J. Mol. Sci.* 22 (21). doi:10.3390/ijms222111773

Ponnambalam, S., and Baldwin, S. A. (2003). Constitutive protein secretion from the trans-Golgi network to the plasma membrane. *Mol. Membr. Biol.* 20 (2), 129–139. doi:10.1080/0968768031000084172

Progida, C., Cogli, L., Piro, F., De Luca, A., Bakke, O., and Bucci, C. (2010). Rab7b controls trafficking from endosomes to the TGN. *J. Cell. Sci.* 123 (9), 1480–1491. doi:10.1242/jcs.051474

Puertollano, R., Aguilar, R. C., Gorshkova, I., Crouch, R. J., and Bonifacino, J. S. (2001). Sorting of mannose 6-phosphate receptors mediated by the GGAs. *Science* 292 (5522), 1712–1716. doi:10.1126/science.1060750

Purchio, A. F., Cooper, J. A., Brunner, A. M., Lioubin, M. N., Gentry, L. E., Kovacina, K. S., et al. (1988). Identification of mannose 6-phosphate in two asparagine-linked sugar chains of recombinant transforming growth factor-beta 1 precursor. *J. Biol. Chem.* 263 (28), 14211–14215. doi:10.1016/S0021-9258(18)68207-9

Puthenveedu, M. A., Lauffer, B., Temkin, P., Vistein, R., Carlton, P., Thorn, K., et al. (2010). Sequence-dependent sorting of recycling proteins by actin-stabilized endosomal microdomains. *Cell.* 143 (5), 761–773. doi:10.1016/j.cell.2010.10.003

Quinn, D., Orci, L., Ravazzola, M., and Moore, H. P. (1991). Intracellular transport and sorting of mutant human proinsulins that fail to form hexamers. *J. Cell. Biol.* 113 (5), 987–996. doi:10.1083/jcb.113.5.987

Reck, J., Beuret, N., Demirci, E., Prescianotto-Baschong, C., and Spiess, M. (2022). Small disulfide loops in peptide hormones mediate self-aggregation and secretory granule sorting. *Life Sci. Alliance* 5 (5). doi:10.26508/lsa.202101279

Reitz, C. (2018). Retromer dysfunction and neurodegenerative disease. *Curr. Genomics* 19 (4), 279–288. doi:10.2174/1389202919666171024122809

Ren, X., Farias, G. G., Canagarajah, B. J., Bonifacino, J. S., and Hurley, J. H. (2013). Structural basis for recruitment and activation of the AP-1 clathrin adaptor complex by Arf1. *Cell.* 152 (4), 755–767. doi:10.1016/j.cell.2012.12.042

Rindler, M. J. (1998). Carboxypeptidase E, a peripheral membrane protein implicated in the targeting of hormones to secretory granules, co-aggregates with granule content proteins at acidic pH. *J. Biol. Chem.* 273 (47), 31180–31185. doi:10.1074/jbc.273.47.31180

Robinson, M. S. (2004). Adaptable adaptors for coated vesicles. *Trends Cell. Biol.* 14 (4), 167–174. doi:10.1016/j.tcb.2004.02.002

Rojas, R., van Vlijmen, T., Mardones, G. A., Prabhu, Y., Rojas, A. L., Mohammed, S., et al. (2008). Regulation of retromer recruitment to endosomes by sequential action of Rab5 and Rab7. *J. Cell. Biol.* 183 (3), 513–526. doi:10.1083/jcb.200804048

Rojo Pulido, I., Nightingale, T. D., Darchen, F., Seabra, M. C., Cutler, D. F., and Gerke, V. (2011). Myosin Va acts in concert with Rab27a and MyRIP to regulate acute von-Willebrand factor release from endothelial cells. *Traffic* 12 (10), 1371–1382. doi:10.1111/j.1600-0854.2011.01248.x

Rose, S. D., Lejen, T., Casaletti, L., Larson, R. E., Pene, T. D., and Trifaro, J. M. (2003). Myosins II and V in chromaffin cells: myosin V is a chromaffin vesicle molecular motor involved in secretion. *J. Neurochem.* 85 (2), 287–298. doi:10.1046/j.1471-4159.2003.01649.x

Rudolf, R., Salm, T., Rustom, A., and Gerdes, H. H. (2001). Dynamics of immature secretory granules: role of cytoskeletal elements during transport, cortical restriction, and F-actin-dependent tethering. *Mol. Biol. Cell.* 12 (5), 1353–1365. doi:10.1091/mbc.12.5.1353

Rudolf, R., Kogel, T., Kuznetsov, S. A., Salm, T., Schlicker, O., Hellwig, A., et al. (2003). Myosin Va facilitates the distribution of secretory granules in the F-actin rich cortex of PC12 cells. *J. Cell. Sci.* 116 (7), 1339–1348. doi:10.1242/jcs.00317

Saito, N., Takeuchi, T., Kawano, A., Hosaka, M., Hou, N., and Torii, S. (2011). Luminal interaction of phogrin with carboxypeptidase E for effective targeting to secretory granules. *Traffic* 12 (4), 499–506. doi:10.1111/j.1600-0854.2011.01159.x

Sannerud, R., Saraste, J., and Goud, B. (2003). Retrograde traffic in the biosynthetic-secretory route: pathways and machinery. *Curr. Opin. Cell. Biol.* 15 (4), 438–445. doi:10.1016/s0955-0674(03)00077-2

Scamuffa, N., Calvo, F., Chretien, M., Seidah, N. G., and Khatib, A. M. (2006). Proprotein convertases: lessons from knockouts. *FASEB J.* 20 (12), 1954–1963. doi:10.1096/fj.05-5491rev

Schmidt, B., Kiecke-Siemsen, C., Waheed, A., Braulke, T., and von Figura, K. (1995). Localization of the insulin-like growth factor II binding site to amino acids 1508-1566 in repeat 11 of the mannose 6-phosphate/insulin-like growth factor II receptor. *J. Biol. Chem.* 270 (25), 14975–14982. doi:10.1074/jbc.270.25.14975

Seaman, M., and Freeman, C. L. (2014). Analysis of the Retromer complex-WASH complex interaction illuminates new avenues to explore in Parkinson disease. *Commun. Integr. Biol.* 7, e29483. doi:10.4161/cib.29483

Seaman, M. N., McCaffery, J. M., and Emr, S. D. (1998). A membrane coat complex essential for endosome-to-Golgi retrograde transport in yeast. *J. Cell. Biol.* 142 (3), 665–681. doi:10.1083/jcb.142.3.665

Seaman, M. N., Harbour, M. E., Tattersall, D., Read, E., and Bright, N. (2009). Membrane recruitment of the cargo-selective retromer subcomplex is catalysed by the small GTPase Rab7 and inhibited by the Rab-GAP TBC1D5. *J. Cell. Sci.* 122 (14), 2371–2382. doi:10.1242/jcs.048686

Seaman, M. N., Gautreau, A., and Billadeau, D. D. (2013). Retromer-mediated endosomal protein sorting: all WASHed up. *Trends Cell. Biol.* 23 (11), 522–528. doi:10.1016/j.tcb.2013.04.010

Seaman, M. N. (2004). Cargo-selective endosomal sorting for retrieval to the Golgi requires retromer. *J. Cell. Biol.* 165 (1), 111–122. doi:10.1083/jcb.200312034

Seaman, M. N. (2007). Identification of a novel conserved sorting motif required for retromer-mediated endosome-to-TGN retrieval. *J. Cell. Sci.* 120 (14), 2378–2389. doi:10.1242/jcs.009654

Seaman, M. N. J. (2018). Retromer and the cation-independent mannose 6-phosphate receptor-Time for a trial separation? *Traffic* 19 (2), 150–152. doi:10.1111/tra.12542

Seidah, N. G., and Prat, A. (2012). The biology and therapeutic targeting of the proprotein convertases. *Nat. Rev. Drug Discov.* 11 (5), 367–383. doi:10.1038/nrd3699

Seidah, N. G., Mattei, M. G., Gaspar, L., Benjannet, S., Mbikay, M., and Chretien, M. (1991). Chromosomal assignments of the genes for neuroendocrine convertase PC1 (NEC1) to human 5q15-21, neuroendocrine convertase PC2 (NEC2) to human 20p11.1-11.2, and furin (mouse 7[D1-E2] region). *Genomics* 11 (1), 103–107. doi:10.1016/0888-7543(91)90106-o

Seidah, N. G., Sadr, M. S., Chretien, M., and Mbikay, M. (2013). The multifaceted proprotein convertases: their unique, redundant, complementary, and opposite functions. *J. Biol. Chem.* 288 (30), 21473–21481. doi:10.1074/jbc.R113.481549

Seidah, N. G. (2011). The proprotein convertases, 20 years later. *Methods Mol. Biol.* 768, 23–57. doi:10.1007/978-1-61779-204-5_3

Shitara, A., Bleck, C. K. E., and Weigert, R. (2020). Cdc42 controls secretory granules morphology in rodent salivary glands *in vivo*. *Commun. Integr. Biol.* 13 (1), 22–26. doi:10.1080/19420889.2020.1724605

Simonetti, B., and Cullen, P. J. (2019). Actin-dependent endosomal receptor recycling. *Curr. Opin. Cell. Biol.* 56, 22–33. doi:10.1016/j.ceb.2018.08.006

Simonetti, B., Danson, C. M., Heesom, K. J., and Cullen, P. J. (2017). Sequence-dependent cargo recognition by SNX-BARs mediates retromer-independent transport of CI-MPR. *J. Cell. Biol.* 216 (11), 3695–3712. doi:10.1083/jcb.201703015

Simonetti, B., Paul, B., Chaudhari, K., Weeratunga, S., Steinberg, F., Gorla, M., et al. (2019). Molecular identification of a BAR domain-containing coat complex for endosomal recycling of transmembrane proteins. *Nat. Cell. Biol.* 21 (10), 1219–1233. doi:10.1038/s41556-019-0393-3

Singla, A., Fedoseienko, A., Giridharan, S. S. P., Overlee, B. L., Lopez, A., Jia, D., et al. (2019). Endosomal PI(3)P regulation by the COMMD/CCDC22/CCDC93 (CCC) complex controls membrane protein recycling. *Nat. Commun.* 10 (1), 4271. doi:10.1038/s41467-019-12221-6

Song, L., and Fricker, L. (1995a). Processing of procarboxypeptidase E into carboxypeptidase E occurs in secretory vesicles. *J. Neurochem.* 65 (1), 444–453. doi:10.1046/j.1471-4159.1995.65010444.x

Song, L., and Fricker, L. D. (1995b). Calcium- and pH-dependent aggregation of carboxypeptidase E. *J. Biol. Chem.* 270 (14), 7963–7967. doi:10.1074/jbc.270.14.7963

Steinberg, F., Gallon, M., Winfield, M., Thomas, E. C., Bell, A. J., Heesom, K. J., et al. (2013). A global analysis of SNX27-retromer assembly and cargo specificity reveals a function in glucose and metal ion transport. *Nat. Cell. Biol.* 15 (5), 461–471. doi:10.1038/ncb2721

Steiner, D. F. (1998). The proprotein convertases. *Curr. Opin. Chem. Biol.* 2 (1), 31–39. doi:10.1016/s1367-5931(98)80033-1

Steveson, T. C., Zhao, G. C., Keutmann, H. T., Mains, R. E., and Eipper, B. A. (2001). Access of a membrane protein to secretory granules is facilitated by phosphorylation. *J. Biol. Chem.* 276 (43), 40326–40337. doi:10.1074/jbc.M011460200

Sudhof, T. C. (2002). Synaptotagmins: why so many? *J. Biol. Chem.* 277 (10), 7629–7632. doi:10.1074/jbc.R100052200

Supattapone, S., Fricker, L. D., and Snyder, S. H. (1984). Purification and characterization of a membrane-bound enkephalin-forming carboxypeptidase, "enkephalin convertase. *J. Neurochem.* 42 (4), 1017–1023. doi:10.1111/j.1471-4159.1984.tb12705.x

Suzuki, S. W., Chuang, Y. S., Li, M., Seaman, M. N. J., and Emr, S. D. (2019). A bipartite sorting signal ensures specificity of retromer complex in membrane protein recycling. *J. Cell. Biol.* 218 (9), 2876–2886. doi:10.1083/jcb.201901019

Tam, W. W., Andreasson, K. I., and Loh, Y. P. (1993). The amino-terminal sequence of pro-opiomelanocortin directs intracellular targeting to the regulated secretory pathway. *Eur. J. Cell. Biol.* 62 (2), 294–306.

Tan, J. Z. A., and Gleeson, P. A. (2019). Cargo sorting at the trans-golgi network for shunting into specific transport routes: role of arf small G proteins and adaptor complexes. *Cells* 8 (6). doi:10.3390/cells8060531

Tanguy, E., Carmon, O., Wang, Q., Jeandel, L., Chasserot-Golaz, S., Montero-Hadjadje, M., et al. (2016). Lipids implicated in the journey of a secretory granule: from biogenesis to fusion. *J. Neurochem.* 137 (6), 904–912. doi:10.1111/jnc.13577

Tanguy, E., Coste de Bagneaux, P., Kassas, N., Ammar, M. R., Wang, Q., Haeberle, A. M., et al. (2020). Mono- and poly-unsaturated phosphatidic acid regulate distinct steps of regulated exocytosis in neuroendocrine cells. *Cell. Rep.* 32 (7), 108026. doi:10.1016/j.celrep.2020.108026

Tatemoto, K., Efendic, S., Mutt, V., Makk, G., Feistner, G. J., and Barchas, J. D. (1986). Pancreastatin, a novel pancreatic peptide that inhibits insulin secretion. *Nature* 324 (6096), 476–478. doi:10.1038/324476a0

Taupenot, L., Harper, K. L., Mahapatra, N. R., Parmer, R. J., Mahata, S. K., and O'Connor, D. T. (2002). Identification of a novel sorting determinant for the regulated pathway in the secretory protein chromogranin A. *J. Cell. Sci.* 115 (24), 4827–4841. doi:10.1242/jcs.00140

Taupenot, L., Harper, K. L., and O'Connor, D. T. (2003). The chromogranin-secretogranin family. *N. Engl. J. Med.* 348 (12), 1134–1149. doi:10.1056/NEJMra021405

Taylor, N. A., Jan, G., Scougall, K. T., Docherty, K., and Shennan, K. I. (1998). Sorting of PC2 to the regulated secretory pathway in AtT20 cells. *J. Mol. Endocrinol.* 21 (2), 209–216. doi:10.1677/jme.0.0210209

Temkin, P., Lauffer, B., Jager, S., Cimermancic, P., Krogan, N. J., and von Zastrow, M. (2011). SNX27 mediates retromer tubule entry and endosome-to-plasma membrane trafficking of signalling receptors. *Nat. Cell. Biol.* 13 (6), 715–721. doi:10.1038/ncb2252

Thiele, C., and Huttner, W. B. (1998a). The disulfide-bonded loop of chromogranins, which is essential for sorting to secretory granules, mediates homodimerization. *J. Biol. Chem.* 273 (2), 1223–1231. doi:10.1074/jbc.273.2.1223

Thiele, C., and Huttner, W. B. (1998b). Protein and lipid sorting from the trans-Golgi network to secretory granules-recent developments. *Semin. Cell. Dev. Biol.* 9 (5), 511–516. doi:10.1006/scdb.1998.0259

Thureson-Klein, A. (1983). Exocytosis from large and small dense cored vesicles in noradrenergic nerve terminals. *Neuroscience* 10 (2), 245–259. doi:10.1016/0306-4522(83)90132-x

Tooze, S. A., Flatmark, T., Tooze, J., and Huttner, W. B. (1991). Characterization of the immature secretory granule, an intermediate in granule biogenesis. *J. Cell. Biol.* 115 (6), 1491–1503. doi:10.1083/jcb.115.6.1491

Tooze, S. A. (1998). Biogenesis of secretory granules in the trans-Golgi network of neuroendocrine and endocrine cells. *Biochim. Biophys. Acta* 1404 (1-2), 231–244. doi:10.1016/s0167-4889(98)00059-7

Torii, S., Saito, N., Kawano, A., Zhao, S., Izumi, T., and Takeuchi, T. (2005). Cytoplasmic transport signal is involved in phogrin targeting and localization to secretory granules. *Traffic* 6 (12), 1213–1224. doi:10.1111/j.1600-0854.2005.00353.x

Traub, L. M., Ostrom, J. A., and Kornfeld, S. (1993). Biochemical dissection of AP-1 recruitment onto Golgi membranes. *J. Cell. Biol.* 123 (3), 561–573. doi:10.1083/jcb.123.3.561

Urbe, S., Dittie, A. S., and Tooze, S. A. (1997). pH-dependent processing of secretogranin II by the endopeptidase PC2 in isolated immature secretory granules. *Biochem. J.* 321, 65–74. doi:10.1042/bj3210065

Urbe, S., Page, L. J., and Tooze, S. A. (1998). Homotypic fusion of immature secretory granules during maturation in a cell-free assay. *J. Cell. Biol.* 143 (7), 1831–1844. doi:10.1083/jcb.143.7.1831

van den Berg, R., and Hoogenraad, C. C. (2012). Molecular motors in cargo trafficking and synapse assembly. *Adv. Exp. Med. Biol.* 970, 173–196. doi:10.1007/978-3-7091-0932-8_8

Varlamov, O., Eng, F. J., Novikova, E. G., and Fricker, L. D. (1999). Localization of metallocarboxypeptidase D in AtT-20 cells. Potential role in prohormone processing. *J. Biol. Chem.* 274 (21), 14759–14767. doi:10.1074/jbc.274.21.14759

Verges, M., Luton, F., Gruber, C., Tiemann, F., Reinders, L. G., Huang, L., et al. (2004). The mammalian retromer regulates transcytosis of the polymeric immunoglobulin receptor. *Nat. Cell. Biol.* 6 (8), 763–769. doi:10.1038/ncb1153

Veugelers, K., Motyka, B., Goping, I. S., Shostak, I., Sawchuk, T., and Bleackley, R. C. (2006). Granule-mediated killing by granzyme B and perforin requires a mannose 6-phosphate receptor and is augmented by cell surface heparan sulfate. *Mol. Biol. Cell.* 17 (2), 623–633. doi:10.1091/mbc.e05-07-0631

Waguri, S., Dewitte, F., Le Borgne, R., Rouille, Y., Uchiyama, Y., Dubremetz, J. F., et al. (2003). Visualization of TGN to endosome trafficking through fluorescently labeled MPR and AP-1 in living cells. *Mol. Biol. Cell.* 14 (1), 142–155. doi:10.1091/mbc.e02-06-0338

Wang, Y., Thiele, C., and Huttner, W. B. (2000). Cholesterol is required for the formation of regulated and constitutive secretory vesicles from the trans-Golgi network. *Traffic* 1 (12), 952–962. doi:10.1034/j.1600-0854.2000.011205.x

Wang, J., Fedoseienko, A., Chen, B., Burstein, E., Jia, D., and Billadeau, D. D. (2018). Endosomal receptor trafficking: retromer and beyond. *Traffic* 19 (8), 578–590. doi:10.1111/tra.12574

Wasmeier, C., Burgos, P. V., Trudeau, T., Davidson, H. W., and Hutton, J. C. (2005). An extended tyrosine-targeting motif for endocytosis and recycling of the dense-core vesicle membrane protein phogrin. *Traffic* 6 (6), 474–487. doi:10.1111/j.1600-0854.2005.00292.x

Welch, M. D., and Mullins, R. D. (2002). Cellular control of actin nucleation. *Annu. Rev. Cell. Dev. Biol.* 18, 247–288. doi:10.1146/annurev.cellbio.18.040202.112133

Wendler, F., Page, L., Urbe, S., and Tooze, S. A. (2001). Homotypic fusion of immature secretory granules during maturation requires syntaxin 6. *Mol. Biol. Cell.* 12 (6), 1699–1709. doi:10.1091/mbc.12.6.1699

Wickner, W., and Schekman, R. (2008). Membrane fusion. *Nat. Struct. Mol. Biol.* 15 (7), 658–664. doi:10.1038/nsmb.1451

Yong, X., Zhao, L., Deng, W., Sun, H., Zhou, X., Mao, L., et al. (2020). Mechanism of cargo recognition by retromer-linked SNX-BAR proteins. *PLoS Biol.* 18 (3), e3000631. doi:10.1371/journal.pbio.3000631

Yong, X., Mao, L., Seaman, M. N. J., and Jia, D. (2022). An evolving understanding of sorting signals for endosomal retrieval. *iScience* 25 (5), 104254. doi:10.1016/j.isci.2022.104254

Yoo, S. H., and Albanesi, J. P. (1991). High capacity, low affinity Ca2+ binding of chromogranin A. Relationship between the pH-induced conformational change and Ca2+ binding property. *J. Biol. Chem.* 266 (12), 7740–7745. doi:10.1016/S0021-9258(20)89511-8

Yoo, S. H., and Lewis, M. S. (1993). Dimerization and tetramerization properties of the C-terminal region of chromogranin A: A thermodynamic analysis. *Biochemistry* 32 (34), 8816–8822. doi:10.1021/bi00085a012

Yoo, S. H. (1994). pH-dependent interaction of chromogranin A with integral membrane proteins of secretory vesicle including 260-kDa protein reactive to inositol 1,4,5-triphosphate receptor antibody. *J. Biol. Chem.* 269 (16), 12001–12006. doi:10.1016/S0021-9258(17)32673-X

Zech, T., Calaminus, S. D., Caswell, P., Spence, H. J., Carnell, M., Insall, R. H., et al. (2011). The Arp2/3 activator WASH regulates alpha5beta1-integrin-mediated invasive migration. *J. Cell. Sci.* 124 (22), 3753–3759. doi:10.1242/jcs.080986

Zhang, C. F., Snell, C. R., and Loh, Y. P. (1999). Identification of a novel prohormone sorting signal-binding site on carboxypeptidase E, a regulated secretory pathway-sorting receptor. *Mol. Endocrinol.* 13 (4), 527–536. doi:10.1210/mend.13.4.0267

Zhang, C. F., Dhanvantari, S., Lou, H., and Loh, Y. P. (2003). Sorting of carboxypeptidase E to the regulated secretory pathway requires interaction of its transmembrane domain with lipid rafts. *Biochem. J.* 369 (3), 453–460. doi:10.1042/BJ20020827

Zhang, X., Bao, L., and Ma, G. Q. (2010). Sorting of neuropeptides and neuropeptide receptors into secretory pathways. *Prog. Neurobiol.* 90 (2), 276–283. doi:10.1016/j.pneurobio.2009.10.011

Zhang, H., Huang, T., Hong, Y., Yang, W., Zhang, X., Luo, H., et al. (2018). The retromer complex and sorting nexins in neurodegenerative diseases. *Front. Aging Neurosci.* 10, 79. doi:10.3389/fnagi.2018.00079

Zhou, A., Webb, G., Zhu, X., and Steiner, D. F. (1999). Proteolytic processing in the secretory pathway. *J. Biol. Chem.* 274 (30), 20745–20748. doi:10.1074/jbc.274.30.20745

Zhu, X., Zhou, A., Dey, A., Norrbom, C., Carroll, R., Zhang, C., et al. (2002). Disruption of PC1/3 expression in mice causes dwarfism and multiple neuroendocrine peptide processing defects. *Proc. Natl. Acad. Sci. U. S. A.* 99 (16), 10293–10298. doi:10.1073/pnas.162352599

frontiers | Frontiers in Physiology

TYPE Review
PUBLISHED 02 November 2023
DOI 10.3389/fphys.2023.1263420

OPEN ACCESS

EDITED BY
Martin Van Der Laan,
Saarland University, Germany

REVIEWED BY
Julia C. Fitzgerald,
University of Tübingen, Germany
Dejana Mokranjac,
Ludwig Maximilian University of Munich, Germany

*CORRESPONDENCE
Nathan N. Alder,
nathan.alder@uconn.edu

†These authors have contributed equally to this work

RECEIVED 19 July 2023
ACCEPTED 02 October 2023
PUBLISHED 02 November 2023

CITATION
Reed AL, Mitchell W, Alexandrescu AT and Alder NN (2023), Interactions of amyloidogenic proteins with mitochondrial protein import machinery in aging-related neurodegenerative diseases.
Front. Physiol. 14:1263420.
doi: 10.3389/fphys.2023.1263420

Interactions of amyloidogenic proteins with mitochondrial protein import machinery in aging-related neurodegenerative diseases

Ashley L. Reed[1†], Wayne Mitchell[2†], Andrei T. Alexandrescu[1] and Nathan N. Alder[1*]

[1]Department of Molecular and Cell Biology, University of Connecticut, Storrs, CT, United States, [2]Department of Medicine, Brigham and Women's Hospital, Harvard Medical School, Boston, MA, United States

Most mitochondrial proteins are targeted to the organelle by N-terminal mitochondrial targeting sequences (MTSs, or "presequences") that are recognized by the import machinery and subsequently cleaved to yield the mature protein. MTSs do not have conserved amino acid compositions, but share common physicochemical properties, including the ability to form amphipathic α-helical structures enriched with basic and hydrophobic residues on alternating faces. The lack of strict sequence conservation implies that some polypeptides can be mistargeted to mitochondria, especially under cellular stress. The pathogenic accumulation of proteins within mitochondria is implicated in many aging-related neurodegenerative diseases, including Alzheimer's, Parkinson's, and Huntington's diseases. Mechanistically, these diseases may originate in part from mitochondrial interactions with amyloid-β precursor protein (APP) or its cleavage product amyloid-β (Aβ), α-synuclein (α-syn), and mutant forms of huntingtin (mHtt), respectively, that are mediated in part through their associations with the mitochondrial protein import machinery. Emerging evidence suggests that these amyloidogenic proteins may present cryptic targeting signals that act as MTS mimetics and can be recognized by mitochondrial import receptors and transported into different mitochondrial compartments. Accumulation of these mistargeted proteins could overwhelm the import machinery and its associated quality control mechanisms, thereby contributing to neurological disease progression. Alternatively, the uptake of amyloidogenic proteins into mitochondria may be part of a protein quality control mechanism for clearance of cytotoxic proteins. Here we review the pathomechanisms of these diseases as they relate to mitochondrial protein import and effects on mitochondrial function, what features of APP/Aβ, α-syn and mHtt make them suitable substrates for the import machinery, and how this information can be leveraged for the development of therapeutic interventions.

KEYWORDS

mitochondria, amyloids, neurodegeneration, protein import, cryptic targeting, targeting signals

1 Introduction

Alzheimer's Disease (AD), Parkinson's Disease (PD) and Huntington's Disease (HD) are distinct neurodegenerative disorders that involve the progressive loss of neuronal structure and function. They are collectively classified as proteopathies, which involve severe disruption in cellular protein homeostasis (proteostasis) associated with protein misfolding as well as disruptions in protein processing and localization (Chowhan et al., 2015). Although the mechanistic causes of these diseases are incompletely understood, each is associated with the pathogenic accumulation of specific proteins. Amyloid-β (Aβ), the proteolytic product of amyloid-β precursor protein (APP), is associated with AD (Rocchi et al., 2003; Tcw and Goate, 2017); α-synuclein (α-syn) is associated with PD and other synucleinopathies (Stefanis, 2012); and expanded polyglutamine (poly-Q) repeats underpin a range of neurodegenerative disorders, including HD which is caused by mutant forms of huntingtin (mHtt) (Li et al., 1993; Schilling et al., 1995). Elucidating the mechanisms by which these proteins precipitate their respective pathogenic cascades will be essential in developing new treatments for their associated neurodegenerative diseases.

As protein deposition diseases, AD, PD and HD are associated with the conversion of soluble monomers or oligomers into highly organized insoluble fibrillar aggregates, called amyloid fibrils, that serve as their primary histopathological markers. Each of these neurodegenerative diseases is associated with a specific composition of protein deposits that target certain neuronal subpopulations within the central nervous system (CNS). For decades the dominant and unifying model to explain the etiology of these cerebral proteopathies has focused on aggregates of amyloid fibrils as the causative agents (Hardy and Higgins, 1992). However, in recent years this model has been challenged on two main fronts. First, there is accumulating evidence that monomers or small oligomers of Aβ, α-syn, and mHtt, rather than the large fibrils themselves, may in fact be the cytotoxic species; and second, the extent of fibrillization is not necessarily correlated with disease progression (Uddin et al., 2020; Wells et al., 2021).

These changes in perspective have been accompanied by an increasing recognition that mitochondrial dysfunction plays a key role in neurodegenerative diseases (Swerdlow et al., 2014). More specifically, APP/Aβ, α-syn, and mHtt have all been shown to negatively impact different mitochondrial functions and to accumulate within different mitochondrial subcompartments. Such observations raise the intriguing mechanistic question of how these amyloids target to mitochondria, given that mitochondria contain a network of machineries that are ostensibly designed to selectively import only polypeptides with defined functions in the organelle. Here we review emerging evidence that APP/Aβ, α-syn, and mHtt may contain "cryptic" sequences that mimic the classic N-terminal targeting information of mitochondrial proteins to interact with mitochondrial import complexes, the implications this may have for the role of mitochondrial dysfunction in neurodegeneration, and how such insights could inform the development of novel therapeutic strategies for AD, PD, and HD.

2 Mitochondria of the central nervous system

The CNS is composed of neurons and glial cells (Figure 1A). Neurons are morphologically complex cells that transmit information by receiving a stimulus at dendrites that is transferred to the cell body and then propagated as an action potential (an electrochemical impulse) along the axon. Glial cells provide physical and metabolic support to neurons and include several subtypes including astrocytes, which serve mainly to support neural function and signaling; oligodendrocytes, which form myelin sheaths around axons; and microglia, the immune cells of the CNS. Neurodegenerative disorders predominantly affect neurons in particular anatomical regions of the brain (Dugger and Dickson, 2017; Fu et al., 2018); however, glial cells are purported to also play a direct role in the pathomechanisms of these diseases (Gleichman and Carmichael, 2020).

Mitochondria are morphologically complex, bound by a mitochondrial outer (MOM) and inner (MIM) membrane that enclose the intermembrane space (IMS), intracristal space (ICS) and matrix aqueous compartments (Figure 1Bi). Mitochondria assume a particularly important role in the physiology of neurons and neuroglia, given the high metabolic and signaling activity of these cells (Kann and Kovacs, 2007). First, mitochondria of the CNS must ensure efficient energy metabolism (Figure 1Bii). The brain comprises only 2%–3% of the human body mass yet accounts for up to 20% of total energy expenditure (Rolfe and Brown, 1997). This high energy demand is due to processes that include the maintenance of ion gradients such as Na^+/K^+-ATPases and Ca^{2+}-ATPases for neuronal excitability, as well as the synthesis, packaging, and cycling of neurotransmitters (Attwell and Laughlin, 2001). To meet this demand, most neuronal ATP is generated by mitochondrial oxidative phosphorylation (OXPHOS) fueled by glycolysis-derived pyruvate, although some glycolysis-derived ATP is utilized directly at nerve terminals during stress to sustain synaptic transmission (Tsacopoulos and Magistretti, 1996; Murali Mahadevan et al., 2021). The astrocyte-neuron lactatae shuttle model proposes that lactate produced by astrocytes is subsequently taken up by surrounding neurons to support high OXPHOS activity; however, the accuracy and relevance of this model has been questioned (Dienel, 2017). Second, mitochondria are the primary source of reactive oxygen species (ROS) in cells (Figure 1Biii), most of which are generated from the partial reduction of dioxygen (O_2) by different enzyme complexes of the electron transport chian (ETC) (Halliwell, 1992). As in other tissues, ROS serve dual roles in CNS cells. On one hand, ROS are critical for signaling processes required for neuronal plasticity and network tuning, and on the other, mitochondrial dysfunction can lead to ROS overproduction and oxidative damage, which is positively associated with neurodegenerative disorders (Milton and Sweeney, 2012; Oswald et al., 2018). Other central functions of mitochondria involve their interactions with the endoplasmic reticulum (ER), specifically at specialized regions of the ER called the mitochondrial-associated membrane (MAM) that is tethered to the MOM at sites termed mitochondria-ER contact sites (MERCSs) (Aoyama-Ishiwatari and Hirabayashi, 2021; Sassano et al., 2022). One function of MERCSs is the regulation of Ca^{2+} homeostasis (Figure 1Biv). The ER serves as the primary Ca^{2+}

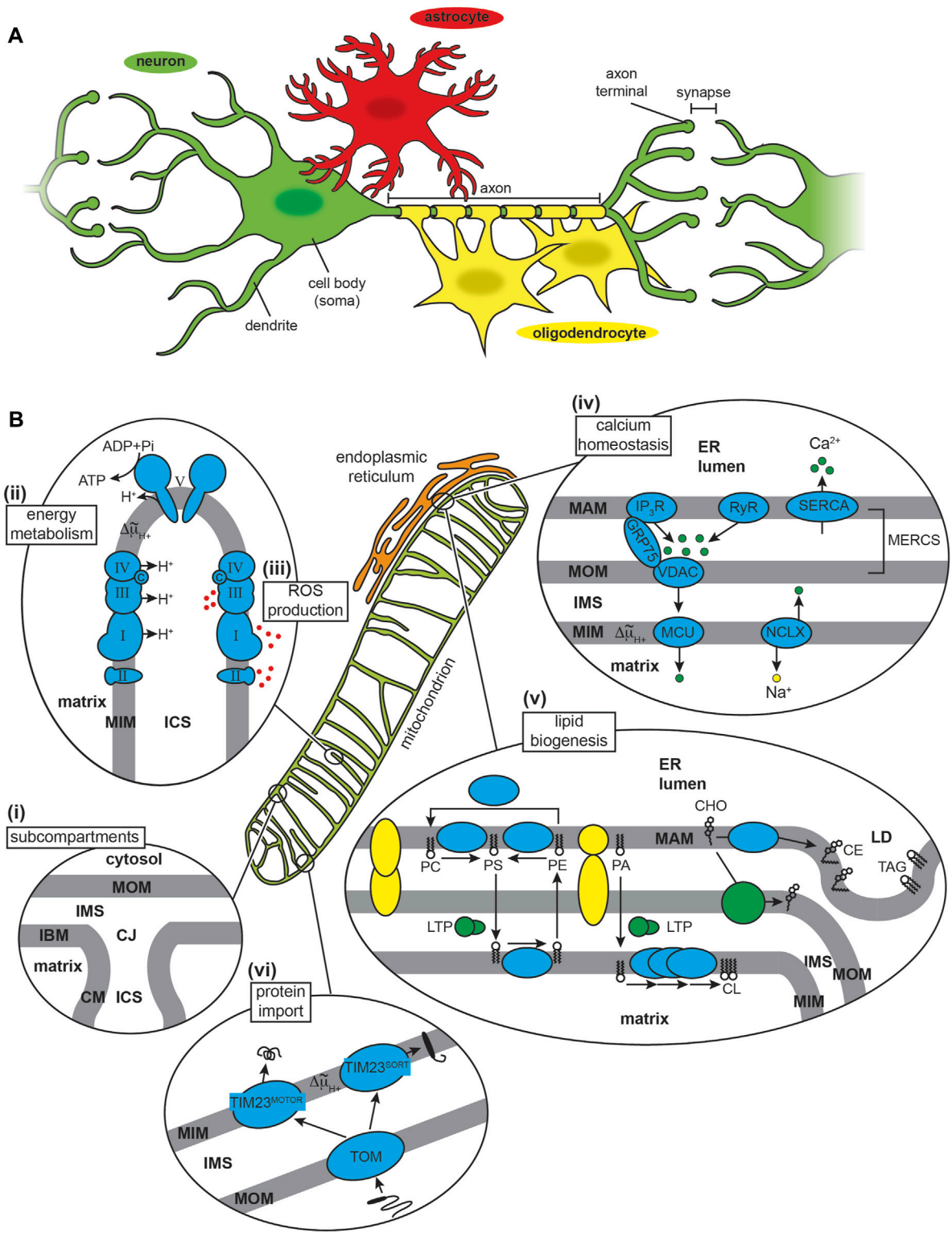

FIGURE 1
The CNS and mitochondria. **(A)** CNS cell types. The neuron (nerve cell, green) typically consists of a cell body (soma), multiple branching dendrites (afferent processes) that receive signals and transmit them to the cell body, and a single axon (efferent process) that forms an extended cable-like structure ending with axon terminals. Glial cells include astrocytes (red) and oligodendrocytes (yellow), amongst other cell types. **(B)** Mitochondria structure and major functions. (i) Subcompartments. Mitochondria have a two-membrane organization with a mitochondrial outer membrane (MOM) and inner membrane (MIM), the latter subdivided into an inner boundary membrane (IBM) closely appressed to the MOM, and the cristae membrane (CM). These membranes delineate the innermost matrix compartment from the intermembrane space (IMS) and intracristal space (ICS) that connect at the functional boundary of the crista junction (CJ). (ii) Energy metabolism. The OXPHOS machinery is parsed into complexes that generate an electrochemical proton potential ($\Delta\bar{\mu}_{H+}$) across the CM (including respiratory complexes I, II, III and IV of the electron transport chain) and the F_1F_O ATP
(*Continued*)

FIGURE 1 (Continued)
synthase (complex V) that uses the energy of the proton gradient to drive ATP synthesis. (iii) ROS production. Mitochondrial complexes I, II and III generate superoxide ($O_2^{\cdot-}$) from the one-electron reduction of O_2, which can subsequently be catalytically dismutated to H_2O_2 (a potent signaling molecule) or converted to the cytotoxic hydroxyl radical ($OH^{\cdot}$). (iv) Calcium homeostasis. The sarco/endoplasmic reticulum acts as a Ca^{2+} repository based largely on Ca^{2+} influx from ATP-dependent SERCA pumps and Ca^{2+} efflux from channels including the inositol (1,4,5)-triphosphate (IP_3R) receptor (tethered to the MOM by GRP75) and ryanodine receptor (RyR). Mitochondrial Ca^{2+} uptake across the MOM occurs through the voltage-dependent anion channel (VDAC) and across the MIM by the mitochondrial calcium uniporter (MCU), with efflux occurring primarily by the Na^+/Ca^{2+} exchanger (NCLX). (v) Lipid biogenesis and trafficking. Lipid biosynthesis complexes (cyan) and lipid transport proteins (LTPs) mediate the production of phospholipids (PC, phosphatidylcholine; PS, phosphatidylserine; PE, phosphatidylethanolamine; PA, phosphatidic acid; and CL, cardiolipin) and cholesterol (CHO). The MAM also mediates formation of lipid droplet (LD), enriched in cholesterol esters (CE) and triacylglycerol (TAG). MAM-MOM tethering complexes are depicted in yellow. (vi) Protein import. Most mitochondrial proteins are nuclear encoded and imported from the cytosol. Nearly all proteins enter mitochondria through the TOM complex, and most are imported to the final destination by modular assemblies of the TIM complex ($TIM23^{MOTOR}$ and $TIM23^{SORT}$).

storage organelle, balancing ion uptake by the sarco/endoplasmic reticulum Ca^{2+}-ATPase (SERCA) pumps with transient release from channels that include the inositol 1,4,5-triphosphate receptor (IP_3R) and the ryanodine receptor (RyR). Mitochondria serve as temporary stores of cellular Ca^{2+} (e.g., during Ca^{2+} transients that occur with action potentials in neurons), taking up ions through the β-barrel voltage-dependent anion channel (VDAC) in the MOM and the mitochondrial calcium uniporter (MCU) of the MIM. Ca^{2+} dyshomeostasis is a central feature of neurodegenerative diseases (Kolobkova et al., 2017; McDaid et al., 2020; Xu et al., 2022a). MERCSs also regulate lipid biosynthesis (Figure 1Bv) by serving as platforms for the non-vesicular trafficking of phospholipids and cholesterol and lipid droplet formation (Giordano, 2018; Benador et al., 2019). Defects in lipid metabolism are also a central feature of neurodegeneration, much of it attributable to alterations at the MAM-mitochondria interface (Block et al., 2010; Alecu and Bennett, 2019; Yin, 2023). Finally, mitochondria contain protein import machinery for the biogenesis of nuclear-encoded proteins (Figure 1Bvi). The role of the import machinery in mediating mitochondrial interactions with amyloidogenic proteins is the focus of this review.

Mitochondria are highly dynamic organelles, constantly undergoing growth, fission into fragments balanced by fusion into interconnected networks, and selective degradation of dysfunctional organelles by mitophagy (Yapa et al., 2021). Furthermore, neuronal mitochondria are distributed to match the local metabolic and signaling requirements of the somatic, dendritic, axonal, and synaptic regions, a process governed by anterograde and retrograde trafficking (Mandal and Drerup, 2019). Mitochondrial biogenesis requires the regulated import of proteins into the organelle to accommodate growth and replacement of damaged proteins to maintain an adequate population of healthy mitochondria.

Mitochondria also have a specialized lipid composition (Claypool and Koehler, 2012; Poulaki and Giannouli, 2022). The glycerophospholipid cardiolipin is of particular relevance because it is unique to mitochondria. Cardiolipin has an unusual structure, with a two-phosphate headgroup that imparts a strong negative charge to the membrane surface and four acyl tails, creating a molecular geometry that affects lipid packing and stabilizes local membrane curvature (Ikon and Ryan, 2017). Cardiolipin is primarily localized to the MIM, where it accounts for approximately 20 mol% of total phospholipid content, and is less abundant in the MOM, where it makes up less than 5 mol% of phospholipids. Externalization of cardiolipin from the MIM to the MOM can occur with cellular stress, which can serve as a signal for selective mitochondrial autophagy (mitophagy) or programmed cell death (apoptosis) (Li et al., 2015).

A key question surrounding neurodegeneration is why neurons are particularly vulnerable to proteostatic imbalance. The answer is manifold: because neurons are terminally differentiated and non-proliferative cells, they cannot rely on asymmetric mitosis to purge aggregated proteins and must therefore rely on robust proteostatic quality control machinery that can fail with age (Heydari et al., 1994; Conconi et al., 1996; Taylor and Dillin, 2011); because neurons are structurally polarized with long processes, the clearance of protein aggregates from distal parts of the cell is energetically costly and prone to dysregulation (Guo et al., 2020); and because neurons have such specialized functional and metabolic demands (e.g., maintenance of ion gradients, calcium regulation, and neurotransmitter cycling), there is a small energetic margin of error to spare in the face of proteostatic stress, particularly with age-related decreases in energy metabolism (Blaszczyk, 2020).

3 Mitochondrial protein import and the proteostatic network

3.1 The mitochondrial protein import and quality control machinery

The biogenesis and steady-state function of mitochondria require a highly regulated system of protein import, sorting, assembly, and quality control (Figure 2; Supplementary Table S1). The human mitochondrial proteome consists of approximately 1200–1500 individual proteins (Morgenstern et al., 2021; Rath et al., 2021). Being semi-autonomous organelles, mitochondria have the genome (mitochondrial DNA) and the biosynthetic machinery (e.g., mitochondrial ribosomes, RNA/DNA polymerases and tRNAs) to synthesize a handful of their resident proteins, which in humans includes 13 subunits of OXPHOS complexes I, III, IV and V. All other mitochondrial proteins are encoded in nuclear DNA, synthesized on cytosolic ribosomes, and subsequently imported into mitochondria. Multiple pathways exist for the targeting and sorting of nuclear-encoded proteins to the proper mitochondrial membrane or aqueous subcompartment (Busch et al., 2023) (Figure 2A). These proteins are synthesized with mitochondria targeting information encoded in the polypeptide sequence itself, which must be recognized by the dedicated import complexes that direct them to their correct

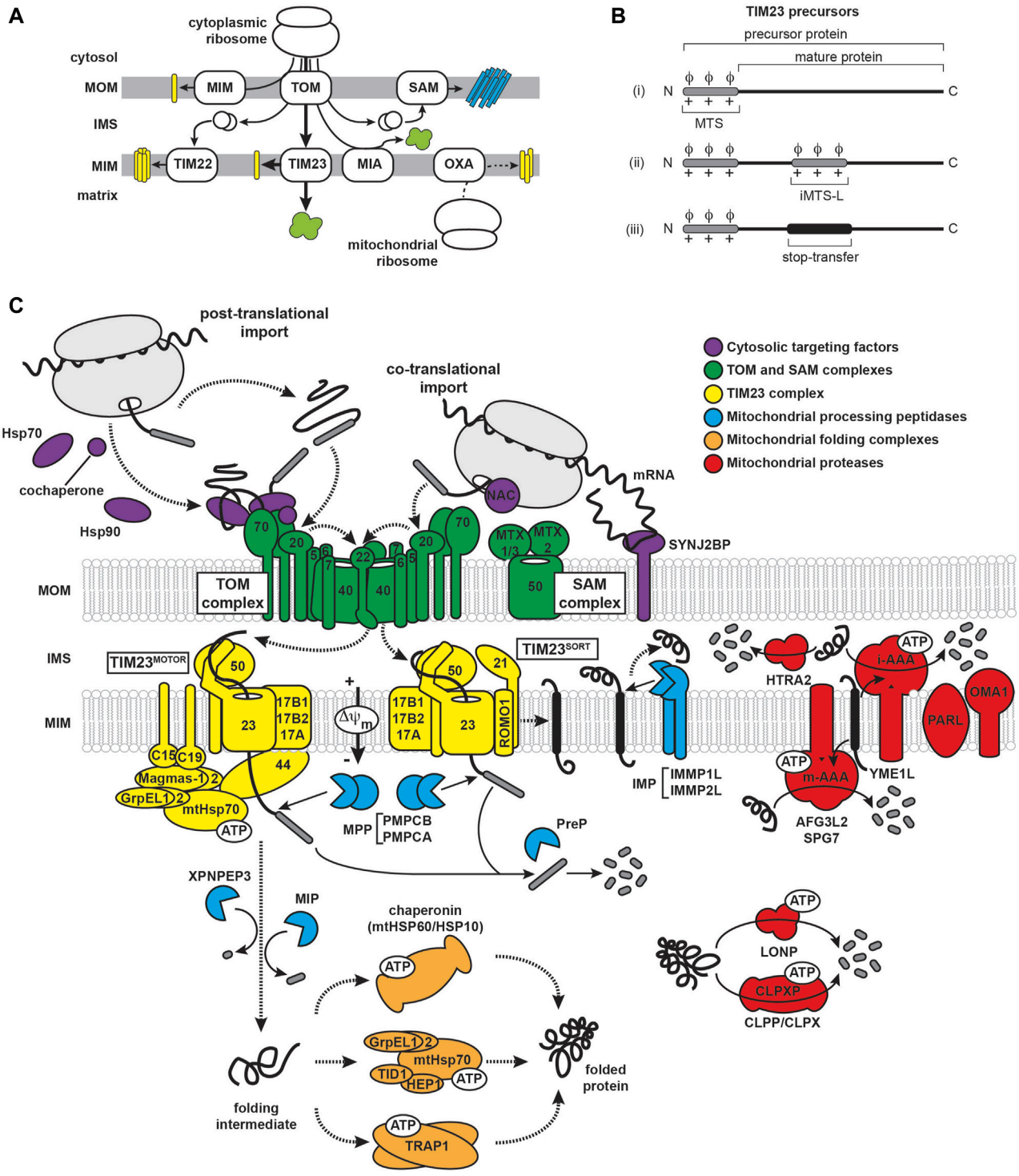

FIGURE 2
Mitochondrial import and proteostatic control. **(A)** Trafficking routes of mitochondrial proteins. Mitochondrial proteins include soluble proteins of the IMS/ICS and matrix (green), α-helical membrane proteins of the MOM and MIM (yellow) and β-barrel proteins of the MOM (cyan). Trafficking routes are depicted for nuclear-encoded proteins (solid lines) and mitochondrial-encoded proteins (dashed line). The major protein transport complexes include the translocase of the outer membrane (TOM) complex, the mitochondrial import (MIM) complex, the sorting and assembly machinery (SAM) complex, translocases of the inner membrane 22 and 23 (TIM22 and TIM23, respectively), the mitochondrial IMS import and assembly (MIA) complex, and the oxidase assembly (OXA) insertase. The trafficking of MTS-containing precursors via the TIM23 pathway is denoted by the thick arrows. **(B)** Targeting and topogenic sequences of TIM23 substrates. The MTSs are depicted in gray as containing basic (+) and hydrophobic (ϕ) residues. The stop-transfer segment is depicted in black. **(C)** The mammalian TIM23 import, processing, and quality control machinery. Components of the biogenesis machinery are categorized as: (i) chaperones that regulate the targeting of precursors from the cytosol to the mitochondrion (violet), (ii) outer membrane (TOM and SAM) complexes (green), (iii) $TIM23^{MOTOR}$ and $TIM23^{SORT}$ complexes (yellow), (iv) proteases that process TIM23 substrates (cyan), (v) matrix chaperones that mediate the folding of TIM23 substrates (orange), and (vi) proteases that mediate the degradation of mitochondrial proteins (red). See Supplementary Table S1 for a listing of all relevant proteins.

destinations. The majority (about two-thirds) of mitochondria-targeted proteins are imported via the translocase of the mitochondrial inner membrane 23 (TIM23) pathway, which mediates the translocation of soluble proteins into the matrix as well as the integration of membrane proteins into the MIM (Sinha et al., 2014). In this section, we summarize our current understanding of TIM23-based protein biogenesis and the associated mitochondrial proteostasis machinery.

3.1.1 TIM23 presequences

A key defining feature of TIM23 substrates is an amino-terminal targeting signal termed the mitochondrial targeting sequence (MTS), or "presequence". These proteins are synthesized as so-called precursors that are recognized by receptors of the mitochondrial import machinery and typically have their respective MTSs cleaved to yield the mature form of the protein upon reaching their destination. The MTS signals lack sequence conservation, are highly variable in length (ranging from about 15 to 60 amino acids), and are unstructured in aqueous solution. However, they all share a capacity to form amphipathic α-helices with one face enriched in hydrophobic residues and the other enriched in basic residues (mostly Arg). This is coupled with a near absence of acidic residues, resulting in a net charge between +3 and +6 (Roise et al., 1986; Roise et al., 1988; Roise and Schatz, 1988; Pak and Weiner, 1990; Vogtle et al., 2009; Calvo et al., 2017). TIM23-targeted precursors have a diversity of targeting elements (Figure 2B): (i) those containing only the N-terminal MTS followed by a soluble mature protein, (ii) those with MTS-like structures (iMTS-Ls) in the mature protein that bind mitochondrial receptors and enhance import efficiency and kinetics (Backes et al., 2018; Hansen et al., 2018), and (iii) those with a bipartite signal sequence that, in addition to the MTS, contain a topogenic (membrane-active) hydrophobic stop-transfer sequence that partitions into the MIM as a transmembrane segment (Glick et al., 1992). It should also be noted that MTS processing is not a strict feature of TIM23-mediated import, as some TIM23 precursors are not processed following translocation and some retain import competence even with their MTSs deleted (Longen et al., 2014; Woellhaf et al., 2014; Weill et al., 2018). Importantly, the variability of the sequence and the locations of MTS and MTS-like sequences may explain the ability of some amyloidogenic polypeptides to present cryptic TIM23 targeting signals, as we discuss later.

3.1.2 Cytosolic trafficking of TIM23 substrates

The biogenesis of TIM23 substrates begins on cytosolic ribosomes and is regulated by several molecular chaperones and piloting factors (Figure 2C, violet). The targeting of these proteins to mitochondria mostly proceeds post-translationally, whereby the polypeptide is completely synthesized and released from the ribosome before engaging the mitochondrial import machinery. In this case, ATP-dependent cytosolic heat shock proteins (HSPs) of the HSP70 (Deshaies et al., 1988; Murakami et al., 1988; Terada et al., 1995; Endo et al., 1996) and HSP90 families (Young et al., 2003; Fan et al., 2006) may bind precursors at different stages to prevent their aggregation and maintain them in partially unfolded states (Becker et al., 2019; Avendano-Monsalve et al., 2020), which is particularly important for precursor proteins with transmembrane segments (Claros et al., 1995). The HSP70/90 chaperones undergo ATPase cycles that are allosterically coupled to substrate binding and release (Rutledge et al., 2022). HSP70s inhibit folding of their client substrates by extensively interacting with low specificity at binding motifs of short hydrophobic segments flanked by charged residues (Rudiger et al., 1997). By comparison, HSP90s have more extended binding sites that recognize later-folding intermediates (Karagoz and Rudiger, 2015). The activity of HSP70s is modulated by co-chaperones that regulate ATP turnover and substrate specificity (Moran Luengo et al., 2019). HSP70 co-chaperones include J domain (HSP40) proteins, which stimulate ATP hydrolysis, and nucleotide exchange factors (NEFs), which promote exchange of bound ADP for ATP (Kampinga and Craig, 2010). Multiple J domain co-chaperones, including DNAJA1, 2, and 4 in mammals and Djp1, Ydj1 and Sis1 in yeast, have been implicated in precursor protein targeting to mammalian mitochondria (Bhangoo et al., 2007; Papic et al., 2013; Jores et al., 2018).

Alternatively, the targeting of TIM23 substrates can proceed co-translationally, wherein the polypeptide engages the mitochondrial import machinery while it is still being translated on the ribosome (Avendano-Monsalve et al., 2020; Lenkiewicz et al., 2021). The existence of cotranslational import in both yeast and mammalian mitochondria is supported by evidence of mitochondria-bound ribosomes and polysomes that is promoted, for example, following treatment with the translation elongation inhibitor cycloheximide (Crowley and Payne, 1998; Williams et al., 2014; Gold et al., 2017). Other studies similarly support cotranslational targeting of different TIM23 substrates (Ahmed et al., 2006; Yogev et al., 2007). Although mitochondria do not appear to have a dedicated cotranslational targeting route (for instance, analogous to the signal recognition particle-mediated pathway of the ER (Akopian et al., 2013)), there are systems in place for promoting cotranslational mitochondrial import under certain conditions. For example, mRNAs encoding mitochondria-targeted proteins are enriched at the mitochondrial surface (Egea et al., 1997; Matsumoto et al., 2012; Williams et al., 2014; Fazal et al., 2019; Kuzniewska et al., 2020), and stabilized by MOM-localized RNA binding proteins Puf3 in yeast (Wang et al., 2018) and perhaps SYNJ2BP in mammals (Qin et al., 2021). Additionally, a translation stimulator at the mitochondrial surface, the MDI-Larp complex, was shown to enhance protein synthesis in the vicinity of import complexes in *Drosophila* (Zhang et al., 2016). Finally, mitochondria-targeted proteins can be recognized by the heterodimeric nascent polypeptide-associated complex (NAC) (Beatrix et al., 2000), which simultaneously binds ribosomes and emerging nascent chains and may promote cotranslational targeting to mitochondria (Wiedmann et al., 1994; George et al., 1998; George et al., 2002; del Alamo et al., 2011; Gamerdinger et al., 2019). In yeast, NAC binds to the SAM complex subunit Sam37 (Ponce-Rojas et al., 2017; Avendano-Monsalve et al., 2022) and the MOM protein OM14 (Lesnik et al., 2014); whether NAC engages homologous proteins in mammalian mitochondria remains an open question. NAC may play a special role in amyloidogenic diseases, as it has recently been shown to suppress aggregation of poly-Q expanded proteins (Shen K. et al., 2019). The critical point is that regardless of whether precursor substrates are imported co- or post-translationally,

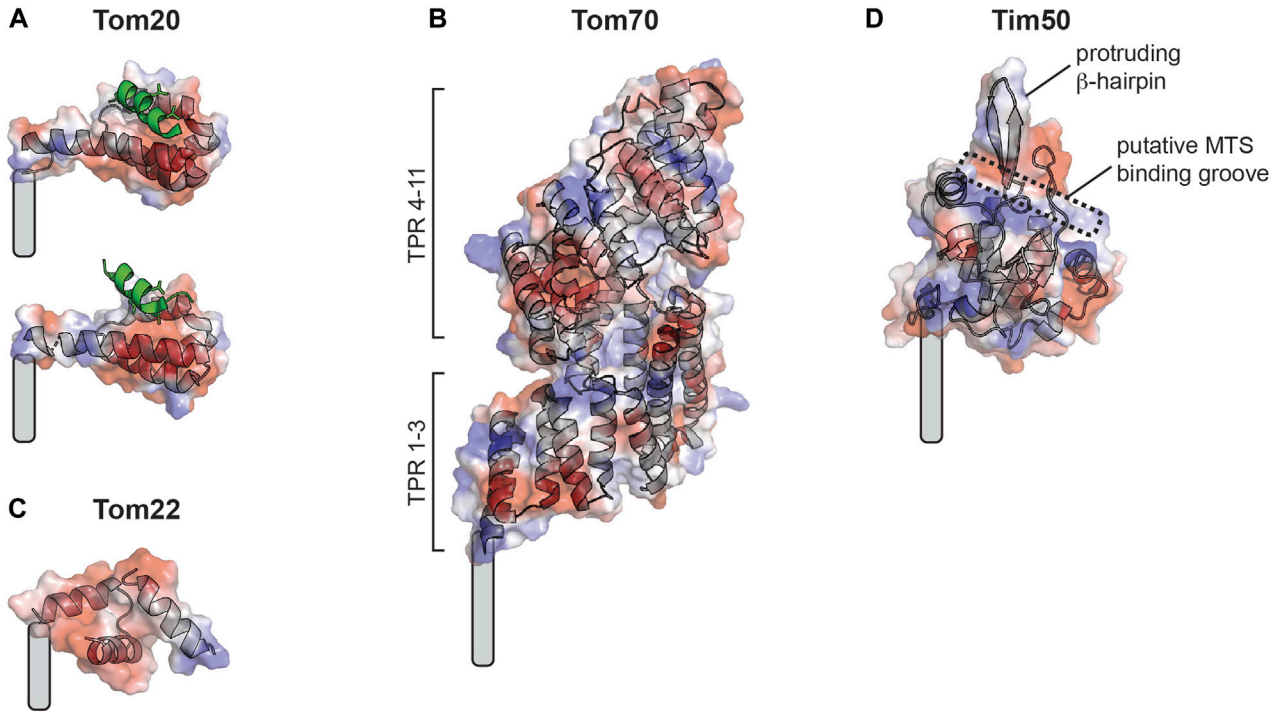

FIGURE 3
Mitochondrial protein import receptors of known structure. Soluble receptor domains are shown as cartoon traces superimposed with electrostatic surfaces (red, acidic; blue, basic; white, neutral). Grey curved rectangles show approximate positions of transmembrane segment attachment. **(A)** Rat Tom20 receptor from crystal structure with disulfide-bound MTS (green) showing two different binding states resolved by distinct MTS-receptor chemical tethering strategies (the so-called A-linker [PDB 2V1T], above; and the Y-linker [PDB 2V1S], below). **(B)** Yeast Tom70 receptor from crystal structure (PDB 2GW1). **(C)** Human Tom22 receptor from cryo-EM structure (PDB 7VDD). **(D)** Tim50 receptor (homology model of human receptor based on yeast Tim50 core domain) from crystal structure (PDB 3QLE), showing the predicted MTS binding pocket and protruding β-hairpin.

the targeting system is designed to maintain the substrate in an unfolded state in order to preserve its import competence.

3.1.3 Structure and function of the TOM complex

The translocase of the outer mitochondrial membrane (TOM) complex of the MOM serves as the entry site for all TIM23 substrates into mitochondria (Figure 2C, green). This complex contains seven different subunits: the Tom40 β-barrel channel that serves as the aqueous transmembrane conduit for precursors; small TOM proteins (Tom5, Tom6, Tom7) that regulate TOM complex assembly; and several receptors, including Tom22, Tom20 and Tom70 (Pitt and Buchanan, 2021; Araiso and Endo, 2022). The core complex appears to form as equi-stoichiometric assemblies of Tom40/22/5/6/7 that can arrange as dimeric or higher order structures (Kunkele et al., 1998; Model et al., 2008; Mager et al., 2010; Shiota et al., 2015; Bausewein et al., 2017; Sakaue et al., 2019); in contrast, the Tom20 and Tom70 receptors appear to be more loosely bound. Thus, these receptors may instead assemble with the TOM complex in an on-demand basis depending on the presence of substrate (Dekker et al., 1998; Bhagawati et al., 2021). Recent cryo-EM structures of the TOM complex in yeast (Araiso et al., 2019; Tucker and Park, 2019) and human (Wang et al., 2020a; Guan et al., 2021; Su et al., 2022) have shed light on the structural interactions among TOM subunits and how precursor proteins are recognized and translocated. For example, the TOM receptors play complementary and partially overlapping roles in the recognition of MTS-containing proteins. Tom20, Tom70, and Tom22 all have receptor domains containing tetratricopeptide repeat (TPR) motifs that mediate protein interactions (Zeytuni and Zarivach, 2012) and appear to have general protein chaperone function in addition to acting as precursor receptors (Yano et al., 2004; Yamamoto et al., 2009). Tom20 serves as the general receptor for preproteins and is paradigmatic for MTS-receptor interactions because it is the only mitochondrial receptor for which high-resolution structural information is available in the MTS peptide-bound state (Abe et al., 2000; Saitoh et al., 2007; Saitoh et al., 2011). The Tom20 cytosolic C-terminal receptor domain contains two helix-turn-helix motifs that define a single prototypical TPR motif with an embedded nonpolar patch flanked by two acidic regions and a region rich in Gln residues (Figure 3A). The binding groove of Tom20 is shallow and short, accommodating only about eight residues of the MTS. The Tom20 recognition motif within MTSs is $\phi\chi\chi\phi\phi$, where ϕ is a nonpolar residue and χ is any residue. This relatively nonspecific recognition motif enables a dynamic, weak-affinity and multi-mode interaction with the substrate, dominated by nonpolar contacts (Muto et al., 2001; Obita et al., 2003). Tom70, by comparison, has a much larger receptor domain containing 11 TPR motifs that are divided into N- and C-terminal parts (Wu and Sha, 2006) (Figure 3B). The N-terminal region of Tom70 contains a homodimerization interface and forms a clamp-like region (TPR motifs 1–3) that binds Hsp70 and Hsp90 chaperones, perhaps serving as a co-chaperone for the

transfer of Hsp70/90-bound precursors to the TOM complex (Young et al., 2003; Wu and Sha, 2006). This function underscores its recently discovered role in recruiting chaperones to the mitochondrial surface (Backes et al., 2021). The C-terminal region of Tom70 (TPR motifs 4–11) forms a large pocket that likely binds polytopic membrane precursor proteins destined for the TIM22 pathway (Wiedemann et al., 2001; Rehling et al., 2003), and may bind targeting signals of TIM23 substrates as well (Hines et al., 1990; Hines and Schatz, 1993; Wu and Sha, 2006; Melin et al., 2015). The central receptor Tom22 regulates TOM complex assembly, and unlike the primary Tom20 and Tom70 receptors, it is tightly bound to the TOM complex. Additionally, Tom22 features receptor domains on both the cytosol-facing (Figure 3C) and IMS-facing sides of the MOM (Bolliger et al., 1995; Honlinger et al., 1995; Dekker et al., 1998; van Wilpe et al., 1999; Yamano et al., 2008). While Tom22 and Tom20 have similar substrate profiles (Mayer et al., 1995; Yamano et al., 2008), the Tom20 receptor mediates hydrophobic interactions with the MTS, whereas Tom22 interactions are dominated by electrostatic attraction between the basic face of the MTS and the partially disordered acidic Tom22 binding pocket (Kiebler et al., 1993). However, the strict requirement of these negatively charged residues has been questioned (Nargang et al., 1998). The dominant model describing how precursor proteins traverse the membrane through the TOM complex is by an "acid chain" of negatively charged patches on TOM subunits that guide the positively charged MTS. By this model, Tom5 and Tom22 make up an acidic pathway on the cytosolic face of the MOM (the *cis* site) (Bolliger et al., 1995; Dietmeier et al., 1997; Schatz, 1997; Komiya et al., 1998), the precursor moves through the Tom40 pore guided by acidic residues on the interior wall of the β-barrel (Suzuki et al., 2000; Gabriel et al., 2003; Shiota et al., 2015), and the precursor then binds sites on the IMS side of the MOM comprised of Tom22, Tom40 and Tom7 (the *trans* site) (Court et al., 1996; Moczko et al., 1997; Rapaport et al., 1997; Kanamori et al., 1999; Esaki et al., 2004). The selective positioning of acidic binding sites with increasing affinity for the MTS from the cytosolic to the IMS sites drives the vectorial movement of the precursor through the TOM complex.

3.1.4 Structure and function of the TIM23 complex

The TIM23 complex is the dedicated machinery of the MIM that mediates the import and sorting of all MTS-containing precursor proteins (Genge and Mokranjac, 2021) (Figure 2, yellow). The general organization of TIM23 is evolutionarily conserved; however, in comparison with the more fully understood yeast complex, human TIM23 forms multiple functionally distinct complexes containing alternate subunit isoforms (Sinha et al., 2014; Pfanner et al., 2019). The core TIM23 complex in humans contains the channel forming Tim23 and Tim17A/B1/B2 isoforms that assemble to make an aqueous conduit across the MIM for the passage of preproteins (Bauer et al., 1999; Moro et al., 1999; Martinez-Caballero et al., 2007; Demishtein-Zohary et al., 2017; Matta et al., 2017). It also contains Tim50, which serves as the main receptor for MTS-bearing precursors (Geissler et al., 2002; Yamamoto et al., 2002; Mokranjac et al., 2003a) and, in mammals, acts as a broad specificity phosphatase (Guo et al., 2004; Chaudhuri et al., 2021). The conserved core domain of the Tim50 receptor contains a putative MTS binding groove lined with negatively charged and hydrophobic residues as well as a prominent β-hairpin (Qian et al., 2011) (Figure 3D). The N-terminal extension of the Tim23 channel is an intrinsically disordered region that specifically interacts with Tim50 near the β-hairpin (Geissler et al., 2002; Yamamoto et al., 2002; Mokranjac et al., 2003a; Meinecke et al., 2006; Alder et al., 2008a; Gevorkyan-Airapetov et al., 2009; Mokranjac et al., 2009; Tamura et al., 2009; Qian et al., 2011; Schulz et al., 2011; Lytovchenko et al., 2013; Malhotra et al., 2017; Dayan et al., 2019; Gunsel et al., 2020). This interaction between the disordered N-terminal extension of Tim23 and Tim50 maintains the Tim23 channel in a quiescent, dimeric state that preserves the transmembrane potential ($\Delta\psi_m$) across the MIM (Bauer et al., 1996; Meinecke et al., 2006; Alder et al., 2008a).

To deliver precursors to their correct destination, the compositionally dynamic TIM23 complex forms two different assemblies adapted to the Tim23/17/50 core. The TIM23^{MOTOR} complex mediates the translocation of soluble precursors into the matrix (Mokranjac, 2020), a process that requires the recruitment of a matrix-localized molecular motor system (the presequence translocase-associated motor, or PAM complex) that includes: the central subunit mitochondrial Hsp70 (mtHsp70, also called mortalin), which serves as the ATP-driven molecular motor (Goswami et al., 2010; Esfahanian et al., 2023); Tim44, which anchors mtHsp70 to the TIM23^{MOTOR} complex (Kronidou et al., 1994; Schneider et al., 1994; Silva et al., 2004); and co-chaperones that modulate the ATPase activity of mtHsp70. The latter include the GrpE-Like 1 and 2 (GrpEL1 and GrpEL2) NEFs (Schneider et al., 1996; Naylor et al., 1998; Srivastava et al., 2017), the paralogous DnaJC15 (C15) and DnaJC19 (C19) that are homologous to the yeast J-protein Pam18/Tim14 (Silva et al., 2003; Mokranjac et al., 2003b; Richter-Dennerlein et al., 2014), and isoforms of the mitochondria-associated granulocyte-macrophage colony stimulating factor (GM-CSF) signaling molecule (Magmas-1 and 2) that are orthologs of the yeast J-like protein Pam16/Tim16 (Elsner et al., 2009; Sinha et al., 2010; Waingankar and Silva, 2021). By contrast, the TIM23^{SORT} complex mediates the lateral sorting of membrane-directed precursor proteins into the MIM. This sorting complex lacks the PAM motor and recruits additional membrane subunits. These include Tim21, which makes specific contacts with Tim23 and Tim50 (Tamura et al., 2009; Lytovchenko et al., 2013; Bajaj et al., 2014) and mediates the assembly of membrane-bound subunits of respiratory complex IV (Mick et al., 2012; Richter-Dennerlein et al., 2016), and ROMO1, a subunit homologous to yeast Mgr2 that promotes the interaction of Tim21 with the TIM23^{SORT} complex and is specifically required for the import of mitochondrial proteases (Ieva et al., 2014; Richter et al., 2019; Matta et al., 2020). Apropos of these proposed discrete TIM23^{SORT} and TIM23^{MOTOR} models for MIM integration and matrix import, it should be noted that other experimental results support a model in which TIM23 is a single structural entity that is actively remodeled to support translocation or integration depending on substrate availability instead of existing in two disparate states (Popov-Celeketic et al., 2008).

The import of MTS-containing substrates by the TIM23 complex is a multistep, energy-requiring process. The transfer of precursor proteins to the TIM23 complex is facilitated by the formation of a TOM-TIM23 supercomplex that is stabilized by interactions of the IMS-facing *trans* site of the TOM complex and

the IMS-facing regions of Tim21, Tim50, and Tim23 subunits of the TIM23 complex (Dekker et al., 1997; Chacinska et al., 2003; Mokranjac et al., 2005; Albrecht et al., 2006; van der Laan et al., 2006; Chacinska et al., 2010; Shiota et al., 2011; Gold et al., 2014), which have been verified primarily by crosslinking experiments done with yeast models and with purified proteins (Chacinska et al., 2005; Mokranjac et al., 2005; Albrecht et al., 2006; Tamura et al., 2009; Shiota et al., 2011; Bajaj et al., 2014; Waegemann et al., 2015; Araiso et al., 2019; Gunsel et al., 2020). Upon emerging from the TOM complex, the MTS first binds the Tim50 receptor, thereby displacing receptor interactions with the Tim23 N-terminus and Tim21 and altering the TOM-TIM23 association (Geissler et al., 2002; Yamamoto et al., 2002; Mokranjac et al., 2003a; Mokranjac et al., 2009; Marom et al., 2011a; Shiota et al., 2011; Lytovchenko et al., 2013; Waegemann et al., 2015). The MTS then binds the now-exposed Tim23 N-terminus (Bauer et al., 1996; de la Cruz et al., 2010; Marom et al., 2011a; Lytovchenko et al., 2013) and is directed to the Tim23 channel which, like Tom40, has specific residues along the channel lumen that interact with substrates (Alder et al., 2008b; Denkert et al., 2017). The dynamic Tim23 channel undergoes conformational alterations in response to substrate and changes in the $\Delta\psi_m$ (Popov-Celeketic et al., 2008; Malhotra et al., 2013) and the presence of the MTS activates the Tim23 channel gating (Bauer et al., 1996; Truscott et al., 2001). The basic MTS is electrophoretically pulled toward the negatively charged matrix through the activated Tim23 channel (Martin et al., 1991), with unidirectional movement imparted by increasing binding affinity between the MTS and Tim23, Tim50, and Tim44 (Marom et al., 2011b). Soluble precursor proteins are then translocated completely into the matrix by the $TIM23^{MOTOR}$ complex, whereby the ATPase activity of mtHsp70, modulated by co-chaperones DnaJC15/19 and Magmas-1/2, pulls the substrate by a Brownian ratchet or active pulling mechanism (Mokranjac et al., 2003a; Mokranjac, 2020; Silva et al., 2003; Mokranjac et al., 2003b; Truscott et al., 2003). By contrast, when a hydrophobic stop-transfer sequence is detected on the substrate, translocation stalls, the complex recruits subunits of the $TIM23^{SORT}$ complex, and the nonpolar segment partitions laterally into the MIM as an α-helical transmembrane segment in a manner driven by the $\Delta\psi_m$ (Gartner et al., 1995; Gruhler et al., 1997) and mediated by the ROMO1 and Tim21 gatekeepers (van der Laan et al., 2006; Mick et al., 2012; Ieva et al., 2014; Richter-Dennerlein et al., 2016; Richter et al., 2019; Lee et al., 2020). Notably, an alternative structure-based model of TIM23 function suggests that instead of forming an aqueous channel, Tim23 and Tim17 together form lipid-exposed cavities that provide a protein translocation pathway (Sim et al., 2023), consistent with evidence that TIM23 precursors are translocated across the MIM at the Tim17-bilayer interface rather than via a channel defined by Tim23 (Fielden et al., 2023).

3.1.5 Processing and quality control of TIM23 substrates

During import, precursor proteins are selectively processed to their mature forms by a set of mitochondria-localized processing proteases (Gomez-Fabra Gala and Vogtle, 2021; Kunova et al., 2022) (Figure 2C, cyan). The vast majority of TIM23 complex substrates are processed in a way that removes the N-terminal targeting sequences (Vogtle et al., 2009). The main protease is the matrix-localized mitochondrial processing peptidase (MPP), a metalloendopeptidase that forms a dimeric complex (PMPCA and PMPCB subunits in human) (Taylor et al., 2001). MPP cleaves at defined recognition sites (predominantly with the scissile bond two or three residues C-terminal to an Arg residue (Calvo et al., 2017)), thereby releasing the MTS which is subsequently degraded by the presequence protease (PreP) (Alikhani et al., 2011a; Kucukkose et al., 2021). Following MTS cleavage, some matrix-targeted precursors require additional maturation steps at the new N-terminus that involve the removal of either a single residue (mediated by the XPNPEP3 protease (Singh et al., 2017)) or an octapeptide (mediated by the MIP protease (Vogtle et al., 2011)), both of which remove destabilizing N-terminal residues to increase protein half-life (Vogtle et al., 2009; Varshavsky, 2011). Additionally, some TIM23-targeted substrates integrated into the MIM are processed by the inner membrane peptidase IMP (IMMP1L and IMMP2L in human), which releases a soluble IMS-facing domain of the imported protein as the mature, functional form (Nunnari et al., 1993).

To ensure the proper folding of newly-imported proteins, mitochondria contain two main chaperone systems in the matrix (Figure 2C, orange). The mitochondrial Hsp60/Hsp10 chaperonin complex, a homolog of the bacterial GroEL/GroES chaperonin, sequesters unfolded or kinetically-trapped folding intermediates inside an Anfinsen cage-like cavity and undergoes ATPase-driven structural changes to release properly folded proteins (Cheng et al., 1989; Ellis, 1996; Nielsen and Cowan, 1998; Apetri and Horwich, 2008; Chakraborty et al., 2010; Nisemblat et al., 2015). In addition, a soluble complex of mtHsp70 (mortalin) resides in the matrix (Horst et al., 1997; Havalova et al., 2021), where it performs its protein folding functions with three co-chaperones that have been identified in human: the Hsp70-escort protein 1 (HEP1) and J-domain protein tumorous imaginal disc protein 1 (TID-1), which regulate ATPase activity of mtHsp70, and the NEFs GrpEL1/2 (Sichting et al., 2005; Zhai et al., 2008; Iosefson et al., 2012; Dores-Silva et al., 2013; Havalova et al., 2021). These main matrix chaperone systems are supplemented in mammals by the HSP90 paralog TRAP1, which performs diverse functions including acting as a late-stage folding chaperone for mitochondrial matrix proteins (Joshi et al., 2022).

In addition, mitochondria contain several proteases for the degradation of misfolded and damaged proteins (Gomez-Fabra Gala and Vogtle, 2021) (Figure 2C, red). In human mitochondria, four main ATP-fueled proteases of the AAA+ (ATPases associated with diverse cellular activities) superfamily are responsible for the surveillance and clearance of proteins. These include the MIM-bound metalloproteases *m*-AAA (homo-oligomers of AFG3L2 or hetero-oligomers of AFG3L2 and SPG7 with catalytic domains facing the matrix) and *i*-AAA (composed of YME1L1 with catalytic domains facing the IMS), both of which can extract and break down MIM proteins (Opalinska and Janska, 2018). Additionally, the matrix contains soluble AAA+ serine proteases. LONP1 is a homohexameric assembly that serves as the central quality control protease in the matrix, degrading misfolded and damaged proteins (Szczepanowska and Trifunovic, 2022) in addition to promoting protein folding by cooperating with mtHsp70 (Shin et al., 2021). The CLPXP complex, on the other hand, is a heterooligomeric

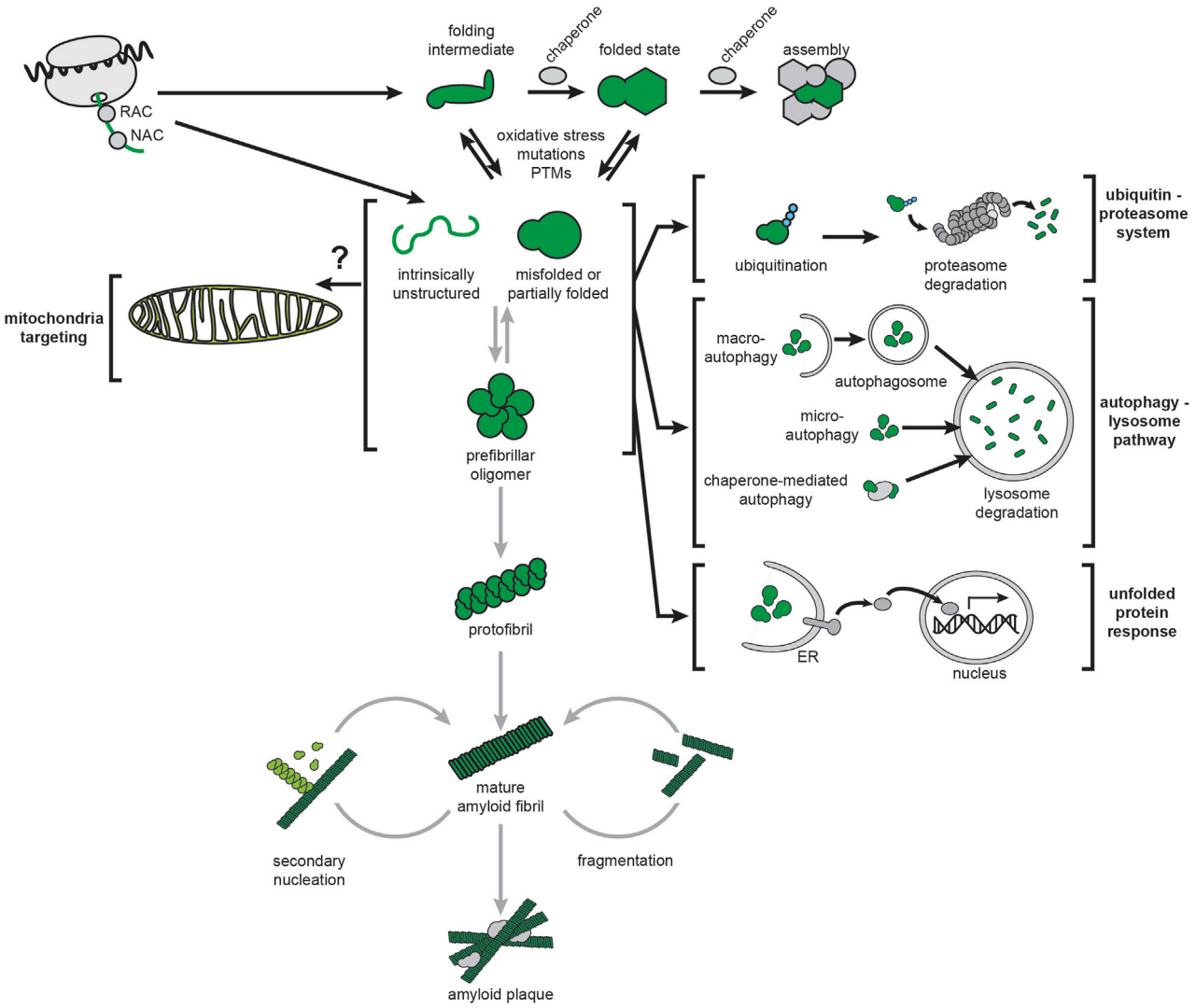

FIGURE 4
Amyloids and cellular proteostasis. The proteostasis network of mammalian cells is depicted by black arrows. Chaperones that guide cotranslational folding on the ribosome include the nascent polypeptide-associated complex (NAC) and the ribosome-associated complex (RAC). Additional chaperones guide monomer folding and assembly into complexes. The ubiquitin-proteasome system (UPS) targets misfolded proteins, or proteins that are no longer needed, by ubiquitination and digestion by the proteasome. The autophagy-lysosome pathway (ALP) targets misfolded proteins (and larger structures such as large aggregates and organelles) by delivering them to the lysosome via distinct pathways (macroautophagy, microautophagy and chaperone-mediated autophagy). Protein unfolding stress can activate complex signal transduction pathways leading to gene expression changes for restoring protein homeostasis, most notably the ER-based unfolded protein response (UPR^{ER}). Amyloidogenesis, depicted by gray arrows, can initiate from intrinsically disordered or misfolded structures and proceed by stepwise formation of oligomers, protofibrils, and finally mature fibrils. It can also be accelerated by secondary nucleation and fragmentation of existing fibrils.

protease assembly involved in diverse functions including mitoribosome and OXPHOS maintenance (Szczepanowska and Trifunovic, 2022). The HTRA2 (high temperature requirement) soluble serine protease of the IMS is involved in caspase-dependent apoptosis and has been implicated in PD progression (Vande Walle et al., 2008). Finally, there are additional MIM-bound proteases, including PARL and OMA1, that have a more specific set of substrate proteins that regulate mitochondrial dynamics, mitophagy, and stress responses (Pellegrini and Scorrano, 2007; Jiang et al., 2014). As discussed below, the quality control machinery for newly imported proteins may also be involved in stress responses involving amyloidogenic proteins.

3.2 Amyloid misfolding and cellular proteostasis

Cellular proteostasis involves the regulation of all stages of the protein life cycle (Labbadia and Morimoto, 2015; Klaips et al., 2018): molecular chaperones guide cotranslational folding of nascent chains during ribosomal synthesis and promote protein folding and assembly of oligomeric complexes, degradation mechanisms such as the ubiquitin-proteasome system (UPS) and the autophagy-lysosome pathway (ALP) remove misfolded and aggregated proteins, and stress response pathways respond to protein folding stress, such as the ER-based unfolded protein response (UPR^{ER})

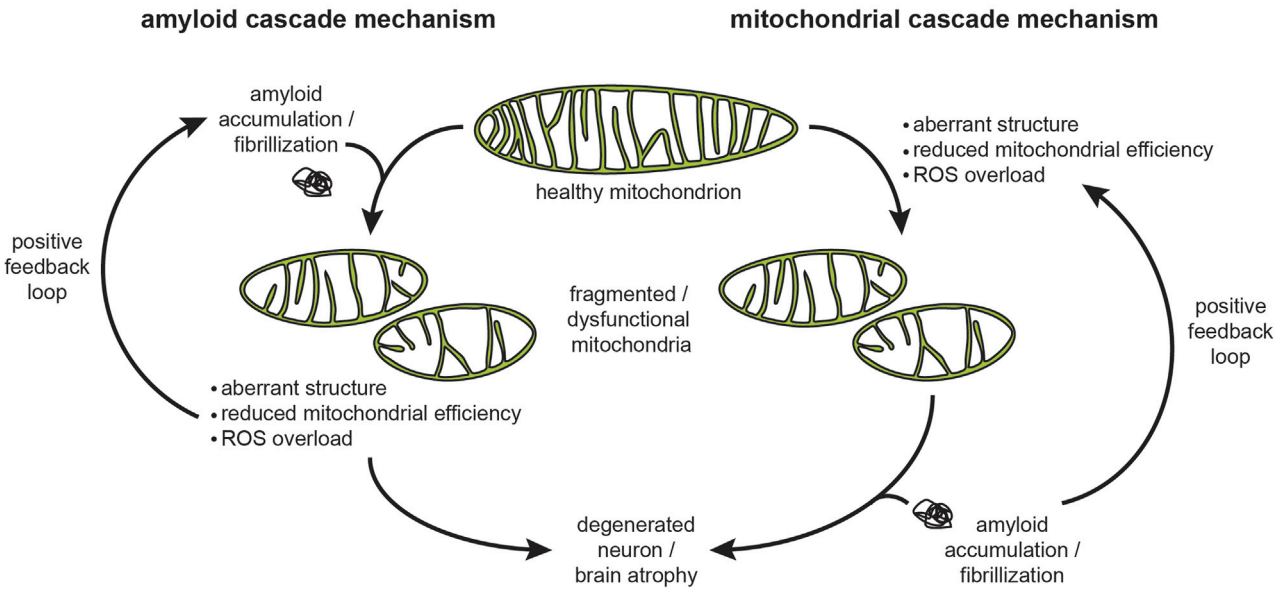

FIGURE 5
The amyloid and mitochondria cascade hypotheses. These two mechanisms describe the cause-and-effect relationships in the progression of neurodegenerative diseases, proposed originally for AD but also relevant for other proteinopathies. The amyloid cascade hypothesis proposes that amyloid accumulation, fibrillization, and plaque formation trigger the pathogenic events, including mitochondrial damage, that lead to neuronal damage. As a corollary to this hypothesis, the most effective interventions would target the accumulation, clearance, and fibril formation of amyloids. The mitochondria cascade hypothesis proposes that mitochondrial dysfunction is the primary driver of neurodegeneration that leads to cellular damage, including amyloid aggregation. As a corollary to this hypothesis, the most effective interventions would be those aimed toward improving mitochondrial physiology. In both mechanisms, amyloid aggregation and mitochondrial dysfunction can be part of a vicious cycle that accelerates disease progression. Note that the interaction of amyloidogenic proteins with the mitochondrial import machinery likely plays a central role in both mechanisms.

(Figure 4, black arrows). All three of these protein quality control processes are implicated in neurodegenerative diseases (Scheper and Hoozemans, 2015; Park et al., 2020; Schmidt et al., 2021).

AD, PD, and HD are proteostatic diseases associated with the misfolding of Aβ, α-syn, and mHtt, respectively, in a process that leads to the formation of amyloid fibrils (Figure 4, grey arrows). This process can begin with precursors that include intrinsically disordered peptides such as Aβ and α-syn, or with partially and misfolded globular proteins. The kinetics of amyloid fibrillization have a marked dependence on protein concentration, as well as factors that affect the tendency for polypeptides to self-associate, including mutations, post-translational modifications (PTMs), cofactors, and oxidative stress (Alexandrescu, 2005; Rezaei-Ghaleh et al., 2016; Hu et al., 2019; Lontay et al., 2020; Chiki et al., 2021; Gottlieb et al., 2021; He et al., 2021; McGlinchey et al., 2021). Fibrillization follows nucleation kinetics, accounting for the "seeding" properties of amyloids (Chiti and Dobson, 2017; Almeida and Brito, 2020). Nucleation can occur through primary or *de novo* processes, or secondary mechanisms whereby mature fibril surfaces act as templates for new fibril growth (Ferrone et al., 1985; Padrick and Miranker, 2002; Patil et al., 2011; Tornquist et al., 2018). Amyloid fibrils share a common structural property of protein association through a cross-β spine motif, stabilized by intermolecular hydrogen-bonded parallel β-sheet layers arranged perpendicular to the long axis of the fibril (Nelson et al., 2005; Chiti and Dobson, 2017; Almeida and Brito, 2020). They also share similar morphologies, often being microns long with widths of ~10 nm and a twisting repeat of ~100 nm (Dobson, 2003; Qiang et al., 2017).

Amyloidogenic aggregates have historically provided the primary histopathological markers of AD, PD, and HD. These aggregates are generally termed "amyloid fibrils" when formed extracellularly and 'inclusions' when formed intracellularly. The hallmarks of AD are extracellular plaques composed primarily of Aβ peptides and intracellular neurofibrillary tangles enriched in hyperphosphorylated variants of the protein tau (Zheng and Koo, 2011). PD is characterized by cytoplasmic aggregates called Lewy bodies and inclusions called Lewy neurites, of which α-syn is the main component (Braak et al., 1999). Intracellular accumulation of mHtt into amyloid-like inclusion bodies is a primary feature of HD (Yamamoto et al., 2000; Arrasate et al., 2004).

The concept that insoluble fibrils, whether extra- or intracellular, are the primary cytotoxic factors that initiate amyloidogenic disease is the core tenet of the "amyloid cascade hypothesis" (Figure 5, left) first proposed by Hardy and Higgins to describe the role of Aβ amyloids in AD pathogenesis (Hardy and Higgins, 1992). Subsequently it was proposed that α-syn fibrils are the primary cytotoxic factors in PD (Stefanis, 2012) and that amyloid fibril-like inclusions of mHtt are the primary cytotoxic factors in HD (Scherzinger et al., 1999). There is considerable controversy, however, on whether amyloid fibrils are the only, or even the principal culprits in pathology. A confounding factor is the heterogeneity of species associated with amyloid formation. Amyloidogenesis involves a hierarchy of structures that starts from the functional, soluble form of a protein or peptide and proceeds to oligomers, nuclei, β-sheets, protofilaments, protofilament bundles, and finally mature fibrils (Serpell, 2000)

(Figure 4). Within the fibrils themselves, there are structural polymorphs that can differ depending on whether they are grown *in vitro* or isolated from patients. In fact, increasing evidence suggests distinct structural polymorphs are associated with specific disease subtypes. Therefore, considerable uncertainty surrounds which species represent the culprits in pathogenicity (Carulla et al., 2005; Lansbury and Lashuel, 2006; Haass and Selkoe, 2007; Zraika et al., 2010), with some recent proposals advancing that soluble oligomers (Larson and Lesné, 2012; Arbor et al., 2016; Cline et al., 2018) or even individual proteins/peptides (Hoffner and Djian, 2014; Hillen, 2019) could initiate the phenotypic cascade of amyloidogenic diseases. Because mature fibrils are insoluble and extremely stable, many view soluble oligomeric precursors as the most likely candidates for cytotoxicity. However, studies on amyloid oligomers have been hampered by the low concentrations and transitory nature of these intermediates (Engel, 2009), thereby contributing to a lack of evidence for this model. Finally, it unclear whether cytotoxicity is associated with intracellular or extracellular forms of amyloidogenic proteins (Cuello, 2005; Gurlo et al., 2010; Aston-Mourney et al., 2011).

Much of the current research on the mechanisms of amyloidogenic diseases has shifted focus towards processes preceding mature fibril formation. As a result, it has now been widely demonstrated that mitochondrial dysfunction occurs early in the pathogenesis of AD (Wang et al., 2020b), PD (Malpartida et al., 2021), and HD (Carmo et al., 2018). The "mitochondrial cascade hypothesis", originally proposed by Swerdlow and colleagues, proposes that it is in fact the progressive decline in mitochondrial function that promotes AD pathology and influences the progression of the disease (Swerdlow et al., 2014) (Figure 5, right). Therefore, exactly how amyloidogenic proteins interact with mitochondria, and specifically how they may engage the mitochondrial protein import machinery, is a key mechanistic question in understanding the pathology of neurodegenerative disorders.

4 Neurodegenerative diseases and pathogenic mechanisms of amyloids

Aβ, α-syn, and Htt/mHtt are among the approximately 50 amyloidogenic proteins associated with human diseases (Chiti and Dobson, 2017). In this section, we review the roles of these proteins in AD, PD, and HD, respectively, with a special emphasis on their interactions with mitochondria.

4.1 Alzheimer's disease and the roles of APP and Aβ

AD is the leading cause of senile dementia, affecting several regions of the brain involved in memory and cognition, including the hippocampus, the neocortex, and the basal forebrain (Auld et al., 2002). While the exact etiology of AD is unknown, it is biologically characterized by the aggregation of two misfolded proteins: Aβ, the primary component of extracellular plaques, and hyperphosphorylated variants of the microtubule-associated protein tau, which form intracellular inclusions known as neurofibrillary tangles (NFTs) (Knopman et al., 2021). Aβ is produced through sequential cleavage of APP, a membrane glycoprotein with isoforms ranging from 100 to 140 kDa that predominantly reside at neuronal synapses (Zhou et al., 2011; Hoe et al., 2012) (Figure 6A). APP plays a vital role in neural development and synaptic plasticity, as it is implicated as a receptor involved in kinesin 1 cargo recognition (Lazarov et al., 2005), the Wnt signaling pathway (Liu T. et al., 2021) and other functions including cell adhesion, synaptogenesis (Baumkötter et al., 2014), and iron export (Duce et al., 2010). As a type I integral membrane protein, APP has a large ectodomain at its N-terminus, a single α-helical transmembrane segment, and a small C-terminal intracellular domain. APP belongs to a highly conserved superfamily of genes (Coulson et al., 2000; Jacobsen and Iverfeldt, 2009). In mammals, alternative splicing generates eight APP isoforms, the three most common being APP_{695}, APP_{751}, and APP_{770}, among which APP_{695} is most highly expressed in neurons (Sandbrink et al., 1996; Belyaev et al., 2010). Like other plasma membrane proteins, the life cycle of APP following synthesis consists of membrane trafficking via the secretory pathway and degradation and recycling by the endocytic system (Lin et al., 2021). The Aβ peptides that form amyloid plaques in AD are derived from the processing of APP through sequential actions of β- and γ-secretases (Selkoe and Hardy, 2016; Zhao et al., 2020) (Figure 6B). The generated Aβ peptides range in size, with the 42-residue $Aβ_{42}$ being much more aggregation-prone than the more abundant 40-residue $Aβ_{40}$ (Seubert et al., 1992; Haass and Selkoe, 2007; Chow et al., 2010). Monomeric $Aβ_{40}$ and $Aβ_{42}$ are intrinsically disordered in solution (Roche et al., 2016), with $Aβ_{42}$ having a transient population of β-sheet structure (Kakeshpour et al., 2021).

The neuropathology of AD has historically been described by the amyloid cascade hypothesis, whereby Aβ deposition is the causative event (Hardy and Higgins, 1992). In support of this hypothesis, early-onset familial AD (FAD) is caused by autosomal dominant inheritance mutations in the genes encoding APP or APP processing enzymes (Bekris et al., 2010; Ricciarelli and Fedele, 2017). However, the vast majority of cases are sporadic, late onset AD (LOAD) occurring without mutations in the genes encoding APP or APP processing enzymes (Bekris et al., 2010). While the correlation between Aβ and AD remains strongly supported (Herrup, 2015), intracellular Aβ in the form of soluble monomers and oligomers are now considered to be the primary toxic species rather than insoluble, fibrillar assemblies of Aβ that form extracellular plaques (Goure et al., 2014; Gallego Villarejo et al., 2022). Despite this, soluble Aβ species precede the formation of plaques, which are found in patient brains prior to the onset of clinical symptoms, and it has been shown that Aβ alone is not sufficient to induce disease pathogenesis (Herrup, 2015). This suggests a more complex pathological mechanism at play that led to the development of a variety of alternative hypotheses surrounding AD etiology.

One prevailing proposal is the ApoE cascade hypothesis (Martens et al., 2022), based on the genetic association of LOAD with the apolipoprotein ε4 allele (APOE4) (Corder et al., 1993). APOE4 carriers have a vastly increased risk of developing LOAD and a reduced age of onset compared to carriers of the

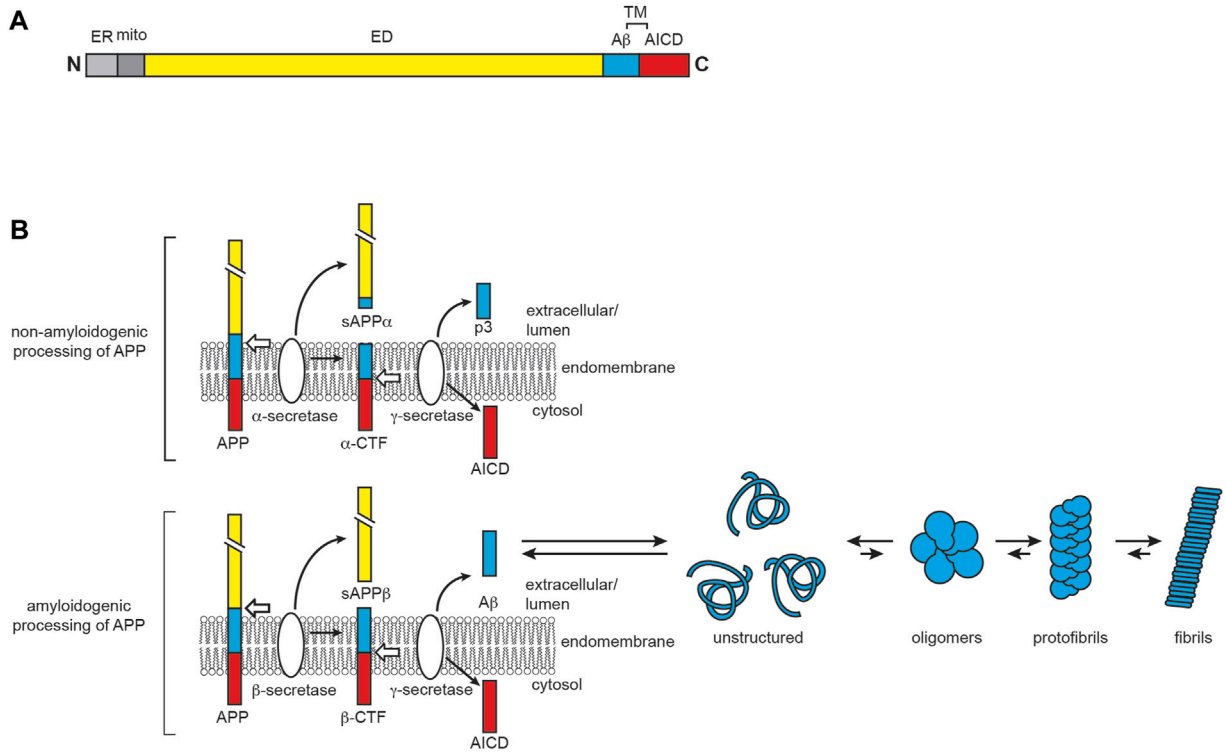

FIGURE 6
AD and the role of APP and Aβ. **(A)** APP domain organization. Full-length APP contains an extracellular domain (ED, yellow), a transmembrane region (TM), and the APP intracellular domain (AICD, red). The proteolysis product corresponding to Aβ is shown in cyan. The N-terminal ER- and mitochondria-targeting sequences are shown in light and dark gray, respectively. **(B)** APP processing and Aβ aggregation. APP has two main proteolytic fates. In the non-amyloidogenic pathway (top), APP is first cleaved by α-secretase to yield soluble APPα (sAPPα) and the α-C-terminal fragment (α-CTF), the latter of which is then cleaved by γ-secretase to produce AICD and the non-amyloidogenic extracellular peptide p3. In the amyloidogenic pathway (bottom), β-secretase proteolyzes full-length APP to yield soluble APPβ (sAPPβ) and the β-C-terminal fragment (β-CTF), the latter of which is then cleaved by γ-secretase to produce AICD and the amyloid beta peptide Aβ. The Aβ peptide, particularly $Aβ_{42}$, is disordered in solution and prone to aggregation and fibrillization.

APOE3 and APOE2 isoforms (Corder et al., 1993; Sando et al., 2008). ApoE is a 34 kDa lipid-binding protein that primarily functions in lipid transport and metabolism (Mahley, 2016), with differences among the ApoE2, E3, and E4 isoforms confined to two sites (residues 112 and 158) (Najm et al., 2019; Martens et al., 2022). The primary functional difference in ApoE4 is its binding preference for very-low density lipoprotein (VLDL) over high-density lipoprotein (HDL), whereas the ApoE2 and ApoE3 isoforms preferentially bind HDL (Raffai et al., 2001; Belloy et al., 2019). While ApoE contributes to Aβ synthesis, accumulation, and clearance in an isoform-dependent manner, there is conflicting evidence on the isoform-specific roles of ApoE in Aβ pathology (Koistinaho et al., 2004; Castellano et al., 2011; Huang and Mahley, 2014; Najm et al., 2019). The ApoE cascade hypothesis does not include Aβ as a contributing factor in disease pathogenesis, stating that the biophysical and structural properties dependent of the ApoE isoform initiate a cascade of events driving AD and aging-related pathogenic condition (Martens et al., 2022). ApoE4 has been shown to alter lipid homeostasis and metabolism, leading to changes in lipid droplet formation, cholesterol turnover, and the PC/PE ratio (Farmer et al., 2019; Lazar et al., 2022; Yang et al., 2023). Consistent with MAM alterations, several lines of work support the involvement of ApoE in mitochondrial dysfunction as a contributing component to disease pathogenesis, including recent findings suggesting mitochondrial dysfunction influences ApoE expression and secretion (Dose et al., 2016; Martens et al., 2022; Wynne et al., 2023).

AD is associated with pronounced defects in mitochondrial function (Cenini and Voos, 2019; Wang et al., 2020c). These include alterations in mitochondrial biogenesis and morphology, and decreases in mitochondrial number (Hirai et al., 2001; Qin et al., 2009; Oka et al., 2016; Brustovetsky et al., 2023); compromised energy metabolism, including glucose hypometabolism (Kumar et al., 2022) and deterioration of the TCA and OXPHOS systems (particularly CIV) (Bubber et al., 2005; Liang et al., 2008; Zhang et al., 2015; Mastroeni et al., 2017; Sorrentino et al., 2017; Adav et al., 2019; Ryu et al., 2021); oxidative stress (Misrani et al., 2021); effects on mitochondrial dynamics, most notably a general increase in fragmentation (Wang et al., 2008a; Wang et al., 2009); impairment of mitochondrial trafficking (Calkins et al., 2011); and altered ER-mitochondria apposition with associated cellular Ca^{2+} dyshomeostasis (Leal et al., 2020; Fernandes et al., 2021; Li et al., 2023). While these effects could be associated with the interaction of APP/Aβ with mitochondria (see below), other AD-related factors could also be involved.

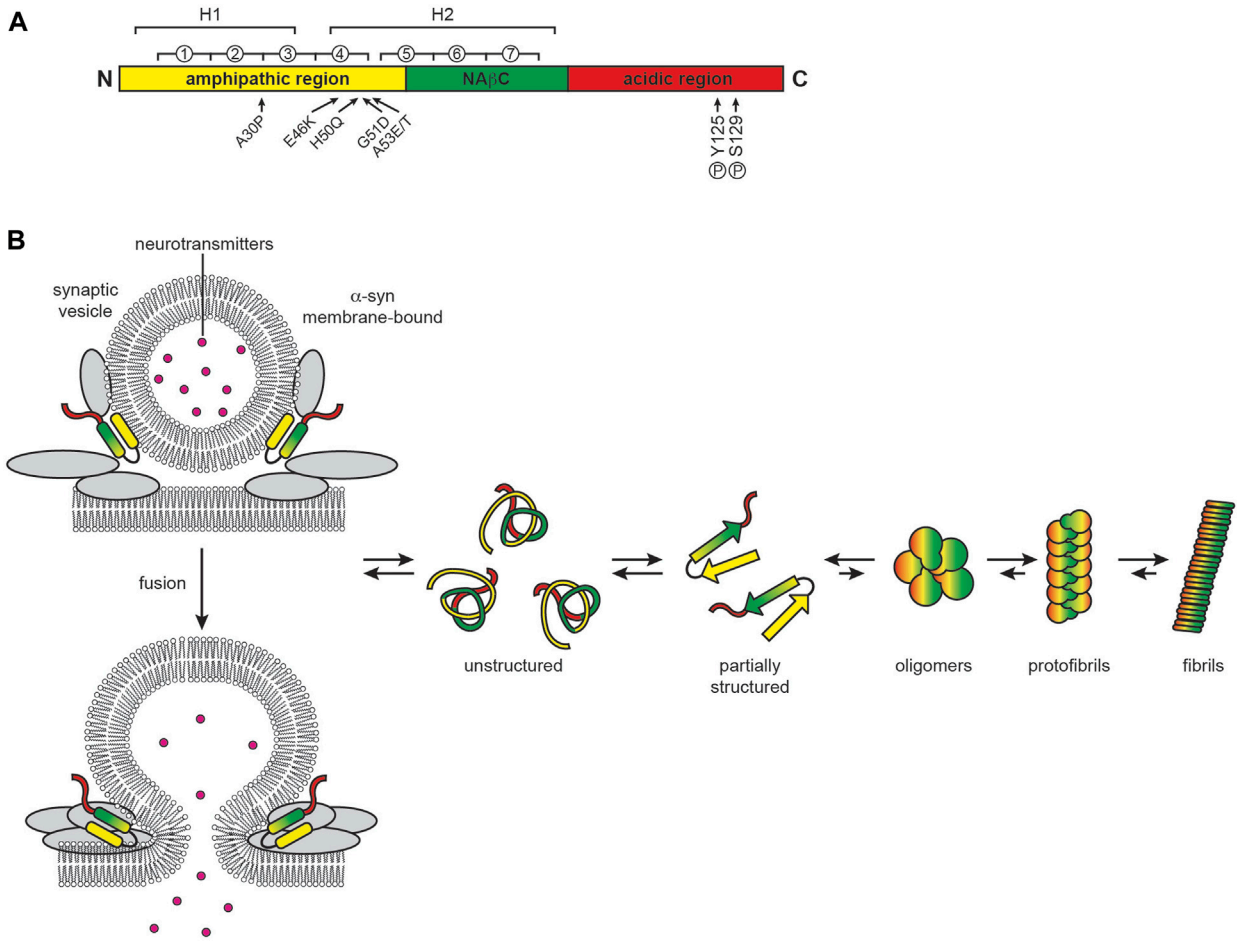

FIGURE 7
PD and the role of α-syn. **(A)** α-syn domain organization. α-syn contains an N-terminal amphipathic region involved in membrane interactions (yellow, residues 1–60), a central non-amyloid β component (NAβC) responsible for protein fibrillization (green, residues 61–95) and a highly acidic C-terminal region (red, residues 96–140). Circled numbers indicate the seven 11-residue repeats containing the KTKEGV motif; H1 and H2 indicate the regions of helical propensity that form two helices in the micelle-bound state or can form an elongated helix when bound to lower-curvature membranes. Arrows indicate sites of point mutations and phosphorylation, as indicated, that enhance α-syn misfolding and aggregation **(B)** α-syn function and aggregation. When membrane bound, α-syn folds into a single elongated helix or forms a two-helix structure. In solution, α-syn is largely disordered and prone to aggregation and fibrillization.

4.2 Parkinson's disease and the role of α-syn

PD involves the selective degeneration of nigrostriatal dopaminergic neurons, manifesting as progressive effects on movement that include rigidity, resting tremor, and bradykinesia (Zhai et al., 2018). The main histological features of PD are cytoplasmic inclusions called Lewy bodies (LBs) and neuritic inclusions called Lewy neurites (LNs) whose core component is α-syn (Baba et al., 1998; Spillantini et al., 1998) but also contain vesicular structures, membranes and fragmented organelles (Shahmoradian et al., 2019; Ericsson et al., 2021). These α-syn aggregates are characteristic of a general group of neurodegenerative disorders termed synucleinopathies. α-syn is a 140 residue protein encoded by the synuclein alpha (*SNCA*) gene that contains three domains: (i) an N-terminal amphipathic region, (ii) a highly hydrophobic region called the non-amyloid-β component (NAβC), and (iii) a C-terminal acidic region (Bisi et al., 2021) (Figure 7A). Being enriched in the axon terminals of presynaptic neurons, α-syn is a membrane-interactive protein that plays a role in synaptic function, including vesicle trafficking and exocytosis by assembly of SNARE complexes, synaptic membrane remodeling, and maintenance of neurotransmitter vesicle pools (Bendor et al., 2013; Burre, 2015). α-syn also localizes to the nucleus, where it regulates gene expression (Somayaji et al., 2021).

Monomeric α-syn is intrinsically disordered in solution, dynamically interconverting among many different conformations that differ with respect to short- and long-range electrostatic interactions and transient secondary structures (Weinreb et al., 1996). The N-terminus of α-syn in solution has helical propensity with a low fractional population assuming α-helix conformation; however, when bound to membranes, it adopts a stable helical structure that is either a continuous helix or two separate helices (Davidson et al., 1998; Bussell and Eliezer, 2003; Chandra et al., 2003; Ulmer et al., 2005; Croke et al., 2008; Georgieva et al., 2008; Jao et al., 2008; Stockl et al., 2008; Cho et al., 2009; Bodner et al., 2010; Rao et al., 2010; Croke et al., 2011; Ullman et al.,

2011; Adao et al., 2020; Musteikyte et al., 2021). Membrane binding is facilitated by seven imperfect repeats of the 11-residue pattern xKTKEGVxxxx that extend from the amphipathic domain into the NAβC domain, a motif also found in apolipoproteins A2 (Bussell and Eliezer, 2003). This membrane-interactive region imparts classic amphitropic behavior to α-syn, which consequently promotes its interaction with curved bilayers, particularly with those enriched in negatively charged phospholipids (Jo et al., 2002) and cholesterol (Fantini et al., 2011). This membrane-binding activity is critical for its function in synaptic vesicle interaction (Fortin et al., 2005; Sarchione et al., 2021). The hydrophobic NAβC domain nucleates α-syn aggregation, forming the canonical β-structure of amyloid fibrils along with parts of the N-terminal domain (Rodriguez et al., 2015). The fraction of α-syn that natively exists in neurons in a membrane-bound state, as an unfolded monomer (Fauvet et al., 2012; Theillet et al., 2016), or as aggregation-resistant folded tetramers (Bartels et al., 2011; Wang et al., 2011) remains an open question.

Familial autosomal dominant PD is linked to defects in several genes, most of which have a connection to mitochondrial physiology (Cieri et al., 2017; Billingsley et al., 2018). Among them, the six known heritable mutations in the *SNCA* gene (A30P, E46K, H50Q, G51D, and A53E/T) all localize to the amphipathic N-terminal region of α-syn and promote aggregation (Flagmeier et al., 2016). α-syn aggregation can also be potentiated by increases in its copy number (Srinivasan et al., 2021). However, PD is primarily an idiopathic disease in which aging-related increases in α-syn aggregation and/or certain post-translational modifications of α-syn are commonly involved (Anderson et al., 2006; Manzanza et al., 2021; Roshanbin et al., 2021). The balance between α-syn function and pathogenicity is depicted in Figure 7B.

Mitochondrial dysfunction plays a key role in the pathogenesis of PD (Vicario et al., 2018). The enhanced expression of α-syn or particular mutants of α-syn known to promote PD cause the disruption of mitochondrial dynamics (Xie and Chung, 2012; Thorne and Tumbarello, 2022) and promote fragmentation (Kamp et al., 2010; Nakamura et al., 2011; Gui et al., 2012; Pozo Devoto et al., 2017), impair mitochondrial trafficking (Pozo Devoto et al., 2017) and autophagic clearance (Gao et al., 2017), impact mitochondrial energetics (Banerjee et al., 2010), and alter Ca^{2+} flux by the enhancement (Cali et al., 2012) or disruption (Guardia-Laguarta et al., 2014; Guardia-Laguarta et al., 2015; Paillusson et al., 2017) of specific ER-mitochondria tethering sites. One of the most prominent effects of PD is the impairment of respiratory Complex I associated with reduced energetic output and an overproduction of ROS (Devi et al., 2008; Marella et al., 2009). This multitude of effects is in line with the many mitochondrial subcompartments α-syn has been found to target, including the MOM (Li et al., 2007; Cole et al., 2008; McFarland et al., 2008; Nakamura et al., 2008; Zhang et al., 2008; Kamp et al., 2010; Nakamura et al., 2011; Di Maio et al., 2016a; Pozo Devoto et al., 2017), the MIM/IMS (McFarland et al., 2008; Nakamura et al., 2011; Zhu et al., 2011; Lu et al., 2013; Robotta et al., 2014; Amorim et al., 2017), the matrix (McFarland et al., 2008; Ludtmann et al., 2016; Ludtmann et al., 2018) and the MAM (Cali et al., 2012; Guardia-Laguarta et al., 2014; Paillusson et al., 2017). Importantly, this extensive interaction of α-syn with mitochondria is mediated in part through lipid bilayer interactions, particularly with regions enriched with the mitochondrial lipid cardiolipin (Ramakrishnan et al., 2003; Cole et al., 2008; Nakamura et al., 2008; Grey et al., 2011; Zigoneanu et al., 2012; Robotta et al., 2014; Ryan et al., 2018) that provides the negative surface, high curvature, and acyl packing defects necessary to promote α-syn binding (Sharon et al., 2003; Nuscher et al., 2004; Middleton and Rhoades, 2010; Pfefferkorn et al., 2012; Ouberai et al., 2013; Gilmozzi et al., 2020).

4.3 Huntington's disease and the role of mHtt

HD is associated with neurodegeneration of the basal ganglion, with preferential deterioration of striatal medium spiny GABAergic neurons, that clinically presents as progressive loss of motor control and cognition (Morigaki and Goto, 2017). This monogenic disease is caused by heritable alterations in Htt (Jurcau and Jurcau, 2022). Structurally, Htt is a 348 kDa protein that contains two domains of HEAT tandem repeats that form α-solenoid structures connected by a bridge domain, and an N-terminal region with a tripartite organization that contains a highly conserved sequence of 17 N-terminal amino acids (Nt17), a stretch of glutamine residues (poly-Q), and a proline-rich domain (PRD) (Saudou and Humbert, 2016; Guo et al., 2018) (Figure 8A). Htt is conformationally dynamic, with an extensive list of interaction partners likely owing to the protein-interaction functions of its HEAT repeats (Shirasaki et al., 2012). As such, it serves as a multivalent molecular scaffold, a function that likely supports its many interactions in synapses including axonal transport, vesicle recycling, autophagy, transcriptional regulation, and endocytosis (Barron et al., 2021).

HD is an autosomal dominant disorder caused by an extension of the poly-Q tracts resulting from polymorphic CAG trinucleotide repeat expansion in exon 1 of the *HTT* gene (MacDonald et al., 1993). HD is part of a larger family of neurodegenerative diseases associated with polyglutamine expansion of proteins (Lieberman et al., 2019). Whereas Htt in healthy individuals contains fewer than 36 CAG repeats, the pathogenically expanded poly-Q region can contain between 42 and 250 CAG repeats, with disease severity and earlier age of onset directly related to the extent of expansion (Rubinsztein et al., 1996; Penney et al., 1997). Because Htt is ubiquitously expressed, HD affects not only the brain but also peripheral tissues with high metabolic activity (Chuang and Demontis, 2021). Poly-Q expansion causes the resulting mHtt protein to have altered folding (Vijayvargia et al., 2016) and interactions (Ratovitski et al., 2012; Greco et al., 2022). This makes mHtt prone to aggregation, forming inclusion bodies in the cytoplasm and nucleus (Davies et al., 1997) with diverse aggregate structures (Tanaka et al., 2001; Poirier et al., 2002) and a complex composition that includes lipids, proteins, and membrane-bound organelles (Kegel-Gleason, 2013; Riguet et al., 2021). Notably, the primary cytotoxic, aggregation-prone species in HD may not be full-length mHtt, but rather heterogeneous populations of N-terminal fragments of mHtt exon 1 (Httex1) (Mangiarini et al., 1996; Cooper et al., 1998; Hackam et al., 1998; Martindale et al., 1998; Hoffner et al., 2005; Barbaro et al., 2015) that can arise by cleavage of the mature protein by caspase, calpain, or other proteases (Goldberg et al., 1996; Wellington et al., 1998; Kim

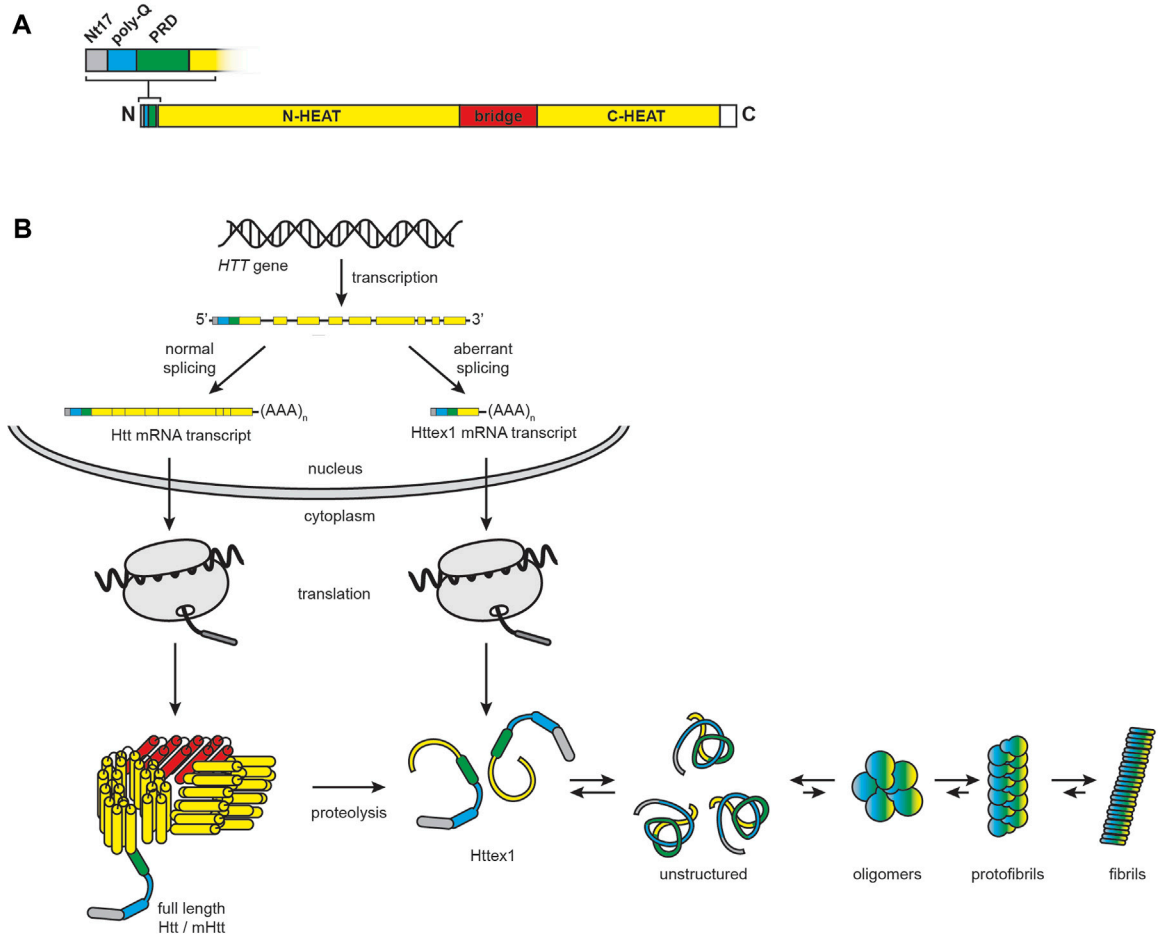

FIGURE 8
HD and the role of mHtt. **(A)** Htt domain organization. Full-length huntingtin is a 3144-residue protein that consists of N-terminal (residues 91–1683) and C-terminal (residues 2092–3057) α-helical solenoid domains containing multiple HEAT (huntingtin, elongation factor 3, protein phosphatase 2A, lipid kinase TOR) repeats (yellow) connected by a helical linker region (red, residues 1684–2091). The full-length protein also features an N-terminal region consisting of the Nt17 sequence (grey, residues 1–17), the poly-Q tract, which is expanded in HD (cyan, residues 18–40), and a proline-rich domain (green, residues 41–90). **(B)** Htt biogenesis, processing, and misfolding. In the nucleus, normal splicing of the *HTT* gene results in a full-length transcript, whereas alternative splicing and premature polyadenylation results in a transcript encoding Httex1. Following translation in the cytosol, full-length Htt is subject to extensive proteolysis, which also contributes to the pool of Httex1 protein. Httex1 is unstructured in solution and prone to aggregation and fibrillization.

et al., 2001; Gafni and Ellerby, 2002; Lunkes et al., 2002; Graham et al., 2006; Schilling et al., 2007; Landles et al., 2010; Tebbenkamp et al., 2012; Martin et al., 2019), or by aberrant splicing and premature polyadenylation of pathogenic *HTT* exon 1 with expanded CAG repeats (*HTT*ex1 transcripts) (Sathasivam et al., 2013; Neueder et al., 2017; Neueder et al., 2018) (Figure 8B).

Mitochondrial dysfunction plays a central role in HD pathogenesis (Bossy-Wetzel et al., 2008; Carmo et al., 2018; Jurcau and Jurcau, 2023). HD is associated with reduced mitochondrial biogenesis and quality control (Steffan et al., 2000; Cui et al., 2006; Weydt et al., 2006; Jin and Johnson, 2010; Wong and Holzbaur, 2014; Khalil et al., 2015; Guo et al., 2016; Dubois et al., 2021; Sonsky et al., 2021), mtDNA heteroplasmy (Wang et al., 2021), defective energy metabolism and OXPHOS activity (Sawa et al., 1999; Klivenyi et al., 2004; Seong et al., 2005; Benchoua et al., 2006; Pandey et al., 2008; Mochel et al., 2012; Silva et al., 2013; Naia et al., 2015; Burtscher et al., 2020), altered mitochondrial Ca^{2+} handling and sensitivity to the mitochondrial permeability transition pore (mPTP) (Panov et al., 2002; Choo et al., 2004; Milakovic et al., 2006; Giacomello et al., 2013), increased mitochondrial oxidative stress (Sorolla et al., 2008; Chae et al., 2012; Ribeiro et al., 2012; Ribeiro et al., 2014; Chen et al., 2017; Moretti et al., 2021; Lopes et al., 2022; Egidio et al., 2023), defective mitochondrial dynamics and hyper-fission (Costa et al., 2010; Song et al., 2011; Shirendeb et al., 2012; Manczak and Reddy, 2015; Cherubini et al., 2020), defective mitochondrial trafficking (Trushina et al., 2004; Chang et al., 2006; Orr et al., 2008; Shirendeb et al., 2012; Berth and Lloyd, 2023), and altered cytochrome *c* release with apoptosis (Chen et al., 2000; Kiechle et al., 2002; Zhang et al., 2006; Wang et al., 2008b). Although many of these effects are related to spurious interactions of mHtt with cytosolic proteins, there are several reports that full-length and N-terminal fragments of Htt/mHtt interact directly with mitochondria (Panov et al., 2002; Choo et al., 2004; Petrasch-Parwez et al., 2007; Orr et al., 2008; Song et al., 2011; Guo et al., 2016). Some

10.3389/fphys.2023.1263420

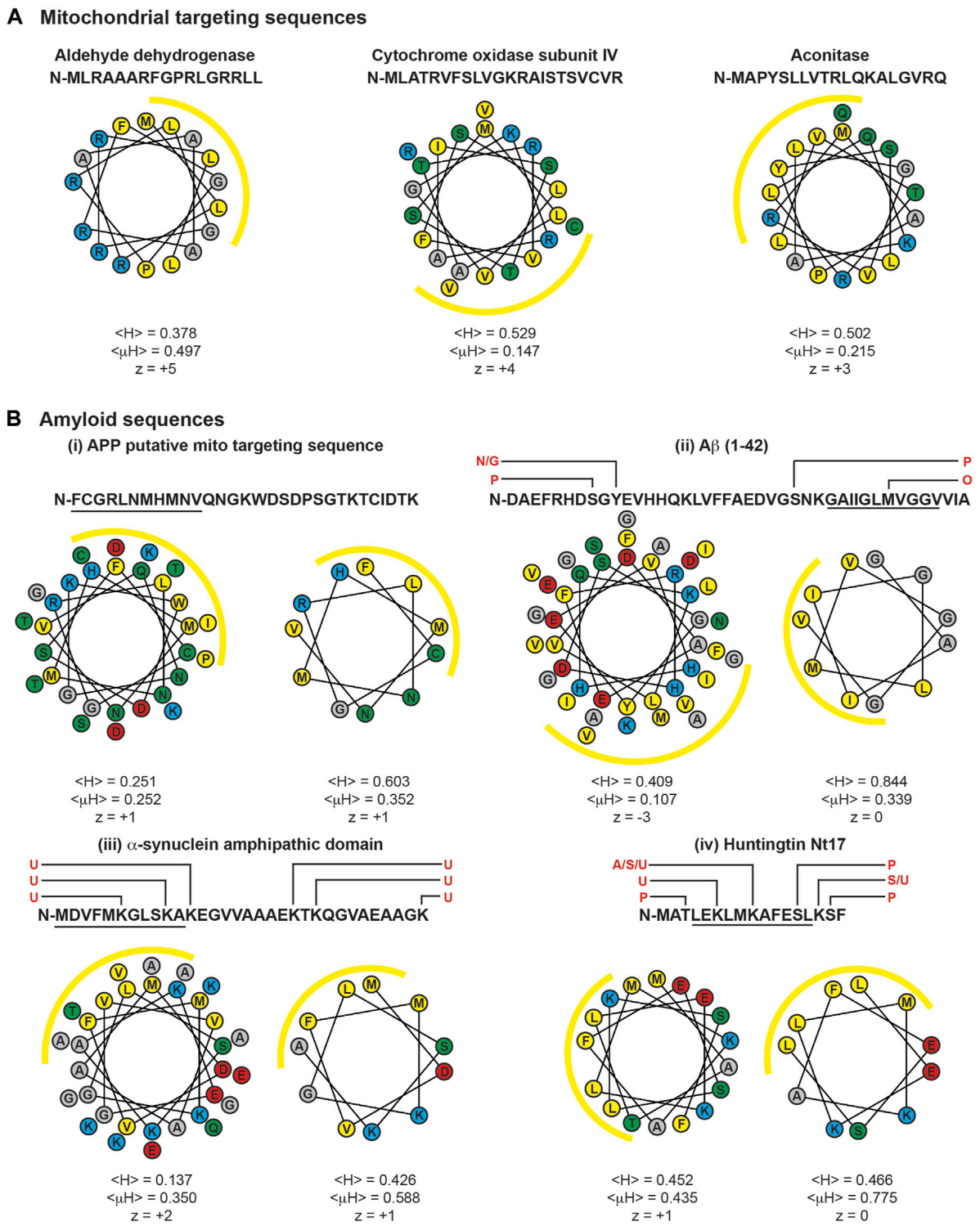

FIGURE 9
MTSs and cryptic targeting sequences of amyloids. Sequences and helical wheel diagrams of MTSs and select regions of amyloidogenic proteins are depicted. Helical projections and parameters were determined using the HeliQuest server (Gautier et al., 2008). Mean hydrophobicity is denoted as <H>, hydrophobic moment as <μH>, and net charge as z. For all projections, the N-terminal residue is oriented due North (0°), and yellow arcs indicate the hydrophobic face of the amphipathic helices determined by <μH> values. **(A)** Example MTSs. Human variants of select TIM23 substrates aldehyde dehydrogenase, subunit IV of Cytochrome *c* oxidase, and aconitase are shown. **(B)** Cryptic targeting signals of amyloidogenic proteins. These include the putative MTS of: (i) APP, (ii) Aβ (1-42), (iii) α-syn (1-32), and (iv) huntingtin (1-17). Helical projections to the left show the entire sequence. Helical projections to the right show the 11-residue (~3 helical turn) section with the strongest amphipathic character, indicated by the underlined residues. Known sites of post-translational modification are indicated above the primary sequences in red (A, acetylation; G, glycosylation; N, nitration; O, oxidation; P, phosphorylation; S, SUMOylation; U, ubiquitinylation). Single letter amino acid codes colored by side chain functionality: yellow, hydrophobic; red, acidic; cyan, basic; green, polar uncharged.

of these studies specifically implicate interactions with the MOM (Hamilton et al., 2020) and some show interactions with internal mitochondrial compartments (Yano et al., 2014; Yablonska et al., 2019). In general, accumulation of N-terminal mHtt fragments with mitochondria increases with age (Orr et al., 2008). Potential interactions between Htt/mHtt and the mitochondrial import machinery are discussed below.

5 Interactions of amyloidogenic proteins with the mitochondrial protein import machinery

5.1 Noncanonical and multi-specific targeting signals

Most proteins that are targeted to cellular compartments other than their site of ribosomal synthesis contain unambiguous targeting sequences that faithfully direct them to a specific location. For example, as described above, the MTSs of TIM23 substrates form an N-terminal amphipathic α-helix that serves as the primary recognition element of the TIM23 import machinery. Three examples of MTSs shown in Figure 9A illustrate their amphipathic character: they have an appreciable number of nonpolar residues quantified as the mean hydrophobicity (<H>) (Fauchere and Pliska, 1983), a net charge (z) that reflects a preponderance of basic residues, and an asymmetric distribution of nonpolar and basic residues quantified by the hydrophobic moment (<μH>) (Eisenberg et al., 1982). Yet it is also notable that MTSs vary significantly with respect to sequence, length, and extent of amphipathicity. Thus, while canonical MTSs encompass a range of physicochemical properties, they are sufficiently well-defined enough to be recognized by a single import pathway.

For some proteins, however, the relationship between the targeting sequence and the organellar import pathway is not straightforward and some targeting sequences can direct passenger proteins to multiple cellular compartments by non-mutually exclusive mechanisms (Karniely and Pines, 2005). Indeed, targeting fidelity requires multiple levels of regulation and precise recognition because mitochondrial MTSs, ER signal peptides, chloroplast transit peptides, and even some peroxisomal targeting signals share similarity in that they all form N-terminal amphipathic α-helices with a hydrophobic face and a basic (or polar) face (Kunze and Berger, 2015).

Some proteins contain an ambiguous (or cryptic) targeting sequence that can be recognized by multiple import machineries (Lu et al., 2004; Ventura et al., 2004; Chatre et al., 2009). Other proteins contain well-defined targeting signals whose accessibility or targeting efficiency can be modified by folding, protein binding, or post-translational modifications (Karniely and Pines, 2005). Still other proteins contain multiple targeting signals that direct them to different compartments (Petrova et al., 2004; Pino et al., 2007). For example, some cytochromes P450 (CYPs) expressed in hepatocytes contain chimeric signals with amino-terminal ER-targeting sequences in tandem with a mitochondrial-targeting sequence (Addya et al., 1997; Anandatheerthavarada et al., 1999; Robin et al., 2001; Robin et al., 2002). The bipartite targeting sequence of these cytochromes contain a cryptic mitochondria localization signal that remains idle until activation. In the case of CYP2E1, the mitochondrial targeting signal is activated by cyclic-AMP-dependent phosphorylation of a Ser residue in the cryptic sequence (Robin et al., 2002). Moreover, an inducible endoprotease has been identified that activates mitochondrial import by cleaving bimodal targeting signals to expose the cryptic mitochondrial targeting signal (Boopathi et al., 2008). It is unclear whether such cleavage of chimeric signals is a general requirement for mitochondrial targeting.

By allowing greater diversity of potential cellular locations, noncanonical targeting imparts flexibility to the functional range of individual proteins that can be subject to regulation by the cell in response to different physiological demands. However, cryptic targeting sequences can also cause the pathogenic accumulation of proteins in organelles. In the following sections, we review the cryptic mitochondria targeting sequences present in Aβ/APP, α-syn, and Htt/mHtt that may facilitate their interactions with the mitochondrial import machinery.

5.2 Interactions of Aβ and APP with the mitochondrial import machinery

Several lines of evidence indicate that full-length APP engages the TIM23 import pathway. The canonical biogenesis route of APP entails targeting to the ER via the SRP/Sec61 pathway, translocation across the ER membrane attendant with glycosylation of the ectodomain, integration as a type I membrane protein, and trafficking by the secretory, endocytic and recycling routes (Muresan and Ladescu Muresan, 2015). APP contains a classic N-terminal Sec-targeting signal with a predicted Signal Peptidase cleavage site (AxA) between positions 17 and 18 (Auclair et al., 2012; Almagro Armenteros et al., 2019). Following this ER-targeting signal is a potential cryptic MTS spanning residues 37 to 67, segments of which could form an amphipathic helix (Figure 9Bi). Thus, together they form a chimeric ER-mitochondria targeting signal (Devi and Anandatheerthavarada, 2010). Indeed, it has been shown using human cortical neuronal cells that a non-glycosylated form of APP_{695} can stall in the mitochondrial import pathway with a predicted N^{mito}/C^{cyto} topology. This stalled intermediate made crosslinking-detected interactions with Tom40, Tim23, and Tim44, in a manner that required the $\Delta\psi_m$ and the positive residues Arg40, His44, and Lys51, all three of which reside on a common face of the putative MTS (Anandatheerthavarada et al., 2003) (Figure 9Bi). Similar translocation intermediates of APP were observed in mitochondria of transgenic AD mouse models (Anandatheerthavarada et al., 2003) and in postmortem samples of AD brains (Devi et al., 2006), the latter showing stable association of APP with ~480 kDa complexes containing the TOM machinery and ~620 kDa complexes containing the TIM23 machinery. The stalling of APP in the import machinery appeared to be due to the tight folding of the APP acidic domain (residues 220–290) blocking transport along the TOM complex, as deletion of this domain facilitated complete translocation (Anandatheerthavarada et al., 2003). This observation is consistent with the formation of stalled translocation intermediates observed with native

10.3389/fphys.2023.1263420

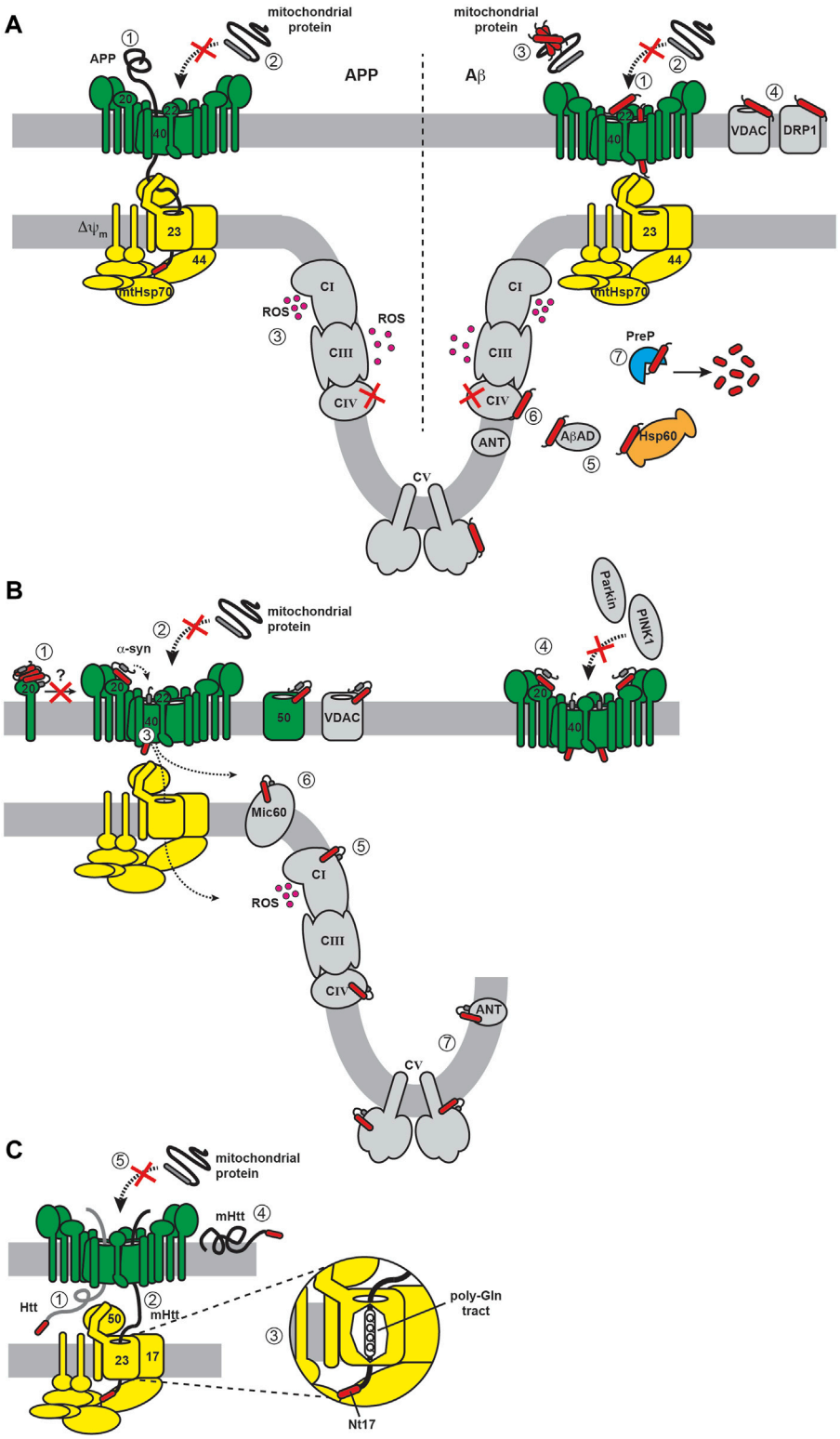

FIGURE 10
Interactions of amyloidogenic proteins with the TIM23 complex. Models show import complex color scheme used in Figure 2 (TOM/SAM complex, green; TIM23 complex, yellow) with other proteins depicted in grey. Subunits known to interact with amyloids are explicitly indicated by their names. Putative cryptic targeting signals of Aβ/APP, α-syn, and Htt/mHtt are shown in red. [**(A)**, left] APP. (1) APP forms a two membrane-spanning intermediate, engaging both TOM and TIM23 complexes in a $\Delta\psi_m$-dependent manner, with complete translocation blocked by the tight folding of the C-terminal AICD domain. (2) Stalled APP intermediates block the import of native mitochondrial precursor proteins. (A, right) Aβ. (1) Aβ interacts with the TOM complex (subunits Tom22 and Tom40), which (2) disrupts the import of native mitochondrial precursors. (3) Aβ forms co-aggregates with mitochondrial precursors in the cytosol. Aβ interacts with proteins of the (4) MOM, (5) matrix, and (6) MIM, most notably CIV and CV. (7) Aβ is degraded by the matrix PreP protease. A general feature of APP/Aβ stress is dysfunctional CIV and excess ROS production by the OXPHOS machinery. **(B)** α-syn. (1) Multimers of α-syn

(*Continued*)

FIGURE 10 (Continued)
interact with free Tom20, blocking its assembly with the TOM complex. The engagement of α-syn with TOM complex receptors and channel may (2) hinder import of native mitochondrial proteins, (3) reduce Tom40 expression, and/or (4) disrupt PINK1/Parkin-mediated mitophagy; (5) Interaction of α-syn with CI or CIV may disrupt ETC activity and cause ROS overproduction; (6) Interaction of α-syn with MICOS subunit Mic60 may affect cristae morphogenesis; (7) Interaction of α-syn with ATP synthase (CV) or the adenine nucleotide translocase (ANT) may disrupt adenine nucleotide flux and/or ATP production. **(C)** Htt/mHtt. (1) Htt may engage the TOM machinery with a tendency to accumulate in the IMS. (2) mHtt engages the TIM23 complex, (3) possibly facilitated by the unstructured poly-Q segment C-terminal to Nt17, which provides a flexible linker for Nt17 to engage TIM23 subunits. (4) mHtt may alternatively accumulate on the cytosolic side of the MOM. (5) Blockage of the import machinery by Htt/mHtt hinders import of mitochondrial precursors.

mitochondria-targeted substrates with tightly folded (cofactor-bound) C-terminal domains and fusion constructs with MTSs fused to cofactor-stabilized domains like DHFR (Schneider, 2018). In agreement with the known effects of AD on mitochondria function, APP translocation intermediates were shown to interfere with the import of native mitochondrial proteins (Devi et al., 2006). The extent to which mitochondrial targeting of APP may be facilitated by endoprotease cleavage of the ER targeting signal to expose the cryptic MTS (Boopathi et al., 2008) is an open question. Figure 10A (*left*) summarizes the interactions of APP with mitochondria.

The Aβ peptide has also been widely reported to accumulate in mitochondria through the import machinery. The presence of Aβ within mitochondria is well documented by its direct interactions with many mitochondrial proteins, including MOM proteins VDAC (Manczak and Reddy, 2012) and Drp1 (Manczak et al., 2011), matrix proteins Hsp60 (Caspersen et al., 2005), Aβ-binding alcohol dehydrogenase (ABAD) (Lustbader et al., 2004) and cyclophilin D (Du et al., 2008), and OXPHOS complexes including Complex IV (Hernandez-Zimbron et al., 2012) and ATP synthase (Beck SJ. et al., 2016). Furthermore, a pronounced feature of AD pathogenesis is the mitochondrial accumulation of Aβ (Caspersen et al., 2005; Manczak et al., 2006; Cha et al., 2012). $A\beta_{42}$ has been shown to enter mitochondria through the TOM complex, associating with the MIM fraction in a $\Delta\psi_m$-independent manner and localizing to cristae in both *in vitro* import systems and in mitochondria from human brain biopsies (Hansson Petersen et al., 2008). The specific interactions of Aβ with the TOM complex were explored using a yeast mitochondria model system, indicating that Aβ binds directly to the Tom22 receptor, but not Tom20 or Tom70, and that Aβ residues 25–42 were indispensable for this interaction (Hu et al., 2018). The accumulation of Aβ within the import machinery is functionally relevant because it inhibits the import of native nuclear-encoded proteins (Sirk et al., 2007). However, it should also be noted that cytosolic Aβ may inhibit the import of mitochondrial proteins by coaggregation in the cytosol that does not involve blocking the mitochondrial import machinery (Cenini et al., 2016). A common theme in these studies is that the more aggregation-prone $A\beta_{42}$ has a stronger interaction with the import machinery than the $A\beta_{40}$ variant (Sirk et al., 2007; Cenini et al., 2016; Hu et al., 2018). Figure 10A (*right*) summarizes the interactions of Aβ with mitochondria.

As mentioned, ApoE4, the primary genetic risk factor for AD, induces increased connectivity between MAMs and mitochondria in different AD models (Area-Gomez et al., 2012; Tambini et al., 2016). MAMs have lipid raft-like membranes, enriched in sphingolipids and cholesterol, which promote the interaction between APP and its processing enzymes (β-secretase and γ-secretase) that have been found to localize at the MAM. The biophysical properties of these microdomains may enhance amyloidogenic processing of APP (Diaz et al., 2015; Del Prete et al., 2017; Area-Gomez et al., 2018). Additionally, the protein interactome of MAMs in cells with mutant APP is enriched in mitochondrial import components Tom22, Tim17b, and Sam50 (Del Prete et al., 2017). Enhanced proximity of APP to the mitochondrial import machinery could contribute to spurious import of APP.

There are some potentially confounding factors regarding the import of the Aβ peptide through the mitochondrial import machinery. The first is that Aβ produced from APP proteolysis is released into exocytoplasmic compartments (ER lumen or the extracellular space), whereas engagement with the mitochondrial import machinery occurs from the cytosol. However, there is evidence that proteolytically produced or externally added Aβ can be taken up by cells via clathrin-dependent or -independent endocytosis, followed by endosomal escape, which could allow it to localize to mitochondria (Saavedra et al., 2007; Hansson Petersen et al., 2008; Berridge, 2010; Friedrich et al., 2010). Furthermore, Aβ produced in the vicinity of mitochondria by MAM-localized secretases could directly access mitochondria (Area-Gomez et al., 2009). The second is that the presence of Aβ in the matrix would necessitate TIM23-mediated translocation; however, to date there is no evidence of a direct interaction between Aβ and the TIM23 complex. One explanation could be that the association between the short Aβ peptide and the TIM23 receptors and channel is too transient to be captured by techniques like crosslinking or immunoprecipitation. Lastly, the Aβ sequence does not contain any segments with strong amphipathicity (opposing basic and nonpolar faces) that are present in canonical MTSs (Figure 9Bii). This feature may hinder transport along the "acid chain" of the TIM23 pathway, possibly explaining how Aβ could stall nonproductively at the TOM complex.

It is noteworthy that AD is associated with a general disruption of the mitochondrial import machinery. Analysis of RNA-seq datasets from brains of AD patients versus age-matched healthy individuals showed that expression of mitochondrial import genes was decreased with AD (Sorrentino et al., 2017), consistent with the observed decrease in expression of Tom20 and Tom70 in postmortem neocortex samples of AD patients that correlate with higher $A\beta_{42}/A\beta_{40}$ ratios (Chai et al., 2018). It has also been proposed that the length of a poly-T polymorphism in the *TOMM40* gene correlates with LOAD, supporting the involvement of the TOM complex channel in AD pathogenesis (Roses et al., 2010); however, this finding has been questioned (Chiba-Falek et al., 2018). It is possible that altered expression of TOM complex subunits could

modulate mitochondrial interactions of APP/Aβ; for instance, decreased Tom20/70 expression relative to Tom22 could promote Aβ binding to the TOM complex (Hu et al., 2018).

The most compelling evidence that the mitochondrial import and processing machinery serves as a mechanism for amyloid clearance comes from the interaction between Aβ and PreP, the matrix-localized protease that digests MTSs (Pinho et al., 2014). This degradation step is critical because MTSs, being amphipathic and membrane-interactive, can disrupt MIM integrity and their buildup can lead to $\Delta\psi_m$ collapse and OXPHOS uncoupling (Teixeira and Glaser, 2013). Importantly, PreP was shown to degrade Aβ variants *in vitro* (Falkevall et al., 2006) and PreP activity is lower in the temporal lobes of AD patients and transgenic AD mice compared with controls, which may be further attributed to disease-related oxidative modifications (Alikhani et al., 2011b). Given the functional coupling between precursor processing and MTS turnover (Kucukkose et al., 2021), the accumulation of Aβ could overcome the MTS-clearing capacity of PreP and cause feedback inhibition of MIP and MPP, thereby inhibiting import by the toxic buildup of precursors and MTSs in the matrix (Mossmann et al., 2014). Conversely, overexpression of PreP in AD mouse models decreases mitochondrial Aβ concentrations and improves organellar function (Fang et al., 2015; Brunetti et al., 2016; Du et al., 2021). Given the key role of PreP in proteostasis (Brunetti et al., 2021), mitochondrial import of Aβ and its subsequent degradation may be essential for balancing cellular Aβ concentrations.

5.3 Interactions of α-syn with the mitochondrial import machinery

Several studies support the entry of α-syn into mitochondria through the import complexes. α-syn was first shown to accumulate in mitochondria in a manner that required the $\Delta\psi_m$ across the MIM and an accessible Tom40 channel (Devi et al., 2008). Furthermore, the possibility that the N-terminus of α-syn targets mitochondria is supported by the indispensable role of residues 1–32 in mitochondrial uptake (Devi et al., 2008) and of residues 1–11 in association of α-syn with isolated mitochondria (Robotta et al., 2014). When folded as an α-helix (stabilized by membrane interactions), the N-terminal 32 residues of α-syn form an amphipathic structure (Figure 9Biii), made up in part by the first two imperfect KTKEGV repeats that produce a Lys-rich basic face and a Val-rich nonpolar face. The N-terminus of α-syn therefore has strong potential to act as a cryptic MTS (Devi and Anandatheerthavarada, 2010).

TIM23-mediated uptake of α-syn is also supported by its physical and genetic interactions with subunits of the import machinery. Based on proteomics analysis of the interactome of the α-syn C-terminal peptide and its variants phosphorylated at Tyr125 and Ser129 that are known to promote aggregation (Samuel et al., 2016; Fayyad et al., 2020), the unmodified and phosphorylated peptides were found to preferentially interact with mitochondrial and cytosolic proteins, respectively (McFarland et al., 2008). In this study, the unmodified α-syn C-terminal peptide bound Tom40, Sam50, and Tom22, with the interaction to MOM proteins Tom40 and Sam50 strongly reduced by phosphorylation, suggesting the preferential import of unmodified α-syn (McFarland et al., 2008). This connection between α-syn aggregation propensity and mitochondrial import is further supported by the fact that all known PD-related missense mutations reside in the N-terminal region (Flagmeier et al., 2016) near the cryptic targeting sequence (Figure 7A). Perhaps more compelling are the specific ways in which N-terminal mutants of α-syn feature altered cellular interactions; namely, the A53T mutant shows increased affinity for mitochondria and the MAM, whereas the A30P mutant shows weaker affinity (Cole et al., 2008; Devi et al., 2008; Guardia-Laguarta et al., 2014; Pozo Devoto et al., 2017). This may be related to the decreased binding affinity of A30P mutant α-syn for lipid membranes (Jo et al., 2002; Fortin et al., 2004). Therefore, these PTMs and site mutations likely alter the aggregation propensity and membrane interactions of α-syn that subsequently affect its interaction with the mitochondrial import machinery in complex ways.

The involvement of the TOM complex in α-syn import was further investigated in two other studies. In one report, brain tissue taken from postmortem PD patients and transgenic mice overexpressing α-syn showed decreased expression of Tom40 concurrent with mtDNA damage, oxidative stress, and reduced bioenergetic efficiency (Bender et al., 2013). Another report used a rotenone-induced Complex I dysfunction model of PD, as well as postmortem brain tissue of PD patients, to show that α-syn (specifically, the S129 phosphomimetic and soluble oligomers) demonstrated strong but reversible binding to Tom20 and reduced Tom20 expression. This binding thereby prevented interactions between the Tom20/Tom22 receptors, inhibited the import of mitochondrial proteins, and inhibited respiration (Di Maio et al., 2016b). In these studies, the overexpression of either Tom40 (Bender et al., 2013) or Tom20 (Di Maio et al., 2016b; De Miranda et al., 2020) reversed α-syn aggregation and its associated mitochondrial defects. Taken together, these results show a direct interaction between α-syn and the TOM complex, although exactly how the oligomeric state of α-syn or its PTMs may modify such interactions remain open questions. It should be noted that to date, there is no strong evidence for the specific interaction between α-syn and the TIM23 import complex of the MIM. However, transport and sorting of α-syn via the TIM23 machinery is highly likely given the submitochondrial distribution of α-syn, which includes the MIM and matrix. Figure 10B summarizes the interactions of α-syn with mitochondria.

Another feature supporting the mitochondria-targeting capacity of the α-syn N-terminus is its membrane-interactive nature. In its functional role of fusing synaptic vesicles with the presynaptic membrane, α-syn binds anionic phospholipid bilayers through its N-terminus, which then adopts a stable α-helical structure and displaces the unstructured C-terminal end resulting in an elongated conformation (Bartels et al., 2010). Similar membrane interactions have long been known for *bona fide* mitochondrial MTSs, which can undergo a coil-to-helix transition upon anchoring to lipid bilayers without perturbing membrane integrity (Skerjanc et al., 1987; Hoyt et al., 1991; Wieprecht et al., 2000). Functionally, this could allow the mitochondrial precursor to undergo a two-dimensional random walk on the membrane surface to seek out its cognate import receptor more efficiently. It is possible that α-syn

adopts a similar mechanism to accumulate on membrane surfaces to increase its local concentration in the vicinity of import complexes.

The interaction of α-syn with the mitochondrial import machinery has important mechanistic implications for mitochondrial stress responses and quality control related to PD (Thorne and Tumbarello, 2022). One of the main pathways for mitophagy-based removal of damaged mitochondria is the PINK1/Parkin system. Under non-stressed conditions, the serine/threonine kinase PINK1 engages mitochondrial import complexes and becomes proteolyzed and efficiently degraded; however, under stress conditions that lower the $\Delta\psi_m$ of the MIM, PINK1 accumulates at the MOM and recruits the E3 ubiquitin ligase Parkin, which ubiquitinylates mitochondrial proteins. This signals for autophagic degradation of dysfunctional organelles and consequently blunts cellular expansion of the damage (Ge et al., 2020). Importantly, defects in PINK1 and Parkin (encoded by *PINK1* and *PRKN* genes, respectively) cause the deregulation of mitochondrial quality control and together they represent the preeminent monogenic forms of heritable PD (Klein and Westenberger, 2012).

Moreover, the specific affinity of the α-syn N-terminal region for cardiolipin (Ramakrishnan et al., 2003; Cole et al., 2008; Nakamura et al., 2008; Grey et al., 2011; Robotta et al., 2014) may explain its interaction with mitochondria during stress. The translocation of cardiolipin from the MIM to the MOM is an early signaling event in mitophagy and apoptosis (Li et al., 2015), and it has been shown using α-syn mutant models of PD that cardiolipin becomes externalized to the cytosol, where it then binds α-syn and promotes the refolding of α-syn monomers from aggregated fibrils (Ryan et al., 2018). This may represent a feed-forward process whereby the stress of α-syn burden causes cardiolipin externalization, thereby resulting in the recruitment of more α-syn to the mitochondrial surface. Mitophagy then results when α-syn burden outmatches the refolding ability of cardiolipin.

It should be emphasized that α-syn may play a physiological role in mitochondria (Faustini et al., 2017). For example, consistent with the general role that α-syn appears to play in cellular lipid metabolism and signaling (Jenco et al., 1998; Golovko et al., 2005; Narayanan et al., 2005; Golovko et al., 2006), the lack of α-syn in *SNCA*$^{-/-}$ mice causes mitochondria to have reduced cardiolipin with altered acyl compositions (Ellis et al., 2005; Barcelo-Coblijn et al., 2007). This effect on cardiolipin in turn alters the physical properties of the MIM coupled with reduced Complex I and III activity (Ellis et al., 2005) and is accompanied by increases in neutral lipids including cholesterol and cholesterol esters (Barcelo-Coblijn et al., 2007). Other studies indicate that α-syn may play critical roles in mitochondrial dynamics, quality control and transport (reviewed in (Pozo Devoto and Falzone, 2017)). While these roles of α-syn could in principle be exerted within or outside the mitochondrion, some reports indicate a role of α-syn within the organelle. For example, α-syn appears to interact directly with the matrix-facing catalytic domain of mitochondrial ATP synthase, with monomers positively regulating its catalytic activity (Ludtmann et al., 2016) and oligomers promoting the mitochondria permeability transition involved in cell death (Ludtmann et al., 2018). This functional duality indicates that, as with cytoplasmic α-syn, it may be the abundance and/or aggregation of α-syn within the mitochondrion and not the mere presence of α-syn itself, that dictates pathogenicity inside the organelle. As such, the TIM23 machinery must then play a key role in regulating this balance of mitochondrial α-syn.

5.4 Interactions of Htt/mHtt with the mitochondrial import machinery

In Htt, the site of pathogenic poly-Q expansion is flanked by the first 17 residues of the N-terminus (Nt17) and the proline-rich domain (PRD) (Figure 8A). The Nt17 sequence has the hallmarks of a moderately amphipathic MTS (Figure 9Biv). Many structural and computational studies have addressed the conformational dynamics of the Nt17 sequence in the context of the tripartite structure of Htt. Nt17 itself does not adopt a stable secondary structure but has the characteristics of a compact coil (Thakur et al., 2009), which is similar to other IDPs (Uversky, 2002), and has the propensity to form α-helical structures, particularly in the presence of membranes (Davies et al., 1997; Tam et al., 2009). Indeed, Nt17 forms α-helices in the context of oligomers or fibrils of Httex1 fragments (Kim et al., 2009; Sivanandam et al., 2011; Michalek et al., 2013). The α-helical Nt17 structure promotes aggregation of Httex1 by promoting helical structure within the poly-Q tract (Thakur et al., 2009). By contrast, the PRD forms a polyproline II structure (PPII), which reduces aggregation propensity (Bhattacharyya et al., 2006). Importantly, Htt constructs lacking the Nt17 fail to localize to mitochondria, supporting a role of this segment in mitochondrial targeting (Rockabrand et al., 2007).

Using a combination of biochemical and microscopy-based analyses with striatum-derived cell lines and murine models of HD, Friedlander and colleagues found that Htt and mHtt (and N-terminal fragments thereof) interact directly with the mitochondrial TIM23 complex and are localized to the IMS (Yano et al., 2014; Yablonska et al., 2019) (Figure 10C). In these studies, immunoprecipitation/mass spectrometry and surface plasmon resonance spectroscopy were used to show interactions with TIM23 complex subunits Tim23, Tim50 and Tim17a. They revealed that mHtt had higher affinity interactions with TIM23 subunits and inhibited the TIM23-mediated import of native mitochondrial proteins to a greater extent than wild type Htt counterparts. Importantly, these studies showed that both the Nt17 segment and the expanded poly-Q tract are crucial for interactions with the TIM23 complex. The authors concluded that this inhibition of mitochondrial import by mHtt is an early event in HD pathology (detected pre-symptomatically) and that this effect alone can result in neuronal cell death. Figure 10C summarizes the interactions of mHtt with the mitochondrial import machinery.

These observations provide potential clues as to how Htt, specifically N-terminal segments of mHtt, may engage and disrupt the TIM23 machinery during HD-related proteostatic stress. First, the requirement of Nt17 for TIM23 interactions suggests that this sequence acts like a MTS, assuming an amphipathic α-helical structure to engage the TOM/TIM23 receptors and accumulate Htt/mHtt at mitochondria during HD progression. Second, because TIM23 substrates must be unfolded to traverse the import pathway, N-terminal fragments of Htt/mHtt may be more likely to engage TIM23 than full-length Htt/mHtt, as this would require significant unfolding for import.

Finally, the selective interaction of mHtt fragments with TIM23 suggests that the poly-Q expansion provides a sufficiently long, unstructured tether for the Nt17 to access the TIM23 binding sites. Indeed, it has been shown that a sufficiently long presequence is required for TIM23 precursors to span both mitochondrial membranes and engage matrix mtHsp70, which translocates substrates by an active power stroke or Brownian ratchet mechanism (Matouschek et al., 1997; Okamoto et al., 2002). The localization of Htt/mHtt to the IMS suggests incomplete translocation of these polypeptides into the matrix, creating stalled translocation intermediates that could explain the inhibition of TIM23 import. It should be noted that the findings of the Friedlander group were subsequently questioned in a study that found mitochondria-localized mHtt to reside only on the cytosolic side of the MOM and to have no measurable effect on the import of TIM23 substrates (Hamilton et al., 2020). Future work will be required to reconcile these contradictory findings.

6 Discussion

We have reviewed current evidence that APP/Aβ, α-syn, and Htt/mHtt interact with the mitochondrial import machinery through their cryptic N-terminal targeting sequences. These interactions have implications for the physiological roles of these proteins as well as their pathogenic interactions in AD, PD, and HD, respectively. They also set the stage for addressing how mitochondrial import may serve as a clearance mechanism for amyloids during proteostatic stress, as well as presenting new directions for developing interventions for neurodegenerative diseases. These two questions are addressed below.

6.1 Proteostatic mechanisms that may involve mitochondrial import

Mitochondrial proteostasis involves many stress response pathways that either directly or indirectly involve the protein import machinery (Figure 11), and any combination of them could be marshalled in response to amyloid burden at the TIM23 complex. First, some responses involve the degradation of toxic peptides or proteins in the matrix subcompartment. As noted above, the MTS-degrading enzyme PreP (Figure 11A) has an established role in the breakdown of Aβ (Falkevall et al., 2006) and may assume a more general role in the clearance of other amyloidogenic peptides. Other pathways have been described whereby mitochondria import unfolded or aggregated proteins into the matrix for degradation, providing a proteostatic mechanism for the clearance of cytotoxic proteins. These mechanisms, termed Mitochondria as Guardian in Cytosol (MAGIC) (Ruan et al., 2017) and the FUNDC1/HSC70 pathway (Li Y. et al., 2019), both entail the uptake of aggregation-prone proteins into mitochondria with subsequent degradation by matrix proteases. Thus, these pathways may explain why some amyloidogenic proteins are ectopically imported into mitochondria (Figure 11B). Alternative quality control pathways involve feedback mechanisms between the mitochondria and the nucleus to signal defects in mitochondrial protein biogenesis. Among them, the best characterized is the mitochondrial unfolded protein response (UPR^{mt}), which senses the accumulation of unfolded proteins and ROS in mitochondrial compartments and activates transcription factors to express nuclear genes encoding mitochondrial chaperones, proteases, and antioxidant systems (Wodrich et al., 2022) (Figure 11C). Indeed, UPR^{mt} activation is implicated in neurodegeneration (Zhu et al., 2021), and particularly in AD (Beck JS. et al., 2016; Sorrentino et al., 2017; Shen Y. et al., 2019), PD (Cooper et al., 2017), and HD (Berendzen et al., 2016; Fu et al., 2019). Other stress responses serve to clear the cytosol of mitochondrial precursor proteins when import is compromised. Namely, the UPR activated by the mistargeting of proteins (UPR^{am}) (Wrobel et al., 2015) and the associated mitochondrial precursor overaccumulation stress (mPOS) response (Wang and Chen, 2015) (Figure 11D) respond to increased cytosolic concentrations of precursors, which are normally very low, by activating the proteasome and downregulating cytosolic protein synthesis, respectively. Other similar responses are designed to extract stalled translocation intermediates from the TOM complex and direct them to the proteasome for degradation. These include the mitochondrial compromised import response (MitoCPR) system (Weidberg and Amon, 2018) and the mitochondrial protein translocation-associated degradation (MitoTAD) system (Martensson et al., 2019) (Figure 11E). Although many of these stress responses have been resolved in lower eukaryotes, there is evidence that they exist in mammalian systems as well, although the mechanistic details have yet to be elucidated.

One confounding factor in these mitochondria-based proteostasis mechanisms is the question of how aggregated proteins in the cytosol could access the TOM/TIM23 machinery, given that the import requires an unfolded precursor. A potential solution may come from the observation that a cytosolic HSP70/co-chaperone system is capable of disaggregating amyloid structures (Wentink et al., 2020). Such a system could in principle dislodge amyloid proteins and deliver them as monomers in a post-translational, chaperone-bound fashion to the mitochondrial import machinery. Indeed, several amyloids are found as distinct disease-associated polymorph structures (Qiang et al., 2017; Yang et al., 2022) that could differ in their stabilities and proclivities to dissociate soluble species. A second possibility is that since amyloid fibril structures feature rigid cores surrounded by disordered "fuzzy coats", the solvent exposure of these flexible regions could promote PTMs and/or dissociation of monomers (Lin et al., 2017). Thus, shed monomers or proteolytic fragments of amyloidogenic proteins from fibrillar aggregates could then be free to interact with the mitochondrial protein machinery.

In summary, the degree to which PreP, MAGIC, and FUNDC1/HSC70 may assist as general clearance systems for amyloidogenic proteins like Aβ, α-syn, or mHtt requires further investigation, as do the pathways by which these amyloids may trigger mitochondrial import-related stress responses.

6.2 Prospects for drug development

The interactions between amyloidogenic proteins and the mitochondrial import machinery may inform strategies for

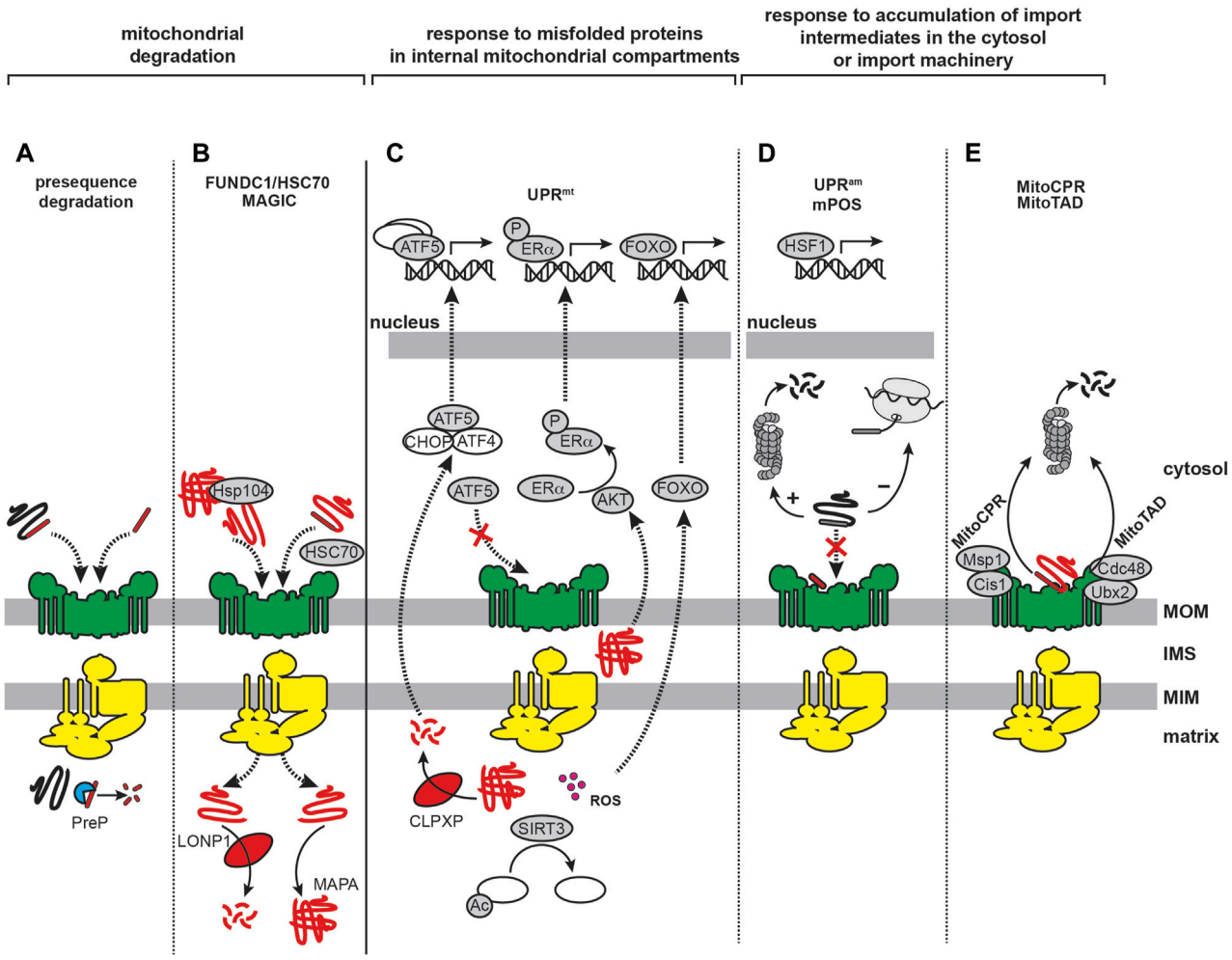

FIGURE 11
Mitochondrial proteostatic stress responses involving the import machinery. Depicted are complementary stress responses of mammalian systems that involve the mitochondrial import machinery and may be upregulated with amyloid burden. **(A)** PreP degradation. The PreP peptidase that cleaves MTSs also degrades Aβ in the matrix and may play a broader role in clearing imported peptides, including amyloids. **(B)** MAGIC and FUNDC1/HSC70. By these processes, cytosolic proteins are imported into mitochondria for sequestration and proteolysis. In the MAGIC pathway, cytosolic Hsp104 dissociates aggregated proteins, which are imported via the TOM complex into the matrix, where they are degraded by the Pim1 (yeast)/LONP1 (human) protease. In the FUNDC1/HSC70 axis, the MOM protein FUNDC1 interacts with cytosolic HSC70 to import unfolded proteins that are either degraded by LONP1 or assembled into non-aggresomal mitochondrion-associated protein aggregates (MAPAs) that can be subsequently degraded by autophagy. **(C)** UPR^{mt}. This process involves transcriptional reprogramming based on mitochondria-nuclear communication in response to protein aggregates in the matrix. The UPR^{mt} involves multiple pathways (1). The ATF5 transcription factor is imported into mitochondria under non-stressed conditions, but when its import is hindered it traffics to the nucleus with other transcription factors (ATF4/CHOP) to activate genes encoding mitochondrial chaperones and proteases. Peptides from the degradation of misfolded mitochondrial proteins, likely produced by CLPXP, may then be exported to facilitate ATF5 translocation (2). Protein aggregates in the IMS activate the AKT kinase, which phosphorylates ERα, serving as a transcription factor to induce expression of IMS-specific proteases (3). Matrix aggregates and ROS activate the sirtuin SIRT3 to deacetylate matrix proteins and activate the FOXO transcription factor that activates mitochondrial antioxidant genes. **(D)** UPR^{am} and mPOS. These reactions respond to cytotoxic accumulation of mitochondrial precursor proteins in the cytosol resulting from defective import. The response of UPR^{am} includes activation of the proteasome, whereas that of the mPOS pathway involves global reduction in cytosolic protein synthesis. Upregulation of the HSP1 transcription factor increases expression of chaperones and other stress response factors. **(E)** MitoTAD and MitoCPR. These systems remove stalled, nonproductive intermediates from the import machinery by continual monitoring of the TOM complex. TOM complex-associated adaptor proteins Cis1/Ubx2 recruit AAA ATPases Msp1/Cdc48 to extract stalled precursors and direct them to the proteasome for degradation.

developing novel therapeutic interventions for neurodegenerative diseases. Clinical studies and drug discovery efforts have led researchers to question the role of amyloid fibrils themselves as the primary causative agents in AD, PD, and HD. For example, the extent of fibril formation does not always correlate with disease severity (Breydo et al., 2012; Ow and Dunstan, 2014), fibrils can be present even in the absence of disease symptoms (Ke et al., 2020), and therapeutic strategies designed to disrupt fibril formation have been met with mixed success (Pardridge, 2016; Barker and Mason, 2019; Paolini Paoletti et al., 2020; Pardridge, 2020; Yiannopoulou and Papageorgiou, 2020). Hence, alternative intervention approaches, including targeting mitochondrial dysfunction, are being developed for neurodegenerative disorders (Xu et al., 2022b). Here we review some promising

interventions that directly or indirectly involve the amyloid-TIM23 pathway interaction.

From a broad perspective, given that AD, PD, and HD are all diseases of aging (Blumenthal, 2004; Taylor and Dillin, 2011), targeting general aging-related mitochondrial dysfunction may be an effective strategy. For example, the efficiency of the UPR^{mt} declines with age (Bennett and Kaeberlein, 2014; Munoz-Carvajal and Sanhueza, 2020) making it a potential target for neurodegenerative diseases (Suarez-Rivero et al., 2022). Indeed, compounds that increase cellular NAD^+ levels, including nicotinamide riboside and olaparib, improved longevity in *C. elegans* models of Aβ proteotoxicity by activation of UPR^{mt} and mitophagy (Sorrentino et al., 2017). Because the UPR^{mt} involves upregulation of the TIM23 machinery (Xin et al., 2022), mitochondrial import may either be an important target of UPR^{mt}-modulating compounds, or serve as a marker for pharmacological UPR^{mt} activation. Another mitochondrial parameter that declines with age is the $\Delta\psi_m$ (Sugrue and Tatton, 2001; Berry and Kaeberlein, 2021; Berry et al., 2023). Caloric restriction (CR) and rapamycin, which extend lifespan in several wild type organisms (Nakagawa et al., 2012; Bitto et al., 2016; Shindyapina et al., 2022), can mediate their effects by regulating $\Delta\psi_m$ (Paglin et al., 2005; Cheema et al., 2021; Berry et al., 2023). These treatments could therefore operate in part by rescuing TIM23-mediated protein import, which functions in a $\Delta\psi_m$-dependent manner. However, thorough pre-clinical testing of these interventions in AD, PD, and HD models would be warranted as CR and UPR^{mt} activation can shorten or extend lifespan depending on the context in which the treatments are applied (Liao et al., 2010; Bennett and Kaeberlein, 2014; Angeli et al., 2021; Xin et al., 2022). Notably, a recent study with rapamycin in a mouse model of AD showed increased amyloid plaque formation upon treatment (Shi et al., 2022).

Given the potential role of mitochondria-resident proteases in amyloid degradation, these may represent pharmacological targets. For instance, as mentioned, the mitochondrial PreP enzyme degrades MTSs and has been implicated in degradation of Aβ in the matrix (Falkevall et al., 2006; Alikhani et al., 2011b; Mossmann et al., 2014; Fang et al., 2015; Du et al., 2021); thus, PreP may represent a potential drug target for neurodegeneration (Brunetti et al., 2021). In fact, researchers using the Senescence Accelerated Mouse Prone 8 (SAMP8) AD model found that restoring global mitochondrial function with metabolic modulators (essential and branched-chain amino acids) was accompanied by a reversal of aging-related declines in PreP levels (Brunetti et al., 2020). Similarly, researchers using the APPswe/PS1dE9 AD model, associated with FAD mutations in APP and γ-secretase, found that treatment with the neuroprotective compound Ligustilide reduced disease progression with a concurrent increase in PreP levels (Xu et al., 2018). Very recently, Pioglitazone, an antagonist of the PPAR-γ transcription factor that regulates mitochondria structure and function, was shown to upregulate PreP and the insulin degrading enzyme IDE, thereby restoring the peptide processing machinery (Di Donfrancesco et al., 2023). Original efforts toward developing agonists of PreP were focused on small molecule benzimidiazole derivatives (Vangavaragu et al., 2014), but these results were called into question (Li NS. et al., 2019). Therefore, the potential efficacy of specific effectors of PreP requires further validation.

Finally, there are several therapeutic compounds effective in treating neurodegenerative diseases that improve mitochondrial function as part of their mechanism of action. Three such compounds, described here, could have direct or indirect effects on mitochondrial protein import. First, the synthetic tetrapeptide SS-31 (elamipretide) targets mitochondria by interacting with the cardiolipin-rich MIM (Szeto, 2014). SS-31 is protective against mitochondrial dysfunction associated with a range of diseases, including myopathy, cardiac, retinal, and kidney diseases, and has demonstrated neuroprotective function (Zhu et al., 2018; Zhao et al., 2019; Liu Y. et al., 2021; Nhu et al., 2021), including efficacy in models of AD (Manczak et al., 2010; Calkins et al., 2011; Reddy et al., 2017; Reddy et al., 2018), PD (Yang et al., 2009), and HD (Yin et al., 2016). In these studies, SS-31 has been shown to restore mitochondrial biogenesis, dynamics and energetic output, reduce oxidative stress, and preserve mitochondria structure, with a notable effect on upregulating TOM complex receptor expression (Reddy et al., 2018). SS-31 and its side chain variants may act by modulating membrane electrostatics (Mitchell et al., 2020; Mitchell et al., 2022), mitigating Ca^{2+} stress at the MIM (Mitchell et al., 2020), and/or preserving the $\Delta\psi_m$ (Zhang et al., 2020). Furthermore, SS-31 has an extensive interactome in mitochondria (Chavez et al., 2020) and may therefore attenuate pathogenic interactions of peptides such as Aβ and α-syn with different mitochondrial proteins. Second, the curcumin derivative J147 is a neuroprotective compound that has been explored as an effective treatment in AD models (Prior et al., 2013; Goldberg et al., 2018; Currais et al., 2019; Goldberg et al., 2020; Kepchia et al., 2021; Kepchia et al., 2022). Based on these studies, several molecular mechanisms have been ascribed to J147, including improved energy metabolism, modulation of Ca^{2+} flux and activation of the AMPK/mTOR pathway, reduction of plasma free fatty acid levels, and regulation of acetyl-CoA metabolism. Third, polyphenols constitute a broad class of phytochemicals, many of which show neuroprotective properties (Naoi et al., 2019). Among them, urolithin A has demonstrated efficacy in models of AD (Ballesteros-Alvarez et al., 2023) and PD (Liu et al., 2022). Mechanistically, urolithin A activates mitophagy (Ryu et al., 2016; Amico et al., 2021), which may reverse defects in PINK1/Parkin mitophagy that are implicated in both familial and sporadic PD (Dawson and Dawson, 2010). Because the PINK1/Parkin mechanism is based on interactions with the TIM23 pathway, urolithin A may help reduce proteostatic stress caused by interactions of α-syn with the import machinery. Notably, SS-31, J147, and polyphenolics are all known to interact with mitochondrial F_1F_O ATP synthase (Ahmad and Laughlin, 2010; Goldberg et al., 2018; Chavez et al., 2020), an enzyme whose dysfunction is implicated in neurodegeneration, particularly AD (Ebanks et al., 2020). Increasing evidence supports that dysfunction of ATP synthase coincides with AD progression (Liang et al., 2008; Terni et al., 2010; Beck SJ. et al., 2016), which may mechanistically occur by interactions of Aβ with the OSCP subunit (Beck SJ. et al., 2016). It has also been shown that loss of OSCP drives the opening of the mPTP and activates the UPR^{mt} (Angeli et al., 2021). Hence, compounds that bind ATP synthase may help maintain its function during amyloidogenic stress and/or inhibit mPTP pore opening induced by the pore initiator cyclophilin D, producing a result similar to the action of cyclosporin A (Connern and Halestrap, 1994; Gauba et al., 2019). Such interventions could increase ATP synthase

activity and prevent membrane depolarization, thereby improving available ATP levels to enhance proteostatic clearance and matrix-directed import through the TIM23 pathway.

7 Conclusion

Aβ/APP, α-syn, and Htt/mHtt all contain MTS-like sequences that promote their interactions with the mitochondrial TIM23 import machinery. These interactions can directly impact mitochondrial protein import function, as well as allow incorporation of amyloids into mitochondrial subcompartments, which could contribute to pathogenicity in AD, PD, and HD, respectively. The engagement of Aβ/APP, α-syn, and Htt/mHtt with the import complexes may be part of the normal physiological function of these proteins, may represent an amyloid clearance mechanism, or may be purely pathogenic. Addressing these questions will be critical in understanding the role of mitochondria in neurodegeneration. We note that evidence for the engagement of amyloids with the import machinery does not necessarily favor either the amyloid or mitochondrial cascade hypotheses, as these interactions could occur under both scenarios. However, determining whether the amyloid-import machinery interaction is an upstream cause, or a downstream effect will help resolve the role of mitochondrial dysfunction in the sequence of events associated with neurodegeneration. Further investigation of the interactions of amyloidogenic proteins with the mitochondrial import machinery will add to our understanding of the role of mitochondria in proteostatic stress and facilitate the development of therapeutic interventions.

Author contributions

AR: Writing–original draft, Writing–review and editing. WM: Writing–original draft, Writing–review and editing. AA: Writing–original draft, Writing–review and editing. NA: Funding acquisition, Writing–original draft, Writing–review and editing.

Funding

The authors declare financial support was received for the research, authorship, and/or publication of this article. This work was supported by a grant from the NIH (R01AG065879) to NA (PI) and AA (co-I).

Conflict of interest

The authors declare that the research was conducted in the absence of any commercial or financial relationships that could be construed as a potential conflict of interest.

Publisher's note

All claims expressed in this article are solely those of the authors and do not necessarily represent those of their affiliated organizations, or those of the publisher, the editors and the reviewers. Any product that may be evaluated in this article, or claim that may be made by its manufacturer, is not guaranteed or endorsed by the publisher.

Supplementary material

The Supplementary Material for this article can be found online at: https://www.frontiersin.org/articles/10.3389/fphys.2023.1263420/full#supplementary-material

References

Abe, Y., Shodai, T., Muto, T., Mihara, K., Torii, H., Nishikawa, S., et al. (2000). Structural basis of presequence recognition by the mitochondrial protein import receptor Tom20. *Cell.* 100 (5), 551–560. doi:10.1016/s0092-8674(00)80691-1

Adao, R., Cruz, P. F., Vaz, D. C., Fonseca, F., Pedersen, J. N., Ferreira-da-Silva, F., et al. (2020). DIBMA nanodiscs keep alpha-synuclein folded. *Biochim. Biophys. Acta Biomembr.* 1862 (9), 183314. doi:10.1016/j.bbamem.2020.183314

Adav, S. S., Park, J. E., and Sze, S. K. (2019). Quantitative profiling brain proteomes revealed mitochondrial dysfunction in Alzheimer's disease. *Mol. Brain* 12 (1), 8. doi:10.1186/s13041-019-0430-y

Addya, S., Anandatheerthavarada, H. K., Biswas, G., Bhagwat, S. V., Mullick, J., and Avadhani, N. G. (1997). Targeting of NH2-terminal-processed microsomal protein to mitochondria: a novel pathway for the biogenesis of hepatic mitochondrial P450MT2. *J. Cell. Biol.* 139 (3), 589–599. doi:10.1083/jcb.139.3.589

Ahmad, Z., and Laughlin, T. F. (2010). Medicinal chemistry of ATP synthase: a potential drug target of dietary polyphenols and amphibian antimicrobial peptides. *Curr. Med. Chem.* 17 (25), 2822–2836. doi:10.2174/092986710791859270

Ahmed, A. U., Beech, P. L., Lay, S. T., Gilson, P. R., and Fisher, P. R. (2006). Import-associated translational inhibition: novel *in vivo* evidence for cotranslational protein import into *Dictyostelium discoideum* mitochondria. *Eukaryot. Cell.* 5 (8), 1314–1327. doi:10.1128/EC.00386-05

Akopian, D., Shen, K., Zhang, X., and Shan, S. O. (2013). Signal recognition particle: an essential protein-targeting machine. *Annu. Rev. Biochem.* 82, 693–721. doi:10.1146/annurev-biochem-072711-164732

Albrecht, R., Rehling, P., Chacinska, A., Brix, J., Cadamuro, S. A., Volkmer, R., et al. (2006). The Tim21 binding domain connects the preprotein translocases of both mitochondrial membranes. *EMBO Rep.* 7 (12), 1233–1238. doi:10.1038/sj.embor.7400828

Alder, N. N., Jensen, R. E., and Johnson, A. E. (2008b). Fluorescence mapping of mitochondrial TIM23 complex reveals a water-facing, substrate-interacting helix surface. *Cell.* 134 (3), 439–450. doi:10.1016/j.cell.2008.06.007

Alder, N. N., Sutherland, J., Buhring, A. I., Jensen, R. E., and Johnson, A. E. (2008a). Quaternary structure of the mitochondrial TIM23 complex reveals dynamic association between Tim23p and other subunits. *Mol. Biol. Cell.* 19 (1), 159–170. doi:10.1091/mbc.e07-07-0669

Alecu, I., and Bennett, S. A. L. (2019). Dysregulated lipid metabolism and its role in alpha-synucleinopathy in Parkinson's disease. *Front. Neurosci.* 13, 328. doi:10.3389/fnins.2019.00328

Alexandrescu, A. T. (2005). Amyloid accomplices and enforcers. *Protein Sci.* 14 (1), 1–12. doi:10.1110/ps.04887005

Alikhani, N., Berglund, A. K., Engmann, T., Spanning, E., Vogtle, F. N., Pavlov, P., et al. (2011a). Targeting capacity and conservation of PreP homologues localization in mitochondria of different species. *J. Mol. Biol.* 410 (3), 400–410. doi:10.1016/j.jmb.2011.05.009

Alikhani, N., Guo, L., Yan, S., Du, H., Pinho, C. M., Chen, J. X., et al. (2011b). Decreased proteolytic activity of the mitochondrial amyloid-beta degrading enzyme, PreP peptidasome, in Alzheimer's disease brain mitochondria. *J. Alzheimers Dis.* 27 (1), 75–87. doi:10.3233/JAD-2011-101716

Almagro Armenteros, J. J., Tsirigos, K. D., Sonderby, C. K., Petersen, T. N., Winther, O., Brunak, S., et al. (2019). SignalP 5.0 improves signal peptide predictions using deep neural networks. *Nat. Biotechnol.* 37 (4), 420–423. doi:10.1038/s41587-019-0036-z

Almeida, Z. L., and Brito, R. M. M. (2020). Structure and aggregation mechanisms in amyloids. *Molecules* 25 (5), 1195. doi:10.3390/molecules25051195

Amico, D., Andreux, P. A., Valdes, P., Singh, A., Rinsch, C., and Auwerx, J. (2021). Impact of the natural compound urolithin A on health, disease, and aging. *Trends Mol. Med.* 27 (7), 687–699. doi:10.1016/j.molmed.2021.04.009

Amorim, I. S., Graham, L. C., Carter, R. N., Morton, N. M., Hammachi, F., Kunath, T., et al. (2017). Sideroflexin 3 is an alpha-synuclein-dependent mitochondrial protein that regulates synaptic morphology. *J. Cell. Sci.* 130 (2), 325–331. doi:10.1242/jcs.194241

Anandatheerthavarada, H. K., Biswas, G., Mullick, J., Sepuri, N. B., Otvos, L., Pain, D., et al. (1999). Dual targeting of cytochrome P4502B1 to endoplasmic reticulum and mitochondria involves a novel signal activation by cyclic AMP-dependent phosphorylation at ser128. *EMBO J.* 18 (20), 5494–5504. doi:10.1093/emboj/18.20.5494

Anandatheerthavarada, H. K., Biswas, G., Robin, M. A., and Avadhani, N. G. (2003). Mitochondrial targeting and a novel transmembrane arrest of Alzheimer's amyloid precursor protein impairs mitochondrial function in neuronal cells. *J. Cell. Biol.* 161 (1), 41–54. doi:10.1083/jcb.200207030

Anderson, J. P., Walker, D. E., Goldstein, J. M., de Laat, R., Banducci, K., Caccavello, R. J., et al. (2006). Phosphorylation of Ser-129 is the dominant pathological modification of alpha-synuclein in familial and sporadic Lewy body disease. *J. Biol. Chem.* 281 (40), 29739–29752. doi:10.1074/jbc.M600933200

Angeli, S., Foulger, A., Chamoli, M., Peiris, T. H., Gerencser, A., Shahmirzadi, A. A., et al. (2021). The mitochondrial permeability transition pore activates the mitochondrial unfolded protein response and promotes aging. *Elife* 10, 10. doi:10.7554/elife.63453

Aoyama-Ishiwatari, S., and Hirabayashi, Y. (2021). Endoplasmic reticulum-mitochondria contact sites-emerging intracellular signaling hubs. *Front. Cell. Dev. Biol.* 9, 653828. doi:10.3389/fcell.2021.653828

Apetri, A. C., and Horwich, A. L. (2008). Chaperonin chamber accelerates protein folding through passive action of preventing aggregation. *Proc. Natl. Acad. Sci. U. S. A.* 105 (45), 17351–17355. doi:10.1073/pnas.0809794105

Araiso, Y., and Endo, T. (2022). Structural overview of the translocase of the mitochondrial outer membrane complex. *Biophys. Physicobiol* 19, e190022. doi:10.2142/biophysico.bppb-v19.0022

Araiso, Y., Tsutsumi, A., Qiu, J., Imai, K., Shiota, T., Song, J., et al. (2019). Structure of the mitochondrial import gate reveals distinct preprotein paths. *Nature* 575 (7782), 395–401. doi:10.1038/s41586-019-1680-7

Arbor, S. C., LaFontaine, M., and Cumbay, M. (2016). Amyloid-beta Alzheimer targets - protein processing, lipid rafts, and amyloid-beta pores. *Yale J. Biol. Med.* 89 (1), 5–21.

Area-Gomez, E., de Groof, A., Bonilla, E., Montesinos, J., Tanji, K., Boldogh, I., et al. (2018). A key role for MAM in mediating mitochondrial dysfunction in Alzheimer disease. *Cell. Death Dis.* 9 (3), 335. doi:10.1038/s41419-017-0215-0

Area-Gomez, E., de Groof, A. J., Boldogh, I., Bird, T. D., Gibson, G. E., Koehler, C. M., et al. (2009). Presenilins are enriched in endoplasmic reticulum membranes associated with mitochondria. *Am. J. Pathol.* 175 (5), 1810–1816. doi:10.2353/ajpath.2009.090219

Area-Gomez, E., Del Carmen Lara Castillo, M., Tambini, M. D., Guardia-Laguarta, C., de Groof, A. J., Madra, M., et al. (2012). Upregulated function of mitochondria-associated ER membranes in Alzheimer disease. *EMBO J.* 31 (21), 4106–4123. doi:10.1038/emboj.2012.202

Arrasate, M., Mitra, S., Schweitzer, E. S., Segal, M. R., and Finkbeiner, S. (2004). Inclusion body formation reduces levels of mutant huntingtin and the risk of neuronal death. *Nature* 431 (7010), 805–810. doi:10.1038/nature02998

Aston-Mourney, K., Hull, R. L., Zraika, S., Udayasankar, J., Subramanian, S. L., and Kahn, S. E. (2011). Exendin-4 increases islet amyloid deposition but offsets the resultant beta cell toxicity in human islet amyloid polypeptide transgenic mouse islets. *Diabetologia* 54 (7), 1756–1765. doi:10.1007/s00125-011-2143-3

Attwell, D., and Laughlin, S. B. (2001). An energy budget for signaling in the grey matter of the brain. *J. Cereb. Blood Flow. Metab.* 21 (10), 1133–1145. doi:10.1097/00004647-200110000-00001

Auclair, S. M., Bhanu, M. K., and Kendall, D. A. (2012). Signal peptidase I: cleaving the way to mature proteins. *Protein Sci.* 21 (1), 13–25. doi:10.1002/pro.757

Auld, D. S., Kornecook, T. J., Bastianetto, S., and Quirion, R. (2002). Alzheimer's disease and the basal forebrain cholinergic system: relations to beta-amyloid peptides, cognition, and treatment strategies. *Prog. Neurobiol.* 68 (3), 209–245. doi:10.1016/s0301-0082(02)00079-5

Avendano-Monsalve, M. C., Mendoza-Martinez, A. E., Ponce-Rojas, J. C., Poot-Hernandez, A. C., Rincon-Heredia, R., and Funes, S. (2022). Positively charged amino acids at the N terminus of select mitochondrial proteins mediate early recognition by import proteins αβ'-NAC and Sam37. *J. Biol. Chem.* 298 (6), 101984. doi:10.1016/j.jbc.2022.101984

Avendano-Monsalve, M. C., Ponce-Rojas, J. C., and Funes, S. (2020). From cytosol to mitochondria: the beginning of a protein journey. *Biol. Chem.* 401 (6-7), 645–661. doi:10.1515/hsz-2020-0110

Baba, M., Nakajo, S., Tu, P. H., Tomita, T., Nakaya, K., Lee, V. M., et al. (1998). Aggregation of alpha-synuclein in Lewy bodies of sporadic Parkinson's disease and dementia with Lewy bodies. *Am. J. Pathol.* 152 (4), 879–884.

Backes, S., Bykov, Y. S., Flohr, T., Raschle, M., Zhou, J., Lenhard, S., et al. (2021). The chaperone-binding activity of the mitochondrial surface receptor Tom70 protects the cytosol against mitoprotein-induced stress. *Cell. Rep.* 35 (1), 108936. doi:10.1016/j.celrep.2021.108936

Backes, S., Hess, S., Boos, F., Woellhaf, M. W., Godel, S., Jung, M., et al. (2018). Tom70 enhances mitochondrial preprotein import efficiency by binding to internal targeting sequences. *J. Cell. Biol.* 217 (4), 1369–1382. doi:10.1083/jcb.201708044

Bajaj, R., Jaremko, L., Jaremko, M., Becker, S., and Zweckstetter, M. (2014). Molecular basis of the dynamic structure of the TIM23 complex in the mitochondrial intermembrane space. *Structure* 22 (10), 1501–1511. doi:10.1016/j.str.2014.07.015

Ballesteros-Alvarez, J., Nguyen, W., Sivapatham, R., Rane, A., and Andersen, J. K. (2023). Urolithin A reduces amyloid-beta load and improves cognitive deficits uncorrelated with plaque burden in a mouse model of Alzheimer's disease. *Geroscience* 45 (2), 1095–1113. doi:10.1007/s11357-022-00708-y

Banerjee, K., Sinha, M., Pham Cle, L., Jana, S., Chanda, D., Cappai, R., et al. (2010). Alpha-synuclein induced membrane depolarization and loss of phosphorylation capacity of isolated rat brain mitochondria: implications in Parkinson's disease. *FEBS Lett.* 584 (8), 1571–1576. doi:10.1016/j.febslet.2010.03.012

Barbaro, B. A., Lukacsovich, T., Agrawal, N., Burke, J., Bornemann, D. J., Purcell, J. M., et al. (2015). Comparative study of naturally occurring huntingtin fragments in Drosophila points to exon 1 as the most pathogenic species in Huntington's disease. *Hum. Mol. Genet.* 24 (4), 913–925. doi:10.1093/hmg/ddu504

Barcelo-Coblijn, G., Golovko, M. Y., Weinhofer, I., Berger, J., and Murphy, E. J. (2007). Brain neutral lipids mass is increased in alpha-synuclein gene-ablated mice. *J. Neurochem.* 101 (1), 132–141. doi:10.1111/j.1471-4159.2006.04348.x

Barker, R., and Mason, S. L. (2019). The hunt for better treatments for Huntington's disease. *Lancet Neurol.* 18 (2), 131–133. doi:10.1016/S1474-4422(18)30448-4

Barron, J. C., Hurley, E. P., and Parsons, M. P. (2021). Huntingtin and the synapse. *Front. Cell. Neurosci.* 15, 689332. doi:10.3389/fncel.2021.689332

Bartels, T., Ahlstrom, L. S., Leftin, A., Kamp, F., Haass, C., Brown, M. F., et al. (2010). The N-terminus of the intrinsically disordered protein α-synuclein triggers membrane binding and helix folding. *Biophys. J.* 99 (7), 2116–2124. doi:10.1016/j.bpj.2010.06.035

Bartels, T., Choi, J. G., and Selkoe, D. J. (2011). α-Synuclein occurs physiologically as a helically folded tetramer that resists aggregation. *Nature* 477 (7362), 107–110. doi:10.1038/nature10324

Bauer, M. F., Gempel, K., Reichert, A. S., Rappold, G. A., Lichtner, P., Gerbitz, K. D., et al. (1999). Genetic and structural characterization of the human mitochondrial inner membrane translocase. *J. Mol. Biol.* 289 (1), 69–82. doi:10.1006/jmbi.1999.2751

Bauer, M. F., Sirrenberg, C., Neupert, W., and Brunner, M. (1996). Role of Tim23 as voltage sensor and presequence receptor in protein import into mitochondria. *Cell.* 87 (1), 33–41. doi:10.1016/s0092-8674(00)81320-3

Baumkötter, F., Schmidt, N., Vargas, C., Schilling, S., Weber, R., Wagner, K., et al. (2014). Amyloid precursor protein dimerization and synaptogenic function depend on copper binding to the growth factor-like domain. *J. Neurosci.* 34 (33), 11159–11172. doi:10.1523/JNEUROSCI.0180-14.2014

Bausewein, T., Mills, D. J., Langer, J. D., Nitschke, B., Nussberger, S., and Kuhlbrandt, W. (2017). Cryo-EM structure of the TOM core complex from neurospora crassa. *Cell.* 170 (4), 693–700. doi:10.1016/j.cell.2017.07.012

Beatrix, B., Sakai, H., and Wiedmann, M. (2000). The alpha and beta subunit of the nascent polypeptide-associated complex have distinct functions. *J. Biol. Chem.* 275 (48), 37838–37845. doi:10.1074/jbc.M006368200

Beck, J. S., Mufson, E. J., and Counts, S. E. (2016b). Evidence for mitochondrial UPR gene activation in familial and sporadic alzheimer's disease. *Curr. Alzheimer Res.* 13 (6), 610–614. doi:10.2174/1567205013666151221145445

Beck, S. J., Guo, L., Phensy, A., Tian, J., Wang, L., Tandon, N., et al. (2016a). Deregulation of mitochondrial F1FO-ATP synthase via OSCP in Alzheimer's disease. *Nat. Commun.* 7, 11483. doi:10.1038/ncomms11483

Becker, T., Song, J., and Pfanner, N. (2019). Versatility of preprotein transfer from the cytosol to mitochondria. *Trends Cell. Biol.* 29 (7), 534–548. doi:10.1016/j.tcb.2019.03.007

Bekris, L. M., Yu, C. E., Bird, T. D., and Tsuang, D. W. (2010). Genetics of alzheimer disease. *J. Geriatr. Psychiatry Neurol.* 23 (4), 213–227. doi:10.1177/0891988710383571

Belloy, M. E., Napolioni, V., and Greicius, M. D. (2019). A quarter century of APOE and alzheimer's disease: progress to date and the path forward. *Neuron* 101 (5), 820–838. doi:10.1016/j.neuron.2019.01.056

Belyaev, N. D., Kellett, K. A., Beckett, C., Makova, N. Z., Revett, T. J., Nalivaeva, N. N., et al. (2010). The transcriptionally active amyloid precursor protein (APP) intracellular domain is preferentially produced from the 695 isoform of APP in a {beta}-secretase-dependent pathway. *J. Biol. Chem.* 285 (53), 41443–41454. doi:10.1074/jbc.M110.141390

Benador, I. Y., Veliova, M., Liesa, M., and Shirihai, O. S. (2019). Mitochondria bound to lipid droplets: where mitochondrial dynamics regulate lipid storage and utilization. *Cell. Metab.* 29 (4), 827–835. doi:10.1016/j.cmet.2019.02.011

Benchoua, A., Trioulier, Y., Zala, D., Gaillard, M. C., Lefort, N., Dufour, N., et al. (2006). Involvement of mitochondrial complex II defects in neuronal death produced by N-terminus fragment of mutated huntingtin. *Mol. Biol. Cell.* 17 (4), 1652–1663. doi:10.1091/mbc.e05-07-0607

Bender, A., Desplats, P., Spencer, B., Rockenstein, E., Adame, A., Elstner, M., et al. (2013). TOM40 mediates mitochondrial dysfunction induced by α-synuclein accumulation in Parkinson's disease. *PLoS One* 8 (4), e62277. doi:10.1371/journal.pone.0062277

Bendor, J. T., Logan, T. P., and Edwards, R. H. (2013). The function of alpha-synuclein. *Neuron* 79 (6), 1044–1066. doi:10.1016/j.neuron.2013.09.004

Bennett, C. F., and Kaeberlein, M. (2014). The mitochondrial unfolded protein response and increased longevity: cause, consequence, or correlation? *Exp. Gerontol.* 56, 142–146. doi:10.1016/j.exger.2014.02.002

Berendzen, K. M., Durieux, J., Shao, L. W., Tian, Y., Kim, H. E., Wolff, S., et al. (2016). Neuroendocrine coordination of mitochondrial stress signaling and proteostasis. *Cell.* 166 (6), 1553–1563. doi:10.1016/j.cell.2016.08.042

Berridge, M. J. (2010). Calcium hypothesis of Alzheimer's disease. *Pflugers Arch.* 459 (3), 441–449. doi:10.1007/s00424-009-0736-1

Berry, B. J., and Kaeberlein, M. (2021). An energetics perspective on geroscience: mitochondrial protonmotive force and aging. *Geroscience* 43 (4), 1591–1604. doi:10.1007/s11357-021-00365-7

Berry, B. J., Mjelde, E., Carreno, F., Gilham, K., Hanson, E. J., Na, E., et al. (2023). Preservation of mitochondrial membrane potential is necessary for lifespan extension from dietary restriction. *Geroscience* 45, 1573–1581. doi:10.1007/s11357-023-00766-w

Berth, S. H., and Lloyd, T. E. (2023). Disruption of axonal transport in neurodegeneration. *J. Clin. Investig.* 133 (11), e168554. doi:10.1172/JCI168554

Bhagawati, M., Arroum, T., Webeling, N., Montoro, A. G., Mootz, H. D., and Busch, K. B. (2021). The receptor subunit Tom20 is dynamically associated with the TOM complex in mitochondria of human cells. *Mol. Biol. Cell.* 32 (20), br1. doi:10.1091/mbc.E21-01-0042

Bhangoo, M. K., Tzankov, S., Fan, A. C., Dejgaard, K., Thomas, D. Y., and Young, J. C. (2007). Multiple 40-kDa heat-shock protein chaperones function in Tom70-dependent mitochondrial import. *Mol. Biol. Cell.* 18 (9), 3414–3428. doi:10.1091/mbc.e07-01-0088

Bhattacharyya, A., Thakur, A. K., Chellgren, V. M., Thiagarajan, G., Williams, A. D., Chellgren, B. W., et al. (2006). Oligoproline effects on polyglutamine conformation and aggregation. *J. Mol. Biol.* 355 (3), 524–535. doi:10.1016/j.jmb.2005.10.053

Billingsley, K. J., Bandres-Ciga, S., Saez-Atienzar, S., and Singleton, A. B. (2018). Genetic risk factors in Parkinson's disease. *Cell. Tissue Res.* 373 (1), 9–20. doi:10.1007/s00441-018-2817-y

Bisi, N., Feni, L., Peqini, K., Perez-Pena, H., Ongeri, S., Pieraccini, S., et al. (2021). α-Synuclein: an all-inclusive trip around its structure, influencing factors and applied techniques. *Front. Chem.* 9, 666585. doi:10.3389/fchem.2021.666585

Bitto, A., Ito, T. K., Pineda, V. V., LeTexier, N. J., Huang, H. Z., Sutlief, E., et al. (2016). Transient rapamycin treatment can increase lifespan and healthspan in middle-aged mice. *Elife* 5, e16351. doi:10.7554/eLife.16351

Blaszczyk, J. W. (2020). Energy metabolism decline in the aging brain-pathogenesis of neurodegenerative disorders. *Metabolites* 10 (11), 450. doi:10.3390/metabo10110450

Block, R. C., Dorsey, E. R., Beck, C. A., Brenna, J. T., and Shoulson, I. (2010). Altered cholesterol and fatty acid metabolism in Huntington disease. *J. Clin. Lipidol.* 4 (1), 17–23. doi:10.1016/j.jacl.2009.11.003

Blumenthal, H. T. (2004). Amyloidosis: a universal disease of aging? *J. Gerontol. A Biol. Sci. Med. Sci.* 59 (4), 361–369. doi:10.1093/gerona/59.4.m361

Bodner, C. R., Maltsev, A. S., Dobson, C. M., and Bax, A. (2010). Differential phospholipid binding of alpha-synuclein variants implicated in Parkinson's disease revealed by solution NMR spectroscopy. *Biochemistry* 49 (5), 862–871. doi:10.1021/bi901723p

Bolliger, L., Junne, T., Schatz, G., and Lithgow, T. (1995). Acidic receptor domains on both sides of the outer membrane mediate translocation of precursor proteins into yeast mitochondria. *EMBO J.* 14 (24), 6318–6326. doi:10.1002/j.1460-2075.1995.tb00322.x

Boopathi, E., Srinivasan, S., Fang, J. K., and Avadhani, N. G. (2008). Bimodal protein targeting through activation of cryptic mitochondrial targeting signals by an inducible cytosolic endoprotease. *Mol. Cell.* 32 (1), 32–42. doi:10.1016/j.molcel.2008.09.008

Bossy-Wetzel, E., Petrilli, A., and Knott, A. B. (2008). Mutant huntingtin and mitochondrial dysfunction. *Trends Neurosci.* 31 (12), 609–616. doi:10.1016/j.tins.2008.09.004

Braak, H., Sandmann-Keil, D., Gai, W., and Braak, E. (1999). Extensive axonal Lewy neurites in Parkinson's disease: a novel pathological feature revealed by alpha-synuclein immunocytochemistry. *Neurosci. Lett.* 265 (1), 67–69. doi:10.1016/s0304-3940(99)00208-6

Breydo, L., Wu, J. W., and Uversky, V. N. (2012). A-synuclein misfolding and Parkinson's disease. *Biochimica Biophysica Acta (BBA) - Mol. Basis Dis.* 1822 (2), 261–285. doi:10.1016/j.bbadis.2011.10.002

Brunetti, D., Bottani, E., Segala, A., Marchet, S., Rossi, F., Orlando, F., et al. (2020). Targeting multiple mitochondrial processes by a metabolic modulator prevents sarcopenia and cognitive decline in SAMP8 mice. *Front. Pharmacol.* 11, 1171. doi:10.3389/fphar.2020.01171

Brunetti, D., Catania, A., Viscomi, C., Deleidi, M., Bindoff, L. A., Ghezzi, D., et al. (2021). Role of PITRM1 in mitochondrial dysfunction and neurodegeneration. *Biomedicines* 9 (7), 833. doi:10.3390/biomedicines9070833

Brunetti, D., Torsvik, J., Dallabona, C., Teixeira, P., Sztromwasser, P., Fernandez-Vizarra, E., et al. (2016). Defective PITRM1 mitochondrial peptidase is associated with Aβ amyloidotic neurodegeneration. *EMBO Mol. Med.* 8 (3), 176–190. doi:10.15252/emmm.201505894

Brustovetsky, T., Khanna, R., and Brustovetsky, N. (2023). CRMP2 participates in regulating mitochondrial morphology and motility in alzheimer's disease. *Cells* 12 (9), 1287. doi:10.3390/cells12091287

Bubber, P., Haroutunian, V., Fisch, G., Blass, J. P., and Gibson, G. E. (2005). Mitochondrial abnormalities in Alzheimer brain: mechanistic implications. *Ann. Neurol.* 57 (5), 695–703. doi:10.1002/ana.20474

Burre, J. (2015). The synaptic function of alpha-synuclein. *J. Park. Dis.* 5 (4), 699–713. doi:10.3233/JPD-150642

Burtscher, J., Di Pardo, A., Maglione, V., Schwarzer, C., and Squitieri, F. (2020). Mitochondrial respiration changes in R6/2 huntington's disease model mice during aging in a brain region specific manner. *Int. J. Mol. Sci.* 21 (15), 5412. doi:10.3390/ijms21155412

Busch, J. D., Fielden, L. F., Pfanner, N., and Wiedemann, N. (2023). Mitochondrial protein transport: versatility of translocases and mechanisms. *Mol. Cell.* 83 (6), 890–910. doi:10.1016/j.molcel.2023.02.020

Bussell, R., Jr., and Eliezer, D. (2003). A structural and functional role for 11-mer repeats in alpha-synuclein and other exchangeable lipid binding proteins. *J. Mol. Biol.* 329 (4), 763–778. doi:10.1016/s0022-2836(03)00520-5

Cali, T., Ottolini, D., Negro, A., and Brini, M. (2012). α-Synuclein controls mitochondrial calcium homeostasis by enhancing endoplasmic reticulum-mitochondria interactions. *J. Biol. Chem.* 287 (22), 17914–17929. doi:10.1074/jbc.M111.302794

Calkins, M. J., Manczak, M., Mao, P., Shirendeb, U., and Reddy, P. H. (2011). Impaired mitochondrial biogenesis, defective axonal transport of mitochondria, abnormal mitochondrial dynamics and synaptic degeneration in a mouse model of Alzheimer's disease. *Hum. Mol. Genet.* 20 (23), 4515–4529. doi:10.1093/hmg/ddr381

Calvo, S. E., Julien, O., Clauser, K. R., Shen, H., Kamer, K. J., Wells, J. A., et al. (2017). Comparative analysis of mitochondrial N-termini from mouse, human, and yeast. *Mol. Cell. Proteomics* 16 (4), 512–523. doi:10.1074/mcp.M116.063818

Carmo, C., Naia, L., Lopes, C., and Rego, A. C. (2018). Mitochondrial dysfunction in huntington's disease. *Adv. Exp. Med. Biol.* 1049, 59–83. doi:10.1007/978-3-319-71779-1_3

Carulla, N., Caddy, G. L., Hall, D. R., Zurdo, J., Gairi, M., Feliz, M., et al. (2005). Molecular recycling within amyloid fibrils. *Nature* 436 (7050), 554–558. doi:10.1038/nature03986

Caspersen, C., Wang, N., Yao, J., Sosunov, A., Chen, X., Lustbader, J. W., et al. (2005). Mitochondrial Abeta: a potential focal point for neuronal metabolic dysfunction in Alzheimer's disease. *FASEB J.* 19 (14), 2040–2041. doi:10.1096/fj.05-3735fje

Castellano, J. M., Kim, J., Stewart, F. R., Jiang, H., DeMattos, R. B., Patterson, B. W., et al. (2011). Human apoE isoforms differentially regulate brain amyloid-beta peptide clearance. *Sci. Transl. Med.* 3 (89), 89ra57. 89ra57. doi:10.1126/scitranslmed.3002156

Cenini, G., Rüb, C., Bruderek, M., and Voos, W. (2016). Amyloid β-peptides interfere with mitochondrial preprotein import competence by a coaggregation process. *Mol. Biol. Cell.* 27 (21), 3257–3272. doi:10.1091/mbc.E16-05-0313

Cenini, G., and Voos, W. (2019). Mitochondria as potential targets in alzheimer disease therapy: an update. *Front. Pharmacol.* 10, 902. doi:10.3389/fphar.2019.00902

Cha, M. Y., Han, S. H., Son, S. M., Hong, H. S., Choi, Y. J., Byun, J., et al. (2012). Mitochondria-specific accumulation of amyloid beta induces mitochondrial dysfunction leading to apoptotic cell death. *PLoS One* 7 (4), e34929. doi:10.1371/journal.pone.0034929

Chacinska, A., Lind, M., Frazier, A. E., Dudek, J., Meisinger, C., Geissler, A., et al. (2005). Mitochondrial presequence translocase: switching between TOM tethering and motor recruitment involves Tim21 and Tim17. *Cell.* 120 (6), 817–829. doi:10.1016/j.cell.2005.01.011

Chacinska, A., Rehling, P., Guiard, B., Frazier, A. E., Schulze-Specking, A., Pfanner, N., et al. (2003). Mitochondrial translocation contact sites: separation of dynamic and stabilizing elements in formation of a TOM-TIM-preprotein supercomplex. *EMBO J.* 22 (20), 5370–5381. doi:10.1093/emboj/cdg532

Chacinska, A., van der Laan, M., Mehnert, C. S., Guiard, B., Mick, D. U., Hutu, D. P., et al. (2010). Distinct forms of mitochondrial TOM-TIM supercomplexes define signal-dependent states of preprotein sorting. *Mol. Cell. Biol.* 30 (1), 307–318. doi:10.1128/MCB.00749-09

Chae, J. I., Kim, D. W., Lee, N., Jeon, Y. J., Jeon, I., Kwon, J., et al. (2012). Quantitative proteomic analysis of induced pluripotent stem cells derived from a human Huntington's disease patient. *Biochem. J.* 446 (3), 359–371. doi:10.1042/BJ20111495

Chai, Y. L., Xing, H., Chong, J. R., Francis, P. T., Ballard, C. G., Chen, C. P., et al. (2018). Mitochondrial translocase of the outer membrane alterations may underlie dysfunctional oxidative phosphorylation in alzheimer's disease. *J. Alzheimers Dis.* 61 (2), 793–801. doi:10.3233/JAD-170613

Chakraborty, K., Chatila, M., Sinha, J., Shi, Q., Poschner, B. C., Sikor, M., et al. (2010). Chaperonin-catalyzed rescue of kinetically trapped states in protein folding. *Cell.* 142 (1), 112–122. doi:10.1016/j.cell.2010.05.027

Chandra, S., Chen, X., Rizo, J., Jahn, R., and Sudhof, T. C. (2003). A broken alpha -helix in folded alpha -Synuclein. *J. Biol. Chem.* 278 (17), 15313–15318. doi:10.1074/jbc.M213128200

Chang, D. T., Rintoul, G. L., Pandipati, S., and Reynolds, I. J. (2006). Mutant huntingtin aggregates impair mitochondrial movement and trafficking in cortical neurons. *Neurobiol. Dis.* 22 (2), 388–400. doi:10.1016/j.nbd.2005.12.007

Chatre, L., Matheson, L. A., Jack, A. S., Hanton, S. L., and Brandizzi, F. (2009). Efficient mitochondrial targeting relies on co-operation of multiple protein signals in plants. *J. Exp. Bot.* 60 (3), 741–749. doi:10.1093/jxb/ern319

Chaudhuri, M., Tripathi, A., and Gonzalez, F. S. (2021). Diverse functions of Tim50, a component of the mitochondrial inner membrane protein translocase. *Int. J. Mol. Sci.* 22 (15), 7779. doi:10.3390/ijms22157779

Chavez, J. D., Tang, X., Campbell, M. D., Reyes, G., Kramer, P. A., Stuppard, R., et al. (2020). Mitochondrial protein interaction landscape of SS-31. *Proc. Natl. Acad. Sci. U. S. A.* 117 (26), 15363–15373. doi:10.1073/pnas.2002250117

Cheema, N. J., Cameron, J. M., and Hood, D. A. (2021). Effect of rapamycin on mitochondria and lysosomes in fibroblasts from patients with mtDNA mutations. *Am. J. Physiol. Cell. Physiol.* 321 (1), C176–C186. doi:10.1152/ajpcell.00471.2020

Chen, C. M., Wu, Y. R., and Chang, K. H. (2017). Altered aconitase 2 activity in huntington's disease peripheral blood cells and mouse model striatum. *Int. J. Mol. Sci.* 18 (11), 2480. doi:10.3390/ijms18112480

Chen, M., Ona, V. O., Li, M., Ferrante, R. J., Fink, K. B., Zhu, S., et al. (2000). Minocycline inhibits caspase-1 and caspase-3 expression and delays mortality in a transgenic mouse model of Huntington disease. *Nat. Med.* 6 (7), 797–801. doi:10.1038/77528

Cheng, M. Y., Hartl, F. U., Martin, J., Pollock, R. A., Kalousek, F., Neupert, W., et al. (1989). Mitochondrial heat-shock protein hsp60 is essential for assembly of proteins imported into yeast mitochondria. *Nature* 337 (6208), 620–625. doi:10.1038/337620a0

Cherubini, M., Lopez-Molina, L., and Gines, S. (2020). Mitochondrial fission in Huntington's disease mouse striatum disrupts ER-mitochondria contacts leading to disturbances in Ca(2+) efflux and Reactive Oxygen Species (ROS) homeostasis. *Neurobiol. Dis.* 136, 104741. doi:10.1016/j.nbd.2020.104741

Chiba-Falek, O., Gottschalk, W. K., and Lutz, M. W. (2018). The effects of the TOMM40 poly-T alleles on Alzheimer's disease phenotypes. *Alzheimers Dement.* 14 (5), 692–698. doi:10.1016/j.jalz.2018.01.015

Chiki, A., Zhang, Z., Rajasekhar, K., Abriata, L. A., Rostami, I., Krapp, L. F., et al. (2021). Investigating crosstalk among PTMs provides novel insight into the structural basis underlying the differential effects of Nt17 PTMs on mutant Httex1 aggregation. *Front. Mol. Biosci.* 8, 686086. doi:10.3389/fmolb.2021.686086

Chiti, F., and Dobson, C. M. (2017). Protein misfolding, amyloid formation, and human disease: a summary of progress over the last decade. *Annu. Rev. Biochem.* 86, 27–68. doi:10.1146/annurev-biochem-061516-045115

Cho, M. K., Nodet, G., Kim, H. Y., Jensen, M. R., Bernado, P., Fernandez, C. O., et al. (2009). Structural characterization of alpha-synuclein in an aggregation prone state. *Protein Sci.* 18 (9), 1840–1846. doi:10.1002/pro.194

Choo, Y. S., Johnson, G. V., MacDonald, M., Detloff, P. J., and Lesort, M. (2004). Mutant huntingtin directly increases susceptibility of mitochondria to the calcium-induced permeability transition and cytochrome c release. *Hum. Mol. Genet.* 13 (14), 1407–1420. doi:10.1093/hmg/ddh162

Chow, V. W., Mattson, M. P., Wong, P. C., and Gleichmann, M. (2010). An overview of APP processing enzymes and products. *Neuromolecular Med.* 12 (1), 1–12. doi:10.1007/s12017-009-8104-z

Chowhan, R. K., Dar, T. A., and Singh, L. R. (2015). "Proteopathies: biological, molecular and clinical perspectives," in *Proteostasis and chaperone surveillance*. Editors L. R. Singh, T. A. Dar, and P. Ahmad (New Delhi: Springer India), 139–169.

Chuang, C. L., and Demontis, F. (2021). Systemic manifestation and contribution of peripheral tissues to Huntington's disease pathogenesis. *Ageing Res. Rev.* 69, 101358. doi:10.1016/j.arr.2021.101358

Cieri, D., Brini, M., and Cali, T. (2017). Emerging (and converging) pathways in Parkinson's disease: keeping mitochondrial wellness. *Biochem. Biophys. Res. Commun.* 483 (4), 1020–1030. doi:10.1016/j.bbrc.2016.08.153

Claros, M. G., Perea, J., Shu, Y., Samatey, F. A., Popot, J. L., and Jacq, C. (1995). Limitations to *in vivo* import of hydrophobic proteins into yeast mitochondria. The case of a cytoplasmically synthesized apocytochrome b. *Eur. J. Biochem.* 228 (3), 762–771. doi:10.1111/j.1432-1033.1995.tb20321.x

Claypool, S. M., and Koehler, C. M. (2012). The complexity of cardiolipin in health and disease. *Trends Biochem. Sci.* 37 (1), 32–41. doi:10.1016/j.tibs.2011.09.003

Cline, E. N., Bicca, M. A., Viola, K. L., and Klein, W. L. (2018). The amyloid-beta oligomer hypothesis: beginning of the third decade. *J. Alzheimers Dis.* 64 (1), S567-S610–S610. doi:10.3233/JAD-179941

Cole, N. B., Dieuliis, D., Leo, P., Mitchell, D. C., and Nussbaum, R. L. (2008). Mitochondrial translocation of alpha-synuclein is promoted by intracellular acidification. *Exp. Cell. Res.* 314 (10), 2076–2089. doi:10.1016/j.yexcr.2008.03.012

Conconi, M., Szweda, L. I., Levine, R. L., Stadtman, E. R., and Friguet, B. (1996). Age-related decline of rat liver multicatalytic proteinase activity and protection from oxidative inactivation by heat-shock protein 90. *Arch. Biochem. Biophys.* 331 (2), 232–240. doi:10.1006/abbi.1996.0303

Connern, C. P., and Halestrap, A. P. (1994). Recruitment of mitochondrial cyclophilin to the mitochondrial inner membrane under conditions of oxidative stress that enhance the opening of a calcium-sensitive non-specific channel. *Biochem. J.* 302 (2), 321–324. doi:10.1042/bj3020321

Cooper, J. F., Machiela, E., Dues, D. J., Spielbauer, K. K., Senchuk, M. M., and Van Raamsdonk, J. M. (2017). Activation of the mitochondrial unfolded protein response promotes longevity and dopamine neuron survival in Parkinson's disease models. *Sci. Rep.* 7 (1), 16441. doi:10.1038/s41598-017-16637-2

Cooper, J. K., Schilling, G., Peters, M. F., Herring, W. J., Sharp, A. H., Kaminsky, Z., et al. (1998). Truncated N-terminal fragments of huntingtin with expanded glutamine repeats form nuclear and cytoplasmic aggregates in cell culture. *Hum. Mol. Genet.* 7 (5), 783–790. doi:10.1093/hmg/7.5.783

Corder, E. H., Saunders, A. M., Strittmatter, W. J., Schmechel, D. E., Gaskell, P. C., Small, G. W., et al. (1993). Gene dose of apolipoprotein E type 4 allele and the risk of Alzheimer's disease in late onset families. *Science* 261 (5123), 921–923. doi:10.1126/science.8346443

Costa, V., Giacomello, M., Hudec, R., Lopreiato, R., Ermak, G., Lim, D., et al. (2010). Mitochondrial fission and cristae disruption increase the response of cell models of Huntington's disease to apoptotic stimuli. *EMBO Mol. Med.* 2 (12), 490–503. doi:10.1002/emmm.201000102

Coulson, E. J., Paliga, K., Beyreuther, K., and Masters, C. L. (2000). What the evolution of the amyloid protein precursor supergene family tells us about its function. *Neurochem. Int.* 36 (3), 175–184. doi:10.1016/s0197-0186(99)00125-4

Court, D. A., Nargang, F. E., Steiner, H., Hodges, R. S., Neupert, W., and Lill, R. (1996). Role of the intermembrane-space domain of the preprotein receptor Tom22 in protein import into mitochondria. *Mol. Cell. Biol.* 16 (8), 4035–4042. doi:10.1128/mcb.16.8.4035

Croke, R. L., Patil, S. M., Quevreaux, J., Kendall, D. A., and Alexandrescu, A. T. (2011). NMR determination of pKa values in α-synuclein. *Protein Sci.* 20 (2), 256–269. doi:10.1002/pro.556

Croke, R. L., Sallum, C. O., Watson, E., Watt, E. D., and Alexandrescu, A. T. (2008). Hydrogen exchange of monomeric alpha-synuclein shows unfolded structure persists at physiological temperature and is independent of molecular crowding in *Escherichia coli*. *Protein Sci.* 17 (8), 1434–1445. doi:10.1110/ps.033803.107

Crowley, K. S., and Payne, R. M. (1998). Ribosome binding to mitochondria is regulated by GTP and the transit peptide. *J. Biol. Chem.* 273 (27), 17278–17285. doi:10.1074/jbc.273.27.17278

Cuello, A. C. (2005). Intracellular and extracellular Abeta, a tale of two neuropathologies. *Brain Pathol.* 15 (1), 66–71. doi:10.1111/j.1750-3639.2005.tb00101.x

Cui, L., Jeong, H., Borovecki, F., Parkhurst, C. N., Tanese, N., and Krainc, D. (2006). Transcriptional repression of PGC-1alpha by mutant huntingtin leads to mitochondrial dysfunction and neurodegeneration. *Cell.* 127 (1), 59–69. doi:10.1016/j.cell.2006.09.015

Currais, A., Huang, L., Goldberg, J., Petrascheck, M., Ates, G., Pinto-Duarte, A., et al. (2019). Elevating acetyl-CoA levels reduces aspects of brain aging. *Elife* 8, e47866. doi:10.7554/eLife.47866

Davidson, W. S., Jonas, A., Clayton, D. F., and George, J. M. (1998). Stabilization of alpha-synuclein secondary structure upon binding to synthetic membranes. *J. Biol. Chem.* 273 (16), 9443–9449. doi:10.1074/jbc.273.16.9443

Davies, S. W., Turmaine, M., Cozens, B. A., DiFiglia, M., Sharp, A. H., Ross, C. A., et al. (1997). Formation of neuronal intranuclear inclusions underlies the neurological dysfunction in mice transgenic for the HD mutation. *Cell.* 90 (3), 537–548. doi:10.1016/s0092-8674(00)80513-9

Dawson, T. M., and Dawson, V. L. (2010). The role of parkin in familial and sporadic Parkinson's disease. *Mov. Disord.* 25(1), S32–S39. doi:10.1002/mds.22798

Dayan, D., Bandel, M., Gunsel, U., Nussbaum, I., Prag, G., Mokranjac, D., et al. (2019). A mutagenesis analysis of Tim50, the major receptor of the TIM23 complex, identifies regions that affect its interaction with Tim23. *Sci. Rep.* 9 (1), 2012. doi:10.1038/s41598-018-38353-1

de la Cruz, L., Bajaj, R., Becker, S., and Zweckstetter, M. (2010). The intermembrane space domain of Tim23 is intrinsically disordered with a distinct binding region for presequences. *Protein Sci.* 19 (11), 2045–2054. doi:10.1002/pro.482

De Miranda, B. R., Rocha, E. M., Castro, S. L., and Greenamyre, J. T. (2020). Protection from α-Synuclein induced dopaminergic neurodegeneration by overexpression of the mitochondrial import receptor TOM20. *NPJ Park. Dis.* 6 (1), 38. doi:10.1038/s41531-020-00139-6

Dekker, P. J., Martin, F., Maarse, A. C., Bomer, U., Muller, H., Guiard, B., et al. (1997). The Tim core complex defines the number of mitochondrial translocation contact sites and can hold arrested preproteins in the absence of matrix Hsp70-Tim44. *EMBO J.* 16 (17), 5408–5419. doi:10.1093/emboj/16.17.5408

Dekker, P. J., Ryan, M. T., Brix, J., Muller, H., Honlinger, A., and Pfanner, N. (1998). Preprotein translocase of the outer mitochondrial membrane: molecular dissection and assembly of the general import pore complex. *Mol. Cell. Biol.* 18 (11), 6515–6524. doi:10.1128/mcb.18.11.6515

del Alamo, M., Hogan, D. J., Pechmann, S., Albanese, V., Brown, P. O., and Frydman, J. (2011). Defining the specificity of cotranslationally acting chaperones by systematic analysis of mRNAs associated with ribosome-nascent chain complexes. *PLoS Biol.* 9 (7), e1001100. doi:10.1371/journal.pbio.1001100

Del Prete, D., Suski, J. M., Oules, B., Debayle, D., Gay, A. S., Lacas-Gervais, S., et al. (2017). Localization and processing of the amyloid-beta protein precursor in mitochondria-associated membranes. *J. Alzheimers Dis.* 55 (4), 1549–1570. doi:10.3233/JAD-160953

Demishtein-Zohary, K., Gunsel, U., Marom, M., Banerjee, R., Neupert, W., Azem, A., et al. (2017). Role of Tim17 in coupling the import motor to the translocation channel of the mitochondrial presequence translocase. *Elife* 6, e22696. doi:10.7554/eLife.22696

Denkert, N., Schendzielorz, A. B., Barbot, M., Versemann, L., Richter, F., Rehling, P., et al. (2017). Cation selectivity of the presequence translocase channel Tim23 is crucial for efficient protein import. *Elife* 6, e28324. doi:10.7554/eLife.28324

Deshaies, R. J., Koch, B. D., Werner-Washburne, M., Craig, E. A., and Schekman, R. (1988). A subfamily of stress proteins facilitates translocation of secretory and mitochondrial precursor polypeptides. *Nature* 332 (6167), 800–805. doi:10.1038/332800a0

Devi, L., and Anandatheerthavarada, H. K. (2010). Mitochondrial trafficking of APP and alpha synuclein: relevance to mitochondrial dysfunction in Alzheimer's and Parkinson's diseases. *Biochimica Biophysica Acta (BBA) - Mol. Basis Dis.* 1802 (1), 11–19. doi:10.1016/j.bbadis.2009.07.007

Devi, L., Prabhu, B. M., Galati, D. F., Avadhani, N. G., and Anandatheerthavarada, H. K. (2006). Accumulation of amyloid precursor protein in the mitochondrial import channels of human Alzheimer's disease brain is associated with mitochondrial dysfunction. *J. Neurosci.* 26 (35), 9057–9068. doi:10.1523/JNEUROSCI.1469-06.2006

Devi, L., Raghavendran, V., Prabhu, B. M., Avadhani, N. G., and Anandatheerthavarada, H. K. (2008). Mitochondrial import and accumulation of alpha-synuclein impair complex I in human dopaminergic neuronal cultures and Parkinson disease brain. *J. Biol. Chem.* 283 (14), 9089–9100. doi:10.1074/jbc.M710012200

Di Donfrancesco, A., Berlingieri, C., Giacomello, M., Frascarelli, C., Magalhaes Rebelo, A. P., Bindoff, L. A., et al. (2023). PPAR-gamma agonist pioglitazone recovers mitochondrial quality control in fibroblasts from PITRM1-deficient patients. *Front. Pharmacol.* 14, 1220620. doi:10.3389/fphar.2023.1220620

Di Maio, R., Barrett, P. J., Hoffman, E. K., Barrett, C. W., Zharikov, A., Borah, A., et al. (2016a). α-Synuclein binds to TOM20 and inhibits mitochondrial protein import in Parkinson's disease. *Sci. Transl. Med.* 8 (342), 342ra78. doi:10.1126/scitranslmed.aaf3634

Di Maio, R., Barrett, P. J., Hoffman, E. K., Barrett, C. W., Zharikov, A., Borah, A., et al. (2016b). α-Synuclein binds to TOM20 and inhibits mitochondrial protein import in Parkinson's disease. *Sci. Transl. Med.* 8 (342), 342ra78. doi:10.1126/scitranslmed.aaf3634

Diaz, M., Fabelo, N., Martin, V., Ferrer, I., Gomez, T., and Marin, R. (2015). Biophysical alterations in lipid rafts from human cerebral cortex associate with increased BACE1/AβPP interaction in early stages of Alzheimer's disease. *J. Alzheimers Dis.* 43 (4), 1185–1198. doi:10.3233/JAD-141146

Dienel, G. A. (2017). Lack of appropriate stoichiometry: strong evidence against an energetically important astrocyte-neuron lactate shuttle in brain. *J. Neurosci. Res.* 95 (11), 2103–2125. doi:10.1002/jnr.24015

Dietmeier, K., Honlinger, A., Bomer, U., Dekker, P. J., Eckerskorn, C., Lottspeich, F., et al. (1997). Tom5 functionally links mitochondrial preprotein receptors to the general import pore. *Nature* 388 (6638), 195–200. doi:10.1038/40663

Dobson, C. M. (2003). Protein folding and misfolding. *Nature* 426 (6968), 884–890. doi:10.1038/nature02261

Dores-Silva, P. R., Minari, K., Ramos, C. H., Barbosa, L. R., and Borges, J. C. (2013). Structural and stability studies of the human mtHsp70-escort protein 1: an essential mortalin co-chaperone. *Int. J. Biol. Macromol.* 56, 140–148. doi:10.1016/j.ijbiomac.2013.02.009

Dose, J., Huebbe, P., Nebel, A., and Rimbach, G. (2016). APOE genotype and stress response - a mini review. *Lipids Health Dis.* 15, 121. doi:10.1186/s12944-016-0288-2

Du, F., Yu, Q., Yan, S., Zhang, Z., Vangavaragu, J. R., Chen, D., et al. (2021). Gain of PITRM1 peptidase in cortical neurons affords protection of mitochondrial and synaptic function in an advanced age mouse model of Alzheimer's disease. *Aging Cell.* 20 (5), e13368. doi:10.1111/acel.13368

Du, H., Guo, L., Fang, F., Chen, D., Sosunov, A. A., McKhann, G. M., et al. (2008). Cyclophilin D deficiency attenuates mitochondrial and neuronal perturbation and ameliorates learning and memory in Alzheimer's disease. *Nat. Med.* 14 (10), 1097–1105. doi:10.1038/nm.1868

Dubois, C., Kong, G., Tran, H., Li, S., Pang, T. Y., Hannan, A. J., et al. (2021). Small non-coding RNAs are dysregulated in huntington's disease transgenic mice independently of the therapeutic effects of an environmental intervention. *Mol. Neurobiol.* 58 (7), 3308–3318. doi:10.1007/s12035-021-02342-9

Duce, J. A., Tsatsanis, A., Cater, M. A., James, S. A., Robb, E., Wikhe, K., et al. (2010). Iron-export ferroxidase activity of beta-amyloid precursor protein is inhibited by zinc in Alzheimer's disease. *Cell.* 142 (6), 857–867. doi:10.1016/j.cell.2010.08.014

Dugger, B. N., and Dickson, D. W. (2017). Pathology of neurodegenerative diseases. *Cold Spring Harb. Perspect. Biol.* 9 (7), a028035. doi:10.1101/cshperspect.a028035

Ebanks, B., Ingram, T. L., and Chakrabarti, L. (2020). ATP synthase and Alzheimer's disease: putting a spin on the mitochondrial hypothesis. *Aging (Albany NY)* 12 (16), 16647–16662. doi:10.18632/aging.103867

Egea, G., Izquierdo, J. M., Ricart, J., San Martin, C., and Cuezva, J. M. (1997). mRNA encoding the beta-subunit of the mitochondrial F1-ATPase complex is a localized mRNA in rat hepatocytes. *Biochem. J.* 322(2), 557–565. doi:10.1042/bj3220557

Egidio, F., Castelli, V., Cimini, A., and d'Angelo, M. (2023). Cell rearrangement and oxidant/antioxidant imbalance in huntington's disease. *Antioxidants (Basel)* 12 (3), 571. doi:10.3390/antiox12030571

Eisenberg, D., Weiss, R. M., and Terwilliger, T. C. (1982). The helical hydrophobic moment: a measure of the amphiphilicity of a helix. *Nature* 299 (5881), 371–374. doi:10.1038/299371a0

Ellis, C. E., Murphy, E. J., Mitchell, D. C., Golovko, M. Y., Scaglia, F., Barcelo-Coblijn, G. C., et al. (2005). Mitochondrial lipid abnormality and electron transport chain impairment in mice lacking alpha-synuclein. *Mol. Cell. Biol.* 25 (22), 10190–10201. doi:10.1128/MCB.25.22.10190-10201.2005

Ellis, R. J. (1996). Revisiting the anfinsen cage. *Fold. Des.* 1 (1), R9–R15. doi:10.1016/S1359-0278(96)00004-1

Elsner, S., Simian, D., Iosefson, O., Marom, M., and Azem, A. (2009). The mitochondrial protein translocation motor: structural conservation between the human and yeast Tim14/Pam18-Tim16/Pam16 co-chaperones. *Int. J. Mol. Sci.* 10 (5), 2041–2053. doi:10.3390/ijms10052041

Endo, T., Mitsui, S., Nakai, M., and Roise, D. (1996). Binding of mitochondrial presequences to yeast cytosolic heat shock protein 70 depends on the amphiphilicity of the presequence. *J. Biol. Chem.* 271 (8), 4161–4167. doi:10.1074/jbc.271.8.4161

Engel, M. F. (2009). Membrane permeabilization by islet amyloid polypeptide. *Chem. Phys. Lipids* 160 (1), 1–10. doi:10.1016/j.chemphyslip.2009.03.008

Ericsson, M., von Saucken, V., Newman, A. J., Doehr, L., Hoesch, C., Kim, T. E., et al. (2021). Crowded organelles, lipid accumulation, and abnormal membrane tubulation in cellular models of enhanced α-synuclein membrane interaction. *Brain Res.* 1758, 147349. doi:10.1016/j.brainres.2021.147349

Esaki, M., Shimizu, H., Ono, T., Yamamoto, H., Kanamori, T., Nishikawa, S., et al. (2004). Mitochondrial protein import. Requirement of presequence elements and tom components for precursor binding to the TOM complex. *J. Biol. Chem.* 279 (44), 45701–45707. doi:10.1074/jbc.M404591200

Esfahanian, N., Knoblich, C. D., Bowman, G. A., and Rezvani, K. (2023). Mortalin: protein partners, biological impacts, pathological roles, and therapeutic opportunities. *Front. Cell. Dev. Biol.* 11, 1028519. doi:10.3389/fcell.2023.1028519

Falkevall, A., Alikhani, N., Bhushan, S., Pavlov, P. F., Busch, K., Johnson, K. A., et al. (2006). Degradation of the amyloid beta-protein by the novel mitochondrial peptidasome, PreP. *J. Biol. Chem.* 281 (39), 29096–29104. doi:10.1074/jbc.M602532200

Fan, A. C., Bhangoo, M. K., and Young, J. C. (2006). Hsp90 functions in the targeting and outer membrane translocation steps of Tom70-mediated mitochondrial import. *J. Biol. Chem.* 281 (44), 33313–33324. doi:10.1074/jbc.M605250200

Fang, D., Wang, Y., Zhang, Z., Du, H., Yan, S., Sun, Q., et al. (2015). Increased neuronal PreP activity reduces Aβ accumulation, attenuates neuroinflammation and improves mitochondrial and synaptic function in Alzheimer disease's mouse model. *Hum. Mol. Genet.* 24 (18), 5198–5210. doi:10.1093/hmg/ddv241

Fantini, J., Carlus, D., and Yahi, N. (2011). The fusogenic tilted peptide (67-78) of alpha-synuclein is a cholesterol binding domain. *Biochim. Biophys. Acta* 1808 (10), 2343–2351. doi:10.1016/j.bbamem.2011.06.017

Farmer, B. C., Kluemper, J., and Johnson, L. A. (2019). Apolipoprotein E4 alters astrocyte fatty acid metabolism and lipid droplet formation. *Cells* 8 (2), 182. doi:10.3390/cells8020182

Fauchere, J., and Pliska, V. (1983). Hydrophobic parameters II of amino acid side-chains from the partitioning of N-acetyl-amino acid amides. *Eur. J. Med. Chem.* 18, 369–375.

Faustini, G., Bono, F., Valerio, A., Pizzi, M., Spano, P., and Bellucci, A. (2017). Mitochondria and alpha-synuclein: friends or foes in the pathogenesis of Parkinson's disease? *Genes. (Basel)* 8 (12), 377. doi:10.3390/genes8120377

Fauvet, B., Mbefo, M. K., Fares, M. B., Desobry, C., Michael, S., Ardah, M. T., et al. (2012). α-Synuclein in central nervous system and from erythrocytes, mammalian cells, and *Escherichia coli* exists predominantly as disordered monomer. *J. Biol. Chem.* 287 (19), 15345–15364. doi:10.1074/jbc.M111.318949

Fayyad, M., Erskine, D., Majbour, N. K., Vaikath, N. N., Ghanem, S. S., Sudhakaran, I. P., et al. (2020). Investigating the presence of doubly phosphorylated alpha-synuclein at tyrosine 125 and serine 129 in idiopathic Lewy body diseases. *Brain Pathol.* 30 (4), 831–843. doi:10.1111/bpa.12845

Fazal, F. M., Han, S., Parker, K. R., Kaewsapsak, P., Xu, J., Boettiger, A. N., et al. (2019). Atlas of subcellular RNA localization revealed by APEX-seq. *Cell.* 178 (2), 473–490. doi:10.1016/j.cell.2019.05.027

Fernandes, T., Resende, R., Silva, D. F., Marques, A. P., Santos, A. E., Cardoso, S. M., et al. (2021). Structural and functional alterations in mitochondria-associated membranes (MAMs) and in mitochondria activate stress response mechanisms in an *in vitro* model of alzheimer's disease. *Biomedicines* 9 (8), 881. doi:10.3390/biomedicines9080881

Ferrone, F. A., Hofrichter, J., and Eaton, W. A. (1985). Kinetics of sickle hemoglobin polymerization. II. A double nucleation mechanism. *J. Mol. Biol.* 183 (4), 611–631. doi:10.1016/0022-2836(85)90175-5

Fielden, L. F., Busch, J. D., Merkt, S. G., Ganesan, I., Steiert, C., Hasselblatt, H. B., et al. (2023). Central role of Tim17 in mitochondrial presequence protein translocation. *Nature* 621, 627–634. doi:10.1038/s41586-023-06477-8

Flagmeier, P., Meisl, G., Vendruscolo, M., Knowles, T. P., Dobson, C. M., Buell, A. K., et al. (2016). Mutations associated with familial Parkinson's disease alter the initiation and amplification steps of alpha-synuclein aggregation. *Proc. Natl. Acad. Sci. U. S. A.* 113 (37), 10328–10333. doi:10.1073/pnas.1604645113

Fortin, D. L., Nemani, V. M., Voglmaier, S. M., Anthony, M. D., Ryan, T. A., and Edwards, R. H. (2005). Neural activity controls the synaptic accumulation of alpha-synuclein. *J. Neurosci.* 25 (47), 10913–10921. doi:10.1523/JNEUROSCI.2922-05.2005

Fortin, D. L., Troyer, M. D., Nakamura, K., Kubo, S., Anthony, M. D., and Edwards, R. H. (2004). Lipid rafts mediate the synaptic localization of alpha-synuclein. *J. Neurosci.* 24 (30), 6715–6723. doi:10.1523/JNEUROSCI.1594-04.2004

Friedrich, R. P., Tepper, K., Ronicke, R., Soom, M., Westermann, M., Reymann, K., et al. (2010). Mechanism of amyloid plaque formation suggests an intracellular basis of Abeta pathogenicity. *Proc. Natl. Acad. Sci. U. S. A.* 107 (5), 1942–1947. doi:10.1073/pnas.0904532106

Fu, H., Hardy, J., and Duff, K. E. (2018). Selective vulnerability in neurodegenerative diseases. *Nat. Neurosci.* 21 (10), 1350–1358. doi:10.1038/s41593-018-0221-2

Fu, Z., Liu, F., Liu, C., Jin, B., Jiang, Y., Tang, M., et al. (2019). Mutant huntingtin inhibits the mitochondrial unfolded protein response by impairing ABCB10 mRNA stability. *Biochim. Biophys. Acta Mol. Basis Dis.* 1865 (6), 1428–1435. doi:10.1016/j.bbadis.2019.02.015

Gabriel, K., Egan, B., and Lithgow, T. (2003). Tom40, the import channel of the mitochondrial outer membrane, plays an active role in sorting imported proteins. *EMBO J.* 22 (10), 2380–2386. doi:10.1093/emboj/cdg229

Gafni, J., and Ellerby, L. M. (2002). Calpain activation in Huntington's disease. *J. Neurosci.* 22 (12), 4842–4849. doi:10.1523/JNEUROSCI.22-12-04842.2002

Gallego Villarejo, L., Bachmann, L., Marks, D., Brachthauser, M., Geidies, A., and Muller, T. (2022). Role of intracellular amyloid beta as pathway modulator, biomarker, and therapy target. *Int. J. Mol. Sci.* 23 (9), 4656. doi:10.3390/ijms23094656

Gamerdinger, M., Kobayashi, K., Wallisch, A., Kreft, S. G., Sailer, C., Schlomer, R., et al. (2019). Early scanning of nascent polypeptides inside the ribosomal tunnel by NAC. *Mol. Cell.* 75 (5), 996–1006. doi:10.1016/j.molcel.2019.06.030

Gao, F., Yang, J., Wang, D., Li, C., Fu, Y., Wang, H., et al. (2017). Mitophagy in Parkinson's disease: pathogenic and therapeutic implications. *Front. Neurol.* 8, 527. doi:10.3389/fneur.2017.00527

Gartner, F., Bomer, U., Guiard, B., and Pfanner, N. (1995). The sorting signal of cytochrome b2 promotes early divergence from the general mitochondrial import pathway and restricts the unfoldase activity of matrix Hsp70. *EMBO J.* 14 (23), 6043–6057. doi:10.1002/j.1460-2075.1995.tb00293.x

Gauba, E., Chen, H., Guo, L., and Du, H. (2019). Cyclophilin D deficiency attenuates mitochondrial F1Fo ATP synthase dysfunction via OSCP in Alzheimer's disease. *Neurobiol. Dis.* 121, 138–147. doi:10.1016/j.nbd.2018.09.020

Gautier, R., Douguet, D., Antonny, B., and Drin, G. (2008). HELIQUEST: a web server to screen sequences with specific alpha-helical properties. *Bioinformatics* 24 (18), 2101–2102. doi:10.1093/bioinformatics/btn392

Ge, P., Dawson, V. L., and Dawson, T. M. (2020). PINK1 and Parkin mitochondrial quality control: a source of regional vulnerability in Parkinson's disease. *Mol. Neurodegener.* 15 (1), 20. doi:10.1186/s13024-020-00367-7

Geissler, A., Chacinska, A., Truscott, K. N., Wiedemann, N., Brandner, K., Sickmann, A., et al. (2002). The mitochondrial presequence translocase: an essential role of Tim50 in directing preproteins to the import channel. *Cell.* 111 (4), 507–518. doi:10.1016/s0092-8674(02)01073-5

Genge, M. G., and Mokranjac, D. (2021). Coordinated translocation of presequence-containing precursor proteins across two mitochondrial membranes: knowns and unknowns of how TOM and TIM23 complexes cooperate with each other. *Front. Physiol.* 12, 806426. doi:10.3389/fphys.2021.806426

George, R., Beddoe, T., Landl, K., and Lithgow, T. (1998). The yeast nascent polypeptide-associated complex initiates protein targeting to mitochondria *in vivo*. *Proc. Natl. Acad. Sci. U. S. A.* 95 (5), 2296–2301. doi:10.1073/pnas.95.5.2296

George, R., Walsh, P., Beddoe, T., and Lithgow, T. (2002). The nascent polypeptide-associated complex (NAC) promotes interaction of ribosomes with the mitochondrial surface *in vivo*. *FEBS Lett.* 516 (1-3), 213–216. doi:10.1016/s0014-5793(02)02528-0

Georgieva, E. R., Ramlall, T. F., Borbat, P. P., Freed, J. H., and Eliezer, D. (2008). Membrane-bound alpha-synuclein forms an extended helix: long-distance pulsed ESR measurements using vesicles, bicelles, and rodlike micelles. *J. Am. Chem. Soc.* 130 (39), 12856–12857. doi:10.1021/ja804517m

Gevorkyan-Airapetov, L., Zohary, K., Popov-Celeketic, D., Mapa, K., Hell, K., Neupert, W., et al. (2009). Interaction of Tim23 with Tim50 Is essential for protein translocation by the mitochondrial TIM23 complex. *J. Biol. Chem.* 284 (8), 4865–4872. doi:10.1074/jbc.M807041200

Giacomello, M., Oliveros, J. C., Naranjo, J. R., and Carafoli, E. (2013). Neuronal Ca(2+) dyshomeostasis in Huntington disease. *Prion* 7 (1), 76–84. doi:10.4161/pri.23581

Gilmozzi, V., Gentile, G., Castelo Rueda, M. P., Hicks, A. A., Pramstaller, P. P., Zanon, A., et al. (2020). Interaction of alpha-synuclein with lipids: mitochondrial cardiolipin as a critical player in the pathogenesis of Parkinson's disease. *Front. Neurosci.* 14, 578993. doi:10.3389/fnins.2020.578993

Giordano, F. (2018). Non-vesicular lipid trafficking at the endoplasmic reticulum-mitochondria interface. *Biochem. Soc. Trans.* 46 (2), 437–452. doi:10.1042/BST20160185

Gleichman, A. J., and Carmichael, S. T. (2020). Glia in neurodegeneration: drivers of disease or along for the ride? *Neurobiol. Dis.* 142, 104957. doi:10.1016/j.nbd.2020.104957

Glick, B. S., Brandt, A., Cunningham, K., Muller, S., Hallberg, R. L., and Schatz, G. (1992). Cytochromes c1 and b2 are sorted to the intermembrane space of yeast mitochondria by a stop-transfer mechanism. *Cell.* 69 (5), 809–822. doi:10.1016/0092-8674(92)90292-k

Gold, V. A., Chroscicki, P., Bragoszewski, P., and Chacinska, A. (2017). Visualization of cytosolic ribosomes on the surface of mitochondria by electron cryo-tomography. *EMBO Rep.* 18 (10), 1786–1800. doi:10.15252/embr.201744261

Gold, V. A., Ieva, R., Walter, A., Pfanner, N., van der Laan, M., and Kuhlbrandt, W. (2014). Visualizing active membrane protein complexes by electron cryotomography. *Nat. Commun.* 5, 4129. doi:10.1038/ncomms5129

Goldberg, J., Currais, A., Ates, G., Huang, L., Shokhirev, M., Maher, P., et al. (2020). Targeting of intracellular Ca(2+) stores as a therapeutic strategy against age-related neurotoxicities. *NPJ Aging Mech. Dis.* 6, 10. doi:10.1038/s41514-020-00048-1

Goldberg, J., Currais, A., Prior, M., Fischer, W., Chiruta, C., Ratliff, E., et al. (2018). The mitochondrial ATP synthase is a shared drug target for aging and dementia. *Aging Cell.* 17 (2), e12715. doi:10.1111/acel.12715

Goldberg, Y. P., Nicholson, D. W., Rasper, D. M., Kalchman, M. A., Koide, H. B., Graham, R. K., et al. (1996). Cleavage of huntingtin by apopain, a proapoptotic cysteine protease, is modulated by the polyglutamine tract. *Nat. Genet.* 13 (4), 442–449. doi:10.1038/ng0896-442

Golovko, M. Y., Faergeman, N. J., Cole, N. B., Castagnet, P. I., Nussbaum, R. L., and Murphy, E. J. (2005). Alpha-synuclein gene deletion decreases brain palmitate uptake and alters the palmitate metabolism in the absence of alpha-synuclein palmitate binding. *Biochemistry* 44 (23), 8251–8259. doi:10.1021/bi0502137

Golovko, M. Y., Rosenberger, T. A., Faergeman, N. J., Feddersen, S., Cole, N. B., Pribill, I., et al. (2006). Acyl-CoA synthetase activity links wild-type but not mutant alpha-synuclein to brain arachidonate metabolism. *Biochemistry* 45 (22), 6956–6966. doi:10.1021/bi0600289

Gomez-Fabra Gala, M., and Vogtle, F. N. (2021). Mitochondrial proteases in human diseases. *FEBS Lett.* 595 (8), 1205–1222. doi:10.1002/1873-3468.14039

Goswami, A. V., Chittoor, B., and D'Silva, P. (2010). Understanding the functional interplay between mammalian mitochondrial Hsp70 chaperone machine components. *J. Biol. Chem.* 285 (25), 19472–19482. doi:10.1074/jbc.M110.105957

Gottlieb, L., Guo, L., Shorter, J., and Marmorstein, R. (2021). N-alpha-acetylation of Huntingtin protein increases its propensity to aggregate. *J. Biol. Chem.* 297 (6), 101363. doi:10.1016/j.jbc.2021.101363

Goure, W. F., Krafft, G. A., Jerecic, J., and Hefti, F. (2014). Targeting the proper amyloid-beta neuronal toxins: a path forward for Alzheimer's disease immunotherapeutics. *Alzheimers Res. Ther.* 6 (4), 42. doi:10.1186/alzrt272

Graham, R. K., Deng, Y., Slow, E. J., Haigh, B., Bissada, N., Lu, G., et al. (2006). Cleavage at the caspase-6 site is required for neuronal dysfunction and degeneration due to mutant huntingtin. *Cell.* 125 (6), 1179–1191. doi:10.1016/j.cell.2006.04.026

Greco, T. M., Secker, C., Ramos, E. S., Federspiel, J. D., Liu, J. P., Perez, A. M., et al. (2022). Dynamics of huntingtin protein interactions in the striatum identifies candidate modifiers of Huntington disease. *Cell. Syst.* 13 (4), 304–320.e5. doi:10.1016/j.cels.2022.01.005

Grey, M., Linse, S., Nilsson, H., Brundin, P., and Sparr, E. (2011). Membrane interaction of α-synuclein in different aggregation states. *J. Park. Dis.* 1 (4), 359–371. doi:10.3233/JPD-2011-11067

Gruhler, A., Arnold, I., Seytter, T., Guiard, B., Schwarz, E., Neupert, W., et al. (1997). N-terminal hydrophobic sorting signals of preproteins confer mitochondrial hsp70 independence for import into mitochondria. *J. Biol. Chem.* 272 (28), 17410–17415. doi:10.1074/jbc.272.28.17410

Guan, Z., Yan, L., Wang, Q., Qi, L., Hong, S., Gong, Z., et al. (2021). Structural insights into assembly of human mitochondrial translocase TOM complex. *Cell. Discov.* 7 (1), 22. doi:10.1038/s41421-021-00252-7

Guardia-Laguarta, C., Area-Gomez, E., Rub, C., Liu, Y., Magrane, J., Becker, D., et al. (2014). α-Synuclein is localized to mitochondria-associated ER membranes. *J. Neurosci.* 34 (1), 249–259. doi:10.1523/JNEUROSCI.2507-13.2014

Guardia-Laguarta, C., Area-Gomez, E., Schon, E. A., and Przedborski, S. (2015). A new role for alpha-synuclein in Parkinson's disease: alteration of ER-mitochondrial communication. *Mov. Disord.* 30 (8), 1026–1033. doi:10.1002/mds.26239

Gui, Y. X., Wang, X. Y., Kang, W. Y., Zhang, Y. J., Zhang, Y., Zhou, Y., et al. (2012). Extracellular signal-regulated kinase is involved in alpha-synuclein-induced mitochondrial dynamic disorders by regulating dynamin-like protein 1. *Neurobiol. Aging* 33 (12), 2841–2854. doi:10.1016/j.neurobiolaging.2012.02.001

Gunsel, U., Paz, E., Gupta, R., Mathes, I., Azem, A., and Mokranjac, D. (2020). InVivo dissection of the intrinsically disordered receptor domain of Tim23. *J. Mol. Biol.* 432 (10), 3326–3337. doi:10.1016/j.jmb.2020.03.031

Guo, Q., Bin, H., Cheng, J., Seefelder, M., Engler, T., Pfeifer, G., et al. (2018). The cryo-electron microscopy structure of huntingtin. *Nature* 555 (7694), 117–120. doi:10.1038/nature25502

Guo, W., Stoklund Dittlau, K., and Van Den Bosch, L. (2020). Axonal transport defects and neurodegeneration: molecular mechanisms and therapeutic implications. *Semin. Cell. Dev. Biol.* 99, 133–150. doi:10.1016/j.semcdb.2019.07.010

Guo, X., Sun, X., Hu, D., Wang, Y. J., Fujioka, H., Vyas, R., et al. (2016). VCP recruitment to mitochondria causes mitophagy impairment and neurodegeneration in models of Huntington's disease. *Nat. Commun.* 7, 12646. doi:10.1038/ncomms12646

Guo, Y., Cheong, N., Zhang, Z., De Rose, R., Deng, Y., Farber, S. A., et al. (2004). Tim50, a component of the mitochondrial translocator, regulates mitochondrial integrity and cell death. *J. Biol. Chem.* 279 (23), 24813–24825. doi:10.1074/jbc.M402049200

Gurlo, T., Ryazantsev, S., Huang, C. J., Yeh, M. W., Reber, H. A., Hines, O. J., et al. (2010). Evidence for proteotoxicity in beta cells in type 2 diabetes: toxic islet amyloid polypeptide oligomers form intracellularly in the secretory pathway. *Am. J. Pathol.* 176 (2), 861–869. doi:10.2353/ajpath.2010.090532

Haass, C., and Selkoe, D. J. (2007). Soluble protein oligomers in neurodegeneration: lessons from the Alzheimer's amyloid beta-peptide. *Nat. Rev. Mol. Cell. Biol.* 8 (2), 101–112. doi:10.1038/nrm2101

Hackam, A. S., Singaraja, R., Wellington, C. L., Metzler, M., McCutcheon, K., Zhang, T., et al. (1998). The influence of huntingtin protein size on nuclear localization and cellular toxicity. *J. Cell. Biol.* 141 (5), 1097–1105. doi:10.1083/jcb.141.5.1097

Halliwell, B. (1992). Reactive oxygen species and the central nervous system. *J. Neurochem.* 59 (5), 1609–1623. doi:10.1111/j.1471-4159.1992.tb10990.x

Hamilton, J., Brustovetsky, T., Khanna, R., and Brustovetsky, N. (2020). Mutant huntingtin does not cross the mitochondrial outer membrane. *Hum. Mol. Genet.* 29 (17), 2962–2975. doi:10.1093/hmg/ddaa185

Hansen, K. G., Boos, F., and Herrmann, J. M. (2018). Accessory signals in protein translocation. *Aging (Albany NY)* 10 (4), 530–531. doi:10.18632/aging.101435

Hansson Petersen, C. A., Alikhani, N., Behbahani, H., Wiehager, B., Pavlov, P. F., Alafuzoff, I., et al. (2008). The amyloid beta-peptide is imported into mitochondria via the TOM import machinery and localized to mitochondrial cristae. *Proc. Natl. Acad. Sci. U. S. A.* 105 (35), 13145–13150. doi:10.1073/pnas.0806192105

Hardy, J. A., and Higgins, G. A. (1992). Alzheimer's disease: the amyloid cascade hypothesis. *Science* 256 (5054), 184–185. doi:10.1126/science.1566067

Havalova, H., Ondrovicova, G., Keresztesova, B., Bauer, J. A., Pevala, V., Kutejova, E., et al. (2021). Mitochondrial HSP70 chaperone system-the influence of post-translational modifications and involvement in human diseases. *Int. J. Mol. Sci.* 22 (15), 8077. doi:10.3390/ijms22158077

He, S., Wang, F., Yung, K. K. L., Zhang, S., and Qu, S. (2021). Effects of α-synuclein-associated post-translational modifications in Parkinson's disease. *ACS Chem. Neurosci.* 12 (7), 1061–1071. doi:10.1021/acschemneuro.1c00028

Hernandez-Zimbron, L. F., Luna-Munoz, J., Mena, R., Vazquez-Ramirez, R., Kubli-Garfias, C., Cribbs, D. H., et al. (2012). Amyloid-beta peptide binds to cytochrome C oxidase subunit 1. *PLoS One* 7 (8), e42344. doi:10.1371/journal.pone.0042344

Herrup, K. (2015). The case for rejecting the amyloid cascade hypothesis. *Nat. Neurosci.* 18 (6), 794–799. doi:10.1038/nn.4017

Heydari, A. R., Takahashi, R., Gutsmann, A., You, S., and Richardson, A. (1994). Hsp70 and aging. *Experientia* 50 (11-12), 1092–1098. doi:10.1007/BF01923466

Hillen, H. (2019). The beta amyloid dysfunction (BAD) hypothesis for Alzheimer's disease. *Front. Neurosci.* 13, 1154. doi:10.3389/fnins.2019.01154

Hines, V., Brandt, A., Griffiths, G., Horstmann, H., Brutsch, H., and Schatz, G. (1990). Protein import into yeast mitochondria is accelerated by the outer membrane protein MAS70. *EMBO J.* 9 (10), 3191–3200. doi:10.1002/j.1460-2075.1990.tb07517.x

Hines, V., and Schatz, G. (1993). Precursor binding to yeast mitochondria. A general role for the outer membrane protein Mas70p. *J. Biol. Chem.* 268 (1), 449–454. doi:10.1016/s0021-9258(18)54172-7

Hirai, K., Aliev, G., Nunomura, A., Fujioka, H., Russell, R. L., Atwood, C. S., et al. (2001). Mitochondrial abnormalities in Alzheimer's disease. *J. Neurosci.* 21 (9), 3017–3023. doi:10.1523/JNEUROSCI.21-09-03017.2001

Hoe, H. S., Lee, H. K., and Pak, D. T. (2012). The upside of APP at synapses. *CNS Neurosci. Ther.* 18 (1), 47–56. doi:10.1111/j.1755-5949.2010.00221.x

Hoffner, G., and Djian, P. (2014). Monomeric, oligomeric and polymeric proteins in huntington disease and other diseases of polyglutamine expansion. *Brain Sci.* 4 (1), 91–122. doi:10.3390/brainsci4010091

Hoffner, G., Island, M. L., and Djian, P. (2005). Purification of neuronal inclusions of patients with Huntington's disease reveals a broad range of N-terminal fragments of expanded huntingtin and insoluble polymers. *J. Neurochem.* 95 (1), 125–136. doi:10.1111/j.1471-4159.2005.03348.x

Honlinger, A., Kubrich, M., Moczko, M., Gartner, F., Mallet, L., Bussereau, F., et al. (1995). The mitochondrial receptor complex: mom22 is essential for cell viability and directly interacts with preproteins. *Mol. Cell. Biol.* 15 (6), 3382–3389. doi:10.1128/mcb.15.6.3382

Horst, M., Oppliger, W., Rospert, S., Schonfeld, H. J., Schatz, G., and Azem, A. (1997). Sequential action of two hsp70 complexes during protein import into mitochondria. *EMBO J.* 16 (8), 1842–1849. doi:10.1093/emboj/16.8.1842

Hoyt, D. W., Cyr, D. M., Gierasch, L. M., and Douglas, M. G. (1991). Interaction of peptides corresponding to mitochondrial presequences with membranes. *J. Biol. Chem.* 266 (32), 21693–21699. doi:10.1016/s0021-9258(18)54692-5

Hu, W., Wang, Z., and Zheng, H. (2018). Mitochondrial accumulation of amyloid β (Aβ) peptides requires TOMM22 as a main Aβ receptor in yeast. *J. Biol. Chem.* 293 (33), 12681–12689. doi:10.1074/jbc.RA118.002713

Hu, Z. W., Vugmeyster, L., Au, D. F., Ostrovsky, D., Sun, Y., and Qiang, W. (2019). Molecular structure of an N-terminal phosphorylated beta-amyloid fibril. *Proc. Natl. Acad. Sci. U. S. A.* 116 (23), 11253–11258. doi:10.1073/pnas.1818530116

Huang, Y., and Mahley, R. W. (2014). Apolipoprotein E: structure and function in lipid metabolism, neurobiology, and Alzheimer's diseases. *Neurobiol. Dis.* 72 Pt, 3–12. doi:10.1016/j.nbd.2014.08.025

Ieva, R., Schrempp, S. G., Opalinski, L., Wollweber, F., Hoss, P., Heisswolf, A. K., et al. (2014). Mgr2 functions as lateral gatekeeper for preprotein sorting in the mitochondrial inner membrane. *Mol. Cell.* 56 (5), 641–652. doi:10.1016/j.molcel.2014.10.010

Ikon, N., and Ryan, R. O. (2017). Cardiolipin and mitochondrial cristae organization. *Biochim. Biophys. Acta Biomembr.* 1859 (6), 1156–1163. doi:10.1016/j.bbamem.2017.03.013

Iosefson, O., Sharon, S., Goloubinoff, P., and Azem, A. (2012). Reactivation of protein aggregates by mortalin and Tid1-the human mitochondrial Hsp70 chaperone system. *Cell. Stress Chaperones* 17 (1), 57–66. doi:10.1007/s12192-011-0285-3

Jacobsen, K. T., and Iverfeldt, K. (2009). Amyloid precursor protein and its homologues: a family of proteolysis-dependent receptors. *Cell. Mol. Life Sci.* 66 (14), 2299–2318. doi:10.1007/s00018-009-0020-8

Jao, C. C., Hegde, B. G., Chen, J., Haworth, I. S., and Langen, R. (2008). Structure of membrane-bound alpha-synuclein from site-directed spin labeling and computational refinement. *Proc. Natl. Acad. Sci. U. S. A.* 105 (50), 19666–19671. doi:10.1073/pnas.0807826105

Jenco, J. M., Rawlingson, A., Daniels, B., and Morris, A. J. (1998). Regulation of phospholipase D2: selective inhibition of mammalian phospholipase D isoenzymes by alpha- and beta-synucleins. *Biochemistry* 37 (14), 4901–4909. doi:10.1021/bi972776r

Jiang, X., Jiang, H., Shen, Z., and Wang, X. (2014). Activation of mitochondrial protease OMA1 by Bax and Bak promotes cytochrome c release during apoptosis. *Proc. Natl. Acad. Sci. U. S. A.* 111 (41), 14782–14787. doi:10.1073/pnas.1417253111

Jin, Y. N., and Johnson, G. V. (2010). The interrelationship between mitochondrial dysfunction and transcriptional dysregulation in Huntington disease. *J. Bioenerg. Biomembr.* 42 (3), 199–205. doi:10.1007/s10863-010-9286-7

Jo, E., Fuller, N., Rand, R. P., St George-Hyslop, P., and Fraser, P. E. (2002). Defective membrane interactions of familial Parkinson's disease mutant A30P alpha-synuclein. *J. Mol. Biol.* 315 (4), 799–807. doi:10.1006/jmbi.2001.5269

Jores, T., Lawatscheck, J., Beke, V., Franz-Wachtel, M., Yunoki, K., Fitzgerald, J. C., et al. (2018). Cytosolic Hsp70 and Hsp40 chaperones enable the biogenesis of mitochondrial beta-barrel proteins. *J. Cell. Biol.* 217 (9), 3091–3108. doi:10.1083/jcb.201712029

Joshi, A., Ito, T., Picard, D., and Neckers, L. (2022). The mitochondrial HSP90 paralog TRAP1: structural dynamics, interactome, role in metabolic regulation, and inhibitors. *Biomolecules* 12 (7), 880. doi:10.3390/biom12070880

Jurcau, A., and Jurcau, C. M. (2023). Mitochondria in Huntington's disease: implications in pathogenesis and mitochondrial-targeted therapeutic strategies. *Neural Regen. Res.* 18 (7), 1472–1477. doi:10.4103/1673-5374.360289

Jurcau, A., and Jurcau, M. C. (2022). Therapeutic strategies in huntington's disease: from genetic defect to gene therapy. *Biomedicines* 10 (6), 1895. doi:10.3390/biomedicines10081895

Kakeshpour, T., Ramanujam, V., Barnes, C. A., Shen, Y., Ying, J., and Bax, A. (2021). A lowly populated, transient β-sheet structure in monomeric $A\beta^{1-42}$ identified by multinuclear NMR of chemical denaturation. *Biophys. Chem.* 270, 106531. doi:10.1016/j.bpc.2020.106531

Kamp, F., Exner, N., Lutz, A. K., Wender, N., Hegermann, J., Brunner, B., et al. (2010). Inhibition of mitochondrial fusion by alpha-synuclein is rescued by PINK1, Parkin and DJ-1. *EMBO J.* 29 (20), 3571–3589. doi:10.1038/emboj.2010.223

Kampinga, H. H., and Craig, E. A. (2010). The HSP70 chaperone machinery: J proteins as drivers of functional specificity. *Nat. Rev. Mol. Cell. Biol.* 11 (8), 579–592. doi:10.1038/nrm2941

Kanamori, T., Nishikawa, S., Nakai, M., Shin, I., Schultz, P. G., and Endo, T. (1999). Uncoupling of transfer of the presequence and unfolding of the mature domain in precursor translocation across the mitochondrial outer membrane. *Proc. Natl. Acad. Sci. U. S. A.* 96 (7), 3634–3639. doi:10.1073/pnas.96.7.3634

Kann, O., and Kovacs, R. (2007). Mitochondria and neuronal activity. *Am. J. Physiol. Cell. Physiol.* 292 (2), C641–C657. doi:10.1152/ajpcell.00222.2006

Karagoz, G. E., and Rudiger, S. G. (2015). Hsp90 interaction with clients. *Trends Biochem. Sci.* 40 (2), 117–125. doi:10.1016/j.tibs.2014.12.002

Karniely, S., and Pines, O. (2005). Single translation-dual destination: mechanisms of dual protein targeting in eukaryotes. *EMBO Rep.* 6 (5), 420–425. doi:10.1038/sj.embor.7400394

Ke, P. C., Zhou, R., Serpell, L. C., Riek, R., Knowles, T. P. J., Lashuel, H. A., et al. (2020). Half a century of amyloids: past, present and future. *Chem. Soc. Rev.* 49 (15), 5473–5509. doi:10.1039/c9cs00199a

Kegel-Gleason, K. B. (2013). Huntingtin interactions with membrane phospholipids: strategic targets for therapeutic intervention? *J. Huntingt. Dis.* 2 (3), 239–250. doi:10.3233/JHD-130068

Kepchia, D., Currais, A., Dargusch, R., Finley, K., Schubert, D., and Maher, P. (2021). Geroprotective effects of Alzheimer's disease drug candidates. *Aging (Albany NY)* 13 (3), 3269–3289. doi:10.18632/aging.202631

Kepchia, D., Huang, L., Currais, A., Liang, Z., Fischer, W., and Maher, P. (2022). The Alzheimer's disease drug candidate J147 decreases blood plasma fatty acid levels via modulation of AMPK/ACC1 signaling in the liver. *Biomed. Pharmacother.* 147, 112648. doi:10.1016/j.biopha.2022.112648

Khalil, B., El Fissi, N., Aouane, A., Cabirol-Pol, M. J., Rival, T., and Lievens, J. C. (2015). PINK1-induced mitophagy promotes neuroprotection in Huntington's disease. *Cell. Death Dis.* 6 (1), e1617. doi:10.1038/cddis.2014.581

Kiebler, M., Keil, P., Schneider, H., van der Klei, I. J., Pfanner, N., and Neupert, W. (1993). The mitochondrial receptor complex: a central role of MOM22 in mediating preprotein transfer from receptors to the general insertion pore. *Cell.* 74 (3), 483–492. doi:10.1016/0092-8674(93)80050-o

Kiechle, T., Dedeoglu, A., Kubilus, J., Kowall, N. W., Beal, M. F., Friedlander, R. M., et al. (2002). Cytochrome C and caspase-9 expression in Huntington's disease. *Neuromolecular Med.* 1 (3), 183–195. doi:10.1385/NMM:1:3:183

Kim, M. W., Chelliah, Y., Kim, S. W., Otwinowski, Z., and Bezprozvanny, I. (2009). Secondary structure of Huntingtin amino-terminal region. *Structure* 17 (9), 1205–1212. doi:10.1016/j.str.2009.08.002

Kim, Y. J., Yi, Y., Sapp, E., Wang, Y., Cuiffo, B., Kegel, K. B., et al. (2001). Caspase 3-cleaved N-terminal fragments of wild-type and mutant huntingtin are present in normal and Huntington's disease brains, associate with membranes, and undergo calpain-dependent proteolysis. *Proc. Natl. Acad. Sci. U. S. A.* 98 (22), 12784–12789. doi:10.1073/pnas.221451398

Klaips, C. L., Jayaraj, G. G., and Hartl, F. U. (2018). Pathways of cellular proteostasis in aging and disease. *J. Cell. Biol.* 217 (1), 51–63. doi:10.1083/jcb.201709072

Klein, C., and Westenberger, A. (2012). Genetics of Parkinson's disease. *Cold Spring Harb. Perspect. Med.* 2 (1), a008888. doi:10.1101/cshperspect.a008888

Klivenyi, P., Starkov, A. A., Calingasan, N. Y., Gardian, G., Browne, S. E., Yang, L., et al. (2004). Mice deficient in dihydrolipoamide dehydrogenase show increased vulnerability to MPTP, malonate and 3-nitropropionic acid neurotoxicity. *J. Neurochem.* 88 (6), 1352–1360. doi:10.1046/j.1471-4159.2003.02263.x

Knopman, D. S., Amieva, H., Petersen, R. C., Chetelat, G., Holtzman, D. M., Hyman, B. T., et al. (2021). Alzheimer disease. *Nat. Rev. Dis. Prim.* 7 (1), 33. doi:10.1038/s41572-021-00269-y

Koistinaho, M., Lin, S., Wu, X., Esterman, M., Koger, D., Hanson, J., et al. (2004). Apolipoprotein E promotes astrocyte colocalization and degradation of deposited amyloid-beta peptides. *Nat. Med.* 10 (7), 719–726. doi:10.1038/nm1058

Kolobkova, Y. A., Vigont, V. A., Shalygin, A. V., and Kaznacheyeva, E. V. (2017). Huntington's disease: calcium dyshomeostasis and pathology models. *Acta Naturae* 9 (2), 34–46. doi:10.32607/20758251-2017-9-2-34-46

Komiya, T., Rospert, S., Koehler, C., Looser, R., Schatz, G., and Mihara, K. (1998). Interaction of mitochondrial targeting signals with acidic receptor domains along the protein import pathway: evidence for the 'acid chain' hypothesis. *EMBO J.* 17 (14), 3886–3898. doi:10.1093/emboj/17.14.3886

Kronidou, N. G., Oppliger, W., Bolliger, L., Hannavy, K., Glick, B. S., Schatz, G., et al. (1994). Dynamic interaction between Isp45 and mitochondrial hsp70 in the protein import system of the yeast mitochondrial inner membrane. *Proc. Natl. Acad. Sci. U. S. A.* 91 (26), 12818–12822. doi:10.1073/pnas.91.26.12818

Kucukkose, C., Taskin, A. A., Marada, A., Brummer, T., Dennerlein, S., and Vogtle, F. N. (2021). Functional coupling of presequence processing and degradation in human mitochondria. *FEBS J.* 288 (2), 600–613. doi:10.1111/febs.15358

Kumar, V., Kim, S. H., and Bishayee, K. (2022). Dysfunctional glucose metabolism in alzheimer's disease onset and potential pharmacological interventions. *Int. J. Mol. Sci.* 23 (17), 9540. doi:10.3390/ijms23179540

Kunkele, K. P., Heins, S., Dembowski, M., Nargang, F. E., Benz, R., Thieffry, M., et al. (1998). The preprotein translocation channel of the outer membrane of mitochondria. *Cell.* 93 (6), 1009–1019. doi:10.1016/s0092-8674(00)81206-4

Kunova, N., Havalova, H., Ondrovicova, G., Stojkovicova, B., Bauer, J. A., Bauerova-Hlinkova, V., et al. (2022). Mitochondrial processing peptidases-structure, function and the role in human diseases. *Int. J. Mol. Sci.* 23 (3), 1297. doi:10.3390/ijms23031297

Kunze, M., and Berger, J. (2015). The similarity between N-terminal targeting signals for protein import into different organelles and its evolutionary relevance. *Front. Physiol.* 6, 259. doi:10.3389/fphys.2015.00259

Kuzniewska, B., Cysewski, D., Wasilewski, M., Sakowska, P., Milek, J., Kulinski, T. M., et al. (2020). Mitochondrial protein biogenesis in the synapse is supported by local translation. *EMBO Rep.* 21 (8), e48882. doi:10.15252/embr.201948882

Labbadia, J., and Morimoto, R. I. (2015). The biology of proteostasis in aging and disease. *Annu. Rev. Biochem.* 84, 435–464. doi:10.1146/annurev-biochem-060614-033955

Landles, C., Sathasivam, K., Weiss, A., Woodman, B., Moffitt, H., Finkbeiner, S., et al. (2010). Proteolysis of mutant huntingtin produces an exon 1 fragment that accumulates as an aggregated protein in neuronal nuclei in Huntington disease. *J. Biol. Chem.* 285 (12), 8808–8823. doi:10.1074/jbc.M109.075028

Lansbury, P. T., and Lashuel, H. A. (2006). A century-old debate on protein aggregation and neurodegeneration enters the clinic. *Nature* 443 (7113), 774–779. doi:10.1038/nature05290

Larson, M. E., and Lesné, S. E. (2012). Soluble Aβ oligomer production and toxicity. *J. Neurochem.* 120(1), 125–139. doi:10.1111/j.1471-4159.2011.07478.x

Lazar, A. N., Hanbouch, L., Boussicaut, L., Fourmaux, B., Daira, P., Millan, M. J., et al. (2022). Lipid dys-homeostasis contributes to APOE4-associated AD pathology. *Cells* 11 (22), 3616. doi:10.3390/cells11223616

Lazarov, O., Morfini, G. A., Lee, E. B., Farah, M. H., Szodorai, A., DeBoer, S. R., et al. (2005). Axonal transport, amyloid precursor protein, kinesin-1, and the processing apparatus: revisited. *J. Neurosci.* 25 (9), 2386–2395. doi:10.1523/JNEUROSCI.3089-04.2005

Leal, N. S., Dentoni, G., Schreiner, B., Naia, L., Piras, A., Graff, C., et al. (2020). Amyloid beta-peptide increases mitochondria-endoplasmic reticulum contact altering mitochondrial function and autophagosome formation in alzheimer's disease-related models. *Cells* 9 (12), 2552. doi:10.3390/cells9122552

Lee, S., Lee, H., Yoo, S., Ieva, R., van der Laan, M., von Heijne, G., et al. (2020). The Mgr2 subunit of the TIM23 complex regulates membrane insertion of marginal stop-transfer signals in the mitochondrial inner membrane. *FEBS Lett.* 594 (6), 1081–1087. doi:10.1002/1873-3468.13692

Lenkiewicz, A. M., Krakowczyk, M., and Bragoszewski, P. (2021). Cytosolic quality control of mitochondrial protein precursors-the early stages of the organelle biogenesis. *Int. J. Mol. Sci.* 23 (1), 7. doi:10.3390/ijms23010007

Lesnik, C., Cohen, Y., Atir-Lande, A., Schuldiner, M., and Arava, Y. (2014). OM14 is a mitochondrial receptor for cytosolic ribosomes that supports co-translational import into mitochondria. *Nat. Commun.* 5, 5711. doi:10.1038/ncomms6711

Li, N. S., Liang, W., Piccirilli, J. A., and Tang, W. J. (2019b). Reinvestigating the synthesis and efficacy of small benzimidazole derivatives as presequence protease enhancers. *Eur. J. Med. Chem.* 184, 111746. doi:10.1016/j.ejmech.2019.111746

Li, S. H., Schilling, G., Young, W. S., 3rd, Li, X. J., Margolis, R. L., Stine, O. C., et al. (1993). Huntington's disease gene (IT15) is widely expressed in human and rat tissues. *Neuron* 11 (5), 985–993. doi:10.1016/0896-6273(93)90127-d

Li, W. W., Yang, R., Guo, J. C., Ren, H. M., Zha, X. L., Cheng, J. S., et al. (2007). Localization of alpha-synuclein to mitochondria within midbrain of mice. *Neuroreport* 18 (15), 1543–1546. doi:10.1097/WNR.0b013e3282f03db4

Li, X. X., Tsoi, B., Li, Y. F., Kurihara, H., and He, R. R. (2015). Cardiolipin and its different properties in mitophagy and apoptosis. *J. Histochem Cytochem* 63 (5), 301–311. doi:10.1369/0022155415574818

Li, Y., Xue, Y., Xu, X., Wang, G., Liu, Y., Wu, H., et al. (2019a). A mitochondrial FUNDC1/HSC70 interaction organizes the proteostatic stress response at the risk of cell morbidity. *EMBO J.* 38 (3), e98786. doi:10.15252/embj.201798786

Li, Z., Cao, Y., Pei, H., Ma, L., Yang, Y., and Li, H. (2023). The contribution of mitochondria-associated endoplasmic reticulum membranes (MAMs) dysfunction in Alzheimer's disease and the potential countermeasure. *Front. Neurosci.* 17, 1158204. doi:10.3389/fnins.2023.1158204

Liang, W. S., Reiman, E. M., Valla, J., Dunckley, T., Beach, T. G., Grover, A., et al. (2008). Alzheimer's disease is associated with reduced expression of energy metabolism genes in posterior cingulate neurons. *Proc. Natl. Acad. Sci. U. S. A.* 105 (11), 4441–4446. doi:10.1073/pnas.0709259105

Liao, C. Y., Rikke, B. A., Johnson, T. E., Diaz, V., and Nelson, J. F. (2010). Genetic variation in the murine lifespan response to dietary restriction: from life extension to life shortening. *Aging Cell.* 9 (1), 92–95. doi:10.1111/j.1474-9726.2009.00533.x

Lieberman, A. P., Shakkottai, V. G., and Albin, R. L. (2019). Polyglutamine repeats in neurodegenerative diseases. *Annu. Rev. Pathol.* 14, 1–27. doi:10.1146/annurev-pathmechdis-012418-012857

Lin, H. K., Boatz, J. C., Krabbendam, I. E., Kodali, R., Hou, Z., Wetzel, R., et al. (2017). Fibril polymorphism affects immobilized non-amyloid flanking domains of huntingtin exon1 rather than its polyglutamine core. *Nat. Commun.* 8, 15462. doi:10.1038/ncomms15462

Lin, T., Tjernberg, L. O., and Schedin-Weiss, S. (2021). Neuronal trafficking of the amyloid precursor protein—what do we really know? *Biomed* 9 (7), 801. doi:10.3390/biomedicines9070801

Liu, J., Jiang, J., Qiu, J., Wang, L., Zhuo, J., Wang, B., et al. (2022). Urolithin A protects dopaminergic neurons in experimental models of Parkinson's disease by promoting mitochondrial biogenesis through the SIRT1/PGC-1α signaling pathway. *Food Funct.* 13 (1), 375–385. doi:10.1039/d1fo02534a

Liu, T., Zhang, T., Nicolas, M., Boussicault, L., Rice, H., Soldano, A., et al. (2021a). The amyloid precursor protein is a conserved Wnt receptor. *eLife* 10, e69199. doi:10.7554/eLife.69199

Liu, Y., Fu, H., Wu, Y., Nie, B., Liu, F., Wang, T., et al. (2021b). Elamipretide (SS-31) improves functional connectivity in Hippocampus and other related regions following prolonged neuroinflammation induced by lipopolysaccharide in aged rats. *Front. Aging Neurosci.* 13, 600484. doi:10.3389/fnagi.2021.600484

Longen, S., Woellhaf, M. W., Petrungaro, C., Riemer, J., and Herrmann, J. M. (2014). The disulfide relay of the intermembrane space oxidizes the ribosomal subunit mrp10 on its transit into the mitochondrial matrix. *Dev. Cell.* 28 (1), 30–42. doi:10.1016/j.devcel.2013.11.007

Lontay, B., Kiss, A., Virag, L., and Tar, K. (2020). How do post-translational modifications influence the pathomechanistic landscape of huntington's disease? A comprehensive review. *Int. J. Mol. Sci.* 21 (12), 4282. doi:10.3390/ijms21124282

Lopes, C., Ferreira, I. L., Maranga, C., Beatriz, M., Mota, S. I., Sereno, J., et al. (2022). Mitochondrial and redox modifications in early stages of Huntington's disease. *Redox Biol.* 56, 102424. doi:10.1016/j.redox.2022.102424

Lu, L., Zhang, C., Cai, Q., Lu, Q., Duan, C., Zhu, Y., et al. (2013). Voltage-dependent anion channel involved in the alpha-synuclein-induced dopaminergic neuron toxicity in rats. *Acta Biochim. Biophys. Sin. (Shanghai).* 45 (3), 170–178. doi:10.1093/abbs/gms114

Lu, Z. H., Chakraborty, G., Ledeen, R. W., Yahya, D., and Wu, G. (2004). N-Acetylaspartate synthase is bimodally expressed in microsomes and mitochondria of brain. *Brain Res. Mol. Brain Res.* 122 (1), 71–78. doi:10.1016/j.molbrainres.2003.12.002

Ludtmann, M. H., Angelova, P. R., Ninkina, N. N., Gandhi, S., Buchman, V. L., and Abramov, A. Y. (2016). Monomeric alpha-synuclein exerts a physiological role on brain ATP synthase. *J. Neurosci.* 36 (41), 10510–10521. doi:10.1523/JNEUROSCI.1659-16.2016

Ludtmann, M. H. R., Angelova, P. R., Horrocks, M. H., Choi, M. L., Rodrigues, M., Baev, A. Y., et al. (2018). α-synuclein oligomers interact with ATP synthase and open the permeability transition pore in Parkinson's disease. *Nat. Commun.* 9 (1), 2293. doi:10.1038/s41467-018-04422-2

Lunkes, A., Lindenberg, K. S., Ben-Haiem, L., Weber, C., Devys, D., Landwehrmeyer, G. B., et al. (2002). Proteases acting on mutant huntingtin generate cleaved products that differentially build up cytoplasmic and nuclear inclusions. *Mol. Cell.* 10 (2), 259–269. doi:10.1016/s1097-2765(02)00602-0

Lustbader, J. W., Cirilli, M., Lin, C., Xu, H. W., Takuma, K., Wang, N., et al. (2004). ABAD directly links Abeta to mitochondrial toxicity in Alzheimer's disease. *Science* 304 (5669), 448–452. doi:10.1126/science.1091230

Lytovchenko, O., Melin, J., Schulz, C., Kilisch, M., Hutu, D. P., and Rehling, P. (2013). Signal recognition initiates reorganization of the presequence translocase during protein import. *EMBO J.* 32 (6), 886–898. doi:10.1038/emboj.2013.23

MacDonald, M. E., Ambrose, C. M., Duyao, M. P., Myers, R. H., Lin, C., Srinidhi, L., et al. (1993). A novel gene containing a trinucleotide repeat that is expanded and unstable on Huntington's disease chromosomes. The Huntington's Disease Collaborative Research Group. *Cell.* 72 (6), 971–983. doi:10.1016/0092-8674(93)90585-e

Mager, F., Sokolova, L., Lintzel, J., Brutschy, B., and Nussberger, S. (2010). LILBID-mass spectrometry of the mitochondrial preprotein translocase TOM. *J. Phys. Condens Matter* 22 (45), 454132. doi:10.1088/0953-8984/22/45/454132

Mahley, R. W. (2016). Central nervous system lipoproteins: apoE and regulation of cholesterol metabolism. *Arterioscler. Thromb. Vasc. Biol.* 36 (7), 1305–1315. doi:10.1161/ATVBAHA.116.307023

Malhotra, K., Modak, A., Nangia, S., Daman, T. H., Gunsel, U., Robinson, V. L., et al. (2017). Cardiolipin mediates membrane and channel interactions of the mitochondrial TIM23 protein import complex receptor Tim50. *Sci. Adv.* 3 (9), e1700532. doi:10.1126/sciadv.1700532

Malhotra, K., Sathappa, M., Landin, J. S., Johnson, A. E., and Alder, N. N. (2013). Structural changes in the mitochondrial Tim23 channel are coupled to the proton-motive force. *Nat. Struct. Mol. Biol.* 20 (8), 965–972. doi:10.1038/nsmb.2613

Malpartida, A. B., Williamson, M., Narendra, D. P., Wade-Martins, R., and Ryan, B. J. (2021). Mitochondrial dysfunction and mitophagy in Parkinson's disease: from mechanism to therapy. *Trends Biochem. Sci.* 46 (4), 329–343. doi:10.1016/j.tibs.2020.11.007

Manczak, M., Anekonda, T. S., Henson, E., Park, B. S., Quinn, J., and Reddy, P. H. (2006). Mitochondria are a direct site of A beta accumulation in Alzheimer's disease neurons: implications for free radical generation and oxidative damage in disease progression. *Hum. Mol. Genet.* 15 (9), 1437–1449. doi:10.1093/hmg/ddl066

Manczak, M., Calkins, M. J., and Reddy, P. H. (2011). Impaired mitochondrial dynamics and abnormal interaction of amyloid beta with mitochondrial protein Drp1 in neurons from patients with Alzheimer's disease: implications for neuronal damage. *Hum. Mol. Genet.* 20 (13), 2495–2509. doi:10.1093/hmg/ddr139

Manczak, M., Mao, P., Calkins, M. J., Cornea, A., Reddy, A. P., Murphy, M. P., et al. (2010). Mitochondria-targeted antioxidants protect against amyloid-beta toxicity in Alzheimer's disease neurons. *J. Alzheimers Dis.* 20(2), S609–S631. doi:10.3233/JAD-2010-100564

Manczak, M., and Reddy, P. H. (2012). Abnormal interaction between the mitochondrial fission protein Drp1 and hyperphosphorylated tau in Alzheimer's disease neurons: implications for mitochondrial dysfunction and neuronal damage. *Hum. Mol. Genet.* 21 (11), 2538–2547. doi:10.1093/hmg/dds072

Manczak, M., and Reddy, P. H. (2015). Mitochondrial division inhibitor 1 protects against mutant huntingtin-induced abnormal mitochondrial dynamics and neuronal damage in Huntington's disease. *Hum. Mol. Genet.* 24 (25), 7308–7325. doi:10.1093/hmg/ddv429

Mandal, A., and Drerup, C. M. (2019). Axonal transport and mitochondrial function in neurons. *Front. Cell. Neurosci.* 13, 373. doi:10.3389/fncel.2019.00373

Mangiarini, L., Sathasivam, K., Seller, M., Cozens, B., Harper, A., Hetherington, C., et al. (1996). Exon 1 of the HD gene with an expanded CAG repeat is sufficient to cause a progressive neurological phenotype in transgenic mice. *Cell.* 87 (3), 493–506. doi:10.1016/s0092-8674(00)81369-0

Manzanza, N. O., Sedlackova, L., and Kalaria, R. N. (2021). Alpha-synuclein post-translational modifications: implications for pathogenesis of lewy body disorders. *Front. Aging Neurosci.* 13, 690293. doi:10.3389/fnagi.2021.690293

Marella, M., Seo, B. B., Yagi, T., and Matsuno-Yagi, A. (2009). Parkinson's disease and mitochondrial complex I: a perspective on the Ndi1 therapy. *J. Bioenerg. Biomembr.* 41 (6), 493–497. doi:10.1007/s10863-009-9249-z

Marom, M., Azem, A., and Mokranjac, D. (2011a). Understanding the molecular mechanism of protein translocation across the mitochondrial inner membrane: still a long way to go. *Biochimica Biophysica Acta (BBA) - Biomembr.* 1808 (3), 990–1001. doi:10.1016/j.bbamem.2010.07.011

Marom, M., Dayan, D., Demishtein-Zohary, K., Mokranjac, D., Neupert, W., and Azem, A. (2011b). Direct interaction of mitochondrial targeting presequences with purified components of the TIM23 protein complex. *J. Biol. Chem.* 286 (51), 43809–43815. doi:10.1074/jbc.M111.261040

Martens, Y. A., Zhao, N., Liu, C. C., Kanekiyo, T., Yang, A. J., Goate, A. M., et al. (2022). ApoE Cascade Hypothesis in the pathogenesis of Alzheimer's disease and related dementias. *Neuron* 110 (8), 1304–1317. doi:10.1016/j.neuron.2022.03.004

Martensson, C. U., Priesnitz, C., Song, J., Ellenrieder, L., Doan, K. N., Boos, F., et al. (2019). Mitochondrial protein translocation-associated degradation. *Nature* 569 (7758), 679–683. doi:10.1038/s41586-019-1227-y

Martin, D. D. O., Schmidt, M. E., Nguyen, Y. T., Lazic, N., and Hayden, M. R. (2019). Identification of a novel caspase cleavage site in huntingtin that regulates mutant huntingtin clearance. *FASEB J.* 33 (3), 3190–3197. doi:10.1096/fj.201701510RRR

Martin, J., Mahlke, K., and Pfanner, N. (1991). Role of an energized inner membrane in mitochondrial protein import. Delta psi drives the movement of presequences. *J. Biol. Chem.* 266 (27), 18051–18057. doi:10.1016/s0021-9258(18)55235-2

Martindale, D., Hackam, A., Wieczorek, A., Ellerby, L., Wellington, C., McCutcheon, K., et al. (1998). Length of huntingtin and its polyglutamine tract influences localization and frequency of intracellular aggregates. *Nat. Genet.* 18 (2), 150–154. doi:10.1038/ng0298-150

Martinez-Caballero, S., Grigoriev, S. M., Herrmann, J. M., Campo, M. L., and Kinnally, K. W. (2007). Tim17p regulates the twin pore structure and voltage gating of the mitochondrial protein import complex TIM23. *J. Biol. Chem.* 282 (6), 3584–3593. doi:10.1074/jbc.M607551200

Mastroeni, D., Khdour, O. M., Delvaux, E., Nolz, J., Olsen, G., Berchtold, N., et al. (2017). Nuclear but not mitochondrial-encoded oxidative phosphorylation genes are altered in aging, mild cognitive impairment, and Alzheimer's disease. *Alzheimers Dement.* 13 (5), 510–519. doi:10.1016/j.jalz.2016.09.003

Matouschek, A., Azem, A., Ratliff, K., Glick, B. S., Schmid, K., and Schatz, G. (1997). Active unfolding of precursor proteins during mitochondrial protein import. *EMBO J.* 16 (22), 6727–6736. doi:10.1093/emboj/16.22.6727

Matsumoto, S., Uchiumi, T., Saito, T., Yagi, M., Takazaki, S., Kanki, T., et al. (2012). Localization of mRNAs encoding human mitochondrial oxidative phosphorylation proteins. *Mitochondrion* 12 (3), 391–398. doi:10.1016/j.mito.2012.02.004

Matta, S. K., Kumar, A., and D'Silva, P. (2020). Mgr2 regulates mitochondrial preprotein import by associating with channel-forming Tim23 subunit. *Mol. Biol. Cell.* 31 (11), 1112–1123. doi:10.1091/mbc.E19-12-0677

Matta, S. K., Pareek, G., Bankapalli, K., Oblesha, A., and D'Silva, P. (2017). Role of Tim17 transmembrane regions in regulating the architecture of presequence translocase

and mitochondrial DNA stability. *Mol. Cell. Biol.* 37 (6), e00491-16. doi:10.1128/MCB.00491-16

Mayer, A., Nargang, F. E., Neupert, W., and Lill, R. (1995). MOM22 is a receptor for mitochondrial targeting sequences and cooperates with MOM19. *EMBO J.* 14 (17), 4204–4211. doi:10.1002/j.1460-2075.1995.tb00094.x

McDaid, J., Mustaly-Kalimi, S., and Stutzmann, G. E. (2020). Ca(2+) dyshomeostasis disrupts neuronal and synaptic function in alzheimer's disease. *Cells* 9 (12), 2655. doi:10.3390/cells9122655

McFarland, M. A., Ellis, C. E., Markey, S. P., and Nussbaum, R. L. (2008). Proteomics analysis identifies phosphorylation-dependent alpha-synuclein protein interactions. *Mol. Cell. Proteomics* 7 (11), 2123–2137. doi:10.1074/mcp.M800116-MCP200

McGlinchey, R. P., Ni, X., Shadish, J. A., Jiang, J., and Lee, J. C. (2021). The N terminus of α-synuclein dictates fibril formation. *Proc. Natl. Acad. Sci. U. S. A.* 118 (35), e2023487118. doi:10.1073/pnas.2023487118

Meinecke, M., Wagner, R., Kovermann, P., Guiard, B., Mick, D. U., Hutu, D. P., et al. (2006). Tim50 maintains the permeability barrier of the mitochondrial inner membrane. *Science* 312 (5779), 1523–1526. doi:10.1126/science.1127628

Melin, J., Kilisch, M., Neumann, P., Lytovchenko, O., Gomkale, R., Schendzielorz, A., et al. (2015). A presequence-binding groove in Tom70 supports import of Mdl1 into mitochondria. *Biochim. Biophys. Acta* 1853 (8), 1850–1859. doi:10.1016/j.bbamcr.2015.04.021

Michalek, M., Salnikov, E. S., and Bechinger, B. (2013). Structure and topology of the huntingtin 1-17 membrane anchor by a combined solution and solid-state NMR approach. *Biophys. J.* 105 (3), 699–710. doi:10.1016/j.bpj.2013.06.030

Mick, D. U., Dennerlein, S., Wiese, H., Reinhold, R., Pacheu-Grau, D., Lorenzi, I., et al. (2012). MITRAC links mitochondrial protein translocation to respiratory-chain assembly and translational regulation. *Cell.* 151 (7), 1528–1541. doi:10.1016/j.cell.2012.11.053

Middleton, E. R., and Rhoades, E. (2010). Effects of curvature and composition on α-synuclein binding to lipid vesicles. *Biophys. J.* 99 (7), 2279–2288. doi:10.1016/j.bpj.2010.07.056

Milakovic, T., Quintanilla, R. A., and Johnson, G. V. (2006). Mutant huntingtin expression induces mitochondrial calcium handling defects in clonal striatal cells: functional consequences. *J. Biol. Chem.* 281 (46), 34785–34795. doi:10.1074/jbc.M603845200

Milton, V. J., and Sweeney, S. T. (2012). Oxidative stress in synapse development and function. *Dev. Neurobiol.* 72 (1), 100–110. doi:10.1002/dneu.20957

Misrani, A., Tabassum, S., and Yang, L. (2021). Mitochondrial dysfunction and oxidative stress in alzheimer's disease. *Front. Aging Neurosci.* 13, 617588. doi:10.3389/fnagi.2021.617588

Mitchell, W., Ng, E. A., Tamucci, J. D., Boyd, K. J., Sathappa, M., Coscia, A., et al. (2020). The mitochondria-targeted peptide SS-31 binds lipid bilayers and modulates surface electrostatics as a key component of its mechanism of action. *J. Biol. Chem.* 295 (21), 7452–7469. doi:10.1074/jbc.RA119.012094

Mitchell, W., Tamucci, J. D., Ng, E. L., Liu, S., Birk, A. V., Szeto, H. H., et al. (2022). Structure-activity relationships of mitochondria-targeted tetrapeptide pharmacological compounds. *Elife* 11, e75531. doi:10.7554/eLife.75531

Mochel, F., Durant, B., Meng, X., O'Callaghan, J., Yu, H., Brouillet, E., et al. (2012). Early alterations of brain cellular energy homeostasis in Huntington disease models. *J. Biol. Chem.* 287 (2), 1361–1370. doi:10.1074/jbc.M111.309849

Moczko, M., Bomer, U., Kubrich, M., Zufall, N., Honlinger, A., and Pfanner, N. (1997). The intermembrane space domain of mitochondrial Tom22 functions as a trans binding site for preproteins with N-terminal targeting sequences. *Mol. Cell. Biol.* 17 (11), 6574–6584. doi:10.1128/mcb.17.11.6574

Model, K., Meisinger, C., and Kuhlbrandt, W. (2008). Cryo-electron microscopy structure of a yeast mitochondrial preprotein translocase. *J. Mol. Biol.* 383 (5), 1049–1057. doi:10.1016/j.jmb.2008.07.087

Mokranjac, D. (2020). How to get to the other side of the mitochondrial inner membrane - the protein import motor. *Biol. Chem.* 401 (6-7), 723–736. doi:10.1515/hsz-2020-0106

Mokranjac, D., Paschen, S. A., Kozany, C., Prokisch, H., Hoppins, S. C., Nargang, F. E., et al. (2003a). Tim50, a novel component of the TIM23 preprotein translocase of mitochondria. *EMBO J.* 22 (4), 816–825. doi:10.1093/emboj/cdg090

Mokranjac, D., Popov-Celeketic, D., Hell, K., and Neupert, W. (2005). Role of Tim21 in mitochondrial translocation contact sites. *J. Biol. Chem.* 280 (25), 23437–23440. doi:10.1074/jbc.C500135200

Mokranjac, D., Sichting, M., Neupert, W., and Hell, K. (2003b). Tim14, a novel key component of the import motor of the TIM23 protein translocase of mitochondria. *EMBO J.* 22 (19), 4945–4956. doi:10.1093/emboj/cdg485

Mokranjac, D., Sichting, M., Popov-Celeketic, D., Mapa, K., Gevorkyan-Airapetov, L., Zohary, K., et al. (2009). Role of Tim50 in the transfer of precursor proteins from the outer to the inner membrane of mitochondria. *Mol. Biol. Cell.* 20 (5), 1400–1407. doi:10.1091/mbc.e08-09-0934

Moran Luengo, T., Mayer, M. P., and Rudiger, S. G. D. (2019). The hsp70-hsp90 chaperone cascade in protein folding. *Trends Cell. Biol.* 29 (2), 164–177. doi:10.1016/j.tcb.2018.10.004

Moretti, D., Tambone, S., Cerretani, M., Fezzardi, P., Missineo, A., Sherman, L. T., et al. (2021). NRF2 activation by reversible KEAP1 binding induces the antioxidant response in primary neurons and astrocytes of a Huntington's disease mouse model. *Free Radic. Biol. Med.* 162, 243–254. doi:10.1016/j.freeradbiomed.2020.10.022

Morgenstern, M., Peikert, C. D., Lubbert, P., Suppanz, I., Klemm, C., Alka, O., et al. (2021). Quantitative high-confidence human mitochondrial proteome and its dynamics in cellular context. *Cell. Metab.* 33 (12), 2464–2483.e18. doi:10.1016/j.cmet.2021.11.001

Morigaki, R., and Goto, S. (2017). Striatal vulnerability in huntington's disease: neuroprotection versus neurotoxicity. *Brain Sci.* 7 (6), 63. doi:10.3390/brainsci7060063

Moro, F., Sirrenberg, C., Schneider, H. C., Neupert, W., and Brunner, M. (1999). The TIM17.23 preprotein translocase of mitochondria: composition and function in protein transport into the matrix. *EMBO J.* 18 (13), 3667–3675. doi:10.1093/emboj/18.13.3667

Mossmann, D., Vogtle, F. N., Taskin, A. A., Teixeira, P. F., Ring, J., Burkhart, J. M., et al. (2014). Amyloid-beta peptide induces mitochondrial dysfunction by inhibition of preprotein maturation. *Cell. Metab.* 20 (4), 662–669. doi:10.1016/j.cmet.2014.07.024

Munoz-Carvajal, F., and Sanhueza, M. (2020). The mitochondrial unfolded protein response: a hinge between healthy and pathological aging. *Front. Aging Neurosci.* 12, 581849. doi:10.3389/fnagi.2020.581849

Murakami, H., Pain, D., and Blobel, G. (1988). 70-kD heat shock-related protein is one of at least two distinct cytosolic factors stimulating protein import into mitochondria. *J. Cell. Biol.* 107 (1), 2051–2057. doi:10.1083/jcb.107.6.2051

Murali Mahadevan, H., Hashemiaghdam, A., Ashrafi, G., and Harbauer, A. B. (2021). Mitochondria in neuronal health: from energy metabolism to Parkinson's disease. *Adv. Biol. (Weinh).* 5 (9), e2100663. doi:10.1002/adbi.202100663

Muresan, V., and Ladescu Muresan, Z. (2015). Amyloid-beta precursor protein: multiple fragments, numerous transport routes and mechanisms. *Exp. Cell. Res.* 334 (1), 45–53. doi:10.1016/j.yexcr.2014.12.014

Musteikyte, G., Jayaram, A. K., Xu, C. K., Vendruscolo, M., Krainer, G., and Knowles, T. P. J. (2021). Interactions of α-synuclein oligomers with lipid membranes. *Biochim. Biophys. Acta Biomembr.* 1863 (4), 183536. doi:10.1016/j.bbamem.2020.183536

Muto, T., Obita, T., Abe, Y., Shodai, T., Endo, T., and Kohda, D. (2001). NMR identification of the Tom20 binding segment in mitochondrial presequences. *J. Mol. Biol.* 306 (2), 137–143. doi:10.1006/jmbi.2000.4397

Naia, L., Ferreira, I. L., Cunha-Oliveira, T., Duarte, A. I., Ribeiro, M., Rosenstock, T. R., et al. (2015). Activation of IGF-1 and insulin signaling pathways ameliorate mitochondrial function and energy metabolism in Huntington's Disease human lymphoblasts. *Mol. Neurobiol.* 51 (1), 331–348. doi:10.1007/s12035-014-8735-4

Najm, R., Jones, E. A., and Huang, Y. (2019). Apolipoprotein E4, inhibitory network dysfunction, and Alzheimer's disease. *Mol. Neurodegener.* 14 (1), 24. doi:10.1186/s13024-019-0324-6

Nakagawa, S., Lagisz, M., Hector, K. L., and Spencer, H. G. (2012). Comparative and meta-analytic insights into life extension via dietary restriction. *Aging Cell.* 11 (3), 401–409. doi:10.1111/j.1474-9726.2012.00798.x

Nakamura, K., Nemani, V. M., Azarbal, F., Skibinski, G., Levy, J. M., Egami, K., et al. (2011). Direct membrane association drives mitochondrial fission by the Parkinson disease-associated protein alpha-synuclein. *J. Biol. Chem.* 286 (23), 20710–20726. doi:10.1074/jbc.M110.213538

Nakamura, K., Nemani, V. M., Wallender, E. K., Kaehlcke, K., Ott, M., and Edwards, R. H. (2008). Optical reporters for the conformation of alpha-synuclein reveal a specific interaction with mitochondria. *J. Neurosci.* 28 (47), 12305–12317. doi:10.1523/JNEUROSCI.3088-08.2008

Naoi, M., Wu, Y., Shamoto-Nagai, M., and Maruyama, W. (2019). Mitochondria in neuroprotection by phytochemicals: bioactive polyphenols modulate mitochondrial apoptosis system, function and structure. *Int. J. Mol. Sci.* 20 (10), 2451. doi:10.3390/ijms20102451

Narayanan, V., Guo, Y., and Scarlata, S. (2005). Fluorescence studies suggest a role for alpha-synuclein in the phosphatidylinositol lipid signaling pathway. *Biochemistry* 44 (2), 462–470. doi:10.1021/bi0487140

Nargang, F. E., Rapaport, D., Ritzel, R. G., Neupert, W., and Lill, R. (1998). Role of the negative charges in the cytosolic domain of TOM22 in the import of precursor proteins into mitochondria. *Mol. Cell. Biol.* 18 (6), 3173–3181. doi:10.1128/mcb.18.6.3173

Naylor, D. J., Stines, A. P., Hoogenraad, N. J., and Hoj, P. B. (1998). Evidence for the existence of distinct mammalian cytosolic, microsomal, and two mitochondrial GrpE-like proteins, the Co-chaperones of specific Hsp70 members. *J. Biol. Chem.* 273 (33), 21169–21177. doi:10.1074/jbc.273.33.21169

Nelson, R., Sawaya, M. R., Balbirnie, M., Madsen, A. O., Riekel, C., Grothe, R., et al. (2005). Structure of the cross-beta spine of amyloid-like fibrils. *Nature* 435 (7043), 773–778. doi:10.1038/nature03680

Neueder, A., Dumas, A. A., Benjamin, A. C., and Bates, G. P. (2018). Regulatory mechanisms of incomplete huntingtin mRNA splicing. *Nat. Commun.* 9 (1), 3955. doi:10.1038/s41467-018-06281-3

Neueder, A., Landles, C., Ghosh, R., Howland, D., Myers, R. H., Faull, R. L. M., et al. (2017). The pathogenic exon 1 HTT protein is produced by incomplete splicing in Huntington's disease patients. *Sci. Rep.* 7 (1), 1307. doi:10.1038/s41598-017-01510-z

Nhu, N. T., Xiao, S. Y., Liu, Y., Kumar, V. B., Cui, Z. Y., and Lee, S. D. (2021). Neuroprotective effects of a small mitochondrially-targeted tetrapeptide elamipretide in neurodegeneration. *Front. Integr. Neurosci.* 15, 747901. doi:10.3389/fnint.2021.747901

Nielsen, K. L., and Cowan, N. J. (1998). A single ring is sufficient for productive chaperonin-mediated folding *in vivo*. *Mol. Cell.* 2 (1), 93–99. doi:10.1016/s1097-2765(00)80117-3

Nisemblat, S., Yaniv, O., Parnas, A., Frolow, F., and Azem, A. (2015). Crystal structure of the human mitochondrial chaperonin symmetrical football complex. *Proc. Natl. Acad. Sci. U. S. A.* 112 (19), 6044–6049. doi:10.1073/pnas.1411718112

Nunnari, J., Fox, T. D., and Walter, P. (1993). A mitochondrial protease with two catalytic subunits of nonoverlapping specificities. *Science* 262 (5142), 1997–2004. doi:10.1126/science.8266095

Nuscher, B., Kamp, F., Mehnert, T., Odoy, S., Haass, C., Kahle, P. J., et al. (2004). Alpha-synuclein has a high affinity for packing defects in a bilayer membrane: a thermodynamics study. *J. Biol. Chem.* 279 (21), 21966–21975. doi:10.1074/jbc.M401076200

Obita, T., Muto, T., Endo, T., and Kohda, D. (2003). Peptide library approach with a disulfide tether to refine the Tom20 recognition motif in mitochondrial presequences. *J. Mol. Biol.* 328 (2), 495–504. doi:10.1016/s0022-2836(03)00288-2

Oka, S., Leon, J., Sakumi, K., Ide, T., Kang, D., LaFerla, F. M., et al. (2016). Human mitochondrial transcriptional factor A breaks the mitochondria-mediated vicious cycle in Alzheimer's disease. *Sci. Rep.* 6, 37889. doi:10.1038/srep37889

Okamoto, K., Brinker, A., Paschen, S. A., Moarefi, I., Hayer-Hartl, M., Neupert, W., et al. (2002). The protein import motor of mitochondria: a targeted molecular ratchet driving unfolding and translocation. *EMBO J.* 21 (14), 3659–3671. doi:10.1093/emboj/cdf358

Opalinska, M., and Janska, H. (2018). AAA proteases: guardians of mitochondrial function and homeostasis. *Cells* 7 (10), 163. doi:10.3390/cells7100163

Orr, A. L., Li, S., Wang, C. E., Li, H., Wang, J., Rong, J., et al. (2008). N-terminal mutant huntingtin associates with mitochondria and impairs mitochondrial trafficking. *J. Neurosci.* 28 (11), 2783–2792. doi:10.1523/JNEUROSCI.0106-08.2008

Oswald, M. C., Brooks, P. S., Zwart, M. F., Mukherjee, A., West, R. J., Giachello, C. N., et al. (2018). Reactive oxygen species regulate activity-dependent neuronal plasticity in Drosophila. *Elife* 7, e39393. doi:10.7554/eLife.39393

Ouberai, M. M., Wang, J., Swann, M. J., Galvagnion, C., Guilliams, T., Dobson, C. M., et al. (2013). α-Synuclein senses lipid packing defects and induces lateral expansion of lipids leading to membrane remodeling. *J. Biol. Chem.* 288 (29), 20883–20895. doi:10.1074/jbc.M113.478297

Ow, S. Y., and Dunstan, D. E. (2014). A brief overview of amyloids and Alzheimer's disease. *Protein Sci.* 23 (10), 1315–1331. doi:10.1002/pro.2524

Padrick, S. B., and Miranker, A. D. (2002). Islet amyloid: phase partitioning and secondary nucleation are central to the mechanism of fibrillogenesis. *Biochemistry* 41 (14), 4694–4703. doi:10.1021/bi0160462

Paglin, S., Lee, N. Y., Nakar, C., Fitzgerald, M., Plotkin, J., Deuel, B., et al. (2005). Rapamycin-sensitive pathway regulates mitochondrial membrane potential, autophagy, and survival in irradiated MCF-7 cells. *Cancer Res.* 65 (23), 11061–11070. doi:10.1158/0008-5472.CAN-05-1083

Paillusson, S., Gomez-Suaga, P., Stoica, R., Little, D., Gissen, P., Devine, M. J., et al. (2017). α-Synuclein binds to the ER-mitochondria tethering protein VAPB to disrupt Ca2+ homeostasis and mitochondrial ATP production. *Acta Neuropathol.* 134 (1), 129–149. doi:10.1007/s00401-017-1704-z

Pak, Y. K., and Weiner, H. (1990). Import of chemically synthesized signal peptides into rat liver mitochondria. *J. Biol. Chem.* 265 (24), 14298–14307. doi:10.1016/s0021-9258(18)77300-6

Pandey, M., Varghese, M., Sindhu, K. M., Sreetama, S., Navneet, A. K., Mohanakumar, K. P., et al. (2008). Mitochondrial NAD+-linked State 3 respiration and complex-I activity are compromised in the cerebral cortex of 3-nitropropionic acid-induced rat model of Huntington's disease. *J. Neurochem.* 104 (2), 420–434. doi:10.1111/j.1471-4159.2007.04996.x

Panov, A. V., Gutekunst, C. A., Leavitt, B. R., Hayden, M. R., Burke, J. R., Strittmatter, W. J., et al. (2002). Early mitochondrial calcium defects in Huntington's disease are a direct effect of polyglutamines. *Nat. Neurosci.* 5 (8), 731–736. doi:10.1038/nn884

Paolini Paoletti, F., Gaetani, L., and Parnetti, L. (2020). The challenge of disease-modifying therapies in Parkinson's disease: role of CSF biomarkers. *Biomolecules* 10 (2), 335. doi:10.3390/biom10020335

Papic, D., Elbaz-Alon, Y., Koerdt, S. N., Leopold, K., Worm, D., Jung, M., et al. (2013). The role of Djp1 in import of the mitochondrial protein Mim1 demonstrates specificity between a cochaperone and its substrate protein. *Mol. Cell. Biol.* 33 (20), 4083–4094. doi:10.1128/MCB.00227-13

Pardridge, W. M. (2016). Re-engineering therapeutic antibodies for Alzheimer's disease as blood-brain barrier penetrating bi-specific antibodies. *Expert Opin. Biol. Ther.* 16 (12), 1455–1468. doi:10.1080/14712598.2016.1230195

Pardridge, W. M. (2020). Treatment of alzheimer's disease and blood-brain barrier drug delivery. *Pharm. (Basel)* 13 (11), 394. doi:10.3390/ph13110394

Park, H., Kang, J. H., and Lee, S. (2020). Autophagy in neurodegenerative diseases: a hunter for aggregates. *Int. J. Mol. Sci.* 21 (9), 3369. doi:10.3390/ijms21093369

Patil, S. M., Mehta, A., Jha, S., and Alexandrescu, A. T. (2011). Heterogeneous amylin fibril growth mechanisms imaged by total internal reflection fluorescence microscopy. *Biochemistry* 50 (14), 2808–2819. doi:10.1021/bi101908m

Pellegrini, L., and Scorrano, L. (2007). A cut short to death: parl and Opa1 in the regulation of mitochondrial morphology and apoptosis. *Cell. Death Differ.* 14 (7), 1275–1284. doi:10.1038/sj.cdd.4402145

Penney, J. B., Jr., Vonsattel, J. P., MacDonald, M. E., Gusella, J. F., and Myers, R. H. (1997). CAG repeat number governs the development rate of pathology in Huntington's disease. *Ann. Neurol.* 41 (5), 689–692. doi:10.1002/ana.410410521

Petrasch-Parwez, E., Nguyen, H. P., Lobbecke-Schumacher, M., Habbes, H. W., Wieczorek, S., Riess, O., et al. (2007). Cellular and subcellular localization of Huntingtin [corrected] aggregates in the brain of a rat transgenic for Huntington disease. *J. Comp. Neurol.* 501 (5), 716–730. doi:10.1002/cne.21272

Petrova, V. Y., Drescher, D., Kujumdzieva, A. V., and Schmitt, M. J. (2004). Dual targeting of yeast catalase A to peroxisomes and mitochondria. *Biochem. J.* 380 (2), 393–400. doi:10.1042/BJ20040042

Pfanner, N., Warscheid, B., and Wiedemann, N. (2019). Mitochondrial proteins: from biogenesis to functional networks. *Nat. Rev. Mol. Cell. Biol.* 20 (5), 267–284. doi:10.1038/s41580-018-0092-0

Pfefferkorn, C. M., Jiang, Z., and Lee, J. C. (2012). Biophysics of alpha-synuclein membrane interactions. *Biochim. Biophys. Acta* 1818 (2), 162–171. doi:10.1016/j.bbamem.2011.07.032

Pinho, C. M., Teixeira, P. F., and Glaser, E. (2014). Mitochondrial import and degradation of amyloid-β peptide. *Biochim. Biophys. Acta* 1837 (7), 1069–1074. doi:10.1016/j.bbabio.2014.02.007

Pino, P., Foth, B. J., Kwok, L. Y., Sheiner, L., Schepers, R., Soldati, T., et al. (2007). Dual targeting of antioxidant and metabolic enzymes to the mitochondrion and the apicoplast of Toxoplasma gondii. *PLoS Pathog.* 3 (8), e115. doi:10.1371/journal.ppat.0030115

Pitt, A. S., and Buchanan, S. K. (2021). A biochemical and structural understanding of TOM complex interactions and implications for human health and disease. *Cells* 10 (5), 1164. doi:10.3390/cells10051164

Poirier, M. A., Li, H., Macosko, J., Cai, S., Amzel, M., and Ross, C. A. (2002). Huntingtin spheroids and protofibrils as precursors in polyglutamine fibrilization. *J. Biol. Chem.* 277 (43), 41032–41037. doi:10.1074/jbc.M205809200

Ponce-Rojas, J. C., Avendano-Monsalve, M. C., Yanez-Falcon, A. R., Jaimes-Miranda, F., Garay, E., Torres-Quiroz, F., et al. (2017). αβ'-NAC cooperates with Sam37 to mediate early stages of mitochondrial protein import. *FEBS J.* 284 (5), 814–830. doi:10.1111/febs.14024

Popov-Celeketic, D., Mapa, K., Neupert, W., and Mokranjac, D. (2008). Active remodelling of the TIM23 complex during translocation of preproteins into mitochondria. *EMBO J.* 27 (10), 1469–1480. doi:10.1038/emboj.2008.79

Poulaki, A., and Giannouli, S. (2022). Mitochondrial lipids: from membrane organization to apoptotic facilitation. *Int. J. Mol. Sci.* 23 (7), 3738. doi:10.3390/ijms23073738

Pozo Devoto, V. M., Dimopoulos, N., Alloatti, M., Pardi, M. B., Saez, T. M., Otero, M. G., et al. (2017). αSynuclein control of mitochondrial homeostasis in human-derived neurons is disrupted by mutations associated with Parkinson's disease. *Sci. Rep.* 7 (1), 5042. doi:10.1038/s41598-017-05334-9

Pozo Devoto, V. M., and Falzone, T. L. (2017). Mitochondrial dynamics in Parkinson's disease: a role for alpha-synuclein? *Dis. Model. Mech.* 10 (9), 1075–1087. doi:10.1242/dmm.026294

Prior, M., Dargusch, R., Ehren, J. L., Chiruta, C., and Schubert, D. (2013). The neurotrophic compound J147 reverses cognitive impairment in aged Alzheimer's disease mice. *Alzheimers Res. Ther.* 5 (3), 25. doi:10.1186/alzrt179

Qian, X., Gebert, M., Hopker, J., Yan, M., Li, J., Wiedemann, N., et al. (2011). Structural basis for the function of Tim50 in the mitochondrial presequence translocase. *J. Mol. Biol.* 411 (3), 513–519. doi:10.1016/j.jmb.2011.06.020

Qiang, W., Yau, W. M., Lu, J. X., Collinge, J., and Tycko, R. (2017). Structural variation in amyloid-beta fibrils from Alzheimer's disease clinical subtypes. *Nature* 541 (7636), 217–221. doi:10.1038/nature20814

Qin, W., Haroutunian, V., Katsel, P., Cardozo, C. P., Ho, L., Buxbaum, J. D., et al. (2009). PGC-1alpha expression decreases in the Alzheimer disease brain as a function of dementia. *Arch. Neurol.* 66 (3), 352–361. doi:10.1001/archneurol.2008.588

Qin, W., Myers, S. A., Carey, D. K., Carr, S. A., and Ting, A. Y. (2021). Spatiotemporally-resolved mapping of RNA binding proteins via functional proximity labeling reveals a mitochondrial mRNA anchor promoting stress recovery. *Nat. Commun.* 12 (1), 4980. doi:10.1038/s41467-021-25259-2

Raffai, R. L., Dong, L. M., Farese, R. V., Jr., and Weisgraber, K. H. (2001). Introduction of human apolipoprotein E4 "domain interaction" into mouse apolipoprotein E. *Proc. Natl. Acad. Sci. U. S. A.* 98 (20), 11587–11591. doi:10.1073/pnas.201279298

Ramakrishnan, M., Jensen, P. H., and Marsh, D. (2003). Alpha-synuclein association with phosphatidylglycerol probed by lipid spin labels. *Biochemistry* 42 (44), 12919–12926. doi:10.1021/bi035048e

Rao, J. N., Jao, C. C., Hegde, B. G., Langen, R., and Ulmer, T. S. (2010). A combinatorial NMR and EPR approach for evaluating the structural ensemble of partially folded proteins. *J. Am. Chem. Soc.* 132 (25), 8657–8668. doi:10.1021/ja100646t

Rapaport, D., Neupert, W., and Lill, R. (1997). Mitochondrial protein import. Tom40 plays a major role in targeting and translocation of preproteins by forming a specific binding site for the presequence. *J. Biol. Chem.* 272 (30), 18725–18731. doi:10.1074/jbc.272.30.18725

Rath, S., Sharma, R., Gupta, R., Ast, T., Chan, C., Durham, T. J., et al. (2021). MitoCarta3.0: an updated mitochondrial proteome now with sub-organelle localization and pathway annotations. *Nucleic Acids Res.* 49 (D1), D1541–D1547. doi:10.1093/nar/gkaa1011

Ratovitski, T., Chighladze, E., Arbez, N., Boronina, T., Herbrich, S., Cole, R. N., et al. (2012). Huntingtin protein interactions altered by polyglutamine expansion as determined by quantitative proteomic analysis. *Cell. Cycle* 11 (10), 2006–2021. doi:10.4161/cc.20423

Reddy, P. H., Manczak, M., and Kandimalla, R. (2017). Mitochondria-targeted small molecule SS31: a potential candidate for the treatment of Alzheimer's disease. *Hum. Mol. Genet.* 26 (8), 1483–1496. doi:10.1093/hmg/ddx129

Reddy, P. H., Manczak, M., Yin, X., and Reddy, A. P. (2018). Synergistic protective effects of mitochondrial division inhibitor 1 and mitochondria-targeted small peptide SS31 in alzheimer's disease. *J. Alzheimers Dis.* 62 (4), 1549–1565. doi:10.3233/JAD-170988

Rehling, P., Model, K., Brandner, K., Kovermann, P., Sickmann, A., Meyer, H. E., et al. (2003). Protein insertion into the mitochondrial inner membrane by a twin-pore translocase. *Science* 299 (5613), 1747–1751. doi:10.1126/science.1080945

Rezaei-Ghaleh, N., Amininasab, M., Kumar, S., Walter, J., and Zweckstetter, M. (2016). Phosphorylation modifies the molecular stability of beta-amyloid deposits. *Nat. Commun.* 7, 11359. doi:10.1038/ncomms11359

Ribeiro, M., Rosenstock, T. R., Cunha-Oliveira, T., Ferreira, I. L., Oliveira, C. R., and Rego, A. C. (2012). Glutathione redox cycle dysregulation in Huntington's disease knock-in striatal cells. *Free Radic. Biol. Med.* 53 (10), 1857–1867. doi:10.1016/j.freeradbiomed.2012.09.004

Ribeiro, M., Rosenstock, T. R., Oliveira, A. M., Oliveira, C. R., and Rego, A. C. (2014). Insulin and IGF-1 improve mitochondrial function in a PI-3K/Akt-dependent manner and reduce mitochondrial generation of reactive oxygen species in Huntington's disease knock-in striatal cells. *Free Radic. Biol. Med.* 74, 129–144. doi:10.1016/j.freeradbiomed.2014.06.023

Ricciarelli, R., and Fedele, E. (2017). The amyloid cascade hypothesis in alzheimer's disease: it's time to change our mind. *Curr. Neuropharmacol.* 15 (6), 926–935. doi:10.2174/1570159X15666170116143743

Richter, F., Dennerlein, S., Nikolov, M., Jans, D. C., Naumenko, N., Aich, A., et al. (2019). ROMO1 is a constituent of the human presequence translocase required for YME1L protease import. *J. Cell. Biol.* 218 (2), 598–614. doi:10.1083/jcb.201806093

Richter-Dennerlein, R., Korwitz, A., Haag, M., Tatsuta, T., Dargazanli, S., Baker, M., et al. (2014). DNAJC19, a mitochondrial cochaperone associated with cardiomyopathy, forms a complex with prohibitins to regulate cardiolipin remodeling. *Cell. Metab.* 20 (1), 158–171. doi:10.1016/j.cmet.2014.04.016

Richter-Dennerlein, R., Oeljeklaus, S., Lorenzi, I., Ronsor, C., Bareth, B., Schendzielorz, A. B., et al. (2016). Mitochondrial protein synthesis adapts to influx of nuclear-encoded protein. *Cell.* 167 (2), 471–483. doi:10.1016/j.cell.2016.09.003

Riguet, N., Mahul-Mellier, A. L., Maharjan, N., Burtscher, J., Croisier, M., Knott, G., et al. (2021). Nuclear and cytoplasmic huntingtin inclusions exhibit distinct biochemical composition, interactome and ultrastructural properties. *Nat. Commun.* 12 (1), 6579. doi:10.1038/s41467-021-26684-z

Robin, M. A., Anandatheerthavarada, H. K., Biswas, G., Sepuri, N. B., Gordon, D. M., Pain, D., et al. (2002). Bimodal targeting of microsomal CYP2E1 to mitochondria through activation of an N-terminal chimeric signal by cAMP-mediated phosphorylation. *J. Biol. Chem.* 277 (43), 40583–40593. doi:10.1074/jbc.M203292200

Robin, M. A., Anandatheerthavarada, H. K., Fang, J. K., Cudic, M., Otvos, L., and Avadhani, N. G. (2001). Mitochondrial targeted cytochrome P450 2E1 (P450 MT5) contains an intact N terminus and requires mitochondrial specific electron transfer proteins for activity. *J. Biol. Chem.* 276 (27), 24680–24689. doi:10.1074/jbc.M100363200

Robotta, M., Gerding, H. R., Vogel, A., Hauser, K., Schildknecht, S., Karreman, C., et al. (2014). Alpha-synuclein binds to the inner membrane of mitochondria in an α-helical conformation. *Chembiochem* 15 (17), 2499–2502. doi:10.1002/cbic.201402281

Rocchi, A., Pellegrini, S., Siciliano, G., and Murri, L. (2003). Causative and susceptibility genes for Alzheimer's disease: a review. *Brain Res. Bull.* 61 (1), 1–24. doi:10.1016/s0361-9230(03)00067-4

Roche, J., Shen, Y., Lee, J. H., Ying, J., and Bax, A. (2016). Monomeric aβ(1-40) and aβ(1-42) peptides in solution adopt very similar ramachandran map distributions that closely resemble random coil. *Biochemistry* 55 (5), 762–775. doi:10.1021/acs.biochem.5b01259

Rockabrand, E., Slepko, N., Pantalone, A., Nukala, V. N., Kazantsev, A., Marsh, J. L., et al. (2007). The first 17 amino acids of Huntingtin modulate its sub-cellular localization, aggregation and effects on calcium homeostasis. *Hum. Mol. Genet.* 16 (1), 61–77. doi:10.1093/hmg/ddl440

Rodriguez, J. A., Ivanova, M. I., Sawaya, M. R., Cascio, D., Reyes, F. E., Shi, D., et al. (2015). Structure of the toxic core of alpha-synuclein from invisible crystals. *Nature* 525 (7570), 486–490. doi:10.1038/nature15368

Roise, D., Horvath, S. J., Tomich, J. M., Richards, J. H., and Schatz, G. (1986). A chemically synthesized pre-sequence of an imported mitochondrial protein can form an amphiphilic helix and perturb natural and artificial phospholipid bilayers. *EMBO J.* 5 (6), 1327–1334. doi:10.1002/j.1460-2075.1986.tb04363.x

Roise, D., and Schatz, G. (1988). Mitochondrial presequences. *J. Biol. Chem.* 263 (10), 4509–4511. doi:10.1016/s0021-9258(18)68809-x

Roise, D., Theiler, F., Horvath, S. J., Tomich, J. M., Richards, J. H., Allison, D. S., et al. (1988). Amphiphilicity is essential for mitochondrial presequence function. *EMBO J.* 7 (3), 649–653. doi:10.1002/j.1460-2075.1988.tb02859.x

Rolfe, D. F., and Brown, G. C. (1997). Cellular energy utilization and molecular origin of standard metabolic rate in mammals. *Physiol. Rev.* 77 (3), 731–758. doi:10.1152/physrev.1997.77.3.731

Roses, A. D., Lutz, M. W., Amrine-Madsen, H., Saunders, A. M., Crenshaw, D. G., Sundseth, S. S., et al. (2010). A TOMM40 variable-length polymorphism predicts the age of late-onset Alzheimer's disease. *Pharmacogenomics J.* 10 (5), 375–384. doi:10.1038/tpj.2009.69

Roshanbin, S., Aniszewska, A., Gumucio, A., Masliah, E., Erlandsson, A., Bergstrom, J., et al. (2021). Age-related increase of alpha-synuclein oligomers is associated with motor disturbances in L61 transgenic mice. *Neurobiol. Aging* 101, 207–220. doi:10.1016/j.neurobiolaging.2021.01.010

Ruan, L., Zhou, C., Jin, E., Kucharavy, A., Zhang, Y., Wen, Z., et al. (2017). Cytosolic proteostasis through importing of misfolded proteins into mitochondria. *Nature* 543 (7645), 443–446. doi:10.1038/nature21695

Rubinsztein, D. C., Leggo, J., Coles, R., Almqvist, E., Biancalana, V., Cassiman, J. J., et al. (1996). Phenotypic characterization of individuals with 30-40 CAG repeats in the Huntington disease (HD) gene reveals HD cases with 36 repeats and apparently normal elderly individuals with 36-39 repeats. *Am. J. Hum. Genet.* 59 (1), 16–22.

Rudiger, S., Germeroth, L., Schneider-Mergener, J., and Bukau, B. (1997). Substrate specificity of the DnaK chaperone determined by screening cellulose-bound peptide libraries. *EMBO J.* 16 (7), 1501–1507. doi:10.1093/emboj/16.7.1501

Rutledge, B. S., Choy, W. Y., and Duennwald, M. L. (2022). Folding or holding? Hsp70 and Hsp90 chaperoning of misfolded proteins in neurodegenerative disease. *J. Biol. Chem.* 298 (5), 101905. doi:10.1016/j.jbc.2022.101905

Ryan, T., Bamm, V. V., Stykel, M. G., Coackley, C. L., Humphries, K. M., Jamieson-Williams, R., et al. (2018). Cardiolipin exposure on the outer mitochondrial membrane modulates alpha-synuclein. *Nat. Commun.* 9 (1), 817. doi:10.1038/s41467-018-03241-9

Ryu, D., Mouchiroud, L., Andreux, P. A., Katsyuba, E., Moullan, N., Nicolet-Dit-Felix, A. A., et al. (2016). Urolithin A induces mitophagy and prolongs lifespan in *C. elegans* and increases muscle function in rodents. *Nat. Med.* 22 (8), 879–888. doi:10.1038/nm.4132

Ryu, W. I., Bormann, M. K., Shen, M., Kim, D., Forester, B., Park, Y., et al. (2021). Brain cells derived from Alzheimer's disease patients have multiple specific innate abnormalities in energy metabolism. *Mol. Psychiatry* 26 (10), 5702–5714. doi:10.1038/s41380-021-01068-3

Saavedra, L., Mohamed, A., Ma, V., Kar, S., and de Chaves, E. P. (2007). Internalization of beta-amyloid peptide by primary neurons in the absence of apolipoprotein E. *J. Biol. Chem.* 282 (49), 35722–35732. doi:10.1074/jbc.M701823200

Saitoh, T., Igura, M., Miyazaki, Y., Ose, T., Maita, N., and Kohda, D. (2011). Crystallographic snapshots of Tom20-mitochondrial presequence interactions with disulfide-stabilized peptides. *Biochemistry* 50 (24), 5487–5496. doi:10.1021/bi200470x

Saitoh, T., Igura, M., Obita, T., Ose, T., Kojima, R., Maenaka, K., et al. (2007). Tom20 recognizes mitochondrial presequences through dynamic equilibrium among multiple bound states. *EMBO J.* 26 (22), 4777–4787. doi:10.1038/sj.emboj.7601888

Sakaue, H., Shiota, T., Ishizaka, N., Kawano, S., Tamura, Y., Tan, K. S., et al. (2019). Porin associates with Tom22 to regulate the mitochondrial protein gate assembly. *Mol. Cell.* 73 (5), 1044–1055. doi:10.1016/j.molcel.2019.01.003

Samuel, F., Flavin, W. P., Iqbal, S., Pacelli, C., Sri Renganathan, S. D., Trudeau, L. E., et al. (2016). Effects of serine 129 phosphorylation on alpha-synuclein aggregation, membrane association, and internalization. *J. Biol. Chem.* 291 (9), 4374–4385. doi:10.1074/jbc.M115.705095

Sandbrink, R., Masters, C. L., and Beyreuther, K. (1996). APP gene family. Alternative splicing generates functionally related isoforms. *Ann. N. Y. Acad. Sci.* 777, 281–287. doi:10.1111/j.1749-6632.1996.tb34433.x

Sando, S. B., Melquist, S., Cannon, A., Hutton, M. L., Sletvold, O., Saltvedt, I., et al. (2008). APOE epsilon 4 lowers age at onset and is a high risk factor for Alzheimer's disease; a case control study from central Norway. *BMC Neurol.* 8, 9. doi:10.1186/1471-2377-8-9

Sarchione, A., Marchand, A., Taymans, J. M., and Chartier-Harlin, M. C. (2021). Alpha-synuclein and lipids: the elephant in the room? *Cells* 10 (9), 2452. doi:10.3390/cells10092452

Sassano, M. L., Felipe-Abrio, B., and Agostinis, P. (2022). ER-mitochondria contact sites; a multifaceted factory for Ca(2+) signaling and lipid transport. *Front. Cell. Dev. Biol.* 10, 988014. doi:10.3389/fcell.2022.988014

Sathasivam, K., Neueder, A., Gipson, T. A., Landles, C., Benjamin, A. C., Bondulich, M. K., et al. (2013). Aberrant splicing of HTT generates the pathogenic exon 1 protein in

Huntington disease. *Proc. Natl. Acad. Sci. U. S. A.* 110 (6), 2366–2370. doi:10.1073/pnas.1221891110

Saudou, F., and Humbert, S. (2016). The biology of huntingtin. *Neuron* 89 (5), 910–926. doi:10.1016/j.neuron.2016.02.003

Sawa, A., Wiegand, G. W., Cooper, J., Margolis, R. L., Sharp, A. H., Lawler, J. F., Jr., et al. (1999). Increased apoptosis of Huntington disease lymphoblasts associated with repeat length-dependent mitochondrial depolarization. *Nat. Med.* 5 (10), 1194–1198. doi:10.1038/13518

Schatz, G. (1997). Just follow the acid chain. *Nature* 388 (6638), 121–122. doi:10.1038/40510

Scheper, W., and Hoozemans, J. J. (2015). The unfolded protein response in neurodegenerative diseases: a neuropathological perspective. *Acta Neuropathol.* 130 (3), 315–331. doi:10.1007/s00401-015-1462-8

Scherzinger, E., Sittler, A., Schweiger, K., Heiser, V., Lurz, R., Hasenbank, R., et al. (1999). Self-assembly of polyglutamine-containing huntingtin fragments into amyloid-like fibrils: implications for Huntington's disease pathology. *Proc. Natl. Acad. Sci. U. S. A.* 96 (8), 4604–4609. doi:10.1073/pnas.96.8.4604

Schilling, G., Klevytska, A., Tebbenkamp, A. T., Juenemann, K., Cooper, J., Gonzales, V., et al. (2007). Characterization of huntingtin pathologic fragments in human Huntington disease, transgenic mice, and cell models. *J. Neuropathol. Exp. Neurol.* 66 (4), 313–320. doi:10.1097/nen.0b013e318040b2c8

Schilling, G., Sharp, A. H., Loev, S. J., Wagster, M. V., Li, S. H., Stine, O. C., et al. (1995). Expression of the Huntington's disease (IT15) protein product in HD patients. *Hum. Mol. Genet.* 4 (8), 1365–1371. doi:10.1093/hmg/4.8.1365

Schmidt, M. F., Gan, Z. Y., Komander, D., and Dewson, G. (2021). Ubiquitin signalling in neurodegeneration: mechanisms and therapeutic opportunities. *Cell. Death Differ.* 28 (2), 570–590. doi:10.1038/s41418-020-00706-7

Schneider, A. (2018). Dihydrofolate reductase and membrane translocation: evolution of a classic experiment: classic landmark papers, irrespective of their age, can teach students how best science is practiced and inspire new experiments. *EMBO Rep.* 19 (3), e45692. doi:10.15252/embr.201745692

Schneider, H. C., Berthold, J., Bauer, M. F., Dietmeier, K., Guiard, B., Brunner, M., et al. (1994). Mitochondrial Hsp70/MIM44 complex facilitates protein import. *Nature* 371 (6500), 768–774. doi:10.1038/371768a0

Schneider, H. C., Westermann, B., Neupert, W., and Brunner, M. (1996). The nucleotide exchange factor MGE exerts a key function in the ATP-dependent cycle of mt-Hsp70-Tim44 interaction driving mitochondrial protein import. *EMBO J.* 15 (21), 5796–5803. doi:10.1002/j.1460-2075.1996.tb00966.x

Schulz, C., Lytovchenko, O., Melin, J., Chacinska, A., Guiard, B., Neumann, P., et al. (2011). Tim50's presequence receptor domain is essential for signal driven transport across the TIM23 complex. *J. Cell. Biol.* 195 (4), 643–656. doi:10.1083/jcb.201105098

Selkoe, D. J., and Hardy, J. (2016). The amyloid hypothesis of Alzheimer's disease at 25 years. *EMBO Mol. Med.* 8 (6), 595–608. doi:10.15252/emmm.201606210

Seong, I. S., Ivanova, E., Lee, J. M., Choo, Y. S., Fossale, E., Anderson, M., et al. (2005). HD CAG repeat implicates a dominant property of huntingtin in mitochondrial energy metabolism. *Hum. Mol. Genet.* 14 (19), 2871–2880. doi:10.1093/hmg/ddi319

Serpell, L. C. (2000). Alzheimer's amyloid fibrils: structure and assembly. *Biochim. Biophys. Acta* 1502 (1), 16–30. doi:10.1016/s0925-4439(00)00029-6

Seubert, P., Vigo-Pelfrey, C., Esch, F., Lee, M., Dovey, H., Davis, D., et al. (1992). Isolation and quantification of soluble Alzheimer's beta-peptide from biological fluids. *Nature* 359 (6393), 325–327. doi:10.1038/359325a0

Shahmoradian, S. H., Lewis, A. J., Genoud, C., Hench, J., Moors, T. E., Navarro, P. P., et al. (2019). Lewy pathology in Parkinson's disease consists of crowded organelles and lipid membranes. *Nat. Neurosci.* 22 (7), 1099–1109. doi:10.1038/s41593-019-0423-2

Sharon, R., Bar-Joseph, I., Frosch, M. P., Walsh, D. M., Hamilton, J. A., and Selkoe, D. J. (2003). The formation of highly soluble oligomers of alpha-synuclein is regulated by fatty acids and enhanced in Parkinson's disease. *Neuron* 37 (4), 583–595. doi:10.1016/s0896-6273(03)00024-2

Shen, K., Gamerdinger, M., Chan, R., Gense, K., Martin, E. M., Sachs, N., et al. (2019a). Dual role of ribosome-binding domain of NAC as a potent suppressor of protein aggregation and aging-related proteinopathies. *Mol. Cell.* 74 (4), 729–741. doi:10.1016/j.molcel.2019.03.012

Shen, Y., Ding, M., Xie, Z., Liu, X., Yang, H., Jin, S., et al. (2019b). Activation of mitochondrial unfolded protein response in SHSY5Y expressing APP cells and APP/PS1 mice. *Front. Cell. Neurosci.* 13, 568. doi:10.3389/fncel.2019.00568

Shi, Q., Chang, C., Saliba, A., and Bhat, M. A. (2022). Microglial mTOR activation upregulates Trem2 and enhances beta-amyloid plaque clearance in the 5XFAD alzheimer's disease model. *J. Neurosci.* 42 (27), 5294–5313. doi:10.1523/JNEUROSCI.2427-21.2022

Shin, C. S., Meng, S., Garbis, S. D., Moradian, A., Taylor, R. W., Sweredoski, M. J., et al. (2021). LONP1 and mtHSP70 cooperate to promote mitochondrial protein folding. *Nat. Commun.* 12 (1), 265. doi:10.1038/s41467-020-20597-z

Shindyapina, A. V., Cho, Y., Kaya, A., Tyshkovskiy, A., Castro, J. P., Deik, A., et al. (2022). Rapamycin treatment during development extends life span and health span of male mice and Daphnia magna. *Sci. Adv.* 8 (37), eabo5482. doi:10.1126/sciadv.abo5482

Shiota, T., Imai, K., Qiu, J., Hewitt, V. L., Tan, K., Shen, H. H., et al. (2015). Molecular architecture of the active mitochondrial protein gate. *Science* 349 (6255), 1544–1548. doi:10.1126/science.aac6428

Shiota, T., Mabuchi, H., Tanaka-Yamano, S., Yamano, K., and Endo, T. (2011). *In vivo* protein-interaction mapping of a mitochondrial translocator protein Tom22 at work. *Proc. Natl. Acad. Sci. U. S. A.* 108 (37), 15179–15183. doi:10.1073/pnas.1105921108

Shirasaki, D. I., Greiner, E. R., Al-Ramahi, I., Gray, M., Boontheung, P., Geschwind, D. H., et al. (2012). Network organization of the huntingtin proteomic interactome in mammalian brain. *Neuron* 75 (1), 41–57. doi:10.1016/j.neuron.2012.05.024

Shirendeb, U. P., Calkins, M. J., Manczak, M., Anekonda, V., Dufour, B., McBride, J. L., et al. (2012). Mutant huntingtin's interaction with mitochondrial protein Drp1 impairs mitochondrial biogenesis and causes defective axonal transport and synaptic degeneration in Huntington's disease. *Hum. Mol. Genet.* 21 (2), 406–420. doi:10.1093/hmg/ddr475

Sichting, M., Mokranjac, D., Azem, A., Neupert, W., and Hell, K. (2005). Maintenance of structure and function of mitochondrial Hsp70 chaperones requires the chaperone Hep1. *EMBO J.* 24 (5), 1046–1056. doi:10.1038/sj.emboj.7600580

Silva, A. C., Almeida, S., Laco, M., Duarte, A. I., Domingues, J., Oliveira, C. R., et al. (2013). Mitochondrial respiratory chain complex activity and bioenergetic alterations in human platelets derived from pre-symptomatic and symptomatic Huntington's disease carriers. *Mitochondrion* 13 (6), 801–809. doi:10.1016/j.mito.2013.05.006

Silva, P. D., Schilke, B., Walter, W., Andrew, A., and Craig, E. A. (2003). J protein cochaperone of the mitochondrial inner membrane required for protein import into the mitochondrial matrix. *Proc. Natl. Acad. Sci. U. S. A.* 100 (24), 13839–13844. doi:10.1073/pnas.1936150100

Silva, P., Liu, Q., Walter, W., and Craig, E. A. (2004). Regulated interactions of mtHsp70 with Tim44 at the translocon in the mitochondrial inner membrane. *Nat. Struct. Mol. Biol.* 11 (11), 1084–1091. doi:10.1038/nsmb846

Sim, S. I., Chen, Y., Lynch, D. L., Gumbart, J. C., and Park, E. (2023). Structural basis of mitochondrial protein import by the TIM23 complex. *Nature* 621, 620–626. doi:10.1038/s41586-023-06239-6

Singh, R., Jamdar, S. N., Goyal, V. D., Kumar, A., Ghosh, B., and Makde, R. D. (2017). Structure of the human aminopeptidase XPNPEP3 and comparison of its *in vitro* activity with Icp55 orthologs: insights into diverse cellular processes. *J. Biol. Chem.* 292 (24), 10035–10047. doi:10.1074/jbc.M117.783357

Sinha, D., Joshi, N., Chittoor, B., Samji, P., and D'Silva, P. (2010). Role of Magmas in protein transport and human mitochondria biogenesis. *Hum. Mol. Genet.* 19 (7), 1248–1262. doi:10.1093/hmg/ddq002

Sinha, D., Srivastava, S., Krishna, L., and D'Silva, P. (2014). Unraveling the intricate organization of mammalian mitochondrial presequence translocases: existence of multiple translocases for maintenance of mitochondrial function. *Mol. Cell. Biol.* 34 (10), 1757–1775. doi:10.1128/MCB.01527-13

Sirk, D., Zhu, Z., Wadia, J. S., Shulyakova, N., Phan, N., Fong, J., et al. (2007). Chronic exposure to sub-lethal beta-amyloid (Abeta) inhibits the import of nuclear-encoded proteins to mitochondria in differentiated PC12 cells. *J. Neurochem.* 103 (5), 1989–2003. doi:10.1111/j.1471-4159.2007.04907.x

Sivanandam, V. N., Jayaraman, M., Hoop, C. L., Kodali, R., Wetzel, R., and van der Wel, P. C. (2011). The aggregation-enhancing huntingtin N-terminus is helical in amyloid fibrils. *J. Am. Chem. Soc.* 133 (12), 4558–4566. doi:10.1021/ja110715f

Skerjanc, I. S., Shore, G. C., and Silvius, J. R. (1987). The interaction of a synthetic mitochondrial signal peptide with lipid membranes is independent of transbilayer potential. *EMBO J.* 6 (10), 3117–3123. doi:10.1002/j.1460-2075.1987.tb02621.x

Somayaji, M., Lanseur, Z., Choi, S. J., Sulzer, D., and Mosharov, E. V. (2021). Roles for α-synuclein in gene expression. *Genes. (Basel)* 12 (8), 1166. doi:10.3390/genes12081166

Song, W., Chen, J., Petrilli, A., Liot, G., Klinglmayr, E., Zhou, Y., et al. (2011). Mutant huntingtin binds the mitochondrial fission GTPase dynamin-related protein-1 and increases its enzymatic activity. *Nat. Med.* 17 (3), 377–382. doi:10.1038/nm.2313

Sonsky, I., Vodicka, P., Vodickova Kepkova, K., and Hansikova, H. (2021). Mitophagy in Huntington's disease. *Neurochem. Int.* 149, 105147. doi:10.1016/j.neuint.2021.105147

Sorolla, M. A., Reverter-Branchat, G., Tamarit, J., Ferrer, I., Ros, J., and Cabiscol, E. (2008). Proteomic and oxidative stress analysis in human brain samples of Huntington disease. *Free Radic. Biol. Med.* 45 (5), 667–678. doi:10.1016/j.freeradbiomed.2008.05.014

Sorrentino, V., Romani, M., Mouchiroud, L., Beck, J. S., Zhang, H., D'Amico, D., et al. (2017). Enhancing mitochondrial proteostasis reduces amyloid-beta proteotoxicity. *Nature* 552 (7684), 187–193. doi:10.1038/nature25143

Spillantini, M. G., Crowther, R. A., Jakes, R., Hasegawa, M., and Goedert, M. (1998). alpha-Synuclein in filamentous inclusions of Lewy bodies from Parkinson's disease and dementia with lewy bodies. *Proc. Natl. Acad. Sci. U. S. A.* 95 (11), 6469–6473. doi:10.1073/pnas.95.11.6469

Srinivasan, E., Chandrasekhar, G., Chandrasekar, P., Anbarasu, K., Vickram, A. S., Karunakaran, R., et al. (2021). Alpha-synuclein aggregation in Parkinson's disease. *Front. Med. (Lausanne)* 8, 736978. doi:10.3389/fmed.2021.736978

Srivastava, S., Savanur, M. A., Sinha, D., Birje, A., and Saha, P. P. (2017). Regulation of mitochondrial protein import by the nucleotide exchange factors GrpEL1 and GrpEL2 in human cells. *J. Biol. Chem.* 292 (44), 18075–18090. doi:10.1074/jbc.M117.788463

Stefanis, L. (2012). α-Synuclein in Parkinson's disease. *Cold Spring Harb. Perspect. Med.* 2 (2), a009399. doi:10.1101/cshperspect.a009399

Steffan, J. S., Kazantsev, A., Spasic-Boskovic, O., Greenwald, M., Zhu, Y. Z., Gohler, H., et al. (2000). The Huntington's disease protein interacts with p53 and CREB-binding protein and represses transcription. *Proc. Natl. Acad. Sci. U. S. A.* 97 (12), 6763–6768. doi:10.1073/pnas.100110097

Stockl, M., Fischer, P., Wanker, E., and Herrmann, A. (2008). Alpha-synuclein selectively binds to anionic phospholipids embedded in liquid-disordered domains. *J. Mol. Biol.* 375 (5), 1394–1404. doi:10.1016/j.jmb.2007.11.051

Su, J., Liu, D., Yang, F., Zuo, M. Q., Li, C., Dong, M. Q., et al. (2022). Structural basis of Tom20 and Tom22 cytosolic domains as the human TOM complex receptors. *Proc. Natl. Acad. Sci. U. S. A.* 119 (26), e2200158119. doi:10.1073/pnas.2200158119

Suarez-Rivero, J. M., Pastor-Maldonado, C. J., Povea-Cabello, S., Alvarez-Cordoba, M., Villalon-Garcia, I., Talaveron-Rey, M., et al. (2022). Activation of the mitochondrial unfolded protein response: a new therapeutic target? *Biomedicines* 10 (7), 1611. doi:10.3390/biomedicines10071611

Sugrue, M. M., and Tatton, W. G. (2001). Mitochondrial membrane potential in aging cells. *Biol. Signals Recept* 10 (3-4), 176–188. doi:10.1159/000046886

Suzuki, H., Okazawa, Y., Komiya, T., Saeki, K., Mekada, E., Kitada, S., et al. (2000). Characterization of rat TOM40, a central component of the preprotein translocase of the mitochondrial outer membrane. *J. Biol. Chem.* 275 (48), 37930–37936. doi:10.1074/jbc.M006558200

Swerdlow, R. H., Burns, J. M., and Khan, S. M. (2014). The Alzheimer's disease mitochondrial cascade hypothesis: progress and perspectives. *Biochim. Biophys. Acta* 1842 (8), 1219–1231. doi:10.1016/j.bbadis.2013.09.010

Szczepanowska, K., and Trifunovic, A. (2022). Mitochondrial matrix proteases: quality control and beyond. *FEBS J.* 289 (22), 7128–7146. doi:10.1111/febs.15964

Szeto, H. H. (2014). First-in-class cardiolipin-protective compound as a therapeutic agent to restore mitochondrial bioenergetics. *Br. J. Pharmacol.* 171 (8), 2029–2050. doi:10.1111/bph.12461

Tam, S., Spiess, C., Auyeung, W., Joachimiak, L., Chen, B., Poirier, M. A., et al. (2009). The chaperonin TRiC blocks a huntingtin sequence element that promotes the conformational switch to aggregation. *Nat. Struct. Mol. Biol.* 16 (12), 1279–1285. doi:10.1038/nsmb.1700

Tambini, M. D., Pera, M., Kanter, E., Yang, H., Guardia-Laguarta, C., Holtzman, D., et al. (2016). ApoE4 upregulates the activity of mitochondria-associated ER membranes. *EMBO Rep.* 17 (1), 27–36. doi:10.15252/embr.201540614

Tamura, Y., Harada, Y., Shiota, T., Yamano, K., Watanabe, K., Yokota, M., et al. (2009). Tim23-Tim50 pair coordinates functions of translocators and motor proteins in mitochondrial protein import. *J. Cell. Biol.* 184 (1), 129–141. doi:10.1083/jcb.200808068

Tanaka, M., Morishima, I., Akagi, T., Hashikawa, T., and Nukina, N. (2001). Intra- and intermolecular beta-pleated sheet formation in glutamine-repeat inserted myoglobin as a model for polyglutamine diseases. *J. Biol. Chem.* 276 (48), 45470–45475. doi:10.1074/jbc.M107502200

Taylor, A. B., Smith, B. S., Kitada, S., Kojima, K., Miyaura, H., Otwinowski, Z., et al. (2001). Crystal structures of mitochondrial processing peptidase reveal the mode for specific cleavage of import signal sequences. *Structure* 9 (7), 615–625. doi:10.1016/s0969-2126(01)00621-9

Taylor, R. C., and Dillin, A. (2011). Aging as an event of proteostasis collapse. *Cold Spring Harb. Perspect. Biol.* 3 (5), a004440. doi:10.1101/cshperspect.a004440

Tcw, J., and Goate, A. M. (2017). Genetics of beta-amyloid precursor protein in alzheimer's disease. *Cold Spring Harb. Perspect. Med.* 7 (6), a024539. doi:10.1101/cshperspect.a024539

Tebbenkamp, A. T., Crosby, K. W., Siemienski, Z. B., Brown, H. H., Golde, T. E., and Borchelt, D. R. (2012). Analysis of proteolytic processes and enzymatic activities in the generation of huntingtin n-terminal fragments in an HEK293 cell model. *PLoS One* 7 (12), e50750. doi:10.1371/journal.pone.0050750

Teixeira, P. F., and Glaser, E. (2013). Processing peptidases in mitochondria and chloroplasts. *Biochim. Biophys. Acta* 1833 (2), 360–370. doi:10.1016/j.bbamcr.2012.03.012

Terada, K., Ohtsuka, K., Imamoto, N., Yoneda, Y., and Mori, M. (1995). Role of heat shock cognate 70 protein in import of ornithine transcarbamylase precursor into mammalian mitochondria. *Mol. Cell. Biol.* 15 (7), 3708–3713. doi:10.1128/mcb.15.7.3708

Terni, B., Boada, J., Portero-Otin, M., Pamplona, R., and Ferrer, I. (2010). Mitochondrial ATP-synthase in the entorhinal cortex is a target of oxidative stress at stages I/II of Alzheimer's disease pathology. *Brain Pathol.* 20 (1), 222–233. doi:10.1111/j.1750-3639.2009.00266.x

Thakur, A. K., Jayaraman, M., Mishra, R., Thakur, M., Chellgren, V. M., Byeon, I. J., et al. (2009). Polyglutamine disruption of the huntingtin exon 1 N terminus triggers a complex aggregation mechanism. *Nat. Struct. Mol. Biol.* 16 (4), 380–389. doi:10.1038/nsmb.1570

Theillet, F. X., Binolfi, A., Bekei, B., Martorana, A., Rose, H. M., Stuiver, M., et al. (2016). Structural disorder of monomeric alpha-synuclein persists in mammalian cells. *Nature* 530 (7588), 45–50. doi:10.1038/nature16531

Thorne, N. J., and Tumbarello, D. A. (2022). The relationship of alpha-synuclein to mitochondrial dynamics and quality control. *Front. Mol. Neurosci.* 15, 947191. doi:10.3389/fnmol.2022.947191

Tornquist, M., Michaels, T. C. T., Sanagavarapu, K., Yang, X., Meisl, G., Cohen, S. I. A., et al. (2018). Secondary nucleation in amyloid formation. *Chem. Commun. (Camb).* 54 (63), 8667–8684. doi:10.1039/c8cc02204f

Truscott, K. N., Kovermann, P., Geissler, A., Merlin, A., Meijer, M., Driessen, A. J., et al. (2001). A presequence- and voltage-sensitive channel of the mitochondrial preprotein translocase formed by Tim23. *Nat. Struct. Biol.* 8 (12), 1074–1082. doi:10.1038/nsb726

Truscott, K. N., Voos, W., Frazier, A. E., Lind, M., Li, Y., Geissler, A., et al. (2003). A J-protein is an essential subunit of the presequence translocase-associated protein import motor of mitochondria. *J. Cell. Biol.* 163 (4), 707–713. doi:10.1083/jcb.200308004

Trushina, E., Dyer, R. B., Badger, J. D., 2nd, Ure, D., Eide, L., Tran, D. D., et al. (2004). Mutant huntingtin impairs axonal trafficking in mammalian neurons *in vivo* and *in vitro*. *Mol. Cell. Biol.* 24 (18), 8195–8209. doi:10.1128/MCB.24.18.8195-8209.2004

Tsacopoulos, M., and Magistretti, P. J. (1996). Metabolic coupling between glia and neurons. *J. Neurosci.* 16 (3), 877–885. doi:10.1523/JNEUROSCI.16-03-00877.1996

Tucker, K., and Park, E. (2019). Cryo-EM structure of the mitochondrial protein-import channel TOM complex at near-atomic resolution. *Nat. Struct. Mol. Biol.* 26 (12), 1158–1166. doi:10.1038/s41594-019-0339-2

Uddin, M. S., Kabir, M. T., Rahman, M. S., Behl, T., Jeandet, P., Ashraf, G. M., et al. (2020). Revisiting the amyloid cascade hypothesis: from anti-aβ therapeutics to auspicious new ways for alzheimer's disease. *Int. J. Mol. Sci.* 21 (16), 5858. doi:10.3390/ijms21165858

Ullman, O., Fisher, C. K., and Stultz, C. M. (2011). Explaining the structural plasticity of alpha-synuclein. *J. Am. Chem. Soc.* 133 (48), 19536–19546. doi:10.1021/ja208657z

Ulmer, T. S., Bax, A., Cole, N. B., and Nussbaum, R. L. (2005). Structure and dynamics of micelle-bound human alpha-synuclein. *J. Biol. Chem.* 280 (10), 9595–9603. doi:10.1074/jbc.M411805200

Uversky, V. N. (2002). Natively unfolded proteins: a point where biology waits for physics. *Protein Sci.* 11 (4), 739–756. doi:10.1110/ps.4210102

van der Laan, M., Wiedemann, N., Mick, D. U., Guiard, B., Rehling, P., and Pfanner, N. (2006). A role for Tim21 in membrane-potential-dependent preprotein sorting in mitochondria. *Curr. Biol.* 16 (22), 2271–2276. doi:10.1016/j.cub.2006.10.025

van Wilpe, S., Ryan, M. T., Hill, K., Maarse, A. C., Meisinger, C., Brix, J., et al. (1999). Tom22 is a multifunctional organizer of the mitochondrial preprotein translocase. *Nature* 401 (6752), 485–489. doi:10.1038/46802

Vande Walle, L., Lamkanfi, M., and Vandenabeele, P. (2008). The mitochondrial serine protease HtrA2/Omi: an overview. *Cell. Death Differ.* 15 (3), 453–460. doi:10.1038/sj.cdd.4402291

Vangavaragu, J. R., Valasani, K. R., Gan, X., and Yan, S. S. (2014). Identification of human presequence protease (hPreP) agonists for the treatment of Alzheimer's disease. *Eur. J. Med. Chem.* 76, 506–516. doi:10.1016/j.ejmech.2014.02.046

Varshavsky, A. (2011). The N-end rule pathway and regulation by proteolysis. *Protein Sci.* 20 (8), 1298–1345. doi:10.1002/pro.666

Ventura, A., Maccarana, M., Raker, V. A., and Pelicci, P. G. (2004). A cryptic targeting signal induces isoform-specific localization of p46Shc to mitochondria. *J. Biol. Chem.* 279 (3), 2299–2306. doi:10.1074/jbc.M307655200

Vicario, M., Cieri, D., Brini, M., and Cali, T. (2018). The close encounter between alpha-synuclein and mitochondria. *Front. Neurosci.* 12, 388. doi:10.3389/fnins.2018.00388

Vijayvargia, R., Epand, R., Leitner, A., Jung, T. Y., Shin, B., Jung, R., et al. (2016). Huntingtin's spherical solenoid structure enables polyglutamine tract-dependent modulation of its structure and function. *Elife* 5, e11184. doi:10.7554/eLife.11184

Vogtle, F. N., Prinz, C., Kellermann, J., Lottspeich, F., Pfanner, N., and Meisinger, C. (2011). Mitochondrial protein turnover: role of the precursor intermediate peptidase Oct1 in protein stabilization. *Mol. Biol. Cell.* 22 (13), 2135–2143. doi:10.1091/mbc.E11-02-0169

Vogtle, F. N., Wortelkamp, S., Zahedi, R. P., Becker, D., Leidhold, C., Gevaert, K., et al. (2009). Global analysis of the mitochondrial N-proteome identifies a processing peptidase critical for protein stability. *Cell.* 139 (2), 428–439. doi:10.1016/j.cell.2009.07.045

Waegemann, K., Popov-Celeketic, D., Neupert, W., Azem, A., and Mokranjac, D. (2015). Cooperation of TOM and TIM23 complexes during translocation of proteins into mitochondria. *J. Mol. Biol.* 427 (5), 1075–1084. doi:10.1016/j.jmb.2014.07.015

Waingankar, T. P., and Silva, P. (2021). Multiple variants of the human presequence translocase motor subunit Magmas govern the mitochondrial import. *J. Biol. Chem.* 297 (6), 101349. doi:10.1016/j.jbc.2021.101349

Wang, M., Oge, L., Perez-Garcia, M. D., Hamama, L., and Sakr, S. (2018). The PUF protein family: overview on PUF RNA targets, biological functions, and post transcriptional regulation. *Int. J. Mol. Sci.* 19 (2), 410. doi:10.3390/ijms19020410

Wang, W., Chen, X., Zhang, L., Yi, J., Ma, Q., Yin, J., et al. (2020a). Atomic structure of human TOM core complex. *Cell. Discov.* 6, 67. doi:10.1038/s41421-020-00198-2

Wang, W., Perovic, I., Chittuluru, J., Kaganovich, A., Nguyen, L. T., Liao, J., et al. (2011). A soluble alpha-synuclein construct forms a dynamic tetramer. *Proc. Natl. Acad. Sci. U. S. A.* 108 (43), 17797–17802. doi:10.1073/pnas.1113260108

Wang, W., Zhao, F., Ma, X., Perry, G., and Zhu, X. (2020c). Mitochondria dysfunction in the pathogenesis of Alzheimer's disease: recent advances. *Mol. Neurodegener.* 15 (1), 30. doi:10.1186/s13024-020-00376-6

Wang, W., Zhao, F., Ma, X., Perry, G., and Zhu, X. (2020b). Mitochondria dysfunction in the pathogenesis of Alzheimer's disease: recent advances. *Mol. Neurodegener.* 15 (1), 30. doi:10.1186/s13024-020-00376-6

Wang, X., and Chen, X. J. (2015). A cytosolic network suppressing mitochondria-mediated proteostatic stress and cell death. *Nature* 524 (7566), 481–484. doi:10.1038/nature14859

Wang, X., Su, B., Lee, H. G., Li, X., Perry, G., Smith, M. A., et al. (2009). Impaired balance of mitochondrial fission and fusion in Alzheimer's disease. *J. Neurosci.* 29 (28), 9090–9103. doi:10.1523/JNEUROSCI.1357-09.2009

Wang, X., Su, B., Siedlak, S. L., Moreira, P. I., Fujioka, H., Wang, Y., et al. (2008a). Amyloid-beta overproduction causes abnormal mitochondrial dynamics via differential modulation of mitochondrial fission/fusion proteins. *Proc. Natl. Acad. Sci. U. S. A.* 105 (49), 19318–19323. doi:10.1073/pnas.0804871105

Wang, X., Zhu, S., Pei, Z., Drozda, M., Stavrovskaya, I. G., Del Signore, S. J., et al. (2008b). Inhibitors of cytochrome c release with therapeutic potential for Huntington's disease. *J. Neurosci.* 28 (38), 9473–9485. doi:10.1523/JNEUROSCI.1867-08.2008

Wang, Y., Guo, X., Ye, K., Orth, M., and Gu, Z. (2021). Accelerated expansion of pathogenic mitochondrial DNA heteroplasmies in Huntington's disease. *Proc. Natl. Acad. Sci. U. S. A.* 118 (30), e2014610118. doi:10.1073/pnas.2014610118

Weidberg, H., and Amon, A. (2018). MitoCPR-A surveillance pathway that protects mitochondria in response to protein import stress. *Science* 360 (6385), eaan4146. doi:10.1126/science.aan4146

Weill, U., Yofe, I., Sass, E., Stynen, B., Davidi, D., Natarajan, J., et al. (2018). Genome-wide SWAp-Tag yeast libraries for proteome exploration. *Nat. Methods* 15 (8), 617–622. doi:10.1038/s41592-018-0044-9

Weinreb, P. H., Zhen, W., Poon, A. W., Conway, K. A., and Lansbury, P. T., Jr (1996). NACP, a protein implicated in Alzheimer's disease and learning, is natively unfolded. *Biochemistry* 35 (43), 13709–13715. doi:10.1021/bi961799n

Wellington, C. L., Ellerby, L. M., Hackam, A. S., Margolis, R. L., Trifiro, M. A., Singaraja, R., et al. (1998). Caspase cleavage of gene products associated with triplet expansion disorders generates truncated fragments containing the polyglutamine tract. *J. Biol. Chem.* 273 (15), 9158–9167. doi:10.1074/jbc.273.15.9158

Wells, C., Brennan, S., Keon, M., and Ooi, L. (2021). The role of amyloid oligomers in neurodegenerative pathologies. *Int. J. Biol. Macromol.* 181, 582–604. doi:10.1016/j.ijbiomac.2021.03.113

Wentink, A. S., Nillegoda, N. B., Feufel, J., Ubartaite, G., Schneider, C. P., De Los Rios, P., et al. (2020). Molecular dissection of amyloid disaggregation by human HSP70. *Nature* 587 (7834), 483–488. doi:10.1038/s41586-020-2904-6

Weydt, P., Pineda, V. V., Torrence, A. E., Libby, R. T., Satterfield, T. F., Lazarowski, E. R., et al. (2006). Thermoregulatory and metabolic defects in Huntington's disease transgenic mice implicate PGC-1alpha in Huntington's disease neurodegeneration. *Cell. Metab.* 4 (5), 349–362. doi:10.1016/j.cmet.2006.10.004

Wiedemann, N., Pfanner, N., and Ryan, M. T. (2001). The three modules of ADP/ATP carrier cooperate in receptor recruitment and translocation into mitochondria. *EMBO J.* 20 (5), 951–960. doi:10.1093/emboj/20.5.951

Wiedmann, B., Sakai, H., Davis, T. A., and Wiedmann, M. (1994). A protein complex required for signal-sequence-specific sorting and translocation. *Nature* 370 (6489), 434–440. doi:10.1038/370434a0

Wieprecht, T., Apostolov, O., Beyermann, M., and Seelig, J. (2000). Interaction of a mitochondrial presequence with lipid membranes: role of helix formation for membrane binding and perturbation. *Biochemistry* 39 (50), 15297–15305. doi:10.1021/bi001774v

Williams, C. C., Jan, C. H., and Weissman, J. S. (2014). Targeting and plasticity of mitochondrial proteins revealed by proximity-specific ribosome profiling. *Science* 346 (6210), 748–751. doi:10.1126/science.1257522

Wodrich, A. P. K., Scott, A. W., Shukla, A. K., Harris, B. T., and Giniger, E. (2022). The unfolded protein responses in health, aging, and neurodegeneration: recent advances and future considerations. *Front. Mol. Neurosci.* 15, 831116. doi:10.3389/fnmol.2022.831116

Woellhaf, M. W., Hansen, K. G., Garth, C., and Herrmann, J. M. (2014). Import of ribosomal proteins into yeast mitochondria. *Biochem. Cell. Biol.* 92 (6), 489–498. doi:10.1139/bcb-2014-0029

Wong, Y. C., and Holzbaur, E. L. (2014). The regulation of autophagosome dynamics by huntingtin and HAP1 is disrupted by expression of mutant huntingtin, leading to defective cargo degradation. *J. Neurosci.* 34 (4), 1293–1305. doi:10.1523/JNEUROSCI.1870-13.2014

Wrobel, L., Topf, U., Bragoszewski, P., Wiese, S., Sztolsztener, M. E., Oeljeklaus, S., et al. (2015). Mistargeted mitochondrial proteins activate a proteostatic response in the cytosol. *Nature* 524 (7566), 485–488. doi:10.1038/nature14951

Wu, Y., and Sha, B. (2006). Crystal structure of yeast mitochondrial outer membrane translocon member Tom70p. *Nat. Struct. Mol. Biol.* 13 (7), 589–593. doi:10.1038/nsmb1106

Wynne, M. E., Ogunbona, O., Lane, A. R., Gokhale, A., Zlatic, S. A., Xu, C., et al. (2023). APOE expression and secretion are modulated by mitochondrial dysfunction. *Elife* 12, e85779. doi:10.7554/eLife.85779

Xie, W., and Chung, K. K. (2012). Alpha-synuclein impairs normal dynamics of mitochondria in cell and animal models of Parkinson's disease. *J. Neurochem.* 122 (2), 404–414. doi:10.1111/j.1471-4159.2012.07769.x

Xin, N., Durieux, J., Yang, C., Wolff, S., Kim, H. E., and Dillin, A. (2022). The UPRmt preserves mitochondrial import to extend lifespan. *J. Cell. Biol.* 221 (7), e202201071. doi:10.1083/jcb.202201071

Xu, J., Du, W., Zhao, Y., Lim, K., Lu, L., Zhang, C., et al. (2022b). Mitochondria targeting drugs for neurodegenerative diseases-Design, mechanism and application. *Acta Pharm. Sin. B* 12 (6), 2778–2789. doi:10.1016/j.apsb.2022.03.001

Xu, J., Minobe, E., and Kameyama, M. (2022a). Ca(2+) dyshomeostasis links risk factors to neurodegeneration in Parkinson's disease. *Front. Cell. Neurosci.* 16, 867385. doi:10.3389/fncel.2022.867385

Xu, Y. J., Mei, Y., Qu, Z. L., Zhang, S. J., Zhao, W., Fang, J. S., et al. (2018). Ligustilide ameliorates memory deficiency in APP/PS1 transgenic mice via restoring mitochondrial dysfunction. *Biomed. Res. Int.* 2018, 4606752. doi:10.1155/2018/4606752

Yablonska, S., Ganesan, V., Ferrando, L. M., Kim, J., Pyzel, A., Baranova, O. V., et al. (2019). Mutant huntingtin disrupts mitochondrial proteostasis by interacting with TIM23. *Proc. Natl. Acad. Sci. U. S. A.* 116 (33), 16593–16602. doi:10.1073/pnas.1904101116

Yamamoto, A., Lucas, J. J., and Hen, R. (2000). Reversal of neuropathology and motor dysfunction in a conditional model of huntington's disease. *Cell.* 101 (1), 57–66. doi:10.1016/S0092-8674(00)80623-6

Yamamoto, H., Esaki, M., Kanamori, T., Tamura, Y., Nishikawa, S., and Endo, T. (2002). Tim50 is a subunit of the TIM23 complex that links protein translocation across the outer and inner mitochondrial membranes. *Cell.* 111 (4), 519–528. doi:10.1016/s0092-8674(02)01053-x

Yamamoto, H., Fukui, K., Takahashi, H., Kitamura, S., Shiota, T., Terao, K., et al. (2009). Roles of Tom70 in import of presequence-containing mitochondrial proteins. *J. Biol. Chem.* 284 (46), 31635–31646. doi:10.1074/jbc.M109.041756

Yamano, K., Yatsukawa, Y., Esaki, M., Hobbs, A. E., Jensen, R. E., and Endo, T. (2008). Tom20 and Tom22 share the common signal recognition pathway in mitochondrial protein import. *J. Biol. Chem.* 283 (7), 3799–3807. doi:10.1074/jbc.M708339200

Yang, L., Zhao, K., Calingasan, N. Y., Luo, G., Szeto, H. H., and Beal, M. F. (2009). Mitochondria targeted peptides protect against 1-methyl-4-phenyl-1,2,3,6-tetrahydropyridine neurotoxicity. *Antioxid. Redox Signal* 11 (9), 2095–2104. doi:10.1089/ars.2009.2445

Yang, L. G., March, Z. M., Stephenson, R. A., and Narayan, P. S. (2023). Apolipoprotein E in lipid metabolism and neurodegenerative disease. *Trends Endocrinol. Metab.* 34 (8), 430–445. doi:10.1016/j.tem.2023.05.002

Yang, Y., Shi, Y., Schweighauser, M., Zhang, X., Kotecha, A., Murzin, A. G., et al. (2022). Structures of α-synuclein filaments from human brains with Lewy pathology. *Nature* 610 (7933), 791–795. doi:10.1038/s41586-022-05319-3

Yano, H., Baranov, S. V., Baranova, O. V., Kim, J., Pan, Y., Yablonska, S., et al. (2014). Inhibition of mitochondrial protein import by mutant huntingtin. *Nat. Neurosci.* 17 (6), 822–831. doi:10.1038/nn.3721

Yano, M., Terada, K., and Mori, M. (2004). Mitochondrial import receptors Tom20 and Tom22 have chaperone-like activity. *J. Biol. Chem.* 279 (11), 10808–10813. doi:10.1074/jbc.M311710200

Yapa, N. M. B., Lisnyak, V., Reljic, B., and Ryan, M. T. (2021). Mitochondrial dynamics in health and disease. *FEBS Lett.* 595 (8), 1184–1204. doi:10.1002/1873-3468.14077

Yiannopoulou, K. G., and Papageorgiou, S. G. (2020). Current and future treatments in alzheimer disease: an update. *J. Cent. Nerv. Syst. Dis.* 12, 1179573520907397. doi:10.1177/1179573520907397

Yin, F. (2023). Lipid metabolism and Alzheimer's disease: clinical evidence, mechanistic link and therapeutic promise. *FEBS J.* 290 (6), 1420–1453. doi:10.1111/febs.16344

Yin, X., Manczak, M., and Reddy, P. H. (2016). Mitochondria-targeted molecules MitoQ and SS31 reduce mutant huntingtin-induced mitochondrial toxicity and synaptic damage in Huntington's disease. *Hum. Mol. Genet.* 25 (9), 1739–1753. doi:10.1093/hmg/ddw045

Yogev, O., Karniely, S., and Pines, O. (2007). Translation-coupled translocation of yeast fumarase into mitochondria *in vivo*. *J. Biol. Chem.* 282 (40), 29222–29229. doi:10.1074/jbc.M704201200

Young, J. C., Hoogenraad, N. J., and Hartl, F. U. (2003). Molecular chaperones Hsp90 and Hsp70 deliver preproteins to the mitochondrial import receptor Tom70. *Cell.* 112 (1), 41–50. doi:10.1016/s0092-8674(02)01250-3

Zeytuni, N., and Zarivach, R. (2012). Structural and functional discussion of the tetra-trico-peptide repeat, a protein interaction module. *Structure* 20 (3), 397–405. doi:10.1016/j.str.2012.01.006

Zhai, P., Stanworth, C., Liu, S., and Silberg, J. J. (2008). The human escort protein Hep binds to the ATPase domain of mitochondrial hsp70 and regulates ATP hydrolysis. *J. Biol. Chem.* 283 (38), 26098–26106. doi:10.1074/jbc.M803475200

Zhai, S., Tanimura, A., Graves, S. M., Shen, W., and Surmeier, D. J. (2018). Striatal synapses, circuits, and Parkinson's disease. *Curr. Opin. Neurobiol.* 48, 9–16. doi:10.1016/j.conb.2017.08.004

Zhang, H., Alder, N. N., Wang, W., Szeto, H., Marcinek, D. J., and Rabinovitch, P. S. (2020). Reduction of elevated proton leak rejuvenates mitochondria in the aged cardiomyocyte. *Elife* 9, e60827. doi:10.7554/eLife.60827

Zhang, L., Guo, X. Q., Chu, J. F., Zhang, X., Yan, Z. R., and Li, Y. Z. (2015). Potential hippocampal genes and pathways involved in Alzheimer's disease: a bioinformatic analysis. *Genet. Mol. Res.* 14 (2), 7218–7232. doi:10.4238/2015.June.29.15

Zhang, L., Zhang, C., Zhu, Y., Cai, Q., Chan, P., Ueda, K., et al. (2008). Semi-quantitative analysis of alpha-synuclein in subcellular pools of rat brain neurons: an immunogold electron microscopic study using a C-terminal specific monoclonal antibody. *Brain Res.* 1244, 40–52. doi:10.1016/j.brainres.2008.08.067

Zhang, Y., Chen, Y., Gucek, M., and Xu, H. (2016). The mitochondrial outer membrane protein MDI promotes local protein synthesis and mtDNA replication. *EMBO J.* 35 (10), 1045–1057. doi:10.15252/embj.201592994

Zhang, Y., Leavitt, B. R., van Raamsdonk, J. M., Dragatsis, I., Goldowitz, D., MacDonald, M. E., et al. (2006). Huntingtin inhibits caspase-3 activation. *EMBO J.* 25 (24), 5896–5906. doi:10.1038/sj.emboj.7601445

Zhao, J., Liu, X., Xia, W., Zhang, Y., and Wang, C. (2020). Targeting amyloidogenic processing of APP in alzheimer's disease. *Front. Mol. Neurosci.* 13, 137. doi:10.3389/fnmol.2020.00137

Zhao, W., Xu, Z., Cao, J., Fu, Q., Wu, Y., Zhang, X., et al. (2019). Elamipretide (SS-31) improves mitochondrial dysfunction, synaptic and memory impairment induced by lipopolysaccharide in mice. *J. Neuroinflammation* 16 (1), 230. doi:10.1186/s12974-019-1627-9

Zheng, H., and Koo, E. H. (2011). Biology and pathophysiology of the amyloid precursor protein. *Mol. Neurodegener.* 6 (1), 27. doi:10.1186/1750-1326-6-27

Zhou, Z. D., Chan, C. H., Ma, Q. H., Xu, X. H., Xiao, Z. C., and Tan, E. K. (2011). The roles of amyloid precursor protein (APP) in neurogenesis: implications to pathogenesis and therapy of Alzheimer disease. *Cell. Adh Migr.* 5 (4), 280–292. doi:10.4161/cam.5.4.16986

Zhu, L., Zhou, Q., He, L., and Chen, L. (2021). Mitochondrial unfolded protein response: an emerging pathway in human diseases. *Free Radic. Biol. Med.* 163, 125–134. doi:10.1016/j.freeradbiomed.2020.12.013

Zhu, Y., Duan, C., Lu, L., Gao, H., Zhao, C., Yu, S., et al. (2011). α-Synuclein overexpression impairs mitochondrial function by associating with adenylate translocator. *Int. J. Biochem. Cell. Biol.* 43 (5), 732–741. doi:10.1016/j.biocel.2011.01.014

Zhu, Y., Wang, H., Fang, J., Dai, W., Zhou, J., Wang, X., et al. (2018). SS-31 provides neuroprotection by reversing mitochondrial dysfunction after traumatic brain injury. *Oxid. Med. Cell. Longev.* 2018, 4783602. doi:10.1155/2018/4783602

Zigoneanu, I. G., Yang, Y. J., Krois, A. S., Haque, E., and Pielak, G. J. (2012). Interaction of alpha-synuclein with vesicles that mimic mitochondrial membranes. *Biochim. Biophys. Acta* 1818 (3), 512–519. doi:10.1016/j.bbamem.2011.11.024

Zraika, S., Hull, R. L., Verchere, C. B., Clark, A., Potter, K. J., Fraser, P. E., et al. (2010). Toxic oligomers and islet beta cell death: guilty by association or convicted by circumstantial evidence? *Diabetologia* 53 (6), 1046–1056. doi:10.1007/s00125-010-1671-6

Frontiers in Physiology

Understanding how an organism's components work together to maintain a healthy state

The second most-cited physiology journal, promoting a multidisciplinary approach to the physiology of living systems - from the subcellular and molecular domains to the intact organism and its interaction with the environment.

Discover the latest Research Topics

See more →

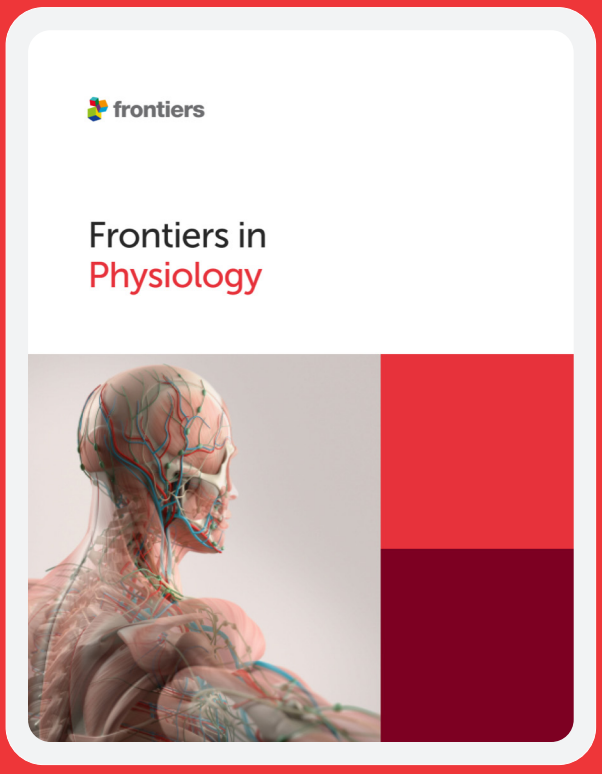

Frontiers

Avenue du Tribunal-Fédéral 34
1005 Lausanne, Switzerland
frontiersin.org

Contact us

+41 (0)21 510 17 00
frontiersin.org/about/contact